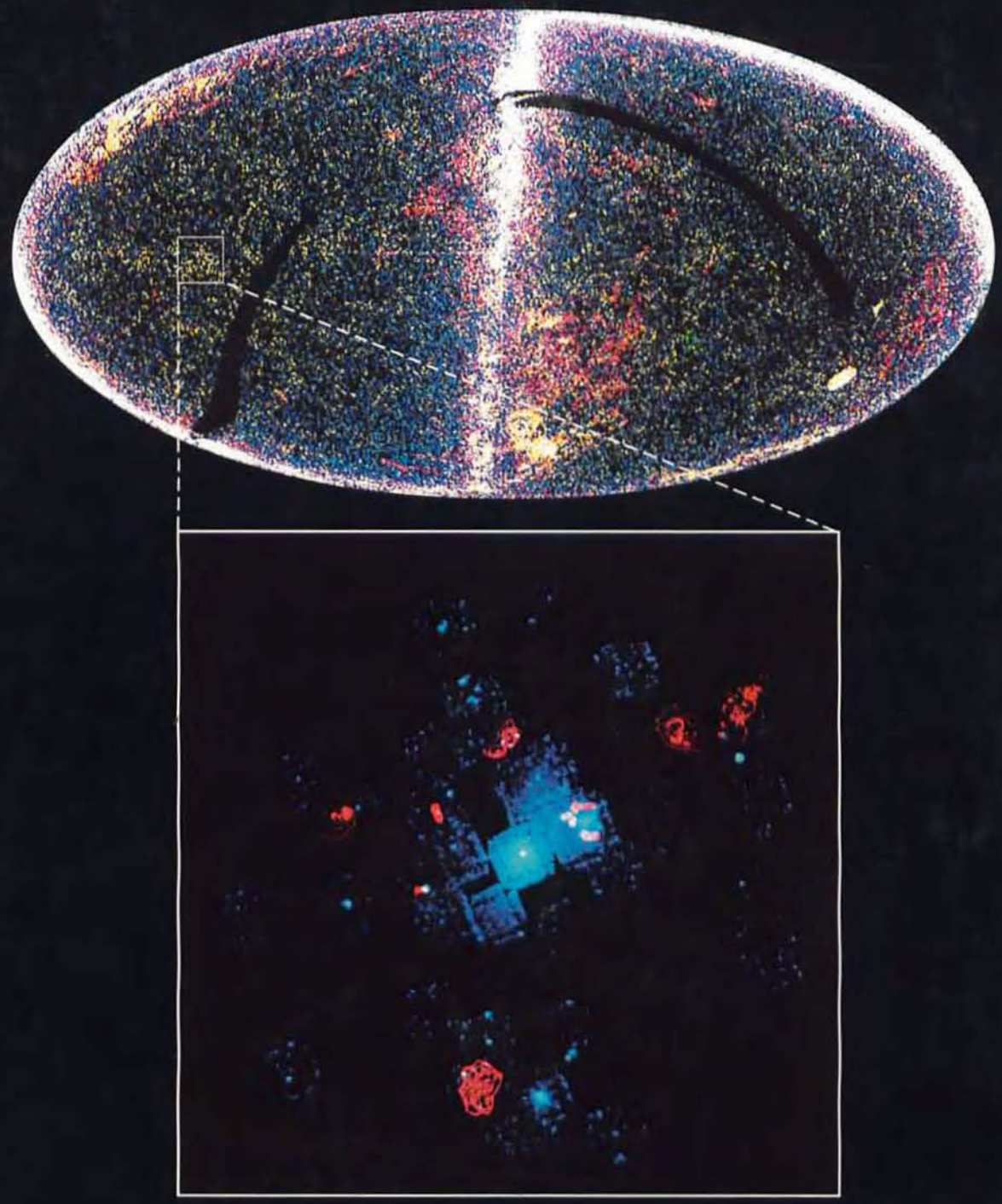
ESO WORKSHOP ON

THE VIRGO CLUSTER

Garching, 4 – 7 September 1984



PROCEEDINGS

Edited by O.-G. Richter and B. Binggeli

European Southern Observatory
ESO
ML 179185
A 24-6
39 a

ESO Libraries

ML 1993 001775

COVER

At the top is a representation of all point sources detected by the IRAS telescope. The point source fluxes are added in each 1/2 deg by 1/2 deg bin on the sky, and the resulting intensity is plotted using blue for the 12 μm band, green for the 60 μm band, and red for the 100 μm band. Supergalactic coordinates are used in this plot, with the Supergalactic equator running along the major axis of the ellipse. The Galaxy runs along the edges and minor axis of the figure; Galactic cirrus appears red. Blue characterizes stars, which concentrate in the Galactic Plane. Yellow is the dominant colour for galaxies. The Virgo cluster of galaxies (inside the little box) stands out prominently. Photograph courtesy of George Helou, JPL, Pasadena, CA, U.S.A.

The bottom picture is a map of the neutral hydrogen emission in the central 10×10 deg^2 of the Virgo cluster superposed on a map of the X-ray emission. The X-ray emission, shown in blue, was observed with the Einstein Observatory. The observed fields have been collected in the mosaic by C. Jones and W. Forman. The bright source in the centre is the X-ray emission from M87. The neutral hydrogen 21cm line emission, shown in red, was observed at the Very Large Array by J. van Gorkom, C. Balkowski and C. Kotanyi. The red contours show the intensity of the integrated 21cm emission in the brightest spiral galaxies. The overlay was made by C. Jones. For an identification of the galaxies see Figure 1 of the paper by J. van Gorkom and C. Kotanyi in this volume. The picture is a normal presentation in right ascension and declination where north is up and east is to the left. Note, therefore, that in reality it does not correspond with the little box in the top picture; neither in orientation nor in angular size. Photograph courtesy of Chris Kotanyi, NRAO, Socorro, NM, U.S.A.

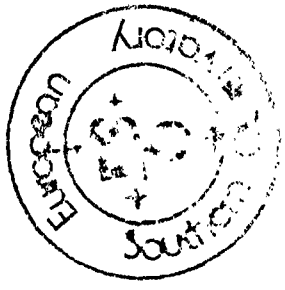


EUROPEAN SOUTHERN OBSERVATORY

ESO WORKSHOP ON

THE VIRGO CLUSTER OF GALAXIES

Garching, 4 – 7 September 1984



PROCEEDINGS

Edited by O.-G. Richter and B. Binggeli

January 1985

ESO Conference and Workshop Proceedings No. 20

EUROPEAN SOUTHERN OBSERVATORY
Karl-Schwarzschild-Str. 2, D-8046 Garching bei München
Federal Republic of Germany

© Copyright 1985 by the European Southern Observatory

ISBN 3-923524-20-X

Foreword

The Virgo Cluster of Galaxies has figured prominently in extragalactic research ever since its beginnings in the 1920's. But, surprisingly, as Prof. Tammann explained in his introduction to this workshop, it is only recently that the cluster of galaxies closest to us has become the focus of intense research. As we now realize, the *Virgo* cluster is likely to play the role of a "Rosetta Stone" for many problems in extragalactic astronomy, being an ideal laboratory in our backyard, cosmologically speaking, in which to study galaxy formation and evolution.

The time was certainly ripe for a workshop devoted exclusively to the *Virgo* cluster of galaxies. Several important surveys of the Virgo region have just been completed or are well underway. Entirely new views of the cluster have been obtained by spaceborne observatories, as shown on the cover of these proceedings. The diversity of observational and theoretical work centred on the *Virgo* cluster is growing fast. It was the idea of this ESO workshop to bring together the people who are working in the field and let them display this diversity of research; to let them survey what has already been done and is currently being done; to discuss what ought to be done next; and, to coordinate their efforts. We think this workshop was a success.

These proceedings contain all the papers that were given at the 4-day workshop. With few exceptions the order of presentation is the same. The camera-ready manuscripts had to be sent in within two months after the meeting, leaving ample time for the authors to respond to the workshop if necessary or desired. These proceedings also include the panel discussion on *"Future Needs for Observations of the Virgo Cluster"* held on the third day of the workshop. The whole discussion was recorded on tape, transcribed, and subsequently smoothed for the sake of clarity and readability. However, the smoothing was kept to a minimum. Our goal was not to write another scientific paper but to give the reader a feeling for the lively and stimulating atmosphere that characterized this workshop. We hope the speakers will agree.

Of course, this ESO workshop could never have taken place without the help of many people who worked "behind the scenes". First, and foremost, is Ms. Christina Stoffer who also did a great job in preparing these proceedings. Without her skills in planning and organizing we had been - and would be - nowhere. Thanks are due to Pam Bristow, Britt Sjöberg, and Harry Neumann, among others, for their excellent help with all local arrangements. We would also like to thank the chairmen of the various workshop sessions for providing stimulation under the constraint imposed by a tight schedule. Kurt Kjär was responsible for all technical aspects of the editorial work. His expertise is gratefully acknowledged. Finally, we are indebted to Massimo Tarenghi who was indispensable in many ways.

Otto-Georg Richter

Bruno Binggeli

TABLE OF CONTENTS

FOREWORD iii

I. INTRODUCTION

Introduction 3
G.A. TAMMANN

II. RADIO OBSERVATIONS

Radio Continuum Emission in the Virgo Cluster 13
C. KOTANYI

HI Observations of Virgo Cluster Galaxies 23
W.K. HUCHTMEIER

The HI Deficiency of the SO Galaxies in the Virgo Cluster 37
C. BALKOWSKI, P. CHAMARAUX, P. FONTANELLI

HI Deficiency in the Virgo Cluster 45
M.P. HAYNES

The HI Distribution in Spiral Galaxies in the Virgo Cluster 51
R.H. WARMELS

Neutral Hydrogen Observations at the VLA 61
J. VAN GORKOM, C. KOTANYI

A Comparison of the Gas Deficiency of Galaxies in Virgo and Other Nearby Clusters 67
R. GIOVANELLI

Rotation Curves of Hydrogen Deficient Galaxies in Virgo 71
G. CHINCARINI, R.E. DE SOUZA

HI Deficiency and Photometric Evolution of Spiral Galaxies in the Virgo Cluster 81
B. GUIDERDONI, B. ROCCA-VOLMERANGE

An HI and Optical Study of the Gas Poor Virgo Cluster Spiral NGC 4571 91
R.C. KENNICUTT, J.M. VAN DER HULST

Radio Continuum and HI Emission from the Spiral Galaxies in the Virgo Cluster Area 95
G. GAVAZZI

HI Observations of Late-type Virgo Dwarfs 101
G.L. HOFFMAN

III. INFRARED AND CO OBSERVATIONS

IRAS Observations of Virgo Cluster Galaxies 111
T. DE JONG

An IRAS Survey of Bright Spirals in Virgo 125
G. HELOU

A Near-Infrared Survey of Bright Virgo Spiral Galaxies 127
R.D. JOSEPH, T.G. HAWARDEN, I. GATLEY

Infrared Observations of Dwarf Elliptical Galaxies in the Virgo Cluster 135
H. ZINNECKER, R.D. CANNON, T.G. HAWARDEN, H.T. MacGILLIVRAY

Molecular Clouds in Spiral Galaxies in the Virgo Cluster 151
J.S. YOUNG

Molecular Clouds in HI-Deficient Virgo Spirals 165
J.D. KENNEY, J.S. YOUNG

IV. OPTICAL OBSERVATIONS

The Virgo Cluster Redshift Survey 181
J.P. HUCHRA

Global Structure of Virgo Cluster Galaxies 201
S. OKAMURA

An Analysis of the Geometrical Properties for Galaxies in the Virgo Cluster Core 217
H.T. MacGILLIVRAY, R.J. DODD

Optical Comparisons of Virgo Cluster Galaxies and Field Galaxies 227
R.C. KENNICUTT, Jr.

Morphological and Physical Characteristics of the Virgo Cluster: First Results from the Las Campanas Photographic Survey 239
A. SANDAGE, B. BINGGELI, G.A. TAMMANN

Search for Young Stars in Virgo Dwarf Elliptical 297
L. VIGROUX, M. LACHIEZE REY, J. SOUVIRON, J.P. VADER

Applications of a Nuclear Spectroscopic Survey of Virgo Spiral Galaxies 301
J.R. STAUFFER

Optical Counterparts of the Radio Source Virgo A (= M87) 311
J.-L. NIETO, G. LELIEVRE

V. X-RAY OBSERVATIONS

X-Ray Survey of the Virgo Cluster and Comparison to Field Galaxies 323
W. FORMAN, C. JONES, M. DeFACCIO

EXOSAT Observations of the Virgo Cluster 345
A. SMITH, G. STEWART

VI. DYNAMICS

Dynamics and Evolution of the Virgo Supercluster 359
A. YAHIL

Dynamics of the Local Supercluster and the Virgo Cluster 375
E.J. SHAYA, R.B. TULLY

The Termination of Galaxy Formation by Cluster Formation 385
R.B. TULLY

The Local Group Velocity and the Virgo Cluster 391
R.D. DAVIES, L. STAVELEY-SMITH

On the Infall Velocity Towards Virgo 397
R.C. KRAAN-KORTEWEG

VII. DISTANCE OF THE VIRGO CLUSTER AND OTHER MATTERS

The Historical Evolution of the Virgo Cluster Distance Modulus 409
O.-G. RICHTER

Distance and Kinematics of the Virgo Cluster 413
G. de VAUCOULEURS

The Virgo Cluster Distance Corrections to Global Parameters 417
R.B. TULLY, P. FOUQUE

Diameters of Galaxies Inside and Outside Clusters 425
A. BOSMA

A Comparison of the Virgo Cluster with (One) Other Nearby Cluster(s) 427
O.-G. RICHTER

The Far Background of the Virgo Cluster 433
G. REAVES

VIII. PANEL DISCUSSION

Future Needs for Observations of the Virgo Cluster 439

IX. SUMMARY

Summary

D. LYNDEN-BELL 471

LIST OF PARTICIPANTS 475

I.

INTRODUCTION

INTRODUCTION

G. A. Tammann
Astronomisches Institut der Universität Basel
European Southern Observatory

The Virgo cluster has not been with us all the time. It was almost discovered by Charles Messier in 1781, if he had only plotted the objects in his catalog of nebulae on a map of the sky. This was actually done by Zwicky (1959) almost two hundred years later. The catalogs of the two Herschels revealed the excess of nebulae in the Virgo region for the first time clearly, such that Alexander von Humboldt could comment in his "Kosmos" (1845-62) that one third of all nebulous objects were lying in one eighth of the sky about the region of Virgo. But the clear concept of Virgo as a real cluster of galaxies emerged only slowly.

Probably the first paper devoted entirely to (the position of 301) Virgo "nebulae" was published by Schwassmann (1902), presumably on the inspiration of Max Wolf.

An all sky map of the distribution of the spirals known at that time delineates the Virgo cluster surprisingly well (Hinks, 1911, 1914) and the author prophesied "it will be prudent for the future to discuss the spiral nebula distribution more on its own merits, and less with an eye to the galactic poles".

More than a decade elapsed before the next important paper appeared on the "cluster of bright spiral nebulae" in Virgo (and partially overlapping into the constellation of Coma!) containing magnitudes, colors, and diameters of 103 NGC galaxies (Shapley and Ames, 1926). The distance of 10 million light years, estimated in this paper, indicates clearly that these authors interpreted the clumpy distribution of nebulae - against a widely held view of that time, but in agreement with Hinks, - not as the effect of patchy Galactic absorption, but as the result of physical clustering. Adelaide Ames (1930) extended the measurements to 2278 nebulae brighter than $\sim 18^{m}$ in what she called correctly, but for us today confusingly the "Coma-Virgo" group or cloud. The analysis of the data by Shapley and Ames was published in several Harvard Bulletins and resulted in impressive maps of the Virgo cluster (Fig. 1) and in the identification of several background clusters (Shapley 1929, 1930a), and of the Southern Extension of

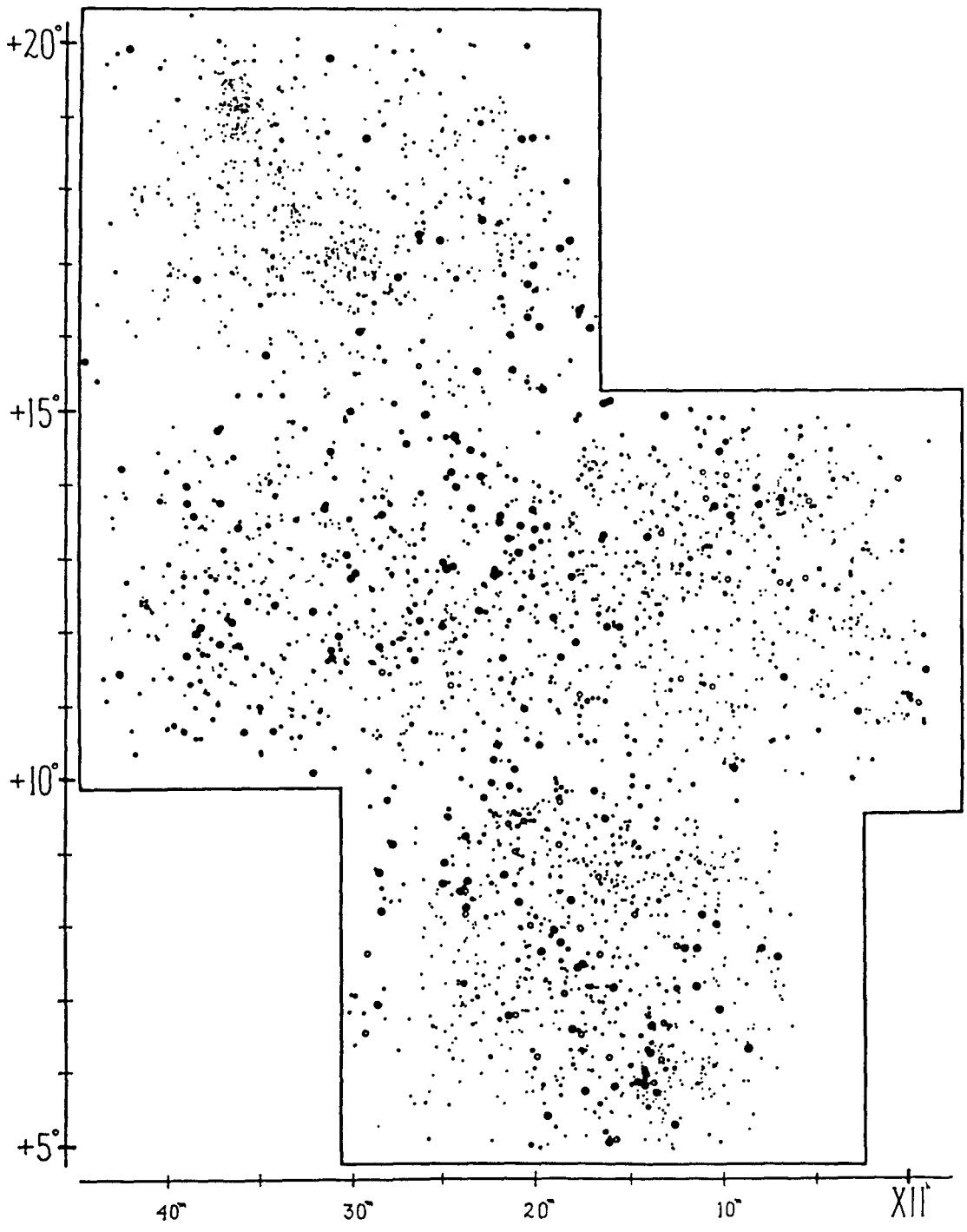


Figure 1. Distribution of 2775 nebulae in Coma-Virgo. Large dots indicate nebulae brighter than magnitude 14; large open circles, those of magnitude 14 to 15; medium dots, 15 to 16; small open circles, 16 to 17; smallest dots, fainter than 17. (From Shapley and Ames, 1929).

the Virgo cluster (Shapley 1930b).

Hubble and Humason (1931) attributed several hundred member galaxies to what they called now the "Virgo cluster", discussed the mixture of galaxian types and gave redshifts for seven members. Interestingly they did not derive a luminosity function for Virgo - as they did for Coma, - clearly because they realized the difficulty of membership assignments for fainter galaxies.

Following Zwicky's (1933) virial mass determination of the Coma cluster, Smith (1936) applied the virial theorem to Virgo for the first time. His result of 10^{15} $\mathfrak{M}_\odot$ (scaled to a distance of $\sim$ 20 Mpc) agrees - one would almost say distressingly - well with the most modern, sophisticated mass determinations of the cluster.

The next important development concerns the realization of an extended halo around the Virgo cluster. Its existence can be clearly seen in plots of the sky distribution of (bright) Shapley-Ames galaxies (Shapley and Ames, 1932) and was further evidenced by Reiz (1941). Beginning in the mid-1950s de Vaucouleurs (1956, 1961, and several later references) studied in great detail the galaxy distribution in function of galaxian type in the Virgo cluster and in its halo; he found that the halo galaxies are concentrated toward a supergalactic plane and that the halo extends out to the Local Group, explaining such the well-known North-South anisotropy of the galaxy distribution.

At this point a remark on the nomenclature may be permitted. When Shapley and Ames (1930b) discovered the Southern Extension of the Virgo cluster they named the whole complex the "Supergalaxy". Subsequently this term was used for the Virgo cluster and its halo. Since about 1960 the term Supergalaxy was frequently replaced by "Local Supercluster". However, by that time the term supercluster was defined by Zwicky (1959) as a spherical system of well defined individual clusters, which according to him does not exist. Indeed the Virgo complex with its halo is not a supercluster in Zwicky's sense. The problem may be a semantic one, particularly in a more modern picture, where galaxies populate the walls of empty cells and concentrate in the intersections of different walls, but one should keep in mind that the term Local Supercluster violates Zwicky's original definition and questions the existence of simple clusters in general, because all typical clusters may have surrounding halos like Virgo.

The following years saw still a number of stimulating review papers on the Virgo cluster (Zwicky 1957, 1959; de Vaucouleurs 1975; Abell 1975), but the interest in the Virgo cluster as a whole stagnated and shifted to more distant clusters, mainly to Coma, even though the general interest in clusters was enormously increasing. The situation can be illustrated by the number of key words used in Astronomy and Astrophysics Abstracts:

Key word	1969-73	1974-78	1979-83
Cluster of gal.	137	1008	1483
Coma cluster	36	73	35
Virgo cluster	10	38	68
% Virgo	7	4	5

The reason why Virgo was overshadowed by Coma, in spite of the six times larger distance of the latter, during the period of about 1965-1980 lies probably less in the fact that the dynamics of an irregular cluster like Virgo seemed more complex than that of a regular cluster, but rather in the very large angular extent of Virgo and the overwhelming effect of the background. The harder one looked, the less one saw of Virgo. This was foreseen by Shapley and Ames (1929) who wrote "the main Coma-Virgo group is seen to fade into the general background at the fifteenth magnitude, but there are clear evidences of its presence at least one magnitude fainter", and it is dramatically shown by P. Wild's isopleth distribution of Shapley-Ames galaxies (down to $\sim 13\overset{m}{.}5$), where the Virgo cluster appears as the most dominant agglomeration in the sky (published by Zwicky, 1957; here Fig. 2), and the Shane-Wirtanen isopleths (down to $\sim 18\overset{m}{.}8$; Shane 1975), where the Virgo cluster is completely lost into the background (cf. Fig. 3).

The era of Sleeping Beauty is over! The realisation that the faint Virgo members were so far systematically missed in catalogs because of their low surface brightness led to systematic searches, which were inaugurated by Reaves (1956), but continued only much later. This development as well as the rapidly increasing redshift data improved our understanding of the cluster population, and they let appear the Virgo cluster now as a clean entity, almost freed from its background contamination. The emerging picture of the kinematics of the Virgo complex together with the unique wealth of individual cluster member data and the exciting

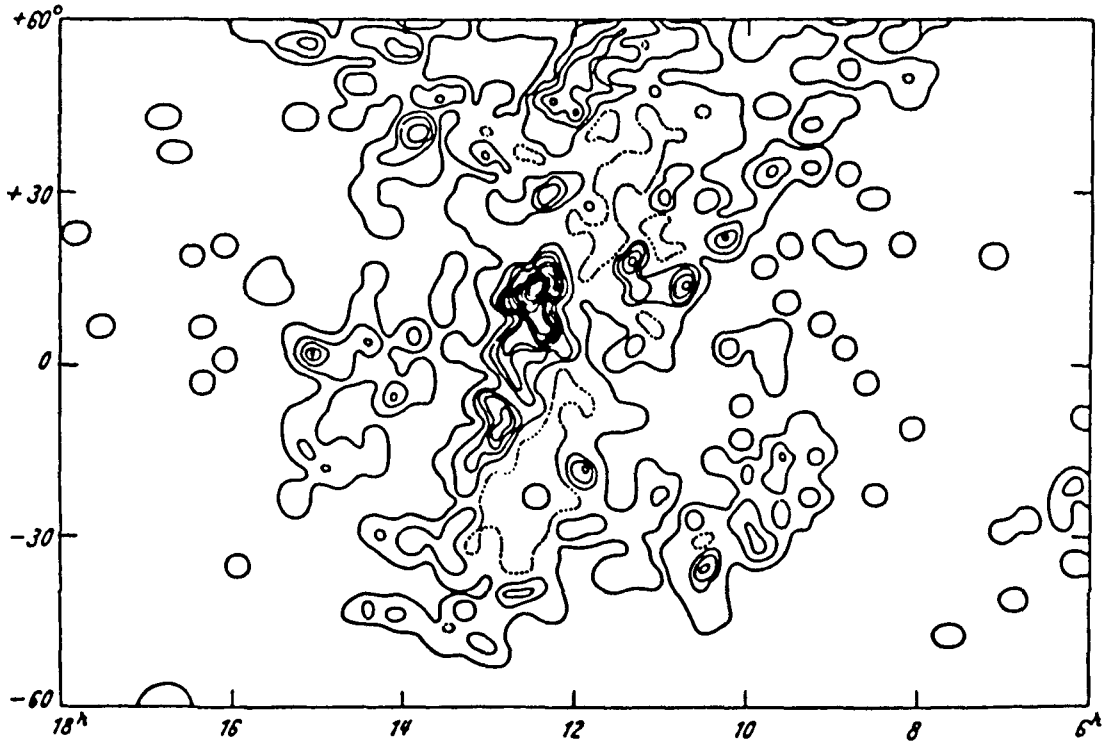


Figure 2. Isopleths of bright galaxies from the Shapley-Ames catalog for the region $6^h < \alpha < 18^h$, $|\delta| < 60^o$.(From Zwicky, 1957).

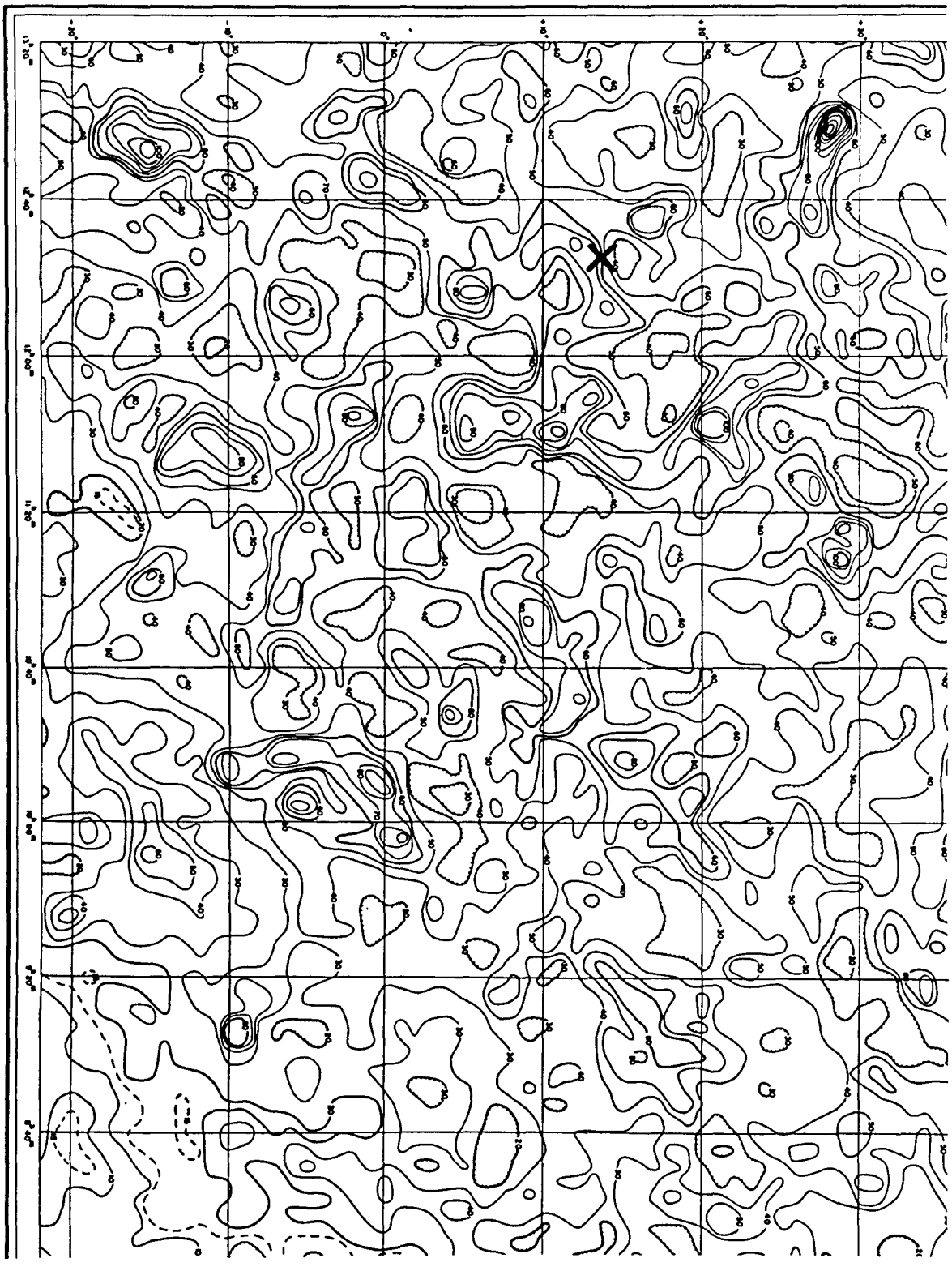


Figure 3. Isopleths of the Shane-Wirtanen counts down to ~ $18^{m}.8$. The position of the Virgo cluster is marked by a cross. (From Shane, 1975).

discovery of the X-ray emitting gas in Virgo, has reborn a new epoch of Virgo research.

In coming years Virgo, the nearest cluster of all, can be expected to play an important role in a variety of fields, e.g.:

1) it will teach us about the formation and evolution of clusters and about the evolutionary effects on its members, which can be studied in greater detail than in any other cluster.

2) it will be the best place to learn about the interaction between an active galaxy (M 87) and the hot, tenuous X-ray gas, and hence may take the leading role which once the Crab nebula played for the development of astrophysics.

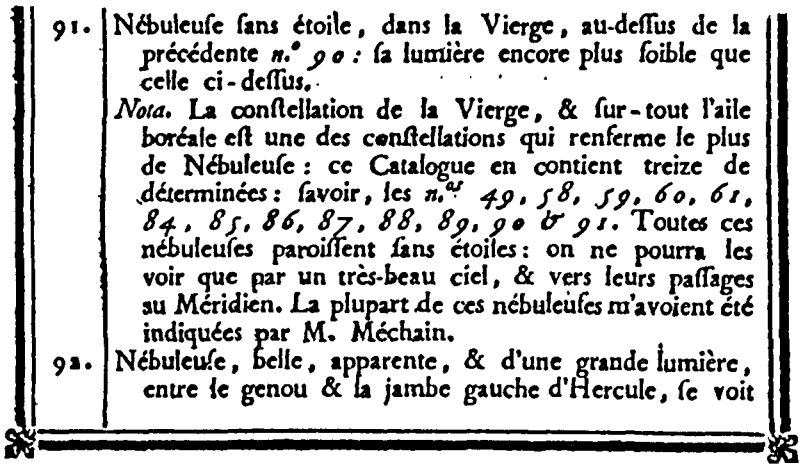
3) it will be essential to solve one of the greatest puzzles in astronomy, i.e. the dark matter in the large clusters of galaxies as apparently required by the virial theorem.

4) it will be, quite unexpectedly, an ideal playing ground for cosmologists, because the different shells around the cluster with different infall velocities exemplify different Friedmann mini-universes which all have their proper expansion rates H_0 (local) and density parameters Ω_0 (local). Once these are understood there is hope that also very good determinations of the global values of H_0 and q_0 will emerge.

In the name of all participants of this workshop and perhaps even of some readers of the resulting Proceedings I thank the Director General of ESO and the organizers of this workshop for the opportunity to plunge into the new excitement of the Virgo cluster.

P.S.

In his welcome address, which preceded this introduction, L. Woltjer pointed out that the present Workshop could be taken as the celebration of the 200th anniversary of the Virgo cluster because Messier did in fact comment on the frequency of nebulae in the northern part of Virgo, viz. in his last catalog of nebulae (Connaissance des Temps pour 1784, Paris 1781, p. 263):



91. Nébuleuſe ſans étoile, dans la Vierge, au-deſſus de la précédente *n.° 90*: ſa lumière encore plus foible que celle ci-deſſus.

Nota. La conſtellation de la Vierge, & ſur-tout l'aile boréale eſt une des conſtellations qui renferme le plus de Nébuleuſe: ce Catalogue en contient treize de déterminées: ſavoir, les *n.os 49, 58, 59, 60, 61, 84, 85, 86, 87, 88, 89, 90 & 91.* Toutes ces nébuleuſes paroiſſent ſans étoiles: on ne pourra les voir que par un très-beau ciel, & vers leurs paſſages au Méridien. La plupart de ces nébuleuſes m'avoient été indiquées par M. Méchain.

92. Nébuleuſe, belle, apparente, & d'une grande lumière, entre le genou & la jambe gauche d'Hercule, ſe voit

References:

Abell, G. O. 1975, in: Galaxies and the Universe, eds. A. and M. Sandage and J. Kristian, Chicago: University of Chicago Press, p. 601.

Ames, A. 1930, Harvard Ann. 88, 1.

de Vaucouleurs, G. 1956, Vistas in Astronomy 2, 1984.

——————— 1961, Ap. J. Suppl. 6, 213.

——————— 1975, in: Galaxies and the Universe, eds. A. and M. Sandage and J. Kristian, Chicago: University of Chicago Press, p. 557.

Hinks, A. 1911, M. N. 71, 588.

——————— 1914, M. N. 74, 707.

Hubble, E., and Humason, M. L. 1931, Ap. J. 74, 43.

Reaves, G. 1956, A. J. 61, 69.

Reiz, A. 1941, Ann. Obs. Lund, No. 9.

Schwassmann, A. 1902, Publ. Astrophys. Obs. Königstuhl-Heidelberg 1, 17.

Shane, C. D. 1975, in: Galaxies and the Universe, eds. A. and M. Sandage and J. Kristian, Chicago: University of Chicago Press, p. 647.

Shapley, H., and Ames, A. 1926, Harvard Circ. 294.

——————— 1929, Harvard Bulletin 865.

——————— 1930a, Harvard Bulletin 873.

——————— 1930b, Harvard Bulletin 880.

——————— 1932, Harvard Ann. 80, 41.

Smith, S. 1936, Ap. J. 83, 23.

Zwicky, F. 1933, Helv. Phys. Acta 6, 110.

——————— 1957, Morphological Astronomy, Berlin: Springer.

——————— 1959, Handb. d. Physik 53, 390.

II.

RADIO OBSERVATIONS

RADIO CONTINUUM EMISSION IN THE VIRGO CLUSTER

C. Kotanyi
NRAO
Socorro, N.M. 87801

1. Introduction

a. General Objectives

Radio observations of rich clusters of galaxies have revealed phenomena which were not predicted from observations at other wavelengths:

1. Head-tail radio sources were a first direct evidence for the existence of a diffuse intergalactic medium in clusters. Its existence implies that spiral galaxies should be affected as well, e.g. through ram-pressure sweeping. Attempts to find differences between the radio emission of cluster and non-cluster spirals have been unsuccessful. Spirals in the Coma cluster have appeared overluminous (Jaffe et al. 1976), in contrast with rather than supporting the expectations from sweeping. This effect needs confirmation. However most clusters are too distant to allow many detections of spirals, and the Virgo cluster may provide the most useful results in this regard.

2. Diffuse intergalactic radio emission has been reported in several clusters (e.g. Coma C in Coma), implying the existence of intergalactic magnetic fields and particles.

3. Strong cluster radio sources are always found within 0.3 of the core radius of the clusters (McHardy, 1979).

This effect may be due to an influence of the cluster environment on enhanced radio emission, i.e. contain clues to the radio galaxy mechanism. It could also be due to the predominance of bright elliptical galaxies in the cluster centres, since the bright giant elliptical galaxies are the most powerful radio sources.

b. Radio Techniques

Early radio observations were mostly done with single antenna telescopes. This allowed in principle to survey a large number of sources in a short time,

yielding a single flux density at one or several frequencies, and some size information in a few cases. The Virgo cluster has been included in two larger surveys of nearby galaxies by Pfleiderer (1977) at Bonn and by Dressel and Condon (1978) at Arecibo.

The first systematic study of the cluster resulted from synthesis observations at the Westerbork telescope (Kotanyi, 1980a). These are now being followed up at the Very Large Array (VLA).

2. Synthesis Observations

The Westerbork survey included 220 bright galaxies listed in the first Reference Catalogue (de Vaucouleurs, 1976). The observations had a resolution of 23" in the EW direction and a sensitivity of 10 mJy at 1.4 Ghz. The analysis of these data is presented in the next section.

The first high-resolution maps with a circular beam have been made at the VLA (except for M87).

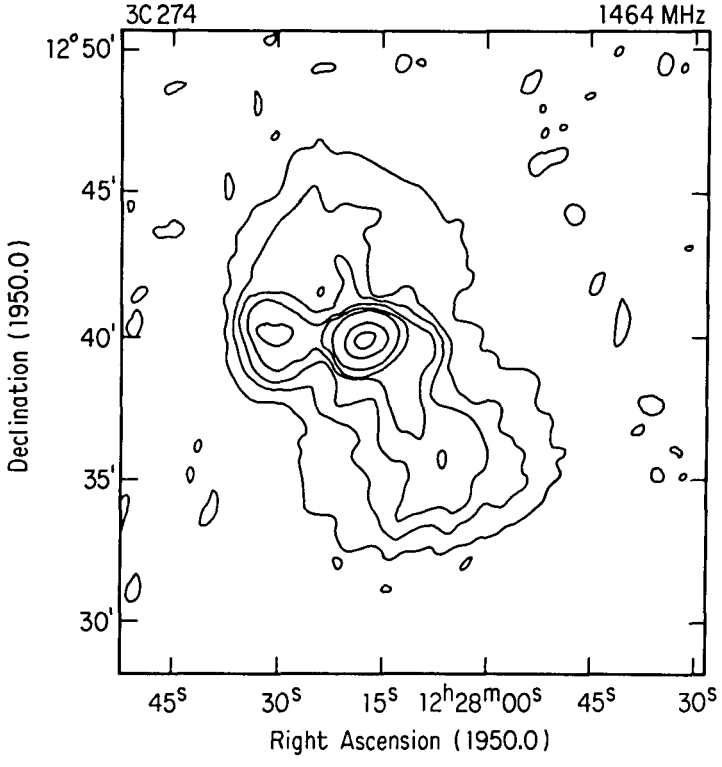


Fig. 1 VLA map of the large-scale radio emission of M87 at 1.5 GHz (Perley, private communication). The resolution is 45". The contour levels are 0.18, 0.36, 0.72, 1.08, 1.62, 4.50, 27.00, 67.50 Jy/beam.

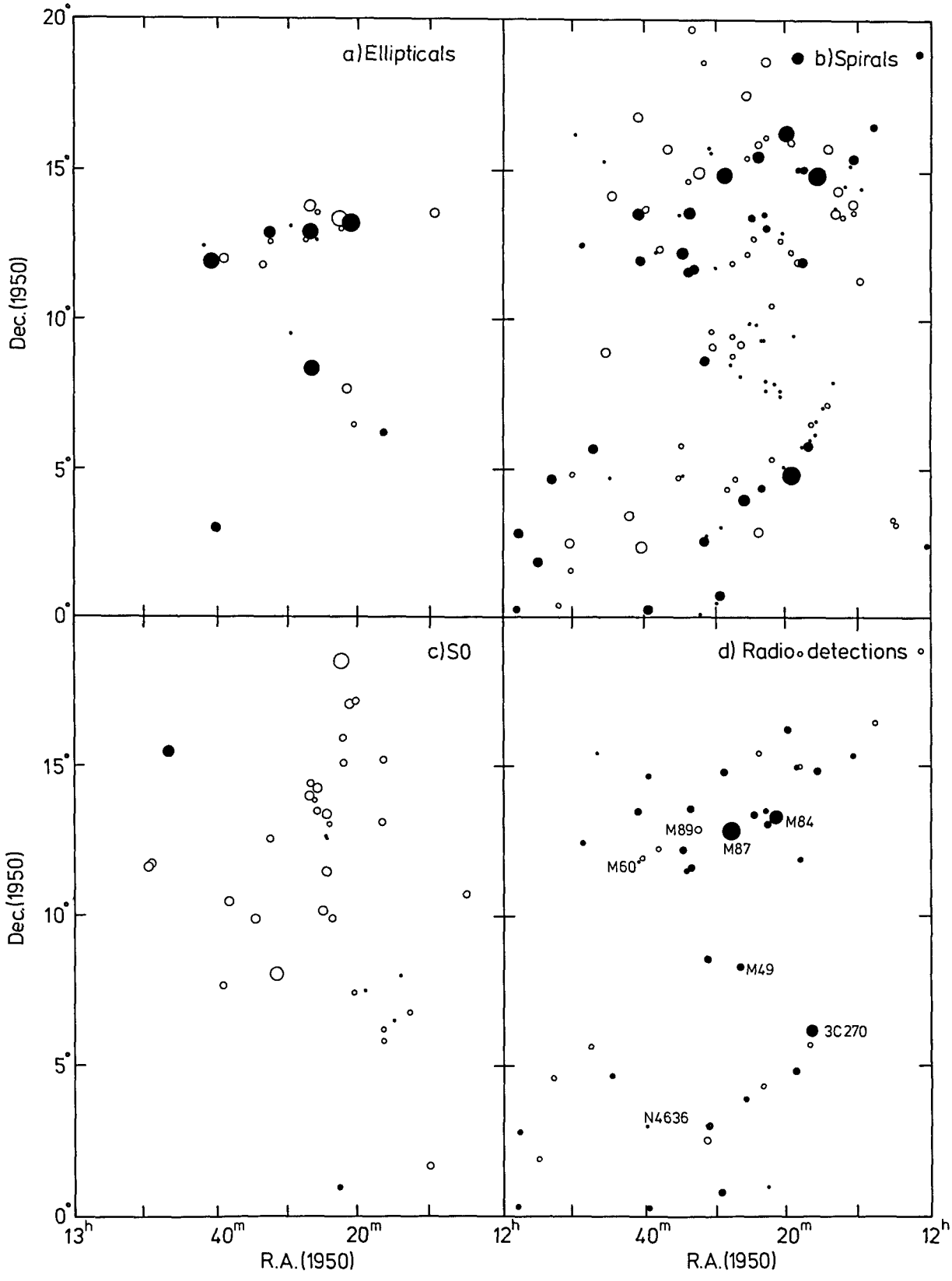


Fig. 2 Distribution over the Virgo cluster area of radio detections in the Westerbork survey. The symbol size increases with optical luminosity and filled symbols are detections in (a) (b) (c). Symbol size increases with radio luminosity in (d) (Kotanyi, 1981).

a. Elliptical Galaxies

The radio emission in the cluster is dominated by M87, which is also one of the strongest sources in the sky (Bolton, 1948). The large-scale emission was mapped by Cameron (1971), Andernach et al. (1979), Costain et al. (1981) and Kotanyi (1980b). The most recent map from the VLA made with a high dynamic range by Perley (private communication) is shown in Fig. 1. The source has a strong core of size about 1' and an extended diffuse component of much lower surface brightness and size 12' x 16'. The diffuse component has an asymmetric, elongated shape with a bend reminiscent of wide-angle head-tail sources (WAT). The X-ray map obtained at the Einstein Observatory shows a similar structure (Schreier et. al. 1984).

The core was mapped by Turland (1975), Forster et al. (1981), and Owen et al. (1983). It shows a double-lobed structure with a one-sided jet associated with the optical jet. The jet observed at a resolution tenfold that attained optically shows interesting structure (Biretta et al. 1983). A nuclear source of size about 1 milliarcsecond and containing 1/100 of the flux of the core at 1.4 GHz is embedded in the core (e.g. Kellermann et al. 1977).

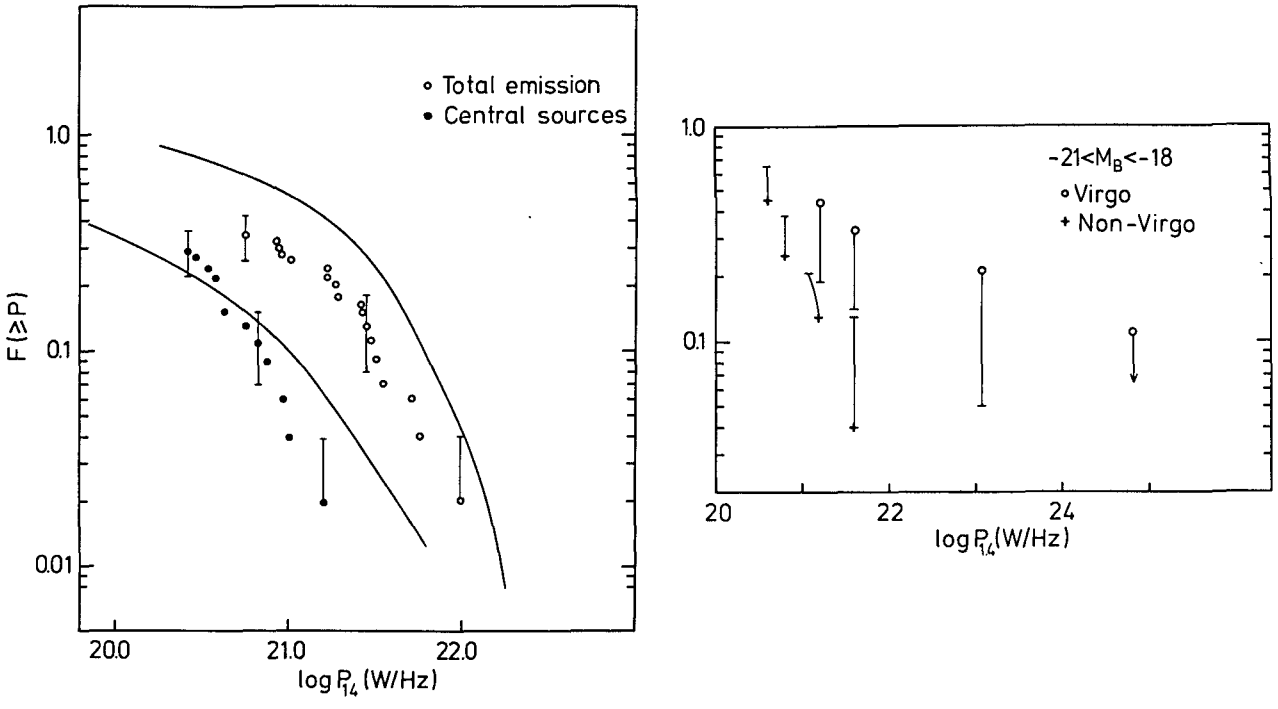


Fig. 3 Radio Luminosity functions of spiral (left) and elliptical galaxies in the Virgo cluster (circles) and in the nearby galaxy sample of Hummel (1981; full line and crosses) from Kotanyi (1981).

M84, the second strongest source in the cluster, is 100 times weaker than M87. It has been mapped by Riley (1972), Jenkins et al. (1977) and Laing and Bridle (in preparation). The source has a fairly symmetric S-shape with two-sided jets and a compact milliarcsecond-size nucleus. The source may show some signs of mild interaction with the environment.

Only three other elliptical galaxies show extended emission. Of these M49 (NGC4472; Kotanyi and Ekers, 1978; Laing et al., in preparation) and M60 (NGC4649) show well-defined double structure whereas NGC4168 may be one-sided. All three are much fainter than M87 and M84 located in the cluster core. They are far out of the cluster core, confirming McHardy's result on 4C sources in Abell clusters. Conversely, not all bright ellipticals in the cluster core are strong radio sources: M86 shows no detectable radio emission at a level below that of the faintest radio elliptical.

b. Spiral Galaxies

Most of the bright spiral galaxies have extended disk emission with size and shape comparable to that of the optical disk. In some cases (M100=NGC4321 and M99=NGC4254) radio emission is associated with the strong spiral arms. In M99 and NGC4654 (Condon, 1983) the radio disk is asymmetric like the optical disk which, in the case of M99 at least, could be attributed to interaction with the cluster environment, e.g. to ram-pressure. In M90=NGC4569, NGC4388 (Hummel et al. 1983), NGC4402 and NGC4438, four bright spirals in the cluster core, the radio disk is smaller than the optical disk. In NGC4438 the extended radio emission as well as the X-ray emission observed at the Einstein Observatory are displaced from the optical disk, possibly due to on-going ram-pressure sweeping (Kotanyi and Ekers, 1983; Kotanyi et al. 1983).

NGC4302 and NGC4647, two spirals in interacting pairs, have radio disks asymmetric with respect to the optical disks, probably as a result of tidal interaction.

c. SO Galaxies

Few SO galaxies have detectable radio emission, although the cluster has a large SO population. Only NGC4710 has extended disk emission.

3. Statistical Properties

Synthesis observations can be used to determine the luminosity, size and spectral properties of the radio emission, and to study the emission from the central core separately from the extended emission. The locations of detections in the Westerbork survey over the cluster area are shown in Fig. 2. Note that the elliptical galaxies are concentrated in an elongated region in the centre. The bright spiral galaxies are mostly distributed in an elongated ring surrounding this region.

a. The Radio Luminosity Function (RLF)

The probability of radio emission in a given optical magnitude and radio luminosity range is given by the bivariate luminosity function (BLF). The RLF of the Virgo cluster galaxies in a broad range of magnitude is shown in Fig. 3, and compared with non-cluster nearby galaxies (Hummel, 1981). The Virgo ellipticals may be overluminous compared to the 'field', which reflects the fact that the two strongest nearby radio ellipticals are in Virgo. The Virgo spirals may have underluminous disks, however a difference in the mean magnitude of the two samples accounts for this effect. Applying a correction for this difference would make the central sources in Virgo spirals overluminous, which might be due to a bias towards early-types in the Virgo spirals.

b. Radio properties versus distance from the cluster centre.

A less biased test of the effects of the cluster environment might be relying on relative location within the cluster. The radio-to-optical sizes and luminosities of spiral galaxies are shown in Fig. 4 against the angular distance from the cluster centre. Small radio disks and strong central sources are found within 3 deg. These effects may be related to an excess of early-type spirals towards the cluster centre (Fig. 5). An even stronger dependence of neutral hydrogen-to-optical disc size on radial distance was found recently (van Gorkom et al., 1984).

c. Radio Continuum Versus Neutral Hydrogen.

A positive correlation between radio continuum and HI line luminosities of

Virgo cluster spirals has been reported (Jaffe and Gavazzi, 1984). Further investigation of this correlation should be the subject of future work.

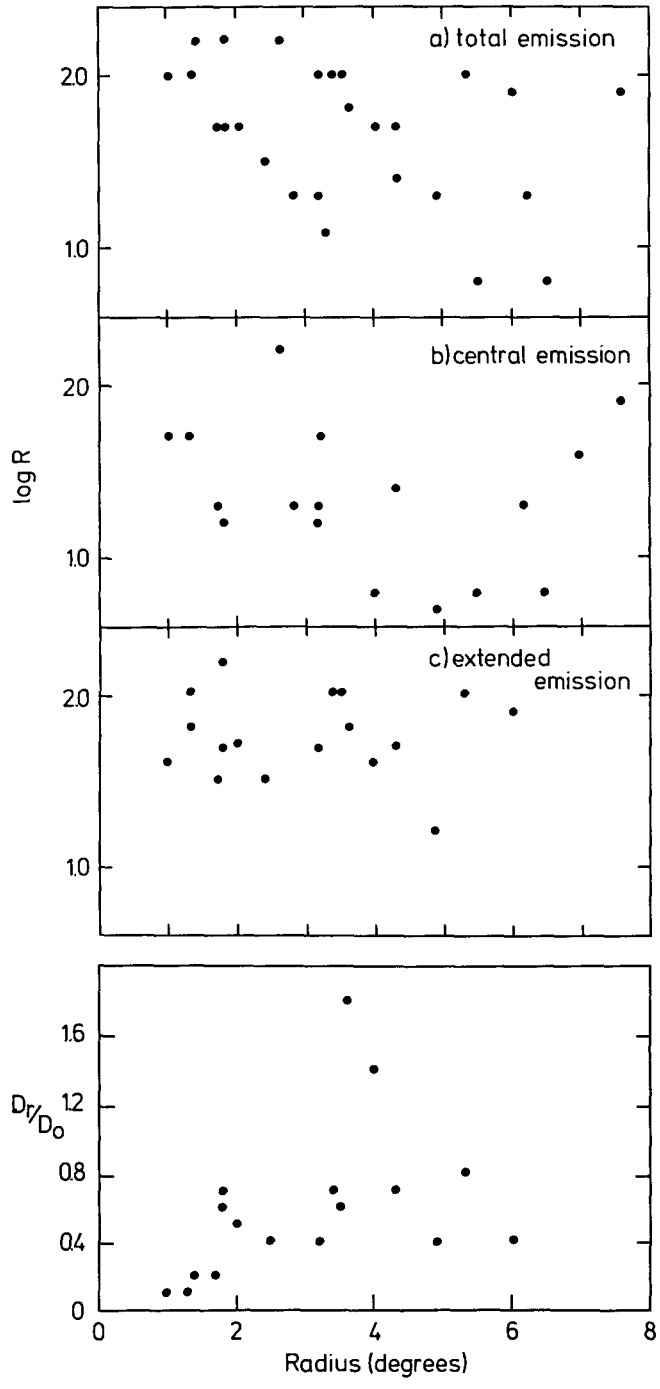


Fig. 4 Radio-to-optical luminosities (log R) and disk sizes of Virgo spirals as a function of angular distance from the cluster centre (Kotanyi, 1981).

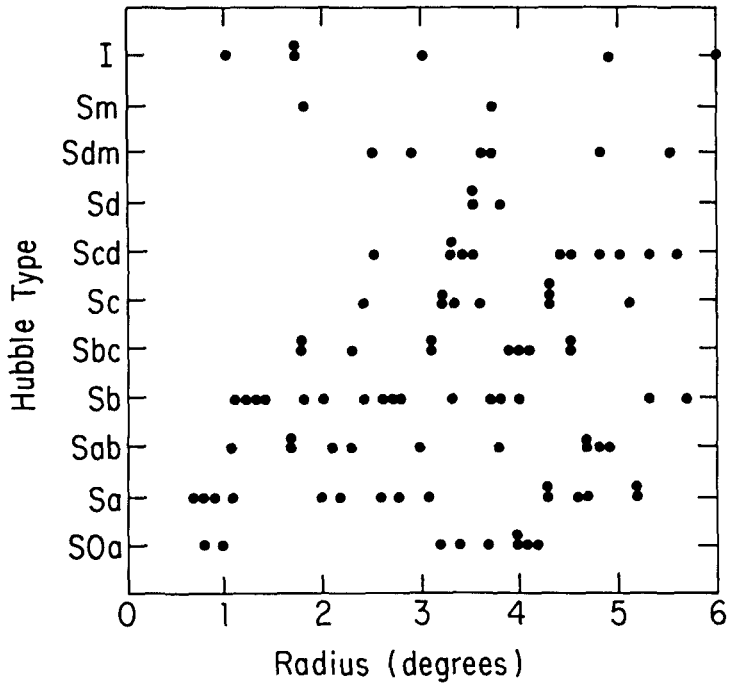


Fig. 5 Frequency of Hubble types for Virgo spirals in the RC2 as a function of distance from the cluster centre.

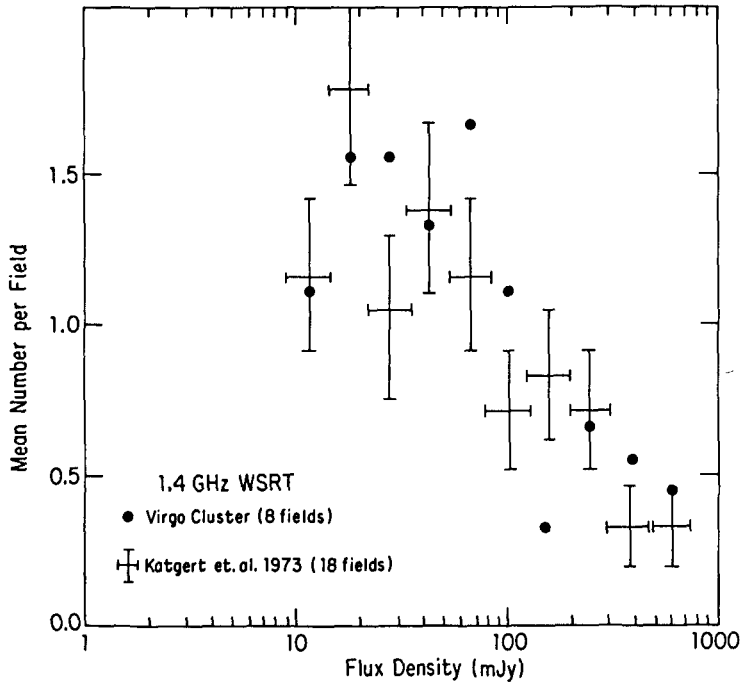


Fig. 6 Flux density distribution of discrete sources in Westerbork synthesis fields in the Virgo cluster (Kotanyi, 1980a) and of sources in the general field (Katgert et al., 1973).

4. General Comments

a. No diffuse intergalactic radio emission has been found at a level tenfold below that of Coma C (Kotanyi, 1981).

b. Many discrete sources not associated with optical galaxies are detected in synthesis observations. Their distribution in the Virgo cluster region is similar to that of the general field (Fig. 6). Any excess of sources in the Virgo region over the field is less than about 10% in the flux density range considered.

This result implies an upper limit on the existence of intergalactic radio sources associated with Virgo.

c. No narrow-angle head-tail (NAT) sources were found in the Virgo cluster. M87 may show features found in wide-angle tail (WAT) sources.

d. Undersized radio continuum and HI disks are only seen within a fraction of the core radius of the Virgo cluster. Hence they would be more difficult to see in other clusters. They could be explained by:

1. ram-pressure sweeping;
2. tidal effects due to a cluster potential with a central cusp (R.H. Miller, in preparation);
3. tidal interaction with a companion.

Acknowledgements

I thank R. Perley for the map of M87 and E. Hummel, J. van Gorkom and P. Crane for their help with the observations.

The National Radio Astronomy Observatory is operated by Associated Universities Inc. under contract with the National Science Foundation.

References

Biretta, J., Owen, F.N., Hardee, P.E. 1983 Ap.J. 274, L27

Bolton, J.G., 1948 Nature 162, 141

Cameron, M.J., 1971. MNRAS 152, 439

Condon, J.J., 1983 Ap.J. Suppl. 53, 459

Costain, G.H., Higgs, L.A., McLeod, R.S., Roger, R.S., 1976 A.J. 81, 1

Dressel, L.L., Condon, J.J., 1978 Ap.J. Suppl. 36, 53

Ekers, R.D., Kotanyi, C. 1978. A.A. 67, 47

Forster, J.R., Dreher, J., Wright, M.C.H., Welch, W.J., 1978, Ap.J. 221, L3.

Hummel, E. 1981 A&A 93, 93

Hummel, E., van Gorkom, J., Kotanyi, C. 1983 Ap.J. 267, L5

Jaffe, W.J., Gavazzi, G. 1984 in Groups and clusters of Galaxies, (ed. Mardirossian).

Jaffe, W.J., Perola, G.C., Valentijn, E.A. 1976 A.A. 49, 179

Jenkins, C.J., Pooley, G.G., Riley, J.M. 1977 MNRAS 84, 61

Katgert, P., Katgert-Merkelijn, J.K., Le Poole, R.S., van der Laan H. 1973 A.A. 23, 171.

Kellermann, K.I. et al. 1977 Ap.J. 211, 658

Kotanyi, C. 1980a A.A. Suppl. 41, 421

1980b A.A. 83, 245

1981 PhD Thesis, University of Groningen

Kotanyi, C., Ekers, R.D. 1983 A.A. 122, 267

Kotanyi, C., van Gorkom, J., Ekers, R.D. 1983 Ap.J. 273, L7

McHardy, I.M. 1979 MNRAS 188, 495

Owen, F.N., Hardee, P.E., Bignell, R.C. 1983. Ap.J. 239, L11

Pfleiderer, J. 1977 A.A. Suppl. 28, 313

Riley, J.M. 1972 MNRAS 157, 349

Schreier, E., Feigelson, E., Fabricant, D. 1984 Ap.J. (in press)

Turland, B.D. 1975 MNRAS 170, 281

Van Gorkom, J., Balkowski, C., Kotanyi, C. 1984 in Groups and clusters of Galaxies, (ed. Mardirossian) p. 261

HI OBSERVATIONS OF VIRGO CLUSTER GALAXIES

by

W.K. Huchtmeier

Max-Planck-Institut für Radioastronomie

Bonn, F.R.G.

Abstract. HI-observations of 456 galaxies in the Virgo cluster area within 10° of M87 are discussed and compared with a sample of nearby galaxies (v_{o} <500 km/s). The total HI-mass (M_{HI}) and the relative HI-content (M_{HI}/L_{B} and σ_{H}) for a given morphological type are the same in both data samples with the exception of the inner 3° of the Virgo cluster where a pronounced HI-deficiency is observed. Application of the Tully-Fisher relation for deriving differential distances in that field is discussed.

Introduction. First observations of neutral hydrogen in Virgo cluster galaxies were performed by Robinson and Koehler (1965) with the 64-m Parkes radiotelescope using a single filter 320 km/s wide centered on the optical radio velocity of each galaxy. They detected 7 spiral galaxies. By 1975 the HI-content of 14 Virgo galaxies was known. Further references are given in Table 1.

This contribution is a report about global properties of a complete sample of Virgo cluster galaxies containing all galaxies brighter than m_{B}=14.2 within 10° of M87 and of morphological type later than S0. The sample is nearly complete to the limit of the Virgo cluster catalogue by Kraan-Korteweg (1982 and 1983 priv. comm.), i.e. to m_{B}=14.95. All published HI-data have been taken into account (e.g. Huchtmeier et al. 1983). Additional observations with the 100-m radiotelescope at Effelsberg were performed to complete the HI-data of the above sample, to improve some high upper limits, and to produce profiles for those galaxies published without this important information. Details of this work will be given by Huchtmeier and Richter (1985, in preparation). 177 of the 456 observed galaxies were detected in HI; this is a detection rate of 39%. The searched radial velocity range generally was between -400 and 3400 km/s. The HI sensitivity limit of the sample is between 0.5 and 3 x 10^{8} $M_{\odot}$ assuming a distance of 21.8 Mpc for the Virgo cluster (Sandage and Tammann, 1976).

A dependence of global galaxian parameters with environment is indicated by the luminosity segregation (Fig. 1). Early-type and bright galaxies are concentrated towards the cluster centre. The HI detection rate of galaxies within 6° of M87 is 32% and increases to 58% in the range 6° to 10°.

Comparison sample. For a thorough discussion of the HI-properties of this sample

Table 1: HI Observations of Virgo Cluster Galaxies

Epstein	1964	1
Robinson, Koehler	1965	9
Gouguenheim	1969	1
McCutcheon, Davies	1970	2
Gallagher	1972	1
Balkowski et al.	1973	1
Bottinelli et al.	1973	1
Knapp, Kerr	1974	1
Roberts	1969,1975	2
Davies, Lewis	1973	11
Huchtmeier et al.	1976	39
Krumm, Salpeter	1976	10
Rots	1980	9
Chamaraux et al.	1980	56
Fisher, Tully	1981	40
Helou et al.	1981	23
Huchtmeier	1982	20
Romanishin et al.	1982	4
Giovannardi et al.	1983	112
Bohnenstengel	1983	12
Giovanelli, Haynes	1983	24
Krishna-Kumar, Thonnard	1983	2
Helou et al.	1983	74
Bottinelli et al.	1982	6
Helou et al.	1984	82
Sulentic, Arp	1983	2
Huchtmeier, Richter	1984	261

total number of observed galaxies within 10° of M87: 456

we need a comparison sample of non-cluster galaxies in order to consider selection effects due to environment, luminosity and type. Global properties of nearby galaxies have been discussed by many authors using different galaxy samples and different magnitude systems. In the case of the Virgo sample luminosities are available in the blue system and therefore we will consider only comparison samples in the same magnitude system. The distance-independent ratio of neutral hydrogen mass to blue luminosity, M_{HI}/L_B, is given in Fig. 2 for data presented by different authors: Shostak (1978) studied spiral galaxies of types Sbc and later, and Bottinelli et al. (1982) of type Sb and later; both are in good agreement. A data collection from the literature was discussed by Li and Liu (1981) covering all morphological types. HI-observations from spiral galaxies with v_o <500 km/s (Kraan-Korteweg and Tammann 1979) from Huchtmeier and Richter (1985, in preparation) enter Fig. 2 as KKT. All these data (i.e. mean values per morphological type) show the same trend as a function of morphological type and are in good agreement. Only for late-type galaxies (Scd and later) the data including great numbers of late-type dwarf systems (Li and Liu (1981) and KKT) show systematically higher M_{HI}/L_B values. (The low value for Sm galaxies from Shostak (1978) depends on two galaxies only).

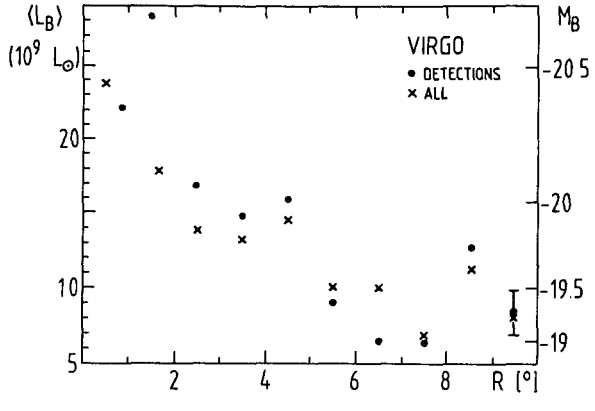


Fig. 1. The luminosity segregation in the Virgo cluster is visualized by luminosity averages over concentric rings 1° wide around M87.

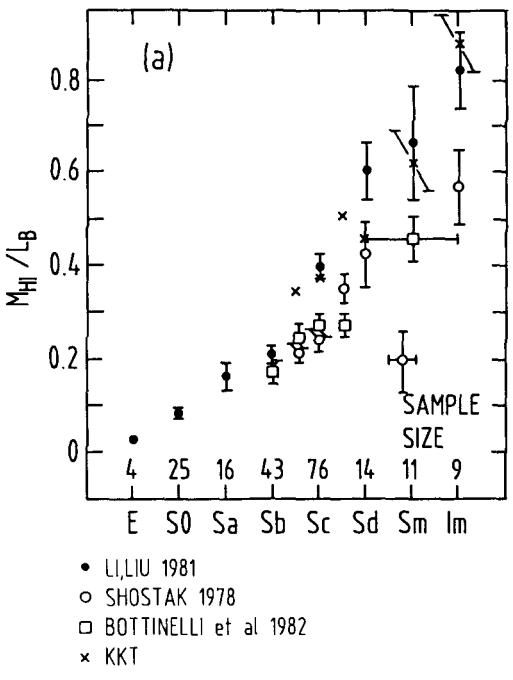


Fig. 2. The relative HI content M_{HI}/L_B for different morphological types from several authors. Error bars correspond to twice the r.m.s. error of the mean. The sample size is given for the Li and Liu sample.

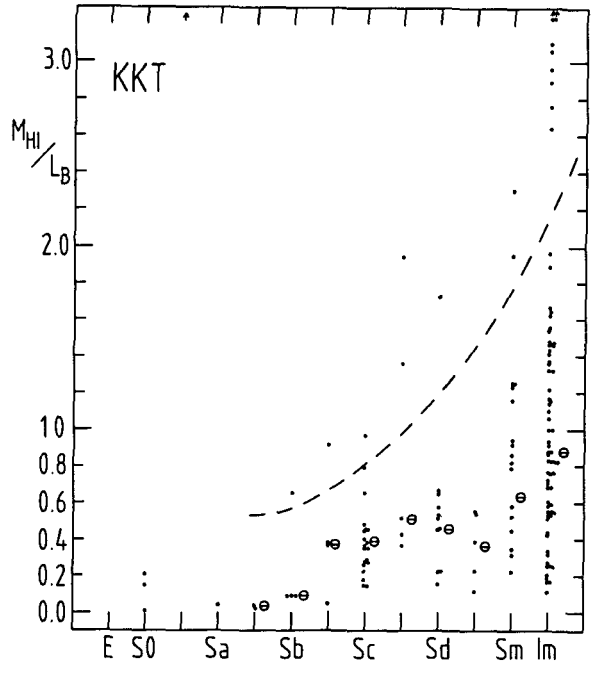


Fig. 3. M_{HI}/L_B for the detected galaxies of the KKT sample. The broken line separates HI-rich from "standard" galaxies. The mean values of this "standard" sample are given by open circles. The few S0 galaxies in the sample have been included for completeness.

The scatter in such a diagram is obvious in Fig. 3 where the M_{HI}/L_B of the KKT sample is given for each galaxy. Apart from the large scatter there is an indication for a HI-rich population (above the broken line); the mean values for the KKT comparison sample shown in Fig. 2 are given by open circles and correspond to the "standard" sample (i.e. entries below the broken line) thus excluding the HI-rich galaxies. However, these mean values of late-type galaxies are still higher than the corresponding values from Shostak (1978) and Bottinelli et al. (1982), demonstrating that (some) global properties depend on the selection of the sample.

Discussion. The mean M_{HI}/L_B values from Shostak (1978) and Bottinelli et al. (1982) from Fig. 2 completed for earlier type galaxies from Li and Liu (1981) are given in Fig. 4 by open squares. A comparison of the M_{HI}/L_B values of the KKT (+) sample with the Virgo sample (•) does not show significant differences for the sample as a whole. The difference for Im galaxies disappears when allowing only those irregulars from the KKT sample brighter than $M_B=-16$. Fig. 5 shows the difference in composition of the Virgo and the KKT sample for morphological types and demonstrates the strong contribution of irregular galaxies to the KKT sample. It has been argued earlier that the M_{HI}/L_B depends on luminosity (e.g. Huchtmeier

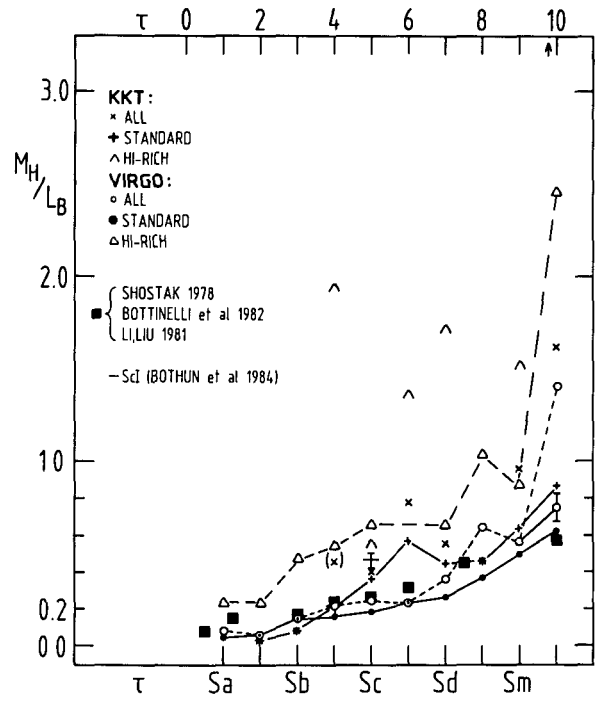


Fig. 4. M_{HI}/L_B as a function of morphological type for the present Virgo sample and comparison samples. Only for the KKT and the Virgo sample HI-rich galaxies were separated from "standard" galaxies.

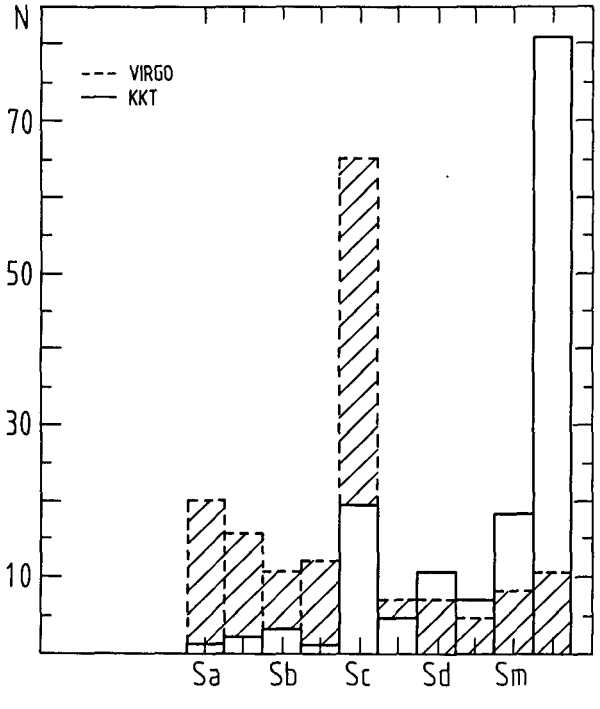


Fig. 5. Frequency of galaxies for various morphological types for the Virgo and the KKT sample.

et al. 1976). In Fig. 6 this is shown for the KKT and Virgo sample. This effect is evident for galaxies fainter than M_B=-18. The dependence of M_{HI}/L_B with type is obvious, too, as the values are grouped into early, median, and late-type spirals. The apparent difference for late-type spirals and irregulars between the Virgo and the KKT sample is another selection effect as our Virgo sample contains only a few HI-rich dwarfs. Hoffman and Helou (this workshop) show a "normal" HI-content for fainter Virgo dwarfs. In order to avoid the luminosity dependence of the M_{HI}/L_B ratio another parameter - σ_H - is given in the lower part of Fig. 6. This "quasi" hydrogen surface density (i.e. M_{HI} devided by the optical area of the galaxy) is independent from the luminosity within observational errors. As the HI-diameter of spiral galaxies seems to be roughly constant in terms of its optical diameter (Bosma, 1978) the parameter σ_H can be taken as a surface density.

The parameter σ_H seems more appropriate for a discussion of the relative HI-content of galaxies which is presented in Fig. 7 for the present sample. There the HI surface density σ_H is given as a function of morphological type for the Virgo and the KKT sample. Here again a separation between HI-rich and "standard" values is apparent (see discussion of Fig. 4). For this para-

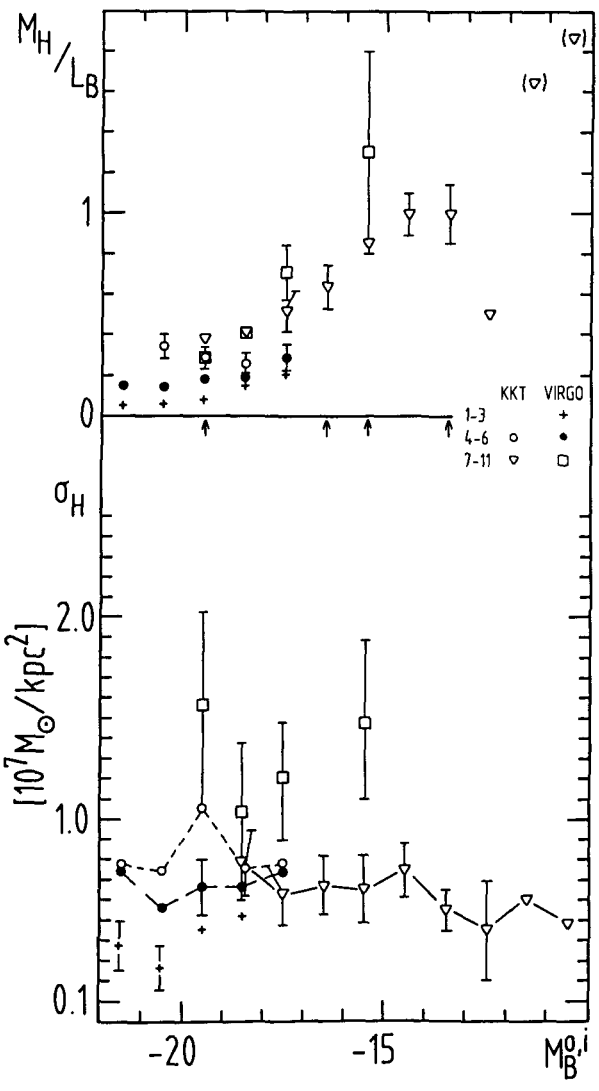


Fig. 6. Mean values of M_{HI}/L_B and HI surface density σ_H against absolute magnitude. Galaxies are grouped for morphological types Sa-Sb(1-3), Sbc-Scd(4-6), Sd-Im(7-10).

meter the HI-rich galaxies separate more clearly from the standard values. The overall scatter for a given type is smaller than compared to the M_{HI}/L_B values. This quantity is type-dependent by a factor of about two to three between types Sa and Im on the average for the "standard" values. The mean value for 137 galaxies from the KKT sample is 0.65±0.05 (10^7 $M_\odot$ kpc^{-2}) and 2.4±0.3 in the same units for 20 HI-rich galaxies from the same sample. This is in agreement with the ratio of HI-rich to normal galaxies as estimated earlier from the frequency of galaxies with extended HI-envelopes (e.g. Huchtmeier and Richter, 1982), i.e. between 10% and 20%.

In terms of the HI column density there is an excellent agreement between the Virgo and the KKT sample. For the irregular galaxies the same discussion applies as for the M_{HI}/L_B value (Fig. 4). A number of nearby galaxies is given by their name. IC1613, NGC253, M81, and M31 are examples for the standard galaxies. HI-rich galaxies known to have extended HI-envelopes greater than two Holmberg diameters

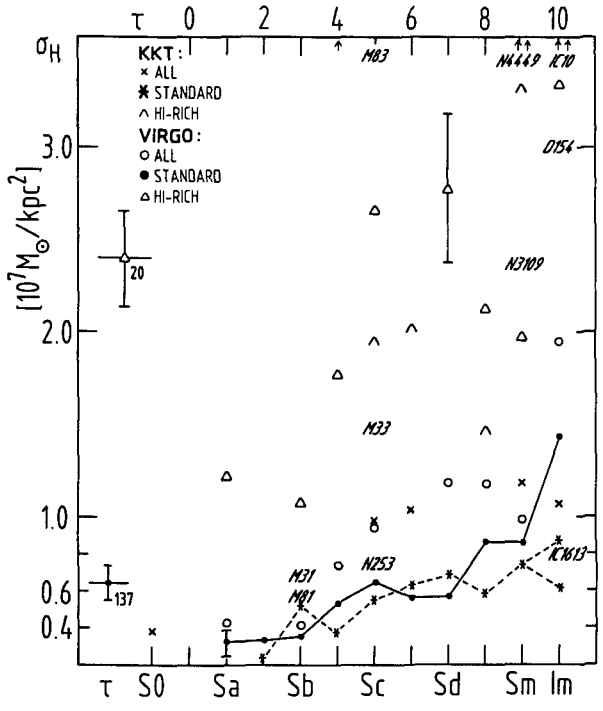


Fig. 7. HI surface density as a functional morphological type for the Virgo and the KKT sample. Mean values of the "standard" galaxies and of the HI-rich galaxies of the KKT sample are given on the left of the diagram.

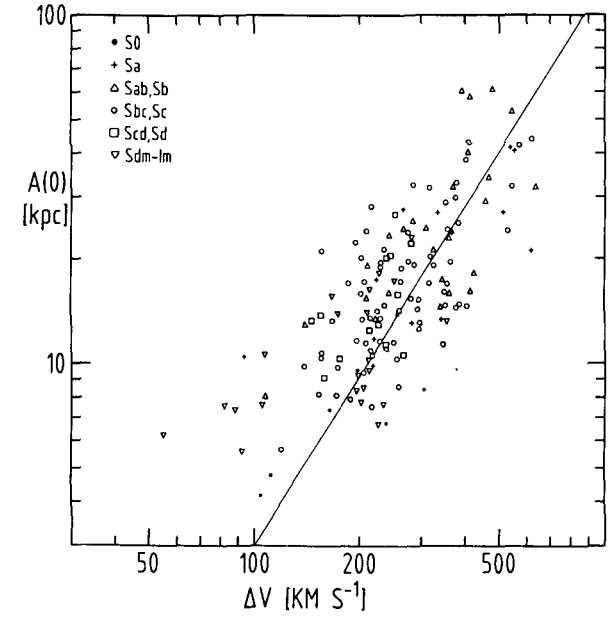


Fig. 8. Linear optical size (A(0)) of Virgo galaxies is given as a function of the corrected 21 cm line profile.

are for example M33, NGC3109, DDO154, NGC4449, IC10 and M83 (e.g. Huchtmeier and Richter, 1982 for discussion and references).

In his classical reference article on extragalactic HI-observations Roberts (1975) demonstrated the excistence of correlations between a great number of global parameters of galaxies. As an example for the present sample we have shown the type-dependence of M_{HI}/L_B (Fig. 4) and of σ_H (Fig. 7). A correlation between the linear optical diameter A(0) (kpc) and the corrected HI-linewidth Δv (km/s) is

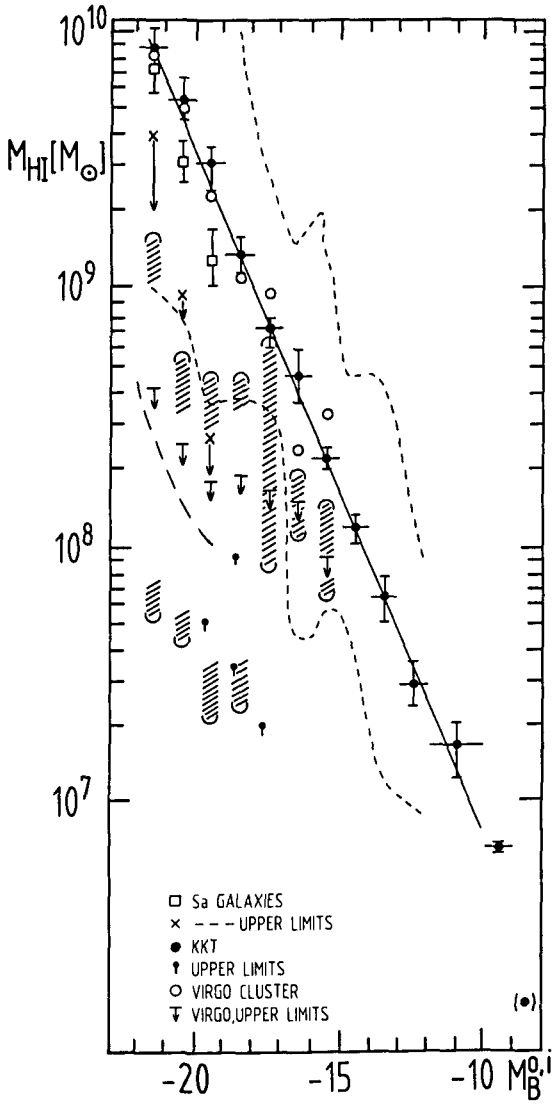


Fig. 9. The correlation of total HI mass with absolute magnitude for different samples. In case of the KKT sample the range of detected galaxies is given by broken lines. There are also a few upper limits for SO galaxies. Hatched areas indicate the upper limits from the Virgo sample.

shown in Fig. 8 for the Virgo sample. There is good agreement with the relation established by Shostak (1978) for nearby galaxies (straight line in Fig. 8) with the exception of the smallest galaxies. For these objects the inclination (needed for the correction of the observed line width) are not well defined. Another well defined correlation which does not depend on distance and should be the same for different samples of galaxies is that between total HI-mass and absolute magnitude which is nicely demonstrated in Figure 9. As virtually all spirals and irregulars of the KKT sample were detected in HI there is a well defined range of observed HI-masses for a given absolute magnitude (area between broken lines in Fig. 9). Values for detected galaxies were averaged in bins half a magnitude wide; error bars represent twice the r.m.s. error of the mean. There is good agreement between the KKT (full circles) and the Virgo sample (open circles). Sa galaxies (open squares) tend to have a lower HI-content (data from Huchtmeier, 1982) reflecting the type dependence. Upper limits of the brightest Sa galaxies fall within the range of actually observed HI masses (KKT) indicating that these data are sensitivity limited. A different behaviour is observed by the partially very low upper limits of the Virgo sample. Averages of upper limits are given by arrows, the ranges of individual upper limits are indicated by the hatched areas. Nearly two thirds of these galaxies are of type SO; their upper limits agree with the low values observed for SO's in the KKT sample. However, one third of the upper limits of the Virgo galaxies are of type Sa and later, some of them with a very low HI-content, which is a form of HI-deficiency. It should be noted that upper limits of only those galaxies of the Virgo sample were used which qualify for cluster membership by location and (optical) radial velocity.

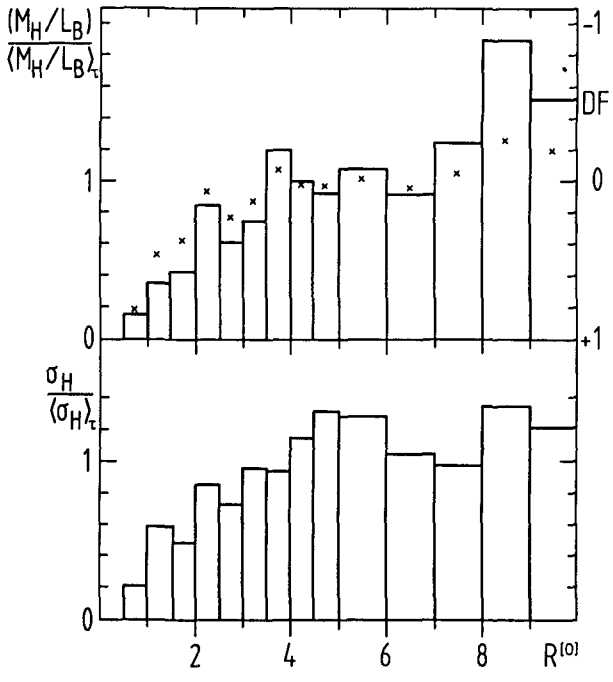


Fig. 10. HI deficiency in the Virgo cluster as a function of angular distance from M87 for two parameters: M_{HI}/L_B and the HI surface density σ_H. The inner 5 degrees are divided into concentric rings 0.5° wide; further out the division is 1 degree.

HI-deficiency. First observational arguments for an HI-deficiency in a cluster environment were put forward by Davies and Lewis (1973) and by Huchtmeier et al. (1976) in the case of the Virgo cluster. For spirals (later than Sb) both derived a relative HI-content ∿1.7 times lower than for galaxies in a reference sample outside the cluster. Krumm and Salpeter (1979) discussed the deficiency of early-type spirals in Virgo. An increased number of HI observations inabled Chamaraux et al. (1980) to demonstrate the HI-deficiency in the inner 2° of the Virgo cluster (by a factor of 2.2). Different parameters have been used to describe the deficiency: M_H/L, $M_H/A(0)^2$, M_H/A_H^2 (A(0) and A_H being the optical and the HI diameter of the galaxy, respectively). Colour indices have been used, too, (e.g. B-V: Bothun et al. 1982). Several authors used a so-called deficiency factor DF defined as the difference of the logarithm of M_H/L for a comparison sample (cs) and the logarithm of the sample of interest:

$$DF = \log(M_H/L)_{cs} - \log(M_H/L)$$

For a discussion of the HI deficiency in the Virgo cluster we will consider the M_H/L_B ratio and the HI surface density σ_H as a function of projected angular separation from M87, i.e. we devide the area in concentric rings each 0.5° wide. In this way we achieve similar numbers of Virgo galaxies in all rings. In each ring the observed parameter, M_H/L_B or σ_H, is normalized by an expected value. The expected value is synthesized from the "standard" values (Fig. 4, Fig. 7) taking into account the number of galaxies and their type. The result is presented in Fig. 10. A low relative HI-content is evident at least to about 3° from M87 for both parameters; hence the deficiency seen in the M_H/L_B is not a selection effect due to luminosity or type segregation. The resulting deficiency (calculated from the projected distribution, σ_H) is as large as 5 within 1° of M87, and about 2 between 1° and 2°, and about 1.5 between 2° and 3.5°.

From Arecibo observations Giovannardi et al. (1983) and Giovanelli and Haynes (1983) concluded that the HI extent of galaxies in the central area of the Virgo cluster is smaller by about 25% on the average compared to galaxies outside the cluster. VLA observations (Van Gorkom et al. 1984) with high spatial resolution convincingly show the HI-depletion in the outer parts of galaxies within 1° of M87. In the outer parts of the cluster the normalized relative HI-content is occasionally greater than one. This is due to HI-rich galaxies, which are not included in the "standard" sample. In addition to the normalized values in Fig. 10, the deficiency factor DF is given, too, for comparison.

In recent years environment of galaxies has been recognized to influence galaxian evolution. Galaxies in areas of high galaxian densities, i.e. central parts of clusters, show definite differences in composition relative to low density areas. In particular we observe segregation by type, luminosity (see Fig. 1), and by mass. Gravitational interaction between galaxies in close encounters have been nicely demonstrated (e.g. Toomre and Toomre 1972; also Huchtmeier and Richter, 1982, for references of observational work). However, this effect does not seem to be very effective for stripping gas off the galaxies as most of the disturbed material will stay within the interacting system. The stripping of gas through ram pressure by galaxies passing through the hot gas in central areas of clusters (demonstrated by extended X-ray emission; e.g. Jones & Forman, 1984) is favored by several authors to be responsible for the observed HI deficiency in six clusters so far (e.g. Haynes et al., 1984 and this workshop).

Absolute Magnitude - HI Line Width Relation. It is well known that luminosity and total mass correlate well (Roberts 1969). With an appropriate mass estimator such a correlation can be used to determine extragalactic distances. Using the observed (and for inclination effects corrected) 21 cm line width for the mass estimation and calibrating the magnitude - line width relation with nearby galaxies of known distances this relation became known as the Tully-Fisher relation (TF) (e.g. Sandage & Tammann, 1976). In Fig. 11a and b we show this relation for blue magnitudes for nearby galaxies and the Virgo cluster, respectively (see Richter and Huchtmeier, 1984 for a detailed description of the nearby galaxies). There are few main comments to this figure:

1. The T-F shows the same slope for the nearby and for the Virgo galaxies allowing distances to be derived and therefore deduce H_{o}.
2. The scatter in the Virgo sample is larger than in the nearby sample. Probably there are not only larger observational errors for the more distant galaxies (M_{B}, i, and Δv) but also some of the scatter will be due to differential distances within the extended cluster.

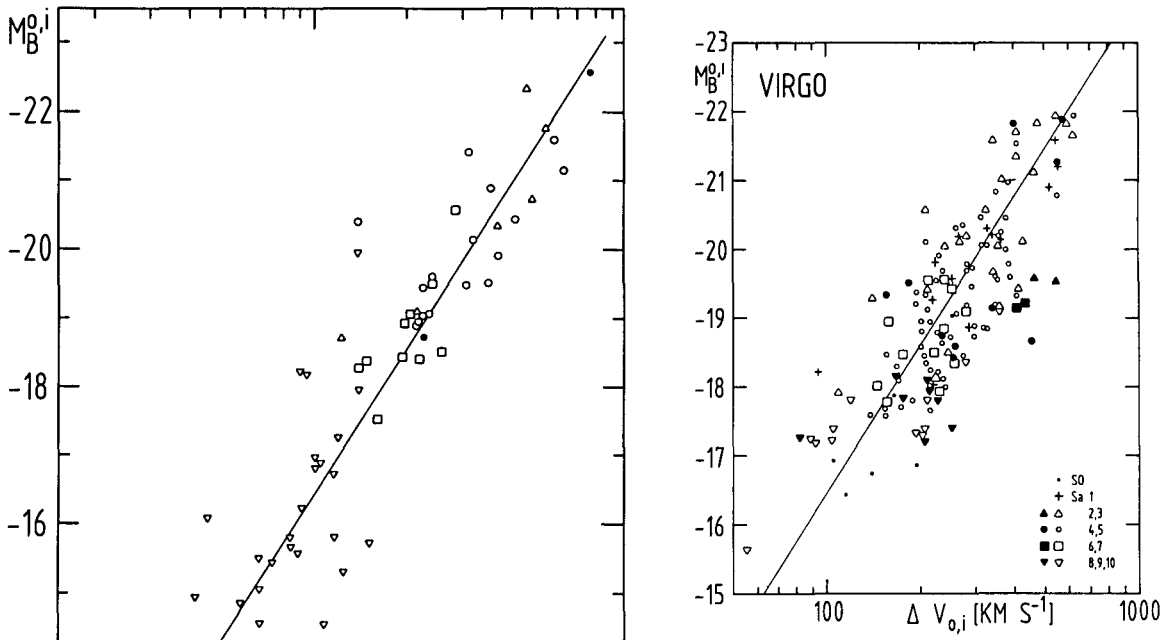


Fig. 11. Absolute magnitude as a function of corrected 21 cm line width a) the calibration sample of nearby galaxies (Richter and Huchtmeier, 1984), b) the present Virgo sample. Galaxies with low inclination (i ≤30°) are given by black symbols.

3. As a consequence of the large scatter of this relation the application to single galaxies might result in unreliable distances.

Richter and Huchtmeier (1984) recalibrated the TF:

$$M_{B_T}^{o,i} = -7.17 \times (\log \Delta v_i) - 2.12$$

which yields a distance of 24±3 Mpc for the Virgo cluster and a Hubble constant of the order of 50 km/s/Mpc. This relation is given in Fig. 11a and b by a straight line. In Fig. 11b we include all galaxies with decent HI profiles. Galaxies with low inclinations (i <30°) are marked by full symbols. These galaxies contribute to the general scatter but are not sufficient to explain its large value.

Applying the TF to subgroups of the Virgo cluster (de Vaucouleurs et al. 1976) could help to derive the three-dimensional structure of the cluster. A first step

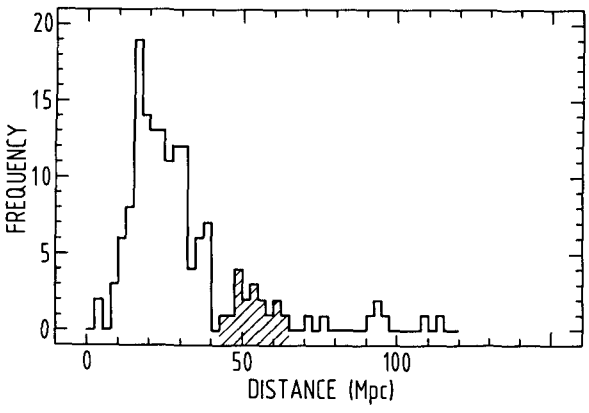


Fig. 12. Frequency distribution of Virgo cluster galaxies for different distance intervals. The hatched area refers to the W group.

was taken by applying it to the Virgo B group which is a member of the Virgo cluster proper. The derived distance is 21±1.5 Mpc. Next the TF was applied to galaxies in the W group which yielded a distance about twice that of the cluster. Applying the TF to all galaxies of the Virgo sample yields the histogram of Fig. 12 showing the frequency of galaxies per distance interval. At half the peak value of the histogram the main distribution is located at 23 Mpc ranging from 15 to 32 Mpc which corresponds to about twice the linear width of the 10° circle. The shaded area in this figure corresponds to the W group. Another indication that application of the TF at least in large terms yields reasonable results is given by retaining only the information nearer (-) or further (+) away than the cluster centre. The distribution of near (-) and far (+) galaxies with radial velocity is regular and symmetric as expected with the exception that for high radial velocities there are greater numbers of distant (+) galaxies. Here we see part of the southern extension at greater distances.

Resumee. The galaxy population in the outer part of the Virgo cluster is similar to the local population of galaxies in terms of global HI properties. Only the central part of the cluster, the area of high galaxian density, shows a clear difference. The type and luminosity segregation is accompanied by a pronounced HI-deficiency. The TF relation seems to be identical for the low and high density environment and might help to disentangle the three dimensional structure of the Virgo cluster.

References

Balkowski, C., Bottinelli, L., Gouguenheim, L., Heidmann, J.: 1973, Astron. Astrophys. 23, 139

Bohnenstengel, H.-D.: 1983, Ph. D. Thesis, Univ. of Hamburg

Bosma, A.: 1978, Ph. D. Thesis, Univ. Groningen

Bothun, G. D., Schommer, R. A., Sullivan, W. T.: 1982, Astron. J. 87, 731

Bothun, G. D., Aaronson, M., Schommer, G. A., Huchra, J., Mould, J.: 1984, Astrophys. J. 278, 475

Bottinelli, L., Gouguenheim, L., Heidmann, J.: 1973, Astron. Astrophys. 25, 451

Bottinelli, L., Gouguenheim, L., Paturel, G.: 1982, Astron. Astrophys. 113, 61

Chamaraux, P., Balkowski, C., Gérard, E.: 1980; Astron. Astrophys. 83, 38

Davies, R. D., Lewis, B. M.: 1973; Mon. Not. Roy. Astr. Soc. 165, 231

de Vaucouleurs, G.: 1975, in Stars and Stellar Systems, Vol. IX, p. 557, ed. A. Sandage, M. Sandage, J. Kristian, Univ. of Chicago Press

de Vaucouleurs, G., de Vaucouleurs, A., Corvin, G. G. Jr.: 1976 (RC2), Second Reference Catalogue of Bright Galaxies, Univ. of Chicago Press

Epstein, E. E.: 1964, Astron. J. 69, 490

Fisher, R. J., Tully, R. R.: 1981, Astrophys. J. Suppl. 47, 139

Gallagher, J. S.: 1972, Astron. J. 77, 568

Giovanardi, C., Krumm, N., Salpeter, E. E.: 1983, Astrophys. J.

Giovanelli, R., Haynes, M. P.: 1983, Astron. J. 88, 881

Gouguenheim, L.: 1969, Astron. Astrophys. 3, 281

Haynes, M., Giovanelli, R., Chincarini, G. L.: 1984 in Ann. Rev. Astron. Astrophys. 22, 445

Helou, G., Giovanardi, G., Salpeter, E. E., Krumm, N.: 1981,

Helou, G., Hoffman, G. L., Salpeter, E. E.: 1984, Astrophys. J. Suppl. 55, 433

Huchtmeier, W. K.: 1982, Astron. Astrophys. 110, 121

Huchtmeier, W. K.: 1984 in Clusters and Groups of Galaxies, p. 221, ed. Mardirossian et al., Reidel

Huchtmeier, W. K., Tammann, G. A., Wendker, H. J.: 1976, Astron. Astrophys. 46, 381

Huchtmeier, W. K., Richter, O.-G.: 1982, Astron. Astrophys. 109, 331

Huchtmeier, W. K., Richter, O.-G., Bohnenstengel, H.-D., Hauschildt, M.: 1983, ESO preprint Nr. 250

Jones, C., Forman, W.: 1984 in Clusters and Groups of Galaxies, p. 319, ed. Mardirossian et al., Reidel

Knapp, G. R., Kerr, F. J.: 1974, Astron. J. 79, 667

Kraan-Korteweg, R. C., Tammann, G. A.: 1979, Astron. Nachr. 300, 181

Kraan-Korteweg, R. C.: 1982, Astron. Astrophys. Suppl. 47, 505

Krishna-Kumar, C., Thonnard, N.: 1983, Astron. J. 88, 260

Krumm, N., Salpeter, E. E.: 1979, Astrophys. J. 228, 64

Li Zong-yun, Liu Ru-Liang: 1981, Chin. Astr. Astrophys. 5, 205

McCutcheon, W. H., Davies, R. D.: 1970, Mon. Not. Roy. Astr. Soc. 150, 337

Richter, O.-G., Huchtmeier, W. K.: 1984, Astron. Astrophys. 132, 253

Roberts, M. S.: 1969, Astron. J. 74, 859

Roberts, M. S.: 1975 in Stars and Stellar Systems, Vol. IX, p. 309, ed. A. Sandage, M. Sandage, J. Kristian, Univ. of Chicago Press

Robinson, B. J., Koehler, J. A.: 1965, Nature 208, 993

Romanishin, W., Krumm, N., Salpeter, E. E., Knapp, G., Strom, K. M., Strom, S. E., 1982, Astrophys. J. 263, 94

Rots, A. H.: 1980, Astron. Astrophys. Suppl. 41, 89

Sandage, A., Tammann, G. A.: 1976, Astrophys. J. 210, 7

Shostak, G. S.: 1978, Astron. Astrophys. 68, 321

Sulentic, J. W., Arp, H.: 1983, Astron. J. 88, 489

Toomre, A., Toomre, J.: 1972, Astrophys. J. 178, 623

van Gorkom, J. H., Balkowski, C., Kotanyi, C.: 1984 in Clusters and Groups of Galaxies, p. 261, ed. Mardirossian et al., Reidel

The HI DEFICIENCY OF THE SO GALAXIES IN THE VIRGO CLUSTER

C. Balkowski P. Chamaraux P. Fontanelli
Observatoire de Paris, Section Meudon

Abstract

We analyse the HI contents of a large sample of SO galaxies measured at Arecibo with a high sensitivity, mainly by Giovanardi et al. (1983) and located within and outside the Virgo Cluster. The analysis is carried out using a new statistical method giving the true distribution of the HI contents taking into account the upper limits for the non detections. As a result, the Virgo SO^S have a deficiency factor DF > 2.3 and most probably a much larger value. The estimation of the stripping of cluster galaxies by the ram pressure of the intracluster medium shows that the deficiency of the Virgo cluster SO^S can be caused by this process.

I - Introduction

It is now well established that the disk galaxies in the Virgo Cluster are HI deficient compared to those located in the field or in small groups. This is true for the spiral galaxies later than Sb (Chamaraux et al. 1980, Giovanelli and Haynes 1983) and for early types as well (Giovanardi et al. 1983 and references herein). However the value of the HI deficiency parameter has been derived only for spiral galaxies later than Sb : a factor of about two, independent of the type, has been found. For early types no attempt has still been made in order to estimate that parameter, or at least some limit of it, mainly because of the low percentage of detections.

In the present paper we determine the HI deficiency parameter for the SO galaxies of the Virgo Cluster. It is particularly interesting to get a quantitative value for that parameter for SO galaxies because if the HI deficiency is caused by the interaction between the galaxies and the intracluster gas, as generally thought, then much higher deficiencies are expected for SO galaxies than for late type spirals since the HI in the SO^S is mainly concentrated in an outer ring (van Woerden et al. 1983) and therefore much more sensitive to stripping.

The derivation of the HI deficiences of the SO^S has been made from a large sample of early type galaxies measured with a high sensitivity at Arecibo, mainly by Giovanardi et al. (1983) , and using a new statistical method which gives the true distribution of the HI contents from the values for the detected and for the undetected galaxies.

The statistical method is presented in part II, the sample is displayed in part III, the derivation of the HI deficiencies, the discussion and a tentative interpretation are given in part IV.

II - The Statistical Method

The purpose of the present method is to derive the true distribution of the HI contents of SO galaxies, above a certain limit of content, from the distribution of that quantity for the detected galaxies and of its upper limit for the undetected galaxies. The method is quite general and can be applied to a variety of problems where upper limits are found. Another method has been developed by Avni et al. (1980) in order to solve similar problems ; although it gives results essentially identical to ours in the present case, we prefer to use our method, which is much simpler to understand and to use and gives other informations of interest, too.

The HI content of a SO galaxy will be described by its HI surface density $\sigma_H = M_H/(\pi/4)\ A_o^2$, where M_H is the HI mass in the galaxy and A_o its linear diameter. Indeed it has been already shown this is the best parameter to describe the HI content of spiral galaxies (Chamaraux et al. 1980, Giovanelli and Haynes 1983) ; moreover, one has also $M_H \propto A^{2.4\pm0.5}$ for the detected SO galaxies, so σ_H seems also well suited for the lenticular galaxies.

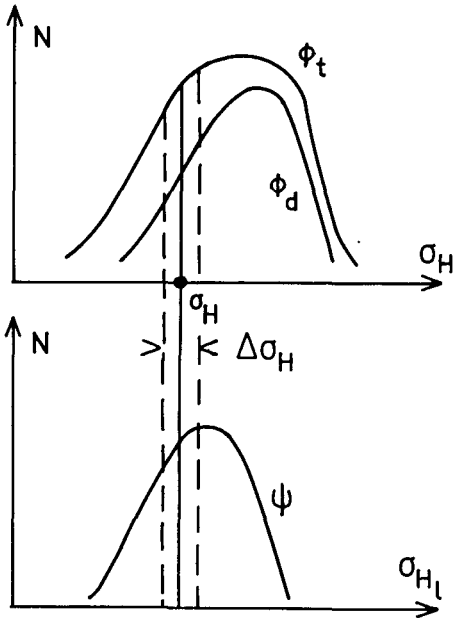


Fig. 1 : Distributions of the σ_H values of the detected objects (Φ_d), of the upper limits (ψ) and the true distribution Φ_t.

So we consider a sample of N_t observed SO galaxies, among which N_d have been detected. Be Φ_t and Φ_d the distributions of the σ_H for the whole sample and the detected galaxies respectively ; of course Φ_t is unknown. (In order to have simpler notations, we will treat the distributions as continuous functions, although they actually are histograms ; that does not change anything for the demonstration). Let us consider a given galaxy of the sample, having an angular diameter a_o and emitting an HI flux F_H (not necessarily detected) ; one has $\sigma_H = \alpha\ F_H/a_o^2$, where α is a numerical constant depending on the units. Be F_{H_ℓ} the minimal HI flux which could have been detected in the observations of that galaxy ; one has : $\sigma_{H_\ell} = \alpha\ F_{H_\ell}/a_o^2$; be ψ the distribution of the σ_{H_ℓ}

values for the N_t galaxies of the sample.

We consider now a small interval $\sigma_H \pm \Delta\sigma_H/2$ around a given value of σ_H. There are n_t galaxies in this interval in the total sample and n_d have been detected, so :

$$n_t = \phi_t \, \Delta\sigma_H \qquad\qquad n_d = \phi_d \, \Delta\sigma_H$$

Be ψ_{σ_H} the distribution of the σ_{H_ℓ} values for those n_t galaxies. The condition of detection of any galaxy in the interval $\sigma_H \pm \Delta\sigma_H/2$ is : $F_{H_\ell} \leqslant F_H$, which is equivalent to : $\sigma_{H_\ell} \leqslant \sigma_H$. Thus :

$$n_t = \int_o^\infty \psi_{\sigma_H} \, d\sigma_{H_\ell} \quad \text{with} \quad n_d = \int_o^{\sigma_H} \psi_{\sigma_H} \, d\sigma_{H_\ell}$$

So if the relative distribution ψ_{σ_H}/n_t of the σ_{H_ℓ} of the n_t galaxies is known, then n_t and ϕ_t can be determined, since n_d is known.

That is the case if ψ_{σ_H} is independent of σ_H ; then $\psi_{\sigma_H} =$ $\psi \, n_t/N_t$ and

$$\phi_t(\sigma_H) = \frac{N_t}{\int_o^{\sigma_H} \psi \, d\sigma_{H_\ell}} \, \phi_d(\sigma_H) \qquad (1)$$

Are we in such a case here ?

We have to check that the distribution of $\sigma_{H_\ell} = \alpha \, F_{H_\ell}/a_o^2$ at a given σ_H does not depend on σ_H.

Obviously, the value of F_{H_ℓ} is independent of σ_H. So the problem is to determine whether the distribution of the apparent diameters a_o at a given σ_H depends on σ_H.

A priori, such a correlation is not expected, since σ_H is an intrinsic parameter and a_o an apparent one. In fact it could exist only if a_o is correlated in the sample to a parameter itself related to σ_H. One thinks immediately to the linear diameter A_o as this intermediate parameter. Indeed σ_H could be correlated to A_o ; in fact one expects only a loose correlation if any since σ_H is nearly independent of A_o for spirals and, for detected $S0^s$, one has : $M_H \quad A^{2.4\pm0.6}$, implying a weak dependence of σ_H on A_o. In the Virgo cluster, a_o and A_o are proportional (galaxies at the same distance), so it could exist a slight correlation between a_o and σ_H. In turn, for the non cluster sample, we have checked that a_o and A_o are independent, so the method is fully applicable. So we will now consider ψ_{σ_H} as independent of σ_H, remembering that it is perhaps not completely true for the Virgo cluster sample ; thus the formula (1) will give the true distribution of the HI contents.

The formula (1) shows that the method gives significant results only if $N_t / \int_o^{\sigma_H} \psi \, d\sigma_{H_\ell}$ is not too large ; otherwise an important uncertainty is expected on

$\Phi_t(\sigma_H)$ for those σ_H. So one is limited to values of σ_H such that the number of galaxies with $\sigma_{H_\ell} < \sigma_H$ is not too small compared to N_t (more than $\sim N_t/5$) ; that gives the lowest value of σ_H for which one can have some information about the true distribution of the HI contents.

III - The Sample

Our purpose is to compare the HI contents of the SO^s located within and outside the Virgo cluster respectively. In order to use the most sensitive measurements, we have restricted to galaxies of these types observed in HI at Arecibo by Bieging and Biermann (1977), Biermann et al. (1979), Krumm and Salpeter (1979), Knapp et al. (1979), Haynes (1981), Giovanardi et al. (1983), Fontanelli et al. (1984) ; the great majority of the measurements used come in fact from Giovanardi et al. (1983). In case of several measurements of the same galaxy, the most sensitive one has been taken. The morphological types are from de Vaucouleurs et al. (1976) ; the lenticulars comprise $T = -3, -2, -1$.

The final sample comprises 122 SO^s among which 67 are outside the Virgo cluster and its extension (24 detections) and 43 belong to the Virgo cluster proper (4 detections), i.e. as being at less than 6° from $\alpha = 12^h27$; $\delta = +13^o.5$ (de Vaucouleurs, 1961) and having $V_r < 2500$ km s^{-1}. The upper limits of the HI fluxes for non detections have been taken as $F_{H_\ell} = 3\sigma \times 300$ (Jy km s^{-1}) where σ is the r.m.s. noise in Jy. For the detections, one has adopted for σ the average for the non-detections of the same series of observations.

On the other hand note that the condition of detection $F_{H_\ell} < F_H$ is valid if F_H is the HI flux measured when pointing at the centre of the galaxy. In principle one could make a correction in order to take into account the gas located outside the central beam, bust most of the sample galaxies have only been observed in the central position, and the HI distribution in SO^s is too poorly known to make a statistical correction. So it must be reminded that σ_H is defined from the HI mass seen by the beam at the center of the galaxy; the true σ_H is somewhat higher, certainly less than twice that value on an average , due to the relatively small diameters. Compared to the range of a factor of 100 in the σ_H values, that correction is negligible and does not affect the conclusions.

At last note that log σ_H has been used as variable instead of σ_H in the application of the statistical method described above.

IV - Results and Discussion

Figure 2 displays the true distribution of the σ_H values for the SO^s located outside the Virgo cluster and having $\sigma_H > 0.022$ computed from our statistical method.

the point at $\sigma_H = 0.032$ is somewhat uncertain, with a possible uncertainty of about a factor 2. One can see that 48(±15) galaxies have $\sigma_H > 0.022$, i.e. ~ 72% (±20%) of the total sample of 67 objects. Thus there is no evidence of an important population of SO^S with extremely low HI contents. On the contrary, the histogram suggests a distribution of the HI contents rather smooth and regular, with a very high dispersion (more than a factor of 5). The median value of σ_H is $\langle\sigma_H\rangle = 0.050$.

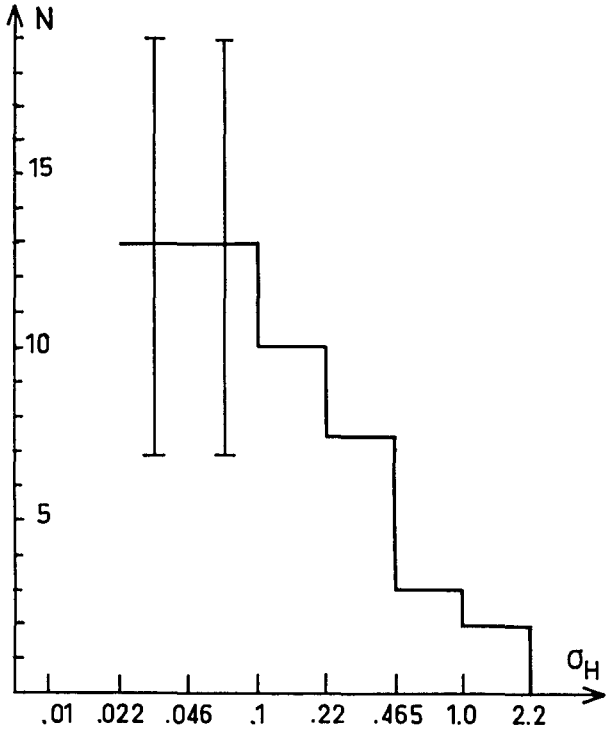


Fig. 2 : True distribution of the σ_H values for SO^S outside the Virgo cluster.

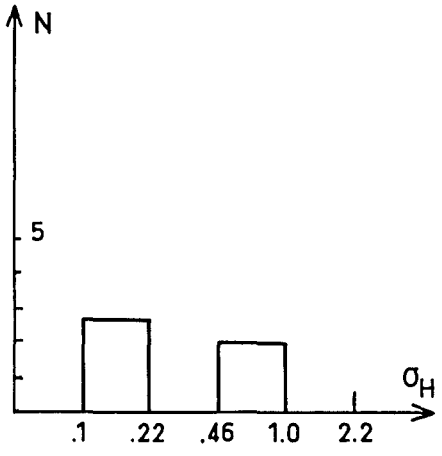


Fig. 3 : True distribution of the σ_H values for SO^S inside the Virgo cluster.

Figure 3 shows the true distribution of the σ_H values for the SO^S of our sample located in the Virgo cluster and having $\sigma_H > 0.022$. That distribution is completely different from the previous one. In particular only 5 galaxies have σ_H values higher than 0.022, that is 11% of the total sample of 43 SO^S. Thus the Virgo cluster SO^S comprise mainly galaxies with very low HI contents. Unfortunately, the measurements are not sensitive enough to push further on the lower limits of the HI content ; one can only say that the median value $\langle\sigma_H\rangle < 0.022$. But it is obvious that $\langle\sigma_H\rangle$ is certainly much lower than that upper limit, obtained in the hypothesis that there is a concentration of σ_H values at 0.022 ; in fact some dispersion of the σ_H values is expected, at least as high as that for the SO^S outside Virgo, then a $\langle\sigma_H\rangle$ value at most 1/3 or even 1/10 that limit can be foreseen.

Thus there is a clear HI deficiency of Virgo cluster SO^S, with a deficiency factor DF > 2.3, and more likely at least 3 times that value ; so the Virgo SO^S are at least as deficient as the spirals and probably much more.

If the HI deficiencies in the Virgo cluster are caused by stripping by the intracluster gas, higher deficiencies are indeed expected for SO^S since the stripping affects primarily the external regions of the galaxies and since the HI is more centrally concentrated in late types than in SO galaxies. Van Woerden et al. (1983) have found that HI in SO^S is mainly concentrated in a ring with a mean radius of 1.5 r_{25} (r_{25} being the radius of the isophote 25 m/□"). The curves of the HI distribution within the SO^S (van Driel, private communication) show that there is no "severe" stripping (DF < 3) as long as the stripping radius is larger than about r_{25}. Using Takeda et al.'s (1984) stripping model we can estimate the percentage of SO^S of the cluster which are not severely stripped. Indeed these authors compute the stripping radius r_s of a galaxy having a velocity dispersion σ along the line of sight, and moving with a velocity v_o through an intracluster medium of density ρ_o. With $\sigma = 100$ km s^{-1}, $\rho_o > 6\ 10^{-30}$ g cm^{-3} (value at 5° from the center, after Bahcall and Sarazin, 1977) the condition $r_s > r_{25}$ leads to $v_o < 440$ km s^{-1}, which gives $v_r < 250$ km s^{-1} ; taking into account the dispersion $\sigma(v_r) \simeq 600$ km s^{-1} of the SO^S of our sample, it comes that 32% at most are expected not to be highly HI deficient. That is an upper limit which assumes in particular no motion in the intracluster medium, an assumption obviously wrong. On the other hand, one can estimate that proportion p from the true distributions of σ_H obtained above. Indeed let us assume that (i) the deficiency factor does not depend on the initial σ_H of the galaxy before stripping and that (ii) the initial relative distribution of σ_H for Virgo SO^S was that obtained for non cluster SO^S. Then let us consider all the Virgo SO^S having an initial $\sigma_H \geq 3 \times 0.022 = 0.066$, i.e. 19 objects from our histogram and using the hypothesis (ii) ; among these galaxies, n have undergone a non severe HI deficiency characterized by DF $\leq$ 3, so resulting in a final $\sigma_H \geq 0.022$. Now 5 galaxies in the Virgo cluster have such σ_H values ; one obtains a maximum value of p assuming that none of these objects has been severely stripped, i.e. : p $\leq$ 25%.

The agreement between the theoretical and the observed values of p is very good, showing that our results are fully compatible with the stripping by ram pressure as responsible for the HI deficiencies of SO^S in the Virgo cluster.

In conclusion, we have compared the HI contents of SO^S located in the Virgo cluster and outside of it, using a new statistical method giving the true distribution of the HI contents when taking into account the upper limits for the undetected objects. The SO galaxies located in the Virgo cluster have an HI deficiency of at least a factor 2.3 and probably much larger. The results are compatible with the stripping by the Virgo intracluster medium as the cause of the gas deficiency.

References

Avni, Y., Soltan, A., Tananbaum, H., Zamorani, G., 1980, Astrophys. J. 238, 800.

Bahcall, J.N., Sarazin, C.L., 1977, Astrophys. J. Letters213, L99.

Bieging, J.H., Biermann, P., 1977, Astron. Astrophys. 60, 361.

Biermann, P., Clarke, J.N., Fricke, K.J., 1979, Astron. Astrophys. 75, 7.

Chamaraux, P., Balkowski, C., Gérard, E., 1980, Astron. Astrophys.83, 38.

Fontanelli, P., Balkowski, C., Chamaraux, P., 1984, in preparation.

Giovanardi, C., Krumm, N., Salpeter, E.E., 1983, Astron. J. 88 , 1719.

Giovanelli, R., Haynes, M.P., 1983, Astron. J. 88, 881.

Haynes, M.P., 1981, Astron. J. 86, 1126.

Knapp, G.R., Kerr, F.J., Henderson, A.P., 1979, Astrophys. J. 234, 448.

Krumm, N., Salpeter, E.E., Astrophys. J. 227, 776.

Takeda, H., Nulsen, P.E.J., Fabian, A.C., 1984, Mon. Not. R. Astr. Soc. 208, 261.

Van Woerden, H., Van Driel, W., Schwarz, U.J., 1983, in Internal Kinematics and dynamics of Galaxies, I.A.U. Symposium 100, ed. E. Athanassoula (Dordrecht - Reidel), p.99.

Vaucouleurs, G. de, 1961, Astrophys. J. Suppl. 6, 213.

Vaucouleurs, G.de, Vaucouleurs, A.de, Corwin, H.C., 1976, Second Reference Catalogue of Bright Galaxies, Univ. of Texas Press, Austin.

HI DEFICIENCY IN THE VIRGO CLUSTER

Martha P. Haynes

National Astronomy and Ionosphere Center[1] and
Astronomy Department, Cornell University

Because of its proximity to us, the Virgo cluster has been the continued subject of numerous studies exploring the effect on galaxy evolution of the environment via investigations in the 21 cm line of neutral hydrogen. In the Virgo core, galaxies are known to have not only lower HI contents (Davies and Lewis 1973; Chamaraux et al. 1980) but also reduced HI sizes (Giovanardi et al. 1983; Giovanelli and Haynes 1983; see talks by Kotanyi and by Warmels in this volume). Here I summarize the comparative studies of both the HI content and HI extents of Virgo and isolated galaxies undertaken by myself, R. Giovanelli and J. N. Hewitt which can now be combined with other results in order to investigate the pattern of HI deficiency seen in the Virgo cluster.

HI Deficiency: DEF

As part of the Arecibo survey of isolated galaxies (Haynes and Giovanelli 1984), the large angular diameter galaxies ($a \geq 2'.5$) from that sample were mapped at major axis points using the Arecibo flat feed system (Hewitt et al. 1983). These galaxies provide a comparison data set of galaxies which lie in low density regions but which are otherwise similar to the Virgo spirals. The isolated galaxy sample includes galaxies which are included both in the Catalog of Isolated Galaxies (Karachentseva 1973) and in the Uppsala General Catalog (Nilson 1973), and which lie in the declination range $-1° < \text{Dec.} < +38°$. The analysis of the galaxian properties derived from these observations leads to the conclusion that the diameter of a spiral disk is a more important determining parameter for the HI mass of a galaxy than is the morphological type. In agreement with Shostak (1978), we find that the HI surface density is nearly constant when averaged over the disk. For the entire isolated galaxy sample, the relation between the HI mass h^2M_H and the optical linear diameter hD_ℓ is nearly independent of morphological type and is given by

$$\log h^2M_H = 7.16 + 1.74 \log hD_\ell \ ,$$

[1] The National Astronomy and Ionosphere Center is operated by Cornell University under contract with the National Science Foundation.

where $h = H_0/100$. We may use this relation, or the slightly modified one obtained for each morphological class separately, to measure the relative HI deficiency DEF, defined as the difference in the logarithm of the galaxy's observed HI mass from that expected for a "normal" galaxy of similar morphological type T and optical linear diameter

$$DEF = \langle \log M_H(T,D_\ell) \rangle - \log M_H(obs).$$

For 19 large angular diameter galaxies within the 5° Virgo core, Giovanelli and Haynes (1983) found that the average HI deficiency of Virgo spirals is a factor of 2.7 with respect to the isolated galaxies, in agreement with the results obtained via other approaches taken by Chamaraux et al. (1980) and Giovanardi et al. (1983).

HI Sizes

Using the major axis mapping observations of the large angular diameter isolated galaxies and the large spirals in the Virgo core, we have measured a characteristic effective diameter D_{70} derived from the best fit comparison of the observed fluxes with a numerical convolution of a model HI surface density distribution and a Bessel function expression for the beam response (Hewitt et al. 1983; Giovanelli and Haynes 1983). Seventy percent of the best-fit model's HI mass lies interior to the corresponding radius R_{70}. The total observational sample includes 24 galaxies in Virgo, 19 of which are found within the 5° core, and 56 comparison galaxies. We have found that, for a given optical size, a Virgo core galaxy has, on the average, a smaller HI extent than a galaxy in a low density region by more than a factor of 1.6. The derived ratios of the HI to Holmberg diameters are $D_{70}/D_{Ho} = 0.78 \pm 0.28$ for galaxies in the 5° Virgo core and $D_{70}/D_{Ho} = 1.10 \pm 0.30$ for the others. Subsequent aperture synthesis observations at both Westerbork (Warmels, this volume) and the VLA (Kotanyi, this volume) confirm our results.

We see, therefore, in Virgo that not only are the spiral galaxies HI poor with respect to their counterparts in the field, but the sizes of their HI disks are also reduced. The use of comparative criteria which are nearly independent of morphological type shows that Virgo core spirals are truly distinct from galaxies in lower density regions.

HI Observations of Faint Virgo Galaxies

The proximity of Virgo also renders unique to it the opportunity to study

its low luminosity members. Other papers given here by Sandage, Tammann, Binggeli and Hoffman contain much valuable insight into the dwarf population. Because the disks of low mass late-type systems are expected to be even more fragile to the hostile cluster environment, we have undertaken new Arecibo HI observations of 66 faint galaxies in the Virgo core in order to investigate their degree of HI deficiency. Most of these "faint" Virgo galaxies have magnitudes fainter than +14.5 and are included in the UGC (Nilson 1973). At the time of the observations, many had optical redshifts either from Karachentsev and Karachentseva (1982) or from the CfA survey (Huchra et al. 1983; Huchra, private communication). However, some had no known redshift, and we conducted the HI search in the usual mode, described in Haynes and Giovanelli (1984). Of the 66 observed galaxies, 50 have heliocentric velocities less than +3000 kms^{-1}; the other 16 are found mostly in the Coma supercluster.

The faint Virgo galaxies are mainly low luminosity dwarfs, characterized by $<\log h^2L> = 8.35 \pm 0.45$ $(L_\odot)$ and $<\log hD_\ell> = 0.64 \pm 0.19$ (kpc). In order to compute DEF, a suitable comparison sample was obtained from 150 galaxies of types Sc, Sd, Sm and Irr with $+500 < V_\odot < +3000$ kms^{-1} observed by us at Arecibo. Figure 1 shows the relationship between $\log h^2M_H$ and $\log(hD_\ell)^2$ for this comparison sample (left panel) and separately for the faint Virgo spirals (right panel). The comparison sample dwarfs are on the average larger (the Virgo spirals have lower surface brightness), but the relationship between h^2M_H and hD_ℓ extends to smaller linear diameters.

We have computed DEF in comparison with the appropriate sample,

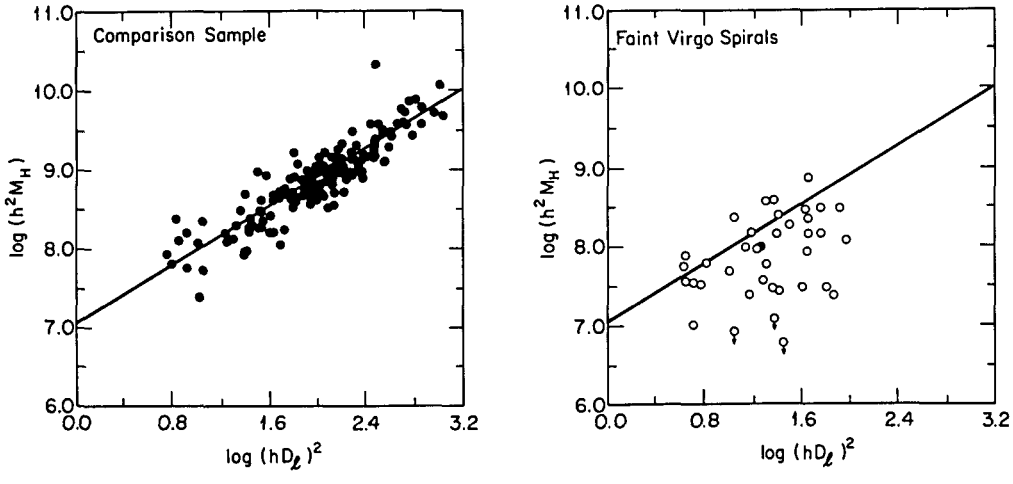


Figure 1. The relationship between HI mass h^2M_H and optical linear diameter hD_ℓ for galaxies in the comparison (left) and the faint Virgo spiral sample (right). Solid lines show the least squares fit for the comparison sample.

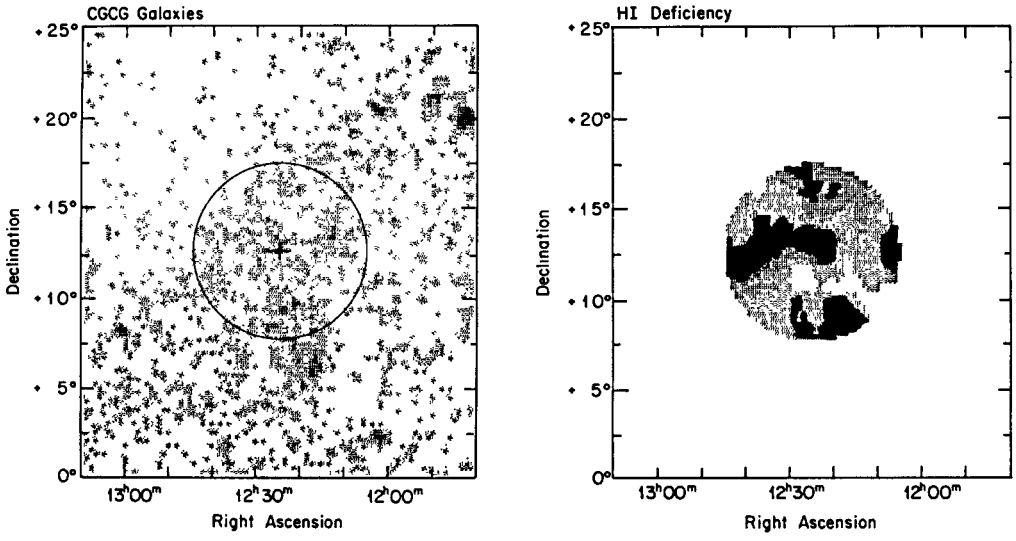


Figure 2. Shade plots showing the galaxy distribution (left) and the HI deficiency pattern (right) in the Virgo cluster core. The circle shown in the left panel outlines the Virgo 5° core; average deficiencies are computed only in that region in the right panel by computing the mean for the three galaxies nearest to the pixel center.

depending on the optical size of the galaxy: for log hD_ℓ greater than 0.8, we use the isolated galaxy sample alone, while for smaller values, the late type dwarf sample is employed. As seen in the comparison of the two panels in Figure 1, the faint Virgo core spirals include a population of very HI poor galaxies. The average value of DEF for all the faint galaxies in Virgo is $\langle DEF \rangle = 0.36$, but in fact the distribution appears bimodal. A substantial number of Virgo dwarfs are HI deficient by up to a factor of ten.

The Pattern of HI Deficiency

In trying to understand the cause of the depletion of the atomic component of the interstellar medium in the outer parts of cluster spirals, we have compiled a list of 120 Virgo galaxies, including the fainter spirals reported here, which have good HI measures reported in the literature. We have remeasured DEF in a systematic fashion in terms of M_H/D^2. Many spiral galaxies within the Virgo 5° core are systematically HI poor with respect to isolated galaxies of similar optical characteristics. Certainly a fraction of the Virgo galaxies with normal HI contents may be mere projections on the cluster core.

Figure 2 shows a comparison of the galaxy distribution and the pattern of HI deficiency. The left panel shows a shade plot of the surface density distribution of galaxies in the Zwicky catalog (Zwicky et al. 1961); no correction is made for the background in this representation, but the enhancements discussed by others around NGC 4472 and M87 are visible. The right panel illustrates the HI deficiency pattern within the 5° core. The shade level for each pixel is computed as the average of the DEF values for the three galaxies nearest to the cell center. The white area shows the locations of galaxies which are normal or deficient by less than a factor of two, while the darkest areas contain galaxies deficient by a factor of five. Within the 5° core, a systematic pattern with radius is not evident, most likely because of the same clumpiness seen in the galaxy distribution. HI deficiency is most prominent in the region around M87, with a secondary peak around NGC 4472.

Summary

The case for HI deficiency in the Virgo cluster is now based not only on the measurement of the lower HI content with respect to a sample of isolated galaxies, but also on the observed reduction in the HI disk sizes. A correlation also appears between DEF and the (U-B) color index obtained from the mid-ultraviolet photometry of Smith and Cornett (1982), in the sense that deficient galaxies have systematically less ultraviolet flux (Giovanelli and Haynes 1983). The lower UV flux and the shrunken HI disks argue against the depletion of HI by stimulated star formation. As discussed by Giovanelli and Haynes (1984) and summarized by Giovanelli in this volume, the HI deficiency seen in nine clusters including Virgo correlates best with the presence of a hot intergalactic medium, and is likely the result of stripping by ram pressure or evaporative processes.

Acknowledgements: Since the time of the meeting, the catalog of Binggeli, Sandage and Tammann was made available to me so that this report includes their better morphological classifications. I thank Bruno Binggeli for his promptness in sending me the catalog.

References

Chamaraux, P., Balkowski, C. and Gerard, E. 1980, Astron. Astrophys. 83, 38.

Davies, R. D. and Lewis, B. M. 1973, Mon. Not. R. Astr. Soc. 165, 231.

Giovanardi, C., Helou, G., Krumm, N. and Salpeter, E.E. 1983, Astrophys. J. 267, 35.

Giovanelli, R. and Haynes, M.P. 1983, Astron. J. 88, 881.

_____ 1984, Astrophys. J. (to appear).

Haynes, M.P. and Giovanelli, R. 1984, Astron. J. 89, 758.

Hewitt, J.N., Haynes, M.P. and Giovanelli, R. 1983, Astron. J. 88, 272.

Huchra, J., Davis, M., Latham, D. and Tonry, J. 1983, Astrophys. J. Suppl. 52, 89.

Karachentsev, I.D. and Karachentseva, V.E. 1982, Sov. Astron. Lett. 8, 104.

Karachentseva, V.E. 1973, Comm. Spec. Astrof. Obs. 8, 1.

Nilson, P. 1973, Uppsala Astr. Obs. Ann. 6.

Shostak, G.S. 1978, Astron. Astrophys. 68, 321.

Smith, A.M. and Cornett, R.H. 1982, Astrophys. J. 261, 1.

Zwicky, F., Herzog, E. and Wild, P. 1961, Catalog of Galaxies and Clusters of Galaxies (Pasadena: Calif. Inst. of Tech.) Vol. I.

THE HI DISTRIBUTION IN SPIRAL GALAXIES IN THE VIRGO CLUSTER

Rein H. Warmels
Kapteyn Astronomical Institute, University of Groningen
Postbox 800, 9700 AV Groningen, The Netherlands

Abstract

Neutral hydrogen observations with the Westerbork Synthesis Radio Telescope have revealed the HI distributions in 36 spiral galaxies in the Virgo cluster area. For these galaxies, with morphological types ranging from Sab to Sdm, I present the face-on corrected HI diameter at the surface density level of 1 $M_\odot$ pc^{-2} and the asymmetry of the HI disk at this level. The results show that, for a given optical diameter, the isophotal HI sizes of Virgo spirals become smaller with decreasing distance to the cluster core. In addition, galaxies which are located in the core have more asymmetric HI disks than galaxies at the periphery.

1. INTRODUCTION

The study of clusters of galaxies is important for our understanding of the formation and evolution of galaxies. In recent years, much observation and theoretical work has been concerned with the question how a cluster environment influences the properties (optical size, color, morphology, gas content, etc.) of the constituent galaxies. In particular HI studies of a number of distant clusters with the Arecibo telescope (see e.g. Sullivan et al., 1981, Schommer et al., 1981 and Bothun et al., 1982a, 1982b) and the HI work in the Virgo cluster area at Nancay and Arecibo (e.g. Chamaraux et al., 1980, Giovanardi et al., 1983 and Giovanelli and Haynes, 1983) have provided a partial answer to this question. Results obtained so far suggest that the ratio of the HI content and optical luminosity tends to be smaller in regions with higher galaxy density.

However these observations, with 3-4 arcmin resolution, can only poorly resolve the HI distributions, even of the largest galaxies in the Virgo cluster. Hence, it was unclear what the brightness distributions of galaxies in clusters look like: are the small HI contents the result of a truncation of the HI disk or caused by a general depletion over the whole disk.

Much better information on the HI distributions in cluster galaxies has now been obtained through observation of 36 spiral galaxies in the Virgo cluster with an angular resolution of about 30 arcsec in one direction. In this paper the isophotal diameter at a specific (face-on) surface density, σ_{HI}, and the asymmetry of the HI distributions will be discussed. Part of this work has already been described by Warmels and van Woerden (1983) which paper mainly concerned galaxies outside the central cluster region. The present paper is based on the complete sample including galaxies which have distances between 1 and 3 degrees from M87.

2. OBSERVATIONS AND REDUCTIONS

The morphological types of the galaxies in the sample range from Sab to Sdm; their absolute magnitudes from -19 to -22 and their (heliocentric) radial velocities range from -138 km s^{-1} (NGC 4192) to 2538 km s^{-1} (NGC 4388). The observations, done with the Westerbork Synthesis Radio Telescope (WSRT, Bos et al., 1981), provide a synthesized beam of 12 arcsec in right ascension and about 60 arcsec in declination. Because of the coarse resolution in the declination direction, and because complete (two-dimensional) mapping of the entire sample would be too timeconsuming, the observations and reduction were carried out in two different ways.

1. For most galaxies we obtained one-dimensional (short) observations, which reveal the HI distribution projected upon a resolution axis, to be called the HI strip integral, S_{HI} (p).
2. For some galaxies we obtained two-dimensional observations, which yield the full HI distribution and the velocity field of the galaxy. In order to obtain an HI strip distribution, S_{HI} (p), similar to the S_{HI} (p) of the short observations, we integrated the HI distribution of most of these galaxies in the declination direction (p-axis in the RA direction).

Given the position angle of the resolution axis, the orientation of the galaxy (i.e. inclination and position angle of the major axis) and S_{HI} (p), we compute the HI surface density distribution, σ_{HI} (r), using the iterative method descrited by Lucy (1974) under the assumptions of azimuthal symmetry and planar distribution of the HI distribution. The two halves of each galaxy we treated independently.

3. THE HI SIZES AND ASYMMETRIES OF SPIRAL GALAXIES IN THE VIRGO CLUSTER

In this survey the HI surface density distributions for 36 galaxies were obtained. For 21 galaxies σ_{HI} (r) was derived from one or two one-dimensional observations. An illustration of the results is given in Figures 1 and 2 where an HI strip integral and the derived HI surface density distribution is displayed. For 15 galaxies σ_{HI} (r) was computed from the two-dimensional data. Below I will discuss the HI sizes and the asymmetry of the HI distributions.

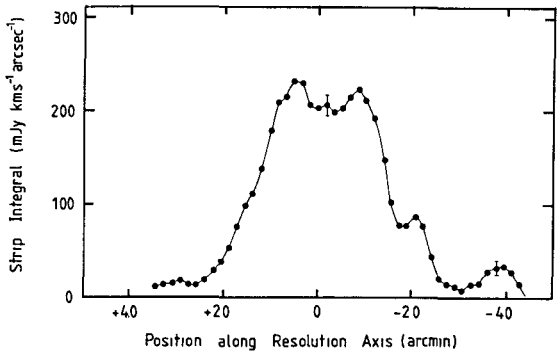


Figure 1. HI strip integral, S_{HI} (p), of the HI distribution in NGC 4519 with the resolution axis along p.a. = 86°.

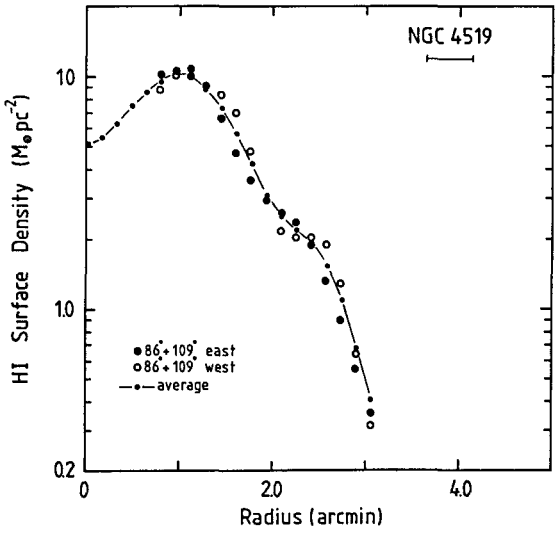


Figure 2. The HI surface density distribution, σ_{HI} (r), in NGC 4519 determined from two short observations. The distribution turns out to be very regular and shows the presence of a hole in the centre.

3.1 The HI sizes

For each of the galaxies in the sample I have determined the HI diameter, D_{HI}, defined as the HI size of the galaxy at the isophotal surface density level of σ_{HI} = 1.0 $M_\odot$ pc^{-2}, and compared this with the optical face-on, extinction-corrected diameter D_0 from the Reference Catalogue of Bright Galaxies (de Vaucouleurs et al., 1976). Figures 3a and 3b show the ratio D_{HI}/D_0 as a function of angular distance R_{M87} to M87, commonly assumed to be located at or

near the centre of the cluster; in Figure 3a the morphological type of the galaxies is indicated; in Figure 3b information about the velocity is given. First however, I will discuss the ratio D_{HI}/D_0 as a function of R_{M87} only, excluding the morphological and velocity information.

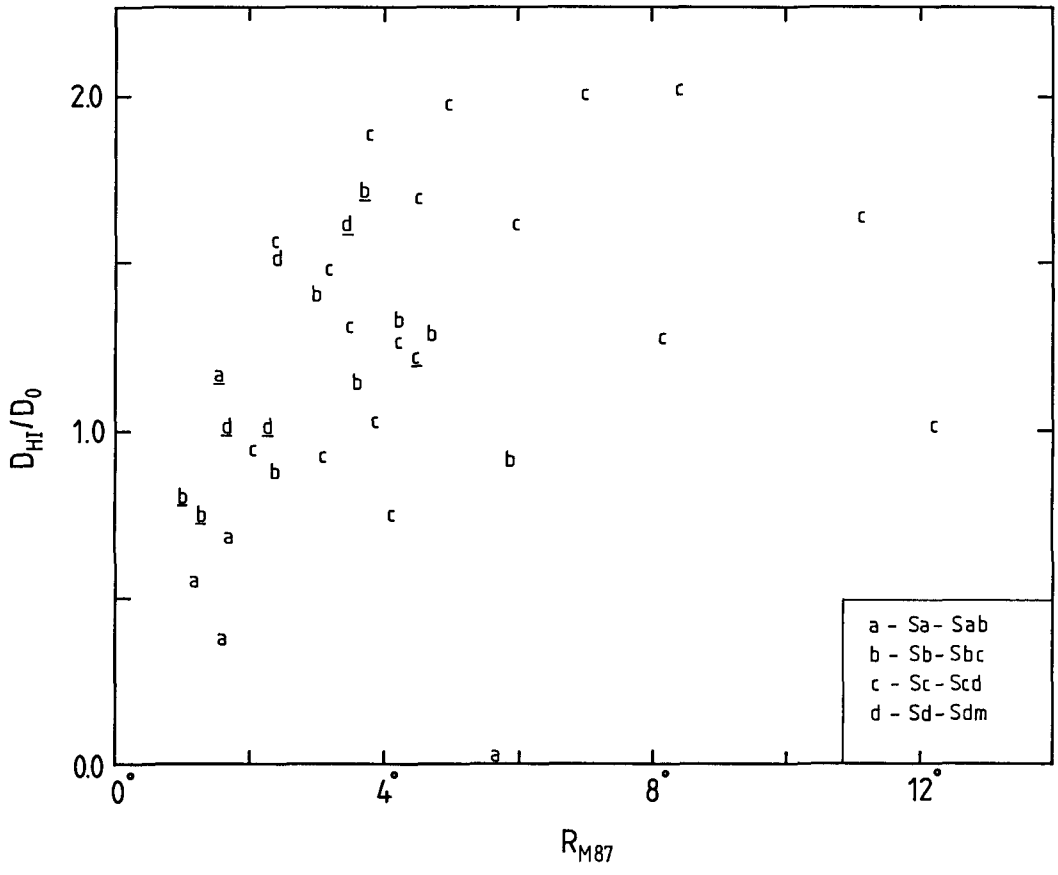


Figure 3a. The ratio of the isophotal HI and optical diameters, D_{HI}/D_0, for 36 galaxies as a function of the angular distance to M87. The morphological type of the galaxies (mostly from Sandage and Tammann, 1982) are indicated different symbols; underlined symbols refer to classification by de Vaucouleurs et al., 1976.

Although the spread of D_{HI}/D_0 is considerable at large R, we see that the average value of D_{HI}/D_0 for galaxies in the core of the cluster is considerably smaller than that for the galaxies at the periphery. In Table 1 this statement is illustrated more quantitatively by showing averages of D_{HI}/D_0 for several distance bins around M87; column (1) lists the distance bin; column (2) the number of galaxies in the bin; column (3) the average angular distance to M87 and its 1σ scatter; column (4) the average ratio D_{HI}/D_0 and its 1σ scatter.

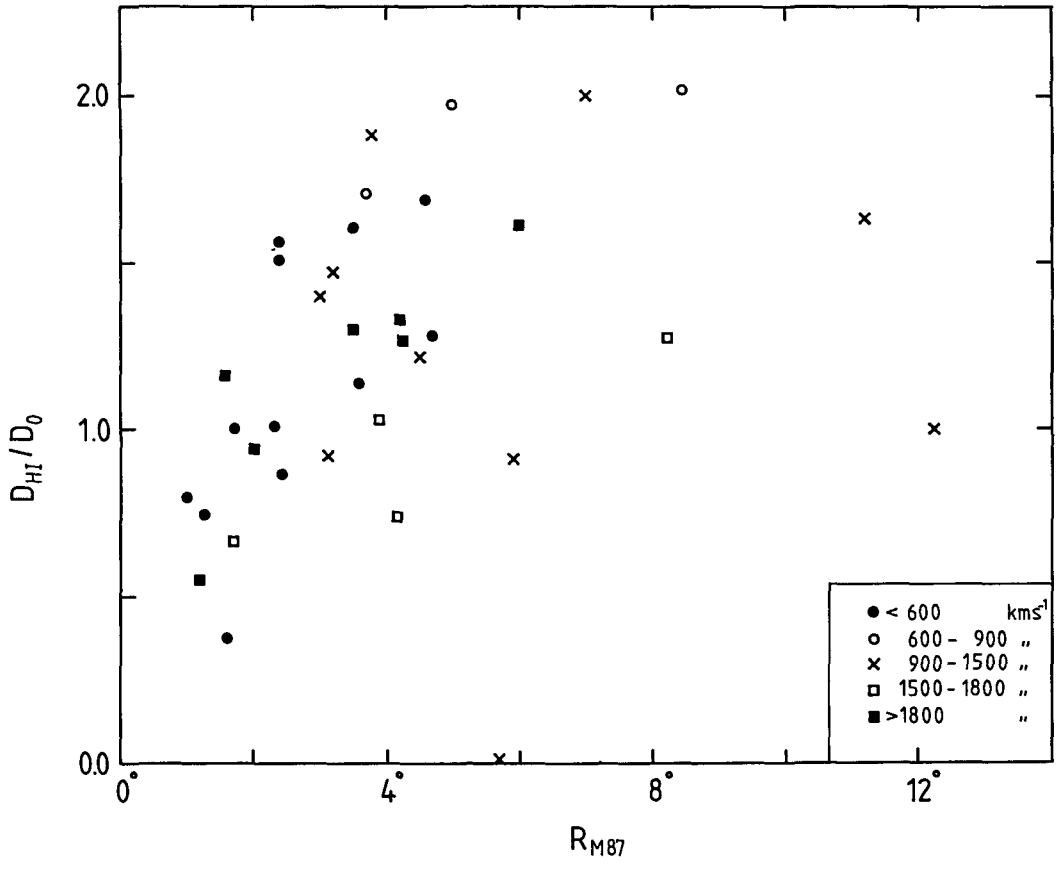


Figure 3b. The ratio of the isophotal HI and optical diameters, D_{HI}/D_0, for 36 galaxies as a function of angular distance to M87. Galaxies in different intervals of heliocentric radial velocity, as derived from the WSRT observations, are indicated by different symbols.

Table 1

RATIO OF THE HI AND OPTICAL DIAMETERS OF VIRGO CLUSTER SPIRALS

Distance range to M87	Number of galaxies	Average distance	Average D_{HI}/D_0 and dispersion
< 2°	7	1.4 ± 0.3	0.75 ± 0.25
2°- 3°	6	2.4 ± 0.3	1.22 ± 0.28
3°- 4°	8	3.5 ± 0.3	1.38 ± 0.32
> 4°	14	6.5 ± 2.6	1.43 ± 0.39
< 3°	13	1.9 ± 0.6	0.97 ± 0.35
> 3°	22	5.4 ± 2.5	1.41 ± 0.37

The average value of D_{HI}/D_0 for the spiral galaxies in the core (less then the 2° from M87) is 0.75 with a 1σ scatter of 0.25. In the outer regions of the cluster (outside the 4° radius around M87) the value increases to 1.43 ± 0.39. So, for galaxies in the core of the Virgo cluster with a given optical diameter the average HI disk size is almost a factor 2 smaller then for such galaxies at the periphery.

Figure 3a clearly shows that the small values of D_{HI}/D_0 in the core of the cluster mainly concern galaxies of early morphological type. This of course, raises the question if these small numbers in the core are the result of an environmental effect or, the reflection of the -early- morphological type. This question has however been answered by high resolution HI observation of galaxies in the field which show no or only a weak correlation of the ratio D_{HI}/D_0 with type (Bosma, 1981). A similar result has been obtained by Giovanelli and Haynes (1983) for the ratio of the effective diameter to the optical diameter. We therefore can conclude that the small values of D_{HI}/D_0 in the cluster core are indeed the result of environmental effects.

The correlation between D_{HI}/D_0, R_{M87} and the radial velocity is given in Figure 3b. As expected on dynamical grounds, the galaxies with extreme velocities with respect to the cluster average are concentrated in the core. From the information in the figure we notice the following main differences between the galaxies in the core ($R_{M87} < 2°$) and outside this region:

- galaxies within a projected distance of 2° from M87 and which have extreme velocities with respect to the cluster average of 1150 km s^{-1} have small D_{HI}/D_0 values.
- galaxies outside this two degrees radius and which have small values for D_{HI}/D_0 do not have extreme velocities. On the other hand, galaxies in this region which have extreme velocities do not have small values for the ratio D_{HI}/D_0.

These facts suggest that galaxies with extreme velocities lose the gas if they pass through the cluster core, with radius 2 or 3 degrees, but not outside this core. On the other hand, galaxies with low velocities relative to the cluster average and small HI diameters may have passed the core region recently.

3.2 The HI asymmetry

Aside from the size at a particular surface brightness level, the WSRT observations can also provide information about large scale disturbances of the HI distributions. Below I present the results concerning the asymmetries of the HI distributions for the galaxies in the sample.

From the HI strip integral, corrected for projection effects, we measured the HI extent on the east and the west side and obtained the asymmetry parameter, A_{HI}, defined as:

$$A_{HI} = \frac{X_{HI}^{E} - X_{HI}^{W}}{X_{HI}^{E} + X_{HI}^{W}}$$

where X_{HI}^{E} and X_{HI}^{W} are the corrected sizes on the east and west side at the level of 25 mJy km s^{-1} $arcsec^{-1}$, respectively. Obviously A_{HI} can vary between -1 (all HI located on the west side) and +1 (all HI located on the east side).

In Figure 4a the absolute values of A_{HI} for all galaxies in the sample are given as a function of the angular distance to M87. Apart from having small isophotal HI diameters (c.f. section 3.1) the galaxies in the centre also exhibit asymmetries in the HI distribution which are larger than for the galaxies at larger distances from M87. We mainly find galaxies with large asymmetries within 2 to 3 degrees from M87, a result also found by Helou et al. (1981).

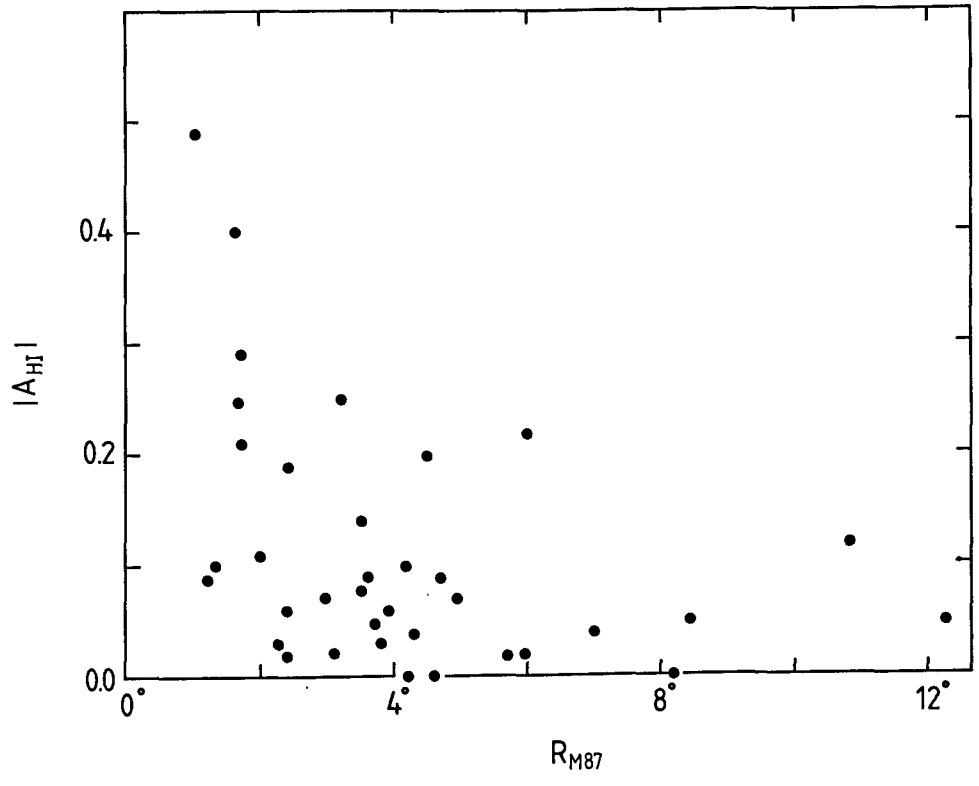


Figure 4a. The absolute asymmetry parameter A_{HI}, as function of angular distance to M87.

In Figure 4b I have investigated whether the sign of the HI asymmetry is correlated with the east-west position of the galaxy with respect to M87. From the figure it seems that at small projected distances from M87 the asymmetry has no preferred direction; however, galaxies in the outer region (R_{M87} > 2 to 3 degrees) seem to prefer an HI distribution which is more extended towards M87. Note, in this connection, that in the western half of the cluster there is not a single galaxy having a greater HI extent on its western side (A_{HI} < 0).

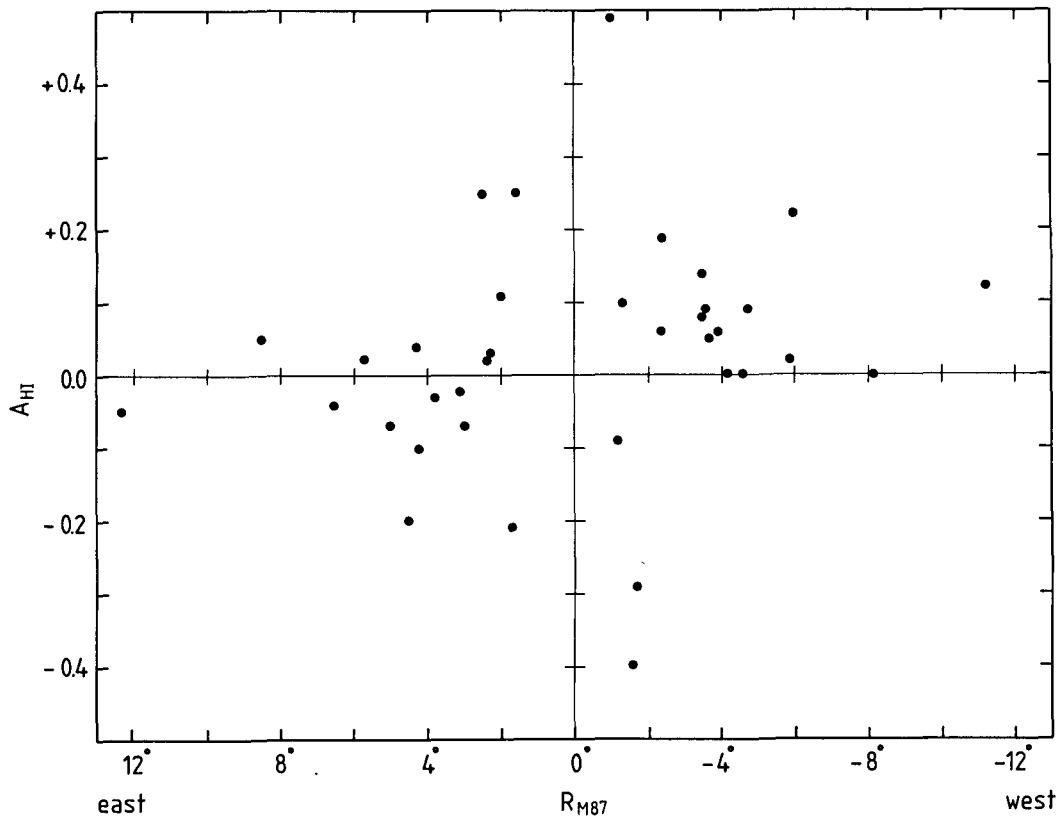


Figure 4b. The asymmetry parameter A_{HI} as a function of angular distance to M87. Negative values of the abscissa indicate positions west of M87; positive values indicate positions east of M87. Galaxies with negative A_{HI} values are more extended to the west; positive A_{HI} values represent larger HI sizes on the eastern side of the galaxies.

4. SUMMARY AND CONCLUSIONS

High resolution HI observations of 36 spiral galaxies in the Virgo cluster have given the following results.

1. The ratio of isophotal HI and optical disk size correlates well with angular distance to the centre of the cluster. A comparison between the galaxies inside the 2° radius around M87 and outside the 4° radius reveals that for a given optical diameter the isophotal HI size of the galaxies in the centre (at the level of 1 $M_\odot$ pc^{-2}) is a factor 1.9 smaller than the HI size of the galaxies in the outer regions.
2. The size ratio D_{HI}/D_0 correlates with the velocity of the galaxies with respect to the cluster average. This is in particular true for galaxies in the cluster core.
3. Galaxies inside the 2° angular distance from M87 show a significantly higher degrees of asymmetry in their HI distribution than galaxies at the periphery of the cluster.

The X-ray measurements of the Einstein Observatory have shown that the hot gas in the Virgo cluster is concentrated around M87, located in the core of the cluster (Forman and Jones, 1982). The strong correlation between the ratio D_{HI}/D_0 and the asymmetry of the hydrogen distribution with the position in the cluster and the velocity, together with the presence of the hot gas in the core, seems to support the idea that ram-pressure stripping (see e.g. Lea and De Young, 1976) is mainly responsible for the HI deficiency. Tidal interactions are not effective at high relative velocities, and galaxy collisions could remove gas both at high and at low relative velocities.

In the cluster core we have observed strong HI asymmetries but without preferential direction. These may be understood if the HI distribution in a galaxy is strongly disturbed when it enters the core and remains disturbed while it passes closest to the centre and travels outwards again. The time-scale for setting up the disturbances must then be of order D sin $1°/\Delta V$ = 3-4 * 10^8 years for D = 15 Mpc, the distance to the Virgo cluster and V = 750 km s^{-1}, the relative galaxy velocity. After a few rotations, i.e. after about 10^9 years, during which the galaxy may travel over 3°, the gas will tend to be redistributed and lose it asymmetry. When the galaxy has left the core region and is "on its way out" the asymmetrical HI distribution will then tend to point towards the core.

After leaving the cluster core, a disturbed galaxy will maintain its asymmetric HI distribution for a limited time.

5. ACKNOWLEDGEMENTS

I would like to thank Drs. H. van Woerden, R. Sancisi, R.D. Ekers and G.S. Shostak for many stimulating and helpful discussions.
I acknowledge financial support from The Netherlands Foundation for Astronomical Research (ASTRON). The Westerbork Radio Observatory is operated by the Netherlands Foundation for Radio Astronomy, with financial support from ZWO.

6. REFERENCES

Bos, A., Raimond, E., van Someren Greve, H.W. 1981, Astron. Astrophys. 98, 251

Bosma, A. 1981, Astron. J. 86, 1825

Bothun, G.D., Schommer, R.A., Sullivan W.T. 1982a, Astron. J. 87, 725

Bothun, G.D., Schommer, R.A., Sullivan W.T. 1982b, Astron. J. 87, 731

Chamaraux P., Balkowski C., Gerard, E. 1980, Astron. Astrophys. 83, 38

Forman, W., Jones, C. 1982, Ann. Rev. Astron. Astrophys. 20, 547

Giovanardi, C., Helou, G., Salpeter, E.E., Krumm, N. 1983, Astrophys. J. 267, 35

Giovanelli R., Haynes, M.P. 1983 Astron. J. 88, 881

Helou, G., Giovanardi, C., Salpeter, E.E., Krumm, N. 1981, Astrophys. J. Suppl. 46, 267

Lea, S.M., De Young, D.S. 1976, Astrophys. J. 210, 647

Lucy, L.B. 1974, Astron. J. 79, 745

Sandage A., Tammann G.A., 1981, Revised Shapley-Ames Calalogue of Bright Galaxies, Carnegie Institute, Washington

Schommer R.A., Sullivan, W.T., Bothun, G.D., Astron. J. 1981, 86, 943

Sullivan, W.T., Bothun, G.D., Bates, B., Schommer, R.A. 1981, Astron. J. 80, 919

de Vaucouleurs, G., de Vaucouleurs, A., Corwin, H.G. 1976, Second Reference Catalogue of Bright Spiral Galaxies, University of Texas Press, Austin

Warmels, R.H., van Woerden, H. 1984, Trieste Symposium, Clusters and Groups of Galaxies, eds. F. Mardirossian et al., Reidel Publishing Company, Dordrecht, p. 251

NEUTRAL HYDROGEN OBSERVATIONS AT THE VLA

J. van Gorkom, C. Kotanyi
NRAO
Socorro, NM 87801

1. Introduction

A survey of the neutral hydrogen line emission from bright spiral galaxies in the Virgo Cluster has been done using the Very Large Array (VLA). The survey was intended as a pilot study to show the capacity of the VLA to observe a large sample of galaxies in the spectral line mode in a fairly short time, and to provide preliminary information on the distribution of neutral gas in Virgo cluster spirals.

The first results on 10 of the brightest spirals close to the cluster centre have been presented previously (paper 1, van Gorkom et al., 1984). They show that the HI disks of spirals within a radius of about 3° from M87 are anomalously small, those outside being normal. The change occurs rather sharply at that radius, suggesting that the dominant mechanism is ram-pressure stripping of the interstellar gas by the diffuse halo of M87. The observations imply that the stripping is instantaneous and nearly complete .

Here we present preliminary data for the full sample, which is nearly complete to a limiting optical magnitude.

2. Sample and Observations

The list of galaxies observed is given in Table 1. The sample includes 17 of the 20 spiral galaxies brighter than magnitude B_T = 12 within a radius of R = 6° to M87 (the cluster core). The full list contains 25 galaxies.

Each galaxy was observed for 1 to 2 hours in the compact configuration of the VLA in the summers of 1982 and 1983. The total bandwidth was 640 km/s and the radial velocity resolution was 20 km/s. The angular resolution was about 40", and the r.m.s. noise per angular and velocity resolution element was about 2.5 mJy. Four galaxies closest to the centre (NGC 4388, 4579, 4569 and 4438) were also observed for 8 hours each in a less compact configuration, at an angular resolution of about 12", and an r.m.s. sensitivity of 1 mJy/beam.

Table 1. Neutral Hydrogen Observations at the VLA

NGC	R (degrees)	D_H/D_O	TYPE	B_T	V_o (km/s)	Δ
4438	1.0	0.2	S0apec	10.85	182	1.28
I3355	1.2	1.4	Im	-	20	-
4388	1.3	0.3	Sb	11.83	2535	1.06
4402	1.4	0.6	Sb	12.50	-77	0.61
4569	1.7	0.3	Sab	10.23	-382	0.99
4579	1.8	0.6	Sb	10.61	1730	1.00
4567	1.8	0.8	Sbc	12.08	2121	-
4568	1.8	1.0	Sbc	11.67	2168	-
4501	2.0	0.9	Sb	10.27	1989	0.47
4548	2.4	1.0	SBb	10.98	403	0.86
4647	3.3	1.2	Sc	11.91	1286	0.51
4654	3.4	1.3	Scd	11.10	970	0.00
4256	3.6	1.5	Sc	10.42	2324	0.02
4216	3.8	0.9	Sb	10.91	-69	0.35
4222	3.8	1.5	Sd	-	139	0.06
4321	4.0	1.0	Sbc	10.10	1543	0.52
4206	4.0	-	Sbc	12.79	619	-0.09
4535	4.3	1.1	Sc	10.66	1853	0.17
4689	4.5	0.8	Sbc	11.59	1616	-
4237	4.5	1.1	Sbc	12.50	781	0.52
4694	4.6	1.8	SOB	12.24	1185	-
4450	4.7	0.8	Sa	10.94	1990	1.31
4178	4.8	1.5	SBdm	11.89	202	-0.13
4192	4.9	1.3	Sab	10.86	-206	0.09
4394	5.9	-	SBb	11.74	717	0.52

3. Results and Discussion

A map summarizing the integrated HI distribution of the first 10 galaxies is shown in Fig. 1. Maps of the velocity fields and rotation curves of the full sample are presently in preparation. Presently we comment on individual galaxies.

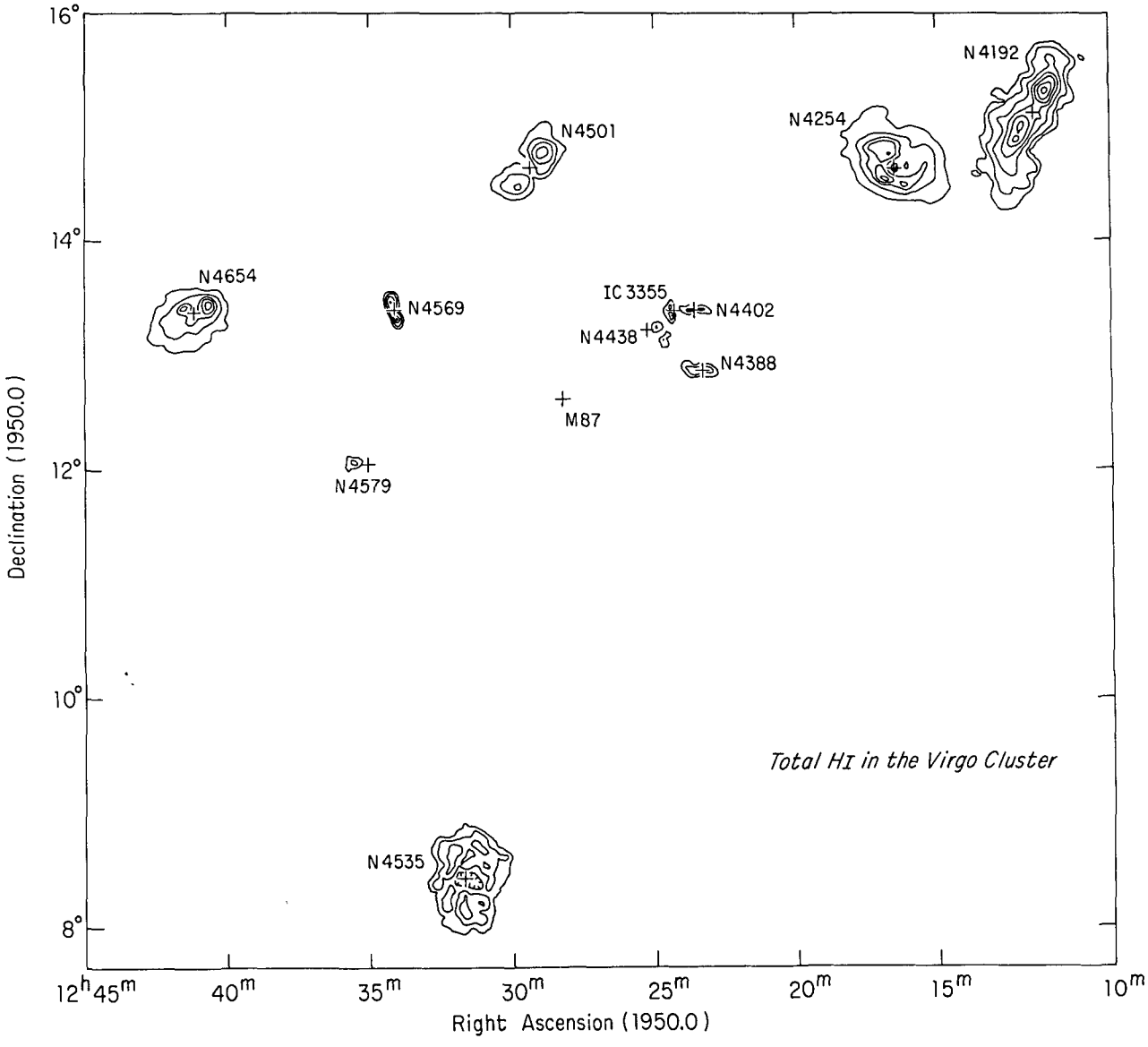


Fig. 1 Integrated neutral hydrogen in 10 of the brightest spiral galaxies (from van Gorkom et al., 1984).

NGC 4438 The gas appears to be in a disordered, rotating disk seen edge-on. The geometry of the stripping assumed by Kotanyi and Ekers (1983) implies that the HI disk has been removed from the galaxy without substantial disruption.

NGC 4388 appears heavily stripped, the total extend of the HI disk being smaller than the optical extent. At higher resolution the disk appears very thin, and the disk may be warped in the outer region. The warp is well within the optical boundaries and as such it is unique. The gas distribution is very asymmetric: the integrated gas peaks on the far side of M87 (West). The velocity gradient is large to the East, whereas the velocity profile is narrow to the West. (see also Huchtmeier et al., 1976). The asymmetry is probably due to stripping rather than tidal interaction, since the galaxy has no close companions and it is strongly redshifted relative to the cluster mean.

NGC 4569 At high resolution the HI appears to be all concentrated in a tilted, thin ring within ½ of the optical extent. The HI boundaries coincide with the outermost dust lanes. Outside these limits no dust is present and the optical disk is very smooth (see photograph in Arp, 1966), suggesting a galaxy aneamic in the outer regions and normal inside. An optical companion is present (IC 3583) but it is red shifted by about 2000 km/s relative to NGC 4569 (Giovanelli, private communication).

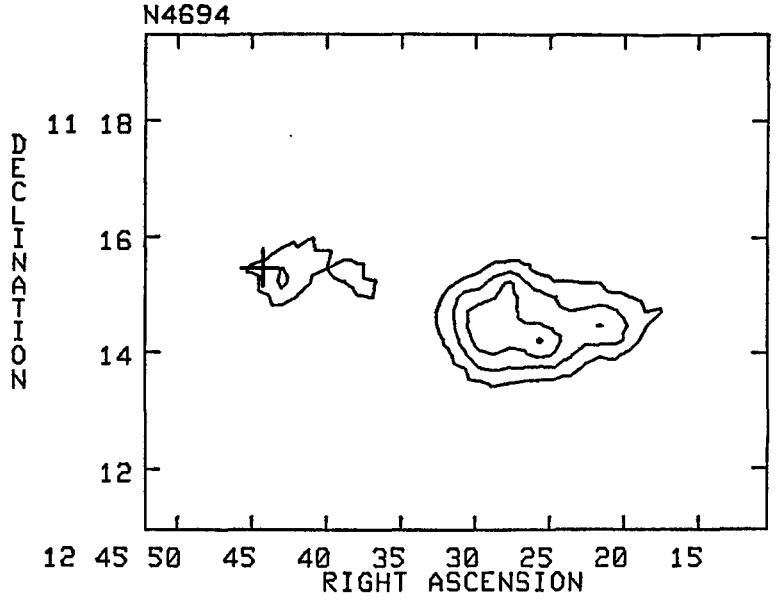


Fig. 2 Integrated neutral hydrogen in NGC4694. The centre of the galaxy is marked by a cross. The contour interval is about 5.10^9 atoms/cm^2.

NGC 4579 is an anaemic galaxy. The neutral hydrogen at high resolution is distributed in a clumpy ring. The gas distribution and velocity field are asymmetric in a way similar to NGC 4388, with the narrow profile peak on the Eastern side (the far side of M87, as in NGC 4388).

NGC 4254 Is optically asymmetric, as is the HI envelope. The absence of nearby companions suggests that the asymmetry is mostly due to stripping.

NGC 4654 The galaxy and its HI envelope are strongly asymmetric. However a nearby companion is present (NGC 4639) with neutral hydrogen connected in redshift with that of NGC4654, suggesting that tidal interaction may be the main cause of the asymmetry.

NGC4694 The HI distribution is shown in Fig. 2. This is a bright SBO galaxy well outside the cluster centre. It shows an anomalously high amount of HI gas for its Hubble type. However, the bulk of the HI is displaced by more than a galaxy diameter from its main body, whereas the main body contains little gas. The HI "tail" points towards the cluster centre. This structure has been found previously at Westerbork (van Woerden and van Driel, private communication). A possible explanation of this most unusual structure is that we see the galaxy long after it has been stripped of gas while crossing the cluster centre. This explanation would require that the galaxy was a spiral with normal HI content

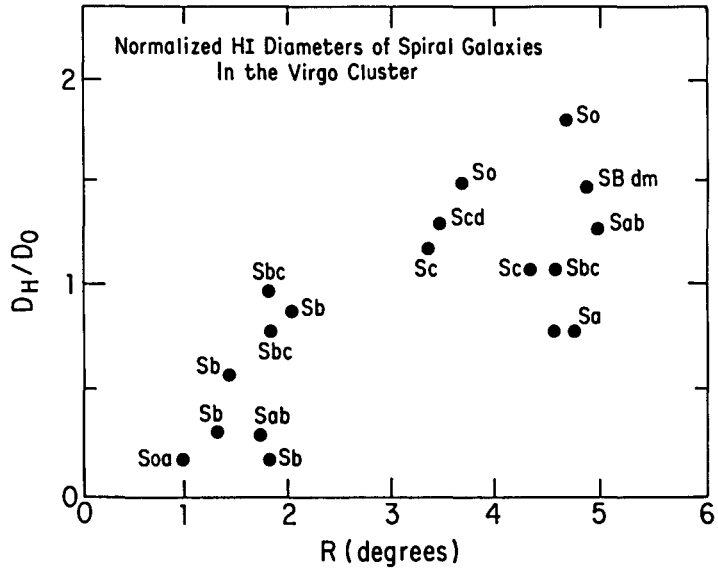


Fig. 3 Normalized HI diameters versus radial distance R from M87.

before the stripping, and that the stripping has modified its Hubble type to SBO. It should be however explained how such a large amount of HI gas can survive outside the galaxy against dynamical disruption and thermal evaporation.

The diameters of the HI disks, measured at the 5 10^{19} atoms/cm^2 contour, are listed in Table 1 normalized to the optical diameters D_{25} from RCBG2 (de Vaucouleurs et al; 1976). The Table also gives the Hubble types, magnitudes B_T and radial velocities from RCBG2, and the deficiency parameters Δ from Giovanelli and Haynes (1983).

The normalized HI diameters are plotted in Fig. 3 as a function of distance R from M87. The HI diameters are seen to be systematically smaller within R $\simeq$ 3° relative to those outside. Some of this effect could be due to a type segregation with radius within the cluster. However the distribution of Hubble types within the diagram suggests that the effect would be also found within a given Hubble type (e.g. Sb) if a larger sample were available.

The National Radio Astronomy Observatory is operated by Associated Universities Inc. under contract with the National Science Foundation.

References

Arp H, 1966 Atlas of Peculiar Galaxies

Chamaraux, P., Balkowski, C., Gerard, E. 1980 A.A. 83 38

Giovanelli R., Haynes M.P. 1983 A. J. 88, 881.

Huchtmeier, W.K., Tammann, G.A., Wendker, H.J. 1976 A.A. 46 381

Kotanyi, C. G., Ekers R. D. 1983 A. A. 122 1976 AA 267

Van Gorkom, J. H., Balkowski, C., Kotanyi, C. G., 1984 in Groups and Cluster of Galaxies, (ed. Mardirossian). P. 261

de Vaucouleurs, G. and A., Corwin H.G. 1976 The Second Reference Catalogue of Bright Galaxies.

A COMPARISON OF THE GAS DEFICIENCY OF GALAXIES IN VIRGO AND OTHER NEARBY CLUSTERS

Riccardo Giovanelli

NAIC, Arecibo Observatory

1. Introduction. Morphological segregation is a well known characteristic of the population of galaxies in clusters: early types tend to dominate the denser regions and spirals the peripheries. Many arguments suggest that to a large degree the segregation dates back to the epoch of galaxy formation or early stages of galaxy evolution. However, a variety of mechanisms could conspire to make cluster cores hostile environments to the member galaxies. To what an extent do such mechanisms contribute a secular component of the morphological segregation phenomenon?

Several studies have approached this question by analyzing the neutral hydrogen content of cluster spirals. A recent review of the subject is given by Haynes et al. (1984). Here we report the summary of a comparative study of the HI content of galaxies in nine nearby clusters, including Virgo. The data base consists of 458 galaxies of type Sa or later (estimated whenever possible from better scale optical data than the Palomar Sky Survey) for which high quality 21 cm line data are available; galaxies with insufficient signal-to-noise or poor upper limits were either re-observed or excluded from the sample. They belong to the clusters A262, Cancer, A1367, Virgo, A1656, Z1400+0949, A2147, A2151 and Pegasus. They were compared with a sample of 324 isolated galaxies observed by Haynes and Giovanelli (1984).

2. HI Deficiency. For each galaxy in the cluster sample, the HI deficiency is estimated in comparison with the sample of isolated galaxies of the same size and type. To a large extent, the expected HI content of a "normal" (i.e. isolated) galaxy is a function of its size; dependence on morphological class within the spiral sequence is a second order effect. It is found that a significant number of HI deficient galaxies is present in the cores of five of the 9 clusters: A262, A1367, Virgo, A1656 and

A2147; the trend is also discernible in A2151, although weak. A galaxy is called deficient when its HI content is in defect of the expected value by a factor of 3 or more; this is a conservative estimate, as the dispersion of HI contents around normalcy for isolated galaxies is, in a log10 scale, on the order of 0.2.

If we measure the global HI deficiency of a cluster as the fraction f of all galaxies observed at 21 cm within one Abell radius, which are HI deficient, then Coma is the most deficient cluster in the sample. Virgo is an intermediate case, similar to A262, A1367 and A2147.

HI deficiency correlates with distance from the cluster center. While in Coma deficient galaxies are observed out to 1.5 times the Abell radius r_A, in other clusters the deficiency pattern is contained within 1 r_A or less. In Virgo, the deficiency pattern is contained with a 5° radius from M87. Inside that distance, however, high deficiency correlates with high galaxian density, observed in clumps.

In deficient cluster cores, the fraction of deficient galaxies is high: most -if not all- spirals passing through the core are affected. In Virgo, if spirals are presently infalling as proposed in some papers in these proceedings, then some have already gone through the core once.

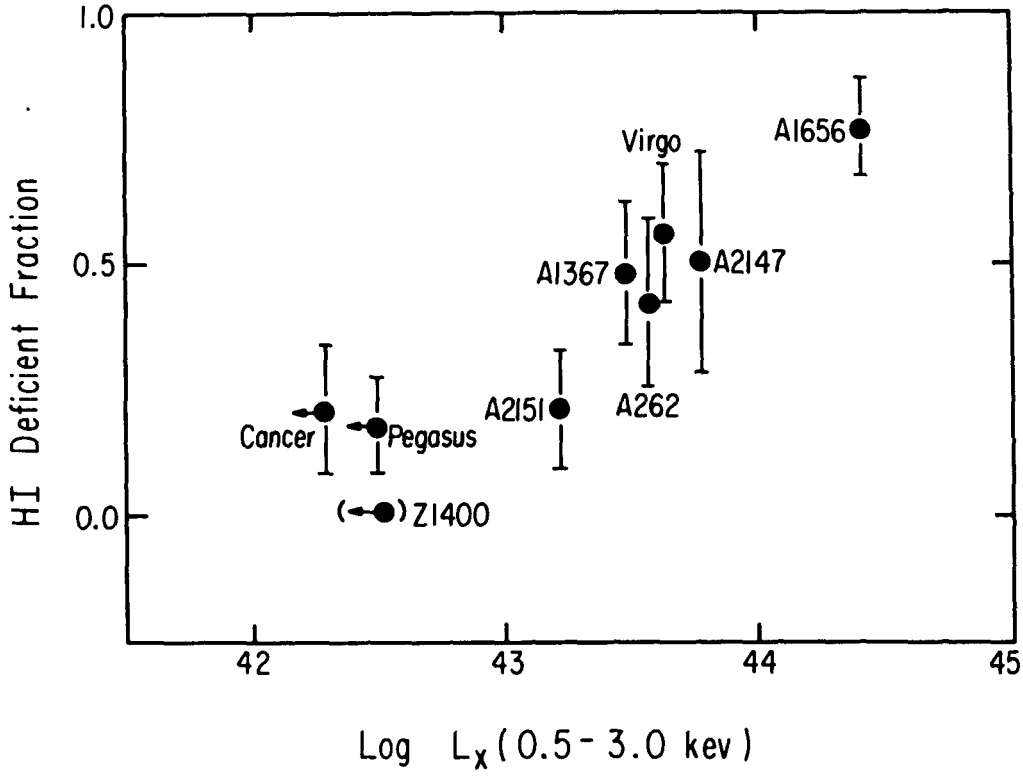
3. HI Deficiency, its cause and Cluster X-ray Luminosity.

Indications exist that the HI gas missing from the cluster spirals has not been removed by vigorous star formation, perhaps stimulated by interactions in the cluster environment: deficient spirals exhibit colors that suggest quenching, rather than stimulation of star formation (see papers by Haynes, by Kennicutt and by Stauffer in these proceedings and Giovanelli and Haynes 1983).

It has been proposed (Larson et al. 1980) that disks grow secularly at the expense of large gas reservoirs that would exist beyond the visible boundaries of disks. Such reservoirs

would be very vulnerable to tidal disruption in high population density environments, which would thus induce arrest of disk growth. Within such a framework, HI deficiency would be a result of arrested disk growth, rather than say, stripping processes. This idea is contradicted by the observation (reported by several papers in these proceedings and others reviewed by Haynes et al. 1984) that HI disks of deficient galaxies are shrunk with respect to the stellar counterpart; if lack of gas were due to arrested disk growth, how did stars and spiral arms form outside the gas disk? Gas must have been removed at recent times.

The removal of the gas from the outer regions of the disks, leaving the stellar component intact, also argues that gas-dynamical processes are responsible, rather than tidally-induced ones which arise from galaxy-galaxy interactions. The most important agent of such processes is the hot intracluster medium which resides in many cluster cores, most easily recognized by its associated, extended X-ray emission. Figure 1 confirms that indication, illustrating a



positive correlation between the cluster deficient fraction f, defined in section 2, and its X-ray luminosity, measured in the 0.5 to 3.0 KeV HEAO-2 IPC Window. Again, as Coma presents the most extreme properties, Virgo is an intermediate case among the clusters studied.

4. The Effect of Interstellar Gas Stripping on Morphological Segregation. The evidence assembled provides strong support for the idea that spiral disks which pass through the cores of clusters containing a healthy intracluster medium suffer severe depletion of their diffuse interstellar gas component. Quenching of the star formation rate thus may result in morphological degeneration of spiral disks, and the morphological segregation of "genetic" origin will be further enhanced by environment-driven mechanisms, which become progressively more severe as the dynamical evolution of clusters proceed. In Virgo, as in A262, A1367 and A2147, such onset appears to be relatively recent.

Further details on the data sample and some of the subjects discussed in this report can be found in a paper by Giovanelli and Haynes (1984).

The National Astronomy and Ionosphere Center is operated by Cornell University under contract with the National Science Foundation.

5. References

Giovanelli, R. and Haynes, M.P. 1984, Ap.J. in press

Giovanelli, R. and Haynes, M.P. 1983, A.J. 88, 881

Haynes, M.P. and Giovanelli, R. 1984, A.J. 89, 758

Haynes, M.P., Giovanelli, R. and Chincarini, G.L. 1984, An.Rev.Ast.Ap. 22, 445

Larson, R.B., Tinsley, B.M. and Caldwell, C.N. 1980, Ap.J. 237, 692.

ROTATION CURVES OF HYDROGEN DEFICIENT GALAXIES IN VIRGO

G. Chincarini[1,2] and R.E. de Souza[2,3]

1) University of Oklahoma, Dept. of Physics & Astronomy, Norman, OK 73019, U.S.A.

2) European Southern Observatory, Karl-Schwarzschild-Str. 2, D-8046 Garching bei München, F.R.G.

3) University of Sao Paulo, Av. Miguel Stefano 4200, 01000 Sao Paulo, Brazil

I. INTRODUCTION

Galaxies inside clusters are more likely to suffer perturbations due to environmental effects. They have a higher probability of participating in direct collisions and of being disturbed by tidal interactions (Richstone, 1975; Strom and Strom, 1978; Dekel et al., 1980). Moreover, the interaction with the hot intracluster gas can partially remove their gaseous content as evidenced by the HI observations (Haynes et al., 1984, and references therein).

An important question to discuss, however, is whether these environmental effects are sufficiently strong to disturb the mass distribution of cluster galaxies. In that case we can, at least in principle, detect these disturbances by comparing the rotation curves of galaxies in clusters with isolated galaxies. An early answer to this matter was given by Rubin (1982) based on a sample of eight member galaxies of the Cancer and Pegasus I clusters. Our data in Virgo agree with her statement, indicating that the rotation curves of cluster galaxies (Virgo and A1060) are similar to those of non-cluster galaxies.

II. OBSERVATIONS

The first sample of galaxies we observed consists of eight galaxies in the Virgo cluster known to be hydrogen deficient (van Gorkom et al., 1983) and two galaxies in the cluster A1060. A list of the observed objects is given in Table 1. The distance from the cluster center is indicated in column 9 and the HI deficiency parameter in column 10. The deficiency parameter is positive for galaxies which have a hydrogen content smaller than the mean content of galaxies in a standard sample and negative if their content of HI is larger.

The optical observations were carried out at La Silla observatory using

the 1.52m and the 3.6m telescopes and the data were reduced at ESO, Garching. We used baked IIIa-J emulsion with a 3-stage EMI image tube and a transfer lens open at f/2. The inverse dispersion at Hα is about 59.5 Å/mm (1.52m) and 38.5 Å/mm (3.6m).

The plates have been digitized with the PDS at ESO using a scanned aperture of 10 × 10 microns. The rotation curve measurements have been done by using an automatic algorithm to detect the peak intensity along a line in the digitized frame and by setting a cross hair on the features seen on the TV screen. All measurements have been done relative to the sky emission lines which were fitted by a II order polynom (a III order does not improve the fit in agreement with the expected distortions of the image tube).

For two galaxies (N4438 and N4569) we have Hα frames using the 2.2m telescope and an RCA thinned back illuminated CCD. The Hα filter we used has an effective wavelength of 6570 Å and an effective pass band of 22 Å. For the adjacent continuum we used a filter centered at 6455.5 Å and a pass band of 60 Å.

TABLE 1: Sample of Observed Galaxies

SPEC #	OBJECT	TYPE(1)	MAG(1)	INCL deg	VEL(1) km/s	TEL	P.A. deg	D.CL. deg	H.DEF.(2)
1	N3312	Sab(r)	11.64	65	2775	3.6m	175	0.1(3)	(4)
2	N3312	"	"	"	"	"	"	"	
3	N3312	"	"	"	"	1.5m	"	"	
4	N3314a	Sc	-	0	2778(5)	3.6m	143	0.2(3)	
	N3314b	S...	-	77	4640(5)	"	"	"	
5	N3314a	Sc	-	0	2778(5)	1.5m	136	"	
	N3314b	S...	-	77	4640	"	"	"	
6	N4254	S(c)I.3	10.11	27	2413	1.5m	90	3.1	0.02
7	N4388	Sab	10.65	74	2614	1.5m	92	0.6	1.06
8	"	"	"	"	"	"	"	"	"
9	N4402	S...	12.91	71	161(6)	3.6m	90	0.9	0.61
10	N4438	Sb-tides	9.97	65	1	1.5m	27	0.6	1.28
11	N4535	SBc(s)	10.12	42	1953	1.5m	18	4.5	0.17
12	N4569	Sab(s)	9.39	61	-261	3.6m	"	2.4	0.99
13	"	"	"	"	"	1.5m	23	"	"
14	N4579	Sab(s)	10.01	36	1805	1.5m	95	2.5	1.00
15	"	"	"	"	"	3.6m	59	"	"
16	"	"	"	"	"	"	"	"	"
17	"	"	"	"	"	"	"	"	"
18	"	"	"	"	"	"	"	"	"
19	N4654	SBc(rs)	10.68	51	1036	1.5m	128	4.1	0.00

(1) Sandage and Tammann, 1981 (RSA)
(2) van Gorkom et al., 1983
(3) Distance relative to N3311
(4) MHI/LB < 0.02, Richter and Huchtmeier, 1983
(5) Velocities from present work
(6) Palumbo et al., 1983

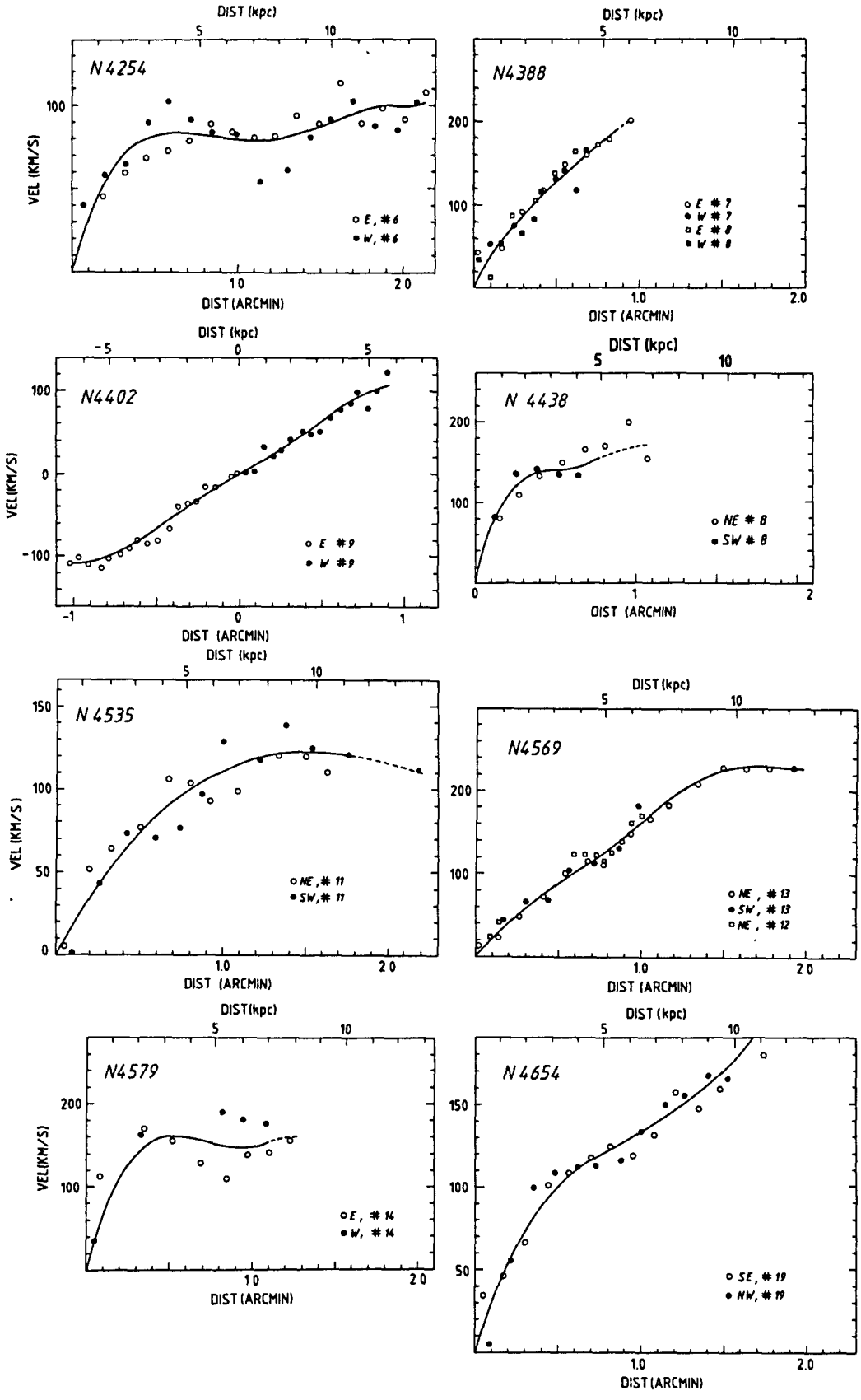


Fig. 1: Rotation curves of Virgo galaxies

III. MASS DISTRIBUTION

The observed velocities have been folded about the center of the galaxy (except for N4402 where the center is not well determined) and the physical parameters determined after fitting the folded rotation curve with a polynom constrained to the point V=0 and R=0. The polynomial fit has been drawn by a continuous line in Figure 1. In those cases where the polynomial is uncertain a dashed line represents a fit done by eye. For Virgo we assumed a distance of 21.9 Mpc as given by Sandage and Tammann (1981).

One important point to note from Figure 1 is that the rotation curves are either flat or still rising at distances of 10-12 kpc from the center of galaxies and are very similar to the one obtained for isolated galaxies.

To derive the mass distribution we have used the same procedure, and relative assumptions, adopted by Burnstein et al. (1982). The integrated mass distribution M(R) at a distance R from the center of the galaxy is estimated as,

$$M(R) = \frac{R \cdot V^2}{G}$$

where V(R) is the velocity in the plane of the galaxy. The density profile d(R), under the assumption of spherical symmetry, is estimated as,

$$d(R) = \frac{1}{4\pi} \frac{dM}{dR}$$

The density distribution is given in Figure 2 and the asymptotic slope of these profiles is about parallel to the line $R^{-1.7}$ as evidenced by Burnstein et al. (1982).

To obtain the luminosity profiles we used the compilation by Longo and de Vaucouleurs (1983) based on published U,B,V, values obtained using circular diaphragms. Due to the inclination of the galaxy, these measurements tend to overestimate the luminosity within a given radius. By comparing with the subsample measured by Grosbøl (1984) we estimate that the error should be at most of a few hundredths of a magnitude. The absolute face-on magnitude was derived using the galactic and internal absorption as given by Sandage and Tammann (1981). For the absolute blue magnitude of the sun we adopted the value 5.48.

The integrated mass profile in our sample increases faster than the derived luminosity profile. From the whole sample we obtain d log M(R)/d log R = 2, while d log L(R)/d log R = 1, that is the ratio between the integrated mass and the integrated luminosity increases roughly with the square root of the mass.

This can be seen from Figure 3 where the mass to luminosity ratio has been plotted against the integrated mass distribution. The curves have been matched by shifting each galaxy in log M by an arbitrary amount. Despite the large scatter in the outer regions we can see that the mass to luminosity ratio is an increasing function of the mass. This is equivalent to saying that the ratio between the luminous and unseen matter is greater near the central region of galaxies.

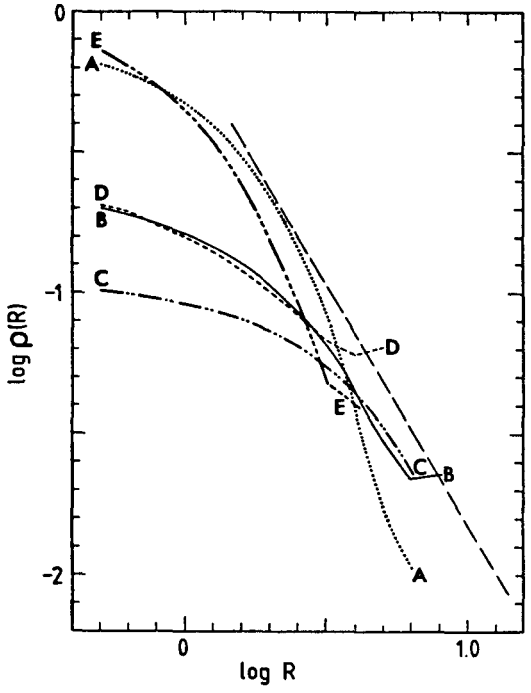


Fig. 2: Density profiles

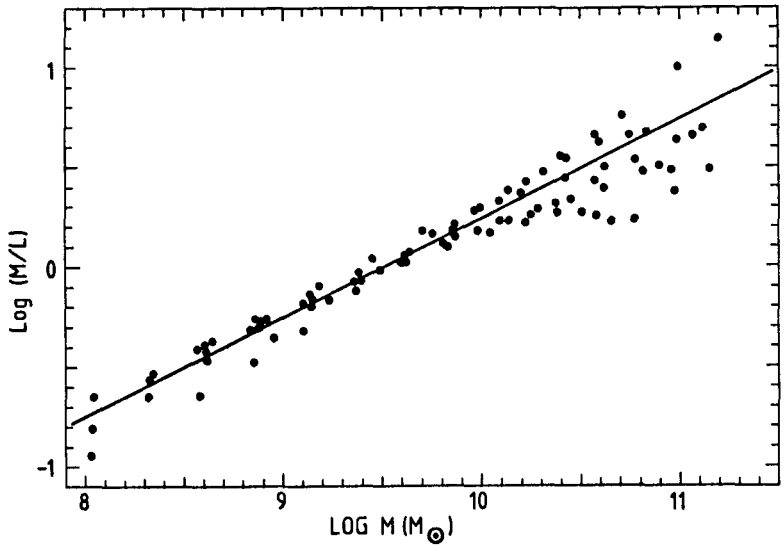


Fig. 3: Mass to luminosity profiles

Up to this point we have implicitly admitted that the mass is dominated by a massive spherical halo. Now we can verify the consequences of this hypothesis if we further assume that the halo has an isothermal distribution. In that case, the rotational velocity is determined by the isothermal halo in a first order approximation and the maximum in the rotation curve defines a characteristic radius that can be used to scale all the rotation curves (Chincarini, de Souza, 1984). The resulting composite rotation curve and mass distribution is shown in Figure 4, together with the asymptotic behaviour of the pure isothermal model.

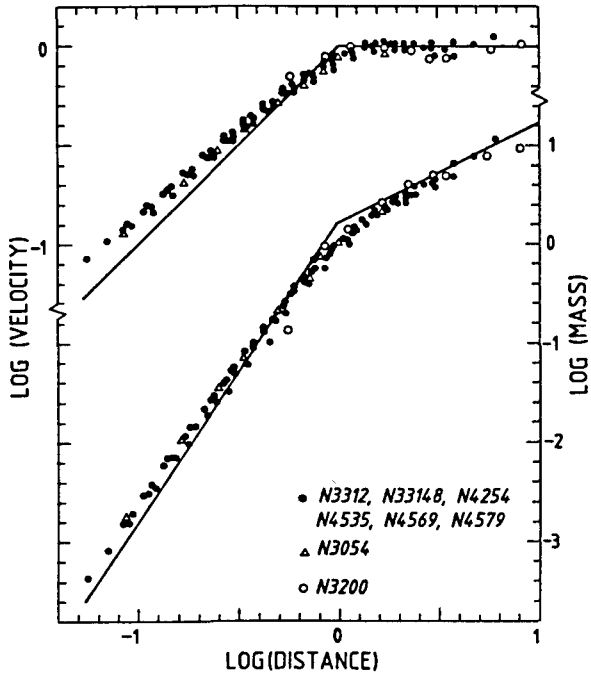


Fig. 4: Composite rotation curve and mass distribution

It is clear from Figure 4 that, compared to the isothermal distribution, we have an excess of mass at small distances from the center and we attribute this mass excess to the visible mass. In that case, and assuming a mass to luminosity ratio nearly constant so that the luminous mass becomes proportional to the radius, we can write,

$$M(x) = M_o x^3 + (1 - M_o)x$$

since the isothermal non-luminous mass distribution goes with the cube of the distance. Here M_o is the non-luminous fraction of mass for $x < 1$ with $x = R/R_{max}$. Writing the equation in terms of log M and log x and using a Taylor expansion near the point x=1 we can write in first approximation,

$$\log M = (2M_o + 1) \log x.$$

Using d log m/d log x = 2.7 as derived from the data in Figure 4, we obtain M_o = .85 corresponding to a contribution of the visible mass to the total mass of about 15%. We further observe that the total mass to luminosity ratio in our sample is of the order of 6-10, implying a mass to light ratio for the visible component of .8-1.5. A more general discussion of these points is the subject of a future paper, de Souza and Chincarini (1985).

IV. NGC 4438

This peculiar galaxy near the core of Virgo was observed by Kotanyi (1981) and Kotanyi et al. (1983) who suggested a strong interaction with the intracluster gas to explain their X-ray and radio observations. The galaxy is clearly perturbed and may interact tidally with the nearby object NGC 4435 at a distance of 4.6 arcmin. However, the velocity difference (>868 km/sec) is too high and the absence of counter tides in N4435 makes it difficult to explain all the observed features as a result of tidal interaction.

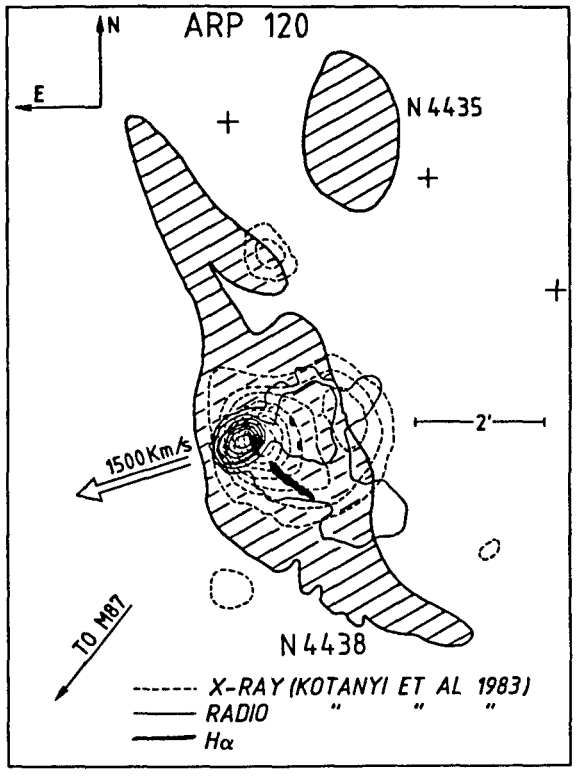


Fig. 5: Shock wave model of N4438

An interesting morphology has been detected in the Hα observations. A fairly strong emission is located south-east of the nucleus, with a faint extension in the south-west quadrant and connected to the nuclear region by an elongated emission about 6 arcsec long. In addition, three faint knots are visible west and north-west of the nucleus (Fig. 5).

The morphology of the HII emission is reminiscent of a bow shock wave. If we assume that the "bow" we observe is in fact the projection of the shock wave it is possible to derive the physical parameters of the shock. N4438 has a line of sight component of 1026 km/sec and owing to the projection effect the speed of the galaxy would be about 1270 km/sec or 1.7 cs. The sound speed was estimated using a temperature of 2.6 kev for the cluster diffuse X-ray component (Lea et al., 1982).

V. CONCLUSIONS

The sample of galaxies belonging to clusters with a known rotation curve is still too small to justify the application of a more refined statistical analysis. Judging only from the material we have, and within the range of sensitivity of our observations, we may tentatively conclude that the rotation curve of cluster galaxies is very similar to the one observed in isolated galaxies. Any influence due to environmental effects is not able to disturb the overall dynamic structure of galaxies within 7-12 kpc from the center. We detect no differences between the rotation curves of hydrogen deficient and non-hydrogen deficient galaxies. Moreover, even galaxies whose optical images are clearly disturbed (N4438, N4654) show no sign of a declining rotation curve.

The total mass to luminosity obtained from our sample is $(M/L)B = (6\text{-}10)$ in solar units. However, in the central regions we have estimated local mass to luminosity ratios which are much lower than this value. One possible explanation is that in these regions there is a higher contribution from a few bright stars or any other form of blue emission. On the other hand, the assumption that the mass is rotationally supported could explain the underestimation of the mass in the central regions where non-circular motions could be more important.

These facts point to a picture where the environment is able to disturb the gaseous component, and perhaps introduces some minor changes in the luminous matter, but leaves the overall mass distribution unchanged. However, it would be highly desirable to extend these observations to a large sample, using more sensitive detectors in order to put more confident limits on the magnitude of the environmental effects.

Acknowledgements

This work was possible thanks to J. Manousoyannaki who kindly provided us with a generous part of the observing time. One of us (R.E.S.) acknowledges partial support by FAPESP (Brazil).

References

Burnstein, D., Rubin, V.C., Thonnard, N., and Ford, W.K., Jr., 1982, Ap.J. 253, 70.

Chincarini, G., and de Souza, R.E., 1984, submitted to Astron. Astroph.

Dekel, A., Lecar, M., and Shaham, J., 1980, Ap.J. 241, 946.

Giovanelli, R., and Haynes, M.P., 1983, Astron. J. 88, 881.

van Gorkom, J.H., Balkowski, C., and Kotanyi, C., 1983, in Clusters and groups of galaxies, p. 251, eds. F. Mardirossian, G. Giuricin, and M. Mezzetti, D. Reidel Publ. Co.

Grosbøl, P., 1984, personal communication.

Haynes, M.P., Giovanelli, R., and Chincarini, G., 1984, Annual Review of Astronomy and Astrophysics (in press).

Kotanyi, C.G., 1981, Ph.D. dissertation, Rijksuniversiteit Groningen.

Kotanyi, C.G., van Gorkom, J.H., and Ekers, R.D., 1983, Ap.J. 273, L7.

Lea, S.M., Mushotzky, R., and Holt, S.S., 1982, Ap.J. 262, 24.

Longo, G., and de Vaucouleurs, A., 1983, The University of Texas Monographs in Astronomy, No. 3.

Palumbo, G., Tanzella-Nitti, G., and Vettolani, G., 1983, Catalogue of Radial Velocities of Galaxies, Gordon and Breach, New York.

Richstone, D.O., 1975, Ap.J. 200, 535.

Rubin, V.C., 1982, International IAU Symposium No. 100, ed. E. Athanassoula, D. Reidel Publ. Co.

Sandage, A., and Tammann, G.A., 1981, A Revised Shapley-Ames Catalog of Bright Galaxies, Carnegie Institution of Washington Publication, No. 635.

de Souza, R.E., and Chincarini, G., 1985, in preparation.

Strom, S.E., and Strom, K.M., 1978, Ap.J. 225, L93.

HI DEFICIENCY AND PHOTOMETRIC EVOLUTION OF SPIRAL GALAXIES IN THE VIRGO CLUSTER

B.Guiderdoni and B.Rocca-Volmerange
Institut d'Astrophysique, 98 bis, bld Arago
F-75014 PARIS

Abstract

From a compilation of HI data of 107 spirals in the Virgo Cluster, with their available UBV, far-UV and Hα photometry, we examine the spatial distribution of HI deficient galaxies and the correlation of the deficiency with morphological type and colors. The history of star formation is studied by means of a model of photometric evolution, together with a consistent dynamical scenario.

I. A sample of spiral galaxies in the Virgo Cluster

The analysis of both HI content and colors properties of cluster spirals can provide useful constraints on the possible environmental influences acting on these galaxies. Since the Virgo Cluster (hereafter VC) is the best site for such studies due to its proximity and spiral richness, we have compiled HI fluxes of 107 spirals mostly located in the VC components Virgo I and Virgo X (de Vaucouleurs, 1961) from nine different sources, as well as the available UBV photometry from de Vaucouleurs et al., 1976, and de Vaucouleurs and Pence, 1979, far-UV (λ 2421 Å) magnitudes from the rocket experiment by Smith and Cornett, 1982, and Hα line equivalent widths from Kennicutt and Kent, 1983. The expected contamination of the sample by non-member objects is weak. Its completeness is very good at the bright end of the luminosity function and exceeds 50 % at B_T =14.00.This sample, possible sources of uncertainties and biases, and a study of the large scale pattern of the HI deficiency are presented in Guiderdoni and Rocca-Volmerange, 1984 (hereafter paper I, submitted). The main conclusions are summarized in paragraph II. Paragraph III reports some preliminary results about the history of star formation in these spirals from a model of photometric evolution (Guiderdoni and Rocca-Volmerange, hereafter paper II, in preparation).

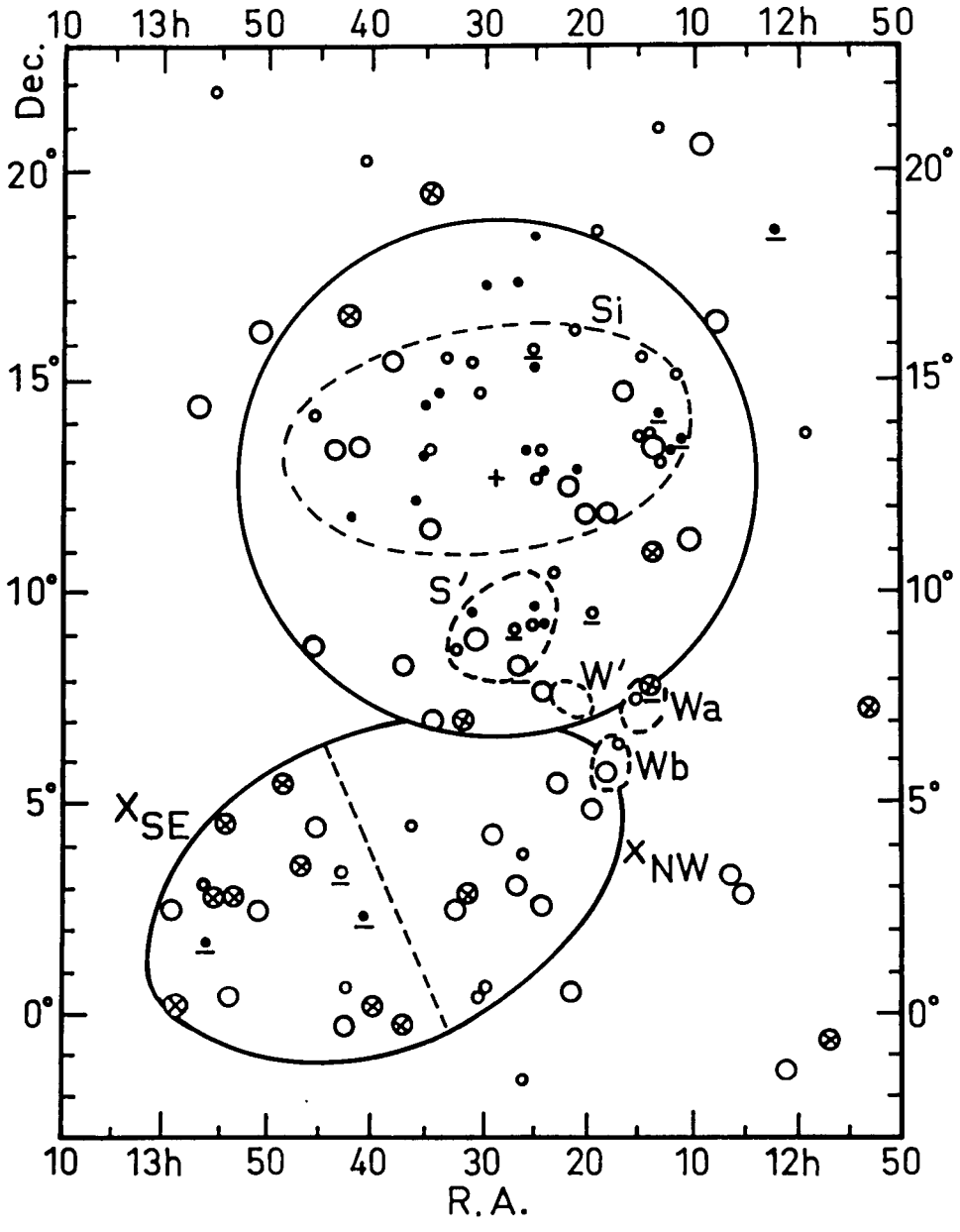


Fig. 1 : Spatial distribution of the Virgo Cluster sample in paper I. The groups from de Vaucouleurs, 1961, are delineated. Dots : $1.5 < Def(\sigma_H)$. Small open circles : $0.5 < Def(\sigma_H) < 1.5$. Large open circles: $-0.5 < Def(\sigma_H) < 0.5$. Large open circles filled with a cross $Def(\sigma_H) < -0.5$. Underlined symbols : lower value of $Def(\sigma_H)$. See text for comments.

II. The large scale pattern of HI deficiency

The distance-independent mixed surface density $\sigma_H = M_H/\frac{\pi}{4}(D_{25}^{\circ})^2$, where M_H is the total HI mass and D_{25}° is the major isophotal diameter at $\mu_B = 25.0$ magarcsec^{-2}, depends only on the coded morphological type T within an intrinsic dispersion σ_T (Chamaraux et al., 1980, Giovanelli and Haynes, 1983). From a reference "field" sample of 405 spirals (HI fluxes from Bottinelli et al., 1980, 1982, and UBV photometry from de Vaucouleurs et al., 1976), we have determined $\langle \log \sigma_H \rangle_T$ and σ_T. With $\Delta \log \sigma_H \equiv \log \sigma_H - \langle \log \sigma_H \rangle_T$, we define a deficiency parameter $Def(\sigma_H) = (-\Delta \log \sigma_H)/\sigma_T$. For a "normal" sample, its mean is zero and its standard deviation is unity. We now present the main results of paper I.

i) For 50 spirals in Virgo I, $\langle \Delta \log \sigma_H \rangle = -0.37 \pm 0.06$ and $\langle Def(\sigma_H) \rangle = 0.94 \pm 0.13$, while for 26 spirals in Virgo X, $\langle \Delta \log \sigma_H \rangle = 0.00 \pm 0.05$ and $\langle Def(\sigma_H) \rangle = -0.06 \pm 0.18$. Among the 20 most deficient galaxies ($Def(\sigma_H) > 1.3$), 18 are located in Virgo I. Both distributions of $Def(\sigma_H)$ are consistent with gaussian laws. In fig.1, one can readily see that most HI deficient spirals are located in subgroups S' and Si from de Vaucouleurs, 1961.

ii) Early-type spirals (or red spirals) are more likely to be very deficient than late-type ones (or blue ones). For S0/a-Sb, $\langle \Delta \log \sigma_H \rangle = -0.72 \pm 0.09$ in Virgo I (18 objects) and $\langle \Delta \log \sigma_H \rangle = -0.35 \pm 0.18$ in Virgo X (4 objects). For Sbc-Im, $\langle \Delta \log \sigma_H \rangle = -0.17 \pm 0.04$ in Virgo I (32 objects) and $\langle \Delta \log \sigma_H \rangle = 0.07 \pm 0.05$ in Virgo X (22 objects). Among the 20 most deficient galaxies, 13 are from S0/a to Sb. Part of this effect is due to the higher number of early-type spirals in Virgo I.

iii) The analysis of the color residues $\Delta(B-V)_T^{\circ}$ and $\Delta(U-B)_T^{\circ}$ shows that deficient spirals are redder than normal counterparts of the same morphological type. The correlation between colors and HI content is roughly that is expected from an extrapolation of the linear regression of the reference sample.

III. History of star formation

The $\log \sigma_H$-equivalent width EW(Hα + [N II]) relation of VC HI deficient and non-deficient spirals is shown in fig.2. It is the same as that of the "field" sample listed by Kennicutt and Kent,

1983(see paper II). Thus Hα photometry only teaches us that a decrease of HI content results in a virtually proportional decrease of star formation, despite the uncertain importance of the molecular component. In short, it seems reasonable to assume that star formation is proportional to the total gas content and that the latter is well probed by HI observations.

This parametrization of the star formation rate has been introduced into a model of photometric evolution of a galactic disk (Rocca-Volmerange et al., 1981, and paper II). We add a bulge

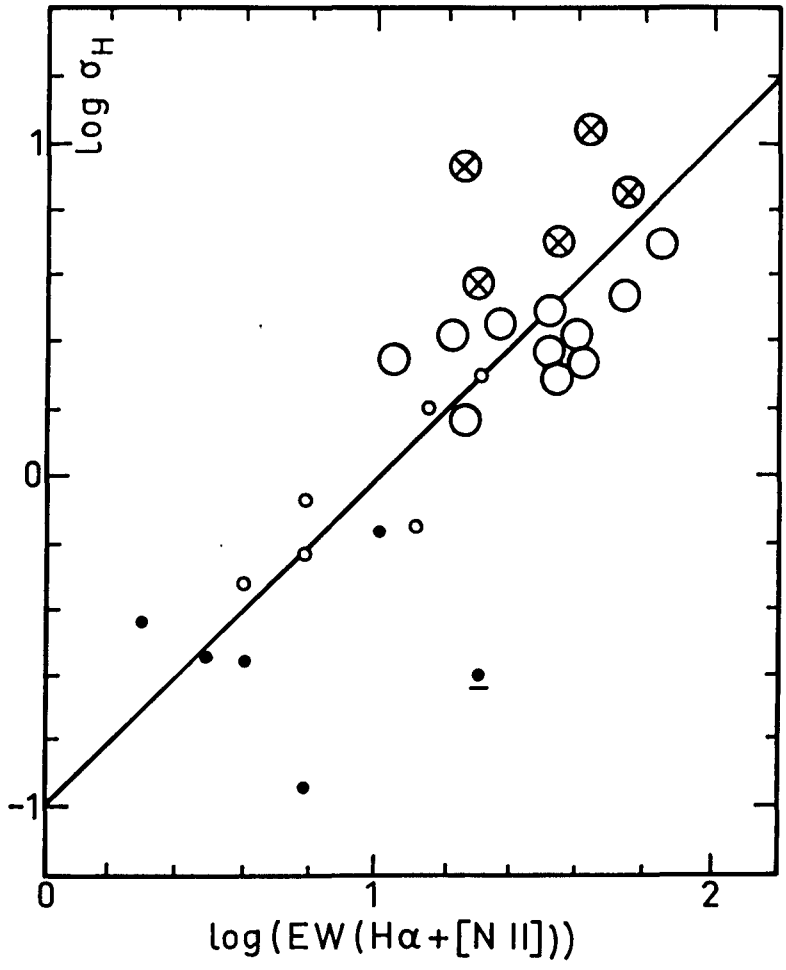


Fig. 2 : log σ_H versus EW(Hα + [N II]) for the Virgo Cluster sample. Symbols as in fig.1. The straight line has a slope equal to unity.

component with elliptical-like colors to an exponential disk according to the dependence of the bulge/disk ratio on T from Yoshizawa and Wakamatsu, 1975. Reasonable assumptions about the mass/luminosity ratio are made. The issues of the model are log σ_{gas}, and extinction-free colors B-V, U-B, m_{2421}-B. They can be compared to the observational log σ_H-face-on color diagrams of the VC sample after estimates of the amount of face-on internal reddening ($E_i(B-V) \simeq 0.06$, $E_i(m_{2421}-B) \simeq 0.40$, conservative values from paper II) and the molecular contribution to the total gas content.

Such a model allows us to study the influence of gas removal on the integrated colors. It turns out from radio continuum observations (Kotanyi and Ekers, 1983) and HI observations (Warmels and Van Woerden, 1984, Van Gorkom et al., 1984) that the most deficient spirals located at the center of Virgo I have very small gaseous disk that can be naturally interpreted in terms of a dramatic stripping of almost all the gas. Most of them exhibit an "anemic" appearance (Van den Bergh, 1976). For such galaxies, we adopt the approximation of a complete gas removal probably associated with the crossing of the denser intracluster medium at the center of the cluster, in a time scale $\simeq$ 0.5 to 1 Gyr. The stripping is followed by gas replenishment from stellar rejections. We have reckoned the location in the log σ_{gas}-color diagrams of a t_0=12 Gyr old Sb galaxy, after complete gas removal during 0.5 Gyr and replenishment, to be compared to observational data. The main free parameter is the age t_1 of the galaxy when this event occurs.

Fig.3 and fig.4 show some preliminary results. Clearly, several complete strippings early occuring in the life of the galaxy would produce too red colors and are ruled out by the data. Most very deficient galaxies are more likely to have experienced one or two recent complete strippings (viz. $t_0-t_1<5$ Gyr). A single early stripping ($t_1\simeq3$ Gyr) would lead to a very low surface brightness galaxy since more than 50 % of the mass of the disk would be removed, which is here again ruled out for the bright spirals of our sample. The decrease of $(m_{2421}-B)^\circ$ due to the dust removal is much lower than the increase due to the cessation of star formation, and an approximate datation of the stripping is allowed. On the contrary, the problem of internal reddening hampers any definitive conclusion from the log σ_H-$(B-V)_T^\circ$ diagram.

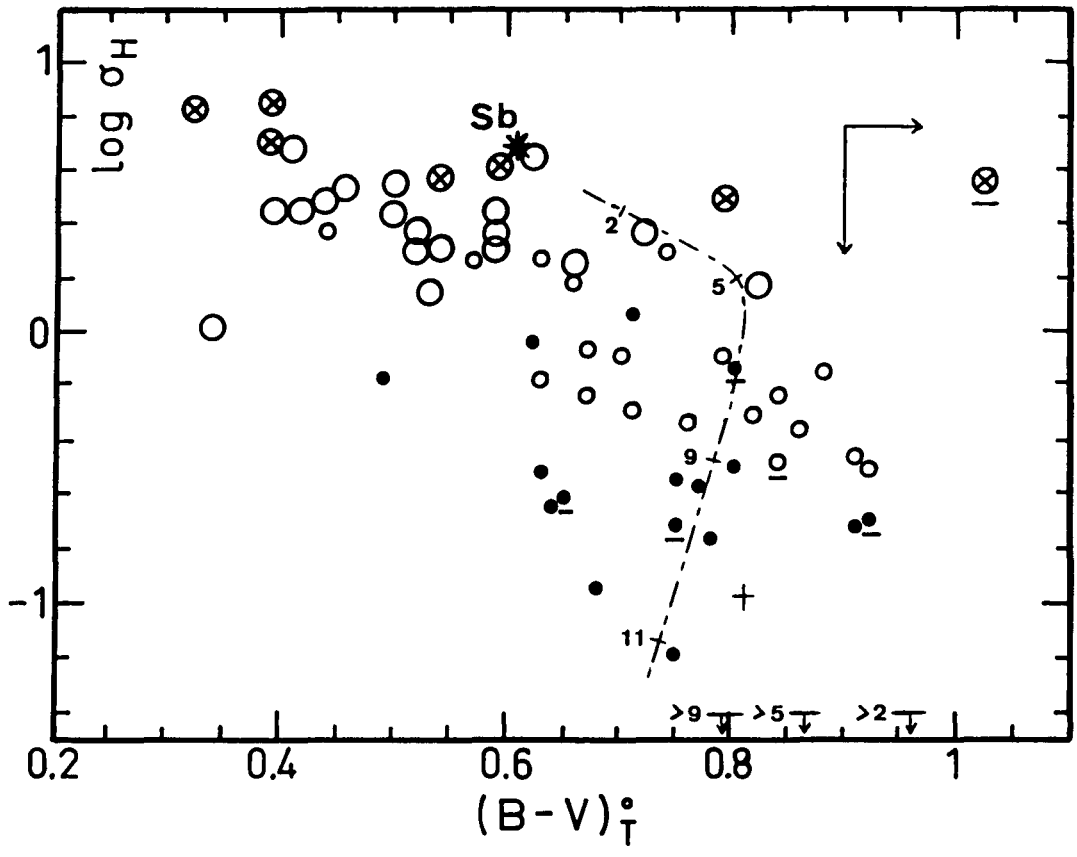


Fig. 3 : log σ_H versus $(B-V)_T^o$ for the Virgo Cluster sample. Symbols as in fig.1. The star denotes the theoretical location of a 12 Gyr old model Sb galaxy in the log σ_{gas}-extinction-free B-V diagram. Model and observations can be compared after shifts of the theoretical locus, allowing for face-on internal extinction (see text for an estimate) and He, H_2 components (Y= 0.30 and $M_{H_2}/M_H \approx 1$ for instance), which are respectively denoted by horizontal and vertical arrows. The dashed curve is the locus of the 12 Gyr old model Sb galaxy after complete gas removal during 0.5 Gyr at age t_l indicated beside the ticks. The cross denotes the location after two complete strippings during 1 Gyr, at ages t_l = 7 Gyr and t_l = 9 Gyr. Smaller shifts are likely to be necessary to compare model and observations. The colors after complete gas removal for age > t_l are indicated by short vertical arrows.

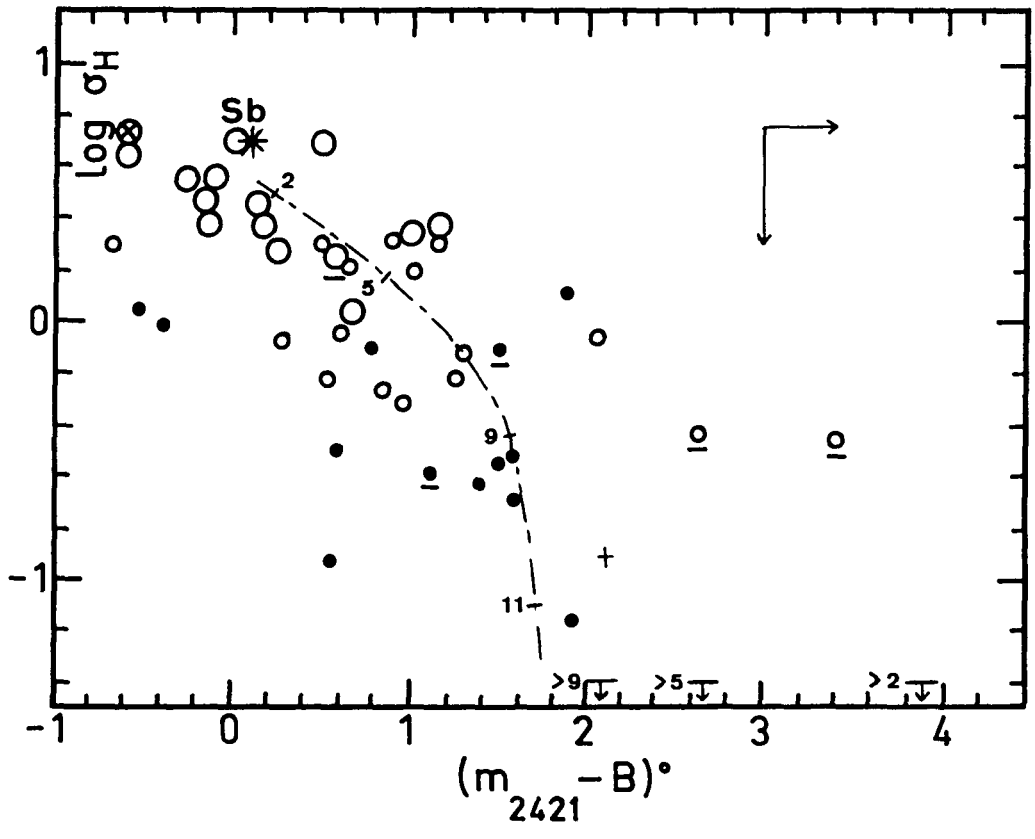


Fig. 4 : log σ_H versus $(m_{2421}-B)^\circ$ for the Virgo Cluster sample. Symbols and comments as in fig. 3.

Most spiral galaxies in Virgo I are likely to be recent arrivants after infall into the core from the outer regions (Tully and Shaya, 1984). According to Rivolo and Yahil, 1983, these spirals would be in motion on their first orbit after rebound, either towards the apapsis or again towards the periapsis. So the probable number of strippings associated with the intracluster medium is one or two, in a time scale of the order of magnitude of one or two crossing times (for the radius of Virgo I, R = 6°, at a distance 16.8 Mpc, from Tully and Shaya, 1984, and a standard

deviation of radial velocities of spiral galaxies equal to 816 kms^{-1}, from Huchra et al., 1984, one obtains $t_{cross} \simeq 2$ Gyr). The high velocity of the arrivals from outer regions supports the plausibily of the explanation of HI deficiency in terms of a ram-pressure mechanism . Because of their poorer gas content, early-type spirals are more likely to be stripped than late-type ones, due to the simple conservation of momentum (see Gisler, 1979). Nevertheless, a spiral probably avoids stripping if its disk lies in the plane of its orbit.

Of course, these spirals can experiment other kinds of interaction with the environment, including evaporation in the hot intracluster medium (Cowie and Songaila, 1977), collision with another disk of spiral (Spitzer and Baade, 1951), or tidal disruption of an extensive gaseous halo that might fuel the star formation in the disk (Larson et al., 1980). Some photometric consequences of these other dynamical scenarios are studied in paper II.

References

Bottinelli, L., Gouguenheim, L., Paturel,G., 1980, Astron. Astrophys., 88, 32

Bottinelli, L., Gouguenheim, L., Paturel, G., 1982, Astron. Astrophys., 113, 61

Chamaraux, P., Balkowski, C., Gérard, E., 1980, Astron. Astrophys., 83, 38

Cowie, L.L., Songaila , A., 1977, Nature, 266, 501

de Vaucouleurs, G., 1961, Ap.J. Suppl., 6, 213

de Vaucouleurs, G., de Vaucouleurs, A., Corwin, H.G., 1976, The Second Reference Catalogue of Bright Galaxies, Austin, University of Texas Press.

de Vaucouleurs, G., Pence, W.D., 1979, Ap.J. Suppl., 40, 425

Giovanelli, R., Haynes, M.P., 1983, An.J., 88, 881

Guiderdoni, B., Rocca-Volmerange, B., 1984, submitted (paper I)

Guiderdoni, B., Rocca-Volmerange, B., in preparation (paper II)

Huchra, J.P., Davis, J.R., Latham, D.W., 1984, in Clusters and Groups of Galaxies, F.Mardirossian et al., D. Reidel, p. 79

Kennicutt, R.C., Kent, S.M., 1983, An.J., 88, 1094
Kotanyi, C., Ekers, R.D., 1983, Astron. Astrophys., 122, 267
Larson, R.B., Tinsley, B.M., Caldwell, C.N., 1980, Ap.J., 237, 692
Rivolo, A.R., Yahil, A., 1983, Ap.J., 274, 474
Rocca-Volmerange, B., Lequeux, J., Maucherat-Joubert, M., 1981, Astron. Astrophys., 104, 177
Smith, A.M., Cornett, R.H., 1982, Ap.J., 261, 1
Spitzer, L., Baade, W., 1951, Ap.J., 113, 413
Tully, R.B., Shaya, E.J., 1984, Ap.J., 281, 31
Van den Bergh, S., 1976, Ap.J., 206, 883
Van Gorkom, J.H., Balkowski, C., Kotanyi, C., 1984 in Clusters and Groups of Galaxies, F.Mardirossian et al., D. Reidel, p.261
Warmels, R.H., Van Woerden, H., 1984, in Clusters and Groups of Galaxies, F. Mardirossian et al., D. Reidel, p. 251
Yoshizawa, M., Wakamatsu, K., 1975, Astron. Astrophys., 44, 363

AN HI AND OPTICAL STUDY OF THE GAS POOR VIRGO CLUSTER SPIRAL NGC 4571 SI

R. C. Kennicutt
Department of Astronomy, University of Minnesota
116 Church St. SE, Minneapolis, MN 55455, USA.

J. M. van der Hulst
Netherlands Foundation for Radio Astronomy
Postbus 2, 7990 AA Dwingeloo, The Netherlands.

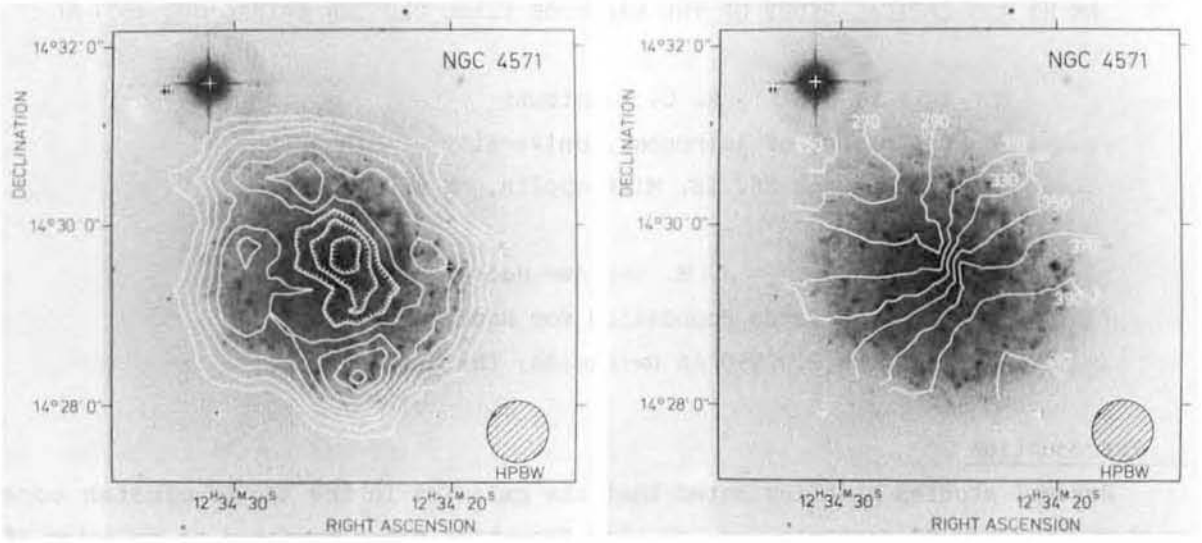
I. Introduction

Several studies have indicated that the galaxies in the Virgo cluster core region have low HI contents and low star formation rates compared to galaxies of similar morphological type in the field. (Kennicutt 1983, Stauffer 1983, Giovanardi et al. 1983, Giovanelli and Haynes 1983, Van Gorkom et al. 1984, Warmels and van Woerden 1984). The most favored interpretation for this effect seems to be stripping by ram pressure when galaxies move through the dense intergalactic medium in the Virgo cluster core. Yet very few galaxies have shown signs of current stripping, two possible exceptions being NGC 4438 (Kotanyi et al. 1983) and NGC 4654 (Warmels, private communication). Kennicutt (1983) identified a few galaxies with extreme properties: galaxies with morphological type Sc, but colors, HI contents and star formation rates which are more typical for field Sb galaxies. We chose one such anemic (van den Bergh 1976) galaxy, NGC 4571, for a detailed study using the National Radio Astronomy Observatory[1] its Very Large Array in its 1 km configuration to study the HI and the Mt. Lemmon, Mt. Palomar and Kitt Peak National Observatory[2] facilities to obtain optical continuum and Hα data.

II. Observations

The VLA observations made in June 1983 provided 16 channel maps with a velocity resolution of 25 km/sec and an angular resolution of 41". From these we determined the distribution of HI column density and the radial (intensity weighted mean) velocity field. These are shown in Figure 1 and 2, superposed on a print of a high resolution plate obtained with the 2.5 m DuPont telescope at Las Campanas. The derived rotation curve (adopting $V_{systemic}$ = 340 km/sec, inclination = 34° and position angle of the line of nodes = 40°) is shown in Figure 3. In the inner part the rotation curve is not well defined because of our poor resolution and because of lack of measurable HI.

Figure 4 summarizes some of the optical data: the blue luminosity profile obtained from surface photometry from a sky limited IIIa-J plate taken in 1979 on



Figures 1 & 2. HI column density distribution (left) and velocity field (right). The HI contours are 0.6, 1.2, 1.7, 2.3, 2.9, 3.5 and 4.1×10^{20} atoms/cm^2. Hatched contours in the central regions indicate decreasing column density. The velocity contours are labelled in km/sec and represent heliocentric velocities.

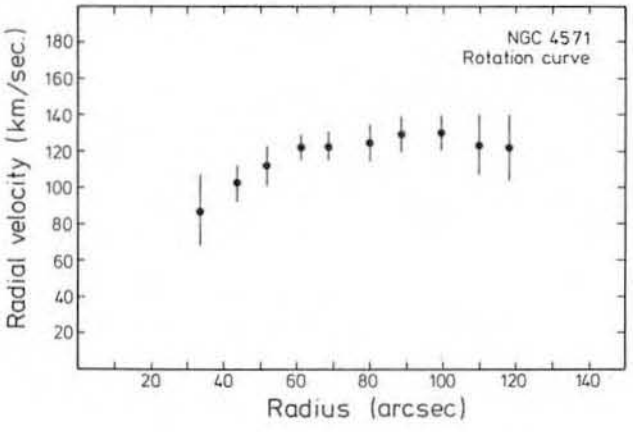
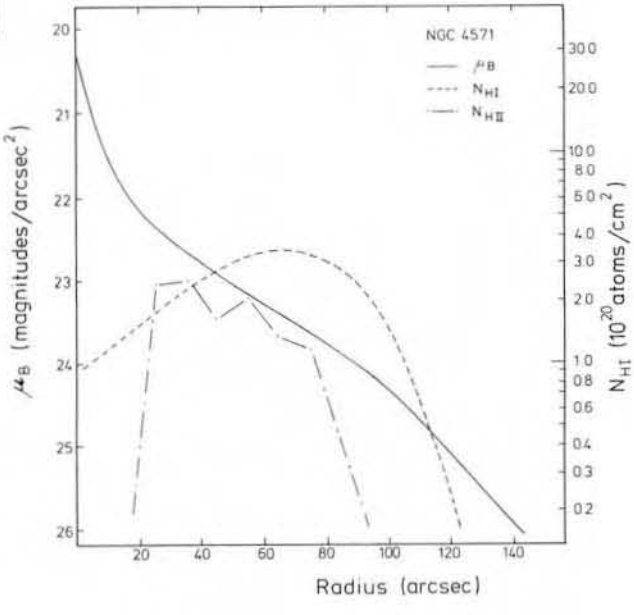


Figure 3. Rotation curve derived from the radial velocity field of Fig. 2 assuming the gas layer exhibits planar, circular motions.

Figure 4. Radial distribution of blue optical surface brightness (μ_B), HI column density (N_{HI}), and surface density of HII regions (N_{HII}).



the 1.3 m Palomar Schmidt telescope, and the radial distribution of HII regions obtained from an Hα plate taken with the Carnegie image tube direct camera on the 2.1 m telescope at KPNO through a 20 A wide interference filter. The surface photometry its zero point was determined from photoelectric BVR photometry obtained in May 1982 using the Schmidt Two-holer photometer on the Mt. Lemmon 1.5 m telescope.

III. Results

NGC 4571 is classified as an Sc galaxy. This is supported by its luminosity profile which is disk dominated and has only a small nuclear or bulge component contributing ~4% to the integrated luminosity. Also the rotation curve, e.g. the implied mass surface density distribution, supports the Sc classification. The slow rise and low maximum velocity of the rotation curve are quite typical for late type galaxies like M33 (Newton 1980) and NGC 2403 (Wevers 1984).

In all other respects, however, NGC 4571 is not a typical Sc galaxy at all as already pointed out by Kennicutt (1983). The current starformation rate in the disk is quite depressed. Both the total Hα luminosity and the characteristic luminosities of the brightest HII regions are at least a factor 3 lower than normal for an Sc galaxy. The broadband colors determined from our BVR photometry are unusually red (B-V ≈ 0.70), consistent with this low starformation rate and indicating that the stellar disk is evolved and has not been subject to active starformation in the past 1-2 billion years. Also the HI properties are quite unusual for an Sc galaxy. There is an HI deficiency in the inner parts (more typical for Sa-Sb galaxies, cf. Bosma 1981, Wevers 1984) and more striking, the column densities are very low everywhere in the disk. Peak values reach only 4×10^{20} atoms/cm^2, a factor 5 below values normal for Sc galaxies and more typical for the outer parts of spiral galaxies and the disks of S0 galaxies (Van Woerden et al. 1983). The total amount of neutral gas is 1.5×10^9 $M_\odot$ for an assumed distance of 21.9 Mpc. The relative gas content is 3%. The overall low gas density is, however, consistent with the low starformation rate and red disk colors, and confirms the findings of Giovanelli and Haynes (1983) and Giovanardi et al (1983) that anemic galaxies have low gas surface densities.

A very striking property of the HI disk, not yet mentioned but very clear in Fig. 4 is its small size compared to the optical diameter. The HI size at 1.83×10^{20} atoms/cm^2 (Bosma 1981, Warmels and van Woerden 1984) is 3.2' while the De Vaucouleurs diameter measures 3.7'. This is very unusual for galaxies in the field but not uncommon for galaxies in the central region of the Virgo cluster (Warmels and van Woerden 1984, Van Gorkom et al. 1984) and is what one expects from simple stripping models. In this case, however, the regularity of the HI

distribution and the velocity field, as well as the red color of the disk argue against very recent stripping.

The HI and optical properties are, however, consistent with a slow gas removal process or one which took place at least a few billion years ago (~one crossing time) so that the disk had time to readjust. It is of interest to note that if 70-90% of the gas was removed a few billion years ago, stellar mass loss would have been able to replenish a large fraction of the observed gas mass over most of the disk, except maybe the very central (bulge) part.

An alternative explanation for the peculiar properties of NGC 4571 is just an inhibition or retardation of the disk formation process. Whether such would result from being in a cluster environment is not absolutely clear, since anemic galaxies have also been found outside clusters of galaxies (Bothun and Sullivan 1980).

We gratefully acknowledge travel support from NATO grant No. 0592/82. RCK acknowledges in addition NSF grant AST 81-11711-01. Mt. Lemmon is supported in part by NSF grant AST 82-14422.

References

Bosma, A. 1981 A.J. 86, 1825.

Bothun, G. C., Sullivan, W. T. 1980 Ap.J. 242, 903.

Giovanardi, C., Helou, G., Salpeter, E. E., Krumm, N. 1983 Ap.J. 267, 35.

Giovanelli, R., Haynes, M. P. 1983, A.J. 88, 881.

Kennicutt, R. C. 1983, A.J. 88, 483.

Kotanyi, C. G., van Gorkom, J. H., Ekers, R. D. 1983 Ap.J. 273, L7.

Newton, K. 1980 M.N.R.A.S. 190, 689.

Stauffer, J. R. 1983, Ap.J. 264, 14.

van den Bergh, S. 1976 Ap.J. 206, 883.

van Gorkom, J. H., Balkowski, C., Kotanyi, C. G. 1984 in "Clusters and Groups of Galaxies", ed. F. Mardirossian et al., Reidel Publ. Co., p.293.

van Woerden, H., van Driel W., Schwartz, U. J. 1983 in "Internal Kinematics and Dynamics of Galaxies", IAU Symp. 100, ed. E. Athanassoula, Reidel Publ. Co.

Warmels, R. H., van Woerden H. 1984 in "Clusters and Groups of Galaxies" ed. F. Mardirossian et al., Reidel Publ. Co., p.251.

Wevers, B. M. H. R. 1984 Ph.D. Dissertation, University of Groningen.

[1]NRAO is operated by Associated Universities Inc., under contract with the National Science Foundation.

[2]KPNO is operated by Associated Universities for Research in Astronomy Inc., under contract with the National Science Foundation.

RADIO CONTINUUM AND HI EMISSION FROM THE SPIRAL GALAXIES IN THE VIRGO CLUSTER AREA

G. Gavazzi, Istituto di Fisica Cosmica, Milano, Italy

I. INTRODUCTORY REMARK

A fundamental, and still open question, on galaxy evolution is whether the observed morphology segregation in clusters of galaxies took place in the early stages of galaxy formation ("genetic" picture), or it was gradually induced by the intergalactic environment ("evolutionary" picture). The study of the environmental effects on galaxy evolution is schematically depicted in Fig.1. The different role played by morphology in diagrams 1a and 1b is fundamental. This remark stresses the need for future studies on the environmental effects on galaxy evolution based on morphology independent parameters (if they exist), or on large data samples allowing to analyze independently galaxies of different morphological types. Unfortunately the limited amount of the presently available observational material does not allow such a detailed work, and all analyses, including the one I am presenting here, could suffer from a selection effect due to improper account of the morphological types of galaxies.

In this paper first I want to show that the statistical method used to derive Luminosity Functions (from radio data to X-ray) can be profitably applied also to HI data. I will apply the method to show quantitatively the amount of HI deficiency among the spiral galaxies in the Virgo area without invoking the deficiency parameter. Secondly I will present some evidence, as a suggestion for future work, that spiral galaxies in Virgo might show a correlation between HI content and radio continuum luminosity which could help us in the understanding of stellar and galaxy evolution and its relation with the intergalactic environment.

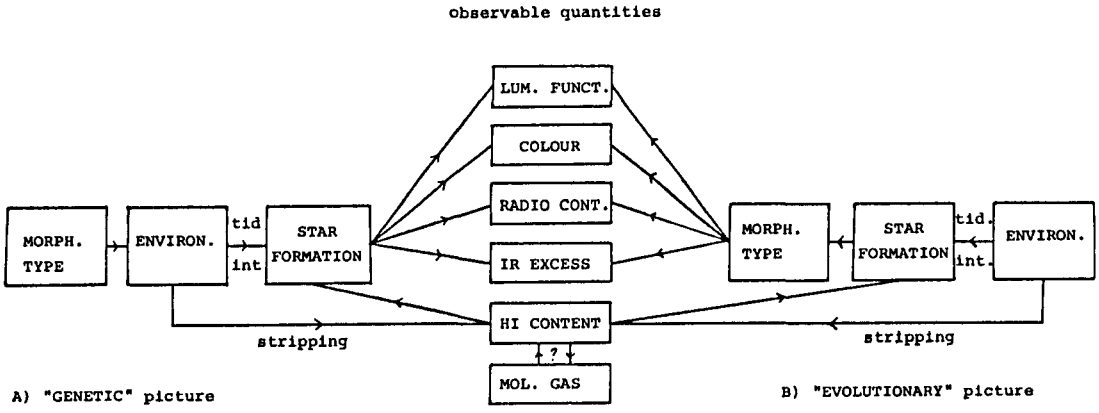


Fig. 1

II. THE SAMPLE

The following analysis is performed on a sample of 101 spiral galaxies brighter than Mp=-17.0 in the Virgo area ($12^h < \alpha < 13^h$; $0^\circ < \delta < 20^\circ$). The sample, which was surveyed in the radio continuum by Kotanyi (1980), is 90% complete at this limiting magnitude and therefore it is suitable for statistical investigations. A subsample (within $\sim 8^\circ$ from M87) belong almost entirely to the sample (complete to $B_T^0 < 12.80$) recently surveyed in the 21 cm line of the Neutral Hydrogen by Helou et al (1981,1984).

III. THE RADIAL DEPENDENCE OF THE HI MASS FUNCTION IN VIRGO

We derive the HI mass function (i.e. the fraction of galaxies having a given Hydrogen mass) of the Virgo galaxies using the method first introduced by Hummel (1981) to determine the Radio Luminosity Function of galaxies. It can be shown analytically that the method is equivalent to that used by Avni et al (1980) to analyze X-ray data of quasars, and I would like to stress that it can be applied to derive the distribution of any particular variable, such as HI surface brightness, which might be a morphology independent parameter, as Haynes and Giovanelli pointed out at this conference.

The use of this method is particularly recommended when upper limits, as well as proper detections, have to be analyzed.
We derive in Fig. 2 a and b the fractional HI Mass Function of the spiral galaxies in Virgo obtained separately in a 3.3 degrees circle centered on M87 and in $3^\circ.3<R<12^\circ$, in bins of $\Delta LogM=0.4$.
The differential MHI Function (Fig.2a) shows the inner and outer distributions have similar "bell" shape (a mean MHI can be determined) with equal height, but the two distributions are peaked at $<MHI> \simeq 2x10^8$ Mo and $<MHI> \simeq 7x10^8$ Mo respectively. The well known HI deficiency of the inner galaxies is quantitatively established with this method without using the deficiency parameter (of course the analysis can be performed in separate subsamples of different optical luminosity or morphological type). The fact that the two distributions have very similar shape indicates that the quantity of stripped gas does not depend on the actual content of the "undisturbed" galaxies. The integral MHI Functions (Fig.2b) shows that 50% of the galaxies in the inner region have $MHI>3x10^8$ Mo, while 50% of the outer galaxies have $MHI>10^9$ Mo.

IV. HI CONTENT AND RADIO CONTINUUM LUMINOSITY

All galaxies having a positive determination of both HI line and radio continuum flux are plotted in Fig.3. Different symbols refer to 3 absolute magnitude bins and to the samples inside and outside $R=3^\circ.3$.
1) A general correlation exists between the plotted quantities, as already pointed out in Gavazzi (1984).
2) The correlation is not entirely due to an optical luminosity effect.
3) The correlation is more marked among the unperturbed ($R>3^\circ.3$) sample.
4) The inner galaxies lie almost entirely below the unperturbed ones in Fig.3: they are HI deficient, as seen in the previous paragraph, but they are not displaced accordingly toward lower radio continuum luminosities. From point 3), however, one should expect to find them on the bottom left corner of the diagram. If one assumes that radio continuum is an indicator of star formation rate, one could argue that in the inner galaxies the star formation rate is higher than inferred from their HI content. A similar conclusion is reached by Helou (this conference) by comparing the HI content and the IR excess on a sample of Virgo galaxies which largely overlaps with ours.

Since in the unperturbed sample star formation and HI content seems to correlate nicely, it can be argued that HI depletion and slowing of the star formation rate have rather different time scales. Perhaps galaxies under the process of stripping lose their Hydrogen first (they move vertically down in Fig.3) and later their star formation rate is slowed down (they move horizontally to the left). This evidence supports the speculation that at the present time Virgo spirals are in their early stripping phase, as many other pieces of evidence seem to indicate, providing evidence that the infall of the spiral galaxies in the Virgo cluster might have been a quite recent phenomenon.

REFERENCES

Avni,Y.,Soltan,A.,Tananbaum,H.,Zamorani,G.:1980,Ap.J.,238,800
Gavazzi,G.,Jaffe,W.,Valentijn,E.:1984,Proc.Conf.Clusters and Groups of Galaxies,p209
Helou,G.,Giovanardi,C.,Salpeter,E.E.,Krumm,N.:1981,Ap.J.Suppl., 46,267
Helou,G.,Hoffman,G.L.,Salpeter,E.E.:1984,Ap.J.Suppl.,55,433
Hummel,K.:1981,Astron.Astrophys.,93,93
Kotanyi,C.:1980,Astron.Astrophys.Suppl.,41,421

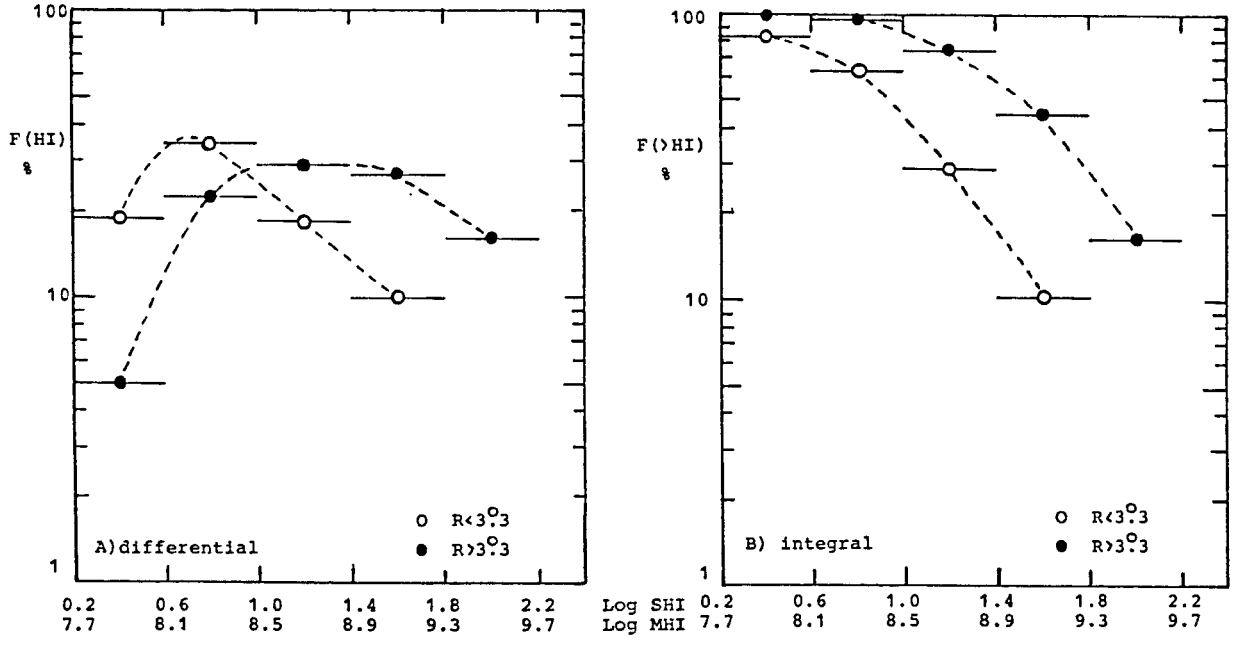


Fig.2

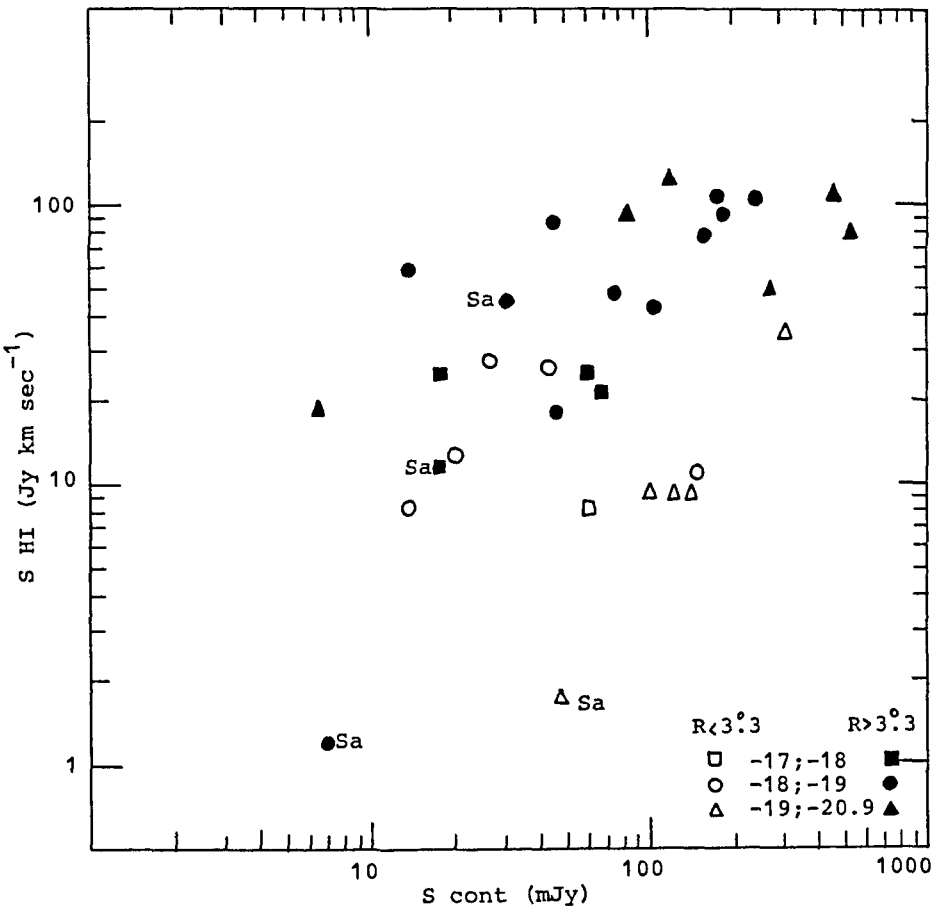


Fig. 3: The correlation between HI line and radio continuum flux.

HI OBSERVATIONS OF LATE-TYPE VIRGO DWARFS

G. Lyle Hoffman, Lafayette College

The Las Campanas optical survey discussed here by Sandage and Binggeli includes 242 galaxies of types Sdm and later which are probable members of the Virgo cluster. In collaboration with G. Helou, E.E. Salpeter and A. Sandage, I am in the midst of an HI detection survey of all these galaxies, and will report here results for the 91 galaxies observed so far at Arecibo. We hope to complete the rest of the sample within 18 months.

These observations allow us to test what fraction of the galaxies, classified as Virgo dwarfs strictly by optical morphology, are in fact in the background (to anticipate a punchline: very few); to assess whether or not the correlations between optical and HI parameters are continuous from giant spirals through dwarf irregulars (as previously claimed by Thuan and Seitzer 1979 and Davies and Kinman 1984); to study the effects of the Virgo environment on galaxies of a wider range of sizes than heretofore available; to put more stringent limits on mass segregation in the cluster; and to evaluate various models of these galaxies, in particular the stochastic star formation model of Gerola et al.(1980).

A breakdown of the galaxies into morphological bins is given in Table 1, with detection statistics. Note first of all that only 10% have been detected at redshifts $v_\odot > 4000$ km/s (and <u>none</u> at $3000 < v_\odot < 4000$ km/s). We conclude that the optical morphological classification is quite successful in predicting membership in the cluster complex. Note also that the undetected galaxies are predominantly the faintest dwarfs, leading us to expect that they have mostly escaped detection because they have intrinsically low M_{HI}, <u>not</u> because they are in the background.

Table I. Detection Statistics

	Number observed	Detected Virgo	Backgd.	Undet.
Sm = Sdm,Sm	21	18	1	2
Imb = ImIII,III-IV	18	12	3	3
IBC = Im/BCD,Sm/BCD,BCD	15	11	2	2
Imf = ImIV,IV-V,V	30	17	2	11
Misc.	7	6	0	1

In Figure 1 we display various mean properties of the galaxies, first as a function of morphological type (left panel), then as a function of luminosity (right panel). The displayed means are for: luminosity, B_T; major diameter, a; optical surface brightness $\sigma_{opt} = 4L/\pi ab$; the detected fraction (background detections omitted); a mixed hydrogen surface

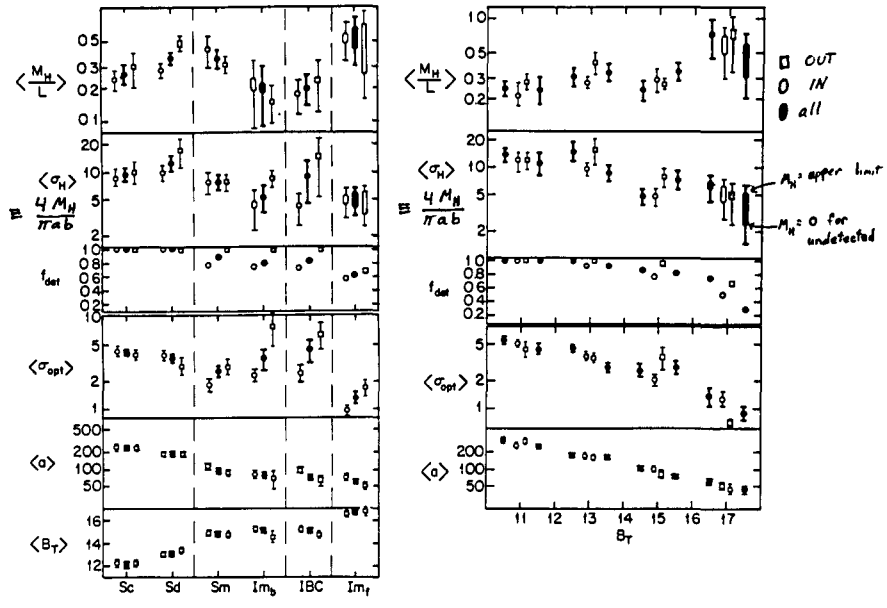


Figure 1. Mean optical and HI properties.

density, $\sigma_H = 4M_H/\pi ab$ using the optical diameters; and the hydrogen mass-to-light ratio. Undetected galaxies are included in the averages; the oblongs extend from the mean taking $M_H = \emptyset$ for nondetections to that taking the full upper limit for M_H. The galaxies in bins Sc (including types ScI+II from the HI sample of Helou, Hoffman and Salpeter 1984) and Sd (types ScIII and Sd) are included for comparison. Focussing on the topmost panels for the moment, we see a general trend for M_H/L to increase from bin Sc through Im_f, with Im_b and IBC falling somewhat below the trend. This is just as expected, since the bright patches in BCD galaxies are presumably sites of active star formation, increasing L with no concomitant increase in M_H. σ_H in general decreases by a factor of 2 from Sc to Im_f; bin IBC may lie slightly above the trend, but that is not yet statistically significant. The trends vs. B_T are not so clear-cut, but in general parallel those vs. morphological type.

A comparison of environmental effects on dwarfs vs. those on large spirals can potentially tell us something about the mechanisms which cause the HI deficiency in cluster spirals. To that end we compare the HI properties of dwarfs and spirals inside a 5° circle centered near M87 with those in our sample outside that circle. In Fig. 1, mean properties for the IN galaxies are shown as open circles, those for OUT galaxies as open squares. First, the positive results: in every bin, Sm and later (or $B_T = 13$ and fainter), the detection rate is higher OUT than IN, and the mixed surface density of HI is larger OUT than IN. However, unexpectedly and confoundingly, the optical surface density is also larger OUT than IN for all dwarf morphological bins (but not for bright spirals). Consequently, M_H/L is not significantly larger OUT than IN. Also, the overall ratio of $\sigma_{H,OUT}/\sigma_{H,IN}$ is only about 2.4 -- not significantly larger than for bright spirals. This poses a

stern challenge to rampressure stripping as the HI removal mechanism, since one would expect the lower surface gravity of the dwarfs to allow much more severe stripping than for bright spirals. One possibility, I suppose, is that we see only the dwarfs that have not yet been stripped (or are only just now being stripped), and that those that were stripped in the past have had their star formation so severely truncated that they have ceased to be recognizable on the Las Campanas plates (or have been converted into something that looks more like a dwarf spheroidal and hence was not included in this survey). If that were the case, however, we would expect the ratio of numbers of dwarfs to bright spirals to be considerably larger OUT than IN, which does not appear to be the case either (as Figure 2

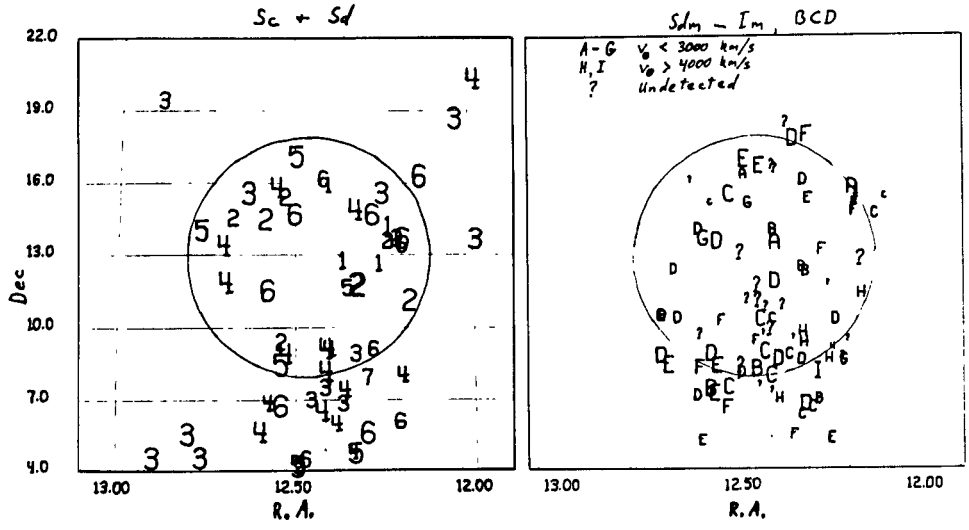


Figure 2. Distribution on the sky.

shows). Nor do we see evidence of mass segregation: the ratio of numbers of dwarfs IN to spirals IN is about the same as OUT, and the velocity dispersions are not significantly greater for dwarfs than for spirals (see Table 2 and Figure 3). In Fig. 3, the histograms of IN velocities are hatched; OUT velocities are shown without shading.

Table II. Mass Segregation.

	Dwarfs $B_T \geq 14.0$		Spirals (Sb-Scd) $B_T \leq 12.5$	
	IN	OUT	IN	OUT
Number	50	29	21	10
σ_v, (km/s)	728	563	785	409

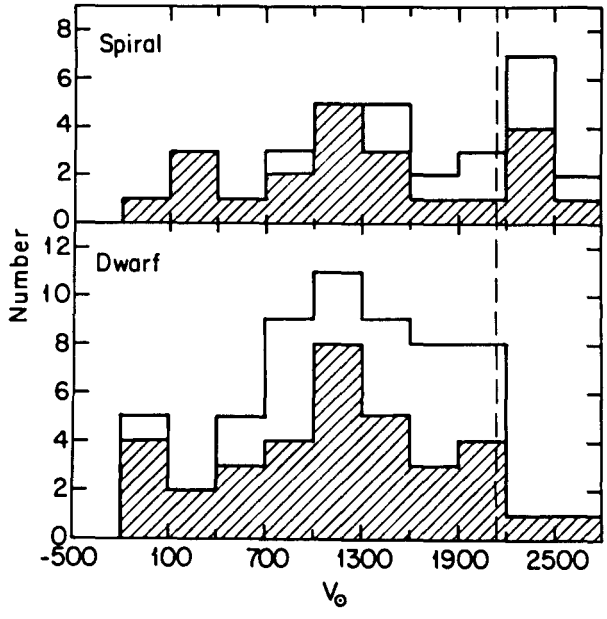


Figure 3. Velocity histograms.

For each detected galaxy we have as well the profile width ΔV and an assignment of the shape of the spectrum to either "double-horned" (DH, similar to the integral profile for an edge-on large spiral) or "gaussian." Figure 4 displays the means of V and the fraction of detections classified as DH vs. morphology and B_T. Evidently regular rotation ceases to be the dominant influence in determining the profiles of the faintest dwarfs, as Thuan and Seitzer (1979) also found for non-cluster

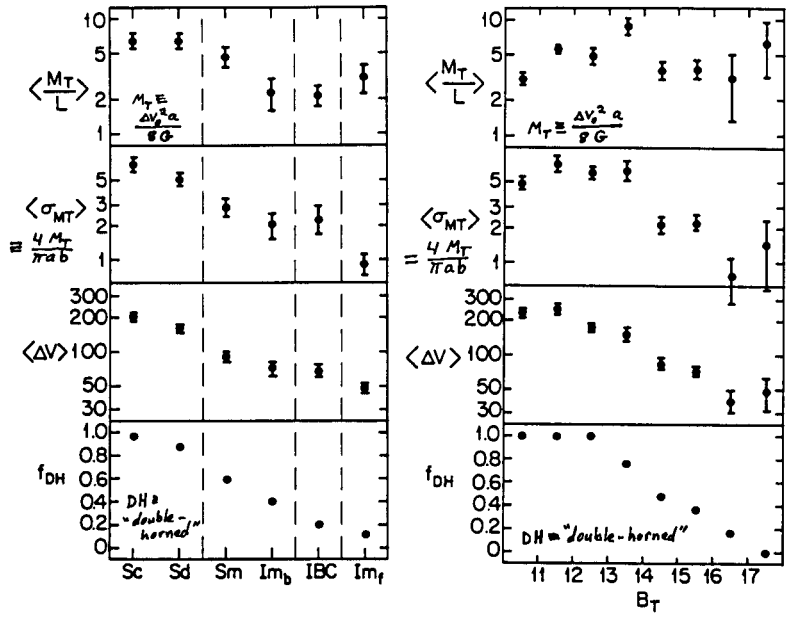


Figure 4. Profile widths and related quantities.

dwarfs. Making conservative corrections for inclination and random motions,

$$\cos^2 i = [(b/a)^2 - 0.04]/0.96,$$

$$\Delta V_o^2 = \Delta V_{obs}^2 + (\Delta V_{obs}^2 - 25^2)(\csc^2 i_> - 1),$$

$$i_> = \max(i, i_c),$$

$$\sin(i_c) = 0.4,$$

we compute the "indicative gravitational mass" $M_T = \Delta V_o^2 a/8G$ and an equivalent mass surface density $\sigma_{MT} = 4M_T/\pi ab$. M_T/L shows no clear trend; σ_{MT} appears to decrease for the fainter dwarfs.

If the most straightforward versions of the stochastic star formation model for these dwarfs were correct, we would expect a rather tight correlation between M_T and the optical

major diameter a whereas the correlation between L and a would be blurred by the effects of recent and current bursts of star formation. Therefore the variance of L about the mean relation

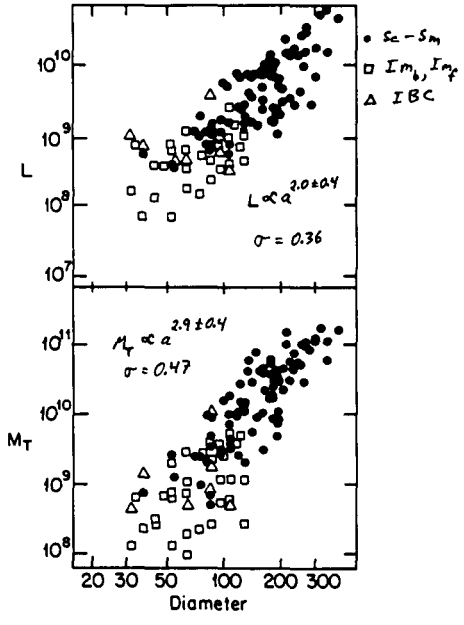


Figure 5.

$L \propto a^{\gamma}$ should be large, as observed in Figure 5. The variance of M_T about its mean relation $M_T \propto a^{\delta}$ should reflect mainly measurement errors (sin i and the like), which admittedly are substantial, but Fig. 5 shows an even larger variance for M_T than for L! We conclude that much of this variance is likely to be intrinsic, and that galaxy size cannot be the only parameter characterizing dwarf irregulars.

The Arecibo Observatory is part of the National Astronomy and Ionosphere Center which is operated by Cornell University under contract with the National Science Foundation.

REFERENCES

Davies, R.D., and Kinman, T.D. 1984, M.N.R.A.S. 207, 173.

Gerola, H., Seiden, P. and Schulman, L. 1980, Ap.J. 242, 517.

Helou, G.T., Hoffman, G.L. and Salpeter, E.E. 1984, Ap.J.Suppl.Ser. 55, 433.

Thuan, T.X., and Seitzer, P.O. 1979, Ap.J. 231, 680.

III.

INFRARED AND CO OBSERVATIONS

IRAS[1] OBSERVATIONS OF VIRGO CLUSTER GALAXIES

Teije de Jong
Astronomical Institute, University of Amsterdam

ABSTRACT

We analyse and discuss infrared data of all 88 galaxies detected by IRAS in the core of the Virgo cluster. Typical infrared energy distributions of the optically brightest galaxies in Virgo - those with Messier numbers - are presented. Two elliptical galaxies, M84 and M87, are detected by IRAS. Masses, removal times and destruction mechanisms of dust in these ellipticals are briefly discussed. The infrared properties of Virgo cluster galaxies are compared with those of field galaxies. Apart from ellipticals, which are not detected in the field sample, the infrared detection probability of galaxies in the Virgo cluster and in the field is similar. The infrared excess distributions of Virgo and field galaxies are identical, with the exception of early-type spirals. Star formation rates in early-type spirals (Sa - Sbc) are more than twice smaller in the Virgo cluster than in the field. A mechanism to explain this anomaly in which slow depletion of interstellar gas is caused by enhanced star formation during galaxy encounters in a cluster environment is suggested. This mechanism is consistent with the infrared data of Virgo galaxies in close pairs.

I. INTRODUCTION

The all-sky survey carried out by the Infrared Astronomical Satellite IRAS has resulted in the detection of about 20000 galaxies in the infrared. This unprecedented rich material constitutes a unique database for studies of star formation in galaxies (de Jong et al. 1984; Soifer et al. 1984; Young et al. 1984). In this paper we present results of a study of the infrared properties of all galaxies in the core of the Virgo cluster detected by IRAS. An accompanying paper by Helou (1985) analyses IRAS observation of a sample of optically bright spirals in Virgo.

****

[1]The infrared Astronomical Satellite was developed and operated by the Netherlands Agency for Aerospace Programs (NIVR), the US National Aeronautics and Space Administration (NASA), and the UK Science and Engineering Research Council (SERC).

Clusters of galaxies are ideal "laboratories" to study the evolution of galaxies, one of the most central but still poorly understood themes in modern astronomy (Dressler 1984). Unravelling the history of star formation is an essential element in such studies because the gradual exhaustion of interstellar matter over the lifetime of a galaxy drastically changes its appearance and observational characteristics. The dynamical, kinematical and chemical evolution of a galaxy are tied in to the history of star formation through their dependence on the amount, the distribution and the physical state of the interstellar matter.

One of the most conspicuous differences between galaxies in clusters and in the field is their different distribution of morphological types: ellipticals and lenticulars are more frequent in clusters while the galaxy population in the field is dominated by spirals. Whether this difference is already established during the early evolution of a cluster or wether it is created later by environmental effects such as merging and tidal stripping of stellar disks or by ram-pressure stripping of interstellar gas in an intercluster medium remains undecided at present (see Dressler 1984 for a review of processes and scenarios).

This first study of IRAS observations of galaxies in the Virgo cluster, the nearest and best studied cluster of galaxies, has greatly benefitted from the recent completion of the Virgo Cluster Catalog (VCC - Binggeli, Sandage and Tammann 1985) kindly made available to us prior to publication by Dr. Binggeli. This catalog is complete to very faint magnitudes ($B_T \lesssim 19$) and it has the additional attractive feature that all optical data are in the system of the Revised Shapley-Ames Catalog of Bright Galaxies (RSA - Sandage and Tammann 1981) which facilitates the comparison of cluster and field galaxies. Both the optical and the infrared data used here are thus taken from uniform data sets.

IRAS data of Virgo cluster galaxies have not been published before so that in many respects this is a research paper rather than a review paper.

II. OBSERVATIONAL DATA

The infrared data used for this study were extracted from the Working Survey Data Base (WSDB), the database from which the IRAS point source catalog will be created. For a discussion of the quality of these pre-catalog data, their calibration and photometric accuracy we refer to Neugebauer et al. (1984). Using criteria developed on the basis of the first IRAS studies of galaxies (de Jong et al. 1984; Soifer et al. 1984) we extracted from the WSDB all month-confirmed

point sources detected at 60 and/or 100 μm within 6 degrees from the adopted Virgo cluster center at RA = $12^h\ 27^m$, DEC = 13° 30' (de Vaucouleurs and de Vaucouleurs 1973). To exclude star-like objects only those sources whose flux densities at 60 or 100 μm exceeded their flux density at 12 μm were kept.

This search resulted in 159 galaxy candidate IRAS sources in the 113 $(\text{degree})^2$ Virgo cluster core region. These were identified using the recently completed Virgo Cluster Catalog (VCC - Binggeli, Sandage and Tammann 1985). The VCC contains about 2100 galaxies down to BT ≃ 19 and covers approximately the same area as searched in the WSDB. Roughly 60% of these are classified as Virgo cluster members, about 30% as possible members and about 10% as background galaxies. Only relatively brigh background galaxies, those also listed in the Catalog of Galaxies and Clusters of Galaxies by Zwicky and co-workers, are included in the VCC.

The identification process yielded the following results:
- 23 sources in the circular area searched fall outside the region covered by the plate material on which the VCC is based
- 88 sources are identified with galaxies classified in the VVC as members or possible members
- 19 sources are identified with background galaxies
- the remaining 29 sources cannot be identified with galaxies in the VCC. They are presumably faint background galaxies not listed in the VCC. The total number of background galaxies of about 50 is then roughly consistent with the number expected on the basis of the estimated 20000 galaxies detected by IRAS over the whole sky.

A comparison of the IRAS positions with the VCC positions, which are estimated to be uncertain by at most about 10 arcseconds (Sandage, private communication), shows that the former are quite accurate. Averaged over all 88 galaxies identified the position difference equals 15 ± 10 arcseconds, a truely remarkable achievement in view of the fact that the infrared detectors have dimensions in the range 0.75 to 5 arcminutes.

Of the 88 Virgo cluster galaxies detected by IRAS 40 lie within 3 degrees from the adopted cluster center and 48 in a 3 degree wide ring centered at 4.5 degrees from the center. Taking into account that several pieces of this ring fall outside the area surveyed by Binggeli et al. (1985) the surface density of detected Virgo cluster members in the central 3 degree radius region is more than three times larger than in the ring.

Due to the proximity of the Virgo cluster several galaxies are resolved by the IRAS detectors so that the point source extraction algorithm used to determine the infrared flux densities is inadequate. To overcome this problem the IRAS data have also been filtered using an extraction algorithm that can handle sources with sizes up to 8 arcminutes. The database resulting from this processing forms the basis for the future production of the Small Extended Source (SES) Catalog. Although the SES processing produces fluxes that are more reliable for extended sources the calibration of the SES fluxes is less well determined than the point source calibration so that the random errors in the SES fluxes are at present appreciably larger than in the point source fluxes (50% versus 15%).

To obtain SES flux densities for the extended galaxies we have cross-correlated the sources in our sample with the SES database. Of the 88 Virgo cluster galaxies detected by the point source processing 18 were also detected by the SES processor at 12 μm, 13 at 25 μm, 22 at 60 μm and 3 at 100 μm. As expected all SES fluxes are larger than the corresponding point source fluxes or upper limits. In Table 1 we list the average values of the SES over point source flux density ratios at each wavelength.

Table 1 SES to Point Source flux density ratios

	12 μm	25 μm	60 μm	100 μm
SES/PS	2.4 ± 0.8	3.9 ± 1.9	1.97 ± 0.74	2.0 ± 0.5
n_{GAL}	11	12	22	3

Taking into account that the detector area is about the same at 12 and 25 μm, increases by a factor 2 from 25 to 60 μm and again by a factor 2 from 60 to 100 μm we conclude that apparently galaxies steadily increase in size with increasing wavelength.

III. RESULTS AND DISCUSSION

Typical spectral energy distributions of galaxies in the infrared are shown in fig.1 where we have plotted data for all Messier galaxies in the Virgo cluster core. All energy distributions are steeply rising into the far-infrared. The 60 - 100 μm color temperatures of the emission are in the range 30 - 40 K, assuming a λ^{-1} wavelength dependence of the dust emissivity. As indicated in fig.1

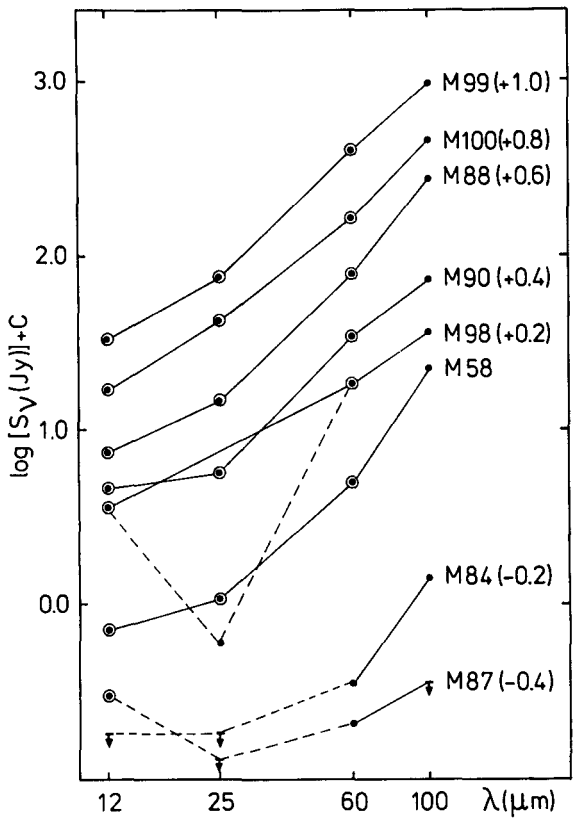


Figure 1
Infrared spectral energy distributions of Messier galaxies in Virgo. Dots represent point source fluxes, circled dots small extended source fluxes and arrows indicate upper limits to point source fluxes. For clarity of illustration the energy distributions are displaced by the amounts listed in brackets

virtually all flux densities at 12, 25 and 60 μm are SES fluxes. This is not surprising since the Messier galaxies are of course the biggest galaxies in the cluster. At 100 μm none of the galaxies is detected by the SES processor so that the point source flux densities are used. One galaxy, M98, was apparently missed by the SES processing at 25 μm.

Due to their cluster membership all galaxies in fig.1 are at approximately the same distance so that their relative intensity is a measure of their relative intrinsic infrared luminosity. The three infrared brightest galaxies, M99 (NGC 4254), M100 (NGC 4321) and M88 (NGC 4501) are late-type spirals. Their 40 - 120 μm luminosities are about 3 10^{10} $L_{\odot}$ at a distance of 21.9 kpc (Sandage and Tammann 1981). The next three galaxies M90 (NGC 4569), M98 (NGC 4192) and M58 (NGC 4579) are early-type spirals with infrared luminosities of order 1 10^{10} $L_{\odot}$. Since the far-infrared radiation of spiral galaxies is predominantly generated by recently formed massive stars still embedded in the molecular clouds from which they were born this result confirms the earlier conclusion that the star formation activity decreases going from late to early spirals (de Jong et al. 1984).

Most noteworthy in fig.1 is the fact that two elliptical galaxies, M84 (NGC

4374) and M87 (NGC 4486), are detected in the infrared. Together with NGC 1052 (Neugebauer et al. 1985) these are the only elliptical galaxies detected by IRAS sofar. Their infrared luminosities are small, 2 10^8 and 6 10^8 $L_\odot$, respectively. Both M84 and M87 are strong radio continuum and X-ray sources (Forman and Jones 1982; Kotanyi and Ekers 1983). While M87 is about two orders of magnitude more luminous than M84 in the radio and in X-rays they are of comparable intensity in the infrared. This suggests that the mechanism causing the infrared emission is of a different nature than that generating the radio or the X-ray emission.

The most straightforward way to explain the infrared emission from M84 and M87 is by assuming that it is generated by interstellar dust particles heated by the radiation of stars in the galaxy. Using the methods employed by Gillett et al. (1985) to analyze the IRAS data of the globular cluster 47 Tuc we derive "dirty silicate" dust masses in M84 and M87 of about 30000 and 3000 $M_\odot$. The uncertainties in these estimates are large, at least a factor 3. In particular the value for M87 is uncertain because it is not detected at 100 μm so that only a lower limit to the dust temperature can be derived.

Adopting masses for M84 and M87 of 2 10^{12} and 4 10^{12} $M_\odot$, using a stellar mass loss timescale of 1 10^{12} yrs (Gisler 1979), equal to that derived for globular clusters by Faulkner and Freeman (1977), and assuming a gas/dust ratio of 1500 we find rates of dust replenisment by mass loss from late-type stars of 1.5 10^{-3} $M_\odot$ yr^{-1} in M84 and 3 10^{-3} $M_\odot$ yr^{-1} in M87. Combining these rates with the estimated dust masses this implies that the dust in elliptical galaxies must be removed in about 2 10^7 yrs in M84 and in about 1 10^6 yrs in M87. The removal of interstellar dust in elliptical galaxies may be related to the existence of a galactic wind driven by supernova explosions (Bregman 1978). At typical wind velocities of about 400 km s^{-1} the dust cannot be swept out of the galaxy in the time available. The alternative is that the dust is destroyed locally, probably by sputtering in collisions with ions in the wind. This is not the place to verify by detailed calculations whether sputtering can destroy the dust fast enough. We just note that the situation in elliptical galaxies is a scaled-up version of that in the globular cluster 47 Tuc recently discussed by Gillett et al. (1985).

In fig.2 we show distributions of morphological types for three samples of galaxies: in the top panel for all galaxies detected by IRAS in the Virgo cluster core, in the middle panel for an optically complete sub-set of those and in the bottom panel for an optically complete sub-sample of RSA field galaxies. The hatched area represents the distribution of the galaxies detected by IRAS,

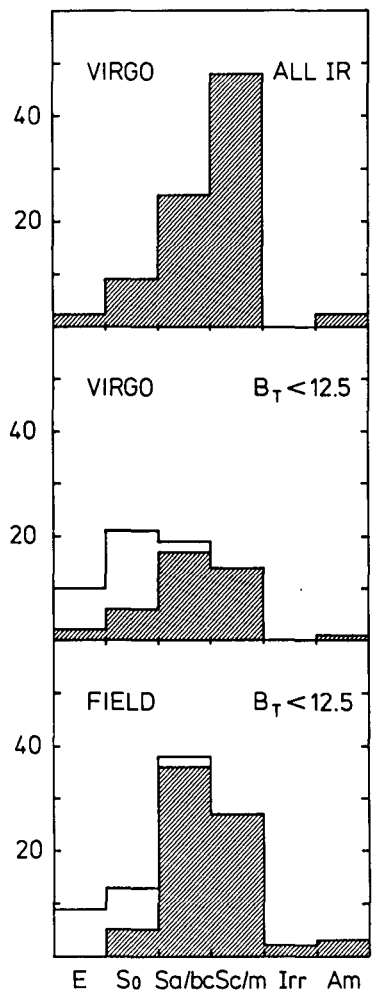


Figure 2
Infrared detection statistics of two samples of Virgo galaxies and of field galaxies as a function of morphological type. The hatched area represents the distribution of the galaxies detected by IRAS. The outer contour includes all galaxies in the sample

the outer contour includes all galaxies in the sample. The field sample consists of all RSA galaxies brighter than B_T = 12.5 in an area of sky delimited by 70° < λ < 130° and 250° < λ < 310° (where λ is the ecliptic longitude). Data for the latter sample were taken from a recent study by de Jong and Brink (1985).

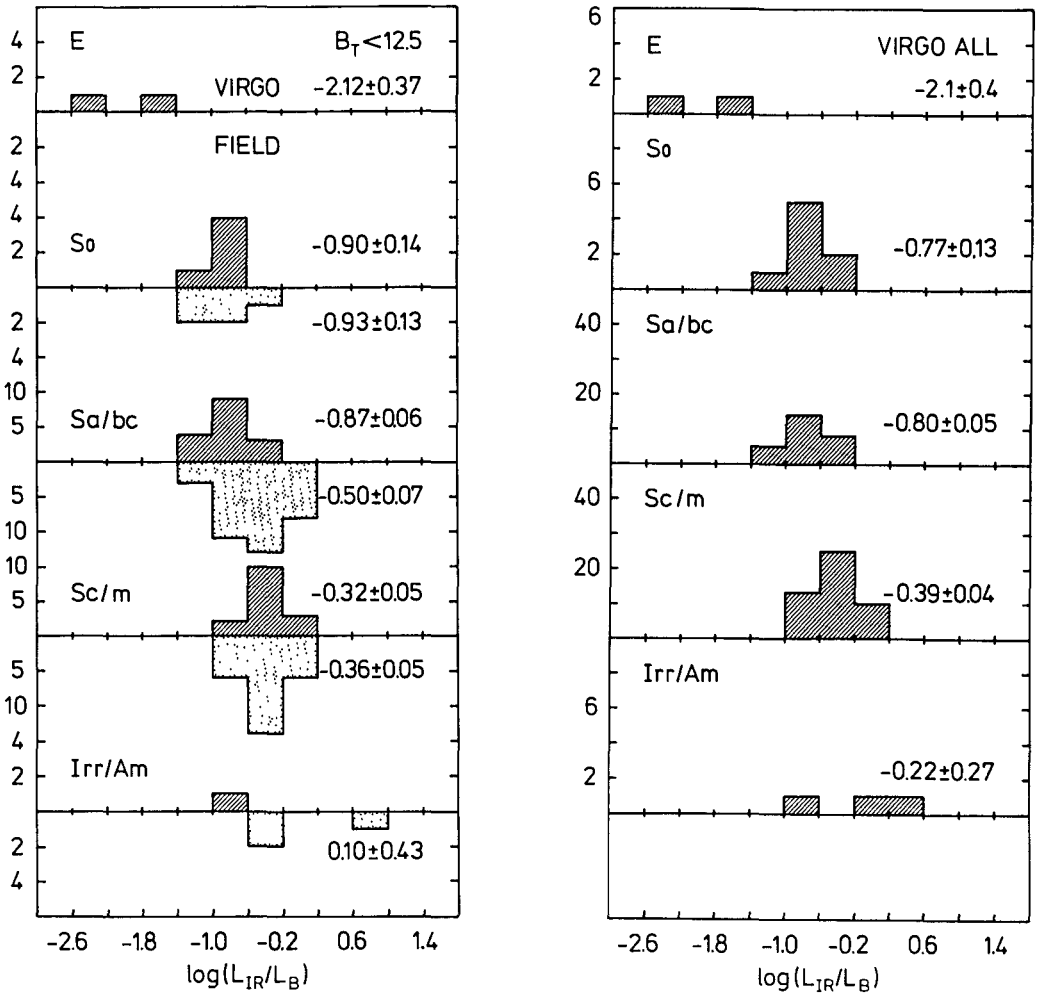
As has been known for a long time the Virgo cluster is richer in early-type galaxies, particularly in lenticulars, than the field. As discussed above the Virgo cluster also differs from the field in the infrared detection of two ellipticals. Otherwise the fractions of galaxies detected by IRAS are similar for cluster and field galaxies. All Sc spirals and later types are detected, about 95% of all early spirals are detected and about 30% of the lenticulars. These results are very similar to those obtained in the first IRAS study of field galaxies by de Jong et al. (1984). The detection statistics in fig.2 indicate that the star formation activity decreases going from late to early spirals.

On the basis of these results it appears that the detection probability of ellipticals may be related to the cluster environment. For instance it has been argued that ellipticals accrete matter from the hot intercluster gas observed in X-rays. Accretion rates of $\sim 10\ M_\odot\ yr^{-1}$ are estimated to occur in the centre of the Virgo cluster (Mathews and Bregman 1978), comparable in magnitude to the rate at which gas is lost by ellipticals in a galactic wind (see above). Since the accreting gas is enriched in heavy elements to about solar abundances (cf. Forman and Jones 1982) a relatively large amount of dust might condense out once it cools and fragments into filaments.

However such a scenario does not explain why M86, the optically second brightest elliptical in Virgo and also an X-ray source (Forman and Jones 1982), is not detected. As an alternative that might be consistent with all observations we offer the possibility that ellipticals in clusters, particularly the giant ones that usually reside in or close to the center where the galaxy density is highest, occasionally swallow irregular dwarf galaxies whose interstellar dust illuminated by the stars in the elliptical may be observed in the infrared as long as it survives.

To compare star formation rates in Virgo cluster and field galaxies we plot in fig.3 the distribution of the infrared excess for galaxies of different morphological type in the two samples. The infrared excess of a galaxy is defined as the ratio of its infrared to its blue luminosity. The infrared luminosity between 40 and 120 μm may to a very good approximation be calculated from the simple relation $L_{IR} = 1.2\ (L_{60} + L_{80})$, where L_{60} and L_{80} are the IRAS in-band 60 and 80 μm luminosities (Helou et al. 1984). The blue luminosity is obtained from B_T^0, the integrated blue magnitude corrected for internal absorption (galactic absorption is negligible in the direction of the Virgo cluster), by calculating the blue flux density and multiplying with the frequency of blue light ($\lambda = 0.44$ μm). The infrared excess has the advantage of being a distance-independent quantity.

The data in fig.3 show that the infrared excess of galaxies both in Virgo and in the field steadily increases along the Hubble sequence. Leaving the two ellipticals that have been discussed above aside this implies that the star formation activity gradually increases. Adopting the schematic two-component model of de Jong et al. (1984) we may explain the infrared excess of lenticulars, where no new stars are formed at present, as due to dust particles heated by the general interstellar radiation field. The magnitude of the infrared excess of ~ 0.1 is consistent with this picture because we expect in



Figures 3 and 4 Infrared excess distributions of optically complete samples of Virgo and field galaxies (fig.3) and of all Virgo cluster galaxies (fig.4) detected by IRAS as a function of morphological type. Averages and mean errors of $\log(L_{IR}/L_B)$ are indicated for each group

that case $L_{IR} \simeq \tau_B L_B$ with $\tau_B \simeq 0.1$ is the dust optical thickness of the disk of the galaxy. Proceeding to later morphological types the contribution of infrared radiation produced by newly-formed stars still embedded in the molecular gas and dust clouds from which they formed gradually increases.

The histograms in fig.3 further show that galaxies in the Virgo cluster and in the field are overall quite similar in their infrared properties. The only clear-cut exception are the early-type spirals. While early-type spirals in the field are intermediate between lenticulars and late-type spirals, as expected, in the Virgo cluster they behave identical to lenticulars. Thus at the present epoch less star formation is going on in early-type spirals in the Virgo cluster than in the field. The data in fig.3 show that the star formation rate in early-

type spirals in the Virgo cluster is more than two times smaller than in the field.

This result is similar but not as extreme as derived from a comparison of Hα data of Virgo cluster and field galaxies by Kennicutt (1983) who found that spirals of all types in Virgo are deficient in star formation. In an earlier more preliminary study of IRAS data of Virgo cluster galaxies (Brink and de Jong 1985) the anomalous behaviour of early-type spirals in Virgo was masked by the fact that all spirals were lumped into one group.

To investigate the generality of our results we have plotted in fig.4 the infrared excess distributions of all Virgo cluster galaxies detected by IRAS. A comparison of figures 3 and 4 shows that the infrared excess distribution of the infrared complete sample and of an optically complete sub-set are identical.

Ways to explain the lower star formation activity in Virgo cluster spirals have been discussed by Kennicutt (1983). Contrary to modern trends in cluster research (Haynes et al. 1984) Kennicutt concludes that recent rapid ram-pressure stripping of interstellar matter from the galaxy by a hot cluster gas cannot be the dominant mechanism. He proposes that the most probable way to explain this effect is by a slow depletion of gas from galaxies during their lifetime. Several mechanisms which could cause this slow depletion in a cluster environment are suggested.

One mechanism not mentioned by Kennicutt but possibly of importance in clusters of galaxies is depletion of gas by enhanced star formation during encounters of galaxies. The IRAS observations of galaxies demonstrate that this is a viable mechanism (Soifer et al. 1984). To investigate the situation in Virgo we have identified 10 galaxies among the 88 in our sample that are members of a close pair (separation less than 4 arcminutes). Seven of these are late-type spirals having an average infrared excess of $\log(L_{IR}/L_B) = -0.10 \pm 0.06$, significantly larger than the average value for late spirals as a group (see fig.4). Moreover the one amorphous galaxy in a close pair, NGC 4383 (Mark 769), has $\log(L_{IR}/L_B) = 0.25$, the largest value of all galaxies in our sample.

On the basis of these results it is attractive to speculate that encounters between galaxies in a cluster may have caused periods of enhanced star formation in spiral galaxies in the past. To be more specific, if we asume a galaxy density of about 1 Mpc^{-3} in the core of the Virgo cluster and a velocity dispersion of about 800 km s^{-1} it follows that each galaxy experiences one

encounter at 100 kpc (~5 galaxy radii) in 1 10^{10} yrs; such encounters last ~ 3 10^{8} yrs, about one galactic rotation period. While these encounters will not be as effective as those in galaxy pairs because they occur at higher relative velocities they might still induce enhanced star formation. In late-type spirals this may lead to minor fluctuations because the star formation rate is appreciable to start out with. In early-type spirals the effect may be more dramatic because the resulting enhanced supernova rate may set up a galactic wind which could drive interstellar matter out of an early-type galaxy more easily because of its low gas content. Such a scenario, however speculative and qualitative it may be, is in any case consistent with the main result of our analysis of infrared properties of Virgo cluster spirals: the deficiency of star formation in early-type spirals.

Early-type spirals in which star formation has come to a halt alltogether may turn into lenticulars. We note that a conversion of early-type spirals into lenticulars comes close to explaining the differences between the morphological type distributions of Virgo cluster and field galaxies in fig.2. Whether it can be made consistent with morphological criteria like bulge/disk ratios remains to be proven by detailed model calculations.

IV. CONCLUSIONS

Our exploratory study of IRAS observations of galaxies in the Virgo cluster core has produced the following results:

(1) 88 galaxies listed in the Virgo Cluster Catalog of Binggeli et al. (1985) are detected by IRAS.

(2) Among those there are two elliptical galaxies, M84 and M87, with derived dust masses of 30 000 and 3000 Msun. This dust has to be removed within 1 10^{6} to 1 10^{7} years. The most probable removal mechanism is sputtering in a galactic wind driven by supernova explosions.

(3) Apart from the ellipticals, none of which are detected among the field galaxies, the infrared detection probability of optically bright Virgo cluster and field galaxies are similar: about 30% of the lenticulars, 90% of the early spirals and all of the later-type galaxies are detected by IRAS.

(4) The infrared properties of Virgo and field galaxies are overall very similar, with the exception of early-type spirals. In the Virgo cluster early-type spirals experience more than two times less star formation than in the

field making them very similar in their infrared properties to lenticulars.

(5) We speculate that the anomalous behaviour of early-type spirals in Virgo may be related to the cluster environment which leads to periods of enhanced star formation during galaxy encounters causing enhanced consumption and possibly expulsion of interstellar matter.

ACKNOWLEDGEMENTS

I would like to express my thanks to the participants of the Virgo cluster workshop for a lively, interesting and very informative meeting. This paper has greatly benefitted from their contributions. Dr. B. Binggeli kindly made the Virgo Cluster Catalog availabele before publication. I thank Karel Brink for a critical reading of the paper.

REFERENCES

Binggeli, B., Sandage, A., and Tammann, G.A. 1985, Astron. J. in press

Bregman, J.N. 1978, Astrophys. J. 224, 768

Brink, K., and de Jong, T. 1985, Proceedings of the 8th European Regional IAU Meeting, Toulouse, in press

de Jong, T., and Brink, K. 1985, in preparation

de Jong, T., Clegg, P.E., Soifer, B.T., Rowan-Robinson, M., Habing, H.J., Houck, J.R., Aumann, H.H., and Raimond, E. 1984, Astrophys. J (Letters) 278, L67

de Vaucouleurs, G., and de Vaucouleurs, A. 1973, Astron. Astrophys. 28, 109

Dressler, A. 1984, Ann. Rev. Astron. Astrophys. 22, 185

Faulkner, D.J., and Freeman, K.C. 1977, Astrophys. J. 211, 77

Forman, W., and Jones, C. 1982, Ann. Rev. Astron. Astrophys. 20, 547

Gisler, G.R. 1979, Astrophys. J. 228, 385

Gillett, F.C., de Jong, T., Neugebauer, G., Rice, W., and Emerson, J.P 1985, in preparation

Haynes, M.P., Giovanelli, R., and Chincarini, G.L. 1984, Ann. Rev. Astron. Astrophys. 22, 445

Helou, G., Good, J., and Lonsdale, C. 1984, JPL IOM SOTS-84-088

Helou, G. 1985, this volume

Kennicutt, R,C. 1983, Astron. J. 88, 483

Kotanyi, C.G., and Ekers 1983, Astron. Astrophys. 122, 267

Mathews, W.G., and Bregman, J.N. 1978, Astrophys. J. 224, 308

Neugebauer, G., Habing, H.J., van Duinen, R.J., Aumann, H.H., Baud, B., Beichman, C.A., Beintema, D.A., Boggess, N., Clegg, P.E., de Jong, T., Emerson, J.P., Gautier, T.N., Gillett, F.C., Harris, S., Hauser, M.G., Houck, J.R., Jennings, R.E., Low, F.J., Marsden, P.L., Miley, G.K., Olnon,

F.M., Pottasch, S.R., Raimond, E., Rowan-Robinson, M., Soifer, B.T., Walker, R.G., Wesselius, P.R., and Young, E. 1984, Astrophys. J. (letters) 278, L1

Neugebauer, G., Soifer, B.T., Rice, W., Rowan-Robinson, M. 1985, Publ. Astron. Soc. Pac., in press

Sandage, A. and Tammann, G.A. 1981, A Revised Shapley-Ames Catalog of Bright Galaxies, Carnegie Institution of Washington Publ. 635, Washington D.C.

Soifer, B.T., Rowan-Robinson, M., Houck, J.R., de Jong, T., Neugebauer, G., Aumann, H.H., Beichman, C.A., Boggess, N., Clegg, P.E., Emerson, J.P., Gillett, F.C., Habing, H.J., Hauser, M.G., Low, F.J., Miley, G.K., and Young, E. 1984, Astrophys. J. (Letters) 278, L71

Young, E., Soifer, B.T., Low, F.J., Neugebauer, G., Rowan-Robinson, M., Miley, G.K., Clegg, P.E., de Jong, T., Gautier, T.N. 1984, Astrophys. J. (Letters) 278, L75

DISCUSSION

J. HUCHRA: I don't think you have to worry about the identification of M87 as the source - the other two faint galaxies (one UGC "galaxy") are not particularly spectroscopically peculiar whereas all of the other faint strong IRAS galaxies in the mini survey are starbursters and show strong H_α emission.

T. DE JONG: That is reassuring. Thank you.

AN IRAS SURVEY OF BRIGHT SPIRALS IN VIRGO

by

George Helou

Jet Propulsion Laboratory/California Institute of Technology

Pasadena, CA

Abstract: This paper presents preliminary results on the analysis of IRAS data for an optically complete sample of spiral galaxies in and around the Virgo Cluster.

The population of galaxies in the cluster core (5° radius) is indistinguishable statistically from the population surrounding the core in terms of far infrared to blue ratio; but in terms of infrared fluxes, the core galaxies dominate the sample, and allow the Virgo Cluster to be easily identified on an all-sky map of IRAS sources (see the cover of these proceedings). The interpretation of these statistical properties are unfortunately complicated by the well known morphological stratification in the Cluster.

A good correlation is established between the 60 μm/100 μm color of galaxies and the mean HI surface density in their disks. The correlation between infrared to blue ratio and infrared color is seen tighter here than in de Jong et al 1984 (Ap.J.(Letters) 278, L67). It is defined by galaxies with a "normal" neutral hydrogen content; galaxies severely depleted (by a factor about 10 or more) in HI fall clearly below that correlation, and are therefore substantically deficient in infrared emission for their infrared color and their blue luminosity. This is not surprising, since HI depletion will lead to lowered dust contents; but the quantitative details of the infrared deficiency (and possible infrared color changes) can discriminate between various models for the depletion mechanisms in HI and infrared.

These results are being prepared for publication in the Astrophysical Journal.

The Infrared Astronomical Satellite (IRAS) was developed and operated by the Netherlands Agency for Aerospace Programs (NIVR), the United States National Aeronautics and Space Administration (NASA), and the United Kingdom Science and Engineering Research Council (SERC). This work was supported at the IRAS Project of the Jet Propulsion Laboratory, of the California Institute of Technology, under contract with NASA.

A NEAR-INFRARED SURVEY OF BRIGHT VIRGO SPIRAL GALAXIES

R.D. Joseph
Imperial College (London)

T.G. Hawarden
Royal Observatory, Edinburgh

Ian Gatley
United Kingdom Infrared Telescope

1. Introduction. One of the major discoveries following the advent of IR astronomy is that the nuclei of many spiral galaxies exhibit large far-IR (i.e. 10-100 μm) luminosities. This "IR activity" is commonly interpreted in terms of a recent burst of star formation. The optical and ultra-violet radiation from massive early-type stars, whose output dominates the luminosity, is largely absorbed by dust associated with the star-formation regions, and re-radiated in the IR.

We know little about the luminosity function of these "starbursts," or how they are correlated with other galaxy properties. One of the most interesting recent attempts to address this question was an IR survey by Becklin, Scoville, Young & Capps (1983) of the 60 spiral galaxies in the Virgo cluster listed in the Revised Shapley-Ames Catalog (Sandage & Tamman 1981). They observed 53 of these galaxies to a uniform sensitivity at 10 μm wavelength. Although they only achieved signal-to-noise ratios > 2 σ for 18 of the 53 galaxies they observed, they made a statistical argument to show that virtually all the galaxies they had observed showed significant 10 μm excesses. They interpreted these excesses in terms of recent star formation, and concluded that star formation activity is occurring in the nuclei of all Virgo spirals, and is uncorrelated with Hubble type or any other large-scale property of these galaxies.

This is a surprising and exciting result, and if true, has far-reaching implications for astrophysics. It is therefore profoundly important that this result be confirmed, especially considering the low signal-to-noise data on which it is based.

2. IR Activity and K-L' Colour Excess. It is clearly desirable to repeat the Becklin et al. (1983) survey at 10 μm, with a significant improvement in

detection sensitivity so that (if the Becklin et al. conclusions are correct) a larger fraction of the galaxies are detected at good signal-to-noise ratio. However even a factor of 3 improvement would require allocation of at least two weeks of large telescope time, an allocation which is probably impossible to obtain. We therefore took another approach. Rather than to work at 10 μm, where sensitivity is most severely limited by photon noise in the emission from the ambient temperature telescope optics, we chose to repeat the survey in the near-IR, working in the JHKL' wavebands (1.2, 1.6, 2.2, and 3.8 μm). We then looked for a K-L' colour index significantly redder than normal galaxy colours as an indication of "IR activity" (cf. Joseph, Meikle, Robertson & Wright 1984). IR colours of "normal" galaxies (e.g. early-type galaxies, spiral bulges) are those of the late-type stars which dominate the light from a galaxy (cf. Joseph et al. 1984 and references therein):

$$J-H = 0.75$$
$$H-K = 0.25$$
$$K-L' = 0.25$$

IR activity will therefore be evident if the K-L' colour index is > 0.3, as illustrated in Fig. 1. By obtaining the mean K-L' colours of various subsets of the Virgo spirals we can investigate the incidence of IR activity in these galaxies.

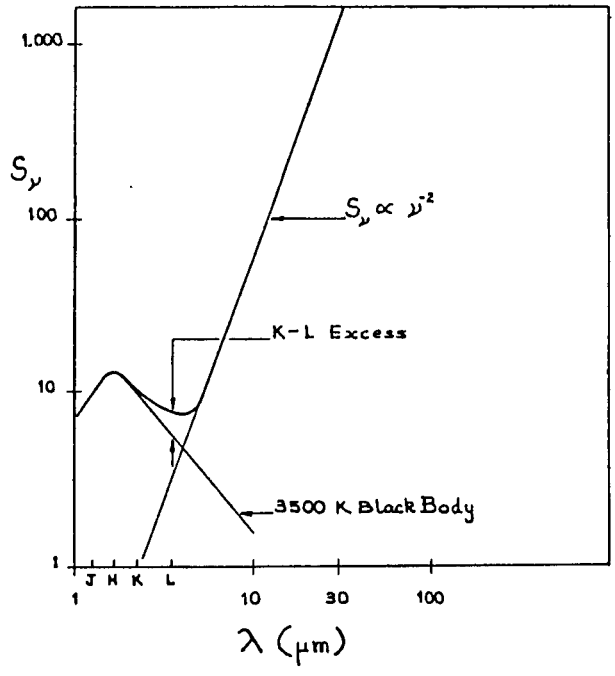


Fig. 1 Illustration of the relationship between a steeply rising far-infrared continuum spectrum and a K-L colour excess.

The major advantage of this observational approach is that detection sensitivity at L' is about 20 times better than that at 10 μm, whereas even the most steeply -rising IR continuum spectrum of "active" galaxies would give a flux density at 10 μm only about 7 times that at L'. Thus we should gain at least a factor of 3 in relative signal-to-noise ratio by working with the K-L' colour index, or a factor of 10 in telescope observing time. In addition one can find the position on the galaxy where the IR signal peaks, and carry out the photometry at this position. (Working at 10 μm one must observe the optical nucleus, if it can be found, and hope that extinction effects have not displaced the optical peak from the IR peak). A disadvantage of the near-IR approach is that one has only qualitative information on the IR luminosity.

3. Observations. The observations were made with the 3.8 m UK Infrared Telescope on Mauna Kea. We used an 8 arcsec aperture, which corresponds to ~ 800 pc at the distance of the Virgo cluster, and a chopper throw of ~ 60 arcsec. We measured the JHKL' magnitudes for 56 of the 60 spiral galaxies listed in the Revised Shapley-Ames Catalog as members of the Virgo cluster or region. The JHK colours are accurate to 2-3%. We achieved signal-to-noise at L' generally in excess of 15, and so the K-L' colours should be accurate to better than .7%.

4. Results and Discussion. The HKL' colours for the entire sample are shown in the two-colour diagram in Fig. 2. The open and filled circles in this diagram represent early and late type spirals, and the horizontal lines denote barred galaxies.

It is evident that at least a third of the sample have significant K-L' colour excesses indicative of nuclear IR activity. It is also clear that there are distinct correlations with morphological types. The tendency toward a K-L' colour excess is very pronounced for late-types, compared to early types, and extremely so for late-type barred spirals. These impressions are made more quantitative in Table 1. If we adopt a criterion that K-L' >0.45 is an indication of IR activity, as exemplified by the continuum spectrum in Fig. 1, then we see that 40% of the late-type normal spirals and 80% of the late-type barred spirals are undergoing nuclear IR activity.

In Table 2 we have presented the mean K-L' colour indices for various subsets of the sample. The subsets with some evidence for K-L' colour excesses indicative of nuclear IR activity are the late types, those more than 4 degrees away from M87 (i.e. the cluster centre), and especially the late-type barred galaxies. These groups are perhaps just those one might naively have expected to show such

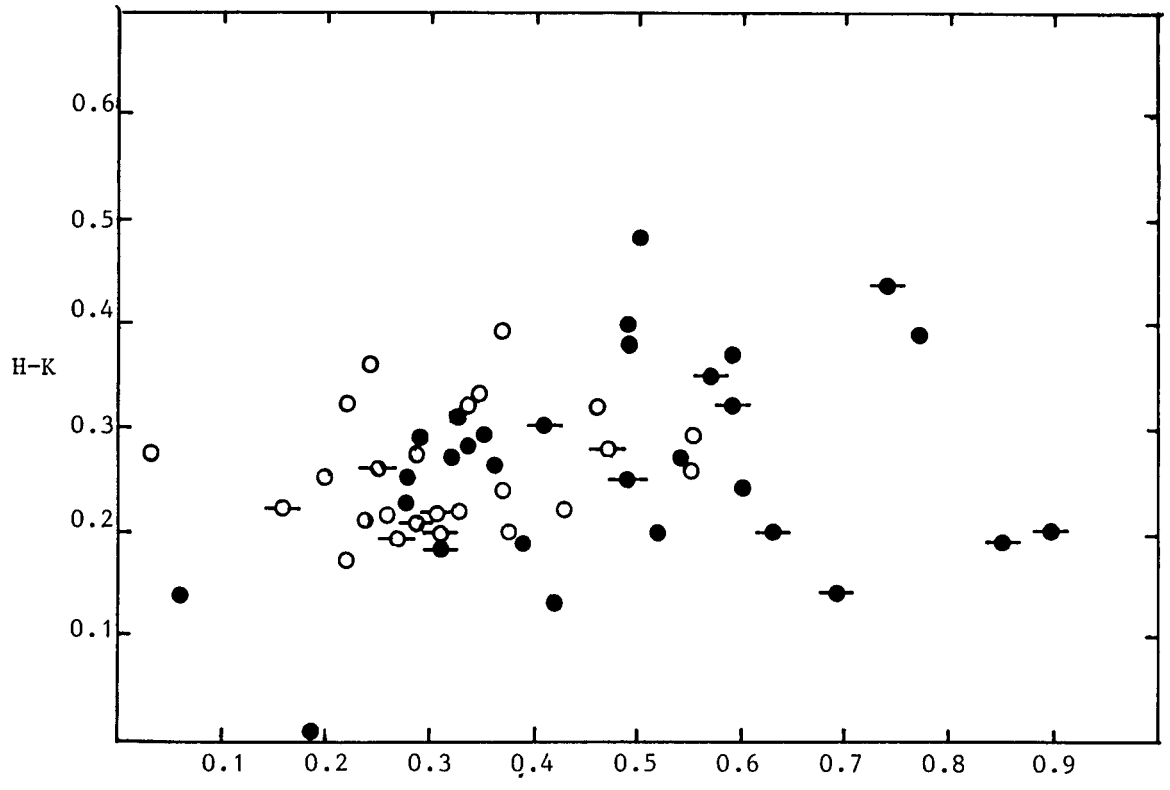


Fig. 2. HKL colours of Virgo cluster spiral galaxies. Open circles are early-type galaxies and filled circles are late-type. Horizontal bars denote barred galaxies.

Table 1. Galaxies with a K-L' Excess

Subset	Number	Number with Excess	Percentage
Sa, Sab, Sb	20	4	20%
SBa, SBab, SBb	6	1	16%
Sbc, Sc, Sd	20	8	40%
SBbc, SBc	10	8	80%

nuclear IR activity. In particular, on both theoretical (e.g. Huntley 1980) and observational (e.g. Meaburn, Terrett, & Walsh 1981) grounds one expects that the dynamical instabilities which are associated with formation of a bar will result in flow of material down the bar toward the nucleus, thus fuelling nuclear activity such as star formation.

Table 2. Mean K-L' Colours of Various Subsets of Virgo Spirals

Subset	Number	<K-L'>
Sa, Sab, Sb	19	0.32 ± 0.03
Sbc, Sc, Sd	20	0.41 ± 0.04
SBa, SBab, SBb	6	0.29 ± 0.05
SBbc, SBc	10	0.62 ± 0.06
$<4^{o}$ from M87	30	0.37 ± 0.03
$>4^{o}$ from M87	25	0.45 ± 0.04

However, there are systematic biases in the morphological makeup of this galaxy sample which make interpretation of these correlations between K-L' colour index and morphological type less straightforward than might be expected. In Fig. 3 we have plotted the K-L' colour as a function of K, with morphological class denoted as in Fig. 2. It is immediately evident from this figure that most of the faint galaxies in the sample are late morphological types and most of the bright galaxies are early-types. This bias makes it impossible to exclude, for example, the possibility that there is a component of non-stellar IR activity in (generally brighter) early-type galaxies as strong as that in (generally fainter) late-type spiral galaxies in the Virgo cluster. Such a component would be small compared to the stellar flux density at L' in bright galaxies, but could dominate the stellar flux in faint galaxies. Correlations between the K-L' colour index and morphological type such as those in Table 2 could therefore be an artifact of this bias, if the emission due to IR activity were small.

To investigate more quantitatively the relation between IR activity and other galaxy properties we have calculated the excess flux density at L' over that due to the stars. We have assumed that the colour index of the stellar continuum is K-L' = 0.25. This excess, $S_{ex}(L')$, is plotted against the nuclear magnitude at

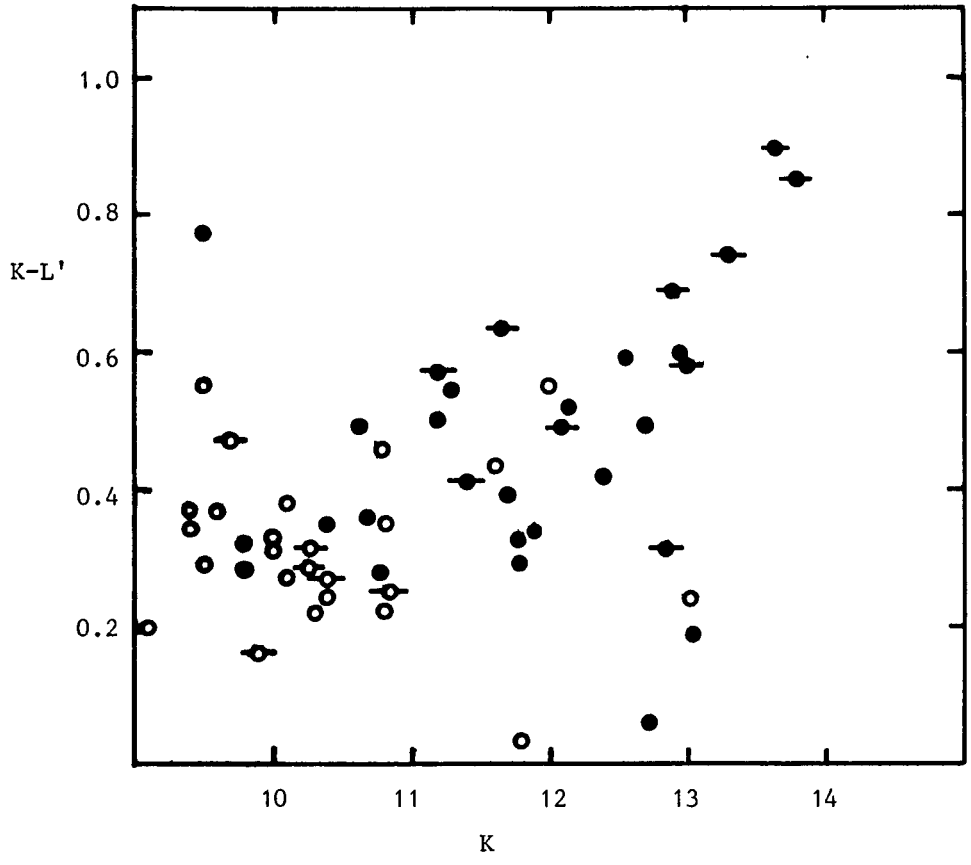


Fig. 3. Colour-magnitude diagram for Virgo spirals. Symbols as in Fig. 2.

H in Fig. 4. Since the stellar spectrum peaks at H, the H magnitude is essentially a measure of the stellar density. Two conclusions can be drawn from this figure. (1) There are IR excesses at L' for most of the galaxies, but certainly not for all of them. (2) The IR excesses correlate more strongly with the number of stars present than with any other galaxy property.

In summary, JHKL' IR photometry is a powerful and efficient tool to investigate IR activity, such as that due to recent star formation, in the nuclei of galaxies. Preliminary analysis of our data for the 60 bright spirals in the Virgo cluster indicates that IR excesses are common, but not universal in these galaxies, and the IR excesses tend to correlate with the stellar density in the nucleus.

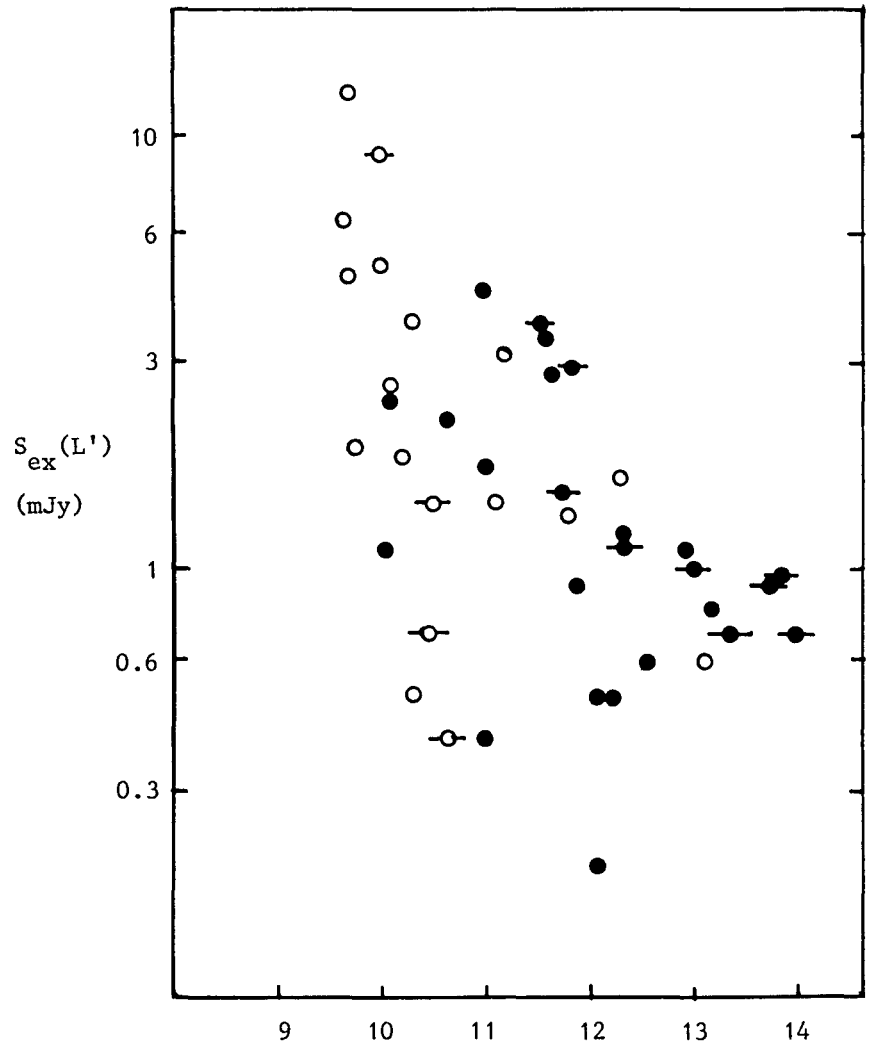


Fig. 4. Excess (i.e. non-stellar) flux density at 3.8 μm vs. H magnitude. Symbols as in Fig. 2.

References

Becklin, E.E., Scoville, N.Z., Young, Judith S. & Capps, R.W. 1983, Ap.J., 271, 512.

Huntley, J.M. 1980, Ap.J., 238, 524.

Joseph, R.D., Meikle, W.P.S., Robertson, N.A. & Wright, G.S. 1984, Mon.Not.R. astr.Soc., 209, 111.

Meaburn, J.M., Terrett, D.L., & Walsh, J.R. 1981, Mon.Not.R.astr.Soc., 195, 39.

Sandage, A. & Tamman, G.A. 1981, A Revised Shapley-Ames Catalog. (Washington: Carnegie Institution).

INFRARED OBSERVATIONS OF DWARF ELLIPTICAL GALAXIES IN THE VIRGO CLUSTER

H Zinnecker, R D Cannon, T G Hawarden, and H T MacGillivray
Royal Observatory, Blackford Hill, Edinburgh, Scotland EH9 3HJ

Abstract

We have obtained JHK photometry of a sample of 10 'nucleated' dwarf elliptical galaxies (dE,N) in the Virgo cluster. The galaxies have been selected from the list of Bingelli, Sandage, and Tarenghi with total B-magnitudes spanning the range 14-17. With the aid of COSMOS, the accuracy of the coordinates of the object centres could be improved to the 1 arcsec level. The infrared data were secured with UKIRT using a 20 arcsec aperture which included most of the light of the objects. It was found that the J-H vs. H-K colour-colour diagram of the dE,N sample is distinctly different from the corresponding diagrams of both the central regions of giant elliptical galaxies and metal-poor galactic globular clusters. The infrared data suggest that the stellar content of dE,N galaxies may be similar to that of fairly metal-rich globular clusters such as M69, and to that of the outermost parts of giant ellipticals.

We were also able to deduce an optical-infrared (B-H) colour for 8 of the 10 dE,N galaxies. The results indicate that the B-H colour of the Virgo dwarf ellipticals is systematically bluer, by 1.0-1.5 mag, than the more luminous elliptical galaxies confirming a similar result of Bothun and Caldwell. It seems that the admixture of a small fraction of younger stars is required to reconcile the B-H colour with the J-K colours. It appears that some star formation occurred in these galaxies up to 3-5 Gyr ago. This conclusion is strengthened by showing that these colours can be reproduced by the superposition of the corresponding colours of the old and intermediate age star clusters in the Magellanic Clouds.

Besides the dE,N study, JHK photometry of two blue compact Virgo dwarf galaxies is reported.

1. Introduction

Little is known about dwarf galaxies beyond the Local Group (eg Tammann 1980), yet an understanding of the properties of these systems may hold important clues to galaxy formation in general (eg Jones 1980). Apart from data on

structural properties, vital information is required on their age, metal abundance, and the nature of their stellar population. Photometric observations of the integrated light from a sufficiently large sample of dwarf galaxies, in the optical and the near infrared, are essential to learn more about these composite stellar systems. In this paper, we will report on infrared photometric observations of ten dwarf elliptical galaxies located in the central region of the Virgo Cluster.

A catalogue of 846 dwarf galaxies (75% of which are dwarf ellipticals) has recently been published by Reaves (1983) covering approximately 200 square degrees in the Virgo Cluster region. The data are based on Palomar 1.2m Schmidt long exposure IIIaJ plates (platescale 67 arcsec/mm) and were taken by A. Sandage in 1976. On the other hand, Sandage in 1979 began a photographic survey at Las Campanas of the Virgo Cluster region using the 2.5m du Pont reflector (plate scale $\sim$ 11 arcsec/mm on 50 x 50 cm plates). This is soon to result in a complete Virgo dwarf galaxy catalogue covering most of a 6° radius around the adopted Virgo Cluster centre at $\alpha(1950) = 12^h25^m$ and $\delta(1950) = 13°06$. In the meantime, Binggeli, Sandage, and Tarenghi (1984) (BST) have published a representative list of $\sim$ 100 dwarf galaxies in the Virgo cluster near the cluster centre to be used as photometric standards for the complete survey. These include $\sim$ 50 dwarf ellipticals (dE), many of which are nucleated (dE,N), i.e. their light distribution exhibits a very pronounced peak at the centre, unresolved on the du Pont plates at the 1 arcsec scale. Some 50% of the BST sample are also Reaves objects. Our sample was chosen from BST (almost exclusively dE,Ns). Half of the dE,N galaxies under study here can be seen in Fig. 9 of BST. The advantage of choosing BST objects is that while Reaves estimated the morphology and the total B-magnitudes of the objects in his catalogue, BST fitted King profiles to the B luminosity distribution of the individual dwarf galaxies. This allows us to calculate the B-flux through the aperture used for the infrared observations and thus to derive not only infrared colours (J-H, H-K) but also a B-H colour (since UBV photometry does not yet exist for the Virgo dwarf galaxies, the commonly used V-K colour cannot be constructed). Note that the B-magnitude of the objects in our sample corresponds approximately to the Local Group M31 dE companions NGC 147, NGC 185, and NGC 205 placed at the distance of the Virgo Cluster ($\sim$ 20 Mpc), while the Milky Way companion 'Fornax' (the brightest dwarf spheroidal satellite) would be somewhat too faint to be in our sample. Note also that the metal abundance of the Local Group dwarf systems (masses 10^8 - $10^9 M_\odot$) is roughly a tenth solar (see eg Table 3 in Vigroux, Chièze and Lazareff, 1981).

The present work extends previous work by Frogel et al. (1978) and by Bothun and Caldwell (1984). Frogel et al. presented infrared photometric observations of the central regions of 51 E/SO galaxies and of 5 galactic globular clusters. Bothun and Caldwell have obtained JHK photometry and the B-H colour for 2 dwarf elliptical galaxies in the Virgo Cluster, namely N4472 Dw8 and N4472 Dw10; they have also obtained the B-H colour for 8 additional dwarf ellipticals near M87. We will compare our results with those of these authors in Section 4.

We first describe the observations (Section 2), then present our results (Section 3) and their discussion (Section 4). We summarise our findings in Section 5. Fuller details of our observational procedures and the complete set of data will be published elsewhere.

2. Observations

The observations were made on the nights of 1984 March 12-14 with the 3.8m United Kingdom Infrared Telescope (UKIRT) on Mauna Kea, Hawaii, under good seeing conditions. We used the infrared system known as UKT 5 which incorporates the usual InSb infrared detector and broad-band infrared filters at J (1.2μm), H (1.6μm), and K (2.2μm). The aperture chosen was 20 arcsec corresponding to 50-90 per cent of the angular size of our objects. The beam profiles for the J,H and K filters were measured by orthogonal scanning of a star across the focal-plane aperture for each of the filters.

Prior to the observing run, precise coordinates of the centres of the dwarf galaxies had to be generated, since many of the objects are too faint to be seen directly. The coordinates given in the list of BST are accurate to ±10 arcsec which is not sufficient for our purpose. Higher accuracy (±1 arcsec) was achieved by measuring the positions of the objects on a glass copy of the deep UK Schmidt plate J2137 of the Virgo field, using the automated plate measuring machine COSMOS at the Royal Observatory, Edinburgh.

We obtained good photometry for ten galaxies and some data for another half dozen. Most have $13.5 < K < 14.5$, and we obtained infrared colours accurate to ± 0.05 mag. Total integration times were around 15 minutes per filter for the fainter galaxies.

In order to tie in with the published JHK photometry of E/SO galaxies (Frogel et al. 1978, hereafter FPAM) we have remeasured some of these galaxies using

the same aperture and the same chopper throw as for the dE,Ns. The comparison of infrared magnitudes and colours between our measurements and those by FPAM is satisfactory. The values of the colours observed by FPAM have all been transformed from the CTIO system to the UKIRT system.

While the J-H colours agree reasonably well, there appears to be a systematic difference regarding the H-K colour in the sense that our colours are bluer than FPAM's colours by about 0.04 mag on average. This suggests that our K-magnitudes may be systematically too faint by 0.04 mag and should be revised accordingly. Investigation of this problem revealed that the reason for this systematic error probably lies in our distorted K-filter beam profile.

For the data given in Table 1 below we have retained our instrumental system of H-K colours and K-magnitudes. On the other hand, the data plotted in the figures are all corrected by 0.04 mag in K to take into account the systematic effect that was noted above.

3. Results

3.1 Basic Data

The basic data resulting from our observations are presented in Table 1, which is divided into the following columns:

(1) : Number under which the objects were listed in BST.
(2,3) : Name and type of the objects, respectively.
(4,5) : Right ascension and declination, as obtained from COSMOS.
(6) : Total B-magnitude from BST (except last 3 entries)[a].
(7) : Radius (in arcsec) containing half the blue light.
(8) : K (2.2μm) flux within 20 arcsec diameter circular aperture[b].
(9,10) : Infrared colours J-H and H-K, respectively (uncorrected).
(11) : Optical-infrared colour B-H, calculating the B-magnitude within a 20 arcsec aperture by using the fitted King profiles from BST.

a The B-magnitudes for the two BCDs (= blue compact dwarf galaxies) are from Sandage and Binggeli (1984), while B(tot) for the last entry, N 4472 Dw8, is from Caldwell (1983).

b Except for the two BCDs for which a circular aperture size of 12 arcsec was used, and for N4472 Dw8 which was measured through an 8 arcsec diameter aperture.

In Table 1, a total of 13 dwarf galaxies with newly observed JHK photometry is listed. The main group comprises 10 dE,N objects, listed in order of

TABLE 1. Infrared Photometry of Virgo dwarf galaxies

BST No.	Name	type	RA(1950)	DEC(1950)	B(tot)	$r_{half-light}$	K(mag)	J-H	H-K	B-H
6	13°50	dEO,N	$12^h23^m34^s.53$	13°08'15".7	17.00	8".7	14.51±0.03	0.69±0.04	0.10±0.04	3.03
11	I3349	dE1,N	12 24 14.90	12 43 48.9	14.93	14.8	13.49±0.02	0.74±0.04	0.09±0.04	2.73
34	I794	dE3,N	12 25 36.46	12 22 10.1	14.12	17.0	12.26±0.09	0.72±0.07	0.19±0.10	3.15
37	13°66	dE6,N	12 25 51.68	13 28 20.2	15.94	13.2	14.56±0.05	0.74±0.05	0.12±0.06	2.33
38	I3388	dE4,N	12 25 56.08	13 06 00.4	15.31	-	13.40±0.02	0.68±0.02	0.12±0.02	
50	13°71	dE5,N	12 26 43.00	13 15 16.7	16.06	8.1	13.94±0.05	0.71±0.04	0.09±0.06	2.45
51	12°52	dE1,N	12 26 51.61	12 43 36.7	15.56	14.5	13.66±0.02	0.74±0.03	0.13±0.03	3.12
71	12°62	dE2,N	12 28 47.74	13 00 50.3	16.49	7.9	14.15±0.03	0.62±0.04	0.08±0.04	2.59
74	10°43	dE2,N	12 29 14.49	10 56 59.6	17.10	-	14.64±0.06	0.73±0.04	0.07±0.07	
77	I3470	dE0,N	12 29 51.53	11 32 16.8	14.29	-	11.74±0.01	0.74±0.01	0.13±0.01	
	I3457	?	12 29 19.64	12 55 58.0	15.0	-	13.78±0.03	0.73±0.04	0.04±0.04	
	N4641	BCD	12 40 36	12 19 24	14.12		12.71±0.02	0.67±0.02	0.27±0.02	
	A1235+08	BCD	12 35 09	8 50 00	14.51		14.49±0.05	0.62±0.05	0.31±0.06	
	N4472Dw8	dE,N	12 27 33	8 21 03	15.68		14.04±0.06	0.70±0.03	0.07±0.06	3.60

Note: All K-magnitudes and colours refer to a 20 arcsec diameter circular aperture except those for the last 3 entries. For the two BCDs a circular size of 12 arcsec was used, and N4472 Dw8 was measured through an 8 arcsec diameter aperture.

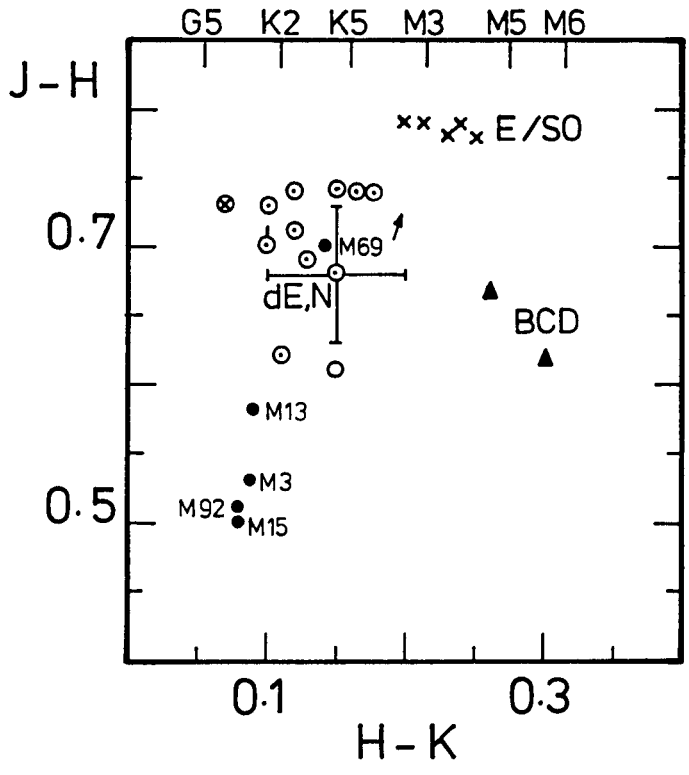


Figure 1: Infrared colour-colour diagram for our sample of nucleated dwarf elliptical galaxies (dE,N) in the Virgo Cluster. dE,N objects are characterised by circled points. The circled point with flag is N4472 Dw8 and the circle with the cross inside is I3467. Crosses indicate our control data on giant elliptical galaxies (E/SO) which are on the same photometric system (UKIRT). Filled circles represent galactic globular cluster data from Frogel et al. (1978, FPAM) transformed to our photometric system and corrected for reddening. The open circle gives the colour coordinates for the Local Group dE N205 (data from Table 4 of FPAM). The colours of the two blue compact dwarf galaxies (BCD) in Virgo - N4641 on the left, A1235+08 on the right - are also plotted as triangles. These were obtained as Service Observations on UKIRT.

Typical error bars (±0.05 mag in each colour) are shown. The Virgo data have been corrected for redshift but not for reddening. (A reddening vector is indicated, though). Spectral types are marked on the top.

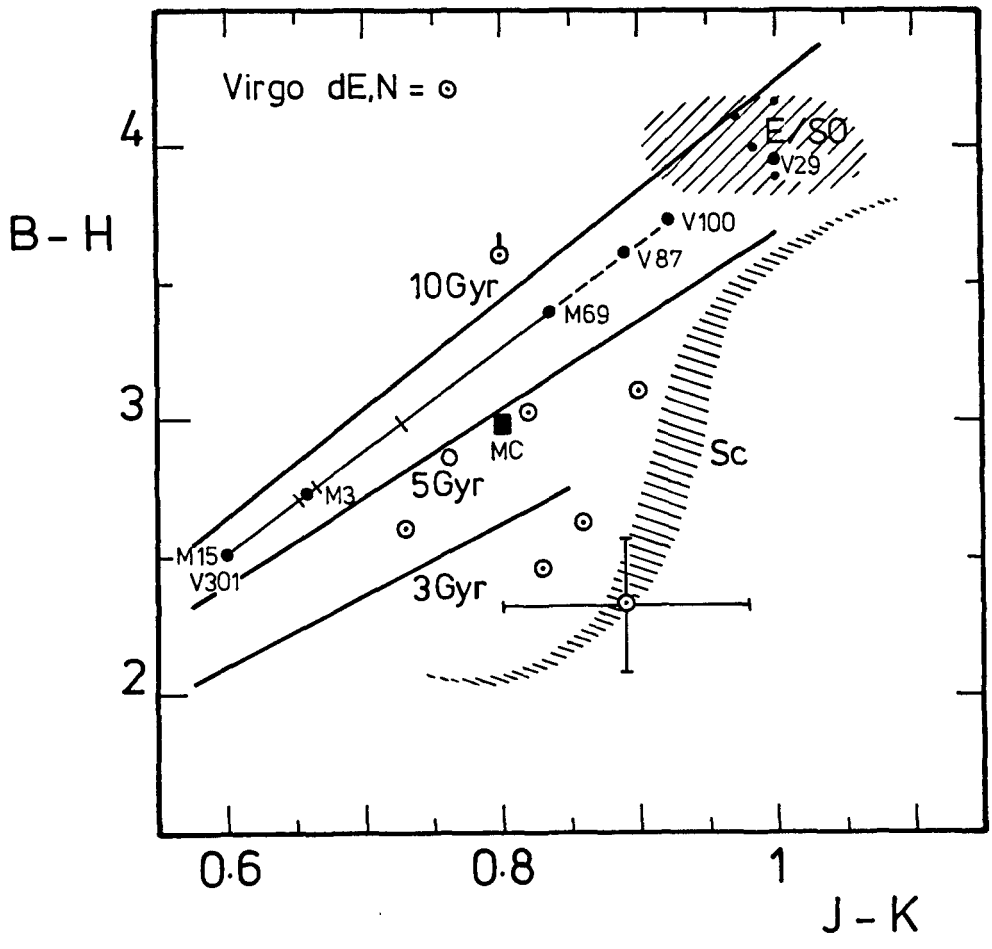


Figure 2: Colour-colour diagram showing the location of the Virgo dE,N galaxies in comparison with the location of a number of other systems: (i) E/SO galaxies (Frogel et al. 1978), indicated by the shaded elliptical area; (ii) Sc galaxies, indicated by the shaded S-shaped area (Bothun et al. 1984); (iii) galactic and M31 globular clusters, indicated by Messier number and Vetesnik number, respectively. Note the very red cluster V29 which, together with four very red NGC 5128 globular clusters (Frogel 1984), lies in the region occupied by the metal-rich E/SO galaxies. The circled point with flag is N4472 Dw8. The open circle is N205. The black square gives the mean colours of 15 old and intermediate age globular clusters in the Magellanic Clouds (Persson et al. 1983). The heavy lines, labelled 3,5, and 10 Gyr, are from Bothun et al. (1984) and represent model predictions of single age populations (with ages as labelled) as a function of metallicity (metallicity increasing along the lines towards the right).

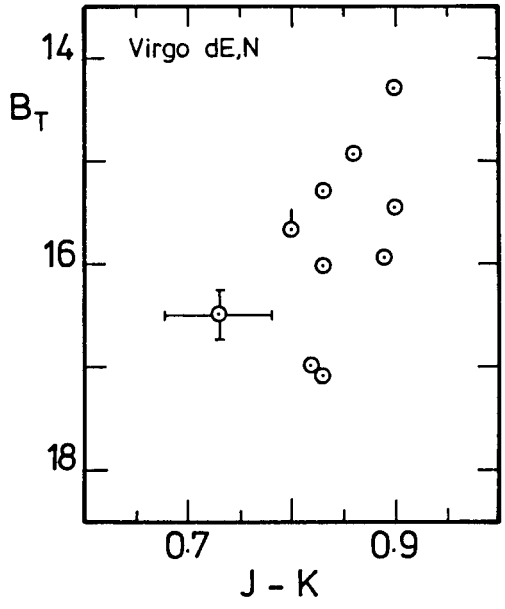


Figure 3a: Colour-magnitude diagram for our sample of nucleated dwarf ellipticals (dE,N) the Virgo Cluster. A typical error box is indicated.

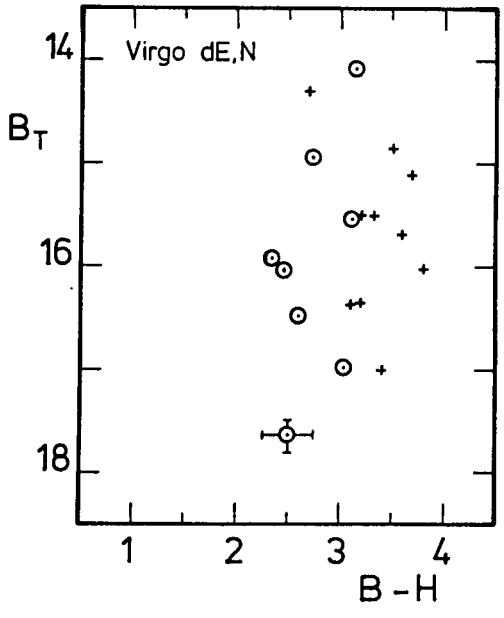


Figure 3b: Colour-magnitude diagram for our sample of Virgo dE,N galaxies (circled points) and for Bothun and Caldwell's sample of Virgo dE,N galaxies (crosses). The B-H colours for the former refer to a 10 arcsec aperture, those for the latter to a 9 arcsec aperture. A typical error box is indicated. Note the offset in B-H between the two samples.

increasing RA. The rest (the unclassified object I3457, the two blue compact dwarfs, and one of Caldwell's N4472 dE,N satellites which we remeasured) are separately listed.

Note that the two BCDs were obtained as Service Observations using UKT 6 on UKIRT in May 1984, not during the main run described above, but that the data were reduced similarly and should be directly comparable.

3.2 J-H vs. H-K diagram

Fig. 1 shows the infrared colour-colour diagram for 9 objects from our sample of 10 Virgo dE,Ns (I794 was excluded because of the large error in its colours). Furthermore N4472 Dw8 and I3467 are shown, as is the Local Group dE N205. Also plotted are the two BCDs which are relatively blue in J-H but surprisingly red in H-K. The five E/SO galaxies which were measured with the same equipment as the dE,Ns are slightly but distinctly redder in both colours than the bulk of the dE,Ns. However, it must be noted that the E/SO colours represent the colours of the inner parts of those galaxies, i.e. within a 1 kpc radius from the centre corresponding to our 20 arcsec aperture at the distance of the Virgo Cluster (4 kpc radius for N1700), while the colours for the dE,Ns are representative for the whole of these stellar systems. From the multi-aperture data of FPAM it appears that the E/SO colours approach the dE,N colours when the colour corrections for larger apertures are extrapolated to the full size of the E/SOs (see however Glass 1984 who does not find such a colour gradient effect in a different sample of galaxies). Five galactic globular clusters, labelled with their Messier numbers, with infrared data taken from FPAM, complete the stellar populations represented in Fig. 1. The globulars range in metallicity from a hundredth solar (M92, M15) to approximately half solar (M69) and become progressively redder in J-H as their metallicity increases. It is seen that the infrared colours of M69 are indistinguishable from the colours of the dE,N sample. Very cool stars (carbon stars or bright M-stars) evidently do not dominate the dE,N infrared light, otherwise H-K would be redder (e.g. Aaronson & Mould, 1980).

3.3 J-K vs. B-H diagram

This colour-colour diagram is potentially more powerful than the purely infrared colour-colour diagram, because it can describe not only a red stellar population but also a mixture between red and blue stars.

Again, many stellar populations are sketched here (Fig. 2): our dE,Ns are surrounded by E/SO (FPAM), Sc spirals (Bothun et al. 1984), and galactic as well as M31 globular clusters (Frogel et al. 1980). The two tick marks near M3 represent the colour coordinates of the globular clusters GC3 and GC5 of the Fornax dwarf spheroidal galaxy (Jones and Hyland 1982) while the third tick mark further along the globular cluster line (Aaronson et al. 1978) represents GC4 also in Fornax. The dashed part of the globular cluster line is populated by M31 globulars only, with V29 being by far the reddest object. Some very red, super-metal-rich globular clusters observed in N5128 (Frogel 1984) are also given (small dots in E/SO shaded area). An important mark is the filled square (denoted "MC" for Magellanic Clusters) indicating the colour position of a population mix consisting of old and intermediate age (SWB class VII and VI-IV) clusters in the Small and Large Magellanic Cloud. Infrared data are from Persson et al. (1983), who also gave V-K. Using the B-V data from van den Bergh and Hagen (1968) the B-H colour could be constructed for 7 SMC and 8 LMC clusters; these include N121, N152, N339, N361, N416, N419, and K3 (SMC), and N1466, N1783, N1806, N1835, N1846, N1978, N1987, and N2019 (LMC).

Furthermore, theoretical lines of constant age of a single age stellar population but with increasing metallicity from the lower left to the upper right along these lines are plotted. These lines are taken from the population synthesis of Bothun et al. (1984) and may help the interpretation of the data later on.

3.4 Colour magnitude diagrams

Figs. 3a,b display the colour-magnitude diagrams. Although the data set is limited, there seems to be a tendency for the infrared colour J-K to become redder for the more luminous dE,N objects; for the optical-infrared colour B-H such a tendency appears to be absent. In the B-H vs. B_T diagram we have plotted not only our own data (circled points) but also other data (pluses); these 10 data points correspond to 8 dE,N satellites of M87 and 2 dE,N satellites of M49, combining B-H from Table 2 in Bothun and Caldwell (1984) and B_T from Caldwell (1983). An offset is discernible between the average B-H colour index of our sample of field dE,Ns and that of the M87/M49 dE,N satellites in the sense that our field sample is bluer by about 0.5 mag. (The size of this colour difference may be uncertain, since the B and H data were obtained in different ways, but it does seem to be a real effect.)

4. Discussion

4.1 The nature of the stellar population

Inspection of Fig. 1 and Fig. 2 suggests the following tentative conclusions about the nature of the stellar population in the Virgo dE,N galaxies.

Firstly, if we assume that we are dealing with an old single age population like globular clusters or (probably) giant ellipticals, we would infer from the infrared colours alone (Fig. 1) that most of the dE,N light comes from moderately metal-rich K-giants as in M69 (=N6637) with metallicity $\sim$ half solar. Certainly, the average dE,N position in the J-H vs. H-K diagram does not coincide with that of extremely metal-poor globulars or of extremely metal-rich cores of giant ellipticals.

Secondly, we infer from the fact that the optical-infrared colour index for dE,Ns is 1.0-1.5 mag bluer than the same B-H colour index for E/SOs (Fig. 2) that there must be an additional blue component in the dwarf ellipticals which is not present in the giant ellipticals. Metal-poor globulars do have such blue B-H colours (Fig. 2) but their J-K colour differs markedly (Fig. 2). This dilemma leaves us with the suggestion that the additional blue component is due to a young stellar population. As an example, one could calculate which main sequence turn-off mass (or age in a single age population) would be consistent with the rather blue B-H colour. From Fig. 2 we would deduce an age less than 3-5 Gyr or a turn-off mass around 1.7-1.3 $M_{\odot}$, since our dE,Ns lie below the lines labelled 3 and 5 Gyr, respectively. However, it is possible that we are dealing with galaxies which have a mixed population, i.e. the galaxies on the whole are not as young as 3-5 Gyr. It may be that the star formation rate in dwarf ellipticals has declined on a longer timescale than in giant ellipticals, such that some star formation was still taking place in dE,Ns 3-5 Gyr ago, or even nearer to the present epoch.

We note that the contribution of asymptotic giant branch stars that have evolved from the slightly more massive blue progenitors is not expected to change the infrared colours of the underlying old population, so that the mixed age population is consistent with the observation (Fig. 1) that the dE,N galaxies have infrared colours similar to M69.

Incidentally, the possibility that any of our dwarf galaxies is actually a faint background galaxy at a redshift of $z \geq 0.2$ can be ruled out a posteriori

on the basis of our data, because in that case one would expect the H-K colour to be much redder than we observe (H-K ≧ 0.5 for z ≧ 0.2 see Lilly and Longair 1982).

4.2 Comparison with other, related work.

As already noted in the introduction, the present work extends the observational work on the near infrared properties of giant ellipticals (Frogel et al. 1978, FPAM) to dwarf ellipticals. Our sample is still small and still restricted to nucleated dwarf ellipticals only. Yet it is the first dwarf elliptical sample on the basis of which an infrared comparison between gEs and dEs can be made. Bothun & Caldwell (1984) have published a comparison of an optical-infrared colour index (B-H) between gEs and dEs based on their study of the M87/M49 dE,N companions. They concluded that B-H for their dE,N sample (10 objects) is systematically bluer, by 0.5 - 1.0 mag, than for the more luminous ellipticals which have B-H in the range 4.1±0.2. We confirm this conclusion noting that our sample of field dE,Ns is even bluer than the Bothun & Caldwell sample (by about 0.5 mag, see Fig. 3b). This may suggest a systematic difference between the dwarf companions and the field dwarfs. Perhaps the field dwarf ellipticals can retain interstellar gas for a longer period than the dwarf elliptical satellites.

Comparison with Local Group dEs is restricted to the M31 dE satellite N205. For this galaxy measured infrared and optical-infrared colours exist and resemble those of our Virgo field dE,Ns (see Fig. 1 and Fig. 2). Young luminous blue and red stars are present in the N205 nucleus (Hodge 1973, Gallagher & Mould 1981) while the stars in the outer parts are probably old (Mould, Kristian, and Da Costa 1984). Vigroux, Souviron, and Vader (1984) have recently obtained CCD photometry of three dwarf ellipticals in the Virgo Cluster and have discovered that one of them (M100Dw5) shows a blue nucleus much like N205.

Bothun et al. (1984) have measured the infrared colours for a sample of 31 Sc galaxies in the Pegasus I and Pisces cluster, and obtained the J-K vs. B-H colour-colour diagram (roughly reproduced in our Fig. 2). They used apertures between 22 and 55 arcsec to get as much disk light as possible, while the contribution of the bulge is minimised for Sc's. We consider the fact that the range in B-H for the Sc galaxies is similar to that for our dE,Ns an indication that the dE,Ns represent a mixed population, similar to spirals which consist of an old population plus progressively smaller fractions of progressively

younger stars. The redder J-K for the spirals compared to the J-K index for the dE,Ns can be attributed to the metallicity effect, the dE,Ns being less metal-rich than the more luminous spirals. It ought to be said here that J-K and B-H do not represent completely orthogonal parameters. While J-K is a metallicity indicator (or, strictly speaking, a measure for the temperature of the giant branch which in turn depends on the [Fe/H]-value), B-H is an indicator for the combined effects of star formation, age, and metallicity. For example, from population synthesis models Bothun et al. predict a change of B-H of $\sim$ 1 mag for a change in J-K of $\sim$ 0.3 mag from metal-abundance variations alone (as shown by the full lines in Fig. 2). The observed range of B-H for our dE,N sample is $\sim$ 1 mag, but the objects with the bluest B-H are too red in J-K to explain the observed range in B-H by a metallicity effect alone.

A few remarks may be in order regarding blue compact dwarfs (BCD) -a seemingly different class of objects as judged from their infrared colours (see Fig. 1). We have obtained only two data points for this object class in the Virgo Cluster so far. The two objects are described in some detail by Sandage & Binggeli (1984). We suspect that the very different infrared colours of these BCDs reflect the presence of M-supergiants and infrared emission from HII regions related to a recent burst of high-mass star formation in these blue galaxies. Thuan (1983) reporting a near infrared study of a large sample of non-Virgo BCDs argued that the infrared light and colours are dominated by the old underlying giant population rather than by a red supergiant population but this view is now strongly challenged by Gondhalekar et al. (1984) and, especially, by the spectrophotometric near infrared observations of Campbell & Terlevich (1984) who have demonstrated that the near infrared luminosity in violent star formation regions is dominated by red supergiants.

5. Conclusions

We summarise our results as follows:

1) The infrared colour-colour diagram (J-H vs. H-K) of 10 dE,N Virgo Cluster galaxies suggests a stellar population whose bulk metallicity is similar to that of the most metal-rich galactic globular clusters, i.e. about half-solar. On the other hand, the dE,Ns are slightly but distinctly bluer in J-H as well as in H-K than the central regions of E/SO's. dE,N-infrared colours may, however, match the infrared colours of the very outer regions of E/SO's. The infrared light is not dominated by very cool stars.

2) The optical-infrared colour, B-H, is significantly bluer for dE,Ns compared with the same colour index for E/SO's (as previously found by Bothun & Caldwell 1984). This is mainly interpreted in terms of different star formation histories for the dwarf and the giant ellipticals: dwarf ellipticals form a larger fraction of their stars closer to the present epoch!

3) A population mix of 7 old and 8 intermediate age star clusters in the LMC/SMC represents the B-H and J-K colours of the Virgo dE,Ns rather well. This suggests that about half the light of a typical dE,N could come from an old population and half from an intermediate age population. The carbon stars from the latter population will not affect the integrated infrared colours as much as in an individual LMC/SMC star cluster because of the averaging effect in a larger stellar system.

4) The B_T vs. J-K diagram suggests a weak mass-metallicity correlation, yet B_T and B-H do not appear to be correlated. This tends to confirm that B-H is not primarily a metallicity indicator, in agreement with the interpretation given above (see 2)).

5) The Local Group dE N205 may be similar in its stellar content to some of the Virgo dE,Ns.

Acknowledgements

Several people have contributed directly or indirectly to this work. First HZ would like to thank Allan Sandage who provided the incentive "to get his hands dirty". We would also like to thank the entire staff at UKIRT, and in particular our telescope operator Dolores Walther for her very competent help. We are greatly indebted to Andy Longmore for taking data for us as part of UKIRT Service Observing. Moreover, we thank Bruno Binggeli and Gibson Reaves for sending relevant material in advance of publication, and Simon Lilly for a constructive discussion. Last but not least, we appreciate the assistance of Fiona Drysdale and Marjorie Fretwell in preparing the manuscript. This work would not have been carried out without the support from the Deutsche Forschungsgemeinschaft for one of the authors (HZ).

References

Aaronson, M., Cohen, J.G., Mould, J., and Malkan, M., 1978. Ap.J. 223, 824.

Aaronson, H., and Mould, J.R., 1980. Ap.J. 240, 804.

Binggeli, B., Sandage, A., and Tarenghi, M., 1984. Astron.J. 89, 64.

Bothun, G.D., and Caldwell, C.N., 1984. Ap.J. 280, 528.

Bothun, G.D., Romanishin, W., Strom, S.E., and Strom, K.M., 1984. Astron.J. 89, 1300.

Caldwell, C.N., 1983. Astron.J. 88, 804.

Campbell, A.W. & Terlevich, R., 1984. M.N.R.A.S. 211, 15.

Frogel, J.A., 1984. Ap.J. 278, 119.

Frogel, J.A., Persson, S.E., and Cohen, J.G., 1980. Ap.J. 240, 785.

Frogel, J., Persson, E., Aaronson, H., and Matthews, K., 1978. Ap.J. 220, 75.

Gallagher, J.S., and Mould, J.R., 1981. Ap.J. 244, L3.

Gerola, H., Carnevali, P., and Salpeter, E.E., 1983. Ap.J. 268, L75.

Glass, I.S., 1984. M.N.R.A.S. 211, 461.

Gondhalekar, P.M., Morgan, D.H., Dopita, M., and Phillips, A.P., 1984. M.N.R.A.S. 209, 59.

Hodge, P.W., 1973. Ap.J. 182, 671.

Jones, B.J.T., 1980. ESO report "Dwarf Galaxies" (eds. Tarenghi and Kjär), p.167.

Jones, T.J., and Hyland, A.R., 1982. M.N.R.A.S. 200, 509.

Klement, R., Yorke, H.W., and Fricke, K.J., 1982. Mitt.Astron.Ges. 60, 462.

Lilly, S.J., and Longair, M.S., 1982. M.N.R.A.S. 199, 1053.

Lynden-Bell, D., 1973. in Dynamical Structure and Evolution of Stellar Systems, Swiss Society of Astronomy and Astrophysics, 3rd Advanced Course, Saas-Fee, p.123ff.

Mould, J.R., Kristian, J., and Da Costa, G.S., 1984. Ap.J. 278, 575.

Persson, S.E., Aaronson, M., Cohen, J.G., Frogel, J.A., and Matthews, K., 1983. Ap.J. 266, 105.

Reaves, G., 1983. Ap.J.Suppl. 53, 375.

Sandage, A., and Binggeli, B., 1984. Astron.J. 89, 919.

Tammann, G.A., 1980. ESO report "Dwarf Galaxies" (eds. Tarenghi and Kjär), p.3.

Thuan, T.X., 1983. Ap.J. 268, 667.

van den Bergh, S., and Hagen, G.L., 1968. Astron.J. 73, 569.

Vigroux, L., Chièze, J.P., and Lazareff, B., 1981. Astron.Astrophys. 98, 119.

Vigroux, L., Souviron, and Vader, J.P., 1984. Astr.Astrophys. 139, L9.

Appendix: On the origin of the nucleus in dE,N galaxies.

The theory of dE galaxies proposed by Gerola et al. (1983) explains dEs as bound remnants of disintegrating more massive dwarf irregular systems after a catastrophic burst of star formation. In that scenario, nucleation would be due to a pre-existing central dense star cluster in the parent galaxy. The gas expulsion would leave the absolute size, mass, and luminosity of the star cluster almost unchanged, thus enhancing the density contrast since the surface density elsewhere would be greatly decreased.

Here we suggest another possibility of how nucleated dwarf galaxies may have become nucleated, a possiblity related to mass loss from old stars. Mass loss from old evolving stars can feed the centre of the galaxy with gas. Galactic winds are probably not effective in dwarf ellipticals (Gallagher & Mould 1981). The angular momentum of the gas is shed in dissipative collisions between gas streams. Once the gas mass exceeds a critical value $M_{crit} \propto \bar{\rho}_*^{-\frac{1}{2}}$, where $\bar{\rho}_*$ is the mean stellar density, the gas begins to collapse. Klement, Yorke and Fricke (1982) have studied this process starting with fully ionized gas ($T \sim 10^4$K) and taking into account radiative hydrodynamics. They find $M_{crit} \simeq 10^6\ M_\odot pc^{-3}$ for $\bar{\rho}_* \simeq 1\ M_\odot pc^{-3}$, not at all unreasonable values for the Virgo dE,Ns (see BST). The answer to the question whether a supermassive object will form or whether the collapsing gas will fragment into ordinary stars is not known, although we favour the latter possiblity (cf. Lynden-Bell 1973). This picture predicts that low-mass dEs should not possess nuclei, as appears to be the case (see BST).

Yet another possiblity to explain the existence of the nuclei might be the spiralling in of globular clusters originally surrounding the dEs, due to dynamical friction.

MOLECULAR CLOUDS IN SPIRAL GALAXIES IN THE VIRGO CLUSTER

Judith S. Young

Department of Physics and Astronomy
and
Five College Radio Astronomy Observatory
University of Massachusetts, Amherst

Abstract

CO observations of the centers of 25 spiral galaxies in the Virgo cluster have been made using the 14 meter telescope of the FCRAO (HPBW=50"; Young, Scoville and Brady 1985). This galaxy sample includes 8 Sa, 7 Sb, and 10 Sc galaxies, covering a wide range in total luminosity within each morphological class. Eighteen of these galaxies were detected at greater than the 3 σ level --- 6 Sa's, 3 Sb's and 9 Sc's. For the Sc galaxies we find that the optical luminosity in the central 5 kpc diameter is proportional to the first power of the CO luminosity in the same region, confirming the relation found previously by us for Sc galaxies in the field. For the early type galaxies (Sa, Sab, Sb) the relation between CO and blue light is slightly displaced from that for the late type galaxies (Sbc, Sc, Scd) in the sense that for a given CO content the early type galaxies are more luminous. This trend may be due to the presence of old stars in the nuclear bulge which contribute significantly to the blue light in the early type galaxies. The maximum CO content observed is similar for the early and late type galaxies; NGC 4569 (Sab) has as much CO emission as NGC 4254 (Sc). However, the fraction of the galaxy mass in molecular form is a factor of $\sim$ 4 smaller in luminous Sa's than Sc's since the early type galaxies have higher dynamical masses for a given luminosity.

We have also mapped the major axis distributions of CO emission in 8 spiral galaxies in the Virgo cluster (Kenney and Young 1984). In NGC 4303, the CO distribution follows the blue light and radio continuum profiles in the disk, as has been found for Sc galaxies in the field. The shapes of the CO distributions with radius in the Virgo cluster and the total CO luminosities also agree well with those found in field galaxies, suggesting that the molecular contents of the galaxies in Virgo are not significantly different from field galaxies of the

same type and luminosity.

I. Introduction

Studies of molecular clouds in external galaxies are important for understanding star formation and the evolution of galactic disks since new generations of stars form in the dense component of the ISM. For several late-type spirals, the CO distribution has been found to follow the roughly exponential blue luminosity profile in the disk out to ~ 10 kpc (Young and Scoville 1982a; Scoville and Young 1983; Solomon et al. 1983). Furthermore, the CO luminosities in the central 5 kpc diameter in a sample of Sc field galaxies have been found to exhibit a one-to-one proportionality with the optical luminosities in the same region (Young and Scoville 1982b). On the other hand, the HI surface densities in these same galaxies show no such correlations with luminosity.

The Virgo cluster provides the ideal setting for a survey of the molecular content of galaxies as a function of morphological type and luminosity. Because the determination of molecular masses depends on the square of the distance to a given galaxy, the fact that the members in the cluster are all at roughly the same distance enables the masses of one galaxy relative to another to be determined with little ambiguity. CO studies of these galaxies also provide information on the effect of environment on the dense component of the ISM, and indicate whether the molecular medium has suffered a similar fate to the less dense clouds of atomic gas.

II. CO Survey of Centers of Virgo Spirals

A survey of the CO emission from the central 50" of 25 spiral galaxies in the Virgo cluster was made using the 14 m millimeter telescope of the Five College Radio Astronomy Observatory (Young, Scoville, and Brady 1985). The goals of this survey were to determine the dependence of CO content on morphological type and luminosity. The 25 galaxies in the sample were chosen to cover a wide range in luminosity within each morphological type. Membership in the Virgo cluster and galaxy classifications were taken from the Revised Shapley-Ames catalogue (Sandage and Tammann 1981, RSA). The sample includes 8 Sa, 7 Sb and 10 Sc galaxies (see Table 1). Figure 1 shows the distribution on the sky for the galaxies in this sample.

Table 1

Virgo Galaxy Sample

Galaxy[a]	Type[a]	I_{CO}[b] (K km s^{-1})	L_{CO}[c] (K km s^{-1} kpc^2)	L_B[d] (10^9 $L_\odot$)	$M(H_2)$[e] (10^8 $M_\odot$)
NGC 4032	S(b)	<0.8	<15	---	<0.9
4237	Sc(r)II.8	2.3	42	---	1.8
4254	Sc(s)I.3	17.6	325	7.5	17
4293	Sa pec	4.4	81	4.1	2.4
4303	Sc(s)I.2	12.4	229	7.5	12
NGC 4321	Sc(s)I	17.1	316	7.5	17
4388	Sab	2.9	54	---	0.9
4394	SBb(sr)I-II	<0.8	<15	---	<0.8
4438	Sb (tides)	4.2	78	6.9	2.0
4450	Sab pec	2.6	48	8.1	2.1
NGC 4501	Sbc(s)II	15.4	285	9.2	9.5
4503	Sa	<0.8	<15	---	<0.4
4535	SBc(s)I.3	5.4	100	2.7	4.4
4548	SBb(rs)I-II	5.1	94	5.7	4.6
4569	Sab(s)I-II	15.6	289	8.1	8.4
NGC 4571	Sc(s)II-III	2.0	37	---	2.0
4579	Sab(s)II	4.7	87	11	4.2
4580	Sbc(r)II	<0.8	<15	---	<0.7
4596	SBa	<0.8	<15	---	<0.8
4635	ScII-III	<1.9	<35	---	<1.6
NGC 4639	SBb(r)II	<0.8	<15	---	<0.6
4651	Sc(r)I-II	7.9	146	6.3	6.2
4654	SBc(rs)II	9.8	181	3.6	6.8
4689	Sc(s)II.3	2.8	52	---	2.7
4698	Sa	1.7	31	---	1.1

[a] Galaxy types and membership in Virgo taken from RSA.

[b] Integrated intensity of CO emission, $I_{CO} = \int T_R^* dV$, where T_R^* is the peak line intensity measured on spectra smoothed to 20 km s^{-1}. I_{CO} is accurate to $\pm$ 0.4 K km s^{-1}.

[c] CO luminosity in 50", $L_{CO} = I_{CO}A$ where A is the area of the beam on the galaxy in kpc^2. For a distance of 20 Mpc to the Virgo cluster, A = 18.5 kpc^2.

[d] Blue luminosity in central 50", calculated from multiaperture photometry (Tifft 1969) and corrected to m_B using NGC 4321 (Schweizer 1976); assuming D = 20 Mpc and $M_B(0) = +5.48$.

[e] $M(H_2) = 6 \times 10^6 L_{CO} \cos i$ gives mass of H_2 corrected to face-on where i is the inclination.

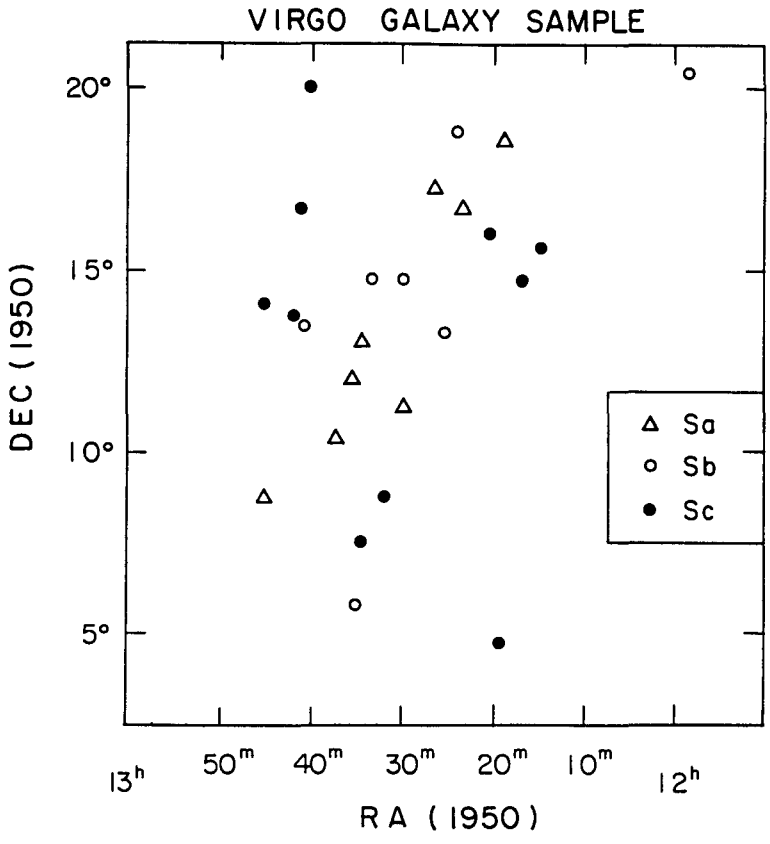


Figure 1. The sample of galaxies in the Virgo cluster in which CO emission was searched for, with different morphological types (from RSA) indicated.

CO emission was detected at greater than the 3σ level in 18 of the 25 galaxies in the Virgo sample --- 6 Sa's, 3 Sb's, and 9 Sc's. Figure 2 shows representative CO spectra (solid lines) for the central 50" in 4 of the Sc galaxies; the upper two panels are spectra from high luminosity galaxies, while the lower two are from low luminosity galaxies. It is immediately apparent from inspection of these CO data that high luminosity galaxies have more CO in their centers than do low luminosity galaxies. The 7 galaxies in which no CO emission was detected are all low luminosity galaxies, with absolute magnitudes fainter than $M_B = -20.4$.

Also shown in Figure 2, are the HI profiles for these same galaxies (dashed lines) obtained at much lower resolution (Chamaraux et al. 1980; Hutchmeier et al. 1976). The HI in these galaxies shows linewidths and velocity centroids which agree well with those obtained from the CO observations. The differences between the CO and HI profiles result from the different resolutions of the

measurements as well as the different shapes and extents of the distributions. For NGC 4321, the CO linewidth is only 70% of the HI linewidth indicating that the rotation curve of the galaxy is still rising at the edge of the CO beam.

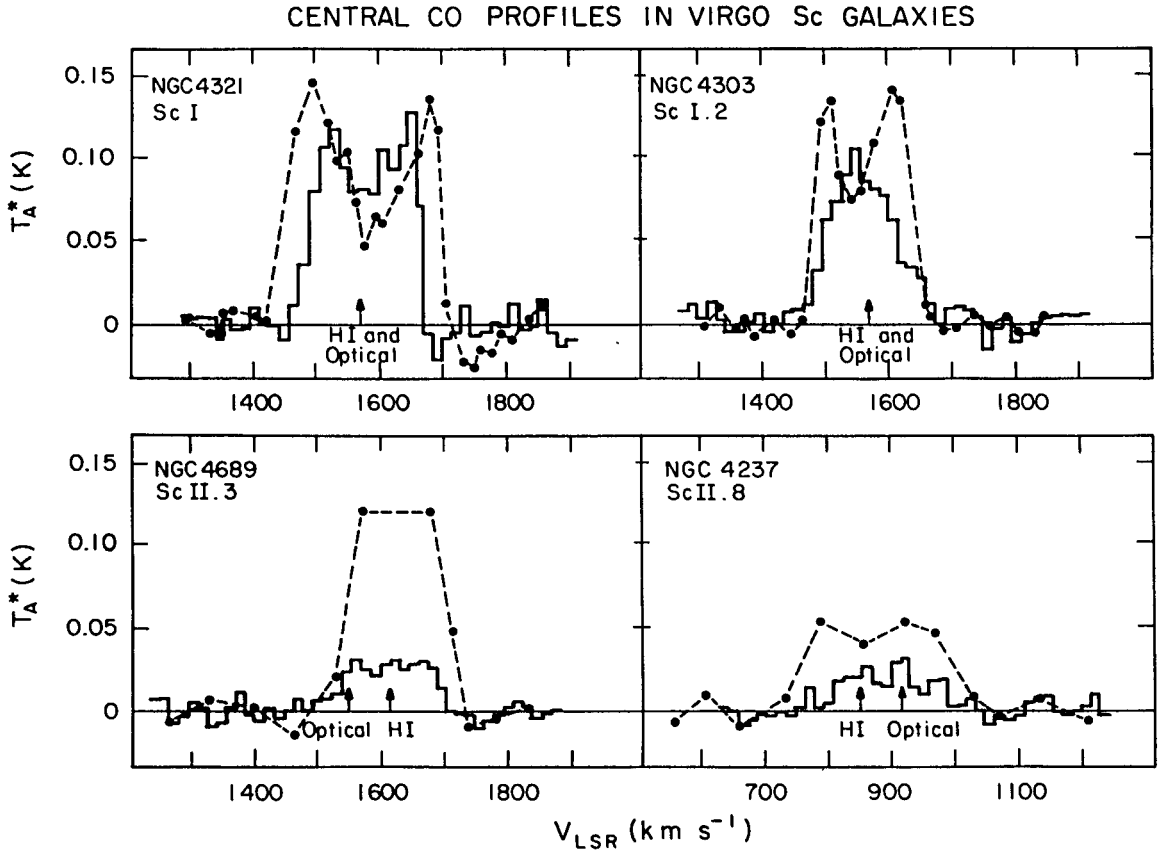


Figure 2. CO spectra in central 50" of 4 Sc galaxies in Virgo (solid histograms). Note that the high luminosity galaxies have more CO in their centers than do the low luminosity galaxies. Also shown are the HI profiles of each galaxy (dashed histograms; Chamaraux et al. 1980; Hutchmeier et al. 1976) obtained at lower resolution.

For the 13 most luminous galaxies in the sample, multiaperture photometry data were used (Tifft 1969) to compute the optical luminosities within the central 50". Figure 3 shows a comparison of the CO and optical luminosities for the central 5 kpc in both Virgo and field spirals, and the elliptical galaxies M86 and M87, with several interesting results. First, the Sc galaxies both in Virgo and the field follow the relation found previously by us for field Sc galaxies (Young and Scoville 1982b), that the optical luminosity in the central 5 kpc is proportional to the CO luminosity in the same region. Second, the

early type galaxies show a similar correlation, although with a wider scatter because of the contribution of the bulge to the luminosity in the central 5 kpc. The difference in the correlation between the early and late type spiral galaxies is also probably due to the luminosity of the nuclear bulge, in that for a given CO luminosity the early type galaxies are more optically luminous. In general, we find that the high luminosity galaxies of a given morphological type have more CO in their centers than do low luminosity galaxies of the same type. The elliptical galaxies, in which no CO was detected, have the highest central 5 kpc optical luminosities, while only upper limits to the CO intensities were obtained.

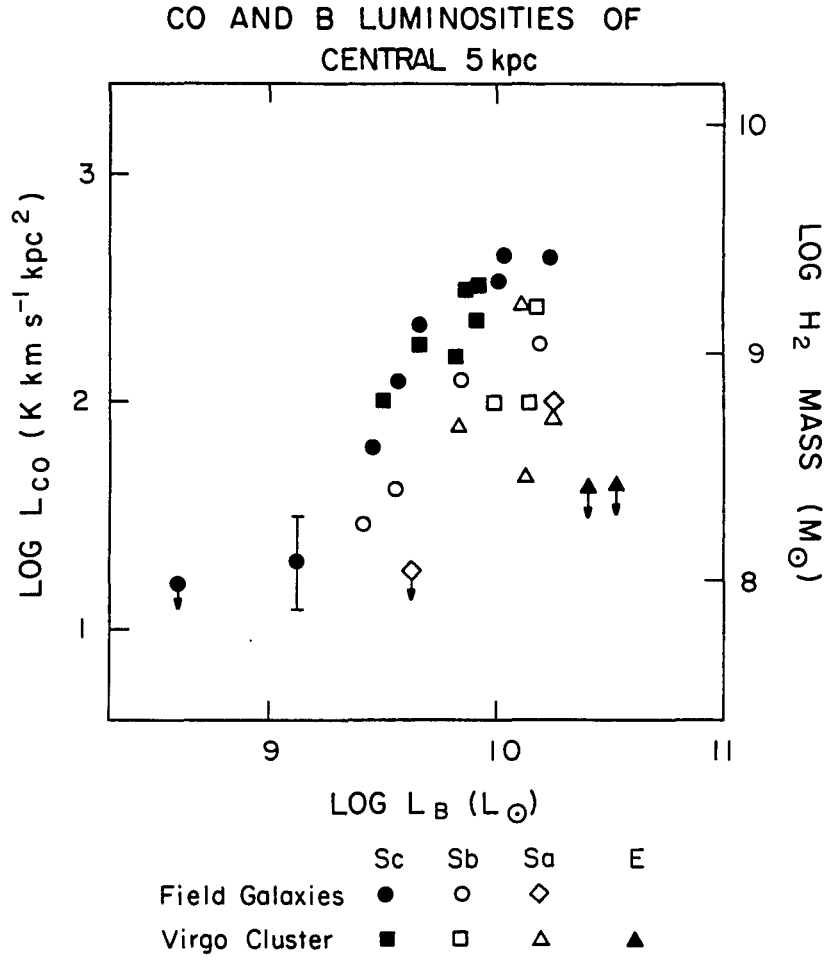


Figure 3. Comparison of the central 5 kpc CO and blue luminosities in 13 Virgo spirals, 2 Virgo ellipticals, and 14 spiral galaxies outside of Virgo. Note that the early type galaxies tend to have higher blue luminosities for a given CO content.

The significance of this correlation is derived from the systematic properties of spiral galaxies as a function of luminosity, and in particular, studies of the optical rotation curves of Sa, Sb, and Sc galaxies. For galaxies of a given morphological type, those with high luminosities are found to have higher rotational velocities at all radii than galaxies with low luminosities (Rubin, Ford, and Thonnard 1980; Rubin et al. 1982). These high rotational velocities translate into high mass densities for the luminous galaxies of a given type. Thus, out to a fixed radius, the luminous galaxies have higher total masses and mass densities than do low luminosity galaxies. The correlation we have found between the molecular content of the central 5 kpc diameter in a galaxy and its total luminosity is probably, in fact, due to the correspondence between mass density and galaxy luminosity. That is, for each morphological type, galaxies with higher mass densities in the central 5 kpc have more molecular gas there.

To derive masses of H_2 for the centers of the Virgo galaxies, we adopt a CO to H_2 conversion of 4×10^{20} H_2 cm^{-2} (K km $s^{-1})^{-1}$ following the analysis of Young and Scoville (1982a). This conversion was determined from observations of dark clouds and giant molecular clouds in our galaxy, and does not account for either the effects of cloud temperature variations or of metallicity variations from galaxy to galaxy. For the Sc galaxies described in Figure 3, the metallicities of the central 5 kpc vary by only a factor of 3 (McCall 1984; Pagel and Edmunds 1981), while the CO luminosities range over almost 2 orders of magnitude. Thus, although metallicity may have some effect on the amount of CO observed per unit H_2 mass, for the present analysis we assume that the conversion from CO integrated intensity to H_2 column density is independent of metallicity. The resulting H_2 masses for the central 5 kpc of the Virgo spirals range from $< 10^8$ $M_\odot$ for the galaxies in which no CO was detected, to 1.7×10^9 $M_\odot$ in the luminous Sc galaxies NGC 4254 and 4321 (see Table 1).

Figure 4 shows a comparison of the H_2 and HI masses for the central 5 kpc in 14 late type spirals. Most of the galaxies have similar values of the HI mass in the central 5 kpc, reflecting primarily the roughly constant HI surface densities seen in the disks of late type spiral galaxies (cf. Rogstad and Shostak 1972). In sharp contrast, the H_2 masses in the same regions in these galaxies vary over almost 2 orders of magnitude with more H_2 in the centers of high luminosity galaxies. That is, the ratio of H_2/HI masses in the central 5 kpc ranges from < 1 in low luminosity galaxies to almost 50 in the luminous normal spirals. NGC 1068 has an anomalously low HI mass and a high H_2 mass, so the H_2/HI mass ratio is ~ 500.

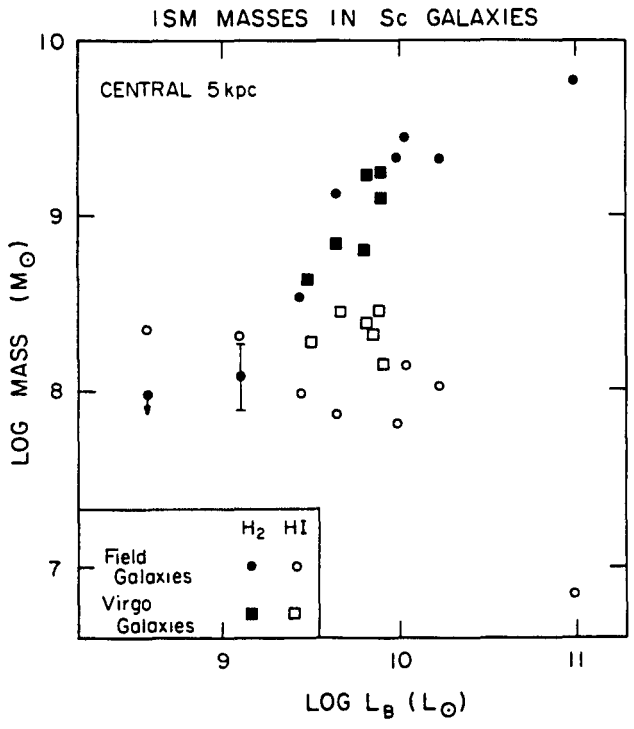


Figure 4. H_2 and HI masses in central 5 kpc of late-type spirals in Virgo and the field. The H_2 masses range over almost 2 orders of magnitude; HI masses (except NGC 1068) are relatively constant from galaxy to galaxy.

The interpretation of the CO-blue light correlation depends on the dominant source of the blue light in the disk of a galaxy. For the late-type spirals, we have used the modeling study of Searle, Sargent and Bagnuolo (1973) to calculate the fraction of blue light in a galactic disk which originates from stars younger than $1\text{-}2\times10^9$ years (corresponding to the young Population I objects which form over the lifetime of molecular clouds; Scoville and Hersh 1979). The results of these calculations are given in Table 2, where the fraction of the total blue light contributed by stars younger than age t is listed as a function of t for several values of β (where β is the reciprocal decay time for an assumed exponential decay in the rate of star formation). The value of β appropriate to a particular galaxy is determined by the measured value of B-V; for 13 of the late-type spirals presented in Figure 3, the values of β implied by the values of B-V (RC2) range from 0.1 to 3.5, with a mean of 1.7. The results in Table 2 suggest that between 35% and 65%, or roughly 50% of the total

blue light in a late-type galaxy is contributed by stars younger than 2×10^9 years old.

Table 2

Fraction f of Blue Light Contributed
by Stars Younger than Age t

t (10^9 years)	$\beta = 0$[a] f	$\beta = 2.5$ f	$\beta = 5$ f
0.25	0.36	0.19	0.05
0.5	0.45	0.23	0.06
1	0.54	0.29	0.08
2	0.64	0.35	0.10
3	0.70	0.39	0.12
5	0.77	0.46	0.14
10	0.88	0.60	0.25
20	1.0	1.0	1.0

[a] The parameter β corresponds to the reciprocal decay time for an assumed exponential decay in the rate of star formation (cf. Searle et al. 1973).

The result presented in Figure 3, that the blue luminosity of the central 5 kpc is proportional to the CO luminosity in the same region can be interpreted as follows. Assuming the CO traces the mass of H_2, and if $\sim$ 50% of the blue luminosity is contributed by stars younger than 2×10^9 years old, the CO-blue light correlation suggests that the amount of star formation averaged over the last 2×10^9 years is proportional to the amount of H_2 present, as suggested previously by us (Young and Scoville 1982b), or that the average star formation rate per nucleon of ISM is constant.

III. CO Radial Distributions in Virgo Spirals

In an investigation of the CO distributions in spiral galaxies in the Virgo cluster, we have undertaken a survey to determine the molecular properties of these systems as a function of morphological type, luminosity, and position in the cluster (Kenney and Young 1984). Thus far, we have mapped the CO radial distributions along the major axes of 8 Virgo spirals (see paper by Kenney and Young in these proceedings).

In NGC 4303, an Sc galaxy 8° from the cluster center, the distribution of CO integratd emission peaks in the center and decreases in intensity with increasing galactocentric distance. Figure 5 shows the CO distribution compared to the profiles of blue light (Whitmore and Kirshner 1982) and 20 cm radio continuum (Condon 1983), both of which exhibit identical radial behavior to the azimuthally averaged CO distribution. In contrast, the distribution of atomic hydrogen is essentially flat over the entire disk (van Gorkom, private communication) unlike the other distributions in the disk. These same features (i.e. similar behavior of the distributions of CO, blue light, and radio continuum, but markedly different HI) have been seen in a number of late type spirals --- IC 342 and NGC 6946 (Young and Scoville 1982), M51 (Scoville and Young 1983), and M101 (Solomon et al. 1983).

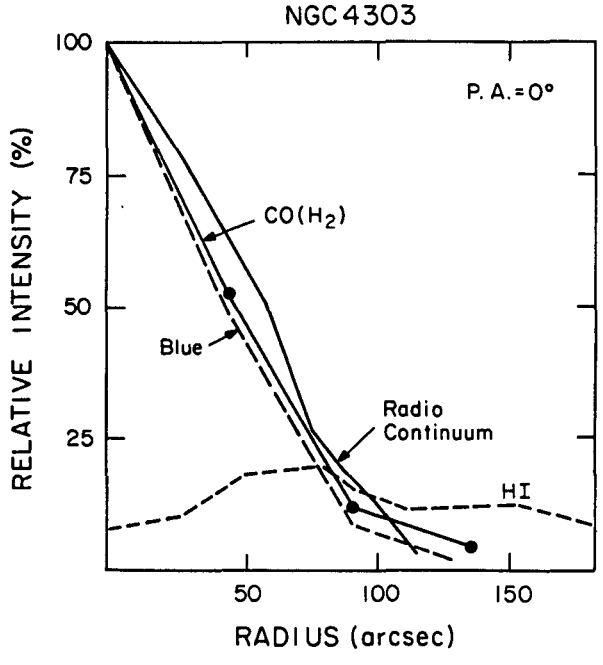


Figure 5. Radial distributions of CO (Kenney and Young 1984), blue light (Whitmore and Kirshner 1982), 20 cm radio continuum (Condon 1983), and HI (van Gorkom, private communication) along the major axis of the Sc galaxy NGC 4303.

In order to compare the overall shapes and extents of the CO distributions in the Virgo spirals with those of nearby Sc galaxies, we plot in Figure 6 the azimuthally averaged CO intensities as a function of galactocentric radius. For the nearby galaxies there is a wide range observed in the CO intensities from galaxy to galaxy. Those objects with high CO intensities and large extents are the large, high luminosity galaxies, while the galaxies with lowest CO intensities and small CO extents (e.g. M33, and NGC 2403) are the small, low luminosity galaxies.

In terms of both the absolute CO intensity in the disk and the radial extent of the emission, the Virgo spirals resemble the nearby galaxies. The fact that the central CO intensities in the Virgo galaxies appear lower than those in the nearby sample reflects the fact that the larger distances of the Virgo galaxies cause their peak intensities to be artificially reduced. Thus, CO distributions in the Virgo spirals appear similar to those in the non-Virgo sample.

IV. Conclusions

(1) From CO observations of the centers of 25 spiral galaxies in the Virgo cluster, we have confirmed the relation found previously by us for Sc field galaxies, that the CO luminosity in the central 5 kpc diameter is proportional to the B luminosity in the same region.

(2) The CO luminosities in the centers of the Virgo galaxies show a strong correlation with the optical luminosities in the same regions, such that the high luminosity galaxies of a given type have more CO in their centers than do the low luminosity galaxies of the same type.

(3) The correlation for the early type galaxies is displaced slightly from that for the late type galaxies in the sense that the early types have higher luminosities for a given CO content. This difference is probably due to the contribution of the stars in the nuclear bulge to the total luminosity.

(4) The maximum CO content observed is similar for early and late spiral types, since the Sab galaxy NGC 4569 has as much CO as the luminous Sc galaxies. However, the fraction of the galaxy mass in molecular form is a factor of ~ 4 smaller in the luminous early types.

(5) For the 8 galaxies in the Virgo cluster whose CO distributions have been mapped, we find that the extents and intensities of the CO emission resemble those of non-Virgo galaxies of similar type and luminosity. Thus, it appears that the molecular medium has not been drastically altered by the dense cluster environment.

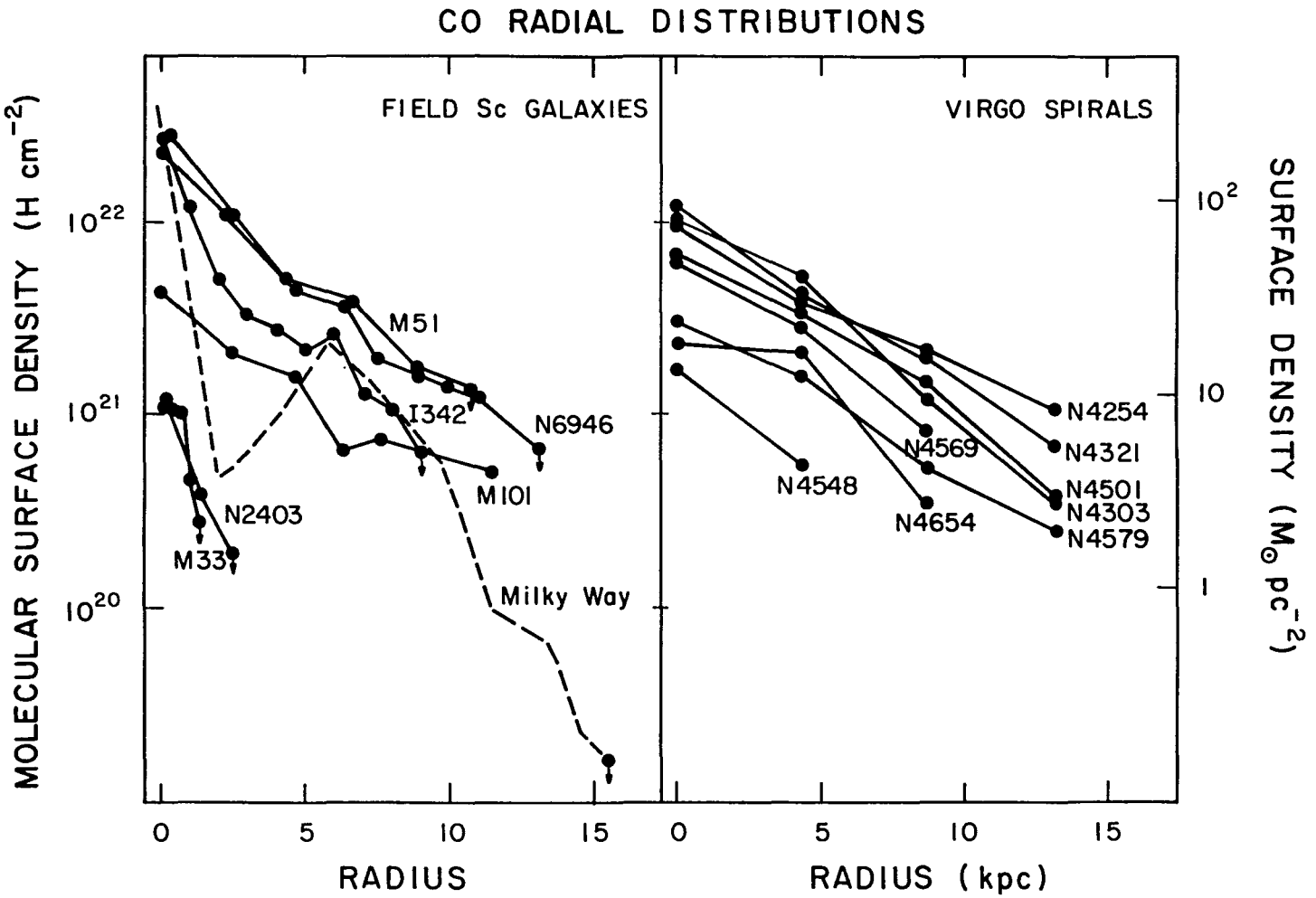


Figure 6. Azimuthally averaged distributions of CO emissivity in spiral galaxies in the Virgo cluster and in the field.

References

Chamaraux, P., Balkowski, C., and Gerard, E. 1980, Astron.Ap., 83, 38.

Condon, J.J. 1983, Ap.J. Suppl., 53, 459.

de Vaucouleurs, G., de Vaucouleurs, A., and Corwin, H.G. 1976, Second Reference Catalogue of Bright Galaxies, (Austin: University of Texas Press) (RC2).

Hutchmeier, W.K., Tammann, G.A., and Wendker, H.J. 1976, Astron.Ap., 46, 381.

Kenney, J. and Young, J. 1984, B.A.A.S., 16, 456.

McCall, M. 1984, Ap.J.Suppl., in press.

Pagel, B.E.J. and Edmunds, M.G. 1981, Ann.Rev.Astr.Ap., 19, 77.

Rogstad, D.H. and Shostak, G.S. 1972, Ap.J., 176, 315.

Rubin, V.C., Ford, W.K., Jr., and Thonnard, N. 1980, Ap.J., 238, 471.

Rubin, V.C., Ford, W.K., Jr., Thonnard, N., and Burstein, D. 1982, Ap.J., 261, 439.

Sandage, A. and Tammann, G. 1980, Revised Shapley-Ames Catalogue, (Washington, DC: Carnegie Institution) (RSA).

Schweizer, F. 1976, Ap.J.Suppl., 31, 313.

Scoville, N. and Hersh, K. 1979, Ap.J., 229, 578.

Scoville, N. and Young, J. 1983, Ap.J., 265, 148.

Searle, L., Sargent, W.L.W., and Bagnuolo, W.G. 1973, Ap.J., 179, 427.

Solomon, P.M., Barrett, J., Sanders, D.B., and de Zafra, R. 1983, Ap.J., 266, L103.

Tifft, W.G. 1969, A.J., 74, 354.

Whitmore, B.C. and Kirshner, R.P. 1982, A.J., 87, 500.

Young, J. and Scoville, N.Z. 1982a, Ap.J., 258, 467.

1982b, Ap.J.(Letters), 260, L11.

Young, J., Scoville, N., and Brady, E. 1985, Ap.J., Jan. 15.

DISCUSSION

S. OKAMURA: Have you ever plotted the correlation diagram between L_{CO} and Luminosity using L_V instead of L_B? Do you think that the diagram will change drastically if you use L_V? It seems to me that you may have relatively good correlation whatever band in visual region (U,B,V,R,I) is used.

J. YOUNG: For the Sc galaxies, for example, the central values of B-V are very similar, so that L_V substituted for L_B in this region would not drastically change the central 5 kpc correlation. However, there are radial gradients in

B-V in a number of galaxies, and the CO distribution is most similar to that of blue light rather than V band, suggesting that blue is the appropriate visual band to use in the comparison.

MOLECULAR CLOUDS IN HI-DEFICIENT VIRGO SPIRALS

Jeffrey D. Kenney and Judith S. Young
Five College Radio Astronomy Observatory
and
University of Massachusetts, Amherst

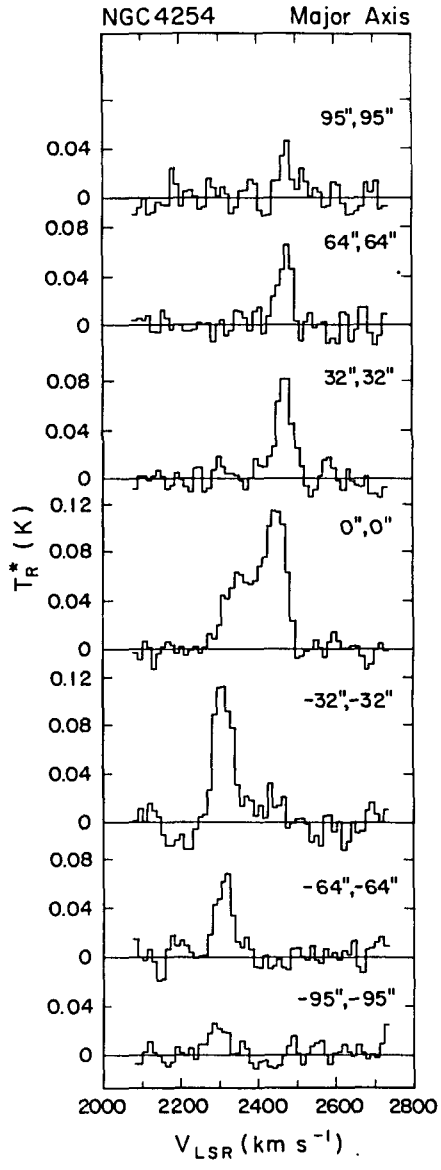
ABSTRACT

We have mapped ^{12}CO along the major axis of 8 bright spiral galaxies in the Virgo cluster. Comparisons of the CO diameters with the HI and optical diameters, and of the CO line fluxes with the HI line fluxes for a sample of Virgo and non-Virgo galaxies show that the molecular gas contents are roughly normal in Virgo spirals, including the severely HI-deficient galaxies NGC4569 and NGC4579. Apparently, some process has removed the low density atomic gas, while leaving the high density molecular gas unscathed. We show that this is consistent with ram-pressure stripping of HI, and discuss the fate of molecular clouds in a galaxy which has lost most of its atomic gas.

I. INTRODUCTION

The molecular gas content of Virgo cluster spiral galaxies holds the key to comprehending the future of star formation in these systems. It is of great interest to know if there is a deficiency of molecular gas in galaxies which are deficient in atomic gas, for this will tell us much about the cause of the HI deficiency and about the relationships between the two gas phases in all galaxies. As the component of the interstellar medium which forms stars, molecular clouds also play a critical role in the evolution of these galaxies. Up until now, attempts to understand the evolution of Virgo systems have been limited to consideration of only the stars and the atomic component of the ISM. Now that it is possible to detect CO in Virgo spirals, evolutionary models can be framed in terms of a more realistic progression of $HI \rightarrow H_2 \rightarrow$ stars.

We are in the midst of mapping ^{12}CO along the major axis of ~40 spirals in Virgo. Thus far, we have completed maps of 8 galaxies, with interesting results about the CO properties of these galaxies relative to HI and blue light. The focus of this paper is the presentation and interpretation of the relationship between the CO, HI, and blue optical diameters in Virgo and non-Virgo galaxies. The CO observations are made with the 14-meter telescope of the Five College Radio Astronomy Observatory located in Amherst, Massachusetts. At the 115 GHz frequency of the ^{12}CO J=1→0 emission line, the beamwidth of the telescope is 45". This is identical to the resolution of the VLA HI maps of van Gorkom,



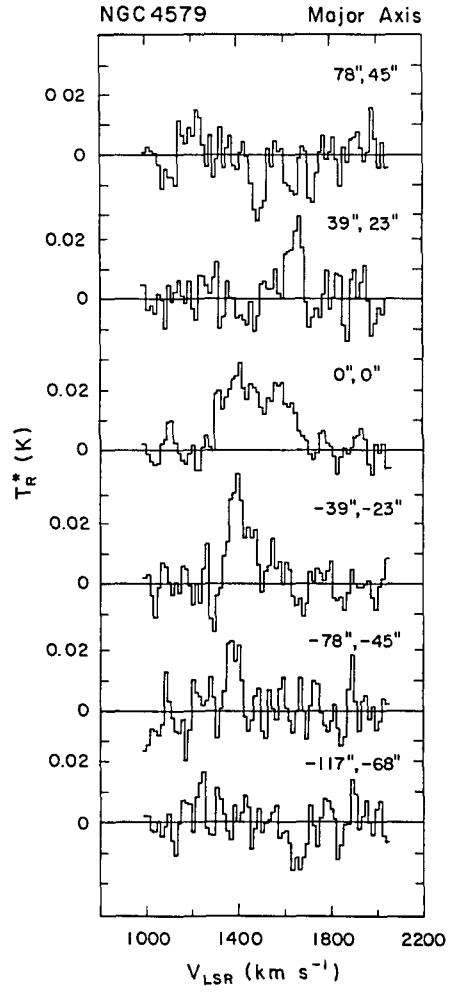


Figure 1. ^{12}CO spectra along the major axes of NGC4254 (position angle 45°) and NGC4579 (position angle 60°). Spectra have been smoothed to a velocity resolution of 15 km s^{-1}. The numbers to the upper right of each spectrum denote the R. A. and Dec. offsets from the nucleus.

Balkowski, and Kotanyi (1984), facilitating the comparison of the CO and HI extents. Further observational details may be found in this volume in the article by Young.

Sample spectra for NGC4254 (Sc) and NGC4579 (Sab), spaced in 45" intervals along the major axis, are shown in Figure 1, where each spectrum represents 2-3 hours of integration time. The CO distributions in all mapped galaxies (except NGC4654) are found to peak on the centers, with decreasing emission at larger galactocentric distances. The reality of the weak features out in the disks is

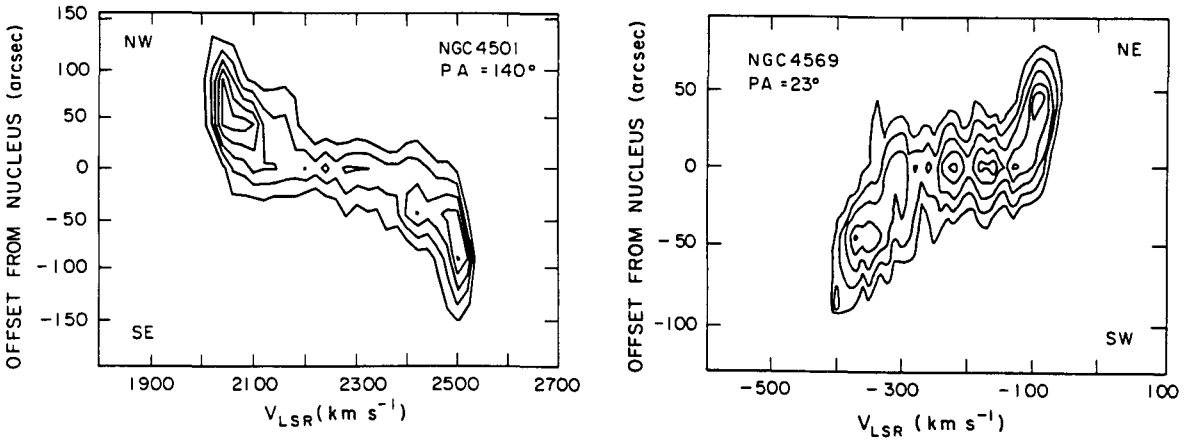


Figure 2. Spatial-velocity plots of ^{12}CO emission along the major axes of NGC4501 and NGC4569. Spectra have been smoothed to a velocity resolution of 15 km s^{-1}. The lowest contour level is 0.013 K for NGC4501 and 0.027 K for NGC4569; the contour increments for both maps are 0.013 K.

confirmed by the agreement in velocity with stronger lines at nearby positions. Data for NGC4501 (Sbc) and NGC4569 (Sab) are displayed in Figure 2 in the form of spatial-velocity plots, where it is clear that the CO emission is associated with the disk of each galaxy.

II. CO AND HI EXTENTS

In order to determine whether or not the molecular cloud contents and CO extents in the Virgo spirals have been altered, it is necessary to make several comparisons between these galaxies and a sample of well-studied galaxies outside of Virgo (see Table 1). We begin by comparing the CO, HI and optical diameters of the galaxies for several reasons. First, gas is less tightly bound to a galaxy far out in the disk due to the overall decreasing mass density; if some process has removed molecular gas from the disk, the effect will most likely show up here. Second, Young, Scoville and Brady (1985) have shown that the central 50" CO luminosities are proportional to the blue luminosities in the same regions for both Virgo and non-Virgo Sc galaxies. However, the bulge contribution to the optical luminosity in Sa-Sb galaxies makes it difficult to establish that early type Virgo galaxies are normal. This problem is avoided by measuring the diameter of a galaxy at some specific disk intensity.

When comparing CO and HI extents, it is necessary to choose appropriate intensity levels for each. A sensible choice would be one where the molecular and atomic hydrogen mass surface densities are equal. Unfortunately, this turns out not to be the best choice, since the weakest ^{12}CO feature which can be

detected in a reasonable amount of time has an integrated intensity $\int T_R^* dv \sim 1$ K km s^{-1}. This corresponds to a face-on surface density $N(H_2) \sim 4 \times 10^{20}$ cos i molecules cm^{-2}, using the conversion factor from ^{12}CO integrated intensity to H_2 surface density derived by Young and Scoville (1982a; hereafter YS82) for the disk of our galaxy, where i is the galaxy's inclination. Some galaxies have HI surface mass densities which never exceed this value. In order to avoid defining an HI extent of zero for galaxies which actually have measurable HI, a face-on surface density $N(HI) = 5 \times 10^{19}$ atoms cm^{-2} has been chosen at which to measure HI extents. This is the lowest contour level on the VLA HI maps of van Gorkom et al., and corresponds to a surface mass density of atomic gas $\sim$16 times smaller than the surface mass density of molecular gas at $N(H_2) \sim 4 \times 10^{20}$ molecules cm^{-2} at which we have measured CO extents.

The ratio of CO to HI extents for 22 Virgo and comparison galaxies is shown as a function of morphological type in Figure 3a. The galaxies comprising the comparison group are those systems in which CO has been mapped out to where the integrated intensity falls to $\sim$1 K km s^{-1}. Included in this group are M31, M51, NGC253, NGC6946, IC342, the peculiar M82, the Seyfert NGC1068, and the galaxies in the Leo Triplet (see Table 1). The Virgo galaxies closest to M87 (NGC4569 and NGC4579, which are both Sab galaxies) stand out in this diagram as systems which have unusually large ratios of CO diameter (D_{CO}) to HI diameter (D_{HI}). There is also a suggestion that some of the Sbc-Sc Virgo galaxies have higher than average values of this ratio. This result is not dependent on the surface density values used. The Virgo and comparison galaxies maintain the same relative positions in this diagram if an HI surface density of 8×10^{20} atoms cm^{-2} is used, corresponding to equivalent atomic and molecular surface mass densities (except in those galaxies in which HI is not detected at this level).

The Virgo spirals with large values for the CO/HI diameter ratio are galaxies which have been shown to be deficient in HI (Huchtmeier, Tammann, and Wendker 1976; Chamaraux, Balkowski, and Gerard 1980; Giovanardi et al. 1983; Giovanelli and Haynes 1983; van Gorkom, Balkowski, and Kotanyi 1984). In order to illustrate that it is the HI deficiency causing the high CO/HI diameter ratio, we have compared both CO and HI extents with optical extents for these same galaxies. For this purpose, D_0 values from the RC2 (deVaucouleurs, deVaucouleurs, and Corwin 1976) are employed. Figure 3b shows the HI to optical diameter ratios as a function of type for the Virgo and comparison galaxies, demonstrating that the HI extents of the Sab galaxies in the center of Virgo are relatively small, as was previously known (Giovanelli and Haynes 1983; van Gorkom, Balkowski, and Kotanyi 1984). In contast, however, there are galaxies of the same morphological type which have much larger HI to optical diameters.

Figure 3c, which displays the CO to optical diameter ratios, shows that the

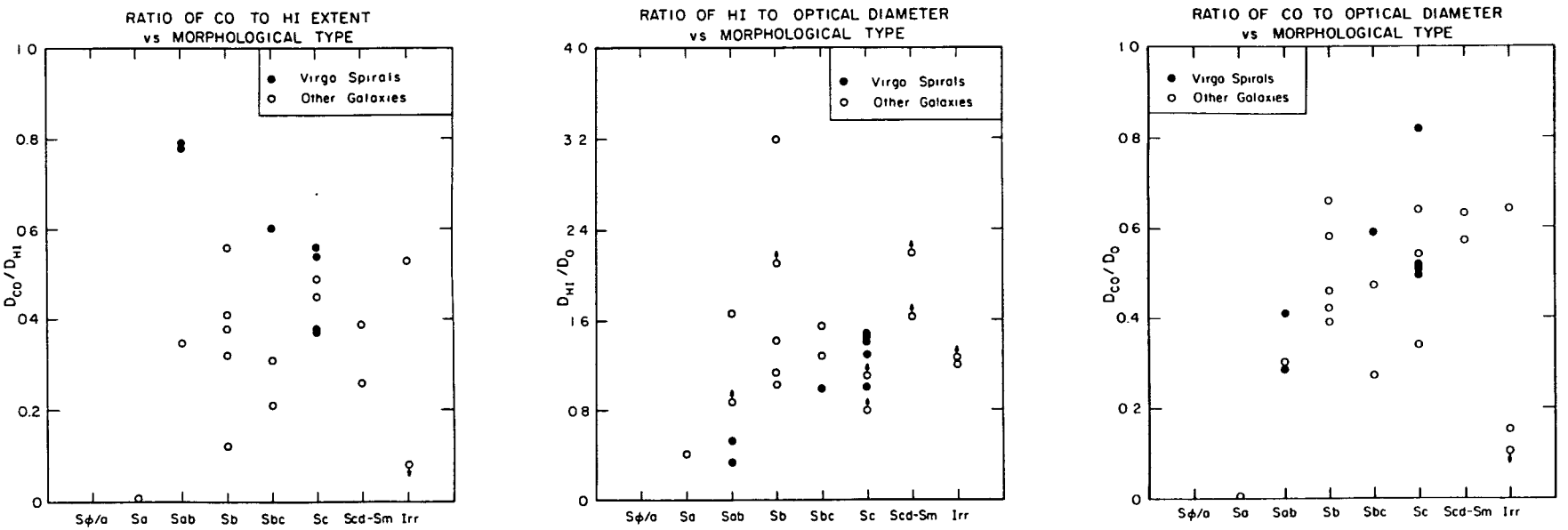


Figure 3. Ratios of the CO, HI, and blue optical diameters as a function of morphological type for Virgo and non-Virgo galaxies. Error bars are not shown, but the errors are dominated by a ~25" uncertainty in the CO diameter, due to the finite resolution of the observations. (a) CO and HI diameter ratios. Typical uncertainty is ~0.10-0.15. The Virgo Sab galaxies NGC4569 and NGC4579 have the largest values of this ratio. (b) HI and optical diameter ratios. Typical uncertainty is ~10-20%. NGC4569, NGC4579 and the Sa galaxy NGC3623 have the smallest values of this ratio. NGC3623 is in the Leo Triplet, and may have a small HI diameter due to galaxy-galaxy interactions within that disturbed group. (c) CO and optical diameter ratios. Typical uncertainties are ~0.05-0.10.

Table 1

GALAXY PROPERTIES

(a) Galaxy	(b) Type	(c) R_{M87}	(d) D	(e) $L_{B_T^o}$	(f) i	(g) D_o	(h) D_{HI}/D_o	(i) D_{CO}/D_o	(j) D_{CO}/D_{HI}	(k) M_{H_2}/M_{HI}	(l) refs
					VIRGO GALAXIES						
N4569	Sab	1.7	20	7.5	61	499	0.34	0.27	0.79	7.0	0,41,21
N4579	Sab	1.8	20	4.6	36	322	0.53	0.42	0.78	4.0	0,41,21
N4548	SBb	2.3	20	3.2	36	322				1.0	0, ,21
N4501	Sbc	2.0	20	7.1	56	379	0.98	0.59	0.60	2.7	0,41,22
N4254	Sc	3.6	20	5.2	27	330	1.47	0.82	0.56	1.6	0,41,21
N4303	Sc	7.9	20	6.4	24	370	1.29	0.49	0.38	1.1	0,40,22
N4321	Sc	3.9	20	7.1	35	425	1.00	0.53	0.54	2.4	0,25,21
N4654	SBc	3.4	20	3.1	51	262	1.40	0.52	0.37	0.3	0,41,21
					NON-VIRGO GALAXIES						
N3623	Sa		7.0	1.0	71	488	0.41	0	0	<0.5	48,19,19
N4736	Sab		6.0	2.1	35	658	>0.87	0.30	<0.35	0.4	14, 6, 6
N 224	Sb		0.7	2.6	77	2090	>2.10	0.66	<0.31	0.5	38,10,10
N 891	Sb		14.0	3.6	~90	628	1.42	0.46	0.32		00,30,30
N1068	Sb		20.0	13.4	35	425	>1.13	0.42	<0.38	4.6	35,27,20
N2841	Sb		7.6	1.3	68	425	3.20	0.39	0.12	0.3	45, 5, 5
N3627	Sb		6.7	1.4	60	466	1.03	0.58	0.56	2.9	48,19,19
N3628	Sc		6.7	1.1	89	673	1.28	0.27	0.21	0.3	48,19,19
N7331	Sbc		20.0	9.7	75	573	1.54	0.47	0.31	0.7	45, 5, 5
N 253	Sc		3.4	2.0	78	1170	>1.10	0.54	<0.49	0.2	00, 8, 8
N5194	Sc		9.6	5.1	20	628	1.43	0.64	0.45	3.0	34,36,36
N5457	Sc		7.2	5.3	25	1691	>0.80	0.34	<0.42	0.2	37, 1, 1
N6946	Scd		10.0	6.4	30	791	>1.62	0.63	<0.39	0.5	44,29,29
IC342	Scd		4.5	2.3	25	1343	>2.19	0.57	<0.26	0.3	44,29,29
N3034	Pec		3.3	0.6	82	382	1.20	0.64	0.53	2.0	46, 9, 9
N4214	Im		5.4	0.4		466	>1.26	<0.10	<0.08	0.002	39, 2, 2

EXPLANATION OF COLUMNS

a) Galaxy name
b) RSA type
c) Angular distance from M87, in degrees
d) Assumed distance in Mpc, used only to calculate blue luminosity
e) Blue luminosity in units of 10^{10} L_o, using B_T^o from RC2, and M_o=5.48
f) Inclination $i=\cos^{-1}(b/a)$ in degrees, where a is major axis, b is minor axis from UGC
g) Blue optical diameter D_o, in arcseconds, corrected for inclination and galactic extinction, from RC2
h) Ratio of HI diameter to blue optical diameter; HI diameter measured to a face-on surface density of $N(HI)=5\times10^{19}$ atom cm^{-2}; 1σ uncertainties are ~10-20%
i) Ratio of CO diameter to blue optical diameter; CO diameter measured to a face-on integrated intensity $\int T_R^* = 1$ K km s^{-1}, corresponding to a face-on surface density $N(H_2) \sim 4\times10^{20}$ molecules cm^{-2}, using the conversion factor from CO to H_2 derived in YS82; 1σ uncertainties are ~0.05-0.10
j) Ratio of CO diameter to HI diameter; 1σ uncertainties are ~0.10-0.15
k) Ratio of H_2 mass to HI mass for entire galaxy, H_2 masses computed using the conversion factor from CO to H_2 in YS82; this column also gives the relative values of the CO to HI line flux ratios with no assumption about the relation between CO line intensity and H_2 surface density; 1σ uncertainties in line flux ratios are ~25%
l) CO reference, HI line flux reference, HI diameter reference: 0 = this paper, 00 = Young, unpublished; all other references numbered at end of paper

CO extents of the Virgo spirals are typical of those in the comparison sample. Furthermore, the CO luminosities of the centers of Virgo galaxies are typical of non-Virgo galaxies, as measured with respect to the blue luminosity in the same aperture (Young, Scoville, and Brady 1985). These two observations, taken together, indicate that the distributions of molecular material in these HI-deficient Virgo galaxies are similar to those in nearby galaxies. It is not yet possible to further quantify this statement since few Sa-Sb galaxies have been mapped in CO; a difference of a factor of ~2 in molecular mass between galaxies in Virgo and the field cannot yet be excluded until more early type spirals have been observed. It is nevertheless clear that the atomic gas in the disks of these Virgo spirals is significantly depleted, while the molecular gas contents are roughly normal.

III. CO AND HI LINE FLUX RATIOS

An additional way to compare the atomic and molecular gas contents is to examine the ratio of CO line flux to HI line flux for the entire galaxy. The total CO line flux for each galaxy may be estimated to ~20% accuracy from major axis observations by assuming that the distribution is azimuthally symmetric in the disk. The HI and CO flux ratios are compared in Figures 4 and 5 as a func-

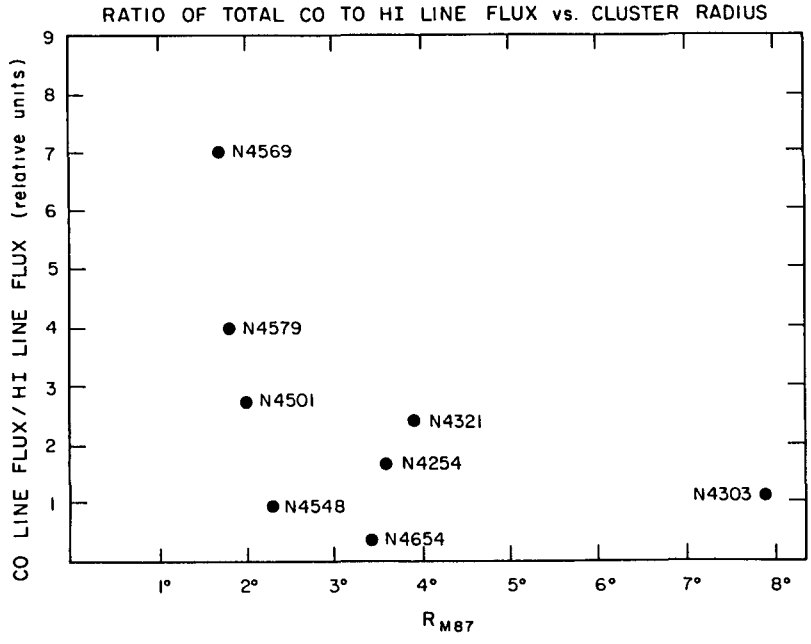


Figure 4. Ratio of CO to HI line flux vs. angular separation from M87. Vertical scale is described in the text. Typical uncertainty in the flux ratio is ~25%.

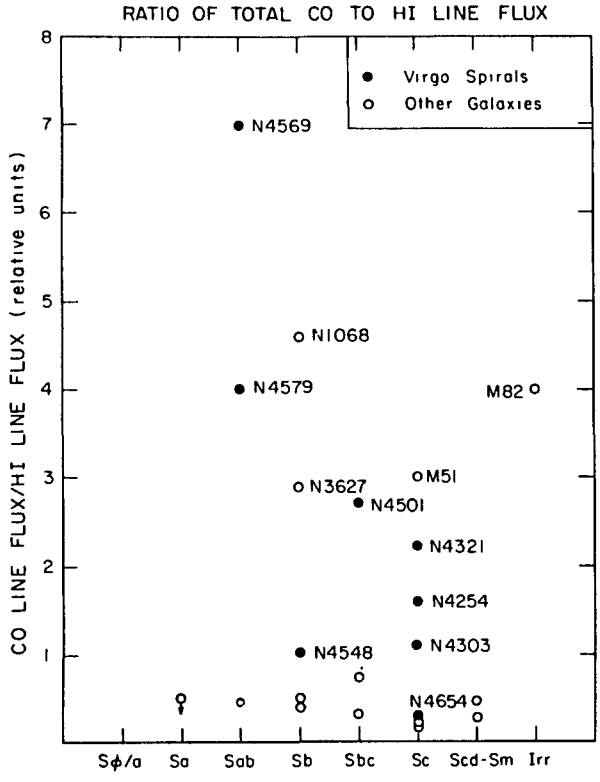


Figure 5. Ratio of CO to HI line flux vs. morphological type. Vertical scale is described in the text.

tion of position in the cluster and morphological type, respectively. Error bars are not shown in these plots, but the variation in this ratio is much larger than the typical uncertainty of ~25%. The numbers on the vertical scale indicate the mass ratio of molecular to atomic gas if the conversion factor between ^{12}CO and H_2 valid in the disk of our our galaxy (YS82) is applied to all the galaxies. This conversion factor is probably the same to within a factor of ~2-3 for most galaxies, based on studies of the $^{12}CO/^{13}CO$ line ratio (Young and Sanders 1985). The one known exception plotted here is M82, whose $^{12}CO/^{13}CO$ line ratio indicates a conversion factor which is ~2-4 times smaller (Young and Scoville 1984).

Figure 4 shows that the Virgo galaxies closest to M87, NGC4569 and NGC4579, have the highest ratios of CO to HI flux. To demonstrate that this result is not the effect of morphological segregation in the cluster, we have plotted in Figure 5 the CO/HI line flux ratios as a function of type for the galaxies listed in Table 1. Even when compared with galaxies of similar morphological type, NGC4569 and NGC4579 have higher than typical values of this flux ratio. Since Virgo disks have average HI surface densities which are typical of those in isolated galaxies (Giovanelli and Haynes 1983), the high CO to HI line flux

ratios reflect the small HI extents of these galaxies. One remarkable feature of Figure 5 is that there are no isolated normal galaxies with high values of the ratio of CO to HI flux. All galaxies in the upper portion of Figure 5 are either in Virgo, experiencing interactions, or suffering other peculiarities: M82 and NGC3627 are each group members, M51 has a companion, and NGC1068 is a Seyfert galaxy. Thus, galaxies with large amounts of CO relative to HI may have suffered stripping of atomic gas, or perhaps unusual conversion of HI into molecular gas.

The HI deficiency of Virgo spirals had been previously measured by comparing the HI and optical properties of the galaxies (see Section II for references). The atomic to molecular gas comparison presented here is not only an independent test of the HI deficiency but valuable since it measures the deficiency with respect to a separate component of the interstellar medium. The existence of roughly normal molecular gas contents in HI-deficient galaxies argues strongly that some mechanism has removed the low density atomic gas, while leaving the high density molecular gas unscathed. In particular, it makes unlikely the possibility that these galaxies are HI-deficient because of less gas infall over the lifetime of the galaxy (Kennicutt 1983). Either ram-pressure stripping or thermal evaporation could account for this present state of the interstellar media. Both effects may be present to some degree, but we will discuss the consistency of the CO observations with ram-pressure stripping in view of the recent evidence for velocity dependent HI deficiencies (Giovanelli and Haynes 1983), and asymmetric HI distributions in the Virgo core (Warmels 1984).

IV. CONSISTENCY WITH RAM-PRESSURE STRIPPING

The effectiveness of ram-pressure stripping is dependent upon the gas surface density. In order for a gas cloud of mass m and area A to be swept from a disk, the ram-pressure force $\rho_{ICM}v^2A$ must exceed the gravitational binding force of the disk $2\pi G\sigma_T m$, where ρ_{ICM} is the mass density of the intracluster medium, v is the velocity of the galaxy through the medium, and σ_T is the total mass surface density of the disk (Gunn and Gott 1972). This leads to the condition for stripping for a disk moving face-on with respect to the intracluster gas:

$$N < \left\{ \frac{n_{ICM}\, v^2}{2\pi\, G\, \sigma_T} \right\}$$

where N is the column density of disk gas, and n_{ICM} is the number density of the

intracluster gas. Using σ_T=0.03 gm cm^{-2}, which is the value for our galaxy at R=8 kpc (Bahcall, Schmidt, and Soneira 1983), the stripping condition becomes

$$N < 5 \times 10^{19} \left\{ \frac{n_{ICM}}{10^{-4} \text{ cm}^{-3}} \right\} \left\{ \frac{v}{780 \text{ km s}^{-1}} \right\}^2 \left\{ \frac{\sigma_T}{.03 \text{ gm cm}^{-2}} \right\}^{-1} \text{ nuclei cm}^{-2}$$

where 780 km s^{-1} is the cluster velocity dispersion for spirals (Ftaclas et al. 1984), and 10^{-4} cm^{-3} is an estimate of the intracluster gas density 2° from M87, based on an isothermal sphere model (Gorenstein et al. 1977; Forman et al. 1979).

Surveys of ^{12}CO line emission in the disk of our galaxy suggest that most of the mass of molecules is contained in several thousand clouds with diameters >22 pc, and masses >10^5 M_o (Sanders et al. 1985). Such clouds have surface densities N> 3x10^{22} nuclei cm^{-2}, and therefore would not be stripped from a galaxy moving with 2 times the cluster velocity dispersion (as high as any Virgo spiral) by the intracluster gas 1° from M87 with a density $n_{ICM} \sim 10^{-3}$ cm^{-3}. Thus, most of the molecular material in a galaxy would survive even the extreme conditions in the center of the Virgo cluster, whereas the HI would not. The fact that the CO distributions and extents in the Virgo spirals are similar to those in non-Virgo galaxies (see paper by J. Young, in these proceedings) suggests that the H_2 has indeed not been stripped, and that the dense component of the ISM has not had sufficient time to respond to the rapidly changing conditions in the galaxy, as discussed below.

V. THE FATE OF MOLECULAR CLOUDS IN HI-STRIPPED GALAXIES

The existence of roughly normal molecular gas contents of HI-deficient galaxies indicates that the lifetime of the molecular gas phase in galaxies is greater than the atomic gas removal time scale. Estimates of cloud lifetimes have ranged from ~10^7 years (Blitz and Shu 1980) to ~10^9 years (Scoville and Hersh 1979). The time scale for ram-pressure stripping is

$$\tau_{RAM} \sim \left\{ \frac{2 \text{ s N}}{n_{ICM} \text{ v}^2} \right\}^{1/2}$$

if the stripping force dominates the gravitational attraction of the disk for a column density of gas N. In this equation, s is the height above the disk at

which the gas has become stripped, i.e. ionized by the hot intracluster gas and no longer detectable as HI. For reasonable estimates of the relevant parameters ($s \sim 1$ kpc, $n_{ICM} \sim 10^{-4}$ cm^{-3}, $v \sim 780$ km s^{-1}, $N \sim 2 \times 10^{20}$ cm^{-2}), $\tau_{RAM} \sim 5 \times 10^{7}$ years. Therefore the fact that we observe normal CO emission in Virgo galaxies suggests that the molecular cloud lifetimes are at least $\sim 10^{8}$ years.

Long-lived molecular clouds will mitigate the impact of even severe stripping events, since star formation will not be truncated due to the survival of the molecular component. However if the medium out of which the H_2 was forming is removed, the formation of molecular clouds will be halted, and the gas consumption mechanisms (star formation, ionization, supernovae) will act to decrease the supply of molecular material. The inevitable disruption of part of the molecular component by processes including ionization, supernovae, and galactic shocks should act to redistribute the gaseous matter in an HI-stripped galaxy from the molecular to atomic phase. While the galaxy is still in the 'stripping zone', this low density gas will tend to be lost; but when the galaxy reemerges from the core region, the redistribution should act to 'resupply' atomic gas at the expense of the molecular phase.

The impact of a stripping event on star formation may depend upon the detailed response of the molecular cloud population. While the GMC's are difficult to strip, smaller clouds ($N \leq 10^{21}$ nuclei cm^{-2}) at large galactic radii may be susceptible to removal when a galaxy is in the cluster core. If GMC's grow by colliding with smaller clouds (Kwan 1979), then the depletion of smaller clouds (both by stripping and removal of the H_2-forming material), coupled with the inevitable consumption of gas within GMC's will lead to GMC masses which shrink with time. Thus, a stripping event may radically alter the size distribution of a galaxy's molecular cloud population. It is not yet known if the star formation efficiency and the initial mass function are strong functions of cloud size, but if they are, ram-pressure stripping of low density gas could irreversibly alter the star formation and evolution of a galaxy.

REFERENCES

1. Allen, R. J., and Goss, W. M. 1979, A. A. Suppl., 36, 135.
2. Allsopp, N. J. 1979, M.N.R.A.S., 188, 765.
3. Bahcall, J. N., Schmidt, M., and Soneira, R. N. 1983, Ap. J., 265, 730.
4. Blitz, L., and Shu, F. H. 1980, Ap. J., 238, 148.
5. Bosma, A. 1978, Ph. D. Thesis, Groningen.
6. Bosma, A., van der Hulst, J. M., and Sullivan, W. T., III 1977, A. A., 57, 373.
7. Chamaraux, P., Balkowski, C., and Gerard, E. 1980, A. A., 83, 38.
8. Combes, F., Gottesman, S. T., and Weliachew, L. 1977, A. A., 59, 181.

9. Cottrell, G. A. 1977, M.N.R.A.S., 178, 577.
10. Cram, T. R., Roberts, M. S., and Whitehurst, R. 1980, A. A. Suppl., 40, 215.
11. deVaucouleurs, G.,deVaucouleurs, A., and Corwin, H. G. 1976, Second Reference Catalouge of Bright Galaxies (Austin: University of Texas Press) (RC2).
12. Forman, W., Schwarz, J., Jones, C., Liller, W., and Fabian, A.C. 1979, Ap. J. (Letters), 234, L27.
13. Ftaclas, C., Fanelli, M. N., and Struble, M. F. 1984, Ap. J., 282, 19.
14. Garman, L. 1984, private communication.
15. Giovanardi, C., Helou, G., Salpeter, E. E., and Krumm, N. 1983, Ap. J., 267, 35.
16. Giovanelli, R., and Haynes, M. P. 1983, A. J., 88, 881.
17. Gorenstein, P., Fabricant, D., Topka, K., Tucker, W., and Harnden, F. R., Jr. 1977, Ap. J. (Letters), 216, L95.
18. Gunn, J. E., and Gott, J. R. 1972, Ap. J., 176, 1.
19. Haynes, M. P., Giovanelli, R., and Roberts, M. 1979, Ap. J., 229, 83.
20. Heckman, T. M., Balick, B., and Sullivan, W. T., III 1978, Ap. J., 224, 745.
21. Helou, G., Giovanardi, C., Salpeter, E. E., and Krumm, N. 1981, Ap. J. Suppl., 46, 267.
22. Helou, G., Hoffman, G. L., and Salpeter, E. E. 1984, Ap. J. Suppl., 55, 433.
23. Huchtmeier, W. K., Tammann, G. A., and Wendker, H. J. 1976, A. A., 46, 381.
24. Kennicutt, R. C., Jr. 1983, A. J., 88, 483.
25. Kotanyi, C. 1984, private communication.
26. Kwan, J. 1979, Ap. J., 229, 567.
27. Liszt, H. 1982, private communication.
28. Nilson, P. 1973, Uppsala General Catalouge of Galaxies (Uppsala) (UGC).
29. Rogstad, D. H., and Shostak, G. S. 1973, A. A., 22, 111.
30. Sancisi, R., and Allen, R. J. 1979, A. A., 74, 73.
31. Sandage, A., and Tammann, G. A. 1981, Revised Shapley-Ames Catalouge of Bright Galaxies (Washington: Carnegie Institution) (RSA).
32. Sanders, D. B., Scoville, N. Z., and Solomon, P. M. 1985, Ap. J., in press (Jan. 1).
33. Scoville, N. Z., and Hersh, K. 1979, Ap. J., 229, 578.
34. Scoville, N. Z., and Young, J. S. 1983, Ap. J., 265, 148.
35. Scoville, N. Z., Young, J. S., and Lucy, L. B. 1983, Ap. J., 270, 443.
36. Shane, W. W., 1975, in Les Dynamiques des Galaxies Spirales, ed. L. Weliachew (CNRS Colloque No. 241), p. 217.
37. Solomon, P. M., Barrett, J., Sanders, D. B., and deZafra, R. 1983, Ap. J. (Letters), 266, L103.

38. Stark, A. A. 1979, Ph. D. Thesis, Princeton University.
39. Tacconi, L. J., and Young, J. S. 1985, Ap. J., in press.
40. van Gorkom, J., private communication.
41. van Gorkom, J., Balkowski, C., and Kotanyi, C. 1984, preprint.
42. Warmels, R. 1984, this volume.
43. Young, J. S., and Sanders, D. B. 1985, Ap. J., in preparation.
44. Young, J. S., and Scoville, N. Z. 1982a, Ap. J., 258, 467 (YS82).
45. Young, J. S., and Scoville, N. Z. 1982b, Ap. J. (Letters), 260, L41.
46. Young, J. S., and Scoville, N. Z. 1984, Ap. J., in press (Dec. 1).
47. Young, J. S., Scoville, N. Z., and Brady, E. 1985, Ap. J., in press (Jan. 15).
48. Young, J. S., Tacconi, L. J., and Scoville, N. Z. 1983, Ap. J., 269, 136.

IV.

OPTICAL OBSERVATIONS

THE VIRGO CLUSTER REDSHIFT SURVEY

J. P. Huchra

Harvard-Smithsonian Center for Astrophysics
60 Garden Street, Cambridge, MA 02138

ABSTRACT

We have measured and collected velocities for 99% of the 471 galaxies brighter that $m_{pg} = 15.5$ and within 6° of the center of the Virgo cluster. In total, there are now 602 galaxies with measured velocities in the 6° circle, of which 362 have velocities less than 3000 km s^{-1} and may be considered for cluster membership.

There is significant correlated velocity and spatial structure in the core of the cluster. There exist individual clumps of galaxies associated with both M87 (NGC4486) and M49 (NGC4472). The velocity dispersion of the M87 clump is 1.6 times larger than that of the M49 clump, probably explaining the distribution of x-ray emission in the cluster. Estimates of the cluster mass made by assuming that the central region is a virialized single "object" overestimate the cluster mass.

The cluster luminosity function is derived with background galaxies removed assuming that all objects with $v < 3000$ km s^{-1} are members. It is surprisingly flat at the faint end. Although the Schechter form is a poor representation, the faint end slope is approximately 1.2, the same as for the CfA redshift survey as a whole.

I. INTRODUCTION

We are now extending the CfA Redshift Survey (Huchra et al. 1982) in the northern hemisphere to a limiting magnitude of 15.5 in the Zwicky et al. catalogue (eg. Zwicky et al. 1961-63). In order to provide intermediate results (funding, you know), our logical first step was to "drill" the centers of nearby clusters of galaxies. The nearest big - although not terribly rich - cluster is Virgo. Virgo lies at the center of the local supercluster and also at the center of several important controversies in extragalactic astronomy: the Hubble constant, the missing mass

problem, Supercluster dynamics, the morphology-density relation, the "stripping" of spiral galaxies by the intracluster medium, and X-ray cooling flows, to name just a few. For these reasons, Virgo was among the first clusters chosen for deep study.

We present here an almost complete (> 99.7%) survey of the 6 degree radius region centered on the Virgo cluster to B(0) = 15.5. With this information it is possible to study the cluster luminosity function, to calculate the mean Virgo velocity (for the Hubble constant and Virgo infall calculations), and to study the cluster's internal dynamics.

II. THE CLUSTER CENTER

There has been considerable controversy over the position of the center of the Virgo cluster. Without velocity information, the problem of finding the cluster center is nontrivial. For example, Figure 1 presents a contour map of the surface number density of galaxies in the Zwicky catalogue. The map is 48 degrees across and is approximately centered on Virgo. The blank strip at the bottom is due to the catalogue cutoff below -3 degrees declination. Virgo is a mess; the Coma and Abell 1367 clusters seen in the top third of the map are considerably better defined. (Note also the large "void" to the NE of Virgo and S of Coma!)

Several centers have been suggested in the literature for Virgo: Sandage and Tammann (1976) give R.A. = 12 25.0 Dec. = +13 06, de Vaucouleurs and de Vaucouleurs (1973) give 12 27.0 +13 30, while the center of the X-ray distribution is undoubtedly M87 at 12 28.3 +12 40 (Fabricant and Gorenstein 1981), and the brightest galaxy in the cluster is NGC 4472 at 12 27.2 +08 16 (Aaronson and Mould 1981). NGC 4472 is over 4° from the other centers. With the completion of the CfA survey to 14.5, it is possible to use velocity information to select member galaxies - as we shall see, the cluster is well isolated from background contamination. Figure 2 shows the isopleths for just those galaxies with velocities less than 3000 km/s and brighter than 14.5. With this sample we find that the luminosity weighted center of the galaxy distribution (assuming that all objects are at the cluster distance) is at R.A. = 12 27.8 Dec. = +12 56 with an error of approximately 3 arcminutes. This is about 20' to the NW of M87 and is the position to which we will refer all following

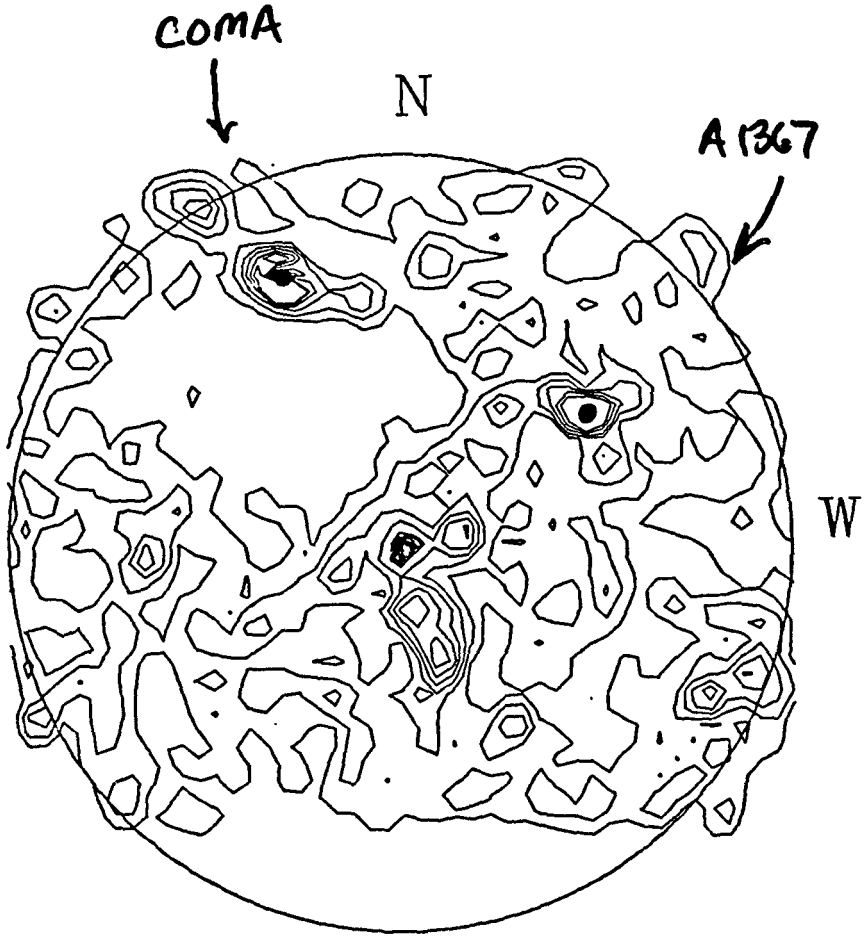


Figure 1. Isopleths of all galaxies in the Zwicky catalog in a 24° radius centered on Virgo.

definitions of the sample. It is in reasonably good agreement with the positions of both Sandage and de Vaucouleurs.

III. THE DATA

The 6 degree radius circle contains 471 galaxies plus 1 plate flaw (Zw1227+1753) with $m_{pg} \leq 15.5$. We now have velocities for 470 of the galaxies in this sample plus an additional 132 velocities for fainter galaxies. 385 of these have been measured with the Whipple Observatory 1.5-m, 10 were measured at the MMT, 88 were measured by Karachentsev and Karachentseva (1983, mostly faint, compact galaxies), 24 were measured at Arecibo by Bothun et al. (1984), Giovanelli and Haynes (1984), and Helou, Hoffman and Salpeter (1984), and the remainder come from various sources in the

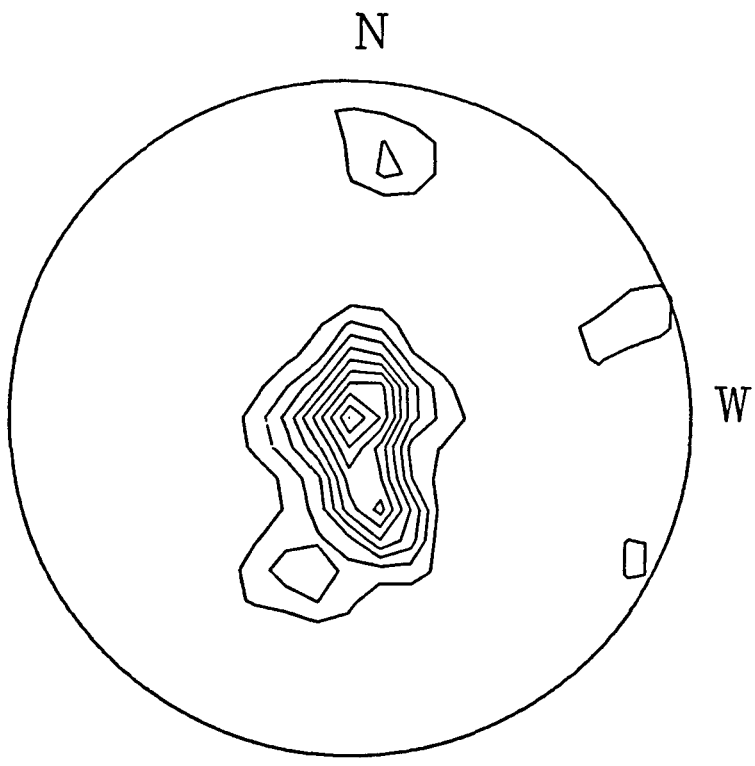


Figure 2. Isopleths for galaxies brighter than 14.5 and with velocities less than 2700 km/sec in the same 24° radius circle around Virgo.

literature (see Huchra et al. 1985). Of the velocities measured with the 1.5-m, approximately 20 are much poorer than average CfA survey quality and will be remeasured with the MMT next spring. Removal of these velocities from the kinematical analysis changes the cluster mean by less than 5 km/s. Figure 3 shows the distribution of all of the 602 galaxies with velocities.

327 of the 470 in the "complete" sample have velocities less than 3000 km/s and are almost certainly cluster members. Only 361 of the total 602 velocities are less than 3000 km/s, which indicates that most of the galaxies fainter than 16th magnitude that have been observed are <u>not</u> cluster members. There is also a very large hole or "void" behind Virgo. Figures 4a and 4b show the velocity histograms for the "complete" cluster and background sample.

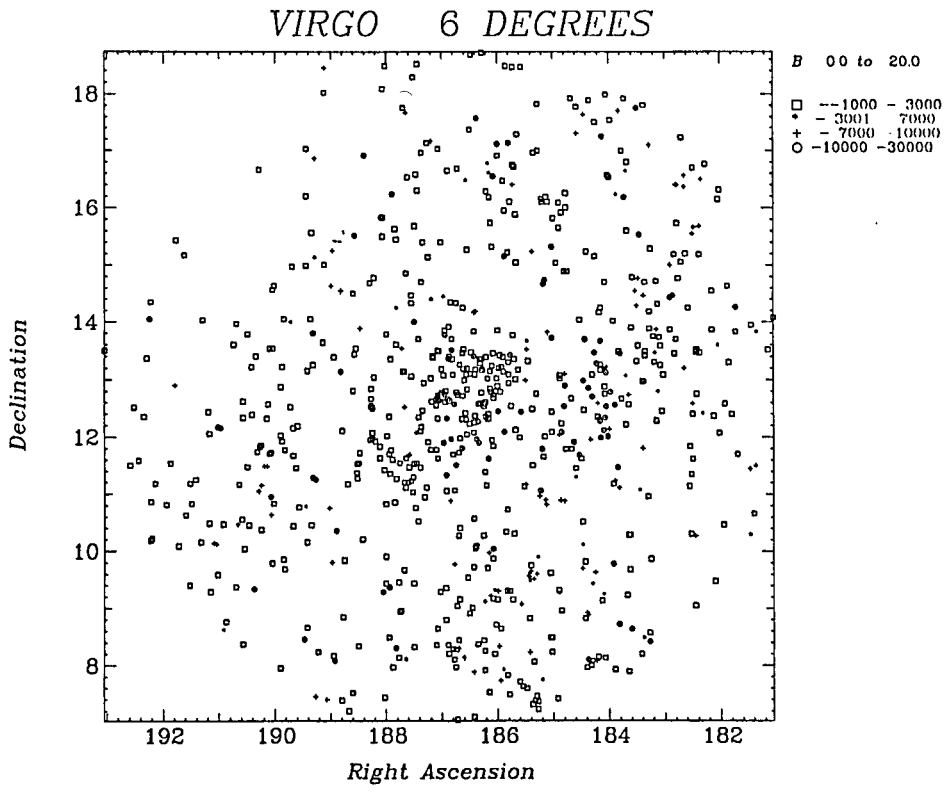


Figure 3. Galaxies with velocities.

Only 4 galaxies have velocities in the interval 2900 to 5900 km/s; this is the velocity range in which the histogram should peak for a randomly distributed sample with a normal luminosity function. This void is underdense by a factor of 10. A large number of galaxies behind the Virgo void have velocities near 7000 km/s, which places them in a southern extension of the Coma supercluster.

Almost all the available evidence supports the hypothesis that most of the galaxies with velocities less than 3000 km/s are cluster members. Of the 60 or so galaxies that have independent distance estimates from the Tully-Fisher relation (Aaronson et al. 1982) or from luminosity class information (de Vaucouleurs 1982), only 6 are questionable members. These are noted in Table 1.

We have also discovered a background cluster of galaxies at a redshift of z = 0.09 almost directly behind M87 (Huchra and Brodie 1984). New measurements by Karachentsev and Karachentseva have brought the total number of galaxies in the velocity range 24,000

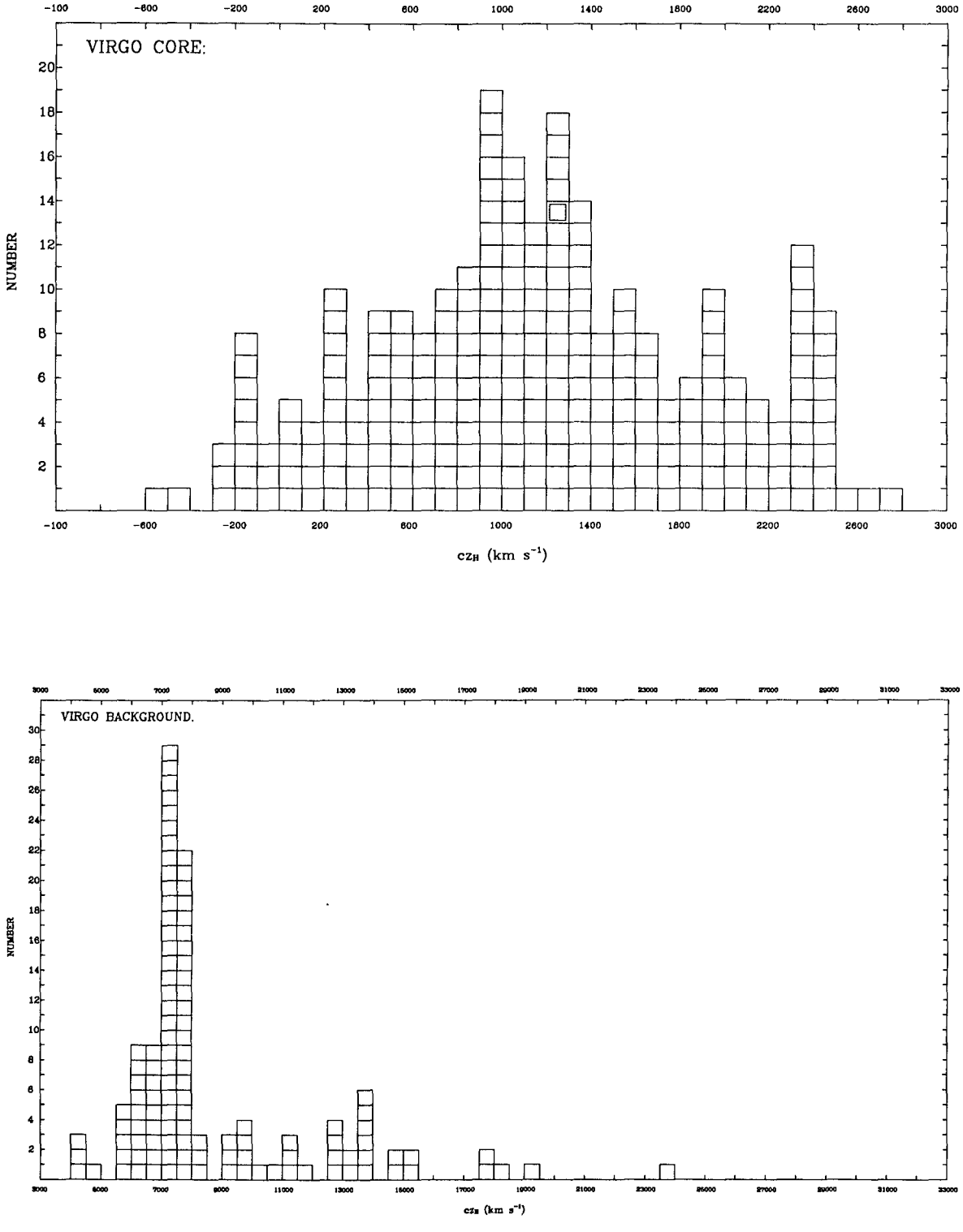


Figure 4. (a) Velocity histogram for galaxies with velocities less than 3000 km/s. (b) Histogram of the background.

Table 1 Suspected Background and Foreground Galaxies

Name	Distance	Velocity (Heliocentric)
NGC 4569	Foreground	-223 km/sec
NGC 4438	Foreground? (AGN)	86
NGC 4192	Foreground	-98
NGC 4189	Background	2123
IC 769	Background	2188
NGC 4152	Background	2161
NGC 4567	Background	2186

Removal of all of these galaxies from the sample lowers the mean cluster velocity by only 1 km/s.

to 29,000 km/s to 18; the mean background cluster redshift is ~ 26,300 km/s and its l.o.s. velocity dispersion is almost 1000 km/s. This probably complicates the X-ray measurements near M87.

IV. LUMINOSITY FUNCTION

The calculation of the luminosity function is essentially straightforward. We assume that all galaxies are at the cluster distance (taken here to be 16 Mpc as found by Mould, Aaronson and Huchra 1981, and by Aaronson and Mould 1983), and we compute the "effective volume" of a 6 degree radius sphere at that distance. This will overestimate the normalization by only a small factor ($\lesssim$1.3) because the volume density in the cluster is falling off by ~ $1/r^2$. The foreground-background contamination is minimal. A quick and dirty estimate of the number of "random" galaxies in a 6 degree cone cut at 3000 km/s was made by examining other regions of the sky that we have sampled to the same limiting magnitude (specifically regions centered on the Coma, Cancer, Hercules, and A194 clusters). The total number of galaxies per square degree in those regions was 1.4 times that in the Virgo cone, nevertheless there were only 15 galaxies between -1000 and 3000 km/s over a comparable surface area.

The sample has also been checked for incompleteness against the lists of faint dwarf galaxies published by Reaves (1983), Caldwell (1983), Binggeli, Sandage and Tarenghi (1984), and Sandage and Binggeli (1984) with photometry in the B_T system. Within the errors in transforming to B(0) and the errors in the Zwicky catalog magnitudes (Huchra 1976), we did not find any galaxies that should have been included in the above sample which were not. The above sample is thus very close to complete.

Figure 5 shows the differential Virgo cluster luminosity function and, for comparison, the luminosity function derived for the entire 2400 galaxy CfA Survey (Davis and Huchra 1981). The Schechter function shape parameters for the two luminosity functions are alpha = -1.18 and -1.30 and M^* = -20.1 and -19.4, respectively. These are identical to within their errors. The cluster function may be rising at absolute magnitudes fainter than -16 as a consequence of the large number of dwarf elliptical galaxies in the cluster (see the papers by A. Sandage and B.

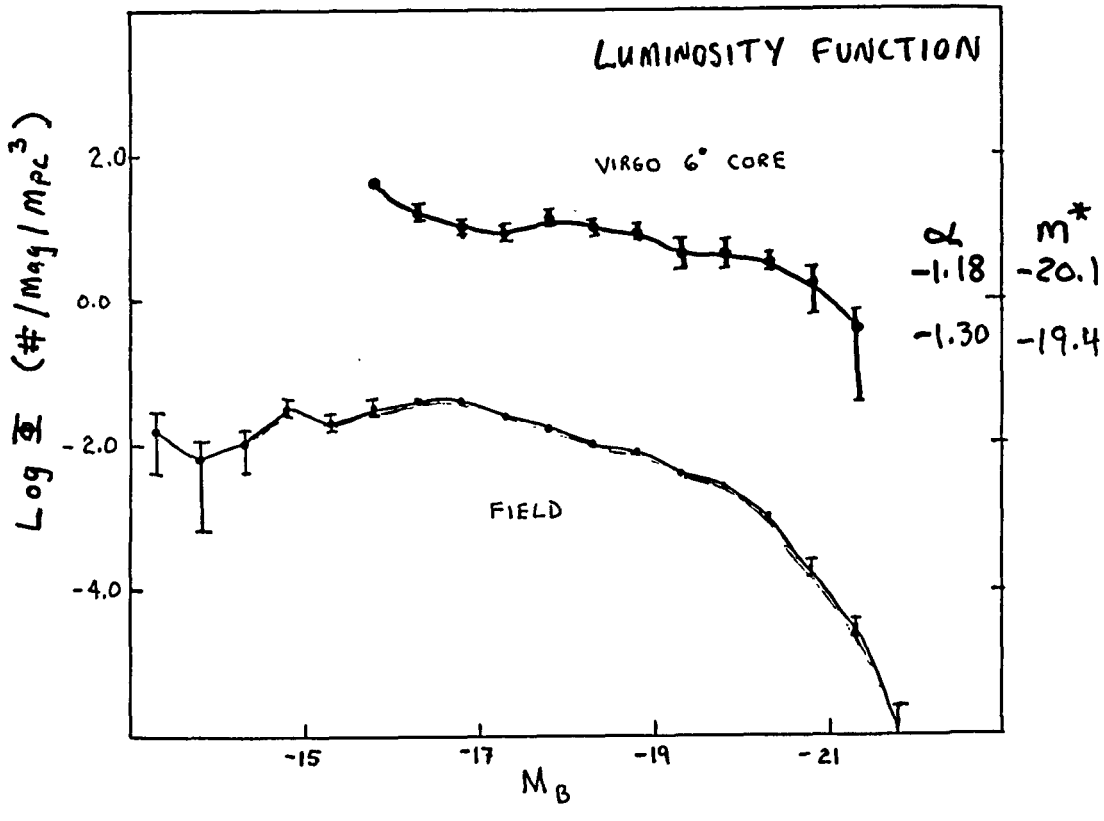


Figure 5. Differential luminosity functions for Virgo and the Field.

Binggeli 1984, and also papers in this conference). Please note that the field function is very poorly determined below magnitude -15.5 because the sample is still very small and very much dominated by the effects of the Local Supercluster. The values for the local function plotted here are partially corrected (maybe even over-corrected) for that overdensity; a more detailed description of the field function is in preparation (Huchra 1985).

V. KINEMATICS

With the complete sample in hand, we can try to answer many of the classical conundrums that have plagued the analysis of the Virgo core. Two such are the question of the behavior of the mean cluster velocity as a function of magnitude and as a function of morphological type (de Vaucouleurs and de Vaucouleurs 1972; Tammann 1972; Sulentic 1977, 1980). Table 2 gives our heliocentric mean velocities for different magnitude cuts and for the early and late type galaxies. There is no correlation between magnitude and either mean velocity or velocity dispersion. The mean velocity for the entire sample of 1151 km/s is very insensitive to the removal of small numbers of suspected background and foreground galaxies. This value is only slightly higher than the unweighted velocity of 1110 51 quoted earlier (Mould, Aaronson and Huchra 1980); the difference is well within the sample statistics. The mean velocities for the E and S0 galaxies is the same as that of the S and Irr galaxies (0.8 sigma). The velocities thus provide no evidence that the ellipticals and spirals are at different mean distances. However, the velocity dispersion for the early types is significantly smaller (4.4 sigma) than that of the late types. We will return to this point later.

Note that we quote straight means and dispersions as opposed to luminosity weighted values; if galaxies really represent test points moving in a global cluster potential, unweighted values are proper for any kinematical or dynamical application (Bahcall and Tremaine 1981).

The next simple kinematical questions are the determinations of the surface density and velocity dispersion as a function of radius. Figure 6 shows the galaxy surface number density as a function of radius, and Table 3 presents the velocity and velocity dispersion as a function of radius. As can be seen, the cluster

Table 2 Velocity and Dispersion vs Magnitude & Type*

Sample	n	V	l.o.s. Disp.
ALL	362	1151 ± 38	721 (+28/-26)
< 11.5	23	970 ± 163	762 (+147/-93)
11.5-12.5	39	1189 ± 106	652 (+90/-63)
12.5-13.5	55	1249 ± 91	667 (+75/-56)
13.5-14.5	53	1169 ± 100	723 (+83/-62)
14.5-15.5	159	1172 ± 58	732 (+45/-38)
< 15.5	326	1172 ± 39	712 (+30/-26)
S's	163	1144 ± 64	817 (+49/-42)
E's	164	1200 ± 46	581 (+35/-30)

* Averages and dispersions from all galaxies with velocities less than 3000 km/s. Mean velocities quoted are heliocentric and are not luminosity weighted.

surface profile is complex and not easily fit with a simple power law. This bodes ill for any of the simple dynamical analyses of the cluster which, like the virial theorem, depend on determining a cluster scale length. The velocity dispersion profile is surprisingly flat and only begins to fall in the outer 1 degree of our circle.

Table 3 Velocity and Dispersion vs Radius*

Sample	n	V	l.o.s. Disp
ALL	362	1151 ± 38	721 (+28/-25)
0° - 1°	35	1174 ± 122	711 (+105/-73)
1° - 2°	58	977 ± 106	803 (+87/-66)
2° - 3°	55	1127 ± 107	785 (+88/-66)
3° - 4°	82	1052 ± 82	740 (+66/-52)
4° - 5°	71	1288 ± 81	678 (+65/-51)
5° - 6°	61	1296 ± 73	565 (+60/-45)

* Units the same as in Table 2.

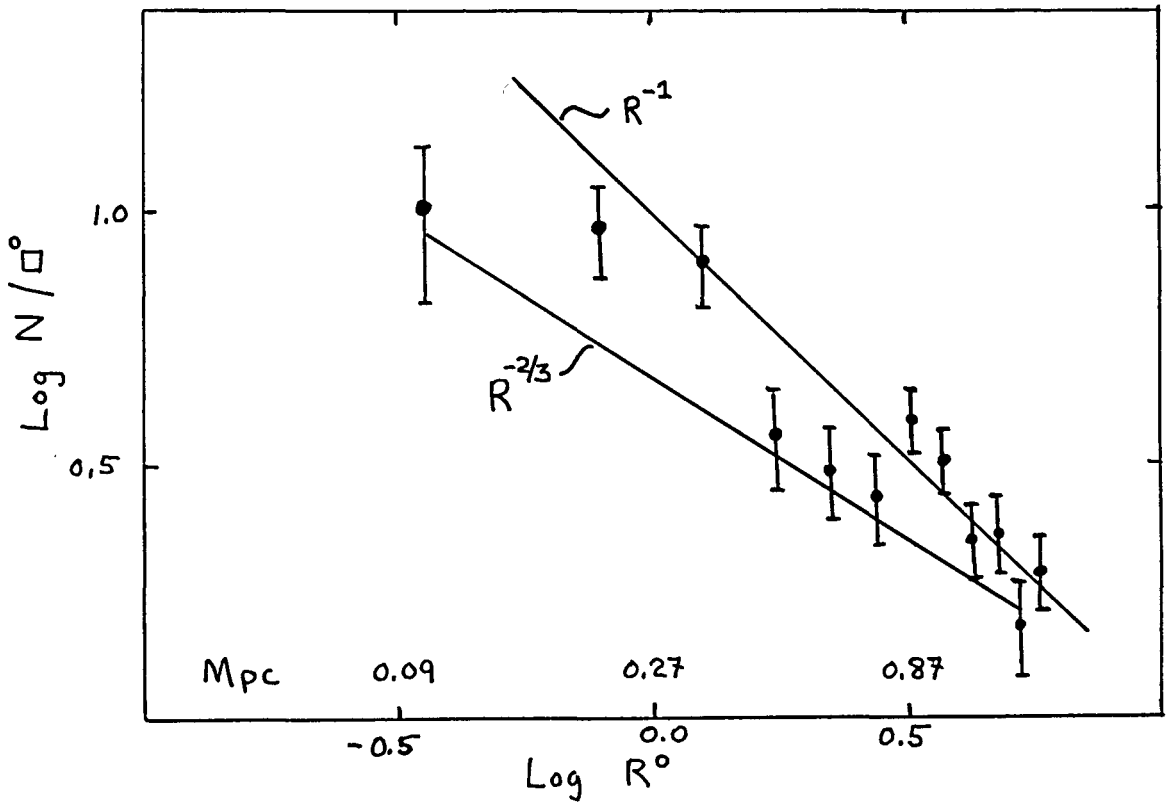


Figure 6. Virgo surface number density profile.

As was pointed out earlier (Bothun et al. 1983; Huchra, Davis and Latham 1984), it is also informative to look at the velocity-position distributions in the cluster. Figure 7 presents four sets of isopleths for the cluster core: (a) all the galaxies in the magnitude limited sample, (b) galaxies between -500 and 500 km/s, (c) galaxies between 500 and 1500 km/s, and (d) galaxies between 1500 and 3000 km/s. The distribution is quite complex. There is a central region about 2° in radius centered near M87 containing galaxies in all velocity ranges - and thus having a fairly high velocity dispersion. This is the center of the cluster X-ray emission as well. The region surrounding NGC 4472 is easily seen only in the central velocity range, and has a much lower velocity dispersion. This probably explains why NGC 4472, despite being the brightest galaxy in the cluster, is not at the center of the x-ray emission: it is not at the center of the dynamical potential well.

To the west are two clumps of galaxies that are well separated in velocity space. One is seen only in the low velocity map and

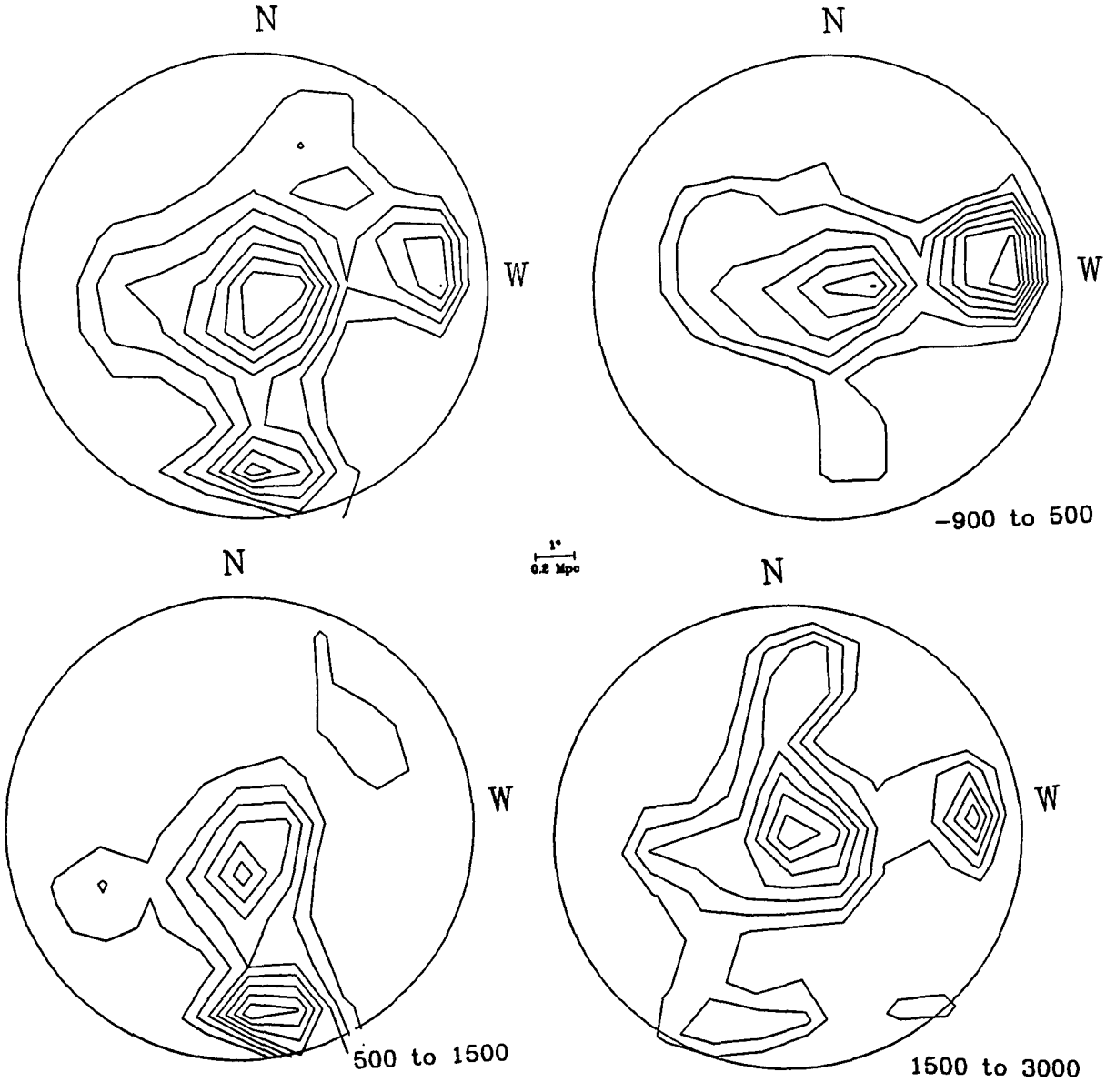


Figure 7. Isopleths for all Virgo galaxies and for galaxies in the velocity ranges -900-500, 500-1500, and 1500-3000 km/s in the 6° circle. These maps have been made with overlapping 2° binning.

the other only in the high. Distance estimates exist for 3 galaxies in each of these condensations and it is very likely that the high velocity clump is background to the cluster as a whole. The low velocity clump is probably at the cluster distance. Removal of all of the members of the high velocity clump lowers our derived cluster velocity by 52 km/s. In that case, the cluster

heliocentric mean velocity is 1099 km/s and its "Local Groupocentric" velocity is only 982 km/s (Yahil, Tammann and Sandage 1977). This is a dangerous exercise until better information is available on both the remaining galaxies in the clump and the general problem of foreground contamination over the cluster (eg. Ftaclas et al. 1984).

We do not find any significant luminosity segregation in the cluster.

VI. DYNAMICS, M/L AND INFALL

The simplest dynamical model treats the entire cluster core as virialized. Using the standard formalism (Bahcall and Tremaine 1981; Beers et al. 1984), and assuming that the cluster is at 16 Mpc, we find that the mean harmonic radius of the galaxies inside the 6° circle is 0.80 Mpc and that the cluster mass is 7.9×10^{14} solar masses. The cluster mass-to-light ratio, M/L, is then 750 in solar units. Note that if the cluster is, in fact, only bound, then the potential energy is equal to the kinetic energy and the mass and M/L are <u>one-half</u> the virialized values. We will argue below that that is more probably the correct dynamical state of the 6° core.

With a superb data set, it is possible to analyse the cluster in somewhat greater detail. Our isopleths, particularly the velocity cuts, suggest an analysis of individual condensations. The two largest concentrations of galaxies are those around M87 and NGC 4472. Figure 8 shows the velocity histograms for the galaxies within 2° of those galaxies.

The clump around M87 has a much higher velocity dispersion. Note also that although the velocity of M87 itself (1286 km/s) differs considerably from the cluster mean and that of NGC 4472 (997 km/s), the mean velocities of the two clumps are almost identical (1061 km/s for M87 and companions versus 1072 km/s for NGC 4472 and companions). If the two clumps are treated as virialized, their masses are 3.1×10^{14} and 1.4×10^{14} solar masses, respectively, yielding M/L's of 1325 and 730! The "closure" M/L in our system is approximately 1700 (note that a Virgo distance of 16 Mpc combined with a Virgocentric infall of the Local Group of about 250 km/s, Aaronson et al. 1982, implies $H_{o} = 80$ km/s/Mpc). The two small

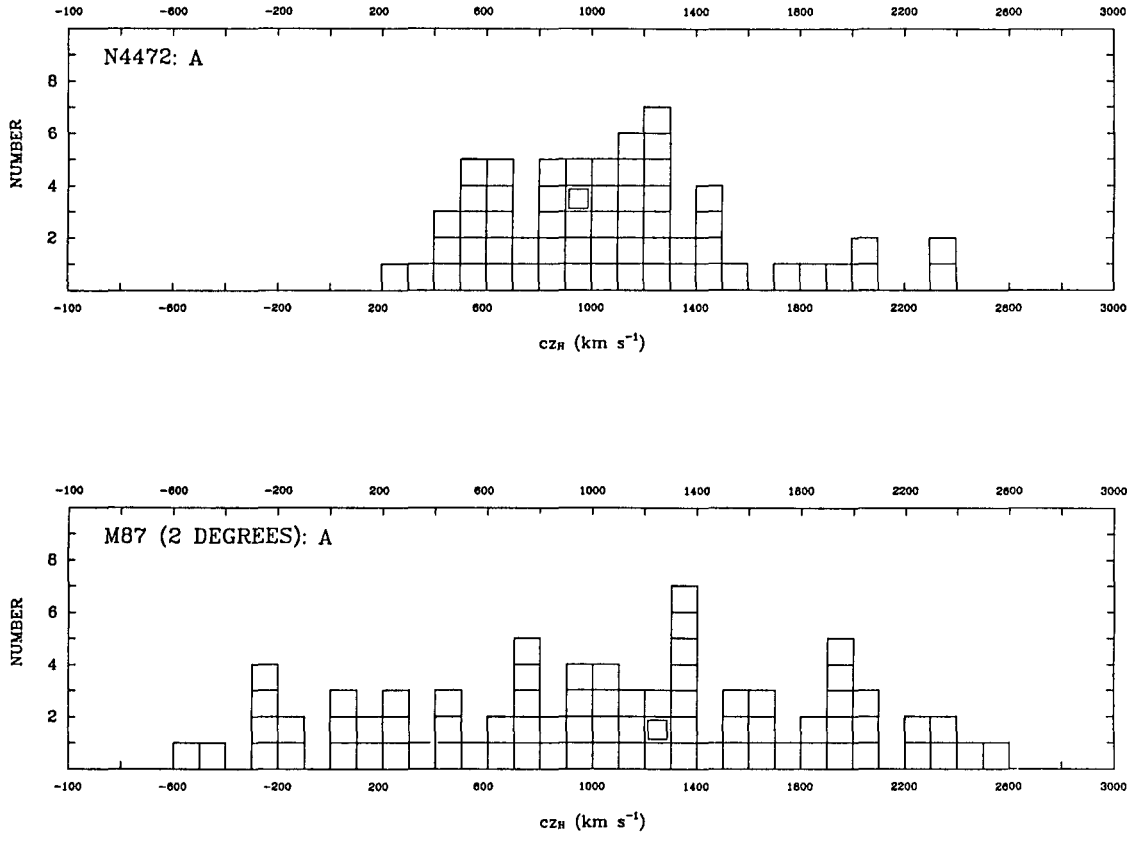


Figure 8. Velocity histograms for the galaxies within 2° of M87 and NGC 4472. The boxes corresponding to M87 and NGC 4472 are marked.

condensations to the W both have very low masses and M/L's (100 for the low velocity clump and 165 for the high velocity clump).

A very interesting difference exists between the distributions of the early versus late type galaxies. We have already noted the difference in their velocity dispersions. This was noted previously by deVaucouleurs on the basis of only 1/6th as many velocities as we now have. We show this again in the velocity histograms of Figure 9.

The distribution for the ellipticals is Gaussian as would be expected for a dynamically relaxed system. The distribution for the spirals is almost flat; certainly very different from the elliptical histogram and not symptomatic of a relaxed system. The gross difference in the distributions of spirals and ellipticals is also see in the spatial distributions. We have morphologically

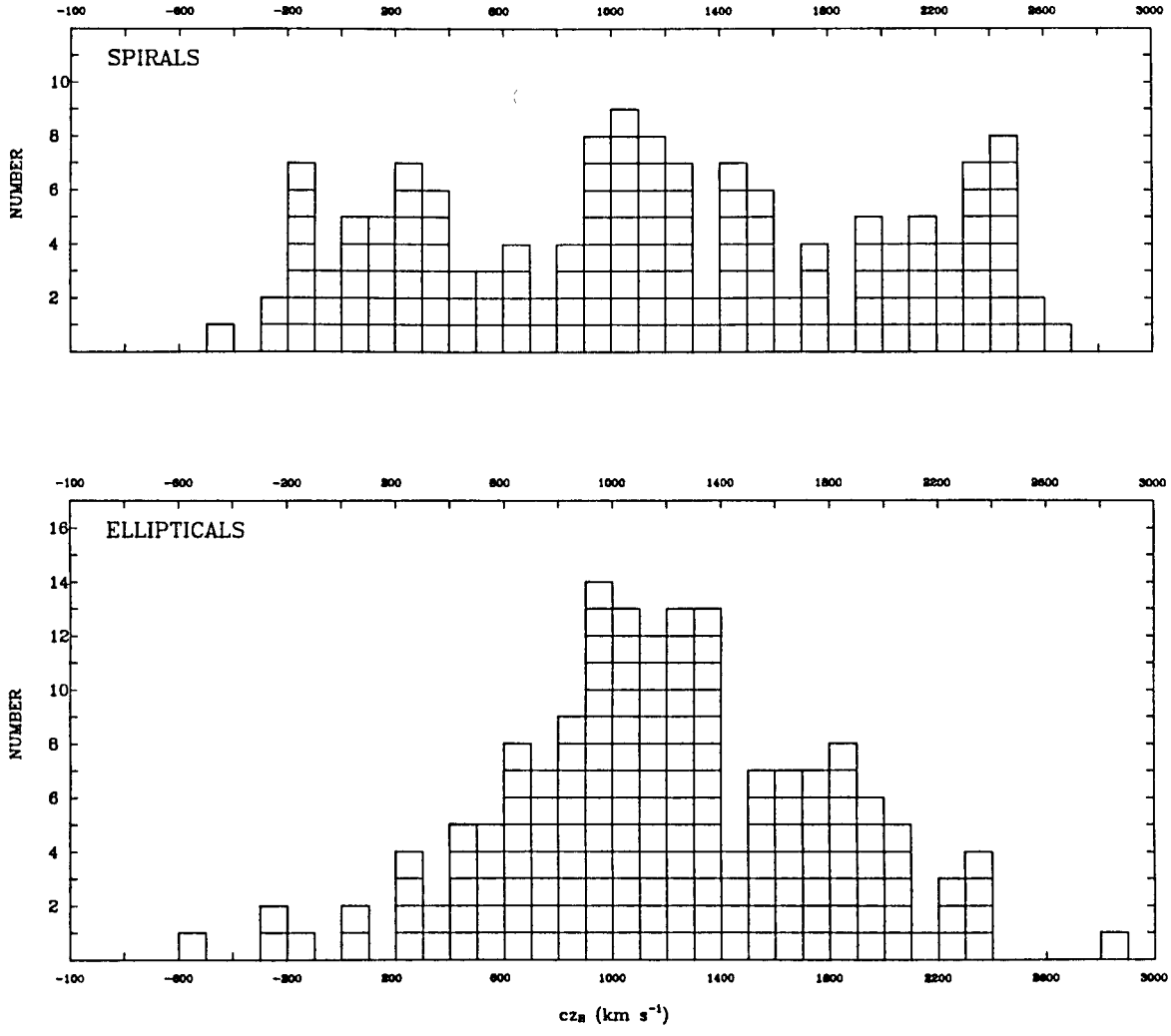


Figure 9. Velocity histograms for the early and late type galaxies in Virgo.

classified the fainter galaxies in the cluster from the Palomar Sky Survey prints with some guidance from the galaxy spectra. These classifications generally agree with the superior classifications of Sandage and collaborators from 2.5-m Dupont plates. Figure 10 presents the isopleths for both the approximately 160 E and S0 galaxies in the magnitude limited sample and a similar number of S and Irr galaxies. The early type galaxies are well condensed towards the cluster center, whereas the spirals are distributed much more uniformly over the cluster. In fact, they exhibit some tendency to be outside of the center (although part of that is due to the large number of spirals in the W clumps).

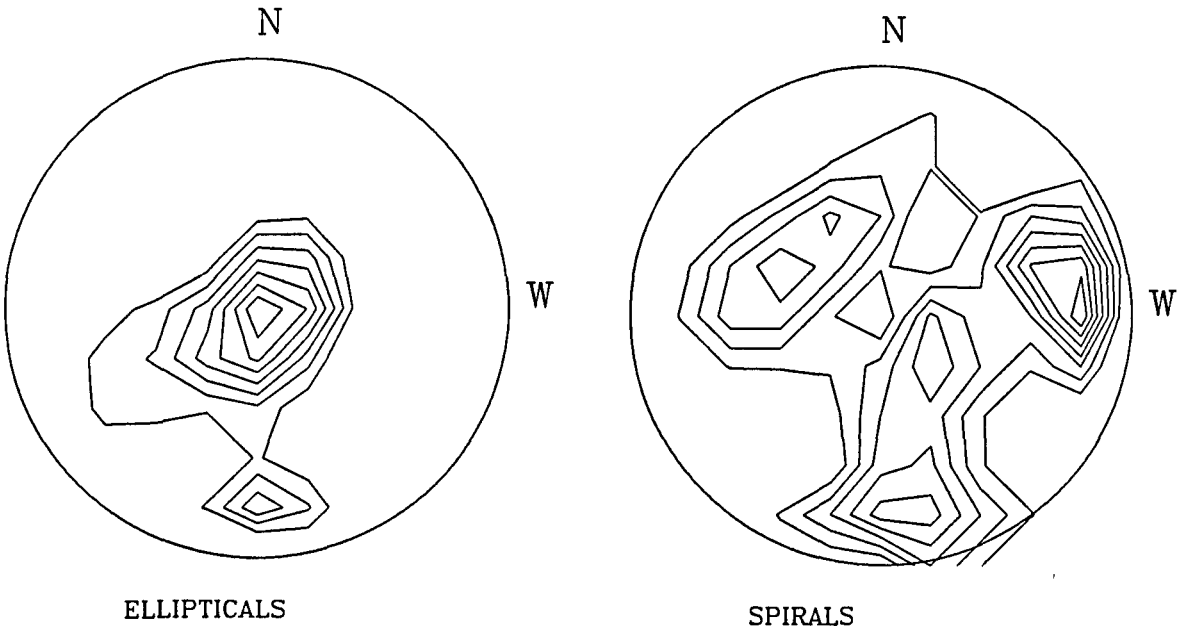


Figure 10. Isopleths for the early and late type galaxies in the 6° radius circle. Again, the binning is 2°. Each map contains approximately 160 galaxies.

The simplest explanation of these distributions is that the late type galaxies are still infalling into the cluster core and that the early type galaxies probably are dynamically relaxed. Is it possible to check this hypothesis? It is difficult to test the part about the early type galaxies other than to say that their velocity distribution is nearly gaussian. On the other hand, if the late type galaxies are infalling, then we might be able to see a distortion of their velocity-distance relation - infall would imply that galaxies on the far side of the cluster would have low velocities along the line of sight while galaxies on the near side would have velocities higher than the cluster mean. About 25 spirals in the cluster core have moderately reliable, velocity-independent distance determinations from the IR-Tully-Fisher relation (Aaronson et al. 1982a). Figure 11 shows the data. There are 12 galaxies with heliocentric velocities less than 1100 km/s and their mean distance is 17.7 ± 1.3 Mpc. There are only 6 galaxies with velocities greater than 1300 km/s, and their mean distance is only 14.1 ± 1.0 Mpc. This is a 2.2 sigma difference and supports the infall hypothesis.

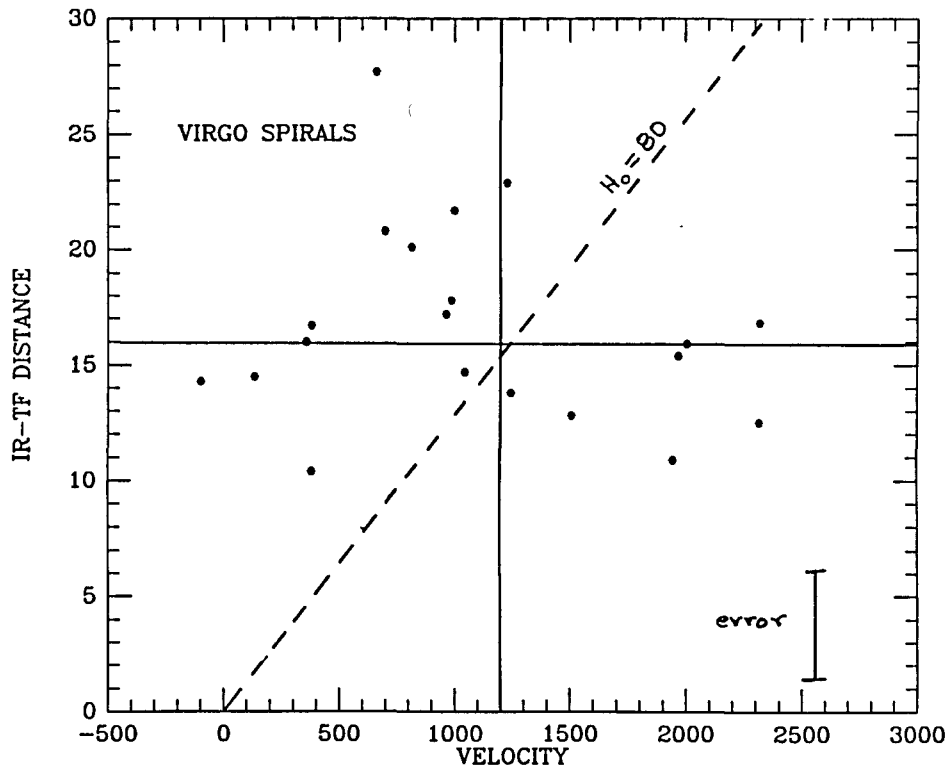


Figure 11. IR-Tully-Fisher distances to spiral galaxies in the Virgo core. The average error in distance is shown in the lower right. A line corresponding to a pure Hubble flow of 80 km/s/Mpc is also indicated.

We have also examined several other distance estimators for galaxies in Virgo, most notably the deVaucouleurs' Luminosity Index (eg. deVaucouleurs 1982), and find that they are not sufficiently precise. It may be possible to use the HI-luminosity correlation, but it is unlikely that a significant number of good distances will be available before the flight of the Hubble Space Telescope.

There is some additional support for the infall of spirals in the cluster core from two circumstantial arguments. Tully and Shaya (1984) have constructed dynamical models of a much larger region around the cluster center and conclude that infall is almost certainly taking place outside the cluster core. In addition, HI observations of spiral galaxies in the 6° region indicate that the galaxies outside a few degree radius are not significantly stripped while those inside are (eg. Giovanelli and Haynes in this conference). That suggests that the spirals outside the center

have not yet been affected by the hot intercluster medium - they haven't yet been through the center.

If the cluster is still collapsing, a straight virial analysis can significantly overestimate the cluster mass; at maximum collapse the kinetic energy is far in excess of the potential energy. Given the observations of the spiral and elliptical distributions, our conservative dynamical description is that the cluster core is bound but not yet relaxed. If the kinetic and potential energies are assumed to be equal, the core mass is about 4×10^{14} and its M/L is 375. This is reasonably close to earlier mass estimates from other techniques (Hartwick 1976 and references therein).

VII. CONCLUSIONS

The conclusions of this work can be summarized as follows:

1. The Virgo Core, taken as a whole, is very complex; it is probably bound but probably <u>not</u> virialized.
2. The E and S0 galaxies in the cluster form a more condensed and concentrated system; they define a "core" that has a relatively low velocity dispersion; this core may be virialized.
3. The S and Irr galaxies have a much smoother distribution as well as a much higher velocity dispersion; indications are that they are still infalling into the cluster "core."
4. The cluster raw mean heliocentric velocity is 1150 km/s; the mean galactocentric velocity is 1075 km/s; the mean "Local Groupocentric" velocity is 1035 km/s.
5. If bound but not virialized, the 6° cluster core has a M/L of 375 $M_{\odot}/L_{\odot}$, which implies that the mean mass density is only 0.2 of the closure value. If the core is analysed (most probably, incorrectly) as virialized, this number doubles - still not enough to close the universe.
6. The cluster luminosity function is indistinguishable from the field luminosity function for magnitudes brighter than $M_B = -15.5$.

This work would not have been possible without the support and assistance of Drs. M. Geller, R. J. Davis, J. Geary and D. Latham and the valiant CfA Redshift survey team - J. Peters, E. Horine, S. Tokarz, B. van Sant, W. Wyatt, D. Danby, and J. Morse. I would

also like to thank Drs. G. Bothun, R. Giovanelli, M. Haynes and G. Helou for communicating data in advance of publication. Financial support has been provided by the Smithsonian Institution for the observations and by NASA Grant NAGW-201 for the dynamical analyses.

REFERENCES

Aaronson, M., Huchra, J., Mould, J., Tully, R. B., Fisher, J. R., van Woerden, H., Goss, W. M., Chamaraux, P., Mebold, U., Seigman, B., Berriman, G. and Persson, S. E. 1982a, Ap. J. Suppl. 50, 241.

Aaronson, M., Huchra, J., Mould, J., Schechter, P. and Tully, R. B. 1982b, Ap. J. 258, 64.

Aaronson, M. and Mould, J. 1981, P.A.S.P. 93, 20.

_____ 1983, Ap. J. 273, 530.

Bahcall, J. and Tremaine, S. 1981, Ap. J. 244, 805.

Beers, T., Geller, M., Huchra, J., Latham D. and Davis, R. 1984, Ap. J. 283 33.

Binggeli, B., Sandage, A. and Tarenghi, M. 1984, A. J. 89, 64.

Bothun, G., Beers, T., Geller, M. and J. Huchra 1983, Ap. J. 268, 47.

Bothun, G., Mould, J., Wirth, A., Caldwell, N. and Strom, S. 1984, Ap. J. in press.

Caldwell, N. 1983, A. J. 88, 804.

de Vaucouleurs, G. 1982, Ap. J. 253, 520.

de Vaucouleurs, G and de Vaucouleurs, A. 1973, Astron and Ap. 28, 109.

de Vaucouleurs, G., Peters, W., Bottinelli, L., Gouguenheim, L. and Paturel, G. 1981, Ap. J. 248, 408.

de Vaucouleurs, G. and Pence, W. 1979, Ap. J. Suppl. 39, 49.

Fabricant, D. and Gorenstein, P. 1983, Ap. J. 267, 535.

Ftaclas, C. Fanelli, M. and Struble, M. 1984, Ap. J. 282, 19.

Giovanelli, R. and Haynes, M. 1984, private communication.

Hartwick, F. D. A. 1976, Ap. J. 208, L13.

Helou, G., Hoffman, G. and Salpeter, E. 1984, private communication.

Huchra, J. 1976, A. J. 81, 952.

Huchra, J. 1985, in preparation.

Huchra, J. and Brodie, J. 1984, Ap. J. 280, 547.

Huchra, J., Davis, R. J. and Latham, D. 1984, in
Clusters and Groups of Galaxies, Mardirossian, Mezzetti
and Giuricin, eds. (Dordrecht: Reidel) p 79.
Huchra, J. et al. 1985, A Catalog of Galaxy Radial Velocities,
SAO Special Report, in preparation.
Karachentsev, I. 1982, Astrofiz. 18, 501.
Karachentsev, I. and Karachentseva, V. 1982,
Pis'ma Astron. Zh. 8, 198.
Mould, J., Aaronson, M. and Huchra, J. 1980,
Ap. J. 238, 458.
Reaves, G. 1983, Ap. J. Suppl. 53, 375.
Sandage, A. and Binggeli, B. 1984, A. J. 89, 919.
Sandage A. and Tammann, G. 1976, Ap. J. 207, L1.
Sulentic, J. 1977, Ap. J. 211, L59.
Sulentic, J. 1980, Ap. J. 241, 67.
Tammann, G. 1972, Astron. and Ap. 21, 355.
Tully, R. B. and Shaya, E. 1984, Ap. J. 281, 31.
Yahil, A., Tammann, G. and Sandage, A. 1977, Ap. J. 217, 903.
Zwicky, F., Herzog, E. and Wild, P. 1961 _1963,
Catalogue of Galaxies and of Clusters of Galaxies,
Vols. I and II, (California Institute of Technology,
Pasadena).

GLOBAL STRUCTURE OF VIRGO CLUSTER GALAXIES

Sadánori Okamura
Kiso Observatory, Tokyo Astronomical Observatory
Mitake-mura, Kiso-gun, Nagano-ken, 397-01 Japan

1. INTRODUCTION

The Virgo Cluster is the nearest rich cluster of galaxies comprising galaxies of all morphological types. Importance of a careful photometric mapping of the Virgo Cluster galaxies was emphasized at the meeting of Working Group on Galaxy Photometry and Spectrophotometry, Commission 28 of IAU (Proc. XVIIIth IAU General Assembly, Patras, p.222).

Six years ago we began a project to obtain detailed luminosity distribution for large number of galaxies using the 105-cm Schmidt telescope of the Kiso Observatory (Takase et al. 1977). Our principal aims in this project are:

(1) To investigate the possibility of developing a quantitative classification system based upon the minimum number of parameters essential to characterize the global structure of galaxies. Such a classification system would be of great help to the understanding of the structure and evolution of galaxies just like the H-R diagram for stars.

(2) To examine if there is a significant difference in the global structure between galaxies residing in dense environments and those in rare environments. Presence or absence of such a difference may impose constraints on acceptable theories on formation of galaxies and clusters of galaxies.

The Virgo Cluster was the first target of the project. The telescope covers a field of 6°X6° when used with 14 inchX14 inch plates. The plate scale is 62".5/mm. The central region of the Virgo Cluster ($\alpha \sim 12^h10^m$ to 12^h50^m; $\delta \sim$ +2° to +18°) was observed. The region was covered by six plates with a small overlap between adjacent fields. Number of plates were taken in various color bands. The near infrared I band would be most appropriate for our study since the effects of internal absorption and young stellar populations become minimum in the I band. A large compilation of good plate material in the I band, however, would take quite a long time. A preliminary analysis of the luminosity distributions in the U, B, V and I bands showed that parameters representing the global structure are rather insensitive to the color bands although small-scale bumpiness in the luminosity distribution of spiral and irregular galaxies increases as we go to shorter wavelengths. The V band, Kodak IIa-D emulsion

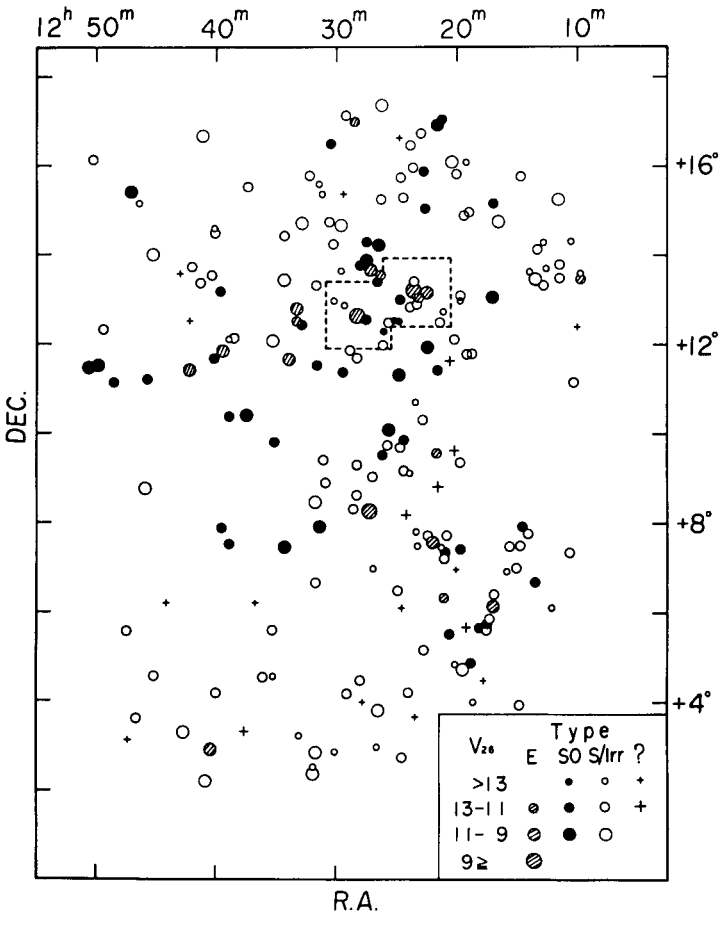


Figure 1a.
Spatial distribution of 213 galaxies in the bright sample. The broken lines show the area covered by du Pont reflector plates.

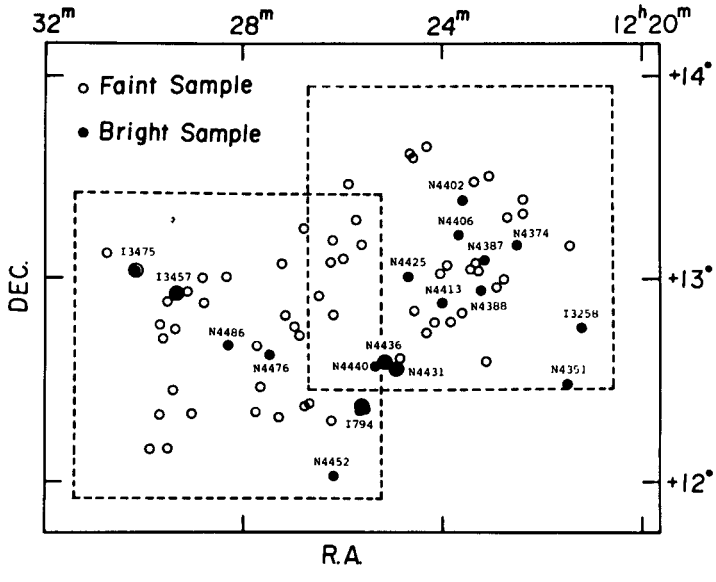


Figure 1b.
Spatial distribution of 64 galaxies in the faint sample (open circles). The filled circles represent galaxies in the bright sample.

behind Schott GG495 filter, was chosen as a compromise. By 1982 a set of six V plates of best quality was obtained for the Virgo Cluster region. Two-dimensional luminosity distribution was derived for 213 bright galaxies. Spatial distribution of the galaxies is shown in figure 1a.

Recently two plates of the Virgo Cluster taken with the 2.5-m du Pont reflector at Las Campanas became available to us by courtesy of Dr. Wakamatsu. They were centered on M87 and NGC 4406 respectively, and covered 1°.5X1°.5 fields as shown by the broken lines in figures 1a and 1b. The plate scale is 10".9/mm. Numerous small faint galaxies which could be easily overlooked on the Kiso Schmidt plates were readily recognized on these large scale plates. We included the faint galaxies in the project to form a more comprehensive sample of Virgo Cluster galaxies. Two-dimensional luminosity distribution has been obtained for 64 faint galaxies so far. Most of them are smaller than the practical limit for surface photometry on the Kiso Schmidt plates. Spatial distribution of the 64 galaxies is shown in figure 1b. The du Pont plates are in the B band, Kodak 103a-O emulsion behind Wratten 2C filter.

We summarize the results of photometric analyses applied to the two samples of Virgo Cluster galaxies, sample of 213 bright galaxies (hereafter bright sample) and sample of 64 faint galaxies (hereafter faint sample). Emphasis is put on a proposed quantitative classification system based upon global luminosity distribution and characteristics of faint (dwarf) galaxies compared with those of bright galaxies. Details of data reductions and analyses are published elsewhere (Watanabe et al. 1982=Paper I; Watanabe 1983=Paper II; Okamura et al.=Paper III; Watanabe et al. 1984=Paper IV; Kodaira et al. 1983; Ichikawa et al. 1984)

It is noted that a comprehensive study of the Virgo Cluster is also being carried out by Sandage and his co-workers (Binggeli et al. 1984, hereafter BST; Sandage and Binggeli 1984, hereafter SB84; see also their papers in this proceedings).

2. COMMENTS ON THE SAMPLE

2.1 Bright Sample

The 213 bright galaxies are selected according to the following criteria (Paper II): (1) The apparent linear size is larger than $\sim$1mm($\sim$1') on the plates and (2) the image is not seriously contaminated by the neighboring images of other galaxies. Radial velocities are available for 169 out of the 213 galaxies in the literature (de Vaucouleurs et al. 1976=RC 2; Eastmond and Abell 1978; Sandage and Tammann 1981; Karachentsev and Karachentseva 1982; Bottinelli et al.

1982; Aaronson et al. 1982). Only two galaxies, NGC 4246 and NGC 4334, have velocities greater than 2600 km/s and they may be backgrounds. A histogram showing the distribution of radial velocities of the remaining 167 galaxies is given as figure 2. We assume the 167 to be confirmed member of the Virgo Cluster. Histograms of morphological type indices in RC 2 and apparent magnitudes are shown in figures 3 and 4, respectively.

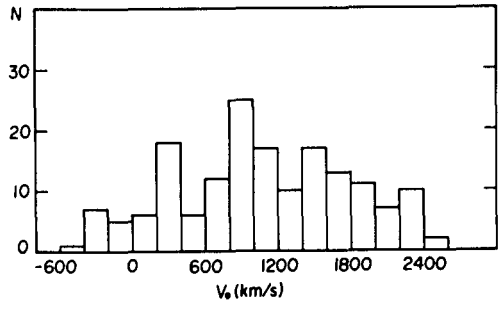


Figure 2. Histogram of radial velocities for 167 galaxies with V_0 less than 2600 km/s in the bright sample.

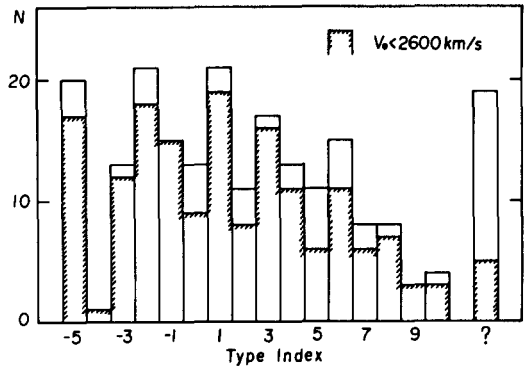


Figure 3. Histogram of morphological type indices in RC 2 for galaxies in the bright sample.

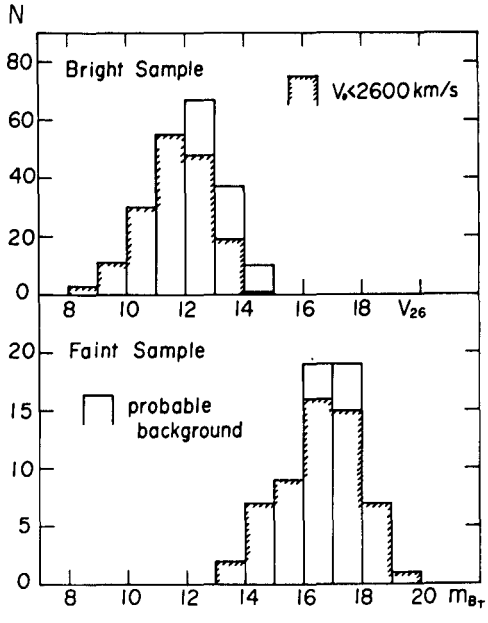


Figure 4. Histograms of apparent V magnitudes for galaxies in the bright sample (upper panel) and of apparent m_{B_T} magnitudes for galaxies in the faint sample (lower panel).

2.2 Faint Sample

Selection criteria for the 64 faint galaxies are: (1) Apparent linear size is between ∿10"(1mm) and ∿100"(1cm) on the plates. (2) The surface brightness is fainter than that of normal galaxies but not prohibitively faint. (3) The image is of approximately elliptical shape and smooth in texture. (4) The image is not seriously contaminated by the neighboring images of bright galaxies

(Ichikawa et al. 1984).

By the criterion (3) above we intended to exclude dwarf irregulars and background spirals and limit the sample to dwarf ellipticals (dEs). We recognized the presence of compact galaxies (diameter $\lesssim$30") of high surface brightness whose appearance would fit that of background normal ellipticals. Seven such galaxies are intentionally included in the sample to see how the difference in their appearances shows up in luminosity profiles and quantitative parameters.

Five galaxies are common to the bright and the faint samples. Out of 64 sample galaxies, 33 appear in the catalogue of dwarf galaxies by Reaves (1983), 19 were photometered by BST and 7 by Caldwell (1983). According to the classification by Reaves (1983), 30 are dEs and 3 are of IC 3475 type, while the new classifications by BST and SB84 available for 27 galaxies give 20 dEs, 2dS0s, 2 dS0/dEs, 1 ImIV or dE, 1 ImIV? and 1 E. It is reasonable to assume that the majority of galaxies in the faint sample comprises dEs. Radial velocity is known for only 9 galaxies, which all have velocities less than 1800 km/s (Karachentsev and Karachentseva 1982). There is, however, convincing evidence that dEs are members of the Virgo Cluster (Reaves 1983). The histogram of apparent magnitudes is shown in the lower panel of figure 4.

3. ANALYSIS OF THE BRIGHT SAMPLE AND A PROPOSED CLASSIFICATION SYSTEM

3.1 Photometric Parameters

We explore the possibility of developing a quantitative classification system on the basis of surface photometric parameters. We reduce the observed two-dimensional luminosity distributions of galaxies in the bright sample into the following parameters characterizing the global structure of galaxies; logarithmic diameter (log D_{26}; D_{26} is in units of 0!1), integrated magnitude (V_{26}), mean surface brightness within D_{26} (SB), and mean concentration index [Xl(P)]. All the parameters are derived using the generalized radial profile $\sigma(r)$, a face-on radial profile calculated numerically under the assumption of optically thin axisymmetric galaxy structure (cf. Papers I and II), within the limiting surface brightness of 26 mag arcsec^{-2}. The last parameter, Xl(P), represents the degree of luminosity concentration towards the galactic center. It is a linear combination of a series of five concentration indices defined by,

$$P_n = 100 \int_0^{r_{26}/2^n} r\,\sigma(r)dr \Big/ \int_0^{r_{26}} r\sigma(r)dr \quad (n=1, 2,..., 5), \qquad (1)$$

where $r_{26}=D_{26}/2$. The parameter Xl(P) is a good measure of both profile shape

and intrinsic surface brightness (Paper III).

3.2 Principal Component Analysis of the Photometric Parameters

In order to characterize the global structure of galaxies on the basis of the above four photometric parameters, it is essential to know the dimensionality, that is, how many significant independent variables are present among the parameters. It is noted that log D_{26}, V_{26} and SB are not independent and the dimensionality of the present sample is at most three. The principal component analysis (hereafter PCA) is an effective tool to find the dimensionality and reduce the original parameters into independent variables, which we call the factor here.

We apply PCA to a sample of 167 members of the Virgo Cluster (Virgo sample). Details of the analysis will be given in Paper IV. Samples on which PCA was performed in previous studies were limited to those of disk galaxies (Brosche 1973; Bujarrabal et al. 1981; Whitmore 1984) or those of ellipticals (Brosche and Lentes 1982; Efstathiou and Fall 1984). Existence of two dominant factors was found in these studies for *respective* samples. In other words, it is known that ellipticals are distributed in a plane (hereafter E-plane) as well as disk galaxies are in a plane (hereafter D-plane). The relationship between E-plane and D-plane is, however, not yet known. The present Virgo sample includes galaxies of all morphological types ranging from ellipticals through lenticulars to spirals and irregulars as shown in figure 3. Such a mixed sample is subjected to PCA for the first time.

Results are summarized below. The main result is that two dominant factors are found also for the present mixed sample; 93.5% of the total variance carried by the four parameters, log D_{26}, V_{26}, SB and Xl(P), can be explained by two factors Y_1 and Y_2. Significance of the third factor, Y_3, which carries 6.5% of the total variance is considered marginal. This result means that the sample galaxies, *both ellipticals and disk/irregular galaxies*, are distributed nearly in a plane defined by Y_1 and Y_2. For comparison, PCA is performed, using the same photometric parameters, on a sample of 34 galaxies in the Ursa Major Clouds (UMa sample). The Clouds and the Virgo Cluster lie at nearly equal distance (Aaronson and Mould 1983). It is remarkable that this UMa sample yields the results almost identical with those for the Virgo sample in spite of its very small sample size as demonstrated in figure 5, which shows the orientation of unit vectors of the original parameters in the factor space. This fact suggests that two factors Y_1 and Y_2 reflect real properties of galaxies and that they are quite stable.

The factors Y_1 and Y_2 are derived using photometric parameters in one color band alone. The previous studies included in PCA kinematical and other

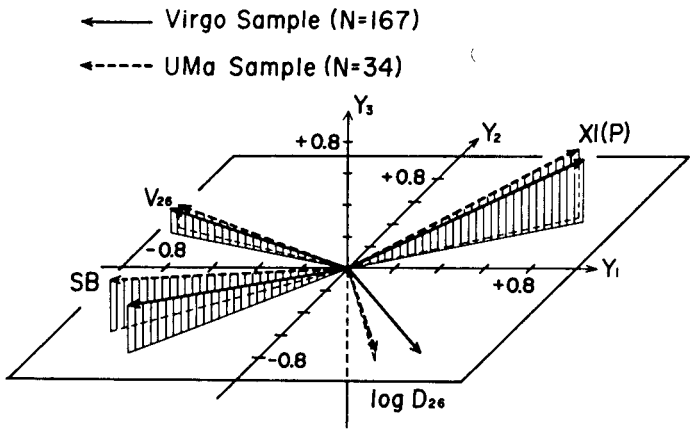


Figure 5. Orientations of unit vectors for the original parameters in factor space. Note that the orientations are almost identical for Virgo and UMa samples.

parameters as well as photometric parameters. Comparisons of results of PCA, especially directions of unit vectors projected onto the plane defined by two dominant factors, between the present and previous studies reveal the following; The plane defined by Y_1 and Y_2 is essentially the same plane as D-plane, and as E-plane as well. Examples of such comparisons are given in paper IV (see also Okamura 1984).

The new findings from our PCA can be summarized in the following three points:

(1) D-plane and E-plane are essentially the same.

(2) As far as the kinematical parameters and color indices etc. included in the previous studies are concerned, inclusion of such parameters *does not* result in the increase of significant dimensions. In other words, there are tight correlations between surface photometric parameters and kinematical parameters etc.

(3) It is highly promising to develop a quantitative classification system based upon Y_1 and Y_2 or a pair of parameters equivalent to them (cf. Whitmore 1984).

3.3 Diameter versus Surface Brightness Diagram (DSBD)

The factors Y_1 and Y_2 are linear combinations of the four original surface photometric parameters. It would be more useful if two original parameters could be used in place of Y_1 and Y_2 with little loss of information. As shown in figure 5, unit vectors for log D_{26} and SB are little inclined to (Y_1,Y_2) plane and nearly orthogonal in factor space. Having this in mind, we propose to use log D_{26} and SB instead of Y_1 and Y_2 as the basis of a quantitative classification of galaxies. The choice of log D_{26} and SB is, of course, tentative because they form the best pair among only the four parameters considered in the present

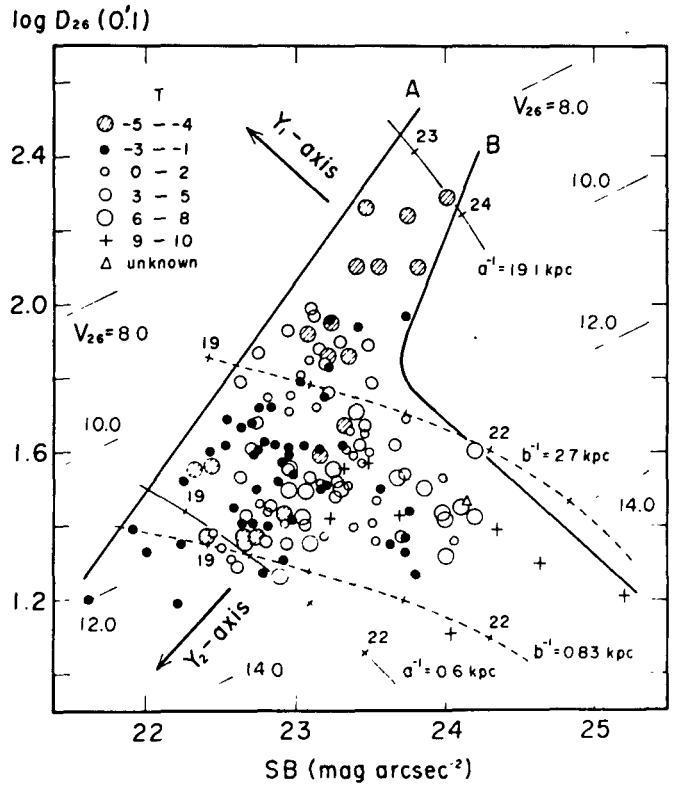


Figure 6. The diameter versus surface brightness diagram for 149 galaxies in the Virgo Cluster and the Ursa Major Clouds. Projections of the axes of two dominant factors and the lines of constant magnitude are shown. The thick solid lines (A and B) show the boundaries of the observed distribution. The thin solid and broken curves represent some model sequences for the $r^{1/4}$-law and exponential law, respectively. The numerals on the ticks indicate the brightness-scale parameter in units of mag arcsec^{-2} while a^{-1} and b^{-1} are the length-scale parameter for respective model sequences.

study. It is, however, an advantage that log D_{26} and SB are parameters which can be obtained rather straightforwardly from surface photometry.

Examples of the log D_{26} versus SB diagram, which we call DSBD, are given in Kodaira et al. (1983) and Takase et al. (1984). A reproduction from the latter is shown in figure 6. We find in DSBD two well-defined boundaries (lines A and B in figure 6) and two branches of distribution which run almost parallel to the projected Y_1 and Y_2 axes. The branch along the projected Y_2 axis is formed mainly by ellipticals and lenticulars while that along the projected Y_1 axis consists of spirals and especially late-type spirals and irregulars. DSBD will be used in section 5 to investigate the characteristics of Virgo Cluster galaxies.

4. PROPERTIES OF GALAXIES IN THE FAINT SAMPLE

4.1 Luminosity Profile

The generalized radial profile and the equivalent profile are constructed from two-dimensional luminosity distributions of 64 faint galaxies. Discussion on the profile shape in this section refers to the equivalent profile.

Equivalent profiles are given in BST for 14 galaxies which are common to the present sample. They are used to assess the consistency of the profile

between the two independent observations. We find a slight systematic difference; our profiles are fainter by $\sim$0.3 mag than those in BST in the very central region ($r \lesssim 3$") for all the galaxies. In the faint parts of the profiles ($\mu_B \gtrsim 26$ mag arcsec^{-2}) our profiles are brighter by 0.3 - 1 mag for seven galaxies while the remaining seven galaxies show very good agreement. Figure 7 shows two examples; one with a good agreement and the other with a bad one. We find a satisfactory agreement with BST in terms of total magnitude. More independent observations may be necessary to obtain more accurate profiles especially in faint outer parts of these faint galaxies. This slight discrepancy, however, does not affect the conclusions of the present study.

A careful inspection of the profile shape in the framework of empirical models results in the following statistics. Out of 64 galaxies 52 have profiles fitted by exponential laws and 7 have profiles consistent with $r^{1/4}$-laws. The remaining 5 have profiles intermediate between the two categories. Profiles of typical examples are shown in figures 8a and 8b. Quite a few galaxies (31 out of 64) have unresolved nuclei and their profiles show central spikes. Profiles of several galaxies fall in outer parts more rapidly than the exponential law. The above classification of the profile shape is based upon the main part of the profile and behaviors in very central parts ($r \lesssim 3$") and in faint outer parts ($\mu_B \gtrsim 26$ mag arcsec^{-2}) are not taken into account.

The most striking result arising from the classification of the profile shape is that seven compact galaxies (section 2.2) have all $r^{1/4}$-law profiles. *Thus, 'normal' dwarf ellipticals all have either exponential profiles or intermediate profiles.* Furthermore, new classifications by BST and SB84 are available for 3 galaxies of intermediate categories. They are $dSO_3(5)$,N: (IC 3303), dSO(5),N (NGC 4431) and dE6/dSO(6),N (NGC 4436). The above statistics lead us to the following supposition; dwarf ellipticals, in the sense of new classification system by BST and SB84, do not have $r^{1/4}$-law profile which normal ellipticals do but have profiles consistent with exponential laws which are characteristics of late-type spiral galaxies.

The same finding was reached by BST on the basis of surface photometry of 46 Es and dEs in the Virgo Cluster. Their finding is confirmed and strengthened by the present study since only 19 dEs are common to both studies. Radial velocity is known for none of the seven compact galaxies and they might be giant ellipticals in the background. Radial velocity measurements of these galaxies are highly desirable.

For the parametrization of the profile shape, equivalent profiles are fitted to King models. King models can express variety of profiles as shown in figure 9, where model profiles are plotted in magnitude versus r plane. It is found that models with $0.75 \lesssim c = \log r_t/r_c \lesssim 1.25$ show profiles consistent with

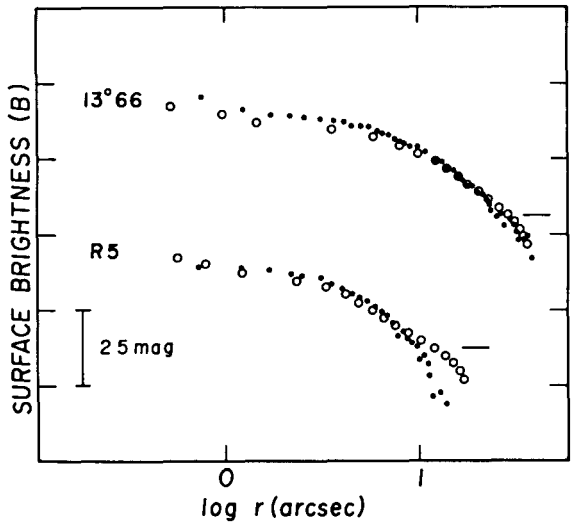


Figure 7. Two examples of equivalent profiles. The open circles represent the present study and the dots are from BST. The horizontal bars indicate the level of 26 mag arcsec^{-2}.

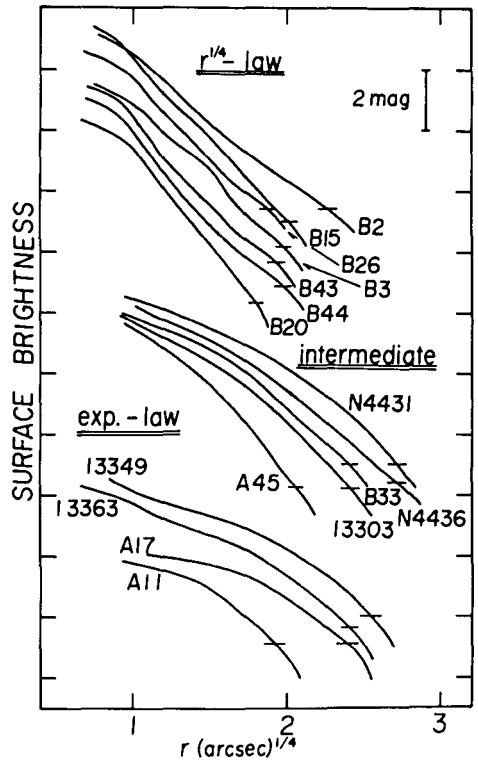


Figure 8a.

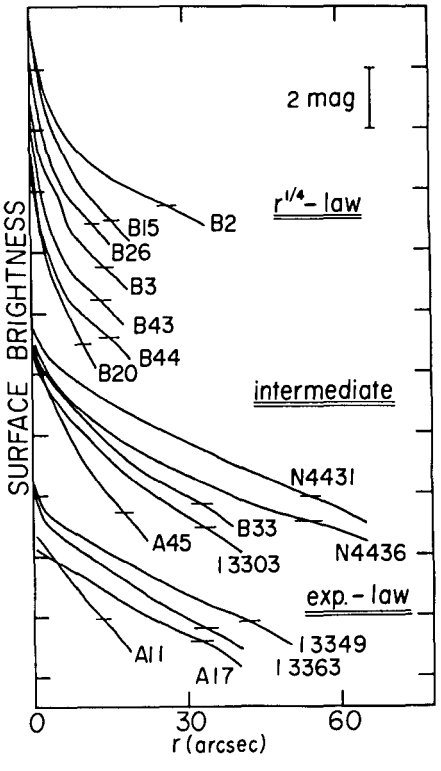


Figure 8b.

Figure 8. Examples of profiles of three categories; $r^{1/4}$-law (all seven galaxies are shown), intermediate (all five are shown) and exponential law. Abscissa is $r^{1/4}$ for (a) and r for (b). Galaxy names other than NGC and IC numbers are tentative. The horizontal bars indicate the level of 26 mag arcsec^{-2}.

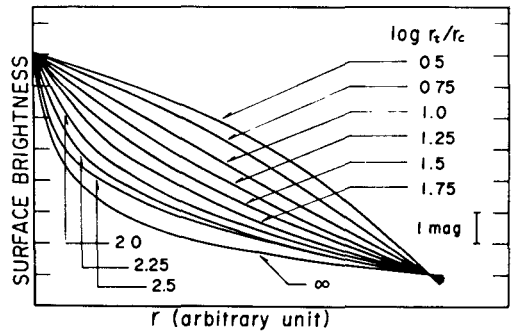


Figure 9. Profiles of King models with different log r_t/r_c. It is noted that models with log $r_t/r_c \sim$ 0.75-1.25 have profiles consistent with exponential laws.

exponential laws, where r_t and r_c are tidal radius and core radius, respectively. The fits are made graphically using a template and the concentration index c is derived as a parameter to characterize the profile shape. In the fitting less weights are put on the data in $r \lesssim 3$" and $\mu_B \gtrsim 26$ mag arcsec^{-2} because in these regions profiles are easily affected by the presence of nucleus and by the incorrect subtraction of sky background.

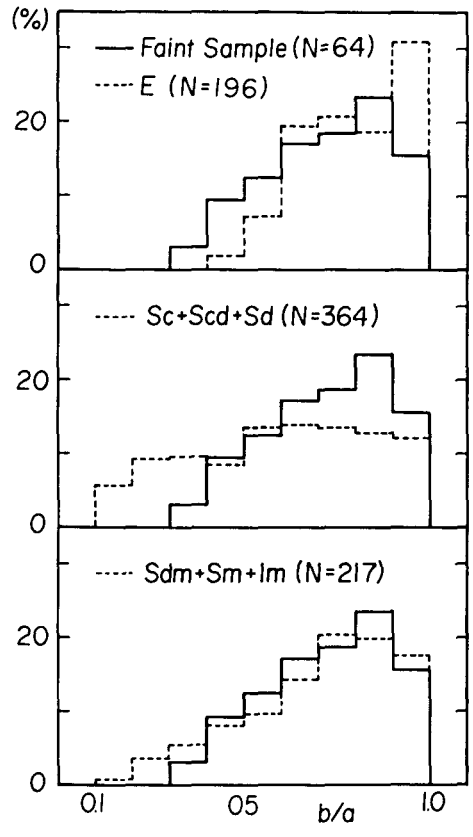
We collected from the literature the concentration indices, c, of normal ellipticals, dwarf ellipticals in Local Group and globular clusters of our Galaxy. All these concentration indices are plotted, together with those of 64 faint galaxies, against their absolute magnitudes (Ichikawa et al. 1984). The variation of the concentration index with the absolute magnitude found by BST is confirmed for the normal E - dE sequence. Globular clusters appear to form a separate sequence in this plot.

4.2 Ellipticity Distribution

In the preceding section, luminosity profiles of the majority of dwarf ellipticals are shown to be fitted by exponential laws very well. Local Group dwarf spheroidals also have profiles consistent with exponential laws (Faber and Lin 1983). These two facts strongly support a view that exponential profile is the intrinsic property of dwarf ellipticals as pointed first by BST. Then the structure of dwarf ellipticals is possibly more related to spiral and irregular galaxies than to normal and giant ellipticals (Faber and Lin 1983). In this context, it is worth while to examine the ellipticity distribution of dwarf ellipticals.

Axial ratio, b/a, is measured at 24 mag arcsec^{-2} for the 64 faint galaxies. The resulting distribution is compared in figure 10 with that of typical normal galaxies, that is, ellipticals, late-type spirals (Sc+Scd+Sd) and latest-type spirals/irregulars (Sdm+Sm+Im). Axial ratios of normal galaxies are taken from the compilation by Binney and de Vaucouleurs (1981), and they are the values at 25 mag arcsec^{-2} in the B band.

Figure 10 clearly demonstrates the following. The axial ratio distribution of dwarf ellipticals is markedly different from that of late-type spirals which are believed to be composed of thin disks while it is similar to that of either



ellipticals or latest-type spirals/ irregulars. There is clear evidence that there are many thick galaxies in latest-type spirals/irregulars (Binney and de Vaucouleurs 1981). The axial ratio distribution presented here supports *thicker intrinsic shape of dwarf ellipticals than late-type spirals in spite of their exponential luminosity profiles.* This suggests that dwarf 'ellipticals' or dwarf 'spheroidals' is a proper nomenclature.

Figure 10. Distribution of axial ratios of dwarf ellipticals is compared with that of normal ellipticals (top), late-type spirals (center), and latest-type spiral/irregulars (bottom).

5. DIAMETER VERSUS SURFACE BRIGHTNESS DIAGRAM FOR VIRGO CLUSTER GALAXIES

We investigate the characteristics of Virgo Cluster galaxies on the basis of the diameter versus surface brightness diagram (DSBD), the proposed quantitative classification system (section 3.3). Since photometric data are compiled in the different color bands between the bright and the faint samples, direct comparison cannot be made between the two samples. In order to construct a composite DSBD for the two samples, we assume that normal ellipticals in the Virgo Cluster have (B-V)=1.0 and no color gradient. This assumption leads to D_{26}(V band)=D_{27}(B band) and SB_{26}(V band)+1.0=SB_{27}(B band).

Figure 11 shows the composite DSBD in the B band, that is, log D_{27} versus SB_{27}, where normal ellipticals in the bright sample are plotted using the transformation above. Boundaries A and B (see figure 6) are also transformed. Spirals are not plotted because transformation cannot be made easily. Spirals are composite systems and have a wide range of (B-V) and color gradient as well. If we assume pure exponential disks with the central surface brightness of 20 - 23 mag arcsec^{-2}, (B-V)=0.5 and no color gradient, we have D_{27}(B band)/D_{26} (V band)$\sim$1.1-1.2 and SB_{27}(B band)=SB_{26}(V band)+$\sim$0.7 mag, exact values depending

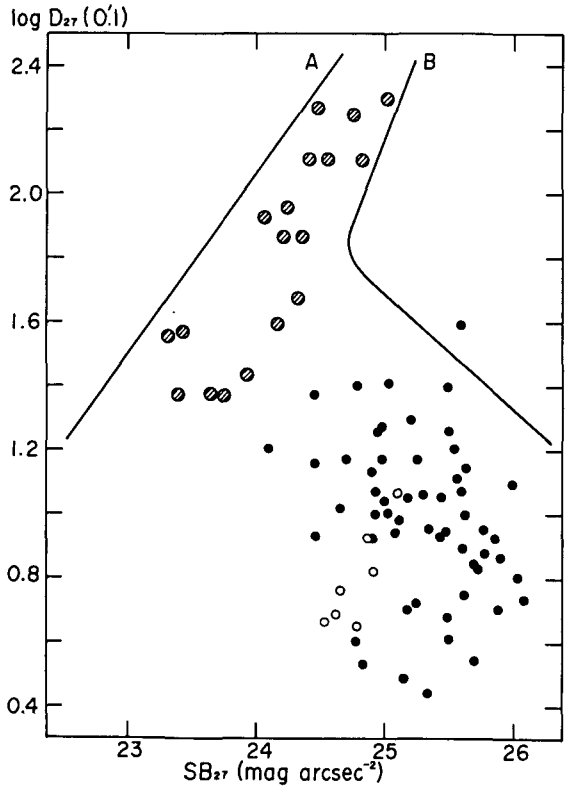


Figure 11. The composite diameter versus surface brightness diagram (DSBD) in the B band for normal ellipticals (hatched circles) and dwarf ellipticals (filled circles) in the Virgo Cluster. The open circles are compact galaxies which are supposed to be background giant ellipticals. It is noted that dwarf ellipticals appear to form a separate branch in this diagram from that of normal ellipticals.

upon the central surface brightness. These values may give us some idea of where spiral galaxies in figure 6 would be distributed in figure 11. In this figure, dwarf ellipticals appear to form a separate branch from that of normal ellipticals. When we include globular clusters in this composite DSBD, we find *three distinct clusterings of data points consisting of normal ellipticals, dwarf ellipticals and globular clusters, respectively* (Ichikawa et al. 1984). This feature may be a hint of possible structural discontinuity originated from different formation histories in the sequence of spheroidal stellar systems comprising giant/normal ellipticals, dwarf ellipticals and globular clusters.

6. SUMMARY

(1) A quantitative classification system, the diameter versus surface brightness diagram (DSBD), is proposed on the basis of a principal component analysis of the bright sample consisting of 213 galaxies of all morphological types in the Virgo Cluster.

(2) Dwarf ellipticals in the Virgo Cluster, which are the majority of the faint sample, are shown to have luminosity profiles consistent with exponential laws.

(3) The intrinsic shape of the dwarf ellipticals is shown to be thicker than that of late-type spirals consisting of thin disks.

(4) Hints are presented, using the concentration index versus absolute magnitude diagram and DSBD, of possible structural discontinuity in the sequence of spheroidal stellar systems comprising giant/normal ellipticals, dwarf ellipticals and globular clusters.

The author wishes to thank all the collaborators who have been working with him on this photometric project and the staff of the Kiso Observatory for their support. This work was supported in part by the Scientific Research Fund of the Ministry of Education, Science and Culture (#59065002).

REFERENCES

Aaronson, M., Huchra, J., Mould, J. R., Tully, R. B., Fisher, J. R., van Woerden, H., Goss, W. M., Chamaraux, P., Mebold, U., Siegman, B., Berriman, G., and Persson, S. E. 1982, Ap. J. Suppl., 50, 241.

Aaronson, M., and Mould, J. R. 1983, Ap. J., 265, 1.

Binggeli, B., Sandage, A., and Tarenghi, M. 1984, A. J., 89, 64. (BST)

Binney, J., and de Vaucouleurs, G. 1981, M. N. R. A. S., 194, 679.

Bottinelli, L., Gouhuenheim, L., and Paturel, G. 1982, Astr. Ap. Suppl., 47, 171.

Brosche, P. 1973, Astr. Ap., 23, 259.

Brosche, P., and Lentes, F. -Th. 1982, in *Internal Kinematics of Galaxies*, IAU Symp. No. 100, ed. E. Athanassoula (Dordorecht, Reidel), p. 377.

Bujarrabal, V., Guibert, J., and Balkowski, C. 1981, Astr. Ap., 104, 1.

Caldwell, N. 1983, A. J., 88, 804.

de Vaucouleurs, G., de Vaucouleurs, A., and Corwin, H. G. Jr. 1976, *Second Reference Catalogue of Bright Galaxies* (Univ. Texas Press, Austin). (RC 2)

Eastmond, T. S., and Abell, G. O. 1978, P. A. S. P., 90, 367.

Efstathiou, G., and Fall, S. M. 1984, M. N. R. A. S., 206, 453.

Faber, S. M., and Lin, D. N. C. 1983, Ap. J. Letters, 266, L17.

Ichikawa, S., Wakamatsu, K., and Okamura, S. 1984, in preparation.

Karachentsev, I. D., and Karachentseva, V. E. 1982, Soviet Astr. Letters, 8, 104.

Kodaira, K., Okamura, S., and Watanabe, M. 1983, Ap. J. Letters, 274, L49.

Okamura, S. 1984, Proc. Specialized Meeting on *New Aspects of Galaxy Photometry*, Eighth European IAU Regional Meeting (Toulouse), ed. J. L. Nieto (in press).

Okamura, S., Kodaira, K., and Watanabe, M. 1984, Ap. J., 280, 7. (Paper III).

Reaves, G. 1983, Ap. J. Suppl., 53, 375.

Sandage, A., and Binggeli, B. 1984, A. J., 89, 919. (SB84).

Sandage, A., and Tammann, G. A. 1981, *A Revised Shapley-Ames Catalog of Bright Galaxies* (Carnegie Institution of Washington, Washington, D. C.).

Takase, B., Ishida, K., Shimizu, M., Maehara, H., Hamajima, K., Noguchi, T., and Ohashi, M. 1977, Annals Tokyo Astron. Obs., 2nd Ser., 16, 74.

Takase, B., Kodaira, K., and Okamura, S. (ed.) 1984, *An Atlas of Selected Galaxies* (Univ. Tokyo Press, Tokyo and VNU Science Press, Holland).

Watanabe, M. 1983, Annals Tokyo Astron. Obs., 2nd Ser., 19, 121. (Paper II).

Watanabe, M., Kodaira, K., and Okamura, S. 1982, Ap. J. Suppl., 50, 1. (Paper I).

Watanabe, M., Kodaira, K., and Okamura, S. 1984, submitted to Ap. J. (Paper IV).

Whitmore, B. C. 1984, Ap. J., 278, 61.

AN ANALYSIS OF THE GEOMETRICAL PROPERTIES FOR GALAXIES IN THE VIRGO CLUSTER CORE

H T MacGillivray[1] and R J Dodd[2]

1. Royal Observatory, Blackford Hill, Edinburgh, Scotland
2. Carter Observatory, PO Box 2909, Wellington, New Zealand

Summary

We have examined (from objective machine measures) the geometrical properties for galaxies in a magnitude-limited sample in a field of 25 square degrees of sky centred on the Virgo cluster. The aim has been to carry out a search for systematic, non-random trends of the type detected in the Local Supercluster (see MacGillivray et al. 1982; MacGillivray and Dodd 1985). No global effect of alignment of Virgo galaxies along the Local Supercluster plane has been detected, in agreement with previous observations. However, galaxies do show a strong effect of alignment with respect to the elliptical galaxy NGC 4406 (M86) in the sense that they are preferentially oriented with their major planes perpendicular to the direction vector to NGC 4406. There is some suggestion for the presence of correlations between the strength of the effect and other parameters of the galaxies (ie position and apparent ellipticity), although statistical support for this is as yet poor. These results and their implications are discussed.

1. Introduction

Investigations of the geometrical properties (eg positions, orientations and shapes) for galaxies in systems such as clusters and superclusters can provide important information for an understanding of the formation of these structures in the early Universe. We are carrying out studies of this nature, mainly from objective measurements made with the COSMOS automatic plate-scanning machine at the Royal Observatory Edinburgh.

The Local Supercluster (hereafter referred to as LSC) is an interesting object for study by virtue of the fact that it is the nearest large-scale structure and hence is a useful starting point for investigations of the global properties of superclusters. In an early study of the properties of

spiral galaxies in the LSC (MacGillivray et al. 1982), evidence was found for an effect (although not strong) of alignment of the major planes of the galaxies along the plane of the LSC. This alignment tendency was most pronounced for galaxies outside the LSC plane and for galaxies which were seen nearly edge-on. Galaxies within the LSC plane itself (including those in the Virgo cluster) displayed, to all intents, random orientations. These observations are in agreement with results obtained by other authors (eg de Vaucouleurs 1978; Helou and Salpeter 1982; Kapranidis and Sullivan 1983). Recently (MacGillivray and Dodd 1985), we have extended the original investigation in a search for correlations with morphological type and spiral winding direction. The results revealed that there is segregation of spiral galaxies according to morphological type within the LSC (spirals of type Sab-Sc being less concentrated towards the plane of the LSC than spirals of other types), that these intermediate-type spirals display preferentially the effect of alignment along the LSC plane and that they are preferentially of winding direction "s" as opposed to "reversed-s" (or "z"). This last effect has also been noted by Borchkadze and Kogoshvili (1976) and Yamagata et al. (1981). Furthermore, in our study a hemispherical dependence of winding direction on supergalactic latitude was detected, intermediate type spirals of winding direction "s" being found preferentially at Southern supergalactic latitudes while galaxies of winding direction "z" are found preferentially at Northern supergalactic latitudes.

The above properties of the galaxies in the LSC were interpreted as indicating that the North poles of spirals of type Sab-Sc are coherently aligned in space both with themselves and with the pole of the LSC. Such properties are consistent with the primeval turbulence model for galaxy formation (Ozernoy 1978) but are not consistent with either the hierarchical clustering scheme (Peebles 1974) nor with the theory of adiabatic perturbations (Zeldovich 1978; Doroshkevich et al. 1978). Clearly, observations such as these are of value in any discussion of the theories for galaxy formation.

The results obtained for galaxies within the LSC and the importance of the Virgo cluster on the dynamics of the LSC as a whole make further investigation (especially of the Virgo cluster itself) desirable. With this aim in mind, we have started to obtain data from the COSMOS automatic plate-scanning machine (see MacGillivray 1981, 1984) for galaxies in the direction to the Virgo cluster. The advantage of machine measurements is in their completely objective nature, providing greater confidence in the reliability of the results.

2. The data

Ultimately, we intend to examine a region of 100 square degrees of sky centred on the Virgo cluster using IIIaJ plates taken with the UK 1.2m Schmidt Telescope (UKST). However, the required plate material was not available at the time this study was initiated and so we were restricted, in the first instance, to an area of 25 square degrees containing the central region of the cluster. Scans were made with COSMOS using pixel size of 16 microns (corresponding approximately to 1 arcsec on the plate) and the normal COSMOS software used to detect images above a fixed isophotal threshold. This threshold was at the 7% above night sky intensity level, corresponding approximately to the $\mu_J = 25$ magnitudes/square arcsec isophote. The software joins together pixels belonging to the same image and calculates various parameters such as image centroid, isophotal magnitude, size, orientation and shape.

An example of the COSMOS pixel data can be seen in Plate I. This is a direct photograph of a colour monitor screen, the raw COSMOS data of 1 arcsec resolution having been compressed by a factor of 15 in each dimension to produce a reduced 512 x 512 pixel frame (with resulting resolution of ~ 16 arcsecs). The plate shows an area of 2.3 x 2.3 square degrees of sky and in figure 1 can be seen the ellipses fitted to the data at the limiting isophote by the COSMOS software. Note that the line-of-sight pair of galaxies N4435/N4438 has been blended in the data thereby producing a single image. The software used at the time the data was produced has been replaced by a new and improved version and this type of situation is now mainly overcome.

Only galaxies brighter than B = 16 are shown in figure 1, star/galaxy separation having been carried out by techniques described in detail in MacGillivray and Stobie (1985). The COSMOS instrumental magnitudes were calibrated using the photometry of Binggeli et al. (1984) for the dwarf galaxies in Virgo. Throughout the rest of this paper the magnitudes referred to will be on the system of Binggeli et al.

3. The results

The distribution of projected ellipticities for the galaxies in our data down to two different limiting magnitudes, B = 15 and B = 16, is shown in figure 2. Two things are noteworthy in this diagram: firstly there is no marked difference in the apparent shapes of bright and faint galaxies, and secondly the ellipticity distributions are slightly dissimilar from those expected for

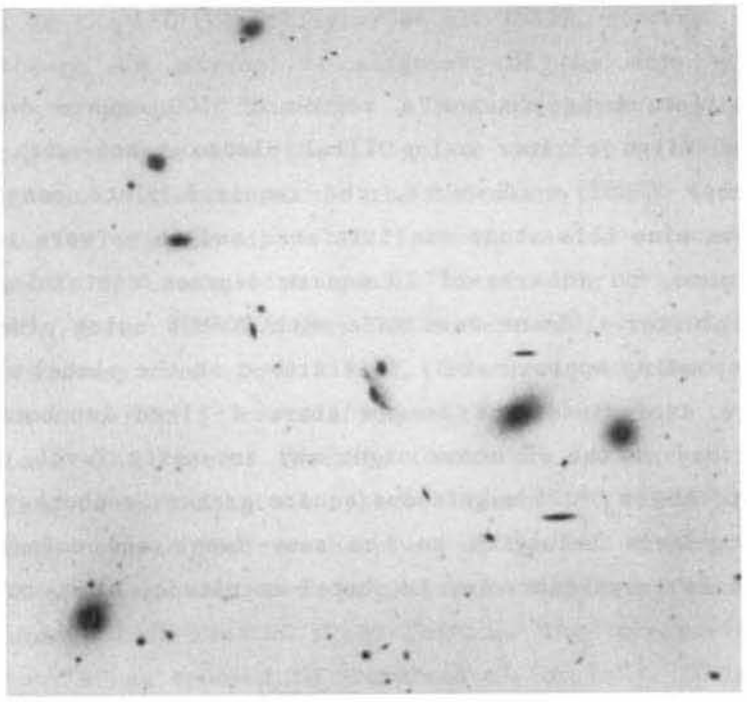


Plate I: Photograph of a colour monitor screen showing the COSMOS pixel data for an area of 2.3^{o} x 2.3^{o} on the UKST plate.

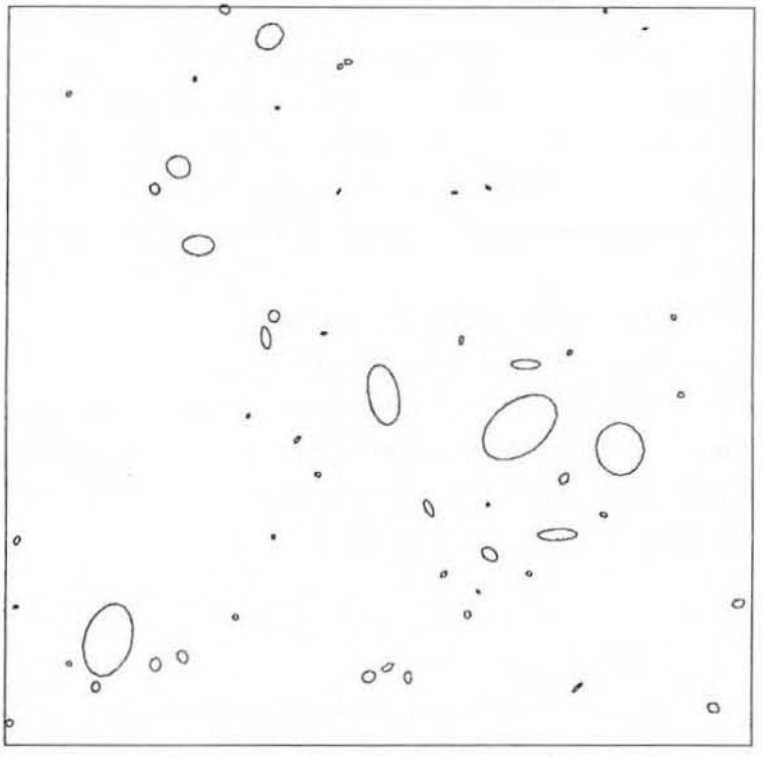


Figure 1 The COSMOS computed ellipses for the galaxies down to B = 16 in the area of Plate I.

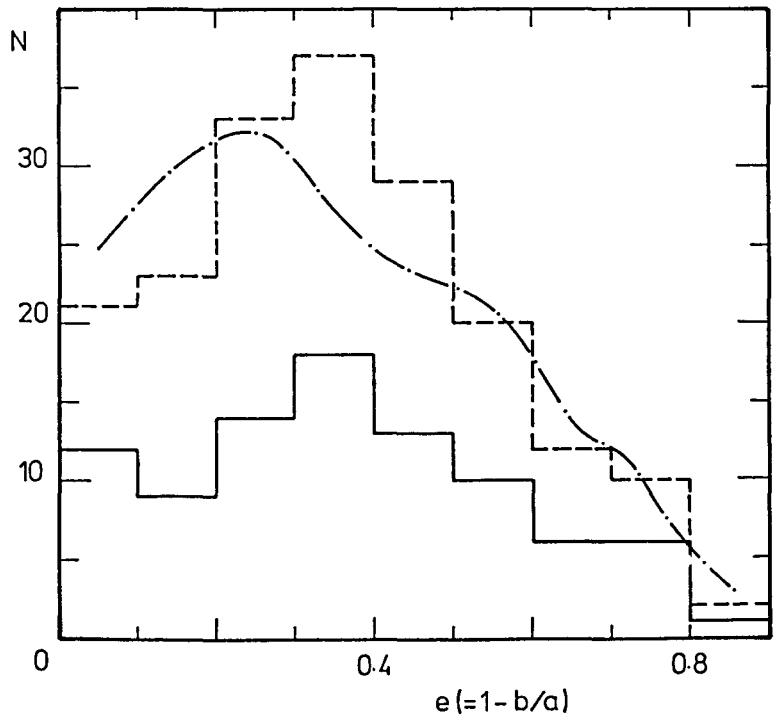


Figure 2 The distribution of galaxy projected ellipticities (e = 1-b/a) for galaxies down to B = 15 (solid histogram) and B = 16 (broken-line histrogram). The curve represents what is expected given a distribution of galaxies with purely random orientations and nomalised for the case down to B = 16.

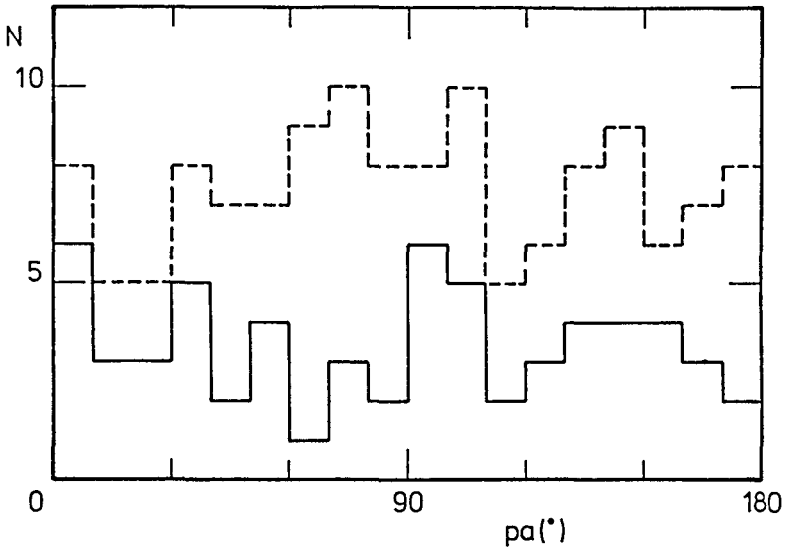


Figure 3 The distribution of position angles (pa) for galaxies with e>0.25 down to B = 15 and B = 16 (solid and broken-line histograms respectively).

a system of galaxies with purely random orientations (the broken-lined curve). This in itself might provide some suggestion for the presence of a non-random effect (see MacGillivray and Dodd 1982).

The distribution of galaxy position angles (pa's) - for those galaxies with $e > 0.25$ - is shown in figure 3. No obvious non-random trend is discernible, certainly not along the plane of the LSC at least (position angle of ~ 160 degrees) indicating no noticeable tendency for the galaxies to be aligned preferentially along the LSC plane. A non-random effect is detected, however, when comparing position angles of the galaxies with the position angle of the direction vector to the elliptical galaxy NGC 4406, M86 (figure 4). In this case, the results are significant on the 92% and 99.9% confidence levels for galaxies down to B = 15 and 16 respectively. The non-random effect is less evident when study is extended to fainter galaxies. It must be stated that the selection of M86 for such a search was based on subjective criteria. However, we have subsequently failed to find any similar effect when taking other galaxies (e.g. M87) as centre.

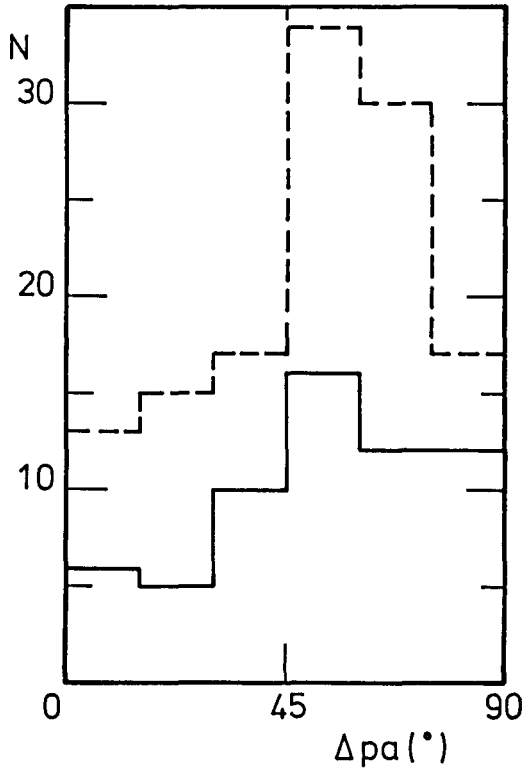


Figure 4 The distribution of the quantity Δpa for the galaxies of figure 3, where Δpa is the difference between the position angle of the major axis of the galaxy and the direction to the galaxy NGC 4406. Small values of Δpa indicate the galaxies are aligned with their major planes pointing towards NGC 4406.

Table 1

Correlations between the parameters for galaxies brighter than B = 16.

e(=1-b/a)

distance from N4406 (mm)	0-0.35	>0.35
0-95	45	49
>95	51	42

Galaxies closer to N4406 appear to be flatter than galaxies further away (66% confidence level).

Δpa(degrees)

distance from N4406 (mm)	0-45	45-90
0-95	36	58
>95	42	51

Galaxies closer to N4406 are more strongly aligned perpendicular to direction vector to N4406 (66% confidence level).

Δpa(degrees)

e (=1-b/a)	0-45	45-90
0-0.35	45	51
>0.35	33	58

Flatter galaxies are more strongly aligned perpendicular to direction vector to N4406 (86% confidence level).

This non-random effect in the orientations of galaxies with respect to M86 is worthy of further investigation in a search for correlations with other properties of the galaxies. In another paper (MacGillivray and Dodd 1982) we have shown from Monte-Carlo simulations of alignments in clusters that such correlations ought to be present. The contingency tables shown in Table 1 do show some interesting trends. However, nothing is supported on a level greater than 86% confidence from application of the χ^2 test, and so the reality of these correlations is as yet not supported by strong quantitative evidence. Analysis of the data for a larger area containing Virgo may provide more significant indications.

4. Discussion

The above results are interesting, perhaps surprising and require interpretation.

The failure to detect an effect of alignment of galaxies along the plane of the LSC is consistent with all previous studies of the LSC in general (see references cited above) and the Virgo cluster in particular (eg Thompson 1976; MacGillivray et al. 1982). It would appear, therefore, that the effect

of coherent alignment of galaxy planes and North poles, observed in the halo regions of the LSC, is indeed absent in the Virgo cluster itself and probably also in the LSC plane. The conclusion must be that primordial effects have been (or are in the process of being) destroyed in these higher density regions.

The effect of alignment of galaxies perpendicular to a central giant elliptical galaxy has been noted in other loose clusters (MacGillivray and Dodd, in preparation). It is unlikely that the effect has a primordial origin, the most likely cause being some dynamical or tidal agency. One possible explanation is that in orbital motions around the centre of a cluster (or in infall towards the cluster centre) the galaxy adopts a position of minimum gravitational potential, ie its major plane aligns itself along the direction of travel. Alternatively, the effect of tidal interactions between a galaxy and a massive cluster core might also lead to this effect. Note that both situations provide properties which are consistent with the observations. They also provide an explanation for the lack of coherent alignment of North poles of galaxies in the Virgo cluster (and also in the LSC plane) as due to disruption of the original alignments by an effect of this nature. In regions of high density in the LSC (eg the Virgo cluster), such interactions are expected to be more frequent and consequently primordial effects more likely to have been destroyed.

Note that in Virgo we are not claiming that M86 is responsible for the re-alignment of galaxies. Indeed, Forman (these proceedings) has shown that M86 is travelling rapidly through the cluster core and spends only a short time therein. Nonetheless, some point at the cluster centre (in the direction of sky coincident approximately with M86) has a profound effect on the properties of nearby galaxies.

A point of interest from comparison of the observations with the Monte-Carlo simulations is in the fact that, in the simulated clusters, the correlations hinted to in Table 1 are of the type to be expected if galaxies were lying with their major planes pointing radially towards NGC 4406 rather than with their poles pointing to NGC 4406. This, however, is consistent with the picture presented above. Also, from simulations of clusters with random orientations for the galaxies, random effects are always observed irrespective of number of galaxies and choice of apparent cluster centre.

Theoretical studies of alignments of galaxies in clusters are still in their infancy. Nonetheless, some progress is being made (eg Miller and Smith 1982;

Wesson 1982). Further work is required to help with an understanding of the origin of the effects reported herein.

Examination of a much larger area of the Virgo cluster from COSMOS data is now underway and it is hoped that this will provide further information for helping with an understanding of the properties of galaxies in Virgo and in other similar clusters. The results will be published in due course.

Acknowledgements

Our thanks are due to the UKST Unit at the ROE for the loan of the photographic material used in this study, and to Photolabs of the ROE for providing Plate I.

References

Borchkadze, T. M. and Kogoshvili, N G., 1976. Astron. Astrophys., 53, 431.

de Vaucouleurs, G., 1978. in The Large Scale Structure of the Universe, IAU Symp. No 79, p.206, D. Reidel, Dordrecht.

Doroshkevich, A. G., Saar, E. M., Shandarin, S. F., 1978. in The Large Scale Structure of the Universe, IAU Symp. No 79, p.423, D. Reidel, Dordrecht.

Helou, G. and Salpeter, E. E., 1982. Astrophys. J., 252, 75.

Kapranidis, S. and Sullivan, W. T., 1983. Astron. Astrophys., 118, 33.

MacGillivray, H. T., 1981. in Astronomical Photography 1981, p.277, eds. J-L Heudier and M. E. Sim.

MacGillivray, H. T., 1984. in Astronomical Photography 1984, ed. M. E. Sim, In press.

MacGillivray, H. T. and Dodd, R. J., 1982. Astrophys, Sp. Sci., 83, 127.

MacGillivray, H. T. and Dodd, R. J., 1985. Astron. Astrophys., submitted.

MacGillivray, H. T. and Stobie, R. S., 1985. Vistas astr., In press.

MacGillivray, H. T., Dodd, R. J., McNally, B. V. and Corwin, H. G. Jr., 1982. Mon. Not. R. astr. Soc., 198, 605.

Miller, R. H. and Smith, B. F., 1982. Astrophys. J., 253, 58.

Ozernoy, L. M., 1978. in The Large Scale Structure of the Universe, IAU Symp. No 79, p.427, D. Reidel, Dordrecht.

Peebles, P. J. E., 1974. Astrophys. J., 189, L51.

Thompson, L. A., 1976. Astrophys. J., 209, 22.

Wesson, P. S., 1982. Vistas Astron., 26, 225.

Yamagata, T., Hamabe, M. and Iye, M., 1981. Ann. Tokyo Astron. Obs., 18, 164.

Zeldovich, Ya. B., 1978. in The Large Scale Structure of the Universe, IAU Symp. No 79, p.409, D. Reidel, Dordrecht.

OPTICAL COMPARISONS OF VIRGO CLUSTER GALAXIES AND FIELD GALAXIES

Robert C. Kennicutt, Jr.
University of Minnesota

I. INTRODUCTION

At this workshop we have seen a great deal of interest in the question of how the gaseous contents of the spiral galaxies in Virgo have been affected by the cluster environment. A related question of some importance is whether the Virgo environment has also altered the stellar populations, star formation, and evolution of the spirals. There are several motivations for answering this question. Gas depletions as severe as often reported should have an observable effect on the stellar populations in the galaxies; by combining the observations one might even hope to place limits on the physical processes and timescales involved. Cluster-field comparisons are important in a more general context as well. Much of the current work on the distance scale, the deceleration parameter, and galaxy evolution is based on studies of nearby or distant clusters, often calibrated against local field galaxies. If galaxies in clusters evolve differently, their effects on those applications may be important.

In this paper I shall summarize what little we know about the optical properties of Virgo cluster versus field spirals. The available statistics indicate that at least some of the Virgo members are different, but not enough is known to unambiguously assign a cause. I shall also try to point out some areas in which future observations would be most helpful.

II. STATISTICAL COMPARISONS OF VIRGO AND FIELD SPIRALS

Classification and Anemia

A convenient, if subjective way to compare cluster and field spirals is to examine their optical morphologies. van den Bergh (1976) and Stauffer (1981) have classified Virgo and field spirals on the Revised DDO (RDDO) system, and have concluded that Virgo contains an abnormally high fraction of "anemic" spirals. An anemic galaxy on van den Bergh's system is one whose Hubble type is defined by disk resolution and smoothness is considerably earlier (i.e., more evolved) than its Hubble type as inferred from its disk-to-bulge ratio. van den Bergh tentatively interpreted the excess of anemics and lenticulars in clusters as an environmental effect, and suggested that stripping would eventually transform most of the cluster spirals first to anemics and then to small-bulge SO systems.

Stauffer (1981) expanded van den Bergh's comparison, classifying a larger sample of Virgo spirals as well as Balkowski's (1973) original HI field sample. He used a common set of photographs (glass copies of the Palomar Sky Survey) to minimize biases in the classifications. Stauffer classified only 9 of 119 field

spirals as anemic, while 17 of 49 Virgo cluster members were classified as anemic. He argued that this strong effect in a large sample could not be explained by subjective errors or by a selection biases between the cluster and field samples.

While these classification statistics are interesting, and are at least generally consistent with results of the more quantitative tests, it is difficult to interpret them unambiguously. One obvious question is how to assess the errors in the subjective classifications. One also should not confuse the RDDO classifications themselves with their preconceived physical interpretation, since the latter is open to some dispute. Smooth-disk small-bulge spirals have been known to galaxy classifiers since Hubble's time, and had been discussed in detail by Sandage (1961) and Sandage, Freeman, and Stokes (1970). "Anemic" spirals are not necessarily gas-poor; indeed many turn out to be abnormally HI-rich (Schommer and Bothun 1983)! Hence it is not clear what relation, if any, there is between anemia and the physical mechanisms such as ram-pressure sweeping which often have been invoked to account for it.

Nevertheless, the classifications suggest that the Virgo members are systematically different, and one should bear this in mind when assessing the more objective comparisons of colors, emission strength, HI, etc. to be discussed below. Most of the optical and radio comparisons are made among galaxies of a given Hubble type, and any ambiguity in the classifications may affect the interpretation of the "objective" data as well.

Integrated Colors

Comparisons of the integrated colors of Virgo cluster and field spirals have been made by Holmberg (1958), Chester and Roberts (1964), Davies and Lewis (1973), Chamaraux et al. (1980), Stauffer (1981, 1983), and Kennicutt (1983). The basic result is that Virgo cluster spirals of a given morphological type are significantly redder on average than their field counterparts.

Figure 1 shows a comparison from my paper. The colors were taken from the Second Reference Catalog of Bright Galaxies (de Vaucouleurs et al. 1976), and the Hubble types from the Revised Shapley-Ames Catalog (Sandage and Tammann 1981). All Shapley-Ames spirals with colors in RC2 are included. In this comparison (and most which follow) "Virgo members" are defined as spirals within 6 degrees of M87. The color distributions in Figure 1 show general features which are similar to those seen in many of the other optical tracers and in HI; galaxies of a given type exhibit a very large spread in color, but the Virgo galaxies are significantly displaced. This displacement is small in comparison with the dispersion at a given type, but is large compared to the statistical uncertainty in the means. In this case the Virgo spirals of types Sb, Sbc (not shown in Fig. 1) and Sc are redder by .07-.08 mag in the medians, while the formal uncertainties

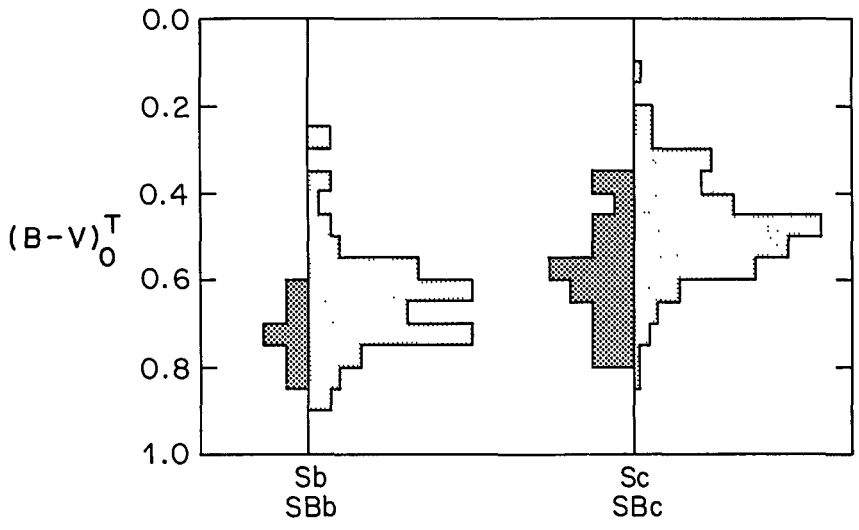


Fig. 1. Comparison of the color distributions of spirals in the Virgo cluster (the left-facing histograms) with field spirals (right-facing).

in the medians are only ±.01 mag in the field and .03-.05 mag in Virgo. The difference is such that an average Virgo Sc galaxy has the color of an average field Sbc galaxy, again consistent with what is seen in HI. There is some evidence for a radial gradient in color, to the extent that spirals in the periphery of the Virgo region (R>6°) have normal colors for their type. Colors are now available for most of the spirals in Virgo, so it is unlikely that these statistics will be improved significantly.

Emission-Line Fluxes, Star Formation, Nuclear Activity

One disadvantage of optical colors of galaxies (especially B-V) is that they are relatively insensitive to small changes in stellar population. As an example, if the star formation rate in an average Sb galaxy suddenly dropped by a factor 2, its integrated B-V color would eventually redden by only .03-.1 mag. This insensitivity is exacerbated by uncertainties from internal reddening and bulge contamination.

The Hα emission from a spiral provides a more linear and sensitive index of current star formation activity, and Stauffer (1983) and Kennicutt (1983) have compared emission line fluxes of Virgo cluster and field spirals. The parameter we use is the emission line equivalent width, the ratio of the Hα + [NII] emission line flux to the continuum flux at 6563Å. Its advantage is that it provides a distance and luminosity-independent index of relative star formation activity. Figure 2 shows the distribution of integrated Hα emission for the 16 Shapley-Ames spirals in Virgo which are classified Sc or SBc by Sandage and Tammann (1981), along with a similar sample in the periphery of Virgo (EXT), and a comparison

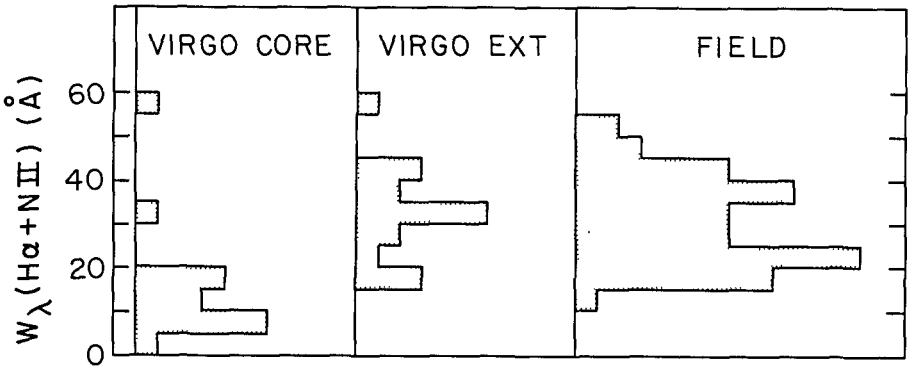


Fig. 2. Distributions of integrated emission-line equivalent widths in Virgo and field Sc-SBc galaxies. Most of the dispersion is the result of real variations in star formation activity.

sample of about 60 field Sc's, all from Kennicutt (1983). Here we see a pronounced difference between the Virgo core and the field, reflecting the increased sensitivity of the emission line index. The median equivalent widths differ by about a factor 2 (15Å in Virgo versus 31Å in the field), similar to the mean HI deficiencies reported in the same galaxies. Note again the strong gradient between the Virgo core and the extension. This is important here, because it reduces any question of selection biases between the complete samples in Virgo and the RC2-selected field sample. An even stronger difference is seen in the Sb-Sbc galaxies, but the sample is small and incomplete. Hα surface photometry has also been obtained for many of the Virgo spirals. The galaxies which are unusually gas-poor generally exhibit much smaller and fainter HII region population. The gas deficiency seems to have altered not only the star formation rate but also the properties of individual star forming regions.

Stauffer (1983) has compared the nuclear emission line fluxes in Virgo and field spirals, and finds quite a different behavior. In contrast to the disk emission, nuclear equivalent widths measured for 48 Virgo spirals are normal for their types. The contradiction should not be too surprising. Among field spirals the nuclear and disk emission line luminosities are only weakly correlated (Kennicutt and Kent 1983), indicating that the nucleus is well isolated from the outer star-forming disk. Stauffer has argued that the combination of a deficiency of gas in the disks and a normal nuclear gas content is precisely what is predicted by simple stripping models (e.g., Kent 1980). While it may be premature to claim observational confirmation of the stripping model on this basis, Stauffer's results do show that the anomalous optical and 21cm properties of the Virgo spirals cannot be easily explained away as due to classification or luminosity biases, because such errors would also show up in the strongly type-dependent nuclear fluxes.

Stauffer also found a significant gradient in spectral excitation ([NII]/Hα) as a function of distance from M87, but could explain it entirely by the well-known gradient in average morphological type as one goes outwards from the center of Virgo. There had been some suggestion that the large [NII]/Hα ratios in the spectra of many Virgo galaxies were produced by shocks generated in ablation or accretion flows, but with the exception of M87 itself, Stauffer can explain all of his spectra in terms of internal galactic properties.

Diameters and Mean Surface Brightnesses

Recently several investigators have compared the distributions of galaxy diameters and surface brightness between Virgo and the field. A primary motivation has been to test the reliability of the IR Tully-Fisher method as an extragalactic distance indicator. For a complete discussion see Bosma's contribution in this volume.

Kraan-Korteweg (1983) and Bosma (1984) have demonstrated that if one forms a distance-independent surface brightness from available infrared magnitudes and catalog diameters, the relationship between surface brightness and 21cm velocity width is different for different clusters (including Virgo), and there is an overall difference between cluster spirals and local field spirals. Bosma also finds residuals in the (B-H) color-velocity width relations which correlate with the surface-brightness residuals. Taken at face-value, we should thus add surface brightness (or optical diameter, since it overwhelmingly influences the surface brightness), as yet another galactic property which is different in Virgo from the field.

In this case, however, it is quite likely that most if not all of the cluster-field differences arises from observational errors. Kraan-Korteweg and Bosma cast considerable suspicion at the RC2 and UGC diameters which are used to derive infrared surface brightness (and aperture-corrected magnitudes), and have suggested that before environmental effects are invoked, diameters based on accurate surface photometry should be measured. The Aaronson-Mould group has obtained such data with a wide-field CCD camera at Kitt Peak, and their preliminary results indicate that most of the cluster-cluster and cluster-field differences indeed arise from systematic errors in the catalog diameters. These errors have a strong effect on the surface brightness tests (which scale as $1/D^2$), and have a significant but smaller effect on the magnitude scales used in the IR Tully-Fisher distance scale. The remaining question is whether some environmental effects will remain. Tully has performed an unpublished analysis similar to Bosma's, believes he has found real differences between Virgo and the Ursa Major cluster. He hopes to publish details in the near future.

Surface Photometry

Accurate photometric profiles would be indispensible, not only to compare diameters, surface brightness, and bulge-disk distributions, but also as an additional check on the subjective morphological types that have been used in comparing Virgo and field spirals. Photographic photometry for Virgo cluster members are available from the work of Fraser (1977), Boronson, Strom, and Strom (1983), and Okamura et al. (1984). One handicap at the moment is the lack of a homogeneous and directly comparable set of data on field spirals. Kent is reducing data from a very large CCD survey, and I suspect that other groups may be collecting similar data. While such data will undoubtedly teach us a great deal about galactic structure, they may not be the panacea to the cluster-field problem that many hope they will be. According to Boroson et al., neither disk scale length nor surface brightness correlate strongly, if at all, with galaxy type, and Boroson's thesis work has demonstrated the difficulty of measuring accurate and physically meaningful bulge-to-disk ratios. So far Boroson et al. find no evidence for environmental modification in Virgo.

III. COMBINED OPTICAL-RADIO COMPARISONS

So far we have only considered the optical properties individually. One way to learn more is to look at the relationships between the various optical and radio properties, independent of galaxy type, and look for differences between cluster and field. As an example, rapidly, recently stripped spirals might show up as anomalously HI and Hα-poor, but blue spirals. Experience with this approach has proven frustrating, however, because while the Virgo spirals of a given type tend to differ systematically from the field, the differences in color, HI, Hα, etc. are usually correlated in a way which parallels the correlations of those properties along the Hubble sequence. In other words, in terms of the optical properties which are easily measured, an "anemic" Sc galaxy in Virgo is often indistinguishable from a field Sb or Sbc galaxy (except for its classification, of course). Figure 3 is one illustration of this problem; it shows the HI-color diagram for Virgo cluster (crosses) and field spirals. If we had not classified these galaxies, we might not consider them as abnormal at all!

This naturally raises the question of whether the assigned Hubble types or luminosities in Virgo might be systematically different from the field. The luminosity distributions have been discussed by Kennicutt (1983), and are similar in Virgo and the field. The possibility of a systematic Virgo-field bias in the Hubble types is more difficult to assess, but it is probably not important in most cases. Stauffer (1981) has intentionally included classification errors in his uncertainty estimates, and finds that the differences with the field are still significant. Kennicutt, Bothun, and Schommer (1984) in turn have compared the

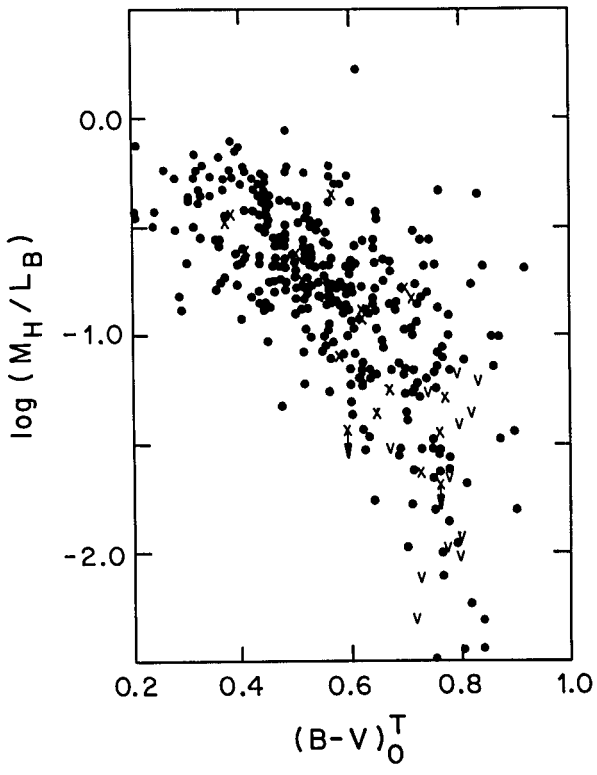


Fig. 3. HI content-color relation for field spirals (plotted as points and upper limit carats), and Virgo spirals (plotted as crosses and upper-limit carats).

Virgo and field galaxy properties with Sb-Sc galaxies lumped together, and still find strong differences. Stauffer's nuclear emission-line statistics also argue against a strong type bias. Finally, there are several extreme cases of individual galaxies (discussed later) which are much too anomalous to be explained by classification errors.

The most extensive comparison of HI and optical data on Virgo that I know about has been made by Stauffer (1981, 1983). He compiled existing data on HI content, B-V colors, and types in Virgo and the field, and computed for each galaxy an HI and a color deficiency factor, the deviation in HI surface density and color from the mean value for field galaxies of the same morphological type. The idea was first applied by Chamaraux et al. (1980). Figure 4 shows the HI and color residuals, for the Balkowski field sample and the Chamaraux et al. Virgo sample, as taken from Stauffer (1981). Stauffer pointed out several features:

a) There is a marked excess of HI-deficient, red galaxies in Virgo, as discussed earlier.

b) There is a corresponding absence of blue, HI-rich galaxies which often are present in the field. The absence of such galaxies is not easily explained by a stripping hypothesis.

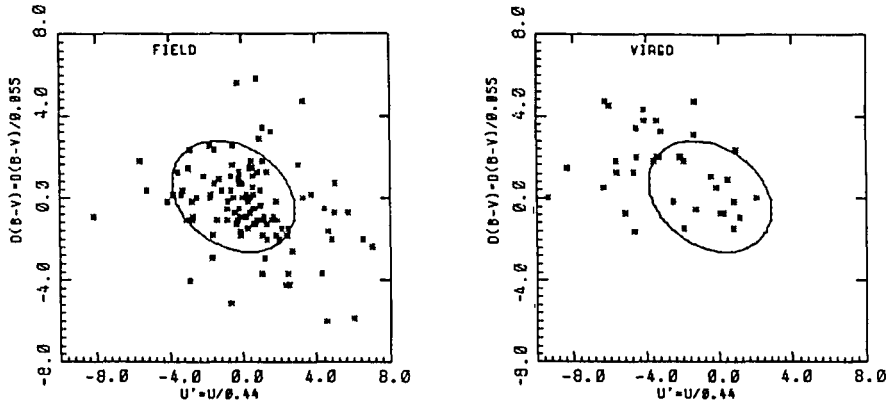


Fig. 4. HI-color correlation diagrams from Stauffer (1981). The two axes measure deviations of a galaxy's integral color and HI content from the mean value for that type. Positive D(B-V) corresponds to being redder than normal, and positive u' corresponds to being HI rich in surface density, following Chamaraux et al. The ellipse is that containing 70% of the field sample, in this case the Balkowski HI sample. The Virgo sample is that of Chamaraux et al. (1980).

c) Most of the HI-deficient galaxies in Virgo are red for their type, but normal in color compared to field spirals of the same HI content. This contradicted a conclusion reached by Chamaraux et al. earlier.

d) There may exist a few blue, HI-poor galaxies in Virgo, candidates for recently stripped spirals. Stauffer offered this last suggestion with some reservations; the galaxies to the lower left in Fig. 4b are all early-type spirals, and the residuals are defined in such a way as to create a bias for early-type blue galaxies in the diagram.

Stauffer's analysis provides a good illustration of how the independent radio and optical data can be combined to isolate significant cluster-field differences, and perhaps even constrain the range of underlying physical causes.

IV. DISCUSSION

The simplest conclusions one can draw from the optical comparisons are that:

1. Some modification of the stellar populations in the Virgo spirals has taken place, on average. The consistency of the optical and radio tracers is a strong argument against selection effects or statistical anomalies.

2. The degree of alteration varies enormously, and many spirals appear to be unaltered.

3. In most cases the differences which can be ascribed to environment are small compared to the intrinsic dispersion in galaxies of a given type. Environmental influences do not dominate the evolution of most Virgo spirals. In particular, we see no evidence for the kind of extreme modification which would be required to manufacture SO galaxies from normal spirals.

Do the available data place any meaningful constraints on possible environmental mechanisms? In Table 1, I have assembled a sort of truth table for 3 straw-man hypotheses:

Hypothesis 1 - No environmental modification is taking place in Virgo. Everything can be explained by selection effects.

Hypothesis 2 - The Virgo spirals are falling into a dense intergalactic medium, and rapid and strong sweeping is taking place at the present time.

Hypothesis 3 - Long-term, slow gas depletion is taking place in Virgo, probably from mechanisms other than ram-pressure sweeping.

TABLE 1

Observation	Hypothesis 1 (Nothing)	Hypothesis 2 (Rapid Stripping)	Hypothesis 3 (Slow Depletion and Several Processes)
overall HI deficiencies	-	+	+
HI diameters	-	+	
integrated colors	-		+
disk Hα emission	-	+	+
nuclear Hα emission		+	+
radio continuum emission		+	
radial gradients in color, HI, Hα	-	+	
strong x-ray sources	-	+	-
extended x-ray source		-(?)	+(?)
many spirals are normal	+	-	
a few spirals are very abnormal	-	+	+
absence of blue HII rich spirals	-	-	+
comparisons with other clusters	-		+

It is clear that no single simple picture can explain everything. The situation would be even more complicated if we included data from other clusters, which often have very different optical properties from Virgo (e.g., Bothun 1981, Kennicutt, Bothun, and Schommer 1984). The null hypothesis is difficult to support - the statistics of the HI, Hα, and colors are too convincing in my view. The stripping hypothesis can account for many of the HI properties, as well as the optical properties of a few unusual spirals in Virgo, but Table 1 includes a long list of observations that cannot be easily explained by stripping alone. The point raised perhaps most often by the optical observers is that the Virgo

spirals appear to have had time to adjust their star formation and stellar populations to the gas shortage. Most sweeping scenarios in Virgo invoke recent, and hence rapid gas removal, because it appears that the Virgo intergalactic medium is a rather young one. The optical observations do not exclude stripping as a viable physical process in Virgo; they just make it difficult to explain everything we see with rapid sweeping alone.

In my mind Hypothesis 3 has many virtues. There are several mechanisms besides ram-pressure sweeping which can deplete the supply of gas in a spiral, and on much longer timescales; tidal encounters (Icke 1984), a cutoff of infalling gas, either at early epochs (e.g., Dressler 1980) or at present (Larson, Tinsley, and Caldwell 1980), or slow moderate ablation of the loosely bound outer HI envelopes (e.g., Kent 1980). One or more of these processes can reproduce virtually all of the observed spiral properties in Virgo, but they will not manufacture SO galaxies in large numbers. The worst aspect of Hypothesis 3 is that it is a vague, slippery, and wishy-washy hypothesis. My bet is that it is the closest to being correct, however.

V. DESIDERATA

Most of the comparisons to date have been statistical tests of some sort. The statistics are rapidly being taken as far as they can; we are running out of galaxies to measure in Virgo, at least spirals. Perhaps the many ongoing studies of the Virgo dwarfs will provide new information, and perhaps someone will find a clever way to combine the various data sets, along the lines of Stauffer's analysis.

If any big breakthroughs are to be made, they may come from detailed, coordinated optical and radio studies of individual galaxies. As an amusing exercise, I have compiled in Table 2 a list of the spirals in Virgo which have been cited in recent papers as favorite candidates for recently stripped or otherwise severely anemic spirals. I shall not defend the choices (except for my own!), and certainly cannot guarantee that they will prove to be Rosetta stones, but their study could prove as rewarding as further surveying of the integrated properties of Virgo members.

As a final caveat, I have appended to the list of "smoking guns" one other galaxy which is as strange as anything in Virgo. NGC 1961 has all of the observational earmarks of a spiral being swept, an asymmetric HI distribution, X-ray emission, peculiar optical colors, and disturbed gas motions (Shostak et al. 1982). If it were situated in Virgo it would be cited as one of the most convincing examples of ongoing sweeping by the cluster IGM. But NGC 1961 is a field spiral, the largest member of what may be a small, loose group. Shostak et al. argue that NGC 1961 <u>is</u> being stripped by hot intergalactic gas. Whatever

the case, any theoretical explanation for manufacturing the unusual spirals in Virgo should also explain how galaxies such as NGC 1961 evolved to the same state without Virgo's help. Caveat emptor!

TABLE 2

Some Favorite Smoking Guns

Galaxy	RSA Type	RDDO Type	$(B-V)_o^T$	$\log(M_H/L_D)$	Ref	Remarks
N4388	Sab	Sb II	.62	-1.3	1	x-ray source
N4406	E3	S0/E3	.89	-	2	elliptical
N4438	Sb(tidos)	Sap	.72	-1.8	1,3	x-ray, radio ridges
N4450	Sabp	Ab II	.74	<-2.0	1	blue HI-poor
N4569	Sab II	AB I-II	.65	$\lesssim$-1.7	1	anemic; anomalous nuclear activity
N4571	Sc II-III	-	.68:	-1.2	4	anemic
N4579	Sab II	A(B)b II	.76	<-1.7	1	blue HI-poor
N4689	Sc II.3	Ab II-III	.60	$\lesssim$-1.2	4	anemic
N1961	Sb IIp	-	.54	-0.5	5	field spiral; suggested as being stripped

References: (1) Stauffer 1981; (2) Forman et al. 1979; (3) Kotanyi et al. 1983; (4) Kennicutt 1983; (5) Shostak et al. 1982.

REFERENCES

Balkowski, C. 1973, Astron. Astrophys. 29, 43.

Boroson, T.A., Strom, K.M., and Strom, S.E. 1983, Astrophys. J. 274, 39.

Bosma, A. 1984, preprint.

Bothun, G.D. 1981, Ph.D. Thesis, University of Washington.

Chamaraux, P., Balkowski, C., and Gerard, E. 1980, Astron. Astrophys. 83, 38.

Chester, C. and Roberts, M.S. 1964, Astron. J. 69, 635.

Davies, R.D. and Lewis, B.M. 1973, Mon.Not.R.A.S. 165, 231.

de Vaucouleurs, G., de Vaucouleurs, A., and Corwin, H.G. 1976, Second Reference Catalog of Bright Galaxies (University of Texas Press).

Dressler, A. 1980, Astrophys. J. 236, 351.

Forman, W., Schwartz, C., Jones, C., Liller, W., and Fabian, A. 1979, Astrophys. J. (Letters) 234, L27.

Fraser, C.W. 1977, Astron. Astrophys. Suppl. 29, 161.

Holmberg, E. 1958, Med. Lund Astr. Obs. Ser. II, No. 36.

Icke, V. 1984, preprint.

Kennicutt, R.C. 1983, Astron. J. 88, 483.

Kennicutt, R.C., Bothun, G.D., and Schommer, R.A. 1984, Astron. J. 89, in press.

Kennicutt, R.C. and Kent, S.M. 1983, Astron. J. 88, 1094.

Kent, S.M. 1980, Ph.D. Thesis, Caltech.

Kotanyi, C., van Gorkham, J.H., and Ekers, R.D. 1983, Astrophys. J. (Letters) 273, L7.

Kraan-Korteweg, R. 1983, Astron. Astrophys. 125, 109.

Larson, R.B., Tinsley, B.M., and Caldwell, C.N. 1980, Astrophys. J. 237, 692.

Sandage, A. 1961, The Hubble Atlas of Galaxies (Carnegie Institute of Washington).

Sandage, A., Freeman, K.C., and Stokes, N.R. 1970, Astrophys. J. 160, 831.

Schommer, R.A. and Bothun, G.D. 1983, Astron. J. 88, 577.

Shostak, G.S., Hummel, E., Shaver, P.A., van der Hulst, J.M., and van der Kruit, P.C. 1982, Astron. Astrophys. 115, 293.

Stauffer, J.R. 1981, Ph.D. Thesis, U.C. Berkeley.

Stauffer, J.R. 1983, Astrophys. J. 264, 14.

van den Bergh, S. 1976, Astrophys. J. 206, 883.

DISCUSSION

O.-G. RICHTER: Do you see in your material (the pictures) any sort of asymmetry in SFRs, especially in galaxies that are by other measures symmetric?

R. KENNICUTT: I have never made a systematic study, but I can give you my impression. Galaxies which are asymmetric in blue light (NGC 4254, NGC 4654) are asymmetric in H_α, and many of the low-luminosity irregulars possess asymmetric distribution, much as you see in the LMC, for example. Such asymmetries are also common in field galaxies, and my impression is that the Virgo members are no different from field galaxies in this respect.

MORPHOLOGICAL AND PHYSICAL CHARACTERISTICS OF THE VIRGO CLUSTER: FIRST RESULTS FROM THE LAS CAMPANAS PHOTOGRAPHIC SURVEY.

ALLAN SANDAGE

Mount Wilson and Las Campanas Observatories
of the
Carnegie Institution of Washington

BRUNO BINGGELI and G.A.TAMMANN

Astronomisches Institut der Universitaet Basel

ABSTRACT

The Las Campanas du Pont 2.5 m telescope has been used for an extensive photographic survey of the Virgo Cluster, the basic results of which will appear in a "Catalog of 2096 galaxies in the Virgo Cluster area" (Figure 1). The Catalog data are currently been used to investigate the structural properties of Virgo Cluster galaxies, and the Virgo Cluster as a whole. This paper reviews the first results of these investigations. Three topics are discussed after a short description of the Catalog. (1), Morphological and physical properties of the dwarfs (Figures 3-10); (2), Luminosity functions for the various morphological types (Figures 11-22); and (3), The projected spatial and velocity distributions (Figures 23-41).

I. INTRODUCTION

In 1979 we began a photographic survey of the Virgo cluster to the faintest convenient limit of the Las Campanas du Pont 2.5 m reflector. The motivation was to study the complexity of both the surface and velocity distributions within the central 6° region (radius) which have been suggested by many previous authors. Our interest was made manifest in 1978 through an unpublished plot by Kraan-Korteweg of the then known velocities in the Virgo cluster region where two velocity concentrations were suggested, one centered near M87 and the other near NGC 4472 which is traditionaly identified as the brightest E member of the cluster. Within each concentration the velocities of the galaxies were somewhat similar, but the mean velocity of the clustering near M87 seemed ~ 200 km s^{-1} higher than that near NGC 4472, and it was not then known if the projected spatial distribution would show a similar clumping if a survey of cluster members were to be made fainter than the ~ 15.7 mag limit in the catalog of de Vaucouleurs and Pence (1979) where two such concentrations are not particularly evident.

The large field (2.3 sq deg), long focal length (18.6 m), and hence large scale (10.9 arc sec mm^{-1}) and faint limiting magnitude (B = 23 for stars) of the du Pont reflector made such a survey to very faint limits possible. A survey to brighter magnitudes had been in progress for some time by Reaves (1983) which was meant to, and indeed has, served as a most valuable aid for the present work.

The goals have been expanded beyond our first expectations. In the following sections are given preliminary summaries of results on two major themes in the study of the cluster. One concerns the physical properties of galaxies as individuals, while the other concerns the structure of the Virgo cluster itself. The first two papers of a series have appeared (Binggeli, Sandage, and Tarenghi 1984, Paper I; Sandage and Binggeli 1984, Paper III) concerning some of the physical and morphological properties of the Virgo dwarfs as individuals, and we shall only summarize the principal results of these as we need them in the following. Greater detail is given for those parts of the work where we have preliminary

results but where publication of the remaining six papers is expected to take some time yet.

A description of the Survey and a discussion of the resulting Catalog is given in the next sections. Section III describes the frequency of galaxy types found and listed in the Catalog. The physical properties of the dwarfs, already discussed in Papers I and III, are summarized in section IV. Luminosity functions for each morphological type separately are given in section V. The progressive change of $< M_{B_T} >$ faintward along the morphological sequence from Sc I through Sm and Im types is shown and leads to a calibration of the de Vaucouleurs Λ luminosity index and a determination of its intrinsic dispersion. Finally, in section VI we summarize the preliminary results on the distribution of galaxies of all types in the two principal sub-clustering regions described earlier, and discuss the velocity distributions over the face of the 6° core for the various galaxy types.

II. THE PHOTOGRAPHIC SURVEY AND CATALOG

A roughly rectangular area of ~150 square degrees was photographed at Las Campanas on 67 blue (Eastman 103aO) plates of size 50 x 50 cm square. The area, covering the nominal center of the cluster at $12^{h}25^{m}$, + $13^{o}06'$, is shown in Fig.1 which also gives the distribution of the 2096 Catalog entries. Not all the listed galaxies are members. The Catalog contains all galaxies in the area brighter than m_{pg} = 15.7 listed in the Zwicky Catalog whether member or not. We consider ~1300 of the entries of our Catalog to be members, ~500 to be possible members, and the remaining ~300 to be "certain" background (so assigned either from a known redshift or from the morphology).

a) The cluster membership sample

Membership was, in large measure, decided by galaxy morphology alone, with only minimum appeal to velocity data. There is no question on membership for most dwarf members of the cluster as

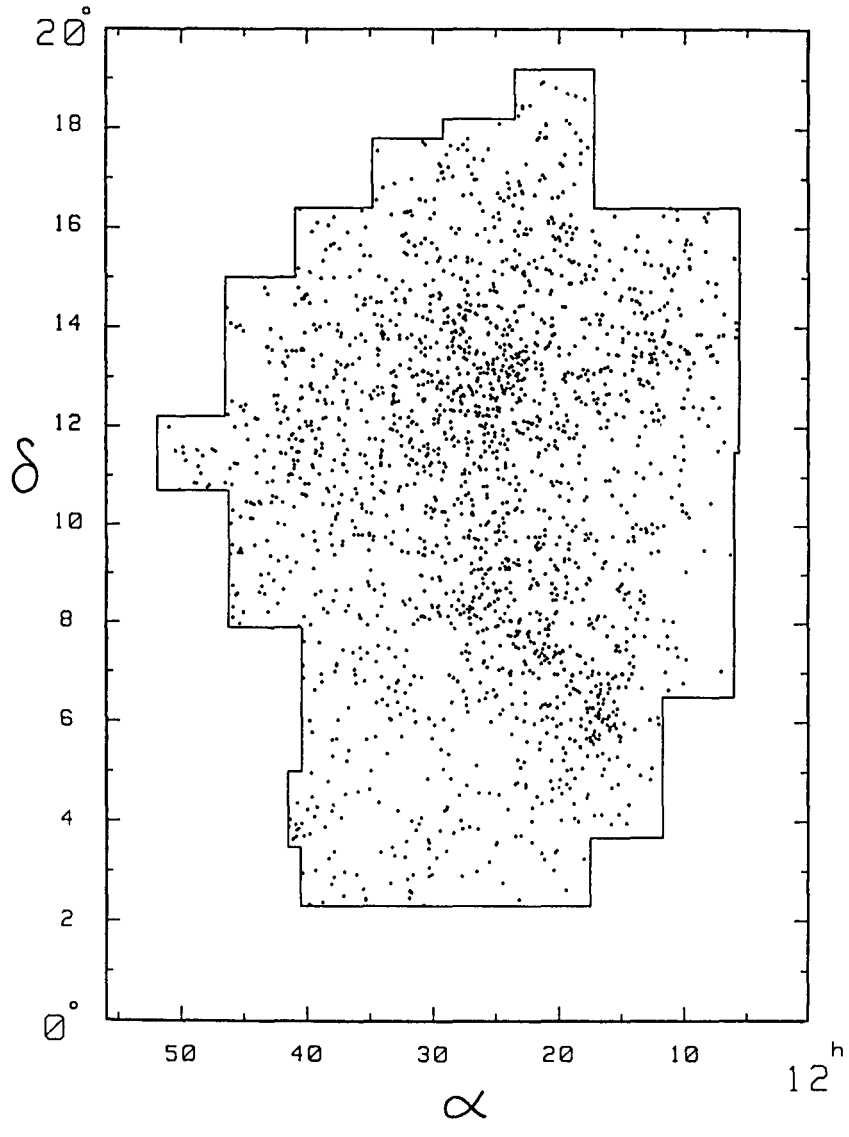


Fig.1 Distribution of the 2096 Catalog galaxies.

there is a well defined surface brightness-absolute magnitude relation (Paper I), and the dwarfs can be recognized beyond question from their unusual surface brightness-diameter relation. This holds for the Im's as well as the dE's.

Membership for the giants is less certain because resolution into stars and stellar associations is not an unfailing criterion for distance. For the few giants, we have relied on the velocity data together with the morphology to assign membership. The velocity

range was from the most negative found to an upper limit of v = 2600 km s^{-1} (heliocentric).

Membership assignment was made during the classification process in which all 67 fields were inspected within a short time. This occured early in the work before all the velocities now in the Catalog were known. A test of the reliability of the membership assignment is available from the 160 new velocities that subsequently became available mostly from Huchra and from a special study by Hoffmann, Helou, and Salpeter (1984) from Arecibo. In 120 out of the 160 cases we predicted correctly the membership or background classification, in the other 40 cases we left open the decision (i.e. the "possible member" class). In only 3 of the 160 cases (2 %) was the predicted membership criteria wrong, suggesting that our membership assignment is correct enough to cause no problems in the following sections.

b) The Catalog

Magnitudes are listed for all 2096 entries. They are based on microphotometer tracings of two particularly galaxy-rich plates of the du Pont telescope measured at ESO headquarters while still in Geneva. Densities were converted to intensities, and the two-dimensional arrays were integrated for 109 galaxies to give total magnitudes on the de Vaucouleurs standard B_T scale. These galaxies served as standards for eye estimates of all other galaxies on all other plates where no other literature value existed. The final magnitudes are a combination of all sources, together with our own determinations. For the eye estimates relative to the 109 standards, our estimated systematic accuracy is better than 0.5 mag, which is sufficient for the luminosity function. Discussion of the physical properties of the dwarf ellipticals (Paper I and section VI here) depend only on the sample actually traced, and there the photometric accuracy is better than $0^m.1$. An independent check of our magnitude system has just now become available through the photometric work of Ichikawa et al. (1984, see Okamura in this Volume). The agreement is very good.

The galaxy types are on the Hubble standard system, with van den Bergh luminosity classes, as estimated by one of us (A.S.), added. Description of the classification of the dwarfs is in Paper III of the series, which also contains an Atlas that illustrates the scheme. A similar Atlas and description of the giants of type Sa and later will be in Paper IV of the series (Sandage, Binggeli, and Tammann 1985). Major and minor diameters and the flattening ratio a/b are listed, from which the distribution of flattenings have been derived discussed in section IV later here.

Velocities are available for ~ 500 entries. Many are new, based on 21 cm radio data, and a major advance has been the CfA catalog, kindly made available by Huchra.

c) Catalog completeness

Special care was taken to achieve completeness in the Catalog to the limit of galaxy detection determined by the galaxian surface brightness against a sky brightness of SB ~22 mag (arc sec)$^{-2}$. We estimate that we have achieved a completeness for galaxies to 25.3 B mag (arc sec)$^{-2}$. The Palomar 1.2 m IIIaJ Schmidt plates previously taken and used by Reaves were inspected continuously in parallel with the large-scale du Pont plates. We believe we are complete for all the spiral types through Sdm and probably Sm as well. The Im types show a large range in surface brightness and are found in numbers even at the faint SB limit just stated, so we are probably not complete for the ImV types. The most serious incompleteness is for dE types that also are found in ever increasing numbers to the detection limit of SB = 25.3 mag (arc sec)$^{-2}$. From an argument based on the intrinsic dispersion of the SB-magnitude relation (Fig.8 of Paper I and repeated later as Fig.3 here) we claim completeness of the Catalog to B_T = 18.0 but do have higher SB entries as faint as B_T = 20. A correction for incompleteness has been made to the dE sample fainter than B = 18.0 in the discussion of the luminosity function in section V.

III. DISTRIBUTION OF THE MORPHOLOGICAL TYPES FOR CLUSTER MEMBERS.

All known galaxy types are found in the sample area, plus a new type of very low surface brightness (~ 25 B mag (arc sec)$^{-2}$), very large diameter (~ 10 000 pc), faint absolute magnitude (M_{B_T} ~ -15) galaxy that comes in both dE and Im types, not yet found in the local neighborhood.

The percentage of Spiral + Im compared to E + dE + S0 + dS0 varies from region to region: it is larger in the NGC 4472 sub-group than in the region near M87, for example, and the detailes of such variations across the area are outlined briefly in section VI where the general projected spatial distribution is discussed. This variation of population type with particular area also makes any concept of a single luminosity function with fixed percentage of Hubble types not so clear. Nevertheless, a general idea of the morphological make-up of the cluster, as averaged over the Catalog area, is useful.

a) Excluded regions

But for this to be meaningful both to this section and for the discussion of the luminosity function, we have excluded certain problem regions of the survey area where membership of particular galaxies is unusually difficult to assign. The best known of these areas is the W cloud in the southwest corner. Galaxies in this region are more distant, on the average, than in the center of the cluster, and although some cluster members must be present in the area, most galaxies probably belong to the background cloud. Another area is the southern extension which is part of the Virgo complex envelope. Still another is the so-called M cloud.

Fig.2 shows the excluded regions, superposed on the distribution of the possible members as judged solely from the morphological classification. From here on in this report, we discuss mainly member galaxies in the non-excluded region of Fig.2.

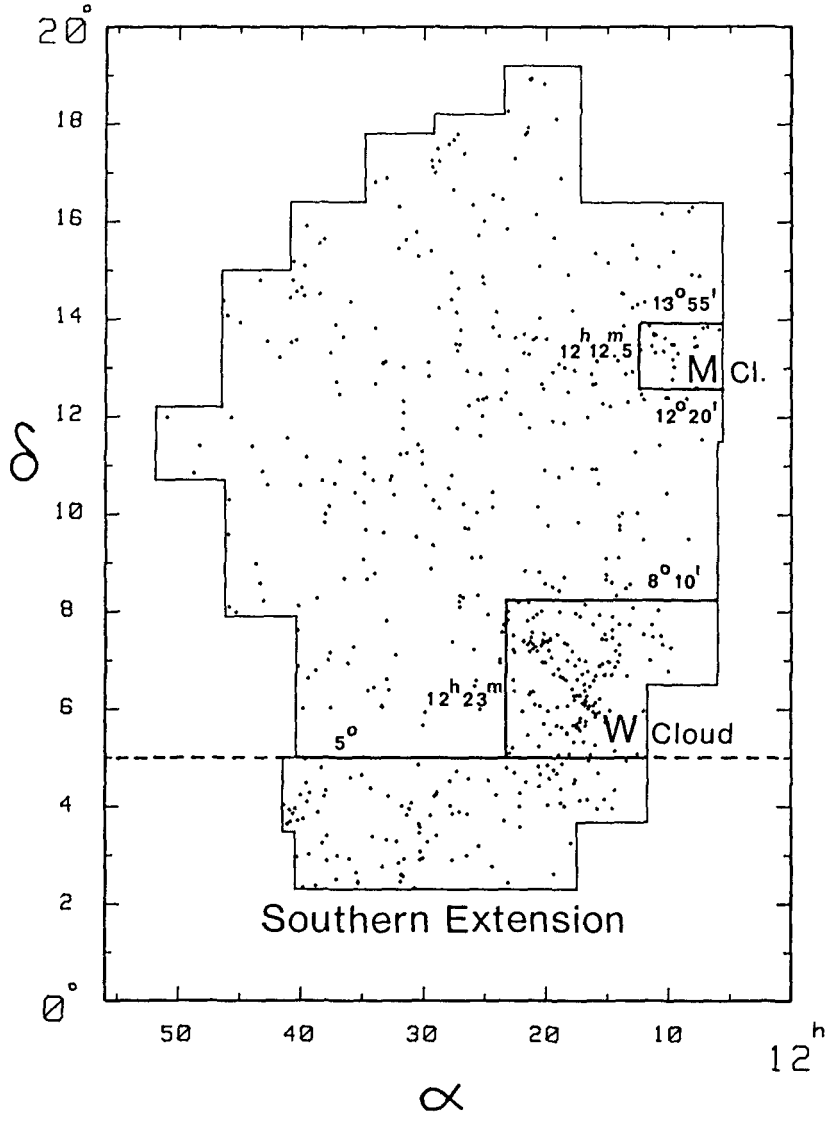


Fig.2 The excluded regions of the Catalog for calculation of the luminosity functions.

b) Percentage of the various morphological types

By far the most frequent type of galaxy in the cluster is the dwarf elliptical and if we add to them the other "non-star producers now" such as the giant E's, the S0, dS0, S0/E, and E/S0 we account for 76 % of the total population to the Catalog limit. However, considering only the giants and not the dwarfs, as divided for example by the two columns in Table 1, and counting

Table 1 Frequency over all magnitudes of VC members and possible members in the standard sample-area shown in Figure 2.

Type	Frequency		
	Member		Possible member
	Ordinary	Barred	
E	22	-	9
E/S0, S0/E	9	-	0
S0	23	15	4
S0/a	3	4	0
Sa	13	4	1
Sab	7	0	0
Sb	5	1	1
Sbc	6	1	0
Sc	32	11	7
Scd	9	1	1
Sd	5	3	2
Sdm	2	0	0
Sm	8	6	2
Sm/BCD	6	0	0
BCD	11	0	0
BCD?	2	0	27

Type	Frequency	
	Member	Possible member
dE	498	11
dE, N	308	0
dE or dS0	8	0
dS0	13	2
dS0, N	11	0
dE(dS0)?	40	119
Im III; III-IV	16	1
Im IV; IV-V	22	2
Im V	21	2
Im III/BCD	8	0
Im?	17	22
dE(dS0) or Im	29	0
?	0	75
Amorphous	4	2

spirals only through Sdm types, the ratio is E + S0/Spirals = 89/99 = 0.9 making the cluster spiral rich at the bright end , but the comparison is entirely misleading when the total sample is considered. In Table 1 there are a total of 1343 members plus possible members that can be well classified. Of this, only 18 % are current star producers; i.e. Sa, Sb, Sc, Sd, Sm, Im, and blue compact dwarf (BCD) types give 244 entries while there are 1099 entries of the early types E, S0, dE, dS0, etc. This suggests

that even spiral rich clusters have most of their members in the dE types.

The detailed data are given in Table 1 which, when combined with the luminosity distributions of section V can be used to give a complete picture of the distribution of morphological types.

IV. MORPHOLOGICAL AND PHYSICAL PROPERTIES OF THE DWARFS

Some of the data on the physical properties of dE galaxies have appeared in Papers I and III and the main points are only briefly given again here, mostly by diagrams. The data and interpretations concerning Im's are mostly new and are given in somewhat more detail.

a) Properties of dwarf E galaxies

Dwarf E galaxies are the most easily identified of all galaxy types because of their uniquely low surface brightness (large angular diameter for a given total magnitude). Even a theoretician with no experience could identify them from photographic plates by the merest of casual inspection. It is this property of low surface brightness that has provided such a positive identifications of cluster membership within the Virgo cluster rather than to confuse them with the background. The distinction is seen in Panel 1 of Paper III (Sandage and Binggeli 1984) where there is no question of the uniqueness of the dE morphology.

There is evidence that dE's form a continuum in their physical properties, merging at the bright end with the giant galaxies and at the faint end with the dwarf spheroidals such as Sculptor, Fornax, Leo I, Leo II, Draco, and the Ursa Minor system of the Local Group. The continuum within the "dE family" is best shown by the photographs in Paper I (Fig.9) and by the correlations with absolute magnitude now to be discussed.

i) The surface brightness-absolute magnitude correlation as derived in Paper I is shown again in Fig.3 here. It is from this diagram (and from Fig.9 of Paper I) that we confirm the continuity within the family of dE's postulated by Baade (1944) where he related the bright dE galaxies NGC 185 and NGC 147 in the Local group with the fainter Sculptor and Fornax dwarfs known already in 1938. His postulated continuum of dE systems is now well seen in the Virgo sample. Figure 3 illustrates the continuum for galaxies in the Virgo cluster itself and shows that the known

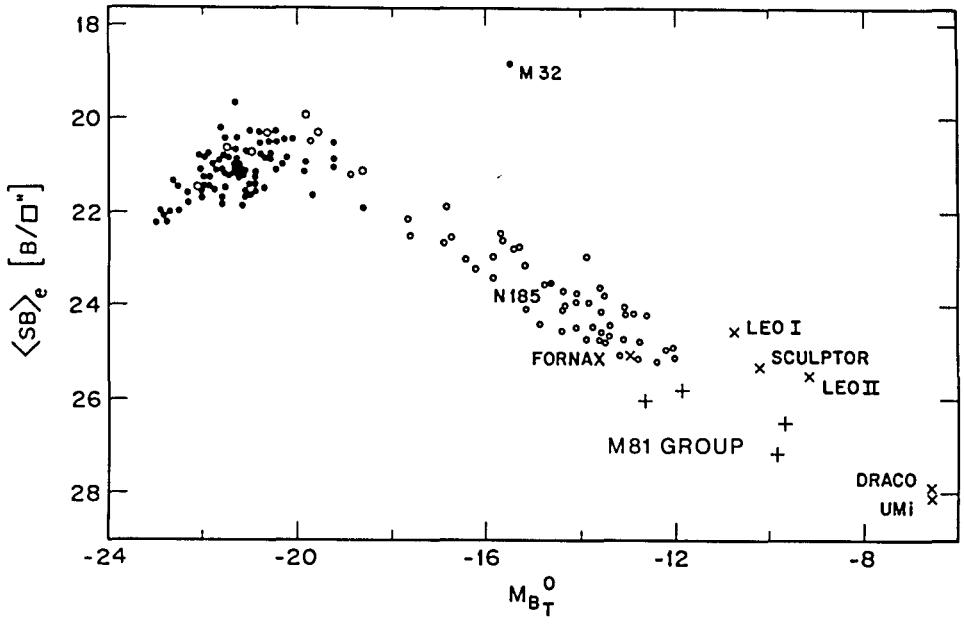


Fig.3 The surface brightness-absolute magnitude diagram for Virgo galaxies (open circles) compared with data for giant E's (closed circles) from the Shapley-Ames Catalog and for dwarf spheroidals of the Local Group (x), and the M81 Group (+).

galaxies of this type in the Local Group fit nicely into the Virgo sequence. Added to the original diagram in Paper I are now four dwarf spheroidals in the M81 group with the data calculated from the detailed photometry of Karachentseva, Schmidt, and

Richter (1984). These also fit very well onto the extension of the Virgo dE's into the region of the dwarf spheroidals. The catalog of dwarfs of this and other types, made with the Tautenburg Schmidt (Boerngen et al. 1982) is, of course, of paramount interest in the present context. We note in passing that the Japanese photometric group of the Tokyo Astronomical Observatory has established a diagram very similar to that shown in Fig.3 (see Okamura in this Volume).

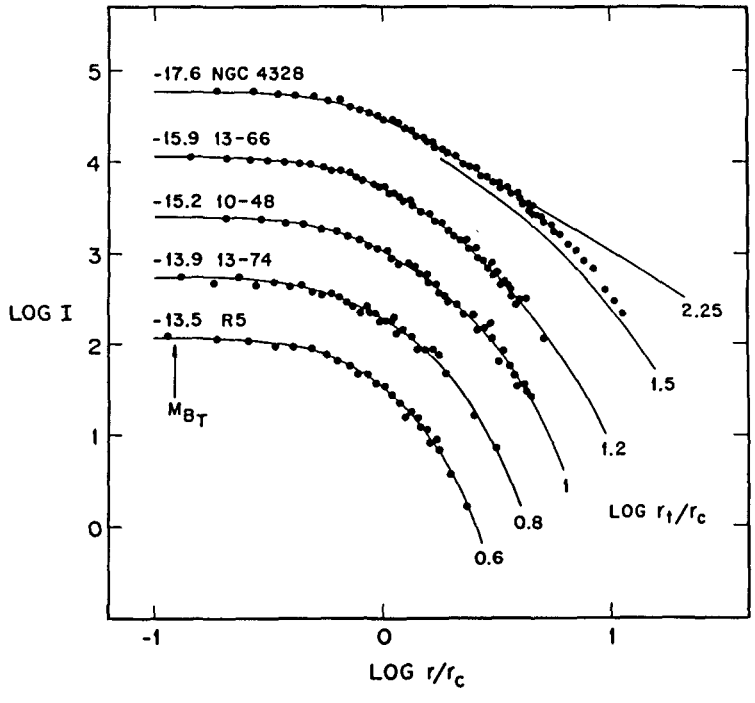


Fig.4 King profile fits to five Virgo dwarfs.

ii) Profiles of the radial luminosity distribution of the Virgo dE dwarfs are well fitted by the manifold of King (1966) models for galaxies fainter than $M_{B_T} = -15.8$ (cf.Fig.5, Paper I). The fitting of King profiles was done as a convenience because the resulting parameter values permit easy conversion of the observed surface photometry into central spatial (i.e. three dimensional) luminosity and mass densities. The remarkably good fits to King profiles of different concentration indices (i.e. log r_t/r_c) is

shown in Fig.4 for five typical mesured profiles (data from Paper I with Tarenghi) for Virgo dwarfs. A special feature of the data is that the core radius r_c is nearly constant at ~ 600 pc for all dE over the total range of ~10 mag from M_{BT} ~ -22 to -12 (cf.Fig.10 of Paper I).

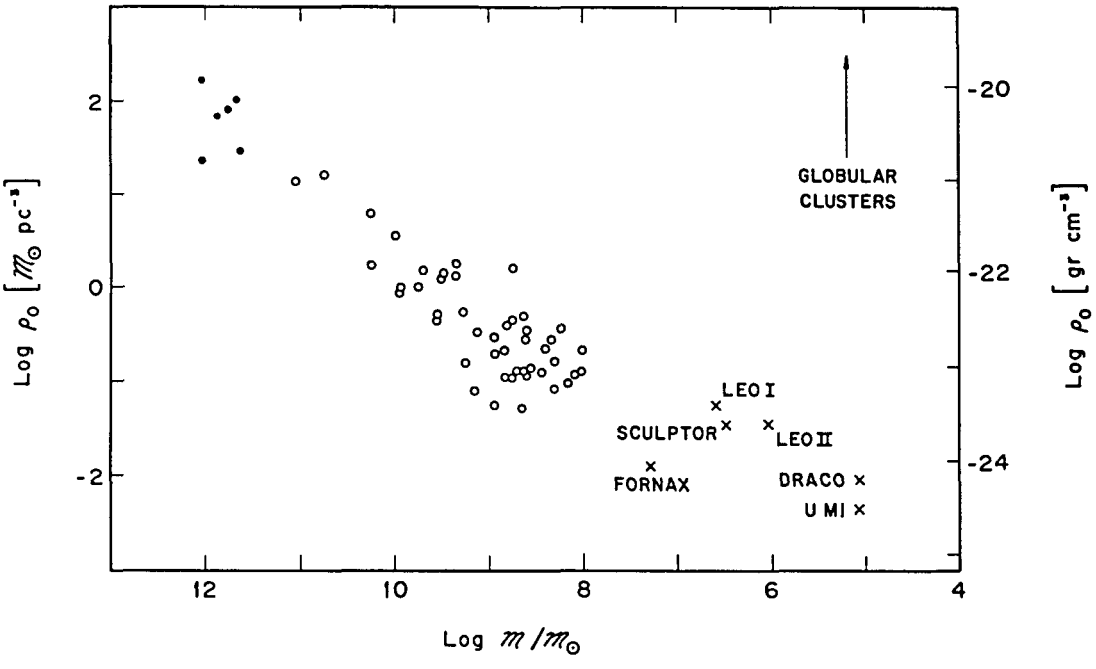


Fig.5 Decrease of the central density (in solar masses pc^{-3}) with total mass of the galaxy. Calculations are based on the King model parameters using $\mathfrak{M}/L_B$ = 10 for Virgo E and dE galaxies (open circles), and giant E's (closed circles), and $\mathfrak{M}/L_B$ = 2 for the local dwarfs (crosses).

iii) The central mass density can now be calculated from the properties of the King models, and is shown over a range of 10^7 in mass in Fig.5 (explained in the text to Fig.11 of Paper I). For giant E's with ~10^{12} solar masses the central mass density is ~ 10^2 solar masses per pc^3, but this decreases nearly linearly with mass to be ~ 10^{-2} solar masses per pc^3 for an aggregate mass of ~ 10^6 solar masses. An "understanding" of this nearly linear

decrease of ρ_o with mass is given in Paper I. Based on the strong correlation of ρ_o and mass, and the nearly constant r_c value over the entire mass range of 10^5 one might call the E family a simple "gestalt".

On the other hand, the globular clusters, so similar in color-magnitude diagram to the dE's in the Local Group, have a much higher central mass density than dE's at the same mass, as shown in Figure 5. It is not yet known if this is a result of a much further dynamical evolution of the globulars since their formation, or of an initial condition difference between the dE and the globular clusters at formation.

iv). Two families of E galaxies may exist, rendering the picture given above oversimplified. It is possible, as argued by Wirth and Gallagher (1984), that a first sequence is given by normal and compact "E" galaxies of increasing surface brightness. In Fig.3 this sequence would span from the giants all the way up to M32. A second sequence would then be defined by the fuzzy "dE" galaxies of ever decreasing surface brightness. It is still an open question if compact E's of relatively low luminosity in the first sequence are a generic feature of the morphological sequence or are a result of tidal stripping, as is suspected for the evolution of M32 itself after it became too friendly with M31. Spurred on by Wirth and Gallagher's insistence that a true (i.e. generic) type of compact E dwarf exists (they cite as evidence their identification of a number of such galaxies in the Fornax cluster), we searched with diligence the very large-scale Campanas plates again and, indeed, did identify a few candidates for Virgo compact E's that we had initially put into the background. But we found only 20 such objects. They are very rare in the cluster, and we have not yet been able to conclude that they are not due to environmental stripping. For us, it is still an open question if a separate sequence should be drawn in Fig.3. The problem is, of course, of great interest and importance to gain an understanding of the formation process and we show in Fig.6 two photographs to illustrate the great morphological differences between the compact E's and the low surface brightness dE's. In any case, the dE galaxies seem to be of secondary origin (see section b), almost certainly in contrast to giant E's. This alone suggests the existence of two E families.

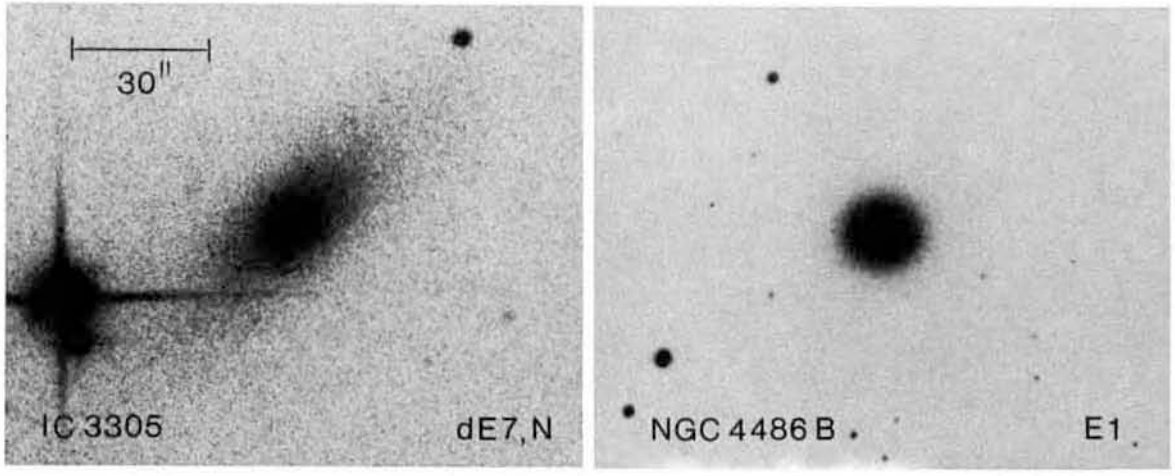


Fig.6 Two faint Virgo galaxies of $B_T \sim 15$ shown on the same scale, illustrating the morphological difference between M32-like, compact E galaxies (such as NGC 4486 B on the right) and low surface brightness dE's (such as IC 3305 on the left). Note the glorious nucleus of IC 3305.

v. The luminosity functions of giant and dwarf E's do not fit together very well, a circumstance that again suggests two families of E's. Fig.7 is the evidence. Shown is the luminosity function [hereafter called $\varphi(M)$] for dE's as solid dots. That for the giant E's has the open circles. There is overlap in the functions near $B_T = 14$, but clearly the two functions do not join onto one another. Fits are shown separately, and an attempted Schechter fit is drawn as dotted for the combined sample of E + dE, which clearly gives an entirely unacceptable representation. This non-merging of the E and dE $\varphi(M)$ is a surprise in view of the continuity of all other physical properties as shown in Figs.3 and 5. The one conclusion that can be drawn from Fig.7, and we emphasize it later in section V, is that $\varphi(M)$ of the regular E's has a maximum, and decreases toward zero at $M_{B_T} \sim -15$. There are no compact E's fainter than this. Wirth and Gallagher reach the same conclusion (1984, their Fig.7) from their Fornax data. On the other hand, $\varphi(M)$ for dE's continues to rise to our survey limit.

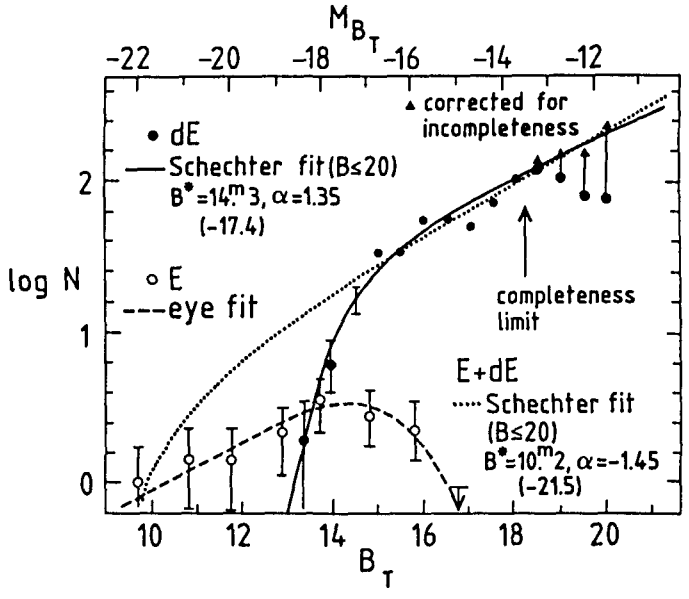


Fig.7 The luminosity functions for E and dE types suggesting that the two types, although part of a continuum of physical properties (cf.Figs.3 and 5), form two families.

vi.) There exist dwarf S0 galaxies characterized either by the presence of an extended envelope or a clear indication of a disk. A discussion and illustration is given in Paper III. It seems that φ(M) for this type has a maximum, decreasing to zero near B_T = 17, but our ability to distinguish dE from dS0 types may be hampered at this faint magnitude.

vii.) But what is clear from the data on luminosity functions is that there are no dwarf spirals, a point we discuss in section V that treats φ(M) for all galaxy types.

b) Properties of the dwarf Im (Magellanic Cloud) types

Of the 1492 members + possible members in the adopted sample, there are many Magellanic Cloud types as listed in Table 1. Although there are only 17 Sm's, i.e. of the Large Magellanic Cloud type, and only 8 of these are of luminosity class III or

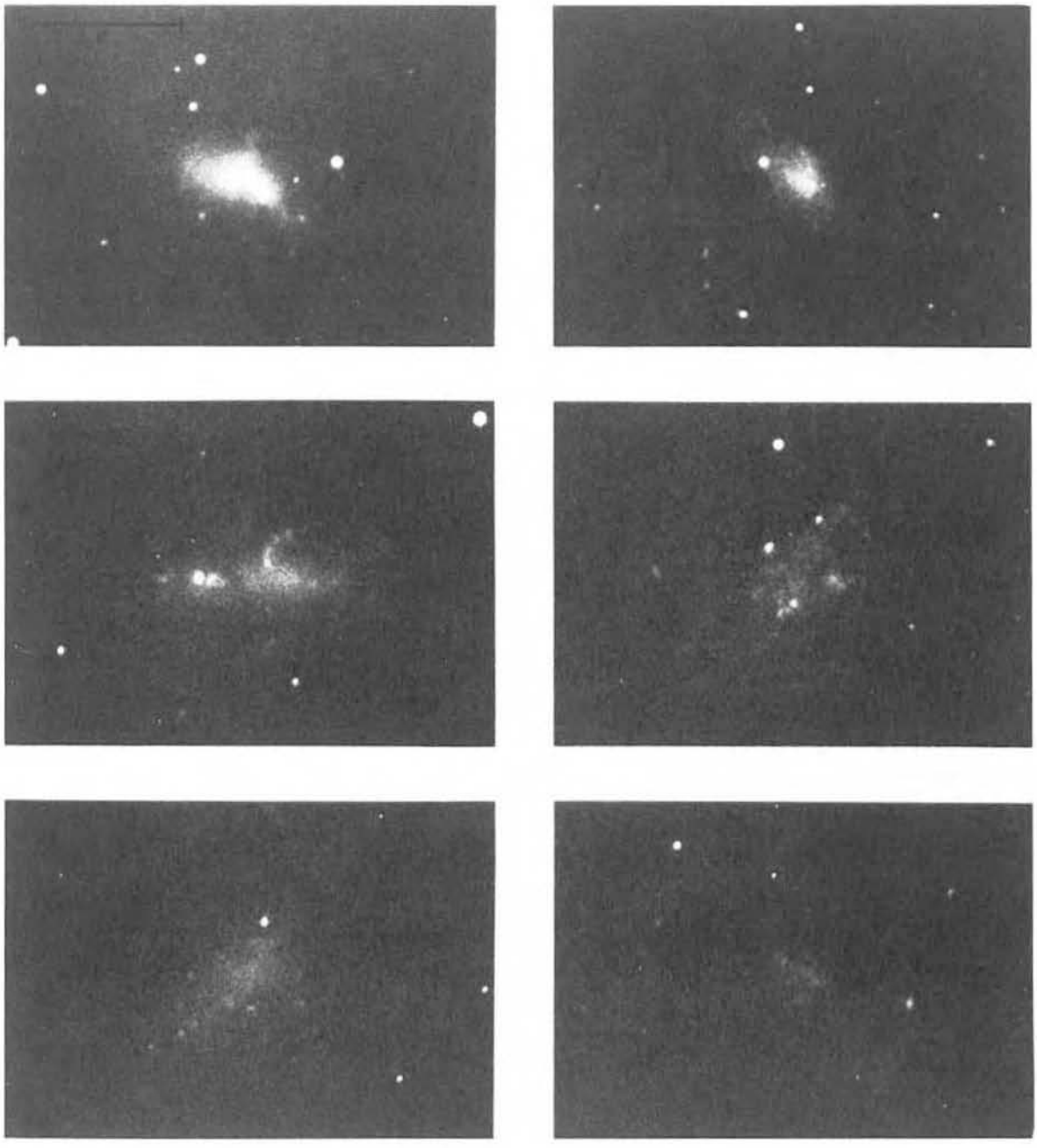


Fig.8 Examples of the Im morphological class.

III-IV, there are very many Im's of the Small Cloud type. Table 1 shows a total of 62 Im's of all luminosity classes, and another 39 with the uncertain classification of "Im..?"

Figure 8 is a collection of 6 typical Im Virgo galaxies, illustrating the distinct morphology. A more complete sample is shown in Panels 14-19 of Paper III. Panels 12 and 13 of the same paper show examples of the Sdm and Sm types which are the brighter cousins of the Im's, and some of the following remarks may apply to them as well.

i.) Is there a physical connection between the dE and the Im types? Panel 19 of Paper III, not reproduced here, shows problems that the classifier faces in deciding between a dE or an Im class for a particular galaxy. It is still an open question with us if this is merely a technical problem of signal-to-noise at these faint levels, or whether physical processes are at work transforming one type into the other.

Ideas of such evolutionary transformation processes have been discussed by Silk and Norman (1979) from theory, Einasto et al. (1974) and Yasov and Karachentseva (1979) from the observational standpoint, and by Faber and Lin (1983) arguing from density profile similarities. In all of these papers the idea is that dE's were once Im's whose gas, and therefore their star forming ability, has been removed. An entirely different idea for the formation of dE galaxies is that of Gerola, Carnevali, and Salpeter (1983) where they propose that the present dwarfs are the bound remains of more massive parents (the giant E's for example) which have lost half or more of their mass by gas ejection leaving behind pockets of negative energy, bound (dE) galaxies. We argue in the next section on the luminosity function that the two families suggested by Fig.7 may favor the Gerola picture. In the following we give two arguments that favor and two arguments that threaten the Im to dE evolutionary transformation idea.

ii.) The distribution on the sky is different for different morphological types over the area of the sample. This is shown in detailed particulars later in section VI where the distributions of spirals, E's and dE's are compared, but we compare here the distribution of faint (B > 18) dE's with the Im types. The projected distributions are in Figure 9. The main cluster at 12^h 25^m, + 13° is defined by the dE's beyond doubt. At this place in

the Im distribution is a hole. Such would be required if Im's were swept clean in the cluster center and were the parents of the present dE's. But, although a necessary condition for the evolutionary transformation hypothesis, it is by no means a sufficient condition, because other causes could be imagined to explain the dearth of Im's in the center such as a high local density restriction on the initial formation. Nevertheless, Figure 9 is one verified prediction of the evolutionary idea.

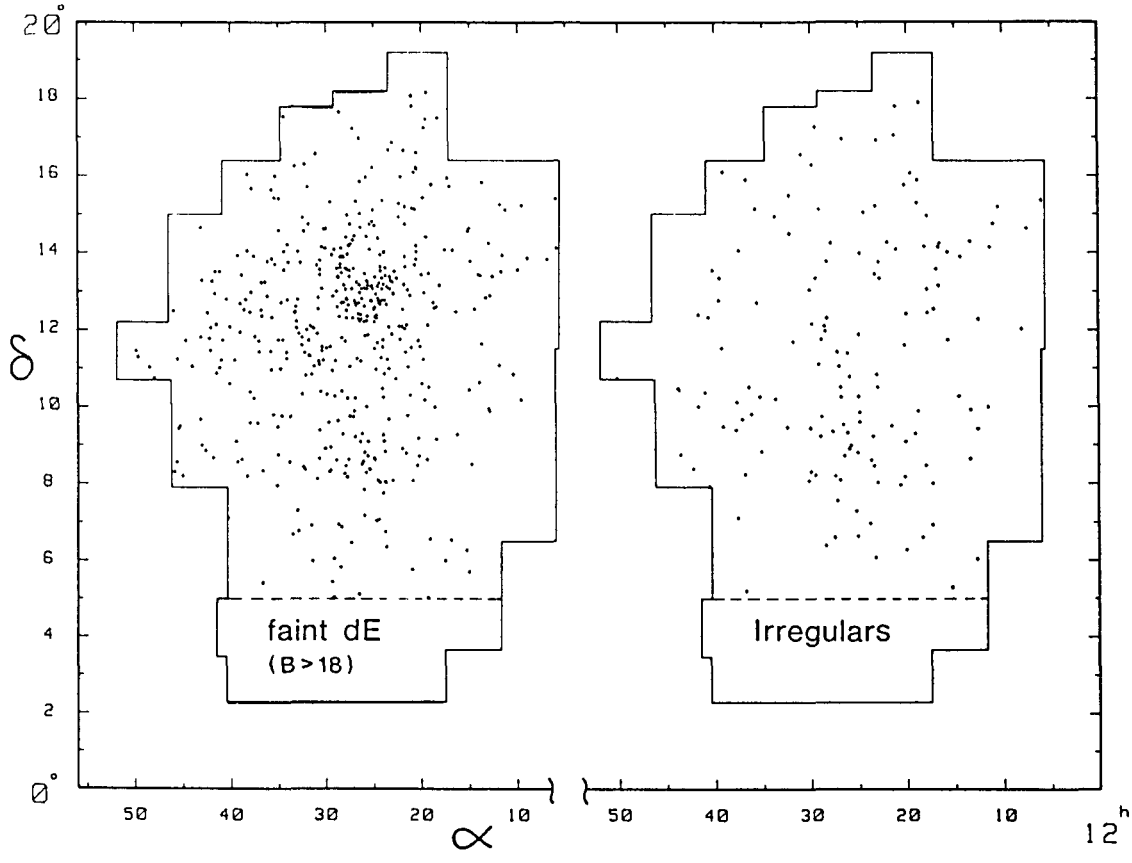


Fig.9 Comparison of the projected distributions of faint dE and Irregulars in the sample area. Note that the cluster core defined by the dE's appears as a hole in the distribution of Irregulars.

iii.) In recent years, following Freeman (1970), it is often argued that galaxies whose luminosity profiles are exponential are disks, while those that follow a Hubble power law are spheroids. Although we believe this to be cannoninicity with scant theoretical support, we can follow the trail to see where it leads. It was shown in the appendix to Paper I that the dE profiles imitate closely an exponential fall off. While at first surprised at this seeming contradiction, since they also obey a King manifold, and necessarily then nearly a Hubble law, it turned out that over the narrow range of King concentration indices of log r_c/r_t near 1 the King profiles imitate the exponential. It was on the basis that the dwarf spheroidals of the Local Group show exponential "disk" profiles that Faber and Lin suggested that dE's are similar to disk irregulars "possibly indicating a closer evolutionary link to spiral-irregular galaxies than to elliptical galaxies". Although our profiles of dE's are indeed exponential, we now argue against this point.

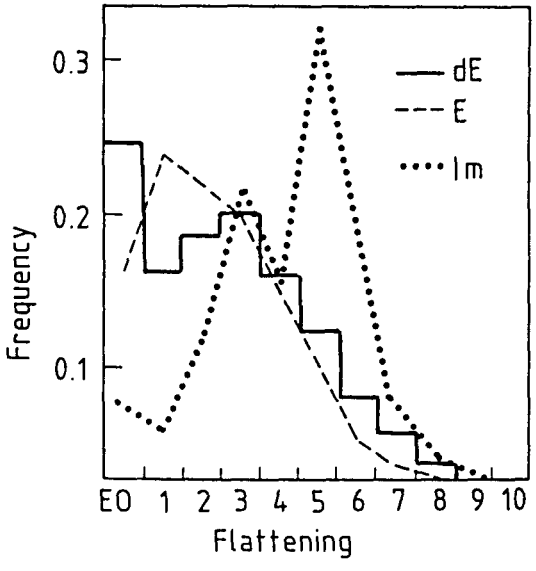


Fig.10

Comparison of the flattening distributions of dE and Im types from data in the Virgo Cluster Catalog, and of E galaxies from data in the RSA (Sandage and Tammann 1981).

iv.) Exponential profiles need not indicate disks. The most powerful way we know to demonstrate disks or spheroids is from the frequency function of the observed flattening, as first applied to elliptical galaxies by Hubble (1926). If dE's come

from Im's, their flattening distributions must be the same. They are not. Data on flattenings taken from the Catalog are shown in Figure 10 for E, dE and Im galaxies separately. The E and dE distributions are almost identical, but both are vastly different from the Im's. This seems to us to be the strongest proof against the evolutionary transformation idea.

v.) Im's have no sharp central nuclei as do dE's. Although it could be argued that upon sweeping, the Im disk brightness fades and that as Im's the disk is so bright as to hide the nucleus that is there, and which will be visible in the daughter dE, the observations belie this. No current Im (with two possible exceptions, see Panel 15 of Paper III) has a bright central nucleus, yet the disk surface brightness of these non-dE's is already fainter than the dE's that do have nuclei.

We believe that these last two arguments are decisive in suggesting that if an evolutionary connection does exist between Im and dE galaxies, it is more subtle than has been given in the literature so far.

c) The BCD galaxies

Discussion of the Blue Compact Dwarfs, parts of which show star bursts overlaying an Sm or an Im disk, has been given extensively in Paper III and illustrated in Panels 20-23 there. It is this class for which we are least certain of completeness in the Catalog. Indeed, in our first durchmusterung we missed all but two of the BCD's that are now listed in the final Catalog version. The high surface brightness and small angular diameter had put most of our present candidates out of contention until redshifts by Karachentsev and Karachentseva (1982) of blue objects found in previous surveys showed them to be Virgo members. We then reinspected the du Pont plates and have a candidate list of ~ 50 objects whose morphology is certainly that of the BCD class. These are easy objects for spectroscopy and suggest that observations for redshift, either in radio or in optical, would be rewarding.

d) The huge low surface brightness dE and Im types

We close this section on the Virgo dwarfs by mentioning the new type of very large galaxy of low surface brightness found by Reaves (1983) and also in this du Pont survey. Four galaxies of this type are described and illustrated in Paper III. The large diameters of 10 000 pc and surface brightness of fainter than 25 mag (arc sec)$^{-2}$ would make detection of such types in the Local neighborhood difficult, but it may, in fact, be that the 11 objects of diameter ~ 3000 pc reported by Boerngen, Karachentseva, and Karachentsev (1984) are smaller examples with the same morphology.

As a summary of this section we state only the obvious. The Virgo cluster contains all known types of dwarfs plus one new kind. This incredible variety of objects, all at the same distance, provides an inclosed zoo that is ideal in which to study fundamental problems of galaxy formation and evolution.

V. LUMINOSITY FUNCTIONS FOR THE VARIOUS MORPHOLOGICAL TYPES

We now approach what was, until recently, a most controversial subject; the luminosity function of galaxies. The most complete early study of the problem was that of Hubble (1936) who concluded that "the luminosity function approximates a normal error-curve with $< M >_{mag} = -14.2$, $\sigma = 0.85$, and $< M >_{vol}$ (corrected for Malmquist bias) = -15.18". He based his study on what he believed to be resolved stars in what we would now call giant spiral galaxies, using a calibration of these "stars" of $< M >_{pg} \sim -6.1$. In a modern system of distances where the modulus of the Virgo cluster is taken to be 31.7, compared to his 26.8 (or another way, with $H_o = 50$ km s^{-1}Mpc^{-1} compared with his 530 giving a factor of 10 difference in the two distance scales) we would translate Hubble's 1936 values to read $< M > \sim -20$ for a distance-limited sample with a dispersion of $\sigma = 0.85$ mag.

Hubble's result was severely criticized by Zwicky (1942) who argued on general grounds that the luminosity function should not

have a maximum. He then proceeded to discover a number of the now well known local Sm and Im systems, and also counted faint galaxies in the nearby clusters of Virgo and Coma, concluding (Zwicky 1957) that no maximum exists in $\varphi(M)$ and that Hubble was fundamentally wrong. The comparison between the two viewpoints is shown in the famous diagram by Zwicky (1957) reproduced here in Fig.11, where the absolute magnitude normalization is on Hubble's old scale, which is 5 magnitudes fainter than that which we now adopt ($H_o = 50$).

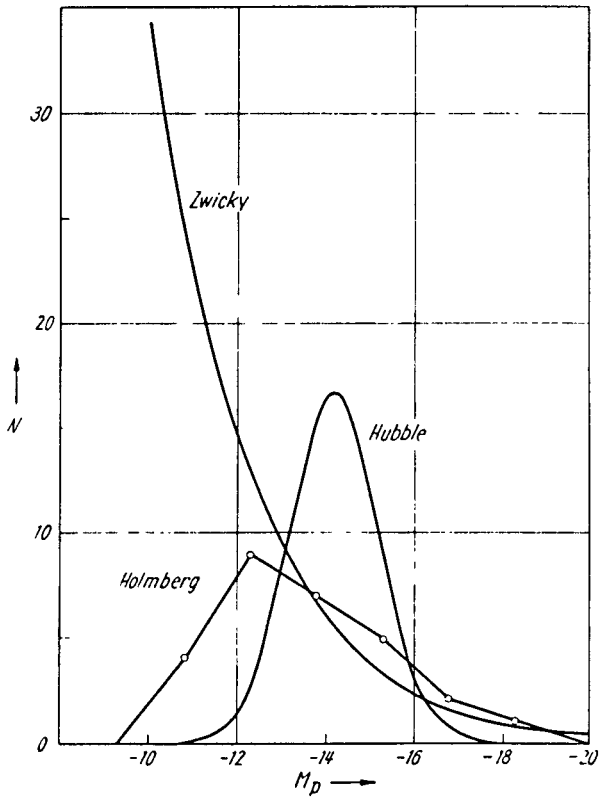


Fig.11

Comparison of the Hubble and the Zwicky claims as to the form of the luminosity function for galaxies (from Zwicky 1957). If $H_o = 50$, the absolute magnitudes along the abscissa should be made brighter by ~ 5 mags.

We now know that Hubble's and Zwicky' conclusions were both correct, but that they were discussing different aspects of the same problem and turning a blind eye to the other's assumptions. Hubble's sample was the nearby "field" galaxies, entirely spirals that showed resolution into "stars" (actually associations of OB stars in the modern understanding), while Zwicky's faint end that

exponentially increases refers entirely to the low surface brightness dE and Im types that were completely discriminated against in Hubble's sample of spirals and in his counts (Hubble 1934) where he did not recognize nor count these types.

We shall see later in this section that the spirals and other currently star producing galaxies do indeed have a maximum in their luminosity function, while the currently dead galaxies (the E, S0, dE, dS0 types when combined into a single luminosity function) do, indeed, have an ever rising φ (M). Hence, as just said, both Hubble and Zwicky were correct within their own contexts but they were not communicating about the same problem.

a) The current data base for the field φ(M) is adequate only brighter than $M_{B_T} \sim -18$.

A large number of studies of φ(M) for field galaxies have appeared during the last two decades, based primarily on redshift and magnitude data on the brighter galaxies in the Shapley-Ames Catalog. A critical summary to ~ 1976 has been given by Felten (1977). With the completion of the Shapley-Ames Catalog in redshift coverage (Sandage and Tammann 1981, the RSA) it became possible to study φ(M) in a truly magnitude-limited sample whose incompleteness function was known. The result (Tammann, Yahil, and Sandage 1979) was, in itself, unsatisfactory because the magnitude grasp of the RSA is insufficient to reach M_{B_T} magnitudes fainter than ~ -18 at best, and at that level none of the φ(M)'s for the various spiral types had reached a convincing maximum. The problem of the general φ(M) was surely not solved with these data. The ideal data base would be a distance-limited sample that was complete to a faint apparent magnitude. We now have such a sample in the Virgo Catalog. In the following subsection we discuss the luminosity function for what can be called star producing galaxies (all the Spirals + Im types) and show that for each type a maximum to φ(M) is reached, and then contrast the situation for the "dead" dwarf ellipticals which exponentiate in their φ(M).

b) The luminosity function for the star producing galaxies

A summary of the distribution of apparent magnitudes for spirals of various types is shown in Fig.12 where the data are taken from the Virgo Catalog but without the strict observance of the sample limits yet imposed on the data in Fig.2, hence these distributions contain the maximum number of galaxies possible. This diagram is taken from Paper IV of the series (Sandage, Binggeli, and Tammann 1985), used to illustrate the distribution of magnitudes in the photographic Atlas of late-type Virgo galaxies. The number of galaxies in each bin is indicated on the left side of each panel. The dispersion of each distribution is shown on the right.

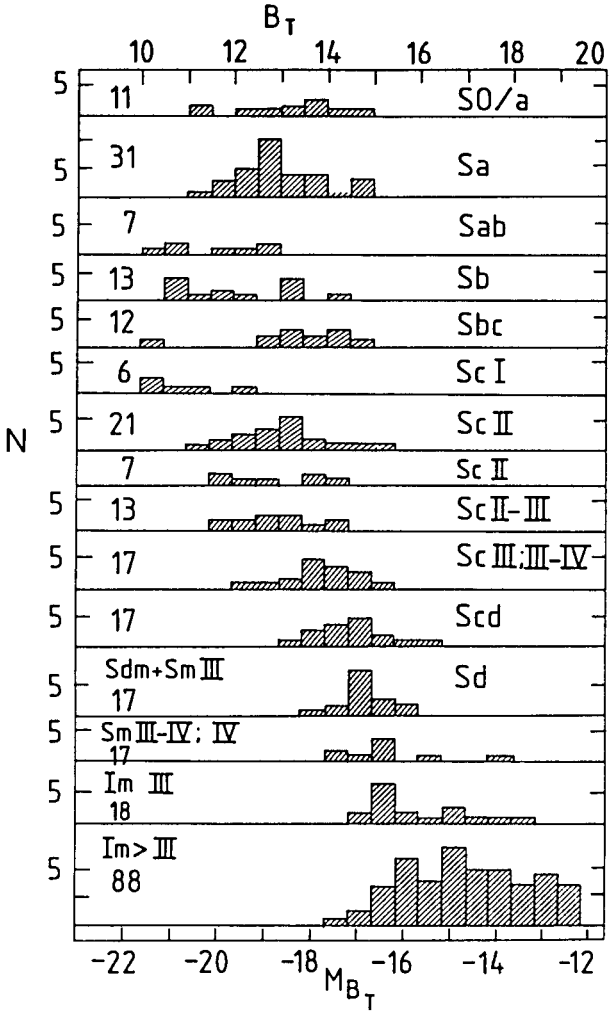


Fig.12

Histogram of the distribution of B_T magnitudes for late type galaxies in the wider sample of the complete Catalog (i.e. not yet the standard sample). Absolute magnitudes are based on a distance modulus of m-M = 31.7.

The principal conclusion is that all types with the probable exception of the Im>III approximate Gauss distributions, bounded on both the bright and the faint end. The faint bound for all distributions is well above our Catalog completeness limit at B_T = 18, indicating that a true maximum for the individual $\varphi(M)$ functions has been reached in every case. As most of the galaxies in Fig.12 are the same type of spirals studied by Hubble, these data confirm his general conclusion of a maximum to $\varphi(M)$ for these galaxy types.

From the top panel of Fig.12 down through the Sdm + SmIII types the peak of the individual functions all occur in the absolute magnitude range between M_{B_T} of -19 to -17. It is just in this range that the determination of the field luminosity functions, using data from the RSA magnitude-limited Catalog terminate (Tammann, Yahil, and Sandage 1979; Kraan-Korteweg, Sandage, and Tammann 1984), but, to be sure, there is a suggested maximum at about M_{B_T} = -19 for most of the functions, except of the ScI galaxies where a real turn around was obtained near M_{B_T} = -21, quite consistent with the data in Figure 12.

Another interesting feature of Fig.12 is the progressive faintening of the mean absolute magnitude for galaxies beginning in the sixth panel down (the ScI's). To see this more clearly, the reader is asked to cover the first five panels and then to inspect the rest. We return to this faintward progression of $< M >$ in section Vc where the calibration of the Λ index is discussed.

Figure 12 is not based on the standard sample which excludes the marked areas of Figure 2, making the conclusion that maxima exist in the individual $\varphi(M)$ functions even stronger. But the standard sample is now used in the next diagrams to illustrate in more detail the individual $\varphi(M)$'s. Figure 13 shows the combined $\varphi(M)$ for all galaxies called spirals. A Gaussian fits the data well, with $< M >_{B_T}$ = -18.4 and σ = 1.5 mag. The individual functions, broken into the detailed types, are shown as dotted curves. Note the same progressive change faintward that is shown in Fig.12 as the types progress from Sa through Sm. Note also that the data are entirely contained in the magnitude interval well above the

completeness limit at B_T = 18. Figure 13 shows what had been suspected before: that there are no dwarf spirals, and we take this to be a principal conclusion of the study.

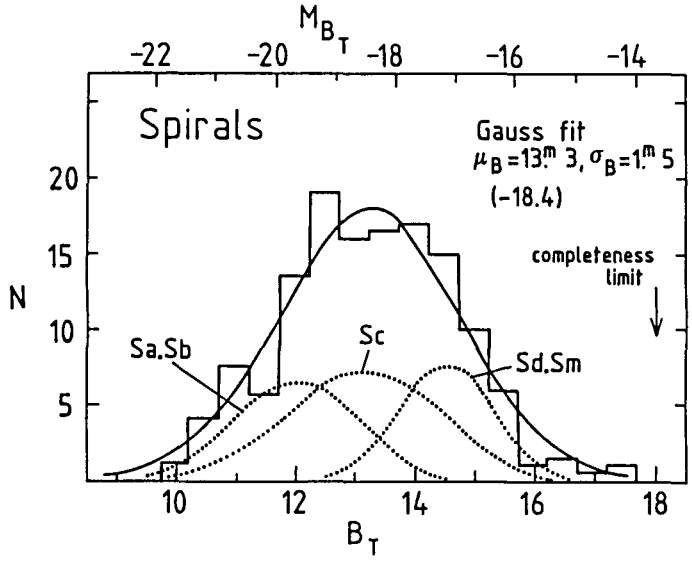


Fig.13 Luminosity function for spiral galaxies showing a maximum at < M > = -18.4. Narrower φ(M)'s exist for galaxies broken into the various Hubble types, shown as the dotted distributions. The principal conclusion is that no dwarf spirals exist.

Figure 14 combines the spiral data in Figure 13 with the distribution of Im galaxies of all luminosity classes. The Im distribution breaches the incompleteness limit at B = 18 so the conclusion that a maximum exists near M_B = -16 is not correct when the Im types are also included. However, Fig.12 shows that it is only for the Im >III that the incompleteness dominates the conclusion.

The point that a maximum is reached in all currently star-producing galaxies, except perhaps for the Im IV and Im V (where, in any case, the classifier has difficulty in distinguishing between the dE and the Im types) is made stronger

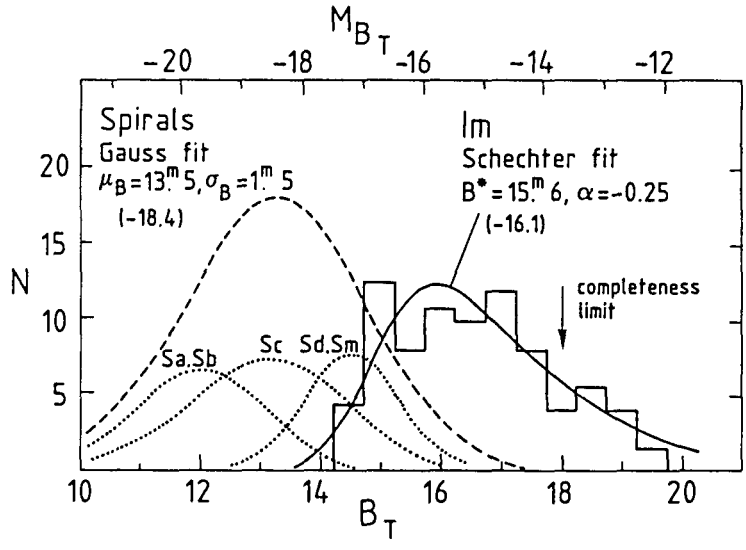


Fig.14 Combining data from Fig.13 with the $\varphi(M)$ for Im types of all luminosity classes, showing the data for essentially all currently star-producing galaxies in the standard Virgo Cluster sample (not included are the Blue Compact Dwarfs).

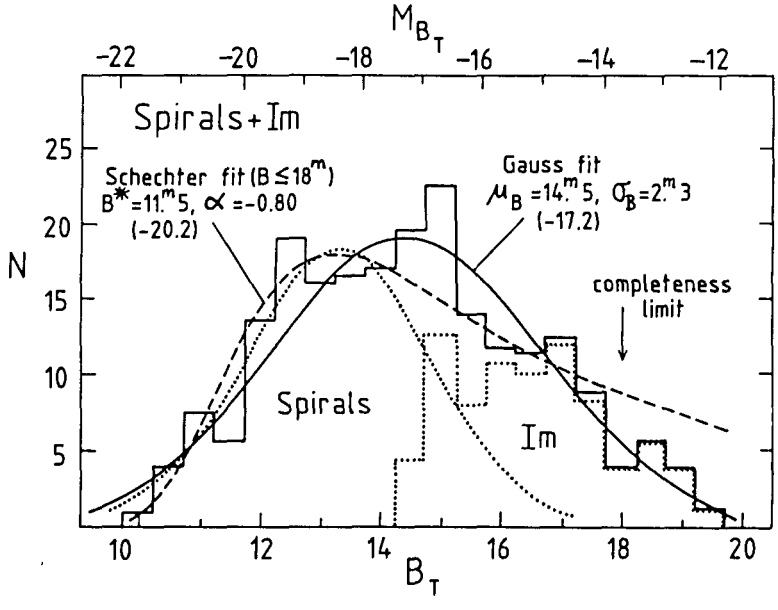


Fig.15 Data from Fig.14 combined into a single distribution.

in Figure 15 where the data in Figure 14 have been combined into a single distribution. The maximum is reached well above the completeness limit. Hence, unless one wishes a bimodal distribution, there is no question of the existence of a maximum. Stated another way: we know that we have missed some Im galaxies fainter than B = 18, and perhaps many. But we certainly have not missed them brighter than say B = 17, and because there are not enough galaxies of any spiral or Im type at B = 17 to shift the maximum to that faintness, we can be certain that a maximum exists, essentially as shown.

c) Calibration of the de Vaucouleurs Λ index

The progressive march of < M > faintward in Figure 12 from types ScI and later is monotonic. This is the essence of the discovery of the luminosity classification by van den Bergh for the Sc galaxies (1960a) and his extension to the later types of Sd, Sm etc. in his reclassification of Shapley-Ames galaxies (van den Bergh 1960b). De Vaucouleurs defined the Λ index which incorporates the van den Bergh discovery by adding the Hubble type (numerically quantized) to a similar numerical description of the luminosity class.

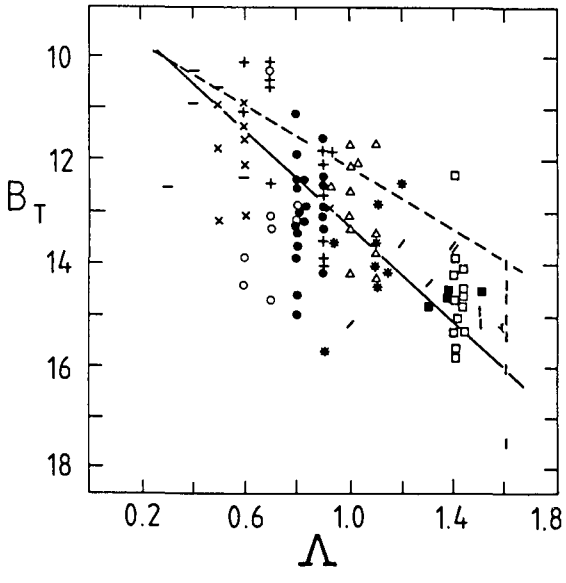


Fig.16

The de Vaucouleurs Λ index for galaxies in the distance-limited Virgo sample. The solid line is the impartial solution through the data. The dotted line is the calibration of de Vaucouleurs (1979).

We have followed the de Vaucouleurs prescription (except we apply no correction to the estimates of luminosity class for inclination) for all galaxies in the sample, with the result shown in Fig.16. The different symbols denote the different galaxy types and classes. As expected from Fig.12 and from the formulation by de Vaucouleurs (1979) and restricting the data to types Sb and later, there is a strong correlation. The correlation coefficient is 0.71 which is highly significant. However, the scatter in Fig.16 is larger than in the calibration by de Vaucouleurs (1979), and our mean line, drawn as solid differs from his, shown as dotted, both in slope and in zero point read at the mid Λ range. Our dispersion, read at constant Λ, is $\varphi(M) = 1.0$ mag, compared with de Vaucouleurs calibration of $\sigma(M) = 0.64$. Figure 16 is similar to an earlier comparison (Tammann and Sandage 1983) which used much fewer data.

The consequences of the different mean lines in Figure 16 and of the large dispersion, which invites a large Malmquist bias in the linearity of a distance scale that is based on the Λ index, is beyond the scope of this report.

d) Luminosity functions for the dE, dS0, E, and S0 galaxies

Figure 17 shows the data for dE alone, and for dE and dS0 galaxies combined, fitted to a Schechter function, which we see later is an upperward exponential of the form $\log \varphi(M) \sim 0.1\ M$ at the faint end. A correction for incompleteness, based on an argument using a surface brightness limit of $\sim$ 25.3 mag (arc sec)$^{-2}$ and the intrinsic dispersion shown in Fig.3, is given as dotted distribution. Such a correction is clearly necessary, and if we have made it properly, the differential luminosity function for dE's is still increasing at $M_{BT} = -12$ in approximately the way suggested by Zwicky.

Also shown in Fig.17 is the fraction of the dE galaxies in our sample that have unresolved central nuclei. Recall that there is no indication of resolution of these nuclei (cf.Paper I) at the 1 arc sec level (corresponding to 100 pc at the Virgo distance of 20 Mpc) and one of the crucial problems for Space Telescope is to

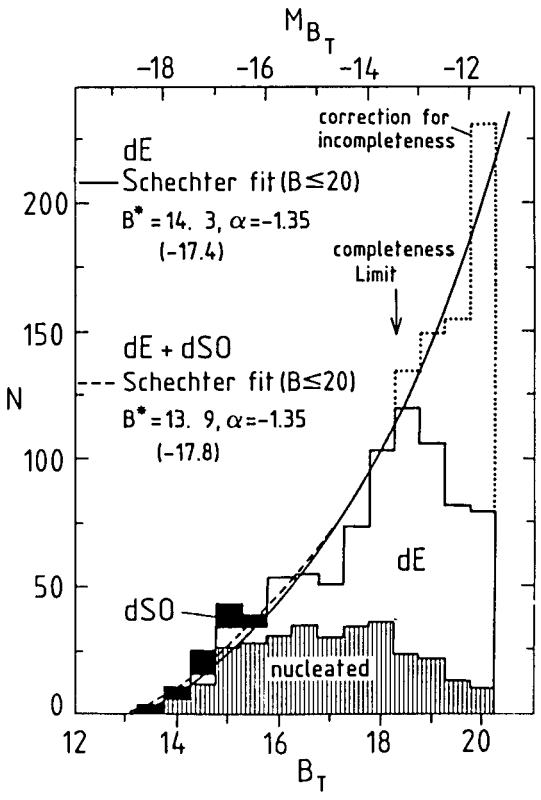


Fig.17

The luminosity function for dE and dS0 galaxies in the standard sample. The fraction of nucleated dE's is shown as the stripped area.

determine the nature of the stars in these nuclei. Figure 17 shows that the percentage of nucleated to non-nucleated dwarfs decreases toward fainter galaxies, but it never approaches zero at our limit of M_{B_I} = -12 for those dE's actually detected near B_T ~20 mag. The change of percentage of the dE,N to the dE types is shown more directly in Fig.18. All of the dwarf ellipticals at

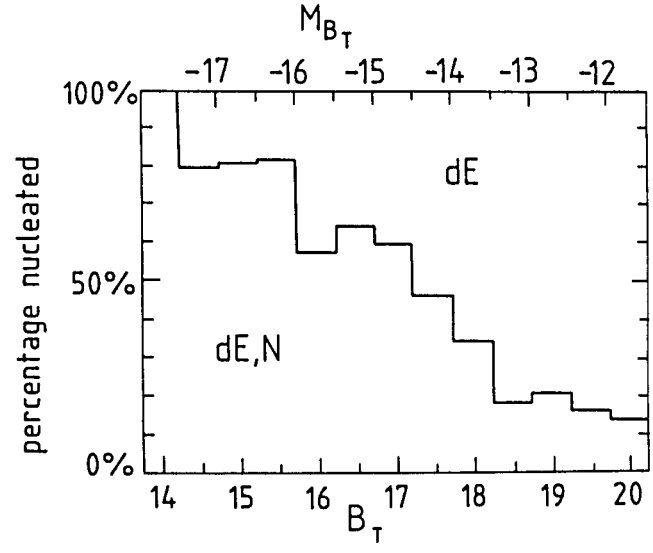


Fig.18

The percentage of nucleated dwarf ellipticals as a function of magnitude.

the brightest magnitude of B = 14 (M = -18) have unresolved nuclei, while only ~15 % of the galaxies at M_{BT} ~-12 are nucleated.

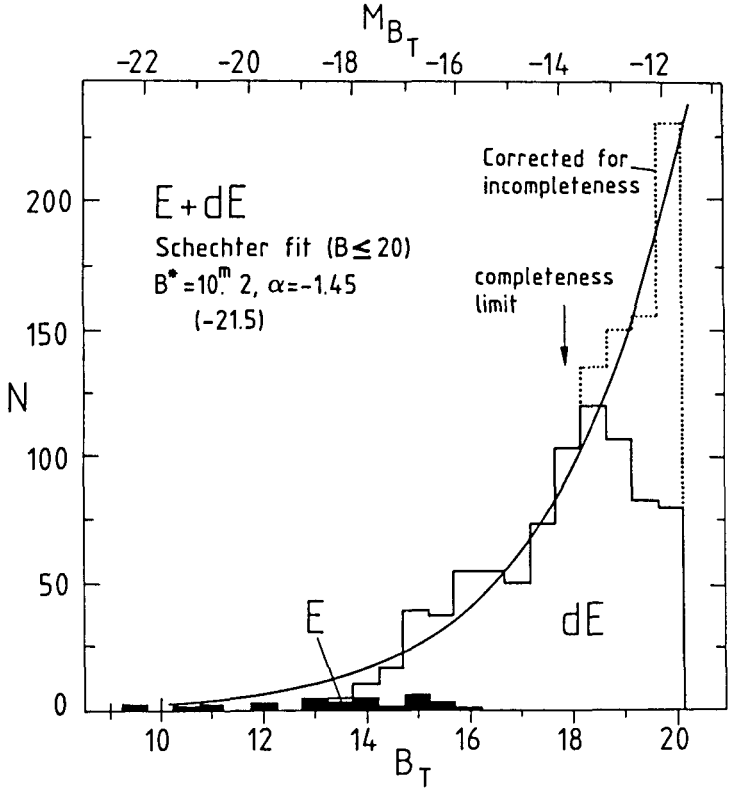


Fig.19 Luminosity functions for E and dE galaxies. Same as Fig.7 except not on a log scale for the ordinate.

Figure 19 shows the combined luminosity function of E and dE types. This is the same diagram as Fig.7 but not in the log presentation. As in Fig.7, a Schechter fit is made, and although it is not as evident here as in Fig.7, the fit is entirely unacceptable judged from a chi square test. The most interesting conclusion is that the $\varphi(M)$ for E galaxies has a maximum, while the dE's do not. The same is true for S0 galaxies themselves, but it is not known yet what the true $\varphi(M)$ is for dS0 because of difficulties in the classification at faint levels of dE compared to dS0. The presence of a maximum in the $\varphi(M)$ for spirals, for E and for S0's is summarized in Fig.20.

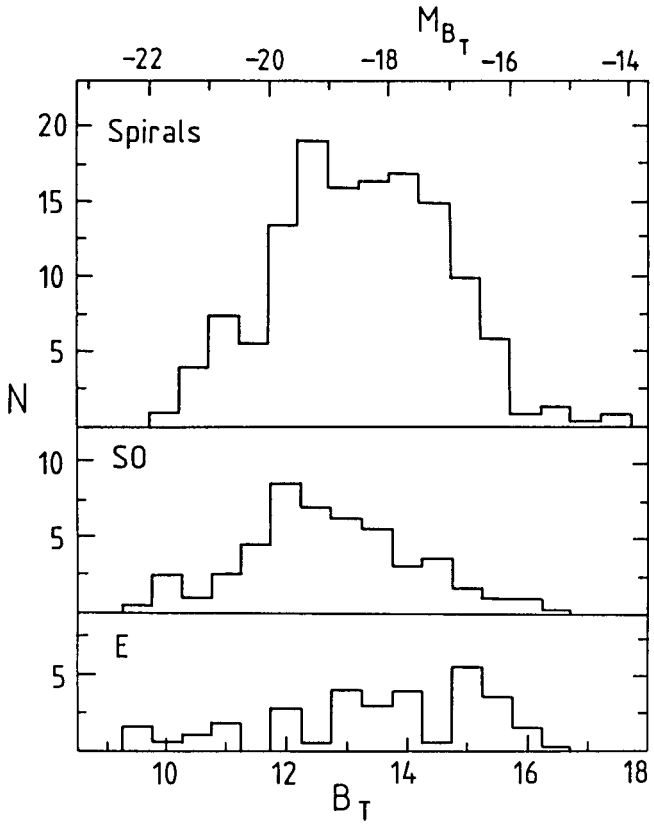


Fig.20

Demonstration that φ(M) for S0 and E galaxies also have a maximum similar to that of spirals.

The meaning of the overlap in the φ(M) functions for E and dE galaxies near $M_{B_T} \sim -18$ was commented on in section III where such a depletion of parent E systems that disperse to populate the dwarf sequence with bound fragments is expected on the formation picture of Gerola et al. (1983), and although our data suggest that such a depletion does, in fact, exist, we leave the question open if this supports the Gerola et al. picture.

e) The total luminosity function for all types combined

The sum total of all the data is shown in Figs.21 and 22, which are the same data, except that Fig.22 is on a log scale. A Schechter function that fits the data well has $\alpha = -1.25$ (in his notation) which at the faint end corresponds to an exponential of about 0.1 as shown in Fig.22. The Zwicky function with 0.2 slope is also shown, as is the divergent condition of 0.4 for infinite luminosity (if φ(M) is foolishly integrated over all luminosities down to zero). Our function does not increase as rapidly as either of the latter, but nevertheless, it has no maximum.

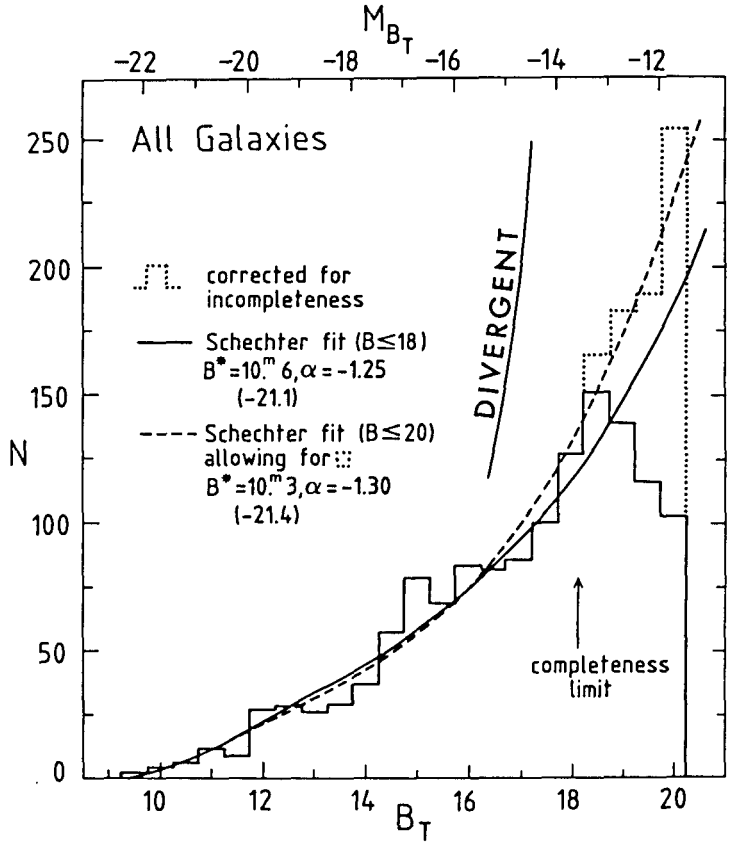


Fig.21 The total luminosity function for the standard sample.

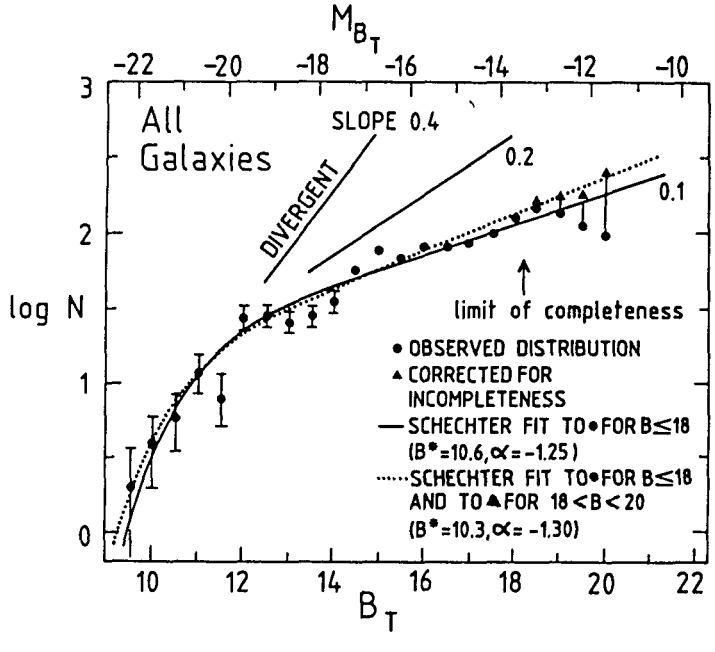


Fig.22 Same as Fig.21 in a log presentation.

VI. THE PROJECTED SPATIAL AND VELOCITY DISTRIBUTIONS

We now come to the problem mentioned in the Introduction as the motivating theme of the work: the presence or absence of two concentrations over the face of the cluster, one near M87, and the other near NGC 4472. And if two concentrations exist, what is their velocity structure? Also of interest is the difference in the distribution of Hubble types over the area, and a comparison of velocities as a function of type and position.

We have looked at the data only in a most preliminary way so as to locate the major trends. With Tarenghi we shall eventually make the correlation analysis to search for any associations of one galaxy type with any other, both in the projected spatial coordinates and in velocity space to answer, for example, if the dE galaxies are associated with the giant E's, or spirals, etc. But in the subsections that follow for this final topic, we present only the obvious correlations, primarily through diagrams, with little commentary. We also consider only those galaxies classed as "members". This excludes the "Southern extension" but not entirely the "W" and "M" cloud regions (cf.Fig.2) where, consequently, true members may be slightly underrepresented in the "member" sample.

a) The projected distributions of various morphological types

Figure 23 shows the distribution of the entire 1267 member sample. The isopleths on the right in this and the following diagrams are constructed from counts in cells of size 0.5°, smoothed by averaging over 9 neighbouring cells. The isopleths in Fig.23 illustrate four points. (1) There is a strong concentration of galaxies in region A near M87. (2) A weaker concentration occurs in region B near M49 (= NGC 4472). Indeed then, as mentioned in the Introduction, there <u>are</u> two major concentrations. (3) Neither M87 nor M 49 lie in the centers of regions A or B. (4) Region A has an elongated outer isopleth defining a major axis of position angle $\sim 48^{\circ}$. Experimentation

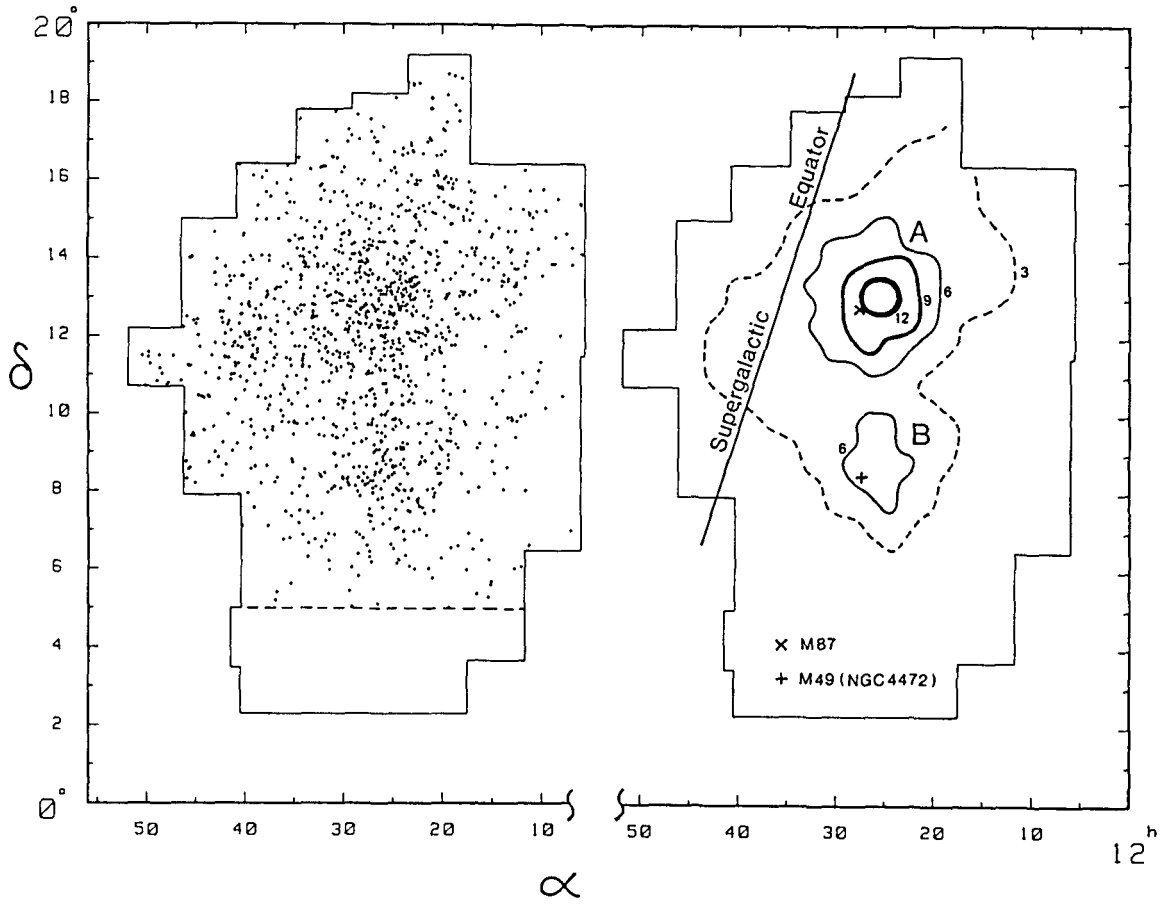


Fig.23 The projected distribution of the 1267 certain members of all morphological types (left). The isopleths on the right were made with a cell size of $0^{\circ}.5 \times 0^{\circ}.5$. The positions of M87 and of M49 (=NGC 4472) are marked.

with various cell sizes showed that the conclusions are quite insensitive to changes of the size. This is a general result throughout this section.

Figure 24 is the same as 23 but the isopleths are now luminosity-weighted. Interestingly, the very bright galaxies M87 and M49 are still not lying in the luminosity centers of region A nor region B. The conclusions from Figure 23 are confirmed, but now region B is more pronounced and the NW-SE extension of region A apprears to be turned toward M59 (= NGC 4621).

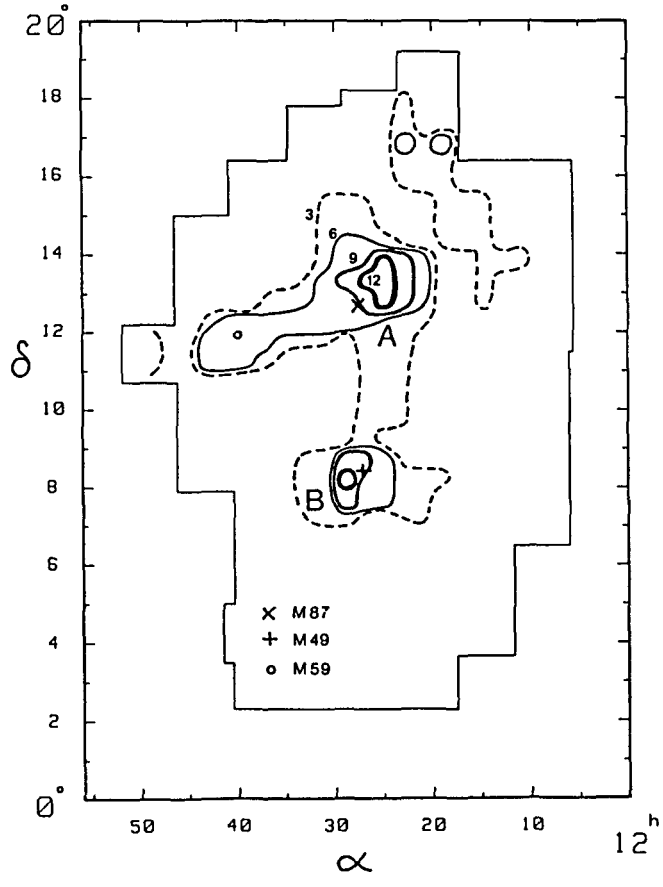


Fig.24 Same as Fig.23 but now with luminosity-weighted isopleths, labeled in units of 10^{10} $L_{\odot}$ per deg^2. The position of M59 (= NGC 4621) is added.

Figure 25 is similar to the preceeding two, but now shows the distribution of only E and S0 galaxies. The number of galaxies is so small that the isopleths have high noise; nevertheless, region A is defined with fair accuracy, region B is visible in the same place as in Figure 23, and a region C around M59 is suggested. As before, the brightest galaxies are not in the center. The luminosity-weighted isopleths in Figure 26 show the same features but now, of course, the bright galaxies dominate the structure.

The distribution of the complete sample of dE galaxies is in Figure 27, which is the most revealing of the diagrams. The region near M87 is quite dominant, whereas region B is relatively

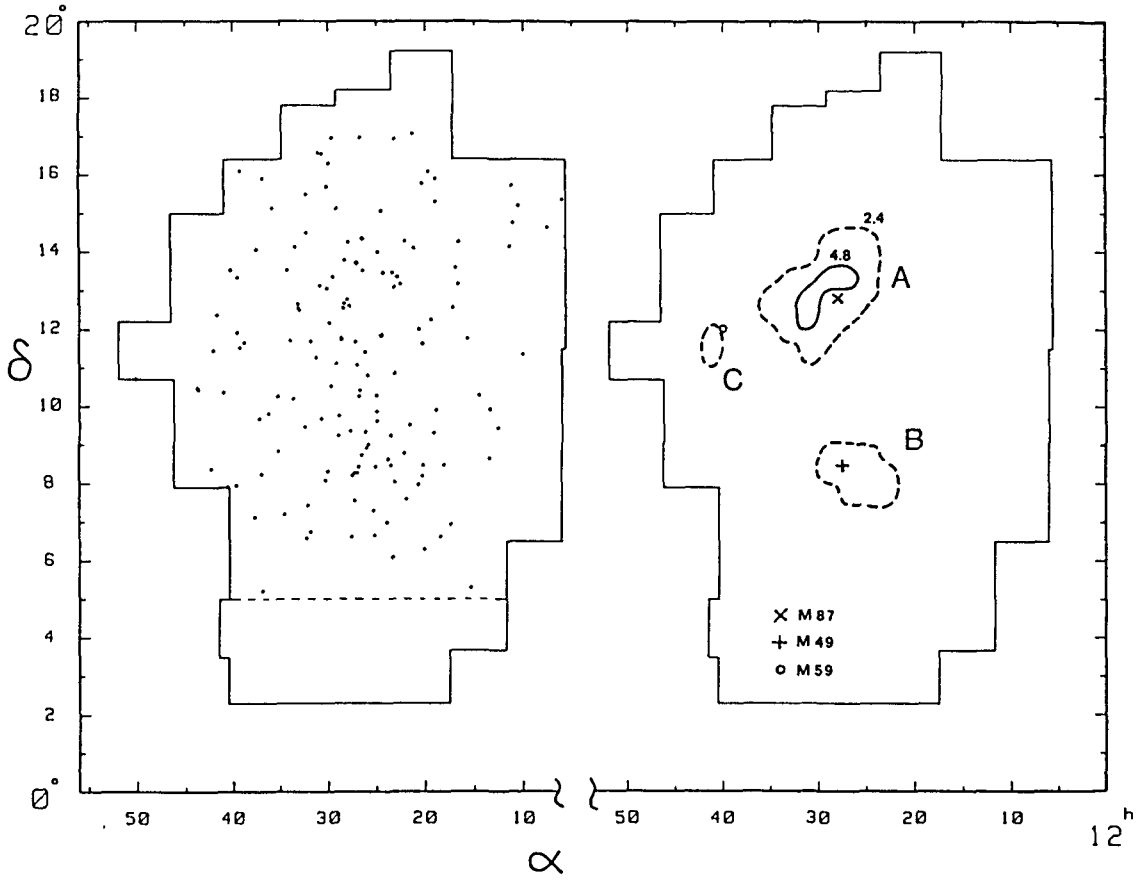


Fig.25 The distribution of the 147 E + S0 galaxies with corresponding isopleths on the right, labeled in units of galaxies per deg^2.

weak, but clearly visible by an isophoth extending from A toward B. The strip counts, to be shown later as Figure 31, suggest indeed a smaller concentration of dE's in region B than in A, while the ratio of spirals to early-type galaxies is significantly higher in B than in A. The impression from Figure 27 is that the Virgo cluster itself is defined by region A, and then, as we shall see, primarily by the dE types.

The distribution of the 128 spiral members is given in Fig.28. By spirals here is meant the true spirals plus the Im's. The isopleths now show a much wider distribution. Region A is displaced $\sim 0.5^{\circ}$ westward from its position in the previous diagrams, while region B is quite pronounced and in its previous

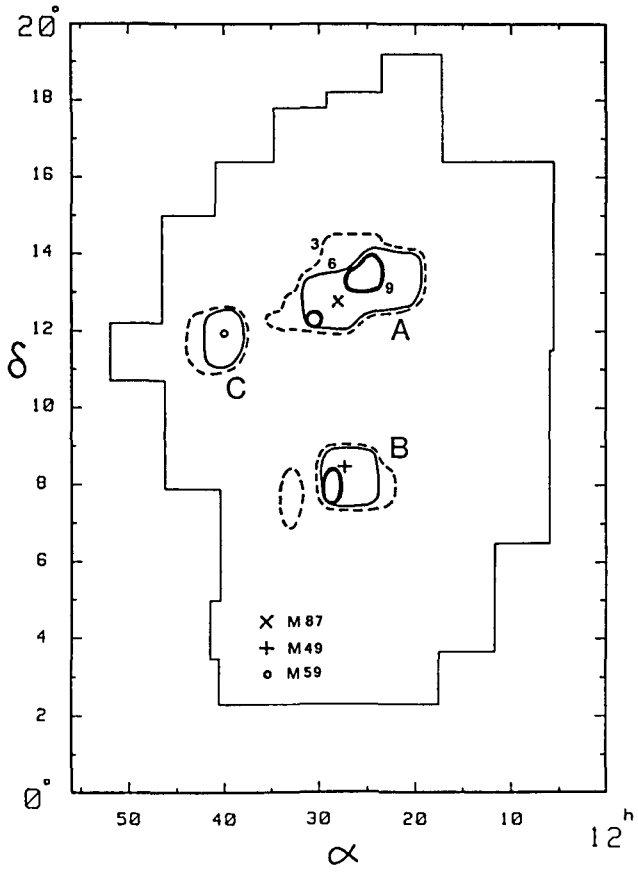


Fig.26 Same as Fig.25 with luminosity-weighted isopleths, labeled in units of 10^{10} $L_{\odot}/deg^2$.

place. Region C is also weakly seen. The fact that also the spirals reflect the concentrations which are primarily defined by the early-type galaxies makes it probable that their distribution centers coincide in space and that they have identical mean distances from the observer.

A most easily readable summary of the difference in the distribution of types in the various regions is found by a study of the counts in two strips, one running north-south and the other east-west.

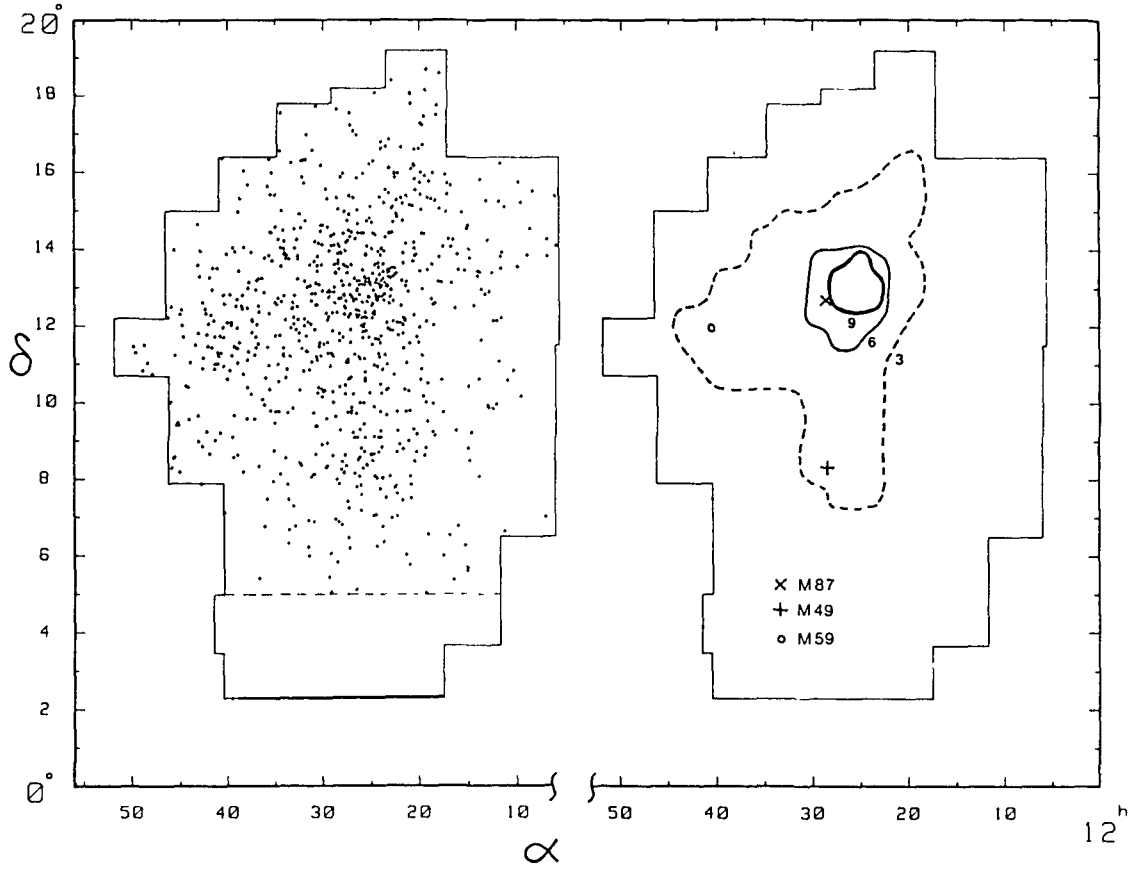


Fig.27 The distribution and isopleths for the complete sample of 828 dE members. Isopleths are labeled in units of galaxies per $0^{\circ}.5 \times 0^{\circ}.5$.

b) Information from strip counts

The geometry of how we counted is shown in Figure 29, and the results are given in Figures 30 and 31. Very much information is contained in these latter two diagrams. In Figure 30 the cluster is certainly seen, as dominated by region A. Region C near 12^h38^m may be weakly visible (hardly above the noise) in the dE's, but seen more definitely at $\sim 0.5^{\circ}$ lower declination in Figure 27. Note especially the more widely spread spiral distribution as compared with the dE's and the E + S0: not a new result, to be sure, but shown well in the strip-counts.

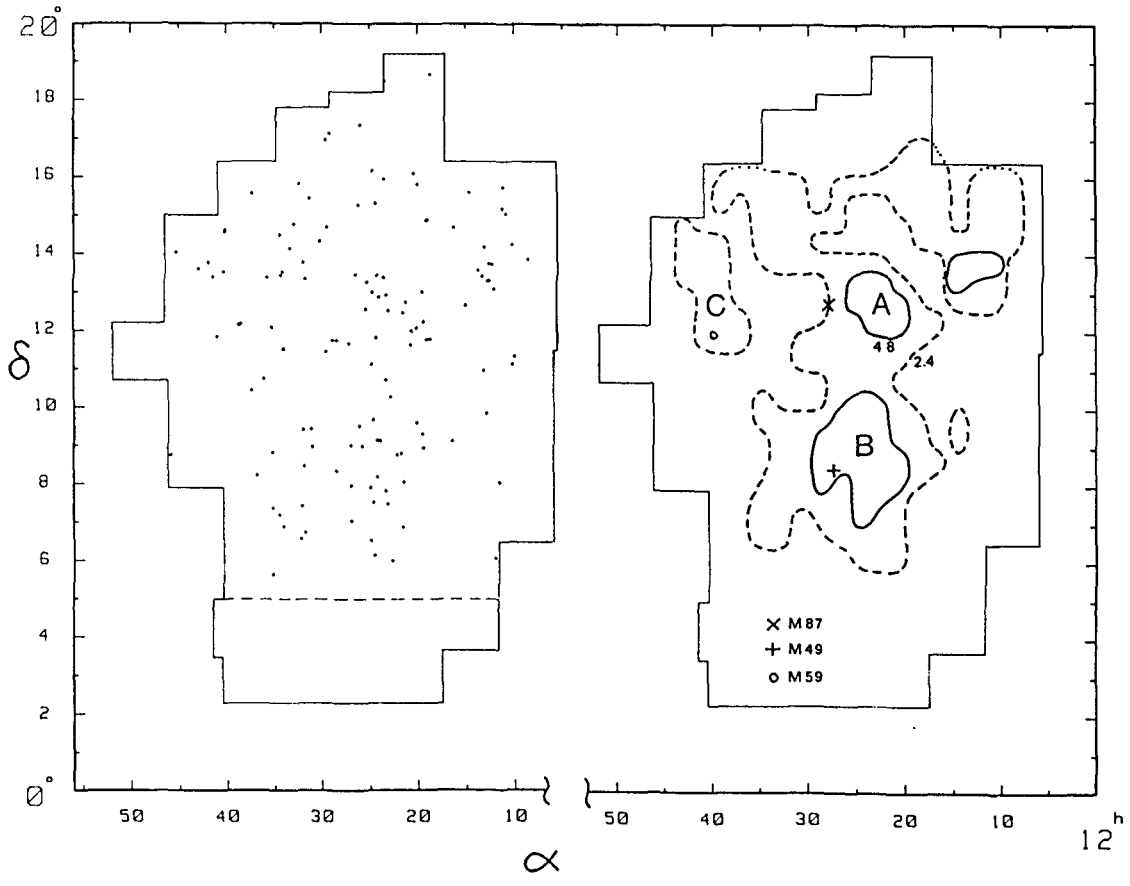


Fig.28 The distribution and isopleths for the spirals plus Im's. Isopleths are labeled in units of galaxies per deg^2.

The N-S cut in Figure 31 goes almost centrally through regions A and regions B. Here it is clear that the ratio of spirals to E's is very much higher in region B than in A. Note also that the ratio of dE's to E + S0's is not the same in region A as in B, a militating fact against the idea that dE's are born from E's.

The luminosity-weighted N-S strip count is shown in Figure 32, which reflects the obvious feature that the light is dominated by M87 and M49, with the rest of the information essentially burried in the noise.

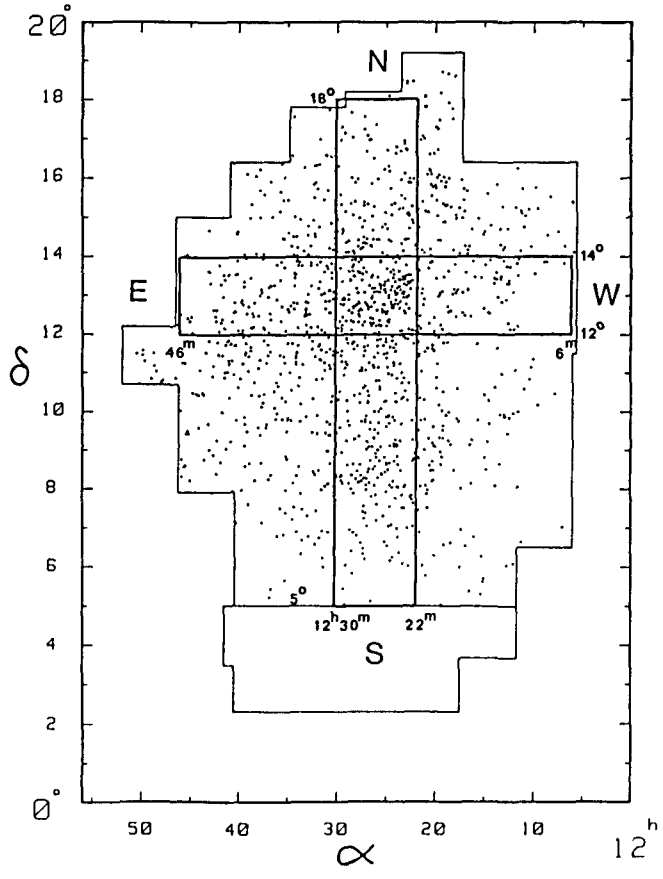


Fig.29

Position of the cuts for the strip counts shown in the following figures.

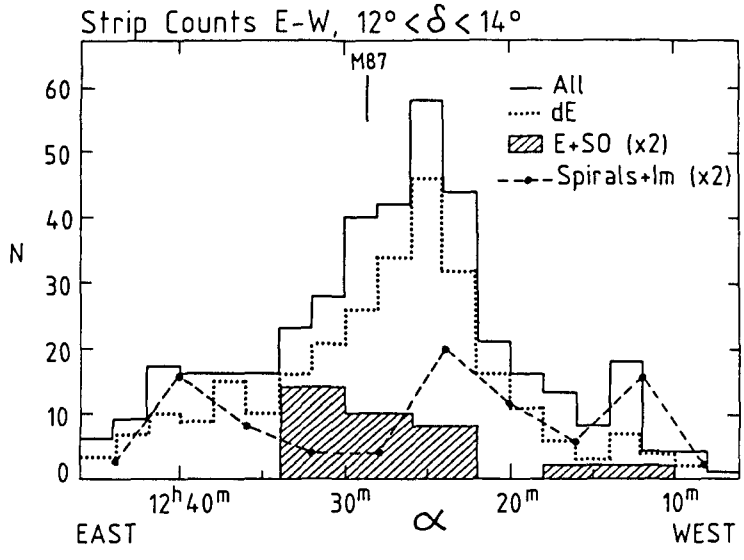


Fig.30 Distribution of the various galaxy types in the E-W strip between declination of 12° and 14°.

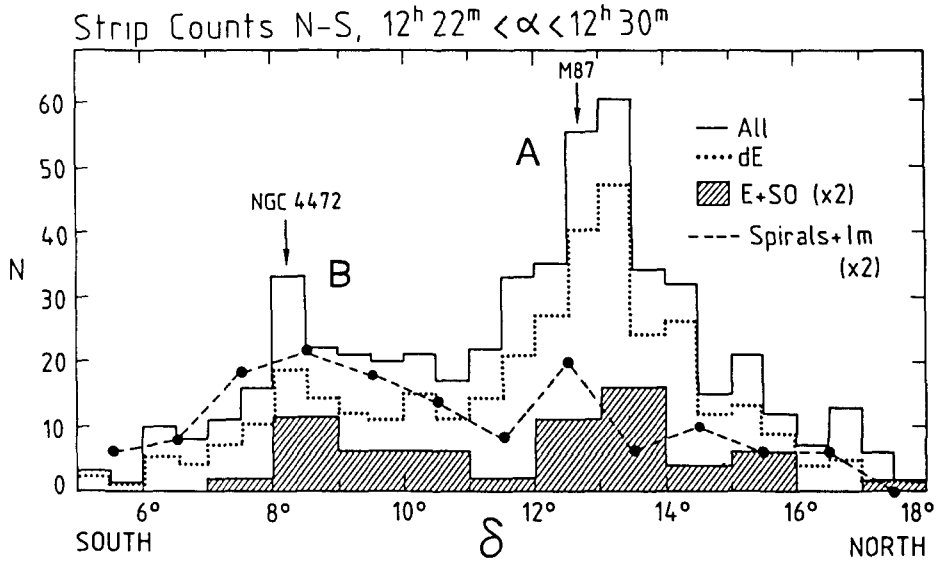


Fig.31 Distribution of various galaxy types in the N-S strip between RA 12^h22^m and 12^h30^m.

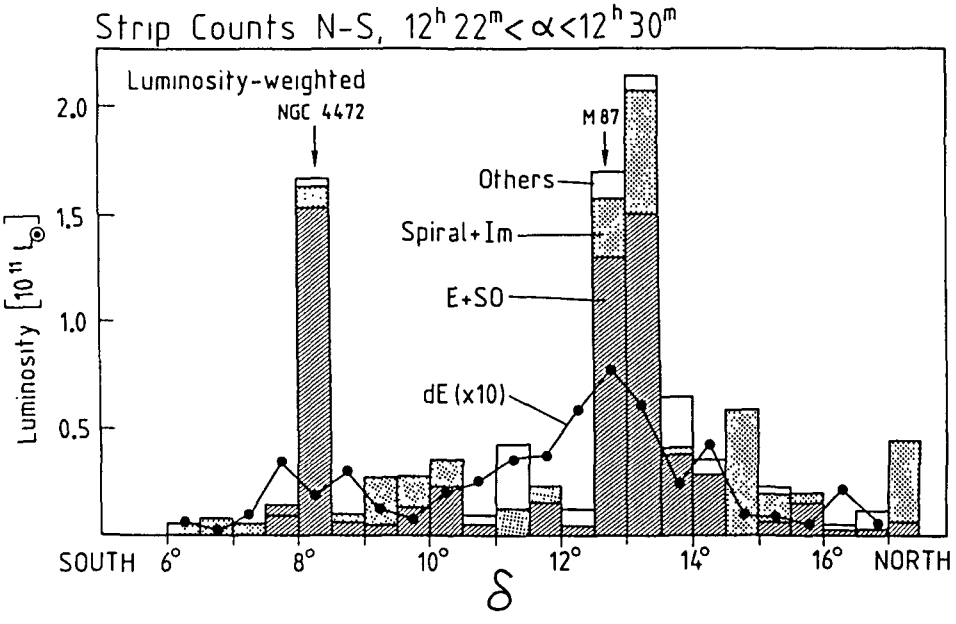


Fig.32 The luminosity-weighted N-S strip counts.

To show more clearly the variation of the population mixture of morphological types across the area, Figure 33 gives lines of equal population mixture, luminosity-weighted. The principal conclusions from this representation are (1) The NW-SE extension through region A is still recognizable, (2) regions A and C both have 60 ± 10 % of all light in the early type galaxies, and in this sense are spiral-poor. Region B has more light than region A in the spirals, about equally divided between spirals and elliptical-like galaxies. (3) There are regions of the sample area where the member galaxies that are E-like contribute only 30 % of the light.

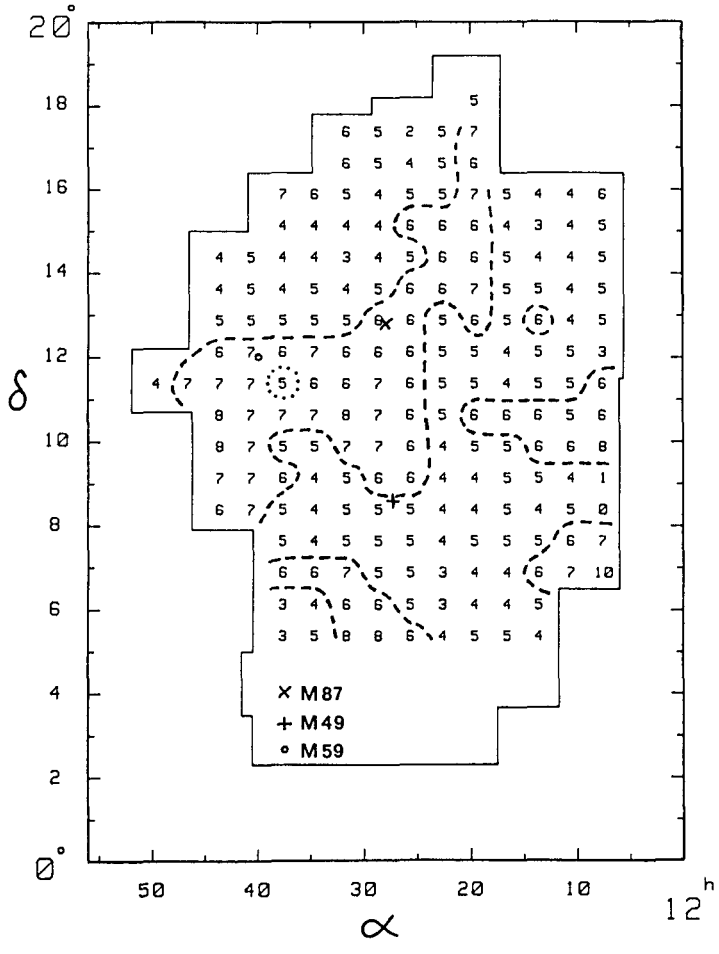


Fig.33 Lines of equal population mixture by luminosity. The members are the luminosity-weighted ratio of the E + S0 + dE + dS0 population to the total times 10.

The main conclusion from Figures 23-33, aside from those directly stated, is that M87 is not in the cluster center but is displaced by ~ 1 degree from the luminosity center of region A. M49 is likewise displaced from the center of region B, but with less significance. The detailed numbers are given in Table 2.

Table 2 Peak positions of clusters A and B compared to the position of M87 and M49.

	A		B	
	α	δ	α	δ
Number density (all)	$12^h25.9^m \pm 0.7^m$	$13^\circ00' \pm 6'$	$12^h25.8^m \pm 1.0^m$	$8^\circ51' \pm 10'$
Luminosity density (all)	12 25.3 ±0.7	13 18 ±8	12 29.0 ±0.7	8 15 ±6
dE + dS0	12 25.2 ±0.9	13 07 ±10		
M87/M49	12 28.3	12 40	12 27.2	8 17

c) Radial density profile fitted to an exponential

The spatial radial density profile over the whole Virgo complex, determined by Yahil, Sandage, and Tammann (1980), was a power law, and so then must the projected density distribution be. We eventually shall analyze the present data of the inner cluster region more completely, but we could not persuade the organizers of this workshop two days before September 4 to postpone for a week, hence the first analysis shown here is made simply with an exponential.

Figure 34 shows the radial density distribution separately for the total sample, and for the dE's, the E + S0's, and the spirals + Im's. Exponential fits through all four samples are shown. Note that since most of the sample is composed of dE's, the top two distributions have, by necessity, nearly the same scale length. Note also these first two distributions are not well fit by an exponential within the first 1° radius; a not unexpected result because we expect a projected power law instead.

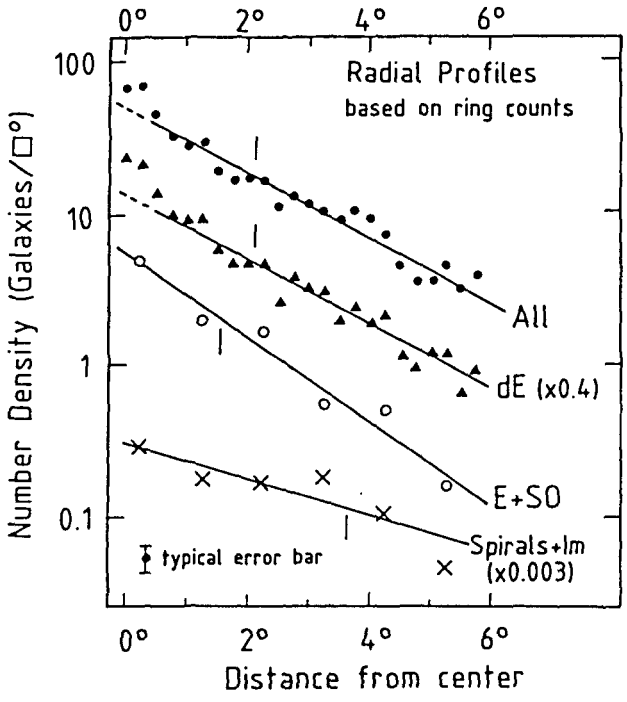


Fig.34 Radial distribution of different morphological types from ring counts based on a center position of RA 12^h 25^m and Dec 13°. Each distribution is fitted to an exponential with a scale-length marked by a tick.

The dE's (outside the inner 1° circle) are less concentrated to the center than the E + S0's, and this may be the long sought after segregation, often claimed, and as often denied; we await a more thorough analysis of our own data. But what is clear is that the spirals + Im's are definitely more widely spread than the E + S0's, again not a new result but we note in passing that the Im's are certainly more widely spread than the dE's (compare Fig.9 of Section IV), and therefore it is not so simple a proposition that dE's come by evolutionary processes from the Im's.

Figure 35 is the same as Figure 34, but now luminosity-weighted. The much shallower fall-off for all galaxy types, except dE's (where the luminosity weighting is not expected to make a difference anyway), shows that the outer galaxies are brighter than the inner on the average!

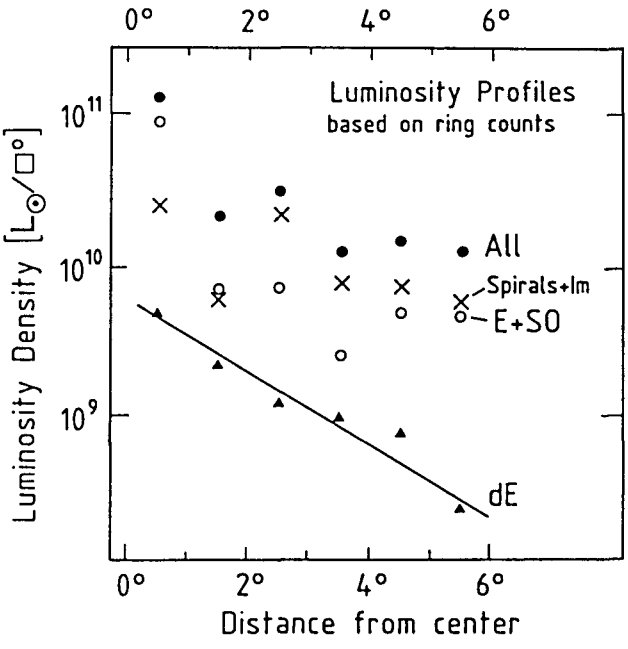


Fig.35 Same as Fig.34 but luminosity-weighted. The flatter distribution for the non-dE types suggest that the outside galaxies of each type are brighter than those near the center.

d) Velocity distributions

Now comes perhaps the most frightening information of all, leading one to doubt that the hypotheticial Virgo Cluster concept we have held so far, of a rather simple entity in space, called the cluster core, might describe reality.

Figure 36 shows the heliocentric velocity distribution as a function of type, averaged over the complete sample area. The conclusions from these data are: (1) The mean velocity of the E + S0's agree very well with that for the spirals + Im's. (2) The dE + dS0's have a higher mean redshift by 2.3 σ than the other distributions. (3) M87 itself has 160 $\pm$ 40 km s^{-1} higher velocity than the mean of the entire sample which is $< v > = 1094 \pm 37$ km s^{-1}. (4) The velocity of M87 agrees well with the high value of $< v > = 1237$ km s^{-1} for the dE + dS0's alone (by coincidence ?).

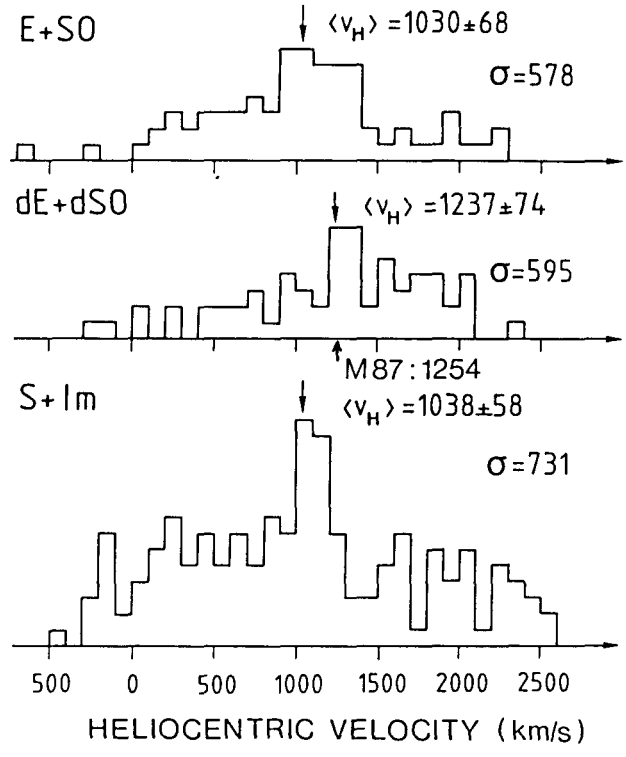


Fig.36 Velocity distribution for the entire sample broken up into three morphological groups.

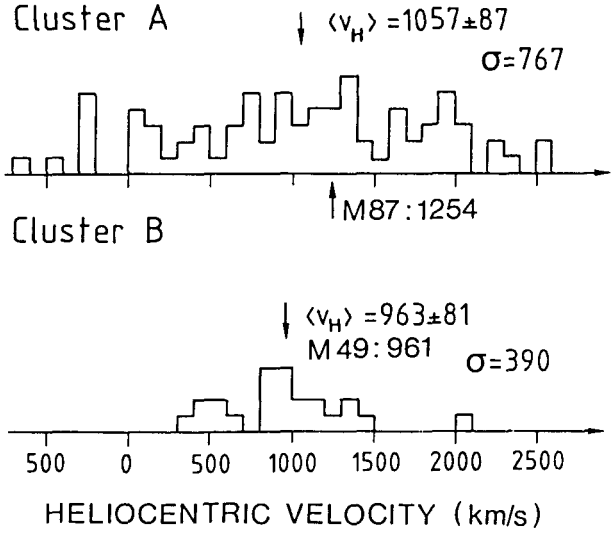


Fig.37 Velocity distribution for all galaxy types within regions A and B. The regions are defined by the two envelopes labeled "6" in Fig.23 (right).

(5) The spirals have, as known before, a very wide distribution whose sigma is 731 km s^{-1}.

Figure 37 shows the velocity distribution of all the galaxies within the A and B regions, where all galaxy types are averaged. The three points to note are: (1) the very wide distribution within region A as if we see a number of subunits that should not be averaged together. (2) The narrow distribution (σ = 390 km s^{-1} only) in region B, suggesting that a real dynamical unit is encountered here, and (3) the difference in mean velocity between region A and B of 94 $\pm$ 120 km s^{-1} which is not significant. Recall that a search for a difference was one of the motivations of this work. A summary of the velocity mean values is in Table 3.

Table 3 Velocity means.

Sample	$\langle v_H \rangle$	σ	n	$\langle v_o \rangle$
All members	1094 ± 37	673	324	976
E+S0	1030 ± 68	578	72	912
dE+dS0	1237 ± 74	595	64	1119
E+S0+dE+dS0	1141 ± 50	585	136	1023
Spirals+Im	1038 ± 58	731	159	920
Region A*	1057 ± 87	767	73	939
Region B*	963 ± 81	390	23	845

$\langle v_H \rangle$ = mean heliocentric velocity in km s^{-1}
σ = mean standard deviation in km s^{-1}
n = number of galaxies
$\langle v_o \rangle$ = mean velocity corrected to the centroid of the Local Group (Yahil et al. 1977) in km/s
* as defined by the isopleths labeled '6' in Fig. 23

e) Velocity dispersions and systematic trends

Shown in Figure 38 is a map of the local velocity dispersions in 1° x 1° cells of the sample-area. Here, as in Figure 39, the values are smoothed by gliding means over 9 cells. Such a map might be said to measure the local temperature. The three points to note in this diagram are: (1) there are three hot spots ($\sigma \sim$ 600 km s^{-1})aligned essentially again NW-SE, (2) there are some quite cold regions with $\sigma \sim$ 300 to 400 km s^{-1}, (3) nowhere is σ (local) as large as the all-sample mean of σ = 673! This is our

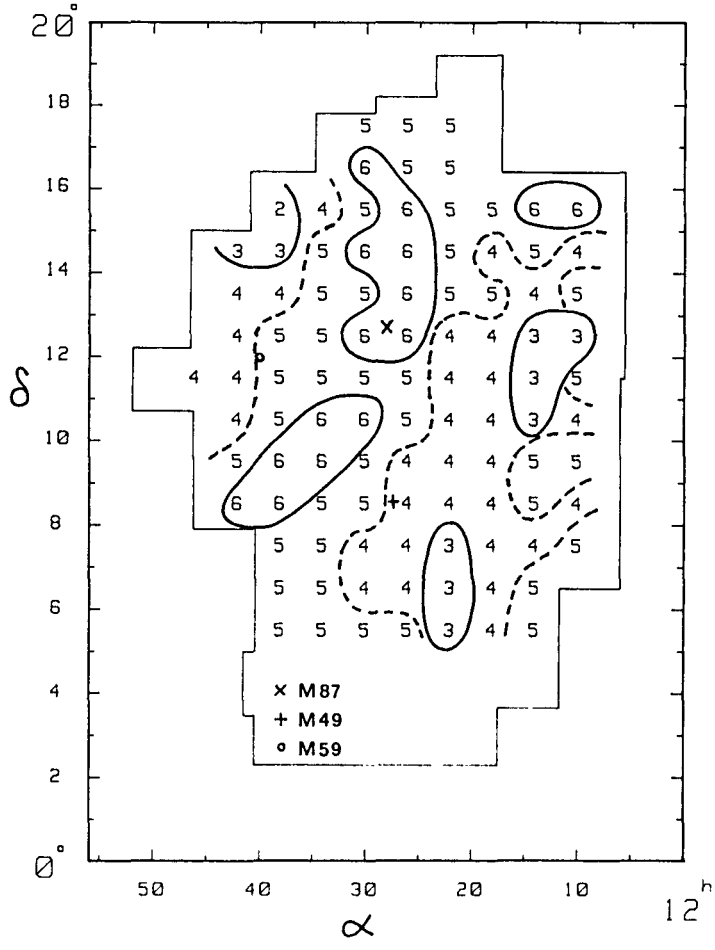


Fig.38 A map of the local velocity dispersion ("local temperature"). The numbers give the mean $\sigma = (v - \langle V \rangle)^2$ > 100 km s^{-1} in 1° square cells, smoothed over 9 neighbouring cells.

most significant finding, also emphasized by Huchra, which again points directly to the non-simple velocity structure of the region. It is as if many small dynamical units co-exist within this region of the centrum. Point (3) shows that there must be systematic variations of $< v >$ with position over the area.

These are, in fact, shown in Figure 39 which gives the map of mean velocities within cells of 1° square. Note the systematic trend of the contours. There are extended regions with low mean values near $< v > \sim 800$ km s^{-1} and high values which exceed 1600 km s^{-1}. The two most extended regions that show the largest range (from 800 to 1800 km s^{-1}) define a "major axis" with position

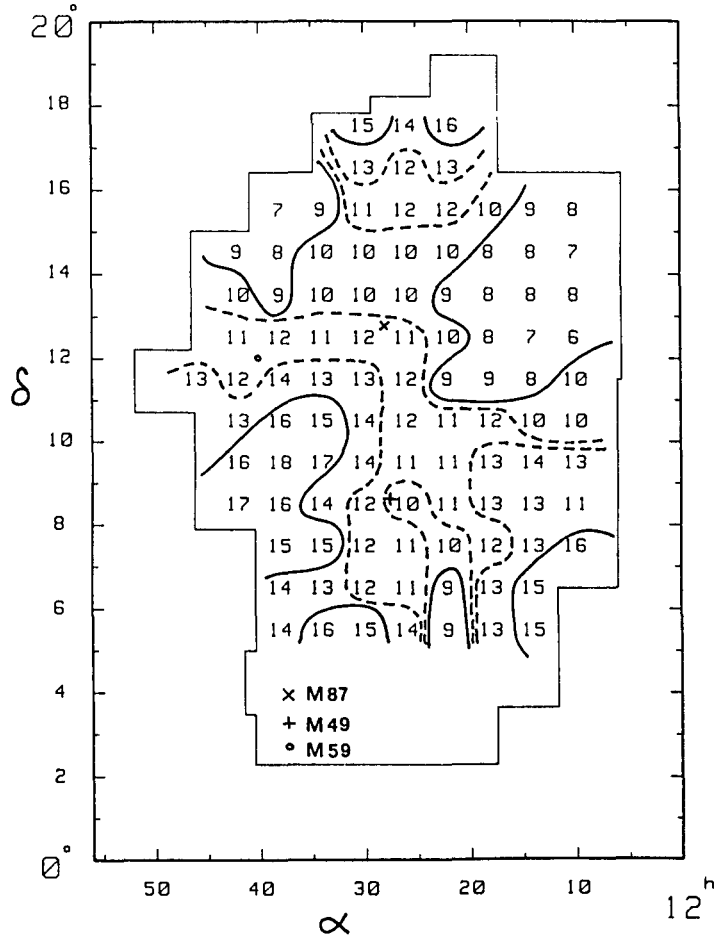


Fig.39 A map of the local mean velocity, $< v > / 100$ km s-1.

angle (north through east) of ~ 55°, passing 2° below M87. As an exercise (a joke ?) we have plotted the velocities within a 4° wide strip along this "major axis" as if the system defined a "rotation curve", with the result shown in Figure 40. And as if this were not enough, we show in Figure 41 the most bizzare distribution of all. Plotted are the positions of all galaxies in the sample with negative velocities. These surely are not uniformly distributed over the "sample-area of the Virgo cluster" as we have naively been assuming in the past pages. The velocity pattern can also be interpreted as different streams falling into the cluster center. Using 21cm-line width distances from data by Richter and Huchtmeier (1984) one could conclude that the high-velocity SE side is 20 % nearer, and that the low-velocity NW side is 10 % more distant than the cluster mean; the result, formally at the 2 sigma level, is, however, yet quite unconvincing. Figure 41 gives the most direct warning that the Virgo Cluster may not, after all, is not in fact, a single dynamical unit, but must be plagued by complex flow pattern.

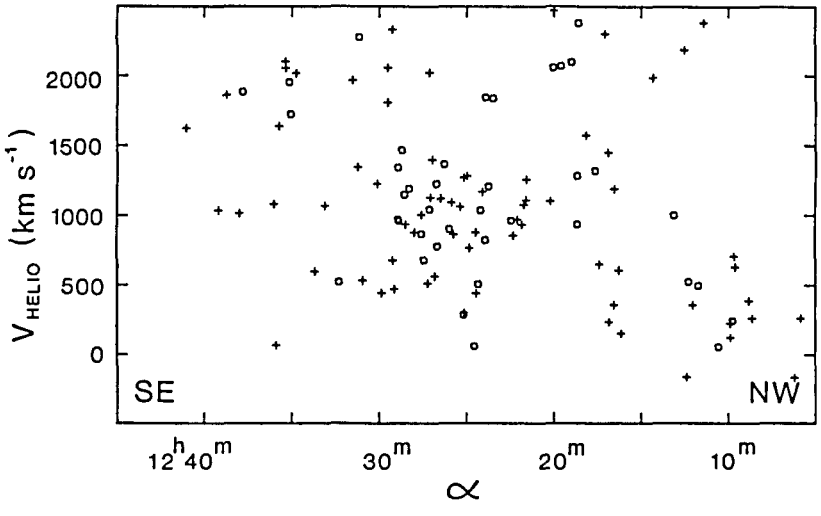


Fig.40 Radial velocities in a 4° wide strip along the "major axis" emerging in Fig.39 (position angle 55° ,passing 2° below M87) - as if to define a "rotation curve". The sample is broken up into E + S0 + dE + dS0 galaxies (open circles) and spirals + Im's (crosses).

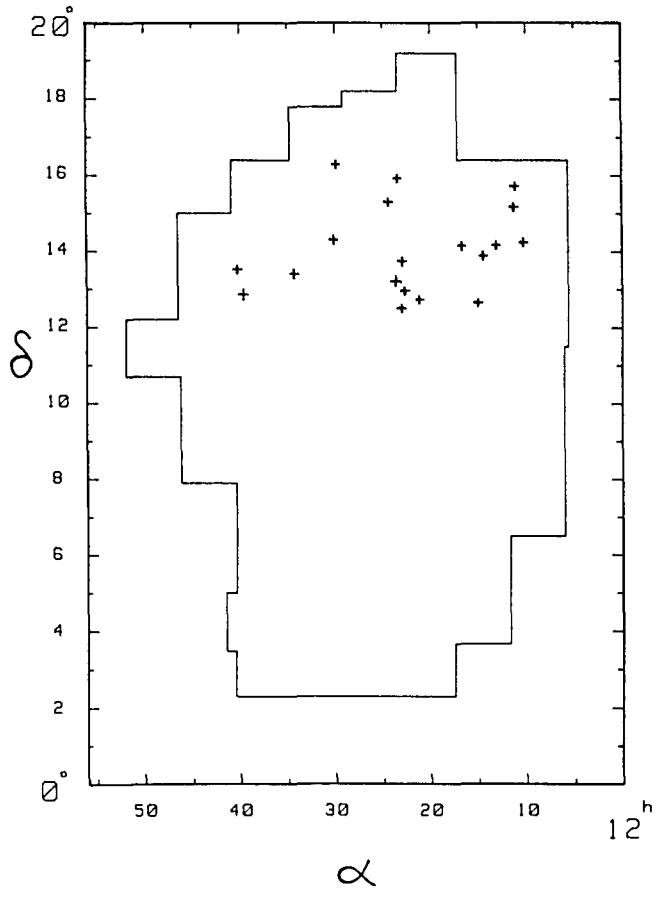


Fig.41 The distribution of all galaxies in the sample that have negative measured velocities.

As this is a workshop, and as the term means to one of us (A.S.) that we are permitted to be as wrong as we wish so as to stimulate ideas for the next round of research by others, we have written these pages as a relaxed progress report. It only remains to thank a number of people who have participated in the work over the past 6 years. First and foremost is Massimo Tarenghi who saved the project from the beginning by his expert work in the reduction of the traced plates, done by R.Shaw. The ESO picture processing lab made this crucial part of the work possible, and we are grateful to Director General Woltjer for making it happen. John Bedke of the Mount Wilson photolab helped at every stage of the photographic reproductions. We are especially indebted to John Huchra for making his velocity catalog available, even more so because he himself is deeply involved with this Virgo problem.

Finally, we wish to thank the Swiss National Science Foundation for support of part of this work, and, for the same reason, NASA in the United States for its support as part of preparation for the launch of Space Telescope.

References

Baade, W. 1944, Astrophys.J.100, 147.

Binggeli, B., Sandage, A., and Tarenghi, M. 1984, Astron.J.89, 64 (Paper I).

Boerngen, F., Karachentseva, V.E., Schmidt, R., Richter, G.M., and Thaenert, W. 1982, Astron.Nachr.303, 287.

Boerngen, F., Karachentseva, V.E., and Karachentsev, I.D. 1984, Astron.Nachr.305, 53.

De Vaucouleurs, G. 1979, Astrophys.J.227, 380.

De Vaucouleurs, G., and Pence, W.D. 1979, Astrophys.J.Suppl.40, 425.

Einasto, J., Kaasik, A., and Saar, E. 1974, Nature 250, 309.

Faber, S., and Lin, D.N.C. 1983, Astrophys.J.Lett.266, L17.

Felten,J.E. 1977, Astron.J.82, 861.

Freeman, K.C. 1970, Astrophys.J.160, 811.

Gerola, H., Carnevali, P., and Salpeter, E.E. 1983, Astrophys.J. Lett.268, L75.

Hubble, E. 1926, Astrophys.J.64, 321.

Hubble, E. 1934, Astrophys.J.79, 8.

Hubble, E. 1936, Astrophys.J.84, 158.

Hoffmann, L., Helon, G., and Salpeter, E.E. 1984, private comm.

Ichikawa, S., Wakamatsu, K., and Okamura, S. 1984, to be publ.

Karachentsev, I.E., and Karachentseva, V.E. 1982, Sov.Astron. Lett.8, 104.

Karachentseva, V.E., Schmidt, R., and Richter, G.M. 1984, Astron. Nachr.305, 59.

King, I.R. 1966, Astron.J.71, 64.

Kraan-Korteweg, R., Sandage, A., and Tammann, G.A. 1984, Astrophys.J.283, 24.

Reaves, G. 1983, Astrophys.J.Suppl.53, 375.

Richter, O.-G., and Huchtmeier, W.K. 1984, Astron.Astrophys.132, 253.

Sandage, A., and Tammann, G.A. 1981, A Revised Shapley-Ames Catalog of Bright Galaxies, Washington: Carnegie Institution of Washington.

Sandage, A., and Binggeli, B. 1984, Astron.J.89, 919 (Paper III).

Sandage, A., Binggeli, B., and Tammann, G.A. 1985, in preparation (Papers IV and V).

Silk, J., and Norman C. 1979, Astrophys.J.234, 86.

Tammann, G.A., Yahil, A., and Sandage, A. 1979, Astrophys.J.234, 775.

Tammann, G.A., and Sandage, A., 1983, in Highlights of Astronomy, ed.R.M.West, Reidel: Dordrecht, p.301.

Van den Bergh, S. 1960a, Astrophys.J.131, 21.

Van den Bergh, S. 1960b, Publ.David Dunlap Obs.II, No.6, 159.

Wirth, A., and Gallagher, J.S. 1984, Astrophys.J.282, 85.

Yahil, A., Tammann, G.A., and Sandage, A. 1977, Astrophys.J.217, 903.

Yahil, A., Sandage, A., and Tammann, G.A. 1980, Astrophys.J.242, 448.

Zasov, A.V., and Karachentseva, V.E. 1979, Pisma Astron.J.5, 259.

Zwicky, F. 1942, Phys.Rev.61, 489.

Zwicky, F. 1957, Morphological Astronomy, Berlin: Springer-Verlag, pp.220-228.

DISCUSSION

R. GIOVANELLI: If sweeping by tides is invoked to turn Im's into dE's, maybe one should not worry too much about differences in flattening. Theoreticians have ways of puffing up disks by means of encounters. These being relatively small systems, the mechanism that is invoked to strip the gas may be quite effective in changing the flattening.

O.E. GERHARD to R. GIOVANELLI: Tidal heating in cluster environments may be described by the impulse approximation, in which case velocity perturbations scale like $\propto r^2$ when averaged over a disk. Rather than thicken the disk of a small spiral by tidal encounters to give an ellipsoidal-like body, such collisions would affect and possibly strip its outer parts.

H. ZINNECKER: You pointed out that there may exist two different families of elliptical galaxies: the loose, low surface brightness family and the compact, high surface brightness family. The Gerola et al. theory of dwarf ellipticals explains the former to be the daughter products of a disintegrated parent galaxy. Which theory explains the latter? Tidal stripping (cf. M32)?

B. BINGGELI: Yes, possibly. Half of the 15 or so M32-type E's in the Virgo Cluster are indeed close companions of giants (like NGC 4486 B), but we have yet to quantify this. We have to wait for velocities to sort out background and members (which is impossible to do morphologically).

O.-G. RICHTER: Is there a continuity from gE and objects like M32 down to the globular clusters? (Are there only <u>two</u> sequences?)

B. BINGGELI: This seems possible, judged from photometric parameters. But the faintest compact E candidate we found is still several magnitudes brighter than the brightest globular cluster. So, one cannot really speak of a "continuity". The globulars would then constitute a third sequence.

J. HUCHRA: What did you do with the 20^{+} high velocity galaxies in the NW region!? Without their removal there is <u>no</u> evidence for "rotation".

G.A. TAMMANN: Our "rotation curve" in Fig. 40 contains indeed only a few galaxies with > 2000 km s^{-1} in the NW corner. Some others we may have left out (a priori!) as doubtful members on morphological grounds; in fact already Shapley and Ames in 1930 considered their Region B, which lies in the NW corner, as a background condensation. For some additional galaxies we may not have known yet your latest velocities. The addition of more member (!) galaxies with > 2000 km s^{-1} in the NW region would indeed disturb our "rotation curve". But the addition of any number of high velocity members in this region cannot restore a normal velocity distribution. The lack of intermediate-velocity members and the excess of low-velocity members already demonstrates the presence of at least some velocity streams.

C. KOTANYI: I think that, from the point of view of the gas dynamics, M87 is the centre of the Virgo cluster. So we have the interesting paradox that the centre of the <u>gas</u> dynamics may be different from the centre of the <u>mass</u> dynamics.

G.A. TAMMANN: We have only presented the evidence for the discrepant positions of the cluster centre(s) and of M87, and we wholeheartedly agree that this discrepancy needs eventually an explanation.

E. SHAYA: Escape velocity is twice virial velocity so the velocity dispersion in the centre of the cluster (Region A) cannot be simply eddy currents. Since it must in the large part represent mass, Region A would tidally disrupt Region B if they are both at the same distance.

G.A. TAMMANN: If Region A has only recently condensed and is not yet virialized, it may still exhibit the larger dispersion of the infall velocities and its more noticeable disruptive action on Region B may still lie in the future.

J. YOUNG: Could you, or someone else, please comment on the non-membership of NGC 4569 in the Virgo Cluster?

G.A. TAMMANN: There is no field galaxy known (outside the Local Group) with a negative corrected velocity in all of the sky with its ~ 40000 deg^2, but 20 deg^2 of the Virgo cluster center contain over two dozen of such galaxies. The latter, including NGC 4569, must therefore be physical members of the cluster and in fact populate the expected low-velocity tail of the cluster velocity distribution. The question remains whether NGC 4569 - as a rare exception - could have been expelled by the young cluster and whether it could lie now at only, say, half of the cluster distance. This would involve, however, an unknown physical process and require an almost exact alignment along the line of sight. For these reasons we find it more appealing to question the reliability of those distance indicators which suggest that NGC 4569 lies in the foreground than to believe that this galaxy is a rocket in the night aiming at us.

SEARCH FOR YOUNG STARS IN VIRGO DWARF ELLIPTICAL

L.Vigroux[1*], M. Lachieze Rey[1*], J.Souviron[1x] and J.P.Vader[2]

1 - Service d'Astrophysique, Centre d'Etudes Nucléaires Saclay, France

2 - Department of Astronomy, Yale University Box 6666, New Haven CTO6511 USA

* Visiting Astronomers at the Canada France Hawaii Telescope, operated by the National Council of Research, Canada, le Centre National de la Recherche Scientifique, France and the University of Hawaii, U.S.A.

Ongoing star formation is known to be present in a small number of dwarf ellipticals. Two of the Andromeda satellites, NGC 185 and 205, are the prototypes of these galaxies. At least 2 more nearby galaxies of this type are known : NGC 4627 and NGC 1531 (Caldwell, 1983). These 2 galaxies have a bright blue nucleus and their spectra exhibit strong Balmer absorption lines which are the signature of young stars. Are these young stars a common feature of all dwarf ellipticals, or are they due to some external causes? These four galaxies are companions of large spiral, but a link between interaction with the large galaxy and ongoing star formation in the companion is still a fair game for theoreticians. Moreover, the star formation in these dwarf galaxies does not seem to be a general behaviour, even for companions of spiral; e.g. NGC 147, close to NGC 185, does not have any young stars.

A better understanding of this phenomena can only be achieved by the observation of a larger sample of galaxies.

Several approaches can be thought off to look for star formation. The best one would be to obtain long slit spectra to derive both metallicity and ages from metallic and Balmer absorption line strengths. Unfortunately these galaxies have a very low surface brightness and even with largest telescopes, the signal to noise ratio is poor. (Bothum and Caldwell 1984).

A safer approach is to perform 2 or 3 colors surface photometry on these galaxies, and to look for color gradients. The presence of a blue excess in the central region may be considered as an evidence of ongoing star formation. However this approach requires exceptional seeing conditions to provide unambiguous information.

For example at the distance of Virgo cluster (m-M 31) the star forming region of NGC 205 would have an angular size of only 4.5 arc.sec. Therefore we decided to perform 3 colors surfaces photometry with the CCD camera of the Canada-France-Hawaii telescope which is known to have generaly a very good seeing. Firsts observations were done in january and may 1984. We have observed 12 dwarf elliptical and we present here preliminary results an selected individual galaxies.

1) M 100 Dwarfs 1,3 and 5

These 3 galaxies belong to the classical list of M 100 dwarfs of Sandage (1972). Observations were made in january 1984 with B and R filters (Vigroux et al 1984). 2 of them, DW1 and DW3 do not present any color gradient while DW5 exhibit a blue excentred nucleus.

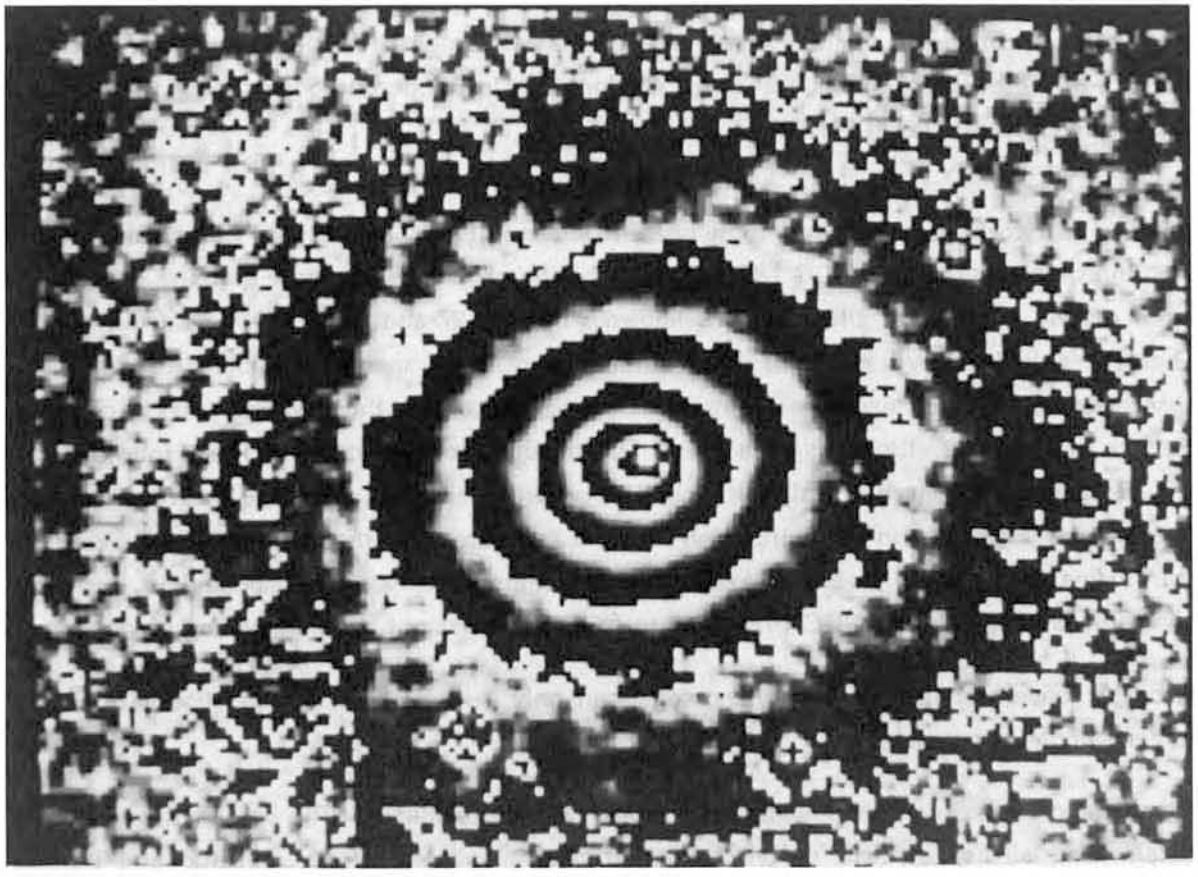


Figure 1: Blue CCD images of M 100 DW5 with a saw tooth black and white lookup table. The excentric position of the nucleus is clearly visible.

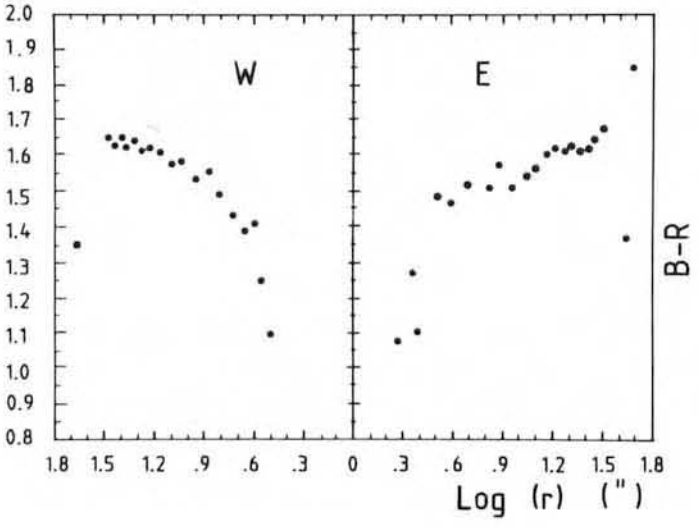


Figure 2: Color profile along the major axis of M 100 DW5. A blue excess centered in the nucleus is present and it extends an 4 arcsec.

If one assumes that this blue spot is due to a young star, this young population is very similar to the one of NGC 205 and NGC 185.

2) NGC 4627

This dwarf elliptical is interacting with the Sc galaxy NGC 4631.

The spectrum of its nucleus (made by Faber and Durstein and quoted by Caldwell 1983) exhibits strong Balmer absorption lines, presumably due to the presence of young stars. Our CCD images, taken in very good seeing condition (0.6 arcsec), show that the nucleus is resolved in 4 condensations. Seeing variation between B and R images prevents us to obtain good colors for each, but they are bluer than the main body of the galaxy. Then NGC 4627 may be the best example of a star forming dwarf elliptical galaxy outside the Local Group.

3) NGC 4472 DW

This is the most nucleated dwarf elliptical of the Caldwell (1983) sample. We have not been able to detect any significatif color gradient. We then confirm in the visible the absence of color gradient between the nucleus and the galaxy found in the infrared (Bothum and Caldwell).

4) IC 3475

This galaxy was proposed by Reaves (1983) as the prototype of a new class of dwarf galaxies intermediate between dwarf elliptical and dwarf irregular. Our CCD images reveales a strange structure. First its photometric profile is very flat. If this galaxy is actually in the Virgo cluster, its radius at = 26/ " is larger than 10 Kpc and its effective aperture is 6 Kpc !

Several bright spots are spread on the galaxy and a loose bar is present. This galaxy is more a reminiscence of an irregular galaxy than of a dwarf elliptical.

CONCLUSION

We are still analyzing about 10 more dwarf elliptical and it may be premature to draw any firm conclusions. However we can already say that :

- Young stars can be found in several dwarf ellipticals but it is not a general feature of these galaxies.

- Interaction with a larger spiral may trigger a burst of star formation. This could be the origin of young stars in NGC 205 and NGC 4627. However young stars can also be found in galaxies isolated or loosely bound such as NGC 185 and M100 DW5.

REFERENCES

Bothum, G.D., Caldwell, C.N., 1984, Ap.J., 280, 528.

Caldwell, C.N., 1983, Astron.J., 88, 804.

Sandage, A.R., 1972, Ap.J., 176, 21.

Reaves, G. 1983, Ap.J.Supp., 53, 375.

Vigroux, L., Souviron, J., Vader, J.P., 1984, Astron.Astrophys., 139, L9.

APPLICATIONS OF A NUCLEAR SPECTROSCOPIC SURVEY OF VIRGO SPIRAL GALAXIES

John R. Stauffer
Dominion Astrophysical Observatory, Herzberg Institute of Astrophysics

My own research during the past two years has been directed primarily toward rather more nearby clusters than Virgo. In particular, I have been studying clusters with names like the Pleiades, the Hyades, and Praesepe. Since it is inappropriate for me to discuss my current research, I will instead spend the majority of my time commenting on two recent Virgo papers published by other authors. My database for these comments will be the nuclear spectrophotometric survey of Virgo and field spirals that I obtained for my thesis (Stauffer 1982a,b; 1983a). I will end my talk with a brief remark concerning the distance of NGC 4569.

1. A Test for Bias in the Morphological Classification of Virgo Spirals

In a 1983 Ap.J. paper (Kennicutt 1983), R. Kennicutt presented new measurements of the integrated Hα emission line equivalent widths for Virgo spiral galaxies. Those data, when compared to the results of a field galaxy survey presented elsewhere (Kennicutt and Kent 1983), showed that Virgo spirals less than six degrees from the cluster core have mean Hα equivalent widths half as strong as field galaxies of the same T type. Kennicutt also reviewed the evidence which shows that Virgo spirals at a given T type are redder (by about 0.1 magnitude) and HI poor (also by about a factor of two) relative to field samples. Such data have often been used to argue that the Virgo galaxies have been affected by their environment, either through ram-pressure stripping (Gunn and Gott 1972), tidal stripping of gas rich companions (Larson, Tinsley and Caldwell 1980), or initial conditions (Dressler 1980). As a caution against facile explanations of the Virgo data, however, Kennicutt also notes that "While galaxies of a given type are different in the Virgo cluster and in the field, Virgo spirals are indistinguishable from field spirals of earlier type, when compared in terms of their HI content, Hα stength, and colors alone. If we did not have access to the Hubble classifications, we would have concluded that the Virgo spirals were completely normal".

Kennicutt's point is not that it is improper to use morphological classifications in this kind of investigation, but that it is necessary to make sure the field and Virgo classifications are consistent with each other. This concern arises primarily because of the subjective nature of galaxy classification. Presumably

there would be no objection if the same Virgo-field differences appeared using B/D ratios or some other objectively determined, type dependent parameter.

I do not intend to measure bulge to disk ratios for Virgo spirals. Such an undertaking would be a worthy but time consuming project. Instead, I propose to construct a parameter Δm_{NT}, which is the difference between a galaxy's nuclear magnitude measured with an 8 arcsecond aperture and its total magnitude B_T^o as listed in the RCBG2. While obviously not equivalent to a bulge to disk ratio since the nuclear magnitude will measure different fractions of the bulge luminosity depending on the actual structural properties of the galaxy, this new parameter should provide a rough index of the galaxy's central concentration.

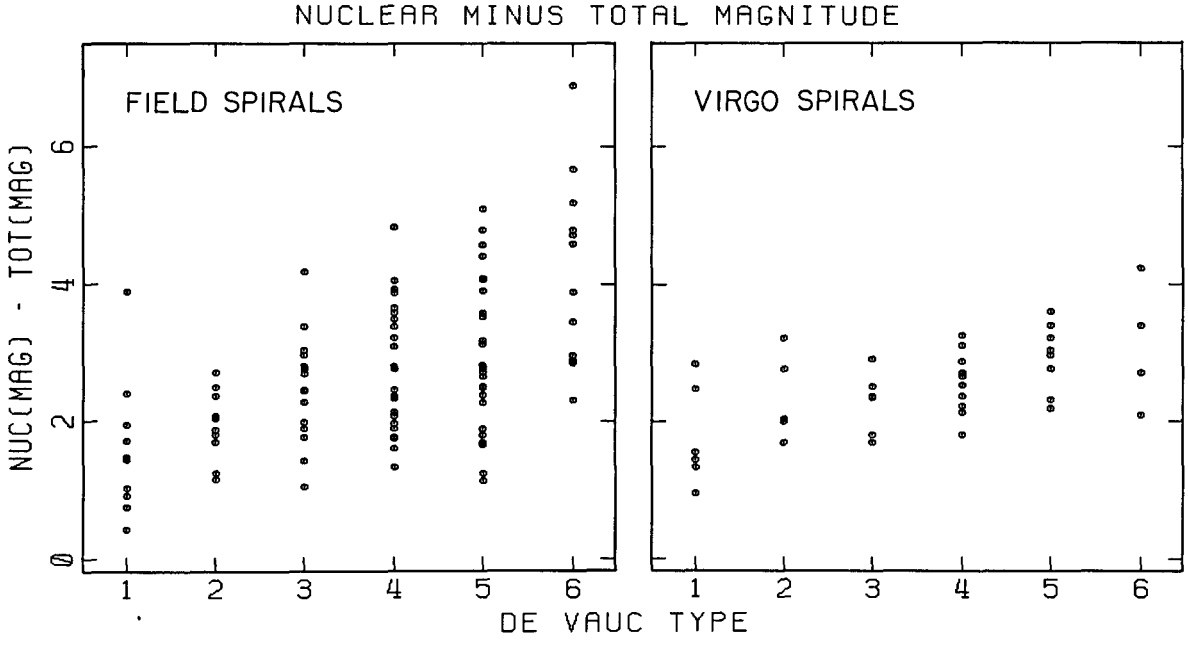


Fig. 1: Nuclear minus integral magnitude versus T type for the field galaxy sample.

Fig. 2: Same as Fig. 1 for the Virgo sample.

The galaxies for which I have nuclear spectrophotometry include about 60 spirals in Virgo (Stauffer 1983a) and 120 spirals and S0's in the field (Stauffer 1982b). The two samples have approximately the same mean absolute magnitude and luminosity function. The field galaxies have heliocentric velocities ranging from 400 km/sec to 2500 km/sec (field galaxies with v > 2500 km/sec in my thesis were excluded since Δm_{NT} is a function of the galaxy's distance). Figures 1 and 2 show the relation between Δm_{NT} and de Vaucouleurs type for the two samples. Both samples show a correlation of Δm_{NT} with type in the expected sense, though with a large amount of scatter. The scatter is larger than desired, but perhaps not unexpected since nearly any other quantity plotted versus T type (B-V,

integral Hα, HI content) also shows a large scatter.

In order to compare the two distributions quantitatively, Figure 3 shows median values of Δm_{NT} as a function of T type for Virgo and the field. The vertical bars are standard deviations of the mean for the field sample. It can be seen that the two distributions are quite similar, with the only major difference being for T = 6.

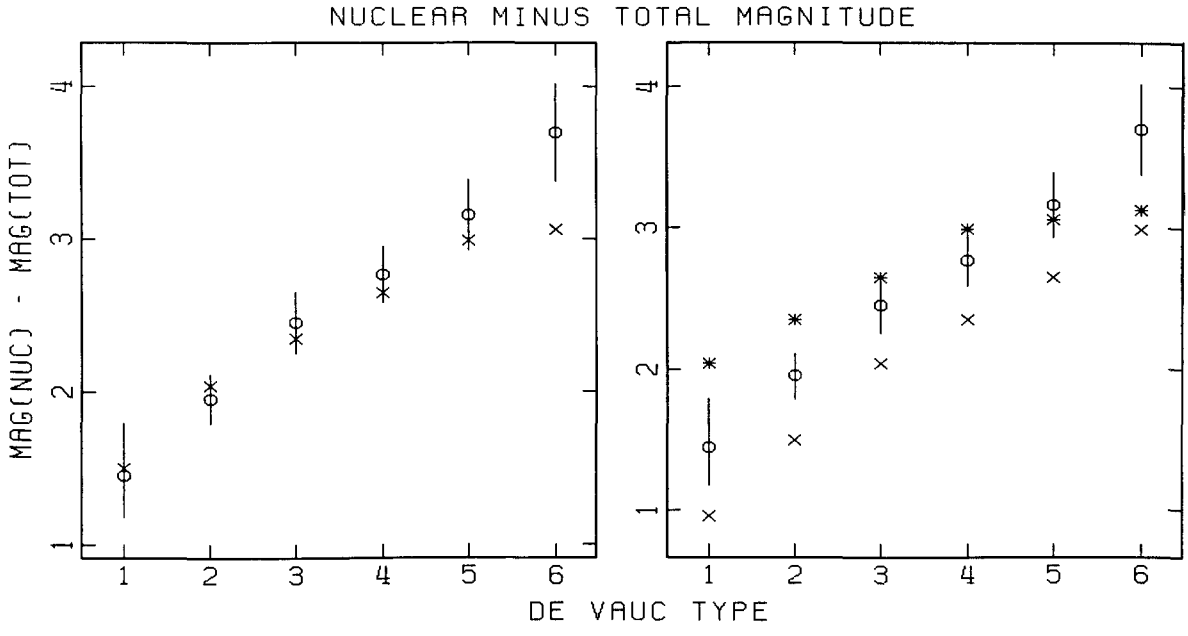


Fig. 3: Comparison of the medians for the nuclear minus integral magnitude distributions for the field (shown as open circles) and Virgo samples (shown as crosses).

Fig. 4: Same as Fig. 3, except the Virgo medians have been shifted by ±1 T type.

I will offer two (slightly) more quantitative comparisons of the two distributions. First, Figure 4 shows the Virgo median values shifted by ±1 T type compared to the observed field medians. The shifted Virgo distributions are much worse fits to the the field data than the observed distribution, indicating that the Virgo classifications are certainly good to 1 T type, and probably good to half a type or better. I have also calculated chi square values for the Virgo distribution shifted by $\Delta T = -1$ to $\Delta T = +1$ in steps of 0.1 T type relative to the field medians. The run of chi square with ΔT is shown in Figure 5. Formally, the test indicates a best shift of 0.2 T type (the Virgo spirals being classified slightly too late) with 90% exclusion points at $\Delta T = -0.4$ and $\Delta T = +0.8$.

I believe that it is encouraging that a test with such relatively meager data shows a credible result. The Virgo T types are consistent with the field classification system, and at least the HI and color difference between the field and Virgo can not now be explained as being due to errors in the T types. A more rigorous test with true bulge to disk data would still be useful, but I doubt if it would turn up any great surprises.

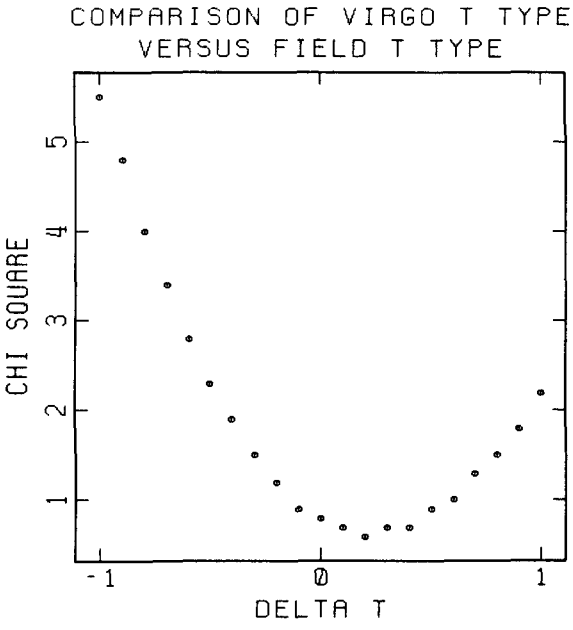


Fig. 5: Chi square comparison of the Virgo and field median distributions.

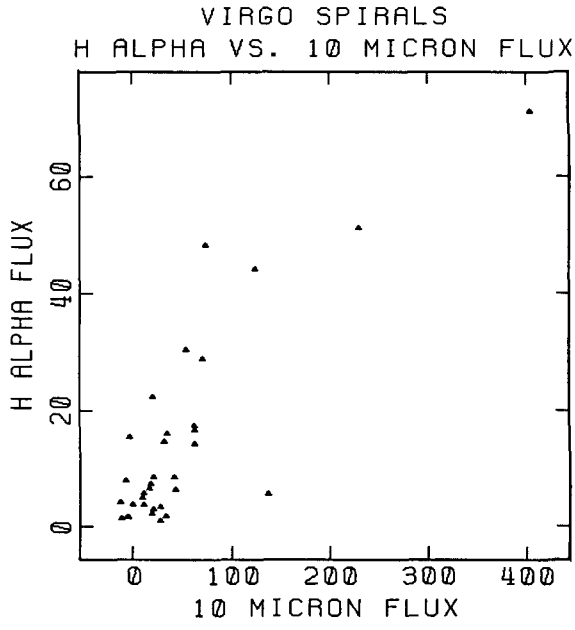


Fig. 6: Correlation between the Hα emission line flux and the 10μ flux from the nuclei of spiral galaxies in the Virgo cluster.

2. Do All Virgo Spirals Have Significant Nuclear Star Formation in Progress?

In another recent paper, Scoville et al (1983) present new 10μ aperture photometry of a sample of 53 Virgo spirals. In their survey, they detected about a third of the galaxies at a significant level, and proposed a statistical argument that all of the nuclei were probably at least weakly "active" at 10μ. Since most nearby normal spirals with 10μ excesses have had their IR emission attributed to star formation (hot dust around protostars), Scoville et al. argued that the 10μ activity indicated that essentially all the Virgo spirals have significant nuclear star-formation in progress. Comparison with scaling laws derived from galactic HII regions then allowed them to estimate that the Virgo spirals would use up their nuclear gas in roughly 2×10^9 years.

Since I have nuclear spectrophotometry through a similar sized aperture (4 or 8

arcseconds for me, 6 arcseconds for the 10μ data) for many of the galaxies observed by Scoville et al., it seemed useful to compare my optical data with the 10μ data. The first two tests provide support to at least some link between IR and optical activity.

Figure 6 provides the most basic comparison between the optical and IR data via a plot of Hα flux versus 10μ flux. A few of the smaller Hα values in the plot are only upper limits, and 10μ fluxes below 30 mJy should also be considered as upper limits. The figure shows a good correlation between the two quantities. The mean Hα flux for the galaxies not detected at 10μ (those with fluxes < 30 mJy) is 5.9 on my arbitrary flux scale, while for the detected galaxies that mean value is 23.1.

I have also derived nuclear colors from my spectra, and it is possible to compare the optical colors of the Virgo galaxies as a function of their 10μ activity. Figures 7 and 8 show the distribution of nuclear colors for the IR detected and non-detected galaxies. The main difference between the two sets of galaxies is that the 10μ active set includes a number of very red (dusty?) and very blue (young stars?) nuclei. Again, this would fit in well with the star formation hypothesis.

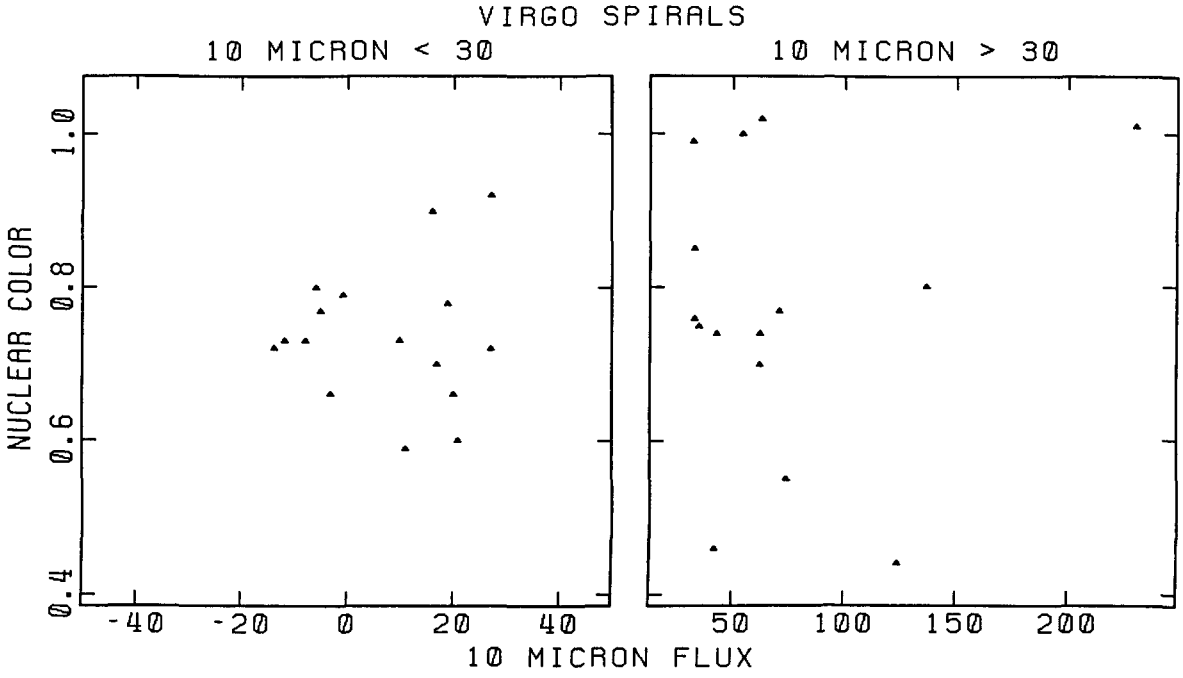


Fig. 7: Nuclear colors (from narrow band magnitudes centered at 4900 and 6500 Å) for the galaxies not detected at 10 microns.

Fig. 8: Same as for Fig. 7 for the 10 micron active nuclei. Not shown in NGC4388 at 10μ = 404, color = 0.60 mag.

When examined in more detail, however, the nuclear spectra do not support a star formation model so well. The emission line spectra of several of the galaxies detected at 10μ have been shown in Stauffer (1983c) to be inconsistent with stellar photoionization. In particular, NGC 4388 is a Seyfert II (see also Phillips and Malin 1982) and NGC's 4438 and 4579 are prototypical LINER's (see also Huchra et al. 1983). All the galaxies detected at 10μ and for which I have sufficient optical data are shown in a [OIII]/Hβ versus [NII]/Hα diagram in Figure 9. The division into stellar photoionized, shock-excited, and power-law photoionized regions follows Baldwin, Phillips and Terlevich (1981) and Stauffer (1983b). Based on this diagram, and on others described by Baldwin et al., some of the nuclear HII regions are stellar photoionized, but at least half have non-thermal excitation sources. The current controversy over whether the LINER's are really shock-excited or instead are power-law photoionized (but with a small ionization parameter, see Ferland 1981) does not affect this conclusion.

The absorption line spectra, in general, also do not support the star formation model since with the exception of NGC 4569 the 10μ detected galaxies do not show enhanced Balmer absorption lines. This argument is not as strong as the emission line result, however, since a small number of hot stars could be present in the nuclei without noticeably affecting the integrating absorption line spectra.

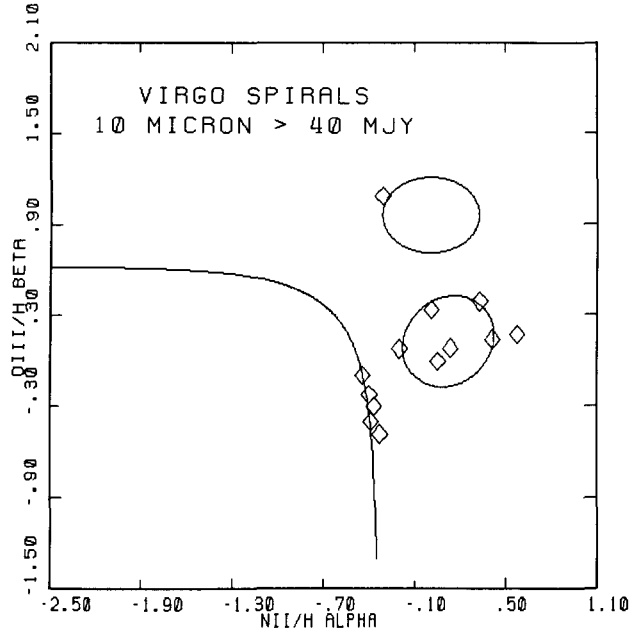


Fig. 9: Log of the flux ratios of [OIII]5007 to Hβ versus [NII]6583 to Hα for the galaxies detected at 10 microns. The smooth curve is a rough locus for normal HII regions, while the upper and lower ellipses enclose regions typical for Seyfert galaxies and LINER's.

In summary, there is no evidence from my optical spectra for continuing nuclear star formation in many of the galaxies detected by Scoville et al. at 10μ. Lacking other evidence, it would seem simplest to attribute the 10μ emission and the optical emission lines to the same source, some type of non-thermal activity. The assertion that "star formation is occurring in the nuclei of virtually all spiral galaxies" should be viewed with considerable caution.

III. What is the Distance to NGC 4569?

The question as to whether NGC 4569 is located relatively near to the center of mass of the Virgo cluster or is significantly in the foreground has been a subject of controversy at this meeting and in the past. Sulentic (1977), Tully (1984), Cowley, Crampton, and McClure (1982), and others have all considered the galaxy to be significantly foreground to the cluster. Because of its optical morphology, HI, and radio continuum characteristics other authors have considered it a good candidate for recent interaction with the Virgo IGM, which would require a location near the center of the Virgo cluster (Stauffer 1983a, Kotanyi 1984).

One distance estimator for NGC 4569 that places it in the foreground to the main body of the Virgo cluster is the Tully-Fisher method (Mould et al. 1983, Tully 1984). As has been pointed out earlier in the conference, however, that method underestimates the distance to NGC 4569 since the galaxy's rotation curve is still rising beyond its VLA determined HI radius. The asymmetry of the HI distribution in NGC 4569 (Kotanyi 1984) may also lead to an underestimate of its true velocity width.

Another commonly quoted argument for the foreground location of NGC 4569 is the nuclear spectroscopy of Cowley, Crampton, and McClure (1982 = CCM). Those authors showed that there exists a correlation between a metals to hydrogen absorption line index for the nuclei of spiral galaxies and the galaxy's bulge luminosity. They interpret that relation as a metallicity sequence - more massive bulges have higher metal abundances. In a diagram comparing bulge luminosity to metal index, NGC 4569 is the most discrepant point, with the difference between observed and predicted bulge luminosity (if NGC 4569 is at the nominal Virgo distance) of nearly 4 magnitudes. In other words, the nuclear spectrum of NGC 4569 is dominated by extremely strong Balmer absorption lines - a fact which is confirmed by my blue IDS spectrum taken at Lick (Figure 10). I will now argue, however, that the CCM method should not be applied to NGC 4569 and does not provide a means of estimating the galaxy's distance.

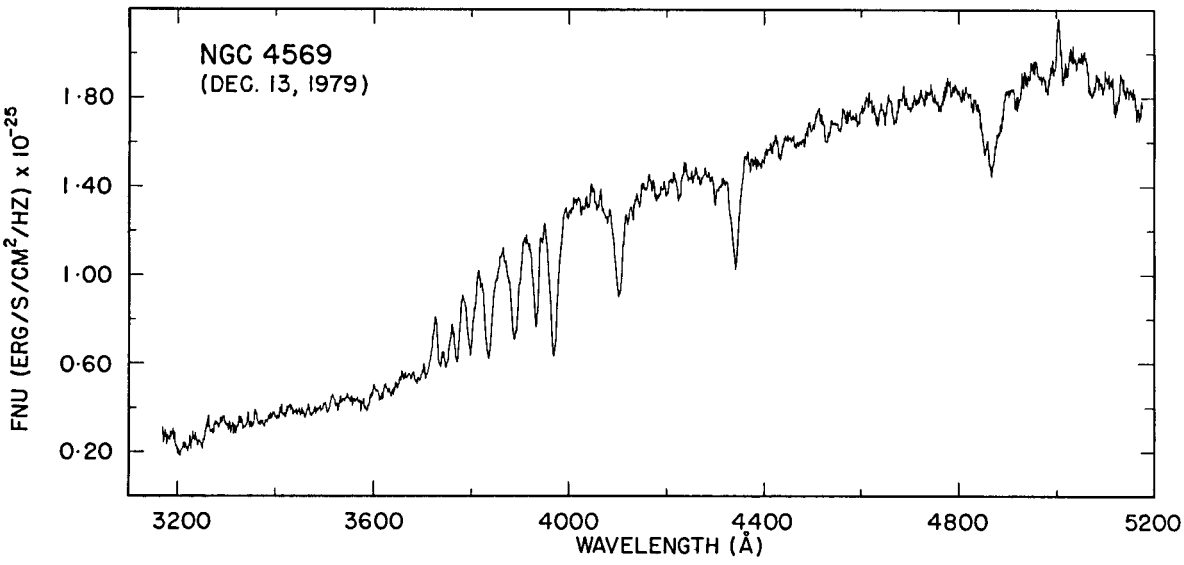


Fig. 10: Nuclear spectrum of NGC 4569.

The primary difficulty with the CCM method when applied to any individual galaxy is that it ignores the possibility of nuclear star formation. Star formation would affect the nuclear "metallicity" index by increasing the strength of the Balmer absorption lines and diluting the metal lines. Some galaxies do have significant nuclear star formation, as shown by the 10μ survey and my optical spectrophotometry. Nuclear star formation adds scatter (toward lower apparent luminosity) in the CCM diagram, with the most strongly star forming nuclei being most affected. Even if the CCM line index versus luminosity diagram is primarily a metallicity sequence, for any given galaxy the method could be significantly in error if there is a Population I contribution to the nuclear spectrum.

More specifically, I believe that the nuclear spectrum of NGC 4569 is indeed dominated by a young stellar population. Various authors have noted that the nucleus of this galaxy is very bright, quite blue and essentially a point source (Humason 1936; Tifft 1969; Weedman 1970). I have obtained blue and red CCD frames of the center of NGC 4569. A color map derived from those two frames, shown in Figure 11, confirms the existence of the blue nucleus. The white hole at the center of the CCD map has a radius of only about 2 arcseconds, and that is still only a limit since the seeing was of that order. As well as being blue, the nucleus is also very bright, contributing essentially all the light to my small aperture spectrum and at least 75% of the light to the CCM spectrum. The bright nucleus has two effects. First, CCM's visual estimate of the bulge luminosity of NGC 4569 will be in error by an unknown (but probably large) amount. Second, and more importantly, the CCM spectrum is not a spectrum of the bulge population but one of the nucleus. A spectrum of the bulge 4 arcseconds

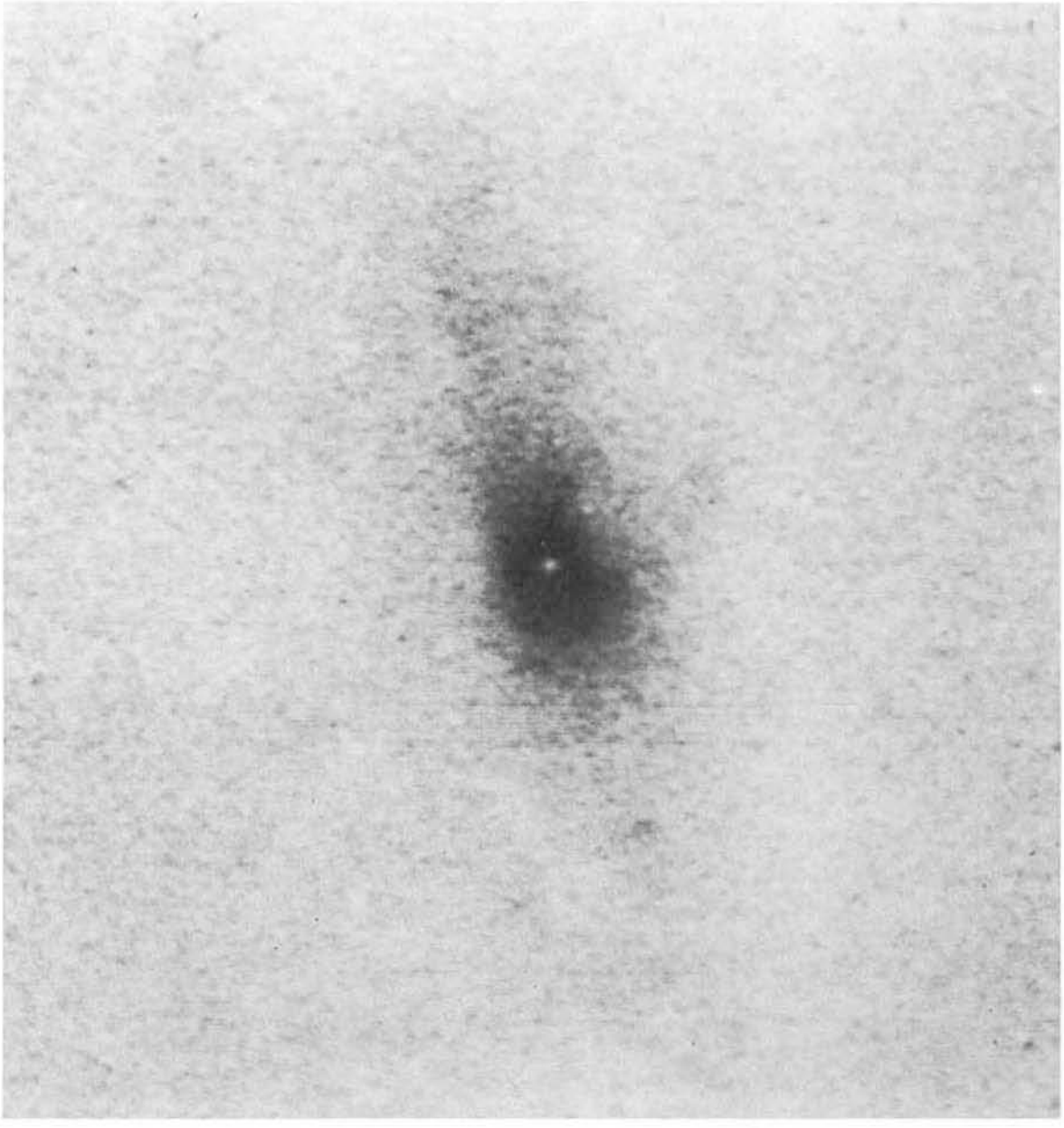


Fig. 11: Color map of the central 2 arcminutes of NGC 4569. The detector used was an RCA CCD, and the filters corresponded roughly to Johnson B and I bands. The nucleus is blue (shown as white or gray), while the bulge is red (shown as darker shades).

north of the nucleus that I have obtained at Lick (as well as the CCD colors) indicates that the true bulge spectrum is much redder, with stronger metal lines and much weaker Balmer absorption lines. Since the stellar metallicity in the center of the galaxy is unlikely to change drastically over a few hundred parsec distance, I conclude that the blue nucleus must be dominated by young stars, rather than being very metal poor. Both effects combine to make the true position of NGC 4569 in the CCM diagram (i.e. bulge metals index versus bulge luminosity) indeterminate. Therefore, the method provides no indication of the true distance of NGC 4569.

References:

Baldwin, J., Phillips, M., and Terlevich, R. 1981, Pub. A. S. P., 93, 5.
Cowley, A., Crampton, D., and McClure, R. 1982, Ap.J., 263, 1.
Dressler, A. 1980, Ap.J., 236, 351.
Ferland, G. 1981, Ap.J., 249, 17.
Gunn, J. R., and Gott, J. 1972, Ap.J., 176, 1.
Huchra, J., Wyatt, W.F., and Davis, M. 1982, Astron. J., 87, 1628.
Humason, M. 1936, Ap.J., 83, 10.
Kennicutt, R. 1983, Astron. J., 88, 483.
Kennicutt, R. and Kent, S. 1983, in preparation.
Kotanyi, C. 1984, this conference.
Larson, R., Tinsley, B., and Caldwell, N. 1980, Ap.J., 237, 692.
Mould, J., Aaronson, M, and Huchra, J. 1980, Ap.J., 238, 458.
Phillips, M., and Malin, D.F. 1982, M.N.R.A.S., 199, 905.
Scoville, N.Z., Becklin, E.E., Young, J.S., and Capps, R.W. 1983, Ap.J., 271, 512.
Stauffer, J. 1982a, Thesis, University of California at Berkeley.
Stauffer, J. 1982b, Ap.J. Supp., 50, 517.
Stauffer, J. 1983a, Ap.J., 264, 14.
Stauffer, J. 1983b, Ap.J., 262, 66.
Sulentic, J. 1977, Ap.J. Lett., 211, L59.
Tifft, W. 1969, Astron. J., 74, 354.
Tully, R. B. 1984, this conference.
Weedman, D. 1970, Ap.J., 159, 405.

OPTICAL COUNTERPARTS OF THE RADIO SOURCE VIRGO A (= M87)

Jean-Luc NIETO
Observatoires du Pic du Midi et de Toulouse
Laboratoire Associé au CNRS n° 285

Gérard LELIÈVRE
Canada-France-Hawaii Corporation

1. Introduction

We present some physical properties of the optical counterparts of the radio source Virgo A. This paper is a compilation of results from a series of optical and UV observations of M87 (1981-1984) essentially at high resolution. These observations were prompted by the first two-dimensional quantitative analysis made by de Vaucouleurs and Nieto (1979b), based on regular-resolution material (FWHM $\sim$ 1".5) obtained at McDonald Observatory. Several runs at the CFH telescope in the last few years have allowed to bring new elements notably with high-resolution (FWHM $\sim$ 0.6-0.7 arc sec) UV observations performed with the Wide-Field Electronographic Camera installed at the Cassegrainian focus (scale : 7 .0 arcsec mm^{-1}).

We describe the optical structure of the M87 jet in Sect.2, compare the optical structure with the radio and X-ray structures in Sect.3, briefly discuss in Sect 4 high resolution polarisation data. We present in Sect 5 preliminary results on the optical counterpart of the radio lobe opposite the jet and on new filamentary regions of ionised gas. Sect 6 is devoted to the suggestion of the existence of possible phenomena in M87 as elements for a plausible scenario. Sect.2,3 and part of Sect. 6 are presented in Lelièvre et al.(1983,1984) in more details. We refer to these papers and to Nieto (1983) for more detailed references.

2. Optical structure of the M87 jet

i) The jet (Figure 1) is made of patches ("complexes" following Nieto and Lelièvre, 1982) quite well separated from each other, with a regular spacing of about 2".9 (= 175 pc if 1" = 60 pc). This seems particularly true for the three inner knots D, E, F. The nucleus fits into this regular frame as well. Beyond knot A, the structure although fitting roughly this periodic spacing, is more complicated.

ii) There is evidence for a continuous component between the knots . This has been a debatable matter. Arp and Lorre (1976) claimed some evidence for it but this was possibly due to some effects such as the limited resolution, the limited signal to noise ratio of their photographic data or the use of a B filter (the galactic background being much stronger in B than in U). The faint continuous component detected here at UV wavelengths is one order of magnitude fainter than that of Arp and Lorre (1976). Remarkably enough this component appears constant between the complexes until it reaches knot I. Simple calculations show that this is not due to the spreading out of the images by seeing.

iii) The jet is not straight, even in its inner part. The inner knots D, E, F and I show slight departures from an elongation following the jet axis. In addition the jet-like feature embedded in the nucleus (figure 2) - which is the cause of the elongation of the nucleus found by Lorre and Nieto (1984) - is slightly bent, in a similar way (although at a scale 10-20 times larger) as the nuclear extension detected by VLBI observations (Reid et al., 1982 ; Reid et al., 1984). We conclude therefore that oscillations start right at the nucleus.

iv) There is a very sharp discontinuity at the level of knot A which appears as on the VLA map (see Biretta et al., 1983) at a projected angle significantly different from a right angle to the main axis of the jet. Beyond knot A, the structure is extremely complex : knots J and K (de Vaucouleurs and Nieto, 1979b) turn out to be filaments linking the bright obvious knots A, B and C, whose two dimensional structures do not suggest perpendicularity with the jet main axis either.

v) Outwards, the tail presents patches at the level of knot C. Broad oscillating extensions are visible at very faint surface brightness levels. Their structure is quite similar to that of the one but last contour level shown in the 6 cm map of Owen et al. (1980). The total length of the visible jet is

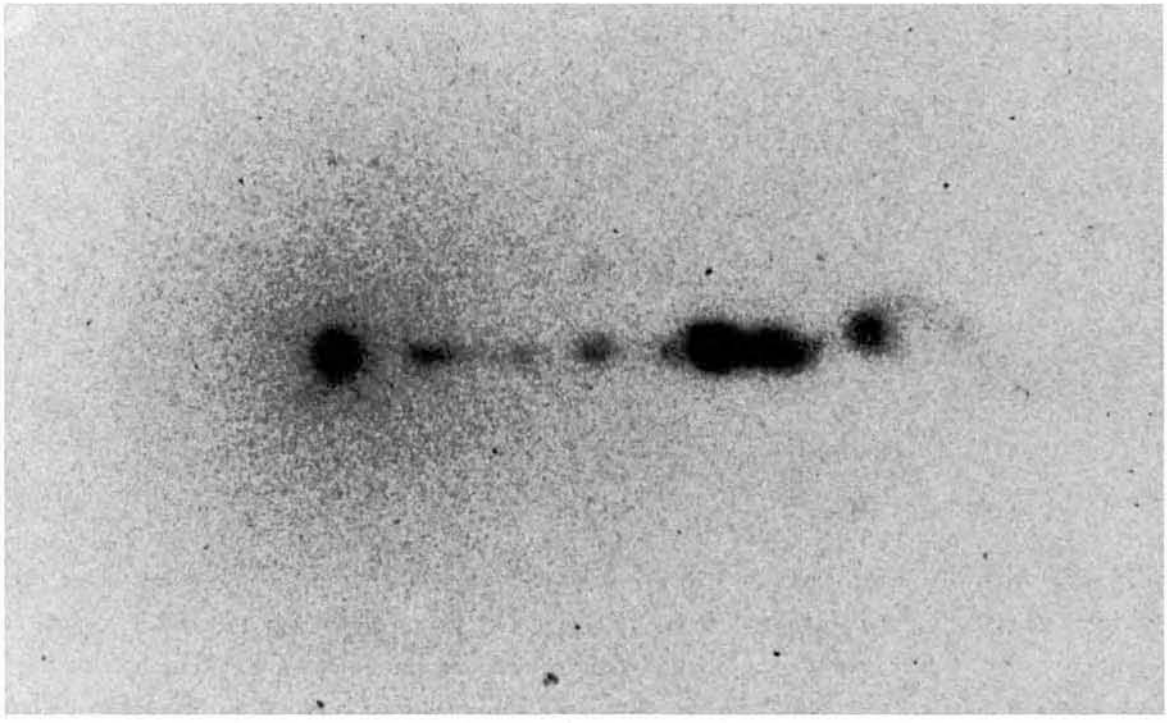


Figure 1 : The M87 jet as seen with a resolution of 0".62 from a 5 mn electronographic plate taken at the CFH telescope with the Wide-Field Electrographic Camera.

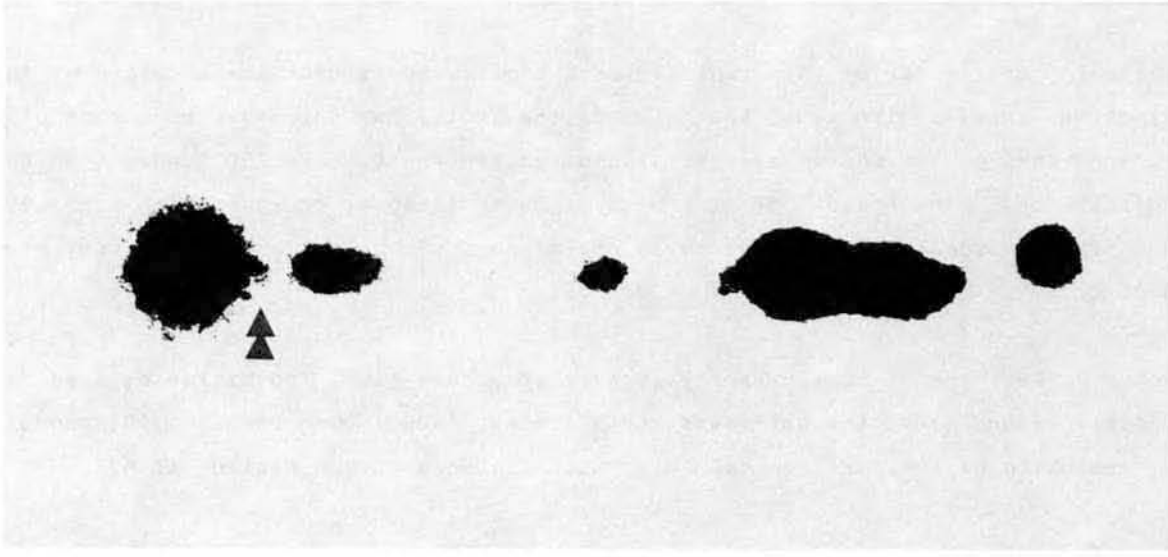


Figure 2 : Contrast enhancement of a U plate showing the nuclear extension bent southwards such as the VLBI jet.

then 26".3.

vi) All knots are resolved in both directions, along and transverse to the jet main axis. The transverse dimensions of the three inner knots D, E, F are respectively 0".5, 0".6 and 0".6.

3. Comparison of the radio, X-ray and optical structures

This optical structure presents a striking similarity with the ∿ 0".6 resolution 2 cm map and the ∿ 1".0 resolution 6 cm map of Owen et al. (1980), as well as the sub-arsec resolution maps of Charlesworth and Spencer (1982) at 408 and 1666 MHz.

Very recent VLA maps with an even better resolution : (0".12 (Biretta et al., 1983)) prompted the use of image restoration techniques to improve the optical resolution. Lorre and Nieto (1984) concluded that the similarity pertained at ∿ 0".2 scale except maybe for the dowstream profile of knot A, very likely to be due to a strong shock. This profile represents the cooling length of the electrons if we assume that the electron acceleration occurs at the shock and that the relativistic electrons lose most of their energy through synchrotron emission. From radio observations (Charlesworth and Spencer, 1982 ; Biretta et al., 1983), the optical cooling length of the electrons should be ∿ 1.5×10^{-3} arcsec in accord with the fact that the profile of knot A is unresolved on the restored maps.

Another consequence of this radio-optical similarity is that the location of the electron acceleration (i.e. the peaks of the knots) has not moved more than 0".2 during the whole characteristic radio synchrotron time, ∿ 250 longer than the optical one. The value of the mean magnetic field at equipartition : B ∿ 250 μG after Hardee (1982) leads to an upper limit of the shock wave velocity of ∿ 0.08 c.

Note however that this similarity is just structure-like. The different spectral indices found for the different knots (Laing, 1980 ; Owen et al. 1980) suggest an evolution of the emission mechanism with distance to the nucleus of M87.

Finally, the X-ray structure of the jet (Schreier et al. 1982), although resolution-limited, is very consistent with both radio and optical structures.

4. Polarisation data

The advantage of studying the polarisation at optical wavelengths is that it is not affected by Faraday rotation. Recently Schmidt et al. (1978) and Visvanathan and Pickles (1981) have studied the optical polarisation of the M87 jet, and found evidence for Faraday rotation between the optical (and 2 cm) data and the 6 cm data.
Moreover, Visvanathan and Pickles found a strong increase of the optical polarisation rate with resolution : for knots A, B, C, the average ratio of 1 arcsec (instrumental) resolution percentage polarisation to that obtained at $\sim$ 2 arcsec resolution is $\sim$ 1.8. This indicates that small-scale structure in the magnetic field exists down to at least one arcsec (1" $\sim$ 60 pc).

It is clear that the detection of a scale threshold within which the polarisation does not increase with resolution would be very informative on the changes in the scale structure of the magnetic field in the jet.
Therefore we have obtained, with the Wide Field Electronographic Camera, high resolution (FWHM $\sim$ 0".75) polarisation data at UV wavelengths in March 1984 consisting in two sets of 4 high resolution exposures 45° apart (Figure 3).

Although these data have not been investigated in detail as yet, some considerations can be drawn :
- the polarisation vector of knots A and C is oriented along the jet, whereas that of knot B is perpendicular to the jet. This confirms Visvanathan and Pickles' results. These recently obtained optical data should be able to reveal by comparison with those of Owen et al. (1980) at about the same resolution the evolution of Faraday rotation at a sub-arcsec scale.
- The polarisation vector of the nuclear extension presented above appears oriented parallel to the jet.

5. The optical counterpart of the eastern lobe

A very deep UV exposure was obtained at the Cassegrain focus of the CFH telescope with the Wide Field Electronographic Camera on March, 1984. Surprisingly the filament of ionised gas firstly discovered by Arp (1967), called n°1 by Ford and Butcher (1979) and located in a direction almost opposite the jet sticks out of the strong stellar background. Other filaments and patches are also readily visible on the plate. Using a specific pass-band filter to extinguish spatial frequencies above 1:0".92 and below 1:8".8 (Roudier, 1985) yields an image where both the random noise and the strong galactic gradient

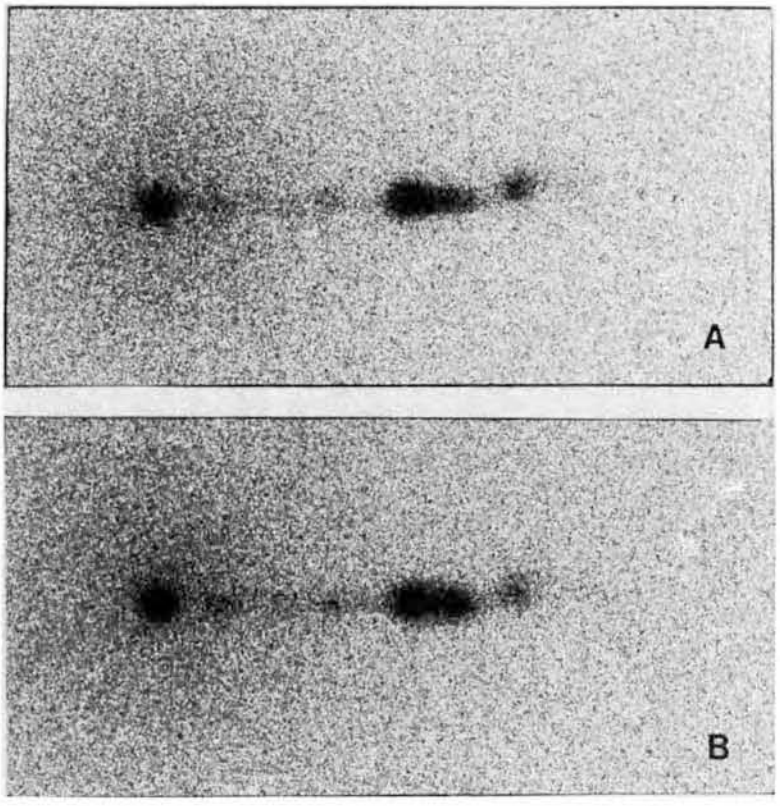


Figure 3 : The M87 jet as seen in the U band through a polarising filter having different orientations : a. parallel to the jet axis (PA = 291°) b. perpendicular to the jet axis (PA = 21°). The resolution of these plates is ≈ 0".75.

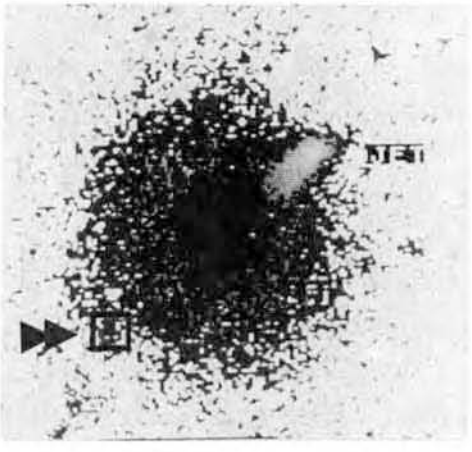


Figure 4 : The optical counterpart of the maximum emission of the eastern radio lobe from a deep UV plate filtered with an appropriate spatial pass band filter.

were suppressed (Figure 4). Several new features are uncovered, some of which being the filaments discussed by Ford and Butcher (1979). The presence of relatively strong UV emission in these ionised regions is something interesting in itself that ought to be investigated more quantitatively.
In addition to these features, a compact blob sticks out about half-way between the ends of filaments 1 and 2 (Ford and Butcher, 1979), at r = 22".9 from the nucleus and PA = 114.1° within 1" of the peak of emission of the eastern radio lobe. The identification with the optical counterpart is quite likely although further observations are needed to confirm it. However it is probably not a region of ionised gas since it does not show up in the Hα maps of Ford and Butcher (1979).

To measure the U magnitude of this object we have integrated its light on a 2".5x2".5 area around its presumed center and subtracted the light from similar areas located at the same distance from the center of M87 chosen to give the same amount of background stellar light (preventing so any spurious effect due to the ellipticity of the galaxy). The blob + background intensity is brighter than the background intensity measured in the three spots only at 3σ level. Assuming $\mu \sim 20.5$ mag arcsec^{-2} at this distance from the center (de Vaucouleurs and Nieto, 1979a) and $\langle U-B \rangle \approx 0.60$ for M87 (Longo and de Vaucouleurs, 1983), the U magnitude of the blob is found to be ≈ 23.85 mag or ≈ 0.63 μJy.
Saslaw et al. (1978) and Crane et al. (1983) have discussed all possible optical emission mechanisms in such radio lobes in radio galaxies : free-free emission from a uniform gas, optical synchrotron emission, inverse Compton emission and others. They seem to favor a synchrotron emission. In the case of M87 however the optical emission of the radio lobe cannot come from the same population of electrons which radiate in the radio region ; extrapolating the radio spectrum to the visible would have given an emission much brighter than that found (U > 20).

6. Emission mechanisms : a possible scenario ?

It is currently believed that the radio and optical emission of the jet is due to synchrotron radiation, from electrons accelerated through shock waves in the jet (Felten, 1968 ; Rees, 1978).

i) Several observational arguments suggest that the M87 jet is not relativistic (Fanti, 1983, Lorre and Nieto, 1984 ; Reid et al., 1984). In addition, since the extended double radio source appears rather symmetrical (Turland, 1975 ; Forster, 1978 ; Laing, 1980), the jet is not likely to be seen very much edge

on. Hence no peculiar geometry of a relativistic jet can hide a two-sidedness nature of the jet : this suggests that the M87 jet is intrinsically one-sided. A similar jet might have existed to feed the eastern radio lobe (both jets may be related by a flip-flap mechanism, see Willis et al., 1978).

ii) It is believed that the presence of gaps and knots might be due to shock waves, either produced by some dynamical effects as the beam goes through the interstellar medium (Blandford and Königl, 1979 ; Norman et al., 1982), by the variability of the source power in the nucleus (Rees, 1978), by Kelvin-Helmholtz instabilities (pinching mode ; see review in Zaninetti and Trussoni, 1983 ; Ferrari et al., 1983), or by the internal structure of the magnetic field, etc.. A critical discussion is in Trussoni et al. (1983).

a) the presence of a continuous component between the knots of the inner jet which oscillates right outside the nucleus of M87 strongly supports the hypothesis of a motion of the power source continuously active and located in the nucleus of the galaxy. If there is a relation between this motion and the periodic 2".9 spacing of the knots (Nieto and Lelièvre, 1982 ; Biretta et al., 1983) this motion should be a precession and periodic events should happen in the nucleus. With $\beta < 0.08$, the precession period would be $> 6.6 \times 10^3$ years (see Lelièvre et al. 1984). It cannot be excluded however that the periodic spacing is due to another cause such as pinching instabilities : theoretical linear calculations of Kelvin-Helmholtz instabilities developped by Hardee (1982) of high Mach number jet flows lead to a periodic spacing of 3".2. In addition any instability in the non linear regime of the flow is expected to develop bubbles having a regular spacing of 1 - 2 jet diameter (Norman et al., 1982).

b) As noticed by Biretta et al. (1983), the strong luminosity gradient at the particular level of knot A suggests a shock. They favor the origin of the shock caused by velocity irregularities in the jet (Rees, 1978). These irregularities are difficult to concile with the very steady jet flow suggested by the constant continuous component between the inner knots. We would like to suggest instead that the shock at the level of knot A might be related to the presence of the (preexisting or being formed by the incoming jet) western lobe material :

- The eastern lobe appears well separated from the nucleus with its inner border located at ≈ 12" from the nucleus of M87. By symmetry, the border of the western lobe (preexisting or being formed) would be is also at ≈ 12" from the nucleus, that is to say at the level of knot A.

- There is a negligible Faraday rotation within knot A (Owen et al., 1980 ; Visvanathan and Pickles, 1981) whereas a ∽ 30° rotation exists for knot A and B, suggesting a new contributor on the line of sight of the jet beyond knot A. This

Faraday rotation may be due to material having the size of the lobe ($d \approx 25'' \approx$ 1500 pc) : $n_e \times B_{//} = 2 \times 10^{-7}$ gauss cm^{-3}. If so, a classical value generally adopted for the magnetic field in radio lobes : $B \backsim 2 \times 10^{-5}$ gauss yields a very likely density of $n_e \approx 10^{-2}$ cm^{-3}.

Acknowledgments

We are very indebted to Th. Roudier and G. Wlérick whose contribution permitted this up-to-date view. Particular thanks go the competence of the Wide-Field Electronographic Camera team : D. Horville, L. Renard and B. Servan.

References

Arp,H.C., 1967, Astrophys. Letters, 1, 1

Arp, H.C., Lorre, J.J., 1976, Astrophys. J., 210, 58

Biretta, J.A., Owen, F.N., Hardee, P.E., 1983, Astrophys. J., 274, L27

Blandford, R.D., Königl, A., 1979, Astrophys. Letters, 20, 15

Charlesworth, M., Spencer, R.E., 1982, Month. Not. Roy. Astr. Soc. 200, 933

Crane, P., Tyson, J.A., Saslaw, W.C., 1983, Astrophys. J., 265, 681

de Vaucouleurs, G., Nieto, J.-L., 1979a, Astrophys. J.,230, 697

de Vaucouleurs, G., Nieto, J.-L. 1979b, Astrophys. J., 231, 364

Fanti, R., 1983, Astrophysical Jets, A. Ferrari and A.G. Pacholczyk Ed, 253

Felten, J.E., 1968, Astrophys. J., 151, 861

Ferrari, A., Trussoni, E., Zaninetti, L., 1983b, Month. Not. Roy. Astr. Soc., 205 515,

Ford, H.C., Butcher, H., 1979, Astrophys. J. Suppl. 41, 147

Forster, J.R., Dreher, J., Wright, M.C.H., Welch, W.J., 1978, Astrophys. J., 221, L3

Hardee, P.E., 1982, Astrophys., 257, 509

Laing, R.A., 1980, Month. Not. Roy. Astr. Soc., 193, 427

Lelièvre, G., Nieto, J.-L., Wlérick, G., Servan, B., Renard, L., Horville,D., 1983, C.R.A.S. Paris, Serie II, 296, 1779

Lelièvre, G., Nieto, J.-L., Horville, D., Renard, L., Servan, B.,, 1984, Astron. Astrophys., 138, 49

Longo, G., de Vaucouleurs, A., University of Texas Monographs in Astronomy n° 3

Lorre, J.J., Nieto, J.-L., 1984, Astron. Astrophys., 130, 167

Nieto, J.-L., 1983, Astrophysical jets, A. Ferrari and A.G. Pacholczyk Ed., 113

Nieto, J.-L., Lelièvre, 1982, Astron. Astrophys., 109, 95

Norman, M.L., Smarr, L., Winkler, K.H.A., Smith M.D., 1982, Astron. Astrophys., 113, 285

Owen, F.N., Hardee, P.E., Bignell, R.E., 1980, Astrophys. J., 239, L11

Rees, M.J., 1978, Month. Not. Roy. Astron. Soc., 184, 61P

Reid, M.J., Schmitt, J.H.M.M., Wilkinson,P.N., Johnston,K.J. 1984, I.A.U., Colloquium 110, 145

Reid, M.J., Schmitt, J.H.M.M., Owen, F.N., Booth, R.S., Wilkinson, P.N., Shaffer, D.B., Johnston, K.J., Hardee, P.E., 1982, Astrophys. J., 263, 615

Roudier, Th. 1985, Thèse de 3e cycle, in preparation

Saslaw, W.C., Tyson, J.A., Crane, P., 1978, Astrophys. J., 222, 435

Schmidt, G.D., Peterson, B.M., Beaver, E.A., 1978, Astrophys. J., 220, L 31

Schreier, E.J., Gorenstein, P., Feigelson, E.D., 1982, Astrophys. J., 261,42

Turland, B.D., 1975, Month. Not. Roy. Astr. Soc., 172, 181

Trussoni, E., Ferrari, A., Zaninetti, L., Astrophysical Jets, A. Ferrari and A.G. Pacholczyk Ed., 281

Visvanathan, N., Pickles, A.J., 1981, Proc. ASA, 4, 177

Willis, A.G., Wilson, A.S., Strom, 1978, Astron. Astrophys., 66, L1

Zaninetti, L, Trussoni, E., Astrophysical Jets, A. Ferrari and A.G. Pacholczyk Ed., 309

V.

X-RAY OBSERVATIONS

X-RAY SURVEY OF THE VIRGO CLUSTER AND COMPARISON TO FIELD GALAXIES

W. Forman, C. Jones, and M. DeFaccio

Harvard-Smithsonian Center for Astrophysics

The observations presented in this review include about 60 galaxies in the Virgo cluster listed in the Shapley-Ames Catalog and about 80 field galaxies. Initially we will combine the Virgo and field samples since the differences in their x-ray properties are rather small (Virgo has a relatively low galaxy density compared to the richest clusters like Coma and hence the Virgo galaxy properties are closer to those of the field than to those of the richest clusters).

The body of this review is divided into three sections. The first describes M87 and its dominance of the cluster in x-rays — it is about one hundred times more luminous in x-rays than any other cluster member and it possesses a massive, dark halo. The second section discusses the x-ray emission from the early type galaxies (E, SO, and Sa) in Virgo and the field. Briefly, these early type galaxies are found to be surrounded by hot gaseous coronae which can be used to probe the masses of these galaxies. In addition, the gas masses of these coronae can be explained as the accumulated gas lost by stellar systems during their evolution. The third section of this review compares the early and late type galaxies in the field to those in the Virgo cluster and discusses the possible effects of the Virgo cluster environment on their x-ray properties.

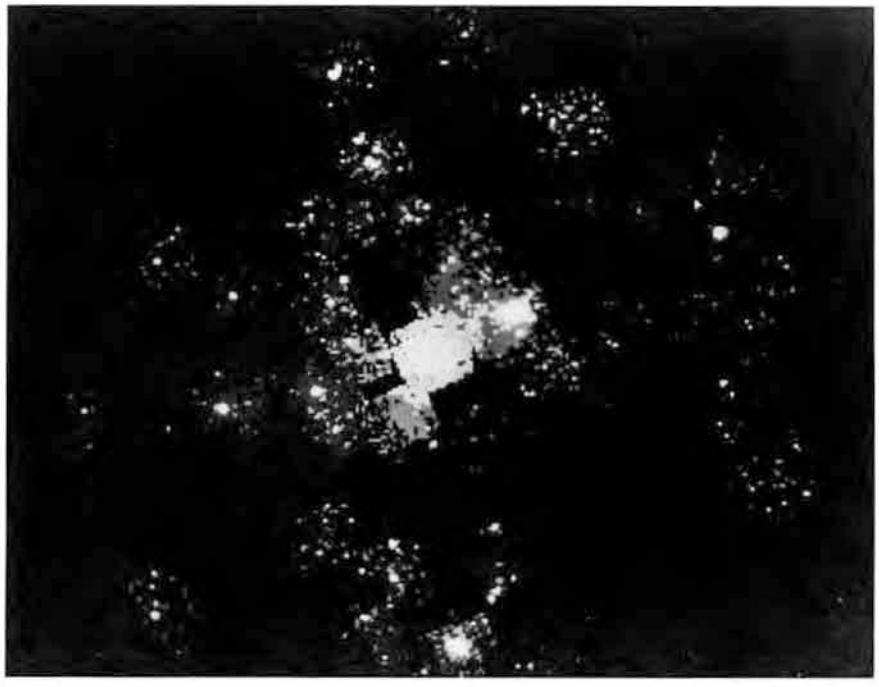


Figure 1: A mosaic of moderate resolution Einstein images of the Virgo cluster shows the dominance of the emission surrounding M87 in the cluster core. Also visible are other galaxies as well as background and foreground objects. The diffuse emission around M87 has been used by Fabricant and Gorenstein (1983) to map the dark matter distribution.

I. The Central Role of M87

Figure 1 shows a mosaic made by combining about 40 1° x 1° images made with the Einstein moderate resolution detector of fields in the Virgo cluster. The cluster, in x-rays, is dominated by the emission from M87. The emission is produced by hot gas which is centered on M87 and extends up to 100 arc minutes from the galaxy. Details of the following discussion of M87, can be found in Fabricant et al. (1980) and Fabricant and Gorenstein (1983; hereafter FG). These authors used the hot gas to map the mass distribution in the core of the Virgo cluster. The basic assumptions which must be valid in order to use the

x-ray distribution to determine the total matter distribution are:

1) the emission is predominantly from hot gas and

2) the hot gas is in hydrostatic equilibrium.

The thermal nature of the emission from the centers of rich clusters has been verified by a number of arguments. First, the spectrum of the emission shows the characteristic emission lines expected from an optically thin hot gas (e.g., Mushotzky et al. 1978). Second, the actual temperature of ~2.5 keV (3×10^7 °K) differs from that of other types of sources (e.g., stars, compact objects, supernova remnants) which might contribute to the emission. Third, the distribution of the x-ray emission (its slow decline with radius compared to the optical light) suggests the emission is not produced by stellar systems. Fourth, the total x-ray luminosity is more than can be explained by the integrated contributions of known types of sources.

The arguments for hydrostatic equilibrium are based on the surface brightness distribution and the gas mass. First, if the gas were in free-fall or free-expansion, its surface brightness distribution would vary with radius as r^{-3} while the x-ray distribution actually varies as r^{-2}. Second, the gas mass observed is ~1.5×10^{12} $M_\odot$ within a one degree radius. To maintain such large amounts of gas in an atmosphere that is not in hydrostatic equilibrium requires unreasonably large replenishment rates. Finally, as Fabricant, et al. (1980) showed, the free fall time of the gas is much smaller than the gas cooling time so the gas has adequate time to establish an equilibrium distribution.

If the gas is in hydrostatic equilibrium and obeys the ideal gas law then the <u>total</u> mass inside a radius r can be written as

$$M_{total}(<r) = \frac{-k\, T_{gas}}{G\, \mu m_H} \left(\frac{d \ln \rho_{gas}}{d \ln r} + \frac{d \ln T_{gas}}{d \ln r}\right) r \qquad (1)$$

where T_{gas} and ρ_{gas} are the gas temperature and density (at radius r), k is Boltzmann's constant, G is the gravitational constant, μ is the mean molecular weight and m_H is the mass of the hydrogen atom (FG). Again we emphasize that

M_{total} is the total gravitational mass including stars, dark matter, and gas. FG used the x-ray observations to determine $\rho_{gas}(r)$ and $T_{gas}(r)$ around M87. Their results are shown in Figure 2 which gives the gravitating mass as a function of radius. They found that out to a radius of 1° the gravitating mass is $\sim 3 \times 10^{13} M_{\odot}$ and the gas mass is a small fraction of the total ($\lesssim$5%). FG used their derived masses to compute mass-to-light ratios and found M/L ~180 (in solar units) at a 20′ radius.

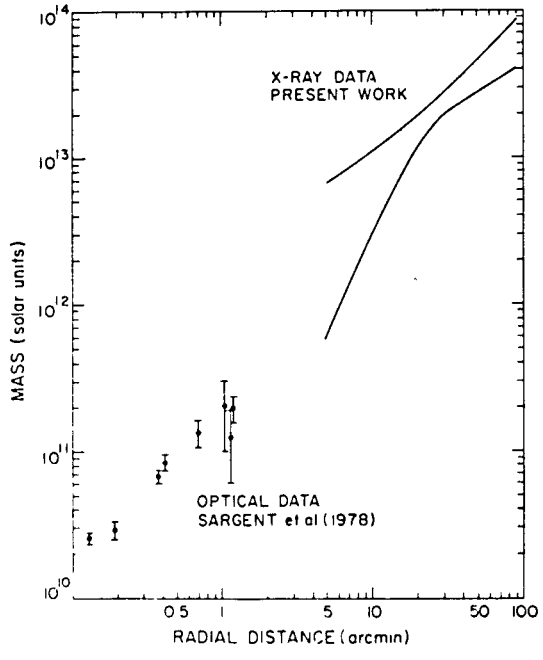


Figure 2: This figure shows the results of the analysis of M87's gaseous envelope by Fabricant and Gorenstein (1983). They plotted total gravitational mass as a function of radius. The data points at small radii are from optical velocity dispersions. It clearly demonstrates the dark halo surrounding M87.

What are the relationships between M87, the cluster, and this envelope of dark matter? Optically, other galaxies are similar to M87 in luminosity and central velocity dispersion. However, as Van den Bergh (1984) has shown, the globular cluster population around M87 is larger (per unit luminosity) than around other galaxies. It appears that M87 is an unusually massive galaxy at (or near) the cluster center which has not been tidally limited by the cluster

gravitational field (see Merritt 1984).

M87 is not unique. There are other x-ray luminous, massive galaxies at the centers of spiral-rich clusters. One such example is NGC 4696 in the Centaurus cluster which has been studied by Matilsky et al. (1984). Both Centaurus and Virgo have comparable properties (e.g., velocity dispersions, spiral fractions). Also, as Matilsky et al. (1984) have shown, NGC 4696 possesses a dark halo of size and mass comparable to that around M87. Table 1 shows a comparison of the Centaurus and Virgo clusters and their central galaxies NGC 4696 and M87.

TABLE 1 - Comparison of Virgo and the Centaurus Clusters

	M87 (Virgo)	NGC 4696 (Centaurus)
X-ray Luminosity (ergs sec^{-1})	3×10^{43}	7×10^{43}
Gas Mass (Solar masses)	1×10^{12}	2×10^{12}
Total Mass within 200 kpc (solar masses)	3×10^{13}	2×10^{13}
Spiral Fraction	55%	45%
Velocity Dispersion (km sec^{-1})	673	507

II. Evidence for Hot Gas Around Early Type Galaxies

Initially, there were several indications that hot gas (~10^7 °K) was present in and around early type galaxies. Gas was seen around M86 in the Virgo cluster (Forman et al. 1979 and Fabian et al. 1980). Bechtold et al. (1983) showed that ~10 early-type galaxies in A1367 contained diffuse x-ray emission probably produced by hot gas. Biermann and Kronberg (1983) found hot gas around galaxies in groups, and Nulsen et al. (1984) discovered hot gas around three relatively isolated galaxies. Using a much larger sample, we find that all bright early type galaxies are associated with diffuse, hot, gaseous coronae. The hot coronae have implications for a variety of problems:

- mass loss rates from stars and galaxies (galactic winds)
- influence on radio emission both as a confining medium and as a source of gas for accretion in order to power the radio source
- presence or absence of cool gas (HI)
- supernova rates and the supernova energy required to heat the coronae or to drive galactic winds
- mass determinations of galaxies by using the gas as a probe of the underlying mass distribution.

We will review in detail the implications of the coronae for masses of galaxies and their mass loss rates.

The sample we studied was a random sub-sample of galaxies in the Shapley-Ames Catalog (Sandage and Tammann 1981). The sample consisted of about 140 galaxies observed with the Einstein Observatory. Of these galaxies, 55 are taken from a paper by Forman, Jones, and Tucker (1984) which describes the x-ray analysis in detail.

What do some of these coronae look like? Figure 3 shows x-ray contours superposed on optical images for several early type galaxies. The parent galaxies have a variety of properties from M86 which is crossing the core of the Virgo cluster at a supersonic velocity, to NGC 4472 farther out in the Virgo cluster (possibly at the center of a subcondensation of galaxies), to NGC 1395, an isolated galaxy.

The x-ray analysis of these coronae involved fitting their surface brightness profiles, S(r), since the profiles plus information on the gas temperature gives the gas density profile and the total mass distribution (as was done by FG for M87). A second aspect of the x-ray data analysis involved measuring the gas temperature.

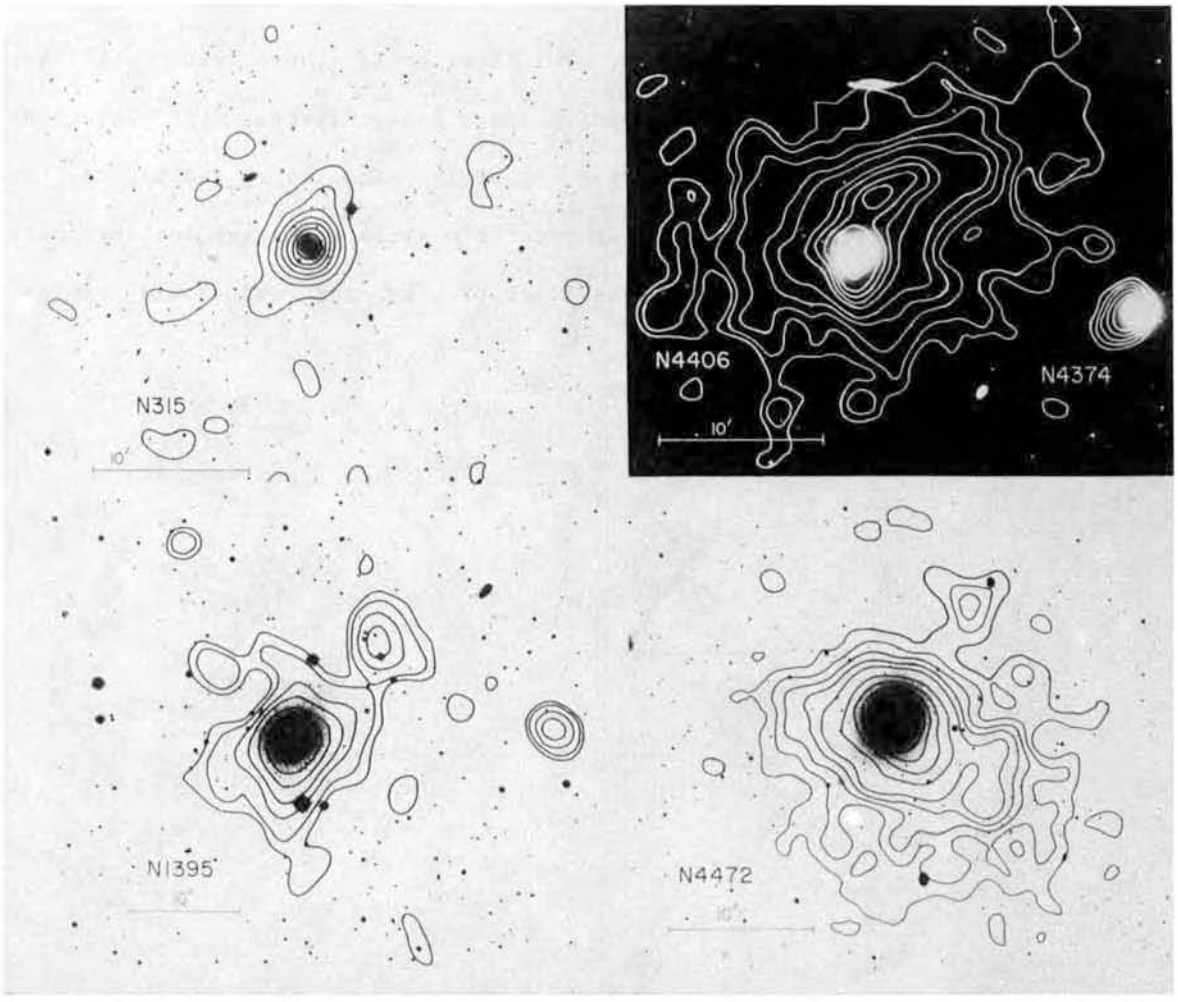


Figure 3: X-ray contours superposed on optical photographs show x-ray coronae in a variety of environments (see text).

Figure 4 shows x-ray surface brightness profiles for four galaxies along with best fit profiles of the form

$$S(r) = S(o)[1+(r/a)^2]^{-3\beta+1/2}$$

where S(o), the central surface brightness, and β are two free parameters. This form is particularly useful in converting from surface brightness to density since the corresponding gas density is (assuming an isothermal gas)

$$n(r) = n(o)[1+(r/a)^2]^{-3\beta/2}$$

where n(o) is the central gas density. For 13 galaxies (those with sufficient counts to allow model fitting) we found $\beta \approx 0.5$ (or consistent with this value for the coronae with the fewest observed counts). The core radius, a, was nominally a few kiloparsecs but is uncertain since radiative cooling in the central regions would increase the emissivity of the gas and could mimic a smaller core radius.

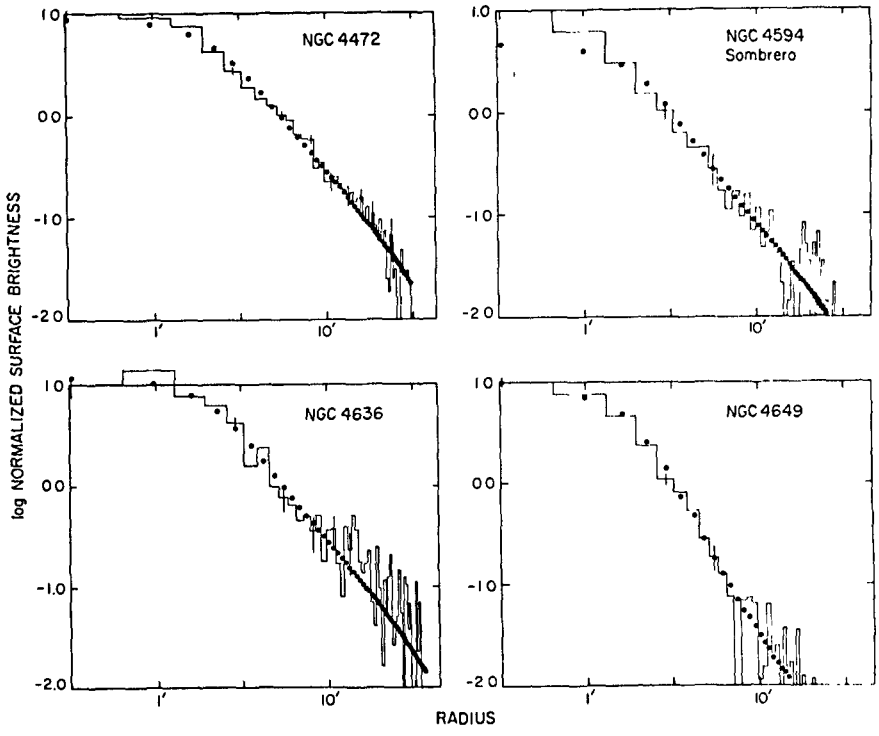


Figure 4: Surface brightness profiles of several coronae are shown along with best fits of the form given in the text. The data are described by the solid histogram and the fits by the symbols.

Eight galaxies in our sample had sufficient counts to permit meaningful spectral fits. Four galaxies gave poor power-law fits but all eight galaxies were well-described by thermal fits (continuum plus lines) with a single gas temperature. For M86, both the galaxy and the plume were better fit by thermal spectra. The characteristic temperatures of the coronae were roughly in the range 0.8-1.5 keV (1×10^7 - 1.8×10^7 °K).

To use the hot coronae as probes of the mass distributions, we rely on the same two assumptions used in studying the dark matter around M87:

1) the emission is thermal from hot gas

2) the emitting gas is in hydrostatic equilibrium.

The thermal assumption has strong support. For example, stellar sources or globular cluster x-ray sources, whose luminosities are known from our own galaxy, cannot provide sufficient x-ray emission. Also, the characteristic temperatures of globular cluster sources and binary x-ray sources are higher than those we observe from the coronae (5 keV compared to 1 keV). For a galaxy like M86, the plume does not correspond to any optical emission and in general the x-ray coronae are more extended than the observed galaxies. An empirical limit on the contribution from compact sources can be derived from the observations of Centaurus A (whose x-ray corona is anomalously weak for such an optically luminous galaxy). We find that if half the extended x-ray emission from Cen A is ascribed to compact sources then these sources can only contribute substantially to the emission from the faintest galaxies in our sample (absolute magnitudes $\gtrsim -19$). As for non-thermal emission, we note that the galaxies we are studying often are resolved in x-rays and generally have no unusual optical emission lines. In addition, their x-ray spectra are poorly characterized by power laws which would be typical of non-thermal sources.

A final argument for the thermal nature of the emission derives from the relation between the x-ray and optical (blue) luminosity. As shown in Figure 5, the x-ray and optical luminosity are related by a relation of the form

$$L_x \propto L_B^{\alpha}$$

where $\alpha \sim 2$. Such a relation can be predicted by taking an estimated mass loss rate from stars of $0.015\ M_\odot\ yr^{-1}\ (10^9\ L_\odot)^{-1}$ as given by Faber and Gallagher (1976), accumulating this material for 10^{10} years, and storing it in a corona with structure like those we observed. Then, since for thermal emission, the

x-ray luminosity is proportional to the gas density squared one finds $L_x \propto L_B^2$. The line drawn in Figure 5 is this relation with the normalization from Faber and Gallagher. Thus, the gas required to produce the coronae has a natural explanation. Also unlike spiral galaxies whose x-ray and optical luminosities are linearly proportional (Long, and Van Speybroeck 1983, Fabbiano and Trinchieri 1984, and Fabbiano et al. 1984), the early type galaxies have a steeper relation (see Trinchieri and Fabbiano 1984 for a detailed discussion).

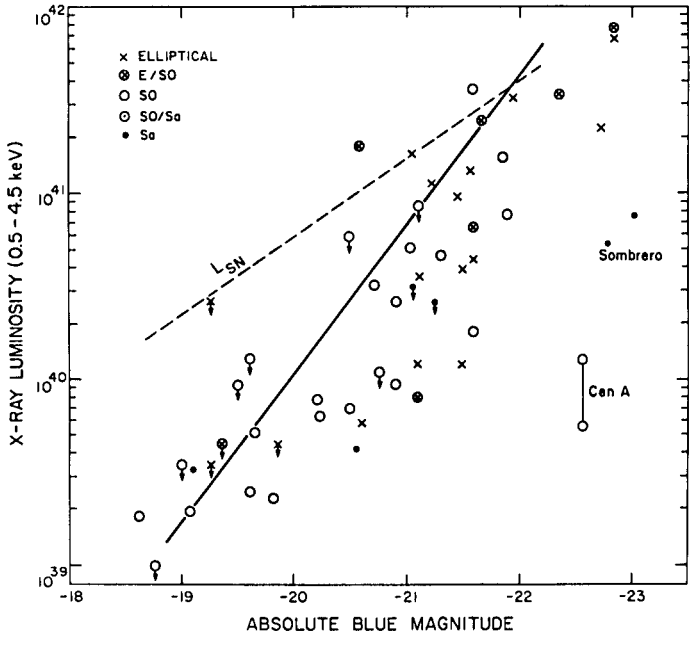


Figure 5: The x-ray luminosity is plotted against the optical luminosity for 55 galaxies taken from Forman, Jones, and Tucker (1984). This figure includes galaxies in and out of the Virgo cluster. The solid line is that predicted from the equation in the text assuming gas is accumulated from stellar mass loss. The dashed line is the predicted supernova luminosity which must be dissipated.

Our second assumption required for determining the total galactic mass is that the gas be in hydrostatic equilibrium. This assumption is supported by two basic arguments. First, if the gas were freely expanding or collapsing its surface brightness distribution would be proportional to r^{-3} while we observe a much flatter distribution (r^{-2}). Second, for galactic winds we require large

stellar mass loss rates to rapidly replenish the gas. Mathews and Baker (1971) computed sweeping times of 4×10^7 years for galactic winds which would imply that the stars in the galaxy would have to replenish the mass at a rate of $100\ M_\odot\ yr^{-1}$ for the more luminous coronae. However, one expects stellar mass loss to provide only a few solar masses per year. Thus, it would be difficult to maintain a non-hydrostatic gas distribution for any substantial period of time.

Having justified the assumptions of thermal emission and hydrostatic equilibrium, we can use the gas distributions to measure the total masses of the underlying galaxies. Equation (1) which was applied by FG to M87 is the basis of the analysis and requires that we determine the derivatives of the gas density and temperature as a function of distance from the galaxy center. If the coronal gas temperature decreases with radius then the mass is larger than that derived for the isothermal case. If the gas temperature increases then the mass would be smaller. An increasing temperature is difficult to explain for galaxies outside clusters and for NGC 4472 the temperature is observed to be roughly constant as a function of radius. Assuming that the gas is nearly isothermal, we find for 13 galaxies with measured surface brightness profiles that the total mass ranges up to $5 \times 10^{12}\ M_\odot$ (for coronae observed out to 100 kpc). Note that $M(<r) \propto r$ and so larger coronae imply larger masses.

The stellar matter in galaxies has a mass-to-light ratio (in solar units) of 6-10 (Faber and Gallagher 1979). With the masses derived above from the x-ray observations we find mass-to-light ratios as large as 100 which suggests that early type galaxies have dark halos.

These dark halos are expected from the detectability alone of the coronae. Compared to galactic wind models, the observed coronae have 1000 times more gas and are 10^6 times more luminous. Therefore, galaxies having coronae must be sufficiently massive to confine the gas. Bregman (1984) has shown that a galaxy will drive a wind if the gas temperature exceeds a critical value given by

$$T_{critical} = 1.2 \times 10^6 \, M_{11}/r_{500} \ ^\circ K$$

where M_{11} is the total galactic mass in units of 10^{11} $M_\odot$ and r_{500} is the core radius in units of 500 pc. Taking a typical gas temperature of 10^7 °K, the galactic mass must be roughly 10^{12} $M_\odot$ to bind the gas.

These dark halos which are implied by the x-ray observations are perhaps not so surprising since clusters, whose predominant constituents are early type galaxies, are known to contain large amounts of dark matter. A comparison of early type galaxies with other systems is shown in Table 2 which is taken from Blumenthal et al. (1984) and to which we have added the results for early type galaxies. One important point made by Blumenthal et al. is that in comparing various systems the mass-to-light ratio alone is not adequate. For example, in rich clusters they note that more mass is in gaseous form (the intracluster medium observed in x-rays) than in stars. Thus, they compute the ratio of total mass to luminous (in any wavelength) mass (last column of Table 2) as a more fundamental quantity. In this regard, early-type galaxies take their proper place with the other types of systems studied by Blumenthal et al. and show a comparable ratio of total to luminous matter.

TABLE 2 - Comparison of Early-Type Galaxies and Other Systems*

System	Total Mass (solar masses)	M_{total}/L_B (solar units)	$M_{total}/M_{luminous}$
Rich Clusters	10^{15}	315±40	8.4(+7,-1)
Poor Elliptical Dominated Groups	5×10^{13}	83(+80,-10)	5.4(+10,-2)
Poor Spiral Dominated Groups	2×10^{13}	40(+50,-10)	14.2(+36,-6)
Milky Way	10^{12}	50	14
Early-type Galaxies	$1\text{-}5 \times 10^{12}$	50-100	8-16

*data from Blumenthal et al. (1984).

An interesting problem for the coronae is the energy balance. The primary energy losses are due to radiation in the x-ray band. The gains are primarily from supernova ejecta whose kinetic energy is thermalized by interaction with the present corona. Taking Tammann's (1982) estimate for Type I supernovae in early-type galaxies of 0.22 supernovae per 100 years per 10^{10} $L_{\odot}$ and a supernova energy input of 5 x 10^{50} ergs per supernova, we find that the supernova energy input to the coronae is $L_{SN} = 3.6 \times 10^{39}$ $(L_B/10^9)$ erg sec^{-1} where L_B is the blue stellar luminosity (in solar luminosities) of the parent galaxy. As shown in Figure 5, this energy source is adequate to power the most luminous x-ray coronae. However, since the x-ray luminosity has a steeper dependence on optical luminosity ($L_x \propto L_B^2$) than the supernova energy input ($L_{SN} \propto L_B$), then for galaxies of lower optical luminosity there is an over abundance of energy. Therefore one possibility is that the supernova rate per unit luminosity decreases with decreasing galaxy luminosity.

In support of the hot gaseous corona model powered by supernovae we note that several galaxies in Figure 5 have rather low x-ray luminosities for their optical luminosities. These galaxies are Sa's plus Centaurus A. Their common feature is that they all possess (notably Cen A) a cool component to their interstellar medium. Therefore, some gas, which would otherwise be radiating in x-rays is tied up in this cool material and also, much of the supernova energy is effectively dissipated and radiated by this cool material. The radiated energy (in the infrared and optical) represents only a few percent of the total emitted luminosity and, thus, does not appreciably alter the appearance of the galaxy.

Also consistent with this idea of supernova energy dissipation by the cool interstellar medium is the lack of hot coronae around late-type spirals. Limits to the x-ray emission from coronae for four galaxies (NGC 4244, NGC 3268 by Bregman and Glassgold 1982; M31 by Van Speybroeck 1984; NGC 253 by Forman, Jones, and Tucker 1984) range from 2 x 10^{38} to 4 x 10^{39} ergs sec^{-1}. Thus, even in late-type spirals where the supernova frequency per unit luminosity is higher

than in early-type systems, no hot coronae are observed.

III. Environmental Effects of the Virgo Cluster on X-ray Properties of Galaxies

We have conducted an x-ray survey of the Virgo cluster. We report here on observations of the bright (Shapley-Ames) galaxies which lie in fields observed with the Einstein Observatory. We will include in our final analysis fainter galaxies as well.

For the spirals, we do know that the cluster does affect the galaxies. As discussed at this conference, the HI content of spiral galaxies in Virgo compared to field samples, does show the effects of ram pressure stripping. NGC 4438 studied by Kotanyi et al. (1983), is an example of a rather spectacular interaction of a spiral passing through the intracluster gas surrounding M87 at supersonic velocity. The effect of the cluster on the x-ray emission of spirals is less dramatic. Figure 6 shows the x-ray luminosity plotted as a function of optical luminosity for a sample of late-type spirals (later than deVaucouleurs type T = 0) taken from the work of Long and Van Speybroeck (1983) which do not lie in the Virgo cluster (open circles). Also shown is our set of spiral galaxies in the Virgo cluster (solid circles). No strong difference between these samples is apparent. Note that NGC 4579 has an anomalously high x-ray luminosity and should be excluded from comparisons of normal galaxies since it is a LINER (Huchra et al. 1982). We would not necessarily expect to see a change in x-ray luminosity between galaxies in VIRGO and those in the field since the x-ray emission from normal spirals is predominantly from the integrated emission of discrete sources (supernova remnants, compact objects, see Long and Van Speybroeck 1983 and Fabbiano et al. 1984) which would be unaffected by sweeping. However, if star formation is extensively decreased as a result of the HI sweeping, then perhaps a decline in the x-ray emission should be expected. Either the effects of depleted star formation are too small to be seen in our sample, or perhaps the HI has been removed only recently and the x-ray emitting systems have not yet evolved significantly.

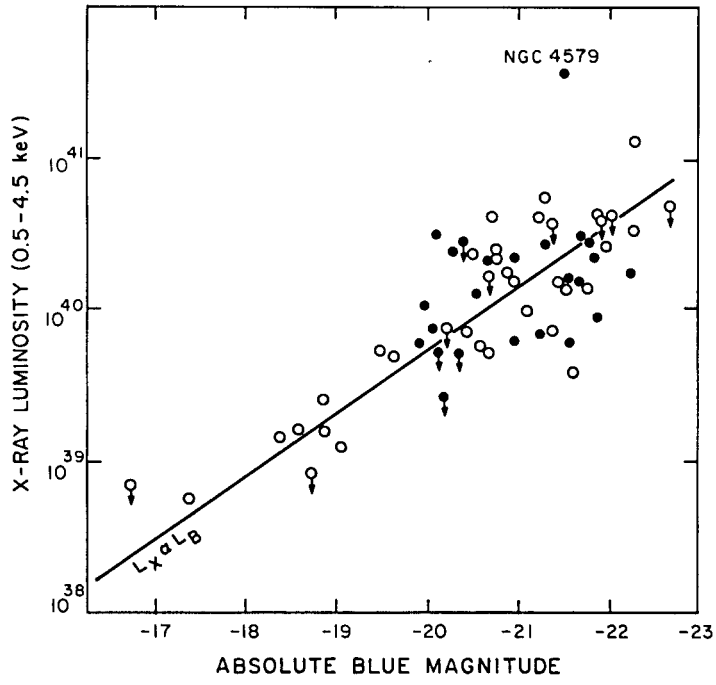


Figure 6: A plot of L_x versus L_B for late-type spiral galaxies is given. Spiral galaxies outside the Virgo cluster are taken from Long and Van Speybroeck (1983) and are shown as open circles. The solid circles are spiral galaxies in the Virgo cluster. No strong differences are seen between the two sets of galaxies. The solid line is drawn such that $L_x \propto L_B$.

For the early-type galaxies with their more extensive, tenuously bound coronae, the intracluster gas has produced some effects which are observable in x-rays. First, as shown in Figure 7, the non-Virgo early-type galaxies (open circles) are, as a class, more luminous than their Virgo counterparts (filled circles). We have performed some model fits using maximum likelihood methods with detections and bounds (see Avni et al. 1980). Formally, the normalization of the Virgo and non-Virgo samples differ at the 95% confidence level (holding the exponent of $L_x = AL_B^{\alpha}$ fixed). Using the derived normalizations, we find that the Virgo galaxies have had ~25% of their gas removed by the environmental effects of the cluster (ram pressure stripping and evaporation). This analysis depends on the relative distances to the Virgo cluster galaxies and the non-Virgo galaxies. Thus, if the Virgo cluster galaxies are actually 30% closer

than the non-Virgo comparison sample, then the two samples would have equal luminosities (our distances were derived using H_o = 50 km sec^{-1} Mpc^{-1} with Shapley-Ames Catalog velocities). We plan to address this question further in our detailed analysis of the Virgo cluster.

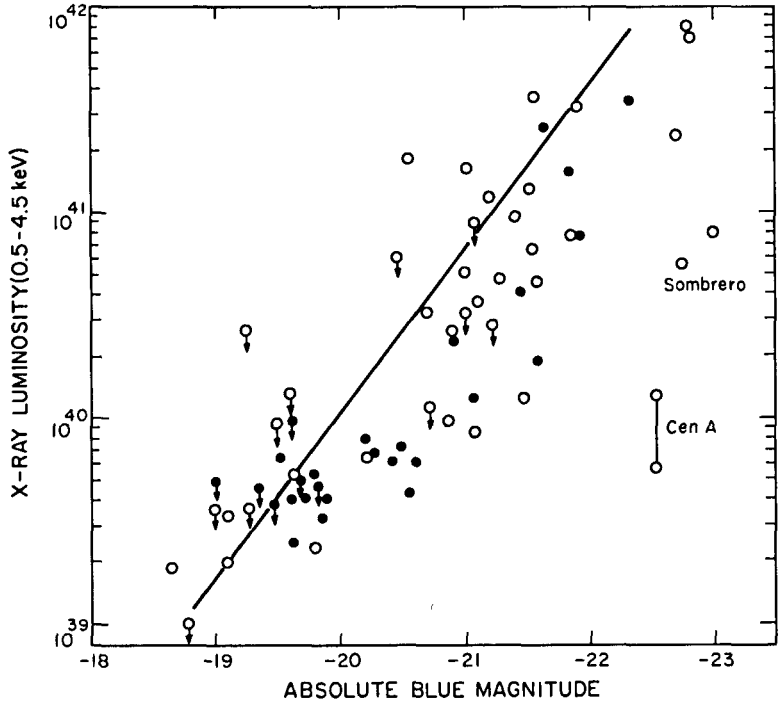


Figure 7: A plot of L_x versus L_B for early-type galaxies (E, SO, Sa) is shown. We have augmented the sample of Forman et al. (1984) with additional Virgo galaxies (solid symbols). Open circles are non-Virgo cluster members. The Virgo galaxies appear to have less luminous coronae suggesting the influence of ram pressure stripping and/or evaporation. The solid line is the same as that from Figure 5.

As with the spiral galaxies, there are some early-type galaxies whose interactions with the intracluster gas are notable. M86 (NGC 4406) is, like the spiral NGC 4438, crossing the cluster core with a supersonic velocity and shows a plume of gas being ram pressure stripped from its corona (see Figure 3 and Forman and Jones 1982, and Fabian et al. 1980). Also we see in Figure 8 the high resolution Einstein image of M84 (NGC 4374). This galaxy is probably a slow moving galaxy within the Virgo core. Its corona is physically small in size and underluminous for the optical luminosity of the galaxy (Forman, Jones,

and Tucker 1984). It is a second example showing the environmental effects of the intracluster gas. Figure 8 suggests motion of M84 to the west (the gas is compressed on the western side of the galaxy). The radio jet morphology is consistent with such a motion (e.g., DeYoung et al. 1980). Thus, there are individual galaxies which are interacting with the intracluster gas and their study should help us to understand the importance of the various environmental effects.

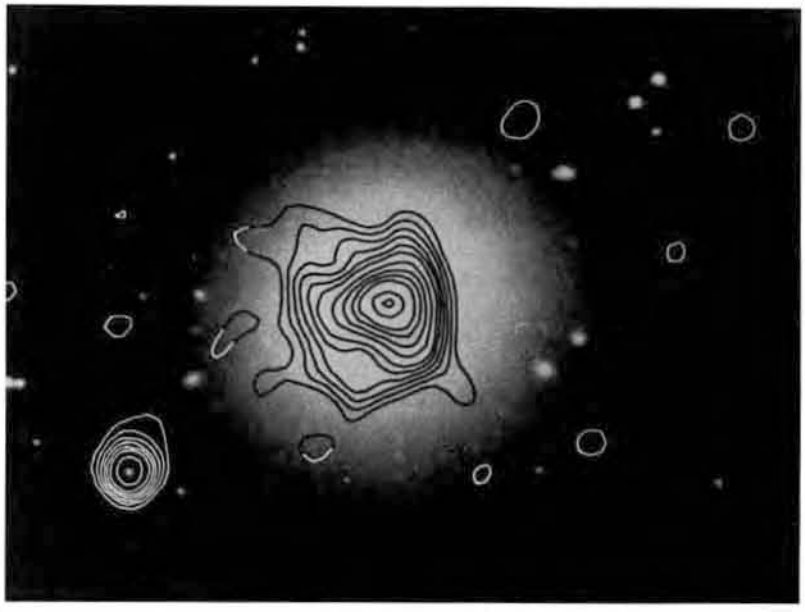


Figure 8: The x-ray contours of M84 (NGC 4374) are shown superposed on an optical photograph. The contours suggest motion of the galaxy through the intracluster gas to the west (compressed contours on the western side of the galaxy).

Summary

We have reviewed three major topics. First, we discussed M87 and its surrounding envelopes of gas and dark matter. The gas, representing only ~5% of the total mass, radiates strongly in x-rays such that M87 dominates the cluster x-ray emission. The gas has been used to trace the distribution of matter

around M87 (Fabricant and Gorenstein 1983) and shows that M87 is surrounded by a dark halo. Second, we presented new observations of early-type galaxies (Forman, Jones, and Tucker 1984) which showed that these galaxies are surrounded by hot, gaseous coronae. The mass of gas is consistent with that thought to be lost by stars. Also we showed that supernovae can play an important role in heating the gas. The existence of the coronae argues that the galaxies are sufficiently massive to suppress galactic winds and, therefore, they probably possess massive, dark halos. Finally, we compared the properties of field galaxies with those in Virgo. While spiral galaxies as a class do show environmental effects at some wavelengths, our presently limited sample did not show any obvious effects in x-rays. On the other hand, there is evidence that the coronae of early-type galaxies in Virgo are smaller and less luminous than their field counterparts. Also several clear examples of ram pressure stripping are observed. Further studies of interesting individual galaxies in Virgo (e.g., M86, M84) along with statistical studies of the entire Virgo sample should provide important information on the interactions of galaxies with their environment and the importance of intragalactic gas on galaxy evolution.

Acknowledgements

We thank K. Modestino for preparing this manuscript. This work was supported by NASA Contract NAS8-30751.

References

Avni, Y., Soltan, A., Tananbaum, H., and Zamorani, G. 1980, Ap.J., 238, 800.

Bechtold, J., Forman, W., Giacconi, R., Jones, C., Schwarz, J., Tucker, W., and Van Speybroeck, L. 1983, Ap.J., 265, 26.

Biermann, P. and Kronberg, P. 1983, Ap.J.(Letters), 268, L69.

Blumenthal, G., Faber, S., Primack, J., and Rees, M. 1984, preprint.

Bregman, J. 1984, Private communication.

Bregman, J. and Glassgold, A.E. 1982, Ap.J., 263, 564.

DeYoung, D.S., Condon, J.J., and Butcher, H. 1980, Ap.J., 243, 11.

Fabbiano, G., Trinchieri, G., and Macdonald, A. 1984, Ap.J., 284, 65.

Fabbiano, G. and Trinchieri, G. 1984, preprint.

Faber, S.M. and Gallagher, J.S. 1976, Ap.J., 204, 365.

Faber, S.M. and Gallagher, J.S. 1979, Ann.Review of Astron.Astrophys. 17, 135.

Fabian, A.C., Schwarz, J., and Forman, W. 1980, Mon.Not.R.Astro.Soc., 192, 135.

Fabricant, D., Lecar, M., and Gorenstein, P. 1980, Ap.J., 241, 552.

Fabricant, D. and Gorenstein, P. 1983, Ap.J., 267, 535.

Forman, W., Schwarz, J., Jones, C., Liller, W., and Fabian, A. 1979, Ap.J.(Letters), 234, L27.

Forman, W., Jones, C., and Tucker, W. 1984, submitted to Ap.J.

Huchra, J., Wyatt, W.F., and Davis, M. 1982, A.J., 87, 1628.

Kotanyi, C., Van Gorkum, H.H., and Ekers, R.D. 1983, Ap.J.(Letters), 273, L7.

Long, K. and Van Speybroeck, L. 1983, Accretion-driven Stellar X-ray Sources, ed. Lewin and van den Heuvel, Cambridge, Univ. Press.

Matilsky, T., Jones, C., and Forman, W. 1984, submitted Ap.J.

Merritt, D. 1984, Ap.J., 276, 26.

Mushotzky, R.F., Serlemitsos, P.J., Smith, B.W., Boldt, E.A., and Holt, S.S. 1978, Ap.J., 225, 21.

Nulsen, P., Stewart, G., and Fabian, A. 1984, Mon.Not.R.Astr.Soc. 208, 185.

Sandage, A. and Tammann, G.A. 1981, The Revised Shapley-Ames Catalog.

Tammann, G.A. 1982, Supernovae: A Survey of Current Research, ed. Rees and Stoneham, Reidel Publishing Co.

Trinchieri, G. and Fabbiano, G. 1984, preprint.

Van den Bergh, S. 1984, PASP, 96, 329.

Van Speybroeck, L. 1984, Private communication.

DISCUSSION

D. LYNDEN-BELL: Surely the dE galaxies are giving as strong an indication of a potential minimum offset from M87!

W. FORMAN: It is certainly puzzling but M87 must lie near the core. M87 could be moving around slowly in the core. Nevertheless, I would emphasize that M87 is a rather special, massive galaxy.

G. HELOU: You have made the comment that the hot corona around M87 would flow out towards the cluster gravitational center if M87 were not at that center. But the gravitational potential must be rather flat at the center of Virgo; have you estimated the tidal radius under these conditions, and how far can M87 be from the cluster center and still keep its corona?

W. FORMAN: The position of M87 could be somewhat off center from the potential defined by the other galaxies in the cluster. However, its mass is sufficiently large that M87 must define the minimum in the potential in its vicinity. Note added: Using the work of Merritt (1984, Ap.J. 276, 26) M87 must be within about 1/5 of a cluster core radius of the cluster center (assuming radial symmetry) since the X-ray gas extends to ~1 degree. For a core radius of 250 kpc, the allowed distance of M87 from the cluster center is then only ~50 kpc. Thus, the cluster center must lie within M87's dark halo.

J.-L. NIETO: The mass determination of M87 which supports that derived from X-ray observations relies upon completely different assumptions. We used the classical von Hoerner's formula of the tidal radius of the tidally stripped companion of M87, NGC 4486 B. This tidal radius was measured from recent surface photometry of this galaxy. We find $M(M87) \sim 5 \times 10^{12}\ M_{\odot}$ within 7!3. This means $M/L_B \sim 70$ (distance to M87 = 15 Mpc). (Nieto and Monnet, Astron. and Astrophys., in press.)

T. DE JONG: I am a little puzzled by the mass balance in the hot coronae around early type galaxies. Are you saying that the hot gas observed has been accumulated in the corona over the lifetime of the galaxy and that none got recycled by undergoing thermal instabilities, cooling and falling back to the galaxy or got blown out of the potential well?

W. FORMAN: The mass you see is consistent with being that produced by stars like those seen at the present epoch. It is initially heated to the virial temperature of the galaxy (unlike spirals, where the relative stellar velocities are small and heating is minimal). Subsequently, the gas can be kept hot by energy input from supernovae. There is no need for recycling the gas, although some at the galaxy center may be involved in a small cooling flow.

E. SHAYA: Do significant amounts of hot gas escape from these galaxies from the tail end of the Maxwellian distribution? After all, the mean velocity of the gas atoms heated by the motions of the stars is nearly one half of escape velocity.

W. FORMAN: I don't know but it certainly is an interesting question.

D. LYNDEN-BELL: Can you not get over the overproduction of energy in low mass galaxies by blowing away some of the corona? Poof!

W. FORMAN: Probably. If you can transfer the energy to the outer portion of the corona, then it might be possible to expel a small amount of gas and yet carry away a large amount of energy. You can't disperse the entire corona since they are generally observed and the mass replenishment rates would be too large.

EXOSAT OBSERVATIONS OF THE VIRGO CLUSTER

A. Smith
Space Science Department of ESA, Estec,
Postbus 299, 2200AG Noordwijk, The Netherlands.
G. Stewart
X-Ray Astronomy Group, Department of Physics,
University of Leicester, University Road,
Leicester, LE1 7RH, England.

Introduction

In X-rays the appearance of the Virgo cluster is dominated by the giant elliptical M87. The imaging proportional counter (IPC) onboard the X-ray astronomy satellite EINSTEIN has determined the extent of the soft X-ray emission associated with M87 and measured the surface brightness as a function of radial distance out to 100 arc minutes (Fabricant and Gorenstein 1983, see Fig.1). Spectral data from the IPC indicates that the temperature of the emitting material is fairly uniform out to at least 25 arc minutes from M87 and possibly much further. The temperature obtained is $\sim$ 3-4 keV. From the assumption of hydrostatic equilibrium it is possible to determine a relationship between mass and radius for M87. From such an analysis it is clear that the X-ray emitting gas has a mass which is small compared with the halo of dark material, (Fabricant and Gorenstein 1983). High spectral resolution instruments have shown that the centre of X-ray emission has a lower temperature than the extended object (e.g. Lea et al 1982, Canizares et al 1982) which has been attributed to the presence of a cooling flow (e.g. Fabian et al 1984).

The higher energy X-ray spectrum of the region around M87 has been determined by a number of instruments. In particular the satellites OSO-8 (Mushotzky et al 1978) and HEAO-1 (Lea et al 1981). These observations have been made with relatively wide field of view instruments (i.e. 5 degrees FWHM circular and 1.5 x 3 degrees FWHM respectively) such that most of the extended emission seen by the IPC is included. These results show a thermal spectrum of temperature $\sim$ 2.5 keV and a line at around 6.7 keV that can be associated with He-like iron. Above 8 keV a harder component is observed (see Fig. 2). The temperature of this harder component would be $\gtrsim$ 10 keV although it may be of non-thermal origin.

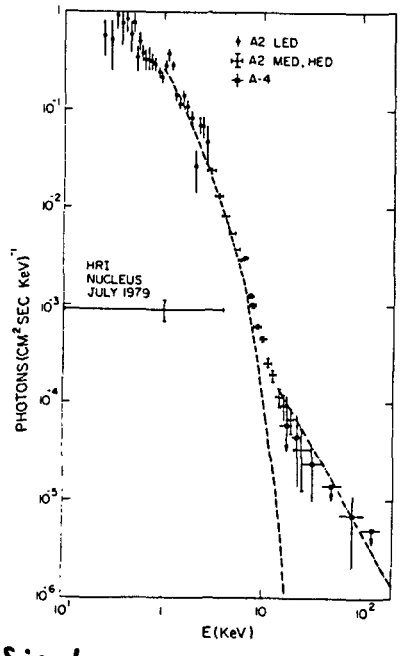


Fig. 1

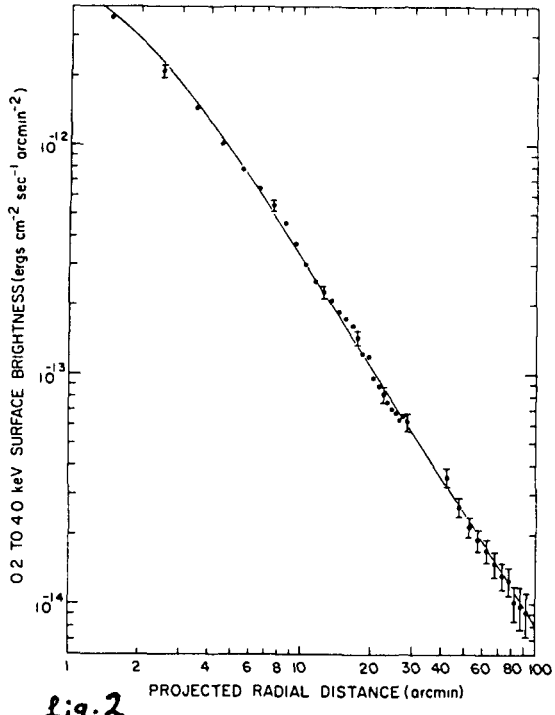


fig. 2

Figure 1. The spectrum of M87 as seen by HEAO-1. This figure is taken from Lea et al 1981. The dashed line is a 2.05 keV thermal bremsstrahlung spectrum. The dot-dash line is an inverse compton fit to the harder component.

Figure 2. The surface brightness of M87 as a function of radial distance. This figure has been taken from Fabricant and Gorenstein 1983.

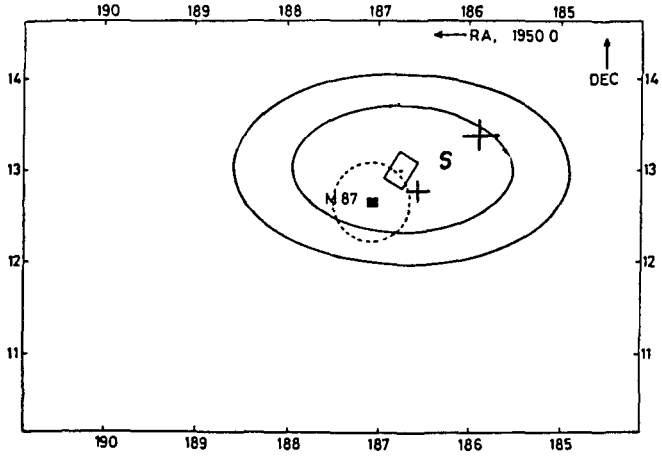


Figure 3. Medium energy X-ray objects in the Virgo Cluster. This figure is based on that given in Lawrence 1978. The elliptical contours refer to the source seen by the SSI instrument on Ariel V. The rectangle corresponds to the centroid of this emission. The crosses refer to the centroids of hard emission seen by Davison (small = 5-8 keV, large = 8-13 keV). The S refers to the cluster centre as determined by Sandage.

Many other galaxies within the Virgo cluster have been observed with EINSTEIN and are discussed by Foreman elsewhere in these proceedings. The experiment whose observations are described here is insensitive to the relatively weak emission from individual galaxies other than M87.

The proportional counter spectrometer on board the Ariel V satellite indicated that the centroid of emission at energies 5 keV is displaced from M87 by 0.5-1 degrees (Davison 1978). The Sky Survey Instrument on board the same satellite observed a very extended source as well as M87 itself. The centroid of emission of this source is in a similar location as that seen by Davison and both are quite close to the centre of the cluster as determined by Sandage. Fig.3 shows a simple map of the cluster including the locations of M87, the Ariel V centres and extents. It is not clear whether the hard tail seen by HEAO-1 is associated with the extended emission seen by Ariel V. It has been speculated that this hard emission is associated with hot intra-cluster gas whilst the emission around M87 is local to the galaxy (e.g. Binney and Cowie 1981).

Reported here are the observations of the Virgo cluster made with the Medium Energy experiment on board EXOSAT. The aims of the observations were to seek further evidence for the presence of the hard very extended object as well as to study M87 and its environment.

Observations

The data reported here were obtained between day 147 17hr 20m and day 150 01hr 54m 1984. The Medium Energy experiment (ME) is sensitive in the range 1.5-20 keV, has a total geometrical area of 1500 cm^2 and a square field of view of 45' FWHM. Further details regarding the ME instrument can be found in Turner et al 1981. The ME experiment is divided into 4 similar quadrants and has the capability of offsetting two of the quadrants up to 110 arc mins from the spacecraft pointing direction in order to monitor the detector background. This is the so called 'Offset configuration'. The narrow field of view of the ME allows the crude mapping of

sources with extents $\gtrsim$ 1/2 degree and so a number of overlapping fields of view were chosen. These are shown in Fig. 4 together with the offset locations.

The eight locations are designated E,D,C,B,A,B',C' and D'. A location at E' was planned but real-time quick-look analysis showed that there was very little emission at either E or D and so the time scheduled at E' was devoted to provide a better sensitivity at D'. Details of the eight locations and exposures are given in Table 1. The observations was made in offset configuration and the aligned and offset quadrants were exchanged approximately half way through each observation for the best possible background estimation.

Very little variability was observed in the detector background during these observations.

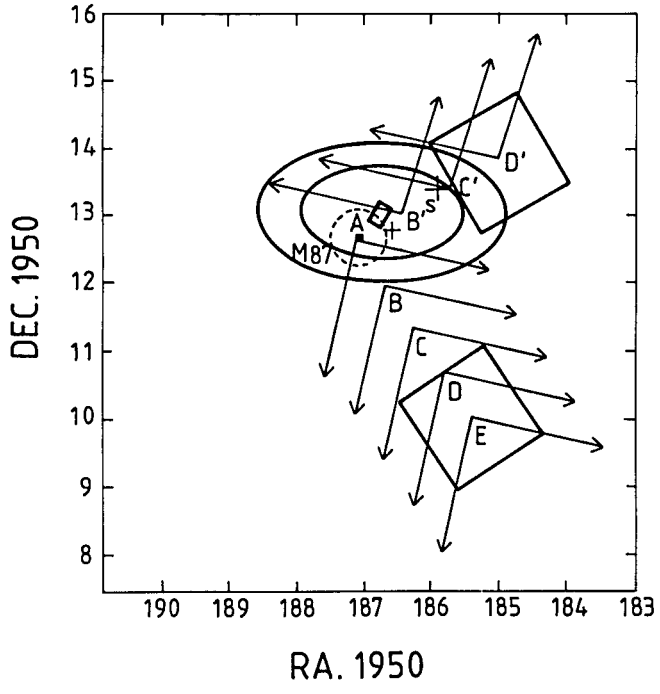
During the observations both the low energy telescope (de Korte et al 1981) and Gas Scintillation proportional counter (Peacock et al 1981) observed the target. The analysis of these data are continuing. Preliminary results from the LE experiment indicate thermal structure at the nucleus of M87 (de Korte private communication).

Table 1

ME observations of the Virgo Cluster								
Location	RA			Dec			Duration	
	Hrs	Min	Sec	°	′	″	Hrs	Min
E	12	21	33	09	57	52	03	39
D	12	24	28	10	46	48	04	39
C	12	26	21	11	23	44	07	30
B	12	27	35	11	54	43	05	49
A	12	28	44	12	36	12	03	01
B'	12	25	25	13	04	38	06	41
C'	12	22	18	13	31	31	09	02
D'	12	20	05	13	50	01	07	40

Figure 4

The ME pointing positions. The zero-intensity field of view is given for positions E and D'. The locations of the offset detector fields are of the ends of the arrows (two for each position). Other features are as in figure 3.



The Results

The onboard computer mode used in this observation provided a 128 channel spectrum for each detector every 10 seconds. These spectra were processed in the following way:

1. For each location there is aligned and offset (background) data. For each detector the offset data was subtracted from the aligned to provide a preliminary source spectrum. The spectra from each group of four detectors that comprise a half array were combined such that for each of the locations two independant spectra were obtained. Although it is more accurate to work with individual detectors throughout the advantage is very small compared with the increased effort involved especially when the source is relatively weak. A fuller study is planned but is not expected to make any major changes to the results.

2. In order to compare the observed strengths at the various locations the count rate in the range 1.5-6 keV (which is the most sensitive) was determined for each spectra. The results are given in Table 2. At locations E,D and D' there is no evidence for emission and the halves have been combined for maximum sensitivity. The difference in observed strengths between the two halves for each location is largely explained by the slightly differing pointing directions of the quadrants and the fact that, except for location A, the centroid of brightness is outside the field of view.
3. For each of the 5 locations where emission was observed the spectral data has been fitted with a thermal bremstralung model. At locations B, A and B' the inclusion of an narrow emission line feature at $\sim$ 6.5 keV was required. The results of the spectral fitting for each location and the details of the fit at location A are given in Table 3. As an example the data and best fits for one half array at positions A, B' and C' are given in Fig. 5.

Table 2

1.5 - 6 keV Count Rates				
Location	Observed		Expected	
	Half #1	Half #2	Half #1	Half #2
E	.09±.06		0	
D	.04±.06		0.10	
C	.69±.03	0.33±.03	0.74	0.44
B	4.49±.04	3.78±.04	4.58	4.07
A	14.88±.08	14.44±.08	14.10	13.97
B'	3.29±.04	2.67±.04	3.80	3.00
C'	0.62±.03	0.52±.03	0.66	0.59
D'	.01±.05		0.07	

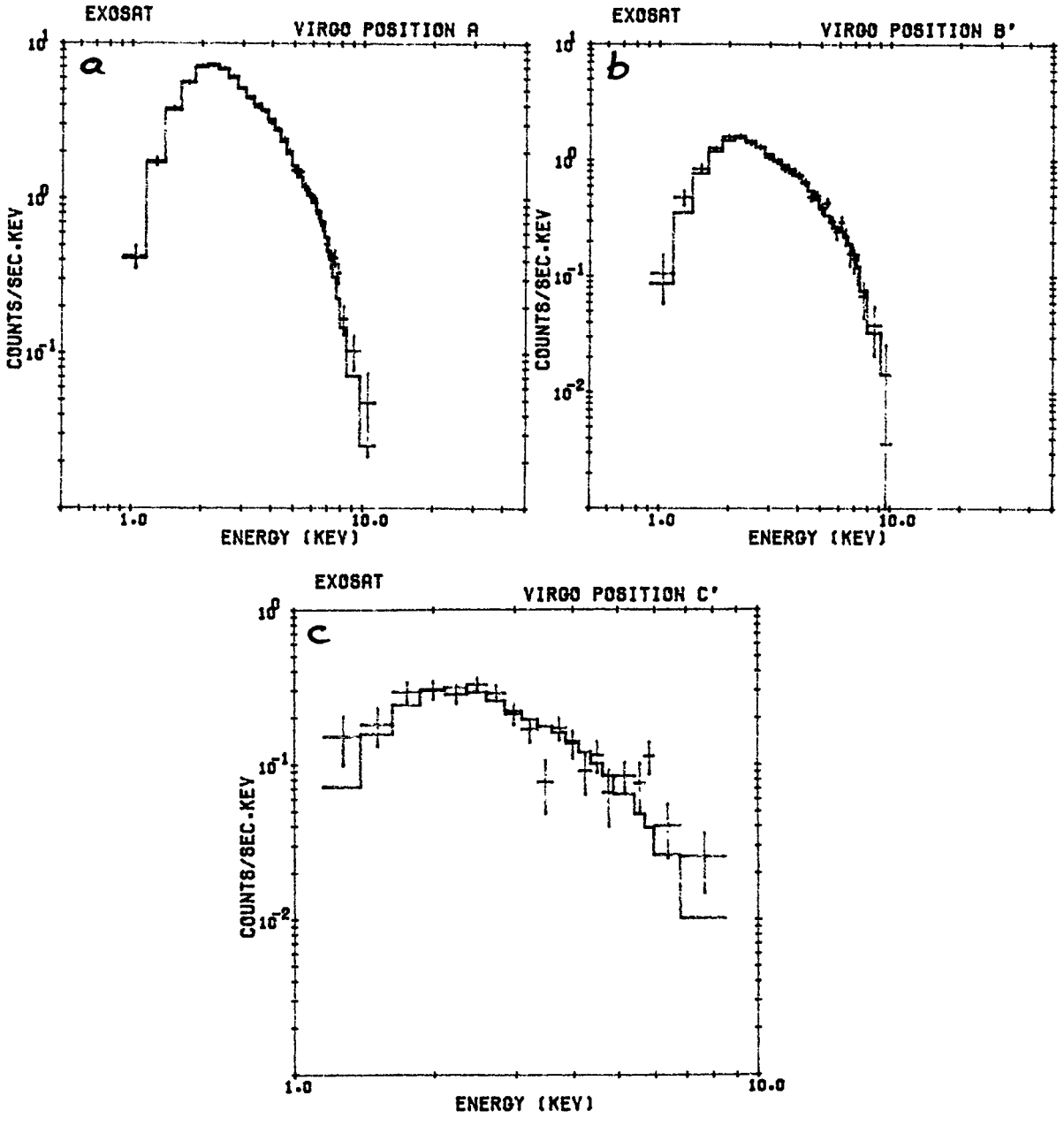


Figure 5.

The pulse height spectra of one half of the ME array for locations A(=a). B'(=b), and C'(=c). The best fits are included. An estimate of the quality of the data can be made from this figure.

Table 3

Best Fit Thermal Bremsstrahlung & Line Spectra						
Location	Mean Radius arcmin	Temperature keV	E(line) keV	E.W. keV	X^2	Dof
C	75	* $2.56^{+.54}_{-.42}$	-	-	33.2	24
B	24	* $2.25^{+.07}_{-.06}$	$6.45^{+.25}_{-.23}$	$0.81^{+.14}_{-.15}$	50.9	44
A	11	+ $2.39^{+.03}_{-.05}$	$6.47^{+.06}_{-.19}$	$0.76^{+.03}_{-.10}$	64.6	53
B'	29	* $2.76^{+.22}_{-.19}$	$6.30^{+.44}_{-.26}$	$0.90^{+.27}_{-.17}$	58.3	44
C'	78	* $2.43^{+.49}_{-.37}$	-	-	50.7	24

\+ Hydrogen column $<10^{21}$ cm^{-2}.

* Hydrogen column fixed at 10^{21}.

Errors are 90% confidence.

Derived luminosity, (assuming the shape of the surface profile given in Fabricant and Gorenstein 1983).		
	2 - 10 keV	0.2 - 3 keV
Within 50' of M87	2.8×10^{-10}	5.0×10^{-10}
Within 100' of M87	4.2×10^{-10}	7.5×10^{-10}

Extropolated and assumes $N_H = 2.5\times10^{20}$ for comparison with IPC results

Discussions

From the results the following points are of interest.

1. The fitted spectrum of M87 indicates a temperature which is consistant with previous maesurements (see Fabricant and Gorenstein 1983 for a review).

   The determined energy of the Fe line is lower than would be expected from a plasma in equilibrium with a tempearture of 2.4 keV (i.e. 6.47 c.f. 6.70 keV). The low red-shift to M87 cannot account for this difference and the object is not likely to be in a non-equilibrium condition. The determined energy may be incorrect because of unknown systematic errors

although the effect is seen in both halves of the ME and such a large discrepancy has not been seen by this author in any other source. It is of interest that the published energy for the iron line seen by OSO-8 is 6.45 keV (Mushotzky et al 1978). The equivelant width of this line is consitant with the OSO-8 value but more accurately determined. For a true energy of 6.7 keV the equivelant width may be used to determine an abundance ratio of Fe/H for the cluster. Using the results of Raymond and Smith 1977 we obtain a ratio of $2.3\ 10^{-5}$ (at location A) which is a little high but generally consistant with the values obtained for other clusters (see Mushotzky et al 1978).

2. The distribution of intensity between the locations is roughly symmetrical about M87. The surface brightness distribution as given by Fabricant et al 1981 does not account for the emission seen at locations C and C' and poorly fits the observations at B and B'. The revised surface brightness profile calculated by Fabricant and Gorenstein 1983 from improved Einstein data is in better agreement. Table 2 gives the observed and predicted count rates for the revised IPC profile. Because the peak surface brightness lies outside the field of view of the ME for all but position A there is a systematic uncertainty related to transmission wings of the collimators. For this reason the EXOSAT results can be said to be consistant with those of Fabricant and Gorenstein 1983.
3. The X-ray distribution is largely isothermal out to a distance of $>$ 70 arc minutes. This is the first direct measurement of temperature at this radius but is entirely consistant with the results of the IPC. In particular it is not consistant with a model in which a hot intra-cluster medium confines a cooling atmosphere. e.g. the model of Binney and Cowie (1981) predicts a temperature of 8 keV at 70 arc minutes.
4. The temperature determined for location B' is significant larger than for M87 and at B. The location of B' is at about the centroid of the harder component seen by Ariel V and also about the cluster centre as measured by Sandage. The method of background estimation adopted in this work discriminates

against the observation of a very extended object with uniform surface brightness. An analysis of the data which is less discriminating is presently underway. One possible interportation of the result for B' is that this is the brightest part of a very extended hard object, (3 x 3 degrees).

Conclusion

The ME experiment has observed emission centred on M87 out to a distance of 1 degree. The surface brightness is generally consistant with the results from the IPC. The emission is seen to be more-or-less isothermal over the observed range but with a significant hardening near the location of the hard X-ray component seen by Ariel V. The question remains:-

Is M87 at the centre of the potential well in the Virgo cluster? Certainly the surface brightness distribution would suggest this since the hot gas observed must be filling the potential well, (otherwise it will simply flow to the potential well). The mass determined for M87 (6 x 10^{13} $M_{\odot}$ within 90 arc mins - see Fabricant and Gorenstein 1983 model 1) is not inconsiderable. The failure to observe a large rise in temperature at large radii argues against a hot intra-cluster medium. Yet M87 does not appear to lie at the dynamical centre of the cluster, (see elsewhere in this volume). There is also the evidence of the harder component seen by Ariel V.

The analysis given above is preliminary and a fuller considerations of the data plus follow-up observations are anticipated.

References

Binney, J., Cowie, L.L., Ap.J., 247, 1981.

Canizares, C.R., Clark, G.W., Jernigan, J.G., Markert, T.H., Ap.J., 262, 33, 1982.

Davison, P.J.N., M.N.R.A.S., 183, 39p, 1978.

Fabian, A.C., Nulsen, P.E.J., Canizares, C.R., Nature, 310, 733, 1984

Fabricant, D., Lear, M., Gorenstein, P., Ap.J., 241, 552, 1980.

Fabricant, D., Gorenstein, P., Ap.J, 267, 535, 1983.

de Korte, P.A.J., Bleeker, J.A.M., den Boggende, G., Branduardi-Raymont, G., Brinkman, A.C., Culhane, J.L., Gronenschild, E.H.B.M., Mason, I., McKechnie, S.P., Sp.Sci. Rev., 30, 495, 1981.

Lawrence, A., M.N.A.R.S., 185, 423, 1978.
Lea, S.M., Reichert, G., Mushotzky, R., Baity, W.A., Gruber, D.E., Rothschild, R., Primini, F.A., Ap.J., 246, 369, 1981.
Lea, S.M., Mushotzky, R., Holt, SS., Ap.J., 262, 24, 1982.
Mushotzky, R.F., Serlemitsos, P.J., Smith, B.W., Boldt, E.A., Holt, S.S., Ap.J., 225, 21, 1978.
Peacock, A., Andresen, R.D., Manzo, G., Taylor, B.G., Villa, G., Re, S., Ives, J.C., Kellock, S., Sp.Sci. Rev., 30, 525, 1981.
Raymond, J., Smith, B., Ap.J. Suppl., 35, 419, 1977.
Turner, M.J.L., Smith, A., Zimmermann, H.U., Sp.Sci. Rev., 30, 512, 1981.

DISCUSSION

E. SHAYA: What is the ratio of the mean densities in the hot spot and the region around M87? Can the difference in temperatures be due to a difference in density?

A. SMITH: Considering the uncertain geometry and line-of-sight effects I could not make a sensible comparison. Basically, the regions involved cannot cool and so density changes could not affect the temperature by cooling.

W. FORMAN: Could the harder component of Virgo actually be the nucleus of M87? Then, if it were variable, you could explain your not detecting it.

A. SMITH: Indeed it could be variable. However, the hard component as seen by HEAO would not have been visible in the ME since it is relatively too faint. The hard source seen by the Ariel instruments would have been visible. I cannot explain the difference in flux between the HEAO and Ariel observations of the hard component.

T. COURVOISIER: Do you see the iron line of M87 in the EXOSAT GSPC spectrum? If yes, is it the same energy (6-7 keV)? Can you say something on the true width of the line?

A. SMITH: A preliminary examination of the GSPC data does strongly indicate the presence of a line at 6-7 keV. However, M87 is a relatively weak source in the GSPC and the line energy is not usefully constrained by the data.

VI.

DYNAMICS

DYNAMICS AND EVOLUTION OF THE VIRGO SUPERCLUSTER

Amos Yahil
Astronomy Program, State University of New York at Stony Brook
and
Institute of Astronomy, University of Cambridge

I. INTRODUCTION

The Virgo Supercluster has been the subject of intensive studies for decades. The advent of complete redshift surveys, which encompass primarily the Virgo Supercluster, have provided the means for confronting dynamical theories with observations. This has resulted in the most reliable observational estimate of the mass content of the universe.

The reader is referred to a number of existing reviews on the subject (Yahil 1981; Davis and Peebles 1983b; Sandage and Tammann 1984). The purpose of this additional one is to add a few recent developments, and to present the subject from the perspective of the author. The observations are summarized in §II, and their standard interpretation is presented in §III, leading to the conclusion that the universe is open, and the cosmological density factor $\Omega_o \ll 1$. Attempts to avoid this conclusion, which runs contrary to some currently popular theories of the early universe, are discussed in §IV. The paper then deals with the process of clustering within the Virgo Supercluster in the standard picture. Small scale clustering is discussed in §V, and the relation between infall in the supercluster and the central virialized cluster is the subject of §VI. A summary is provided in §VII.

II. SUMMARY OF OBSERVATIONS

Observations of the Virgo Supercluster can be divided into determinations of the peculiar velocity field and the density structure. The mass content of the density perturbations is then deduced from these data, III.

Distance estimators other than the radial velocity itself are required in order to measure peculiar velocities. For objects whose distance is comparable to that of the Virgo cluster, distance estimators available to date have typical dispersions $\Delta m \sim 0.4-0.6$ (this is expected to improve significantly with the advent of the Hubble Telescope). An average over many galaxies is therefore required in order to determine the peculiar flow velocity with reasonable accuracy, and attention has consequently focused on global flow models.

The peculiar velocity field can be described as a sum of two terms: the overall velocity of the entire Virgo Supercluster with respect to the Robertson-Walker frame, i.e., the microwave background radiation, and the internal velocities within the Virgo Supercluster. Fortunately, these flow patterns are well decoupled, because the tidal force due to distant density perturbations is small compared with the force induced by the Virgo Supercluster itself.

The internal motions within the Virgo Supercluster have been approximated by a spherical Virgocentric inflow pattern. This can be justified *a posteriori* because of the smallness of the peculiar velocities, and the strong central concentration of the density perturbation (see § IV below). A convenient parametrization of this velocity field is given by the peculiar velocity of the Local Group with respect to the Virgo cluster. A consensus has now emerged (Yahil 1981; Aaronson *et al.* 1982; Dressler 1984; Kraan-Korteweg 1984) that this velocity is

$$u = 250 \pm 50 \text{ km s}^{-1} \qquad (1)$$

where the error bar is both indicative of the internal errors of each measurement and of the scatter between different authors.

Two earlier results, quoting $u \simeq 500$ km s^{-1}, have recently been criticized. Dressler (1984) argues that Tonry and Davis (1981), when

measuring the central velocity dispersions of elliptical galaxies, did not adjust their apertures to the distances of the galaxies, thus obtaining lower velocity dispersions for more distant galaxies. When he corrects for this bias he finds their data to be in agreement with equation (1). Aaronson (private communication) has indicated that he suspects, and is currently investigating, another distance dependent bias in an early determination of the relative distances of Virgo and more distant clusters (Aaronson et al. 1980).

The mean recession velocity of the Virgo Cluster relative to the Local Group (Huchra 1984) is

$$v = 976 \pm 37 \text{ km s}^{-1} \quad . \tag{2}$$

This gives for the dimensionless velocity perturbation of the Virgo Supercluster at the position of the Local Group

$$u/H_o r = u/(u + v) = 0.2 \pm 0.04 \quad . \tag{3}$$

It should be noted that the velocity of the Local Group with respect to the microwave background radiation is

$$u_{MBR} = 550 \pm 50 \text{ km s}^{-1} \quad , \tag{4}$$

toward an apex that is about 45° away from the center of Virgo (Lubin et al. 1983; Fixsen et al. 1983). Accepting equation (1) for the velocity of the Local Group with respect to Virgo, the bulk velocity of the entire Virgo Supercluster with respect to the microwave background radiation therefore has a component in the direction of Virgo of 140 km s^{-1}, and a perpendicular one of 390 km s^{-1}, for a total of 410 km s^{-1}. The only sensible interpretation is that most of this bulk peculiar velocity of the Virgo Supercluster is due to more distant accelerators. The density perturbations responsible for these accelerators, however, have not yet been established.

The density profile of galaxies in the Virgo Supercluster can be determined from a complete redshift survey either by counting galaxies, or by adding up their luminosities. The results are identical, i.e., the shape of the luminosity function is not sensitive to density (Sandage et al. 1979). Yahil et al. (1980) analyzed the Revised Shapley Ames Catalog, and the Center for Astrophysics Catalog was used by Davis et al. (1980) and Davis and Huchra (1982). There is agreement that the excess density varies with Virgocentric

radius as

$$\delta D \propto r^{-2} \tag{5}$$

There is disagreement on the normalization constant. Parametrizing by the mean value of D in a sphere centered on Virgo with the Local Group at its periphery, Yahil et al. find $\langle \delta DLG \rangle / D_o = 3$, while the value of Davis et al. is $\langle \delta DLG \rangle / D_o = 2$.

III. STANDARD INTERPRETATION

The standard assumption is that, at least on large scales as in the Virgo Supercluster, the number (or luminosity) density of galaxies is proportional to the total mass-energy density

$$\rho \propto D \tag{6}$$

Deviations from this assumption are discussed in IV below.

Under this assumption, it is possible to relate the mean density within each shell to its peculiar velocity, since all shells have the same age. This relation, first realized by Silk (1974), can be worked out exactly from the Friedman equations (for details see Schechter 1980). A useful approximation:

$$u/H_o r = \frac{1}{3} \Omega_o^{0.6} \frac{\langle \delta\rho \rangle}{\rho_o} \left[1 + \frac{\langle \delta\rho \rangle}{\rho_o}\right]^{-0.25} , \tag{7}$$

is accurate to better than 5% for $0.1 < \Omega_o < 1$ and $0 < u/H_o r < 1$, which covers the entire range of interest. The approximation is a generalization of a previous one, based on linear perturbation theory, given by Peebles (1980). The (empirical) nonlinear modification is the addition of the last factor on the right hand side of equation (7).

Applying equation (7) with $u/H_o r = 0.2$ and $\langle \delta\rho \rangle / \rho_o = 2\text{–}3$, gives

$$\Omega_o = 0.1\text{–}0.2 \tag{8}$$

Note that the errors in the determination of Ω_o are multiplicative, not additive. An error of a factor of 2 in Ω_o (probably a reasonable estimate) therefore does not alter the conclusion that the universe is open. In fact, given the quoted range of $\langle \delta\rho \rangle / \rho_o = 2\text{–}3$, if $\Omega_o = 1$, then $u/H_o r = 0.5\text{–}0.7$. It

follows that the Virgocentric peculiar velocity of the Local Group is in the range u=1000–2400 km s^{-1}. Such a high value is out of the question.

It is worth emphasizing that a value of $\Omega_o \sim 0.1$ is consistent, within a factor of 2 or so, with two other independent determinations. One is the baryonic density deduced from standard big-bang nucleosynthesis (e.g., Yang et al. 1984 and references therein). The other is the mean density inside galaxies, whether baryonic or not, obtained from the product of their mean emissivity and a mean mass-to-light ratio (see the review by Faber and Gallagher 1979; and the discussion of the validity of virial analyses in §V and §VI below).

The standard interpretation therefore presents a completely consistent picture of an open universe, dominated by baryons, whose mean density at the present epoch is about a tenth of the critical density.

IV. ALTERNATIVE INTERPRETATIONS

In recent years theoretical particle physicists have developed Grand Unified Theories (GUTs), and applied them to the early universe. Several conclusions follow that can be confronted with observations.

One prediction, which has resulted in a series of experiments to detect the decay of the proton, is that the net baryon density of the universe is due to baryon nonconservation in the early universe. The current lower limit on the lifetime of the proton already rules out the simple SU(5) GUT, but can be accommodated by other GUTs (see the review by Fiorini 1984). A cosmological corollary of such theories is that, since the baryon to photon ratio is determined by microphysical processes, density perturbations must be adiabatic, maintaining the same baryon to photon ratio. The limits on small scale anisotropy of the microwave background radiation (Uson and Wilkinson 1984 and references therein) rule out such adiabatic perturbations in a baryon dominated universe.

The above difficulty can be overcome (Bond and Szalay 1983) if the universe is dominated by nonbaryonic matter, such as massive neutrinos, which ceased to interact with baryons or photons long before the recombination epoch ($z \sim 1500$). Adiabatic perturbations whose mass is smaller than about 10^{15} $M_\odot$, however, are attenuated by viscous forces before recombination

(Silk 1968). It has therefore become popular to consider the pancake scenario (Zel'dovich 1970), in which 10^{15} $M_\odot$ clusters form first, and galaxies fragment out later.

Most of the Virgo Supercluster is inconsistent with such a scenario. Gunn (1983) emphasized that the Local Group could not possibly form in this way. The smallest pancake from which it could have formed is the entire Virgo Supercluster. But, at least at the distance of the Local Group from the center of Virgo, the Virgo Supercluster is only now beginning to turn around.

The argument can be strenghtened to include the bulk of the Virgo Supercluster. While it has been argued for some time that there is a supergalactic disk in the Virgo Supercluster (de Vaucouleurs 1976 and references therein), and this might be identified with a pancake, the bulk of the mass of the Virgo Supercluster in not in that disk. The situation is illustrated in Figs. 1 and 2, in which are plotted equal density contours based on the RSA catalog. The higher density contour in Fig. 1, $\rho/\rho_o=10$, indeed does show some flattening, but the lower density contour in Fig. 2, $\rho/\rho_o=2$, only shows an axis ratio ~2. The bulk of the mass of the Virgo Supercluster is in the lower density levels, and therefore the monopole approximation to the gravitational field is very good (Yahil et al. 1980). Furthermore, since the velocity perturbation at the position of the Local Group is still small, $u/H_o r=0.2$, linear perturbation theory is a good approximation (cf. equation [7]), and the peculiar velocity is expected to be in the direction of the peculiar acceleration. This justifies a posteriori the spherical inflow model.

Great attention has recently focused on inflationary universes (Guth 1981; Albrecht and Steinhardt 1982; Linde 1982), in which the coherence length of the initial fluctuations in the universe is stretched during an inflationary phase beyond the size of the present horizon. The advantage of this scenario is that it removes with a stroke the horizon, flatness, and monopole problems (Guth 1981). The disadvantage is that the universe at the present epoch should be flat to a high degree with $|\Omega_o-1|<10^{-8}$. This is at variance with the standard interpretation of the Virgocentric infall. Therefore, if there is reluctance to give up the appealing features of inflation, a modified interpretation of the Virgocentric inflow is required.

It is easy to question the basic assumption of the standard interpretation, namely that the mean mass-energy density is proportional to

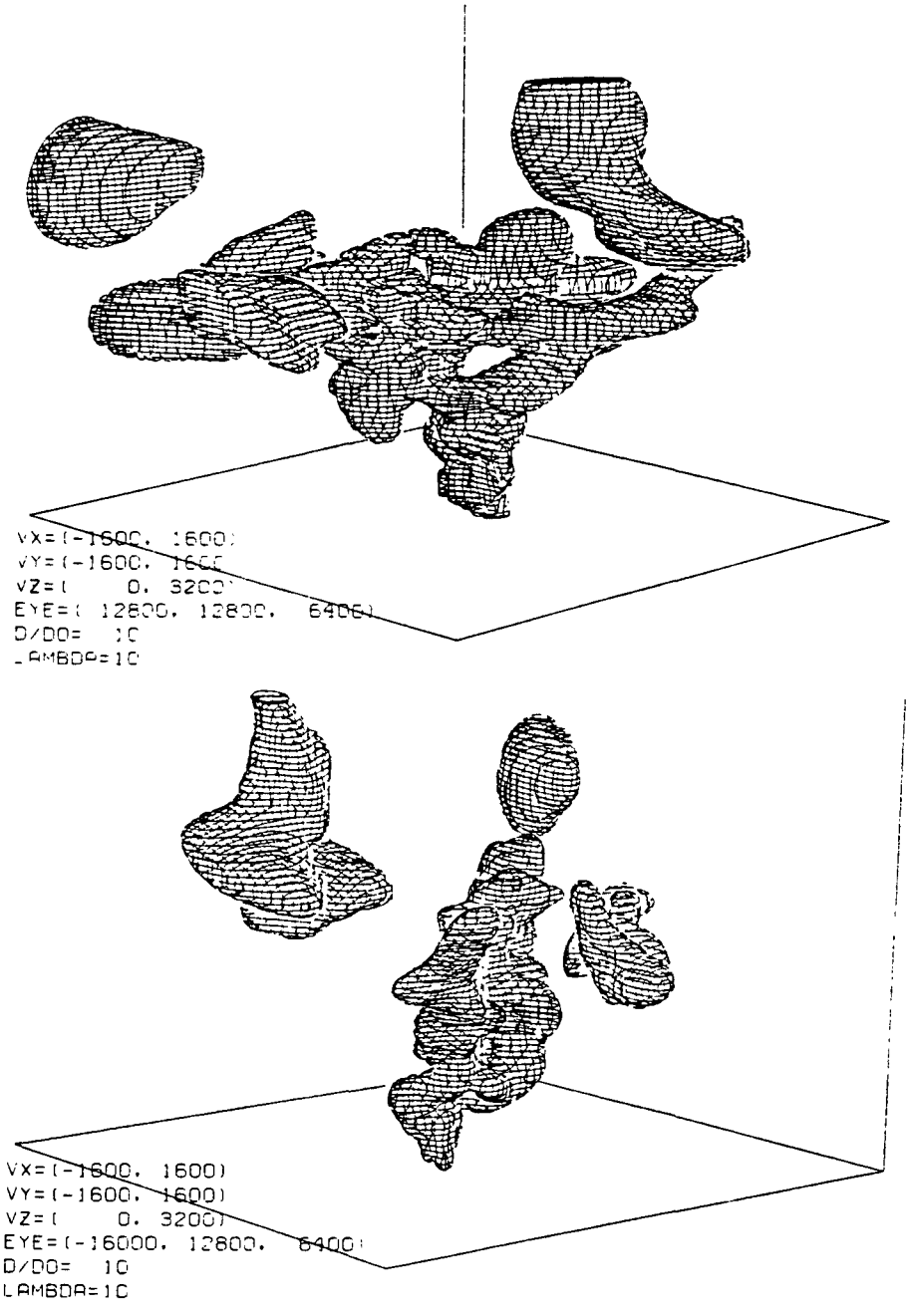


Figure 1: The surface D/D_o=10 of the smoothed density distribution of galaxies in the Local Supercluster (based on the Revised Shapley-Ames Catalog), viewed such that the supergalactic disk is face-on (top), and edge-on (bottom).

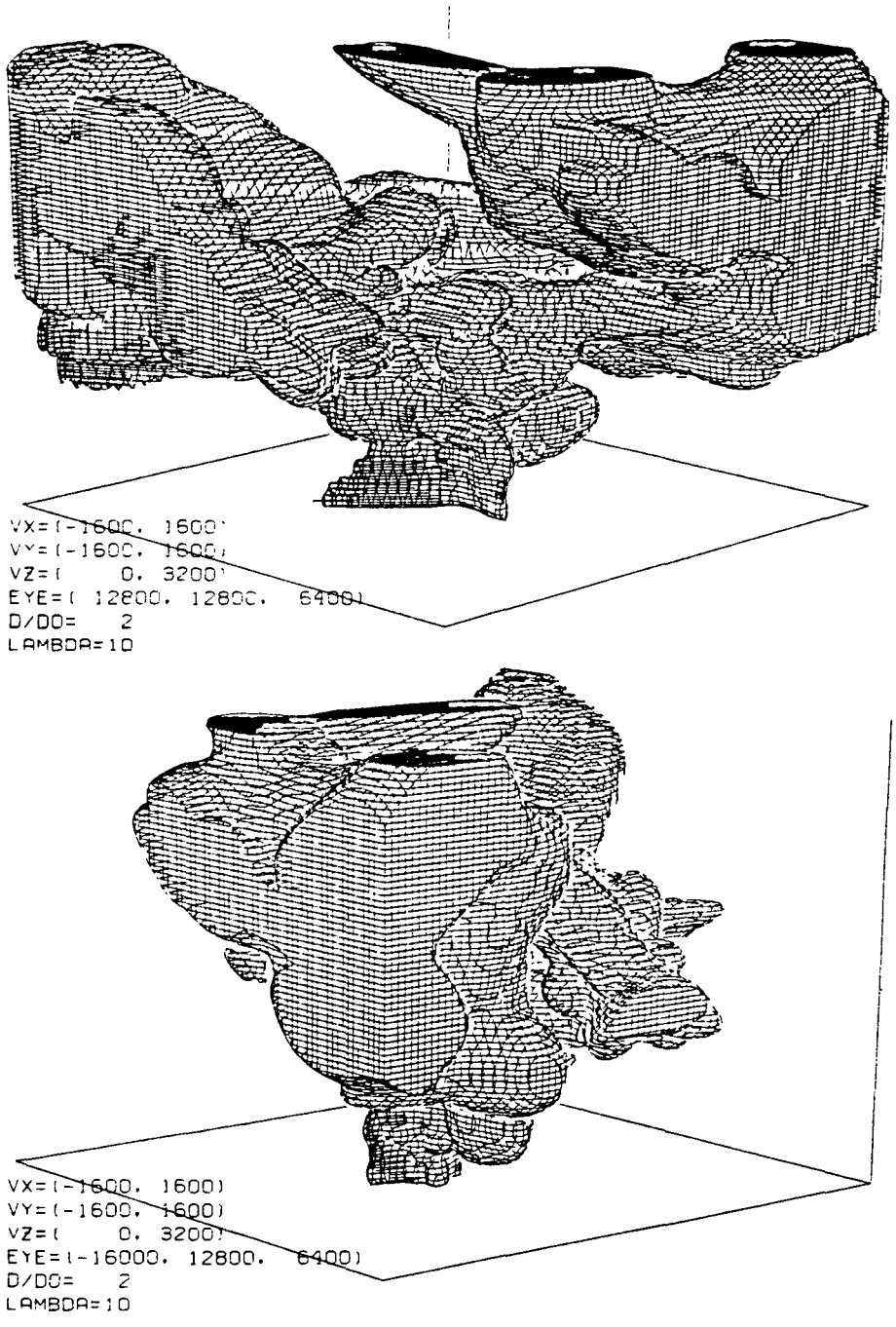


Figure 2: Same as Figure 1, but for the surface $D/D_o=2$. Note that the supergalactic disk has thickened considerably to an axis ratio ~2. Since the bulk of the mass of the Virgo Supercluster is in the lower density regime, this supports the standard interpretation of Virgocentric infall.

the galaxy density. It is another matter to find the requisite alternative scenario, in which the mass distribution on scales of the Virgo Supercluster is dominated by a component that is smoother than the galactic density. Such a smooth component would have to be hot in order not to fall into the potential well created by the galactic distribution, but the existence of a hot component inhibits the growth of gravitational instabilities.

One, somewhat artificial, proposal (Turner, Steigman, and Krauss 1984) is that the smooth component was initially cold, enabling the growth of the perturbations, but then decayed into relativistic particles, and is now smooth. A less exotic possibility is that $\Omega_o<1$, but the universe is still flat because the cosmological constant $\Lambda\neq 0$. Peebles (1984) shows that this possibility is consistent with all existing observations. The difficulty is to explain the the specific value of Λ required; at the end of the inflationary phase the ratio of the thermal energy density to that in Λ is $\sim 10^{-102}$.

Another approach is to argue that the rate of galaxy formation depends on the ambient density, with a higher formation rate in regions of higher density. It is difficult to see how this can come about by gravitational means alone. Galaxies formed at a sufficiently early epoch, when the density perturbation of the Virgo Supercluster was much smaller than it is at the present epoch. How, then, could an incipient 10% perturbation, say, on scales of megaparsecs, affect the gravitational growth of a small scale density perturbation that ends up as a galaxy? But this sort of argument is not tight, since galaxy formation is poorly understood, and some processes might be sensitive to the ambient density. This should be an active area of research in the near future.

Of course, it is also possible that the inflationary scenario is wrong, or that baryogenesis is not due to a microphysical process of baryon nonconservation, or both. In that case, however, we are left to explain the present baryon to photon ratio, and/or the horizon and flatness problems.

V. SMALL SCALE CLUSTERING

Small scale clustering, by which is meant clustering on scales on the order of 1 Mpc and smaller, is of interest in the Virgo Supercluster on two grounds. Ultimately it should provide us with enough information to

understand the process of galaxy formation and clustering, and whether this occurs by hierarchical clustering or by pancake like fragmentation. Of more immediate interest is the answer to the question whether mass estimates based on virial analyses of such small groups and clusters are valid. Since such analyses lead to estimates of the mean mass density of the universe (Faber and Gallagher 1979; Peebles 1976; Huchra and Geller 1982), this question is relevant to the previous discussion.

Burbidge (1975) has argued that there is no evidence against binary galaxies simply being "ships passing by in the night". In that case their relative velocity would be a manifestation of the general galaxian velocity dispersion, and not due to their two-body interaction. If true, this would mean that there is no handle on the mass content in galaxies beyond galactocentric radii of a few tens of kpc, inside which rotation curves can be measured directly (Rubin et al. 1980; Bosma 1983). Rivolo and Yahil (1981) found similar relative velocities for isolated and nonisolated pairs in the RSA Catalog, and concluded that additional criteria were needed to determine if, or which of the pairs were dynamical binaries.

Peebles (1976) argued that for small separations, for which the galaxy two-point correlation function $\xi >> 1$, dynamical equilibrium should be expected. Therefore, the relative force between pairs of galaxies, i.e., the sum of the direct two-body force and the tidal forces due to all the other galaxies, must be balanced by a pressure gradient induced by the relative velocity dispersion. Furthermore, except for a normalization constant, which is proportional to Ω_o, the mean tidal force between pairs of galaxies can be calculated from the three-point correlation function. A measurement of the velocity dispersion thus determines this normalization constant, and hence Ω_o.

Evrard and Yahil (1984a,b) have recently tested both isolated and nonisolated pairs in the end product of the N-body calculation of Efstathiou and Eastwood (1981). They used a very liberal isolation criterion, only that a pair be each other's nearest neighbors. They nevertheless find that at least 75% of such loosely isolated pairs are bound by their two-body force, and satisfy the virial theorem extremely well. While the N-body simulations do not reproduce the observations in detail (see Evrard and Yahil 1984a), the basic conclusion may very well be correct, namely mass estimates based on binary galaxies are valid.

Evrard and Yahil (1984b) also find that virial estimates are satisfied to better than a factor of two for the set of all pairs, which is dominated by the nonisolated pairs. This means that Ω_o can be determined reasonably well from the relative velocity dispersion of galaxy pairs. In the simulations the 1-d relative velocity dispersion for all separations smaller than 1 Mpc is 190 km s^{-1} for the Ω_o=0.1 model, and 825 km s^{-1} for the Ω_o=1.0 model. There is some discussion about the observed value of the velocity dispersion, the quoted range being 100 km s^{-1} to 310 km s^{-1} (Rivolo and Yahil 1981; Davis and Peebles 1983a; Bean et al. 1983). Taking any value in this range, however, comparison with the N-body models clearly favors the case of an open universe. This conclusion is unlikely to be altered by more realistic modeling of extended galaxies and stronger positional correlation, as long as all the mass is assumed to be distributed as the galaxies. A velocity dispersion of 825 km s^{-1} (the Ω_o=1.0 case) can not be dissipated by galaxies whose internal dispersion or rotation velocities are ~150 km s^{-1} (1-d) and stronger clustering will only increase the velocity dispersion.

VI. LARGE SCALE CLUSTERING

Rich clusters are observed to be the "mountain tops" of the galaxian density distribution, with deep saddles separating the peaks. This enables each supercluster, by which is meant one such "mountain", to be treated as a separate dynamical entity. But the central cluster must be included. The Virgocentric infall model used in §III ignores the central cluster. It assumes that galaxies possess only systematic flow velocities, and takes no account of their random velocities. This is a good approximation at large Virgocentric radii, where the effects of pressure gradients are small compared with gravity. But adiabatic compression guarantees that the random velocities do become important further in, and ultimately result in virialization in the central cluster. Any comprehensive theory of the dynamics of superclusters should therefore account for both the central cluster and the infalling supercluster around it.

One attempt at such a theory was recently made by Rivolo and Yahil (1983). They calculated the gravitational growth of a supercluster, maintaining the assumption of the monopole approximation, but allowing each galaxy to have an initial random velocity with both radial and transverse components. While this is admittedly still a very crude model, they were able to reproduce the observational characteristics of both the central

clusters and their surrounding superclusters.

The main conclusions of that investigation were: (1) The density profile of the central cluster is characterized by a peak density $\rho/\rho_o \sim 10^4$, followed by a falloff in which $\rho \propto r^{-2.5}$. (2) The edge of the cluster is delineated by a secondary maximum; this is the point at which galaxies on their first rebound reach the point of maximum expansion. (3) Beyond the edge of the cluster there is pure infall; the density profile depends only on the initial perturbation, and the related peculiar velocity field follows from the standard cold Virgocentric inflow model. (4) The 1-d velocity dispersion of the central cluster in Virgo is predicted to be 750 km s^{-1} (Ω_o=0.1) and 1200 km s^{-1} (Ω_o=0.5); this again favors the lower value of Ω_o. (5) The asymptotic 1-d velocity dispersion of field galaxies as $\delta\rho \to 0$ is 40 km s^{-1} (Ω_o=0.1) and 140 km s^{-1} (Ω_o=0.5); comparison with observations is problematic, because observed values are quoted for complete samples, which contain many pairs that are too close to rich clusters to be considered "asymptotic field galaxies". (6) The initial shells to collapse "soft land", i.e., do not oscillate, and virialize within one dynamical timescale of the collapsed configuration. (7) Subsequent shells, on the other hand, do not relax quickly, and galaxies in them maintain very eccentric orbits; most of the mass observed in the Virgo cluster today is either in its initial infall, or on its first orbit after rebound. (8) Despite the "nonhydrostatic" nature of the cluster, the virial theorem gives a reasonable estimate of the mass of the cluster. (9) The velocity dispersion of the infalling galaxies outside the central cluster is anisotropic, with the transverse dispersion exceeding the radial one. (10) There is a hint that clusters could be late collapsers, with $z_c \sim 0.5$; this can be tested by deep searches for clusters.

VII. SUMMARY

Existing observations are all consistent with a standard baryonic universe with a cosmological density factor Ω_o=0.1-0.2. This includes a comparison of the abundances of the light elements with those predicted from standard big-bang nucleosynthesis, as well as virial estimates of the mass content of galaxies with their massive halos. To that is added the determination of Ω_o from the Virgocentric infall, which is especially important, because it provides an estimate of the mean density on scales of tens of Mpc, both in and out of galaxies, and whether baryonic or not.

N-body simulations support the standard interpretation of a baryonic universe in at least two ways. First, they show that mass estimates based on virial analyses are basically correct. Secondly, they are able to reproduce in detail the observed characteristics of rich clusters of galaxies and the infalling superclusters surrounding them.

An open baryonic universe is inconsistent with some recent theories of elementary particle physics in the early universe, such as baryogenesis by baryon nonconservation, and the existence of an inflationary phase of exponential expansion. Either these theories are wrong, or Virgocentric infall needs to be explained in some other way. Suggestions made so far seem somewhat artificial, but such possibilities need to be explored further.

ACKNOWLEDGEMENTS

This research was supported in part by USDOE grant DE-AC02-80ER10719 at the State University of New York and by a John Simon Guggenheim Fellowship. The hospitality of the Institute of Astronomy at Cambridge, where part of this work was done, is gratefully acknowledged.

REFERENCES

Aaronson, M., Huchra, J., Mould, J.R., Schechter, P.L., and Tully, R.B. 1982, Astrophys. J., **258**, 64.

Aaronson, M., Huchra, J., Mould, J.R., Sullivan, W.T., Schommer, R.A., and Bothum, G.D. 1980, Astrophys. J., **239**, 12.

Albrecht, A., and Steinhardt, P.J. 1982, Phys. Rev. Letters, **48**, 1220.

Bean, A.J., Efstathiou, G., Ellis, R.S., Peterson, B.A., and Shanks, T. 1983, Mon. Not. Roy. Astr. Soc., **204**, 615.

Bond, J.R., and Szalay, A.S. 1983, Astrophys. J., **274**, 443.

Bosma, A. 1983, Internal Kinematics and Dynamics of Galaxies (I.A.U. Symp. 100), ed. E. Athanassoula, (Dordrecht: Reidel) p. 11.

Burbidge, G.R. 1975, Astrophys. J. (Letters), **196**, L7.

Davis, M., and Huchra, J. 1982, Astrophys. J., **254**, 437.

Davis, M., and Peebles, P.J.E. 1983a, Astrophys. J., **267**, 465.

. 1983b, Ann. Rev. Astr. Astrophys., **21**, 109.

Davis, M., Tonry, J., Huchra, J., and Latham, J.W. 1980, Astrophys. J. (Letters), **238**, L113.

de Vaucouleurs, G. 1976, Astrophys. J., **203**, 33.

Dressler, A. 1984, Astrophys. J., **281**, 512.

Efstathiou, G., and Eastwood, T.W. 1981, Mon. Not. Roy. Astr. Soc., **194**, 503.

Evrard, A.E., and Yahil 1984a, preprint.

_____. 1984b, preprint.

Faber, S.M., and Gallagher, J.S. 1979, Ann. Rev. Astr. Astrophys., **17**, 135.

Fiorini, E. 1984, First ESO-CERN Symp., eds. G. Setti and L. van Hove, (Geneva: CERN) p. 81.

Fixsen, D.J., Cheng, E.S., and Wilkinson, D.T. 1983, Phys. Rev. Letters, **50**, 620.

Gunn, J.E. 1983, Internal Kinematics and Dynamics of Galaxies, (I.A.U. Symp. 100), ed. E. Athanassoula, (Dordrecht: Reidel), p. 379.

Guth, A. 1981, Phys. Rev., **D23**, 347.

Huchra, J. 1984, this volume.

Huchra, J.P., and Geller, M.J. 1982, Astrophys. J., **257**, 423.

Kraan-Korteweg, R.C. 1984, this volume.

Linde, A.D. 1982, Phys. Letters, **114B**, 431.

Lubin, P.M., Epstein, G.L., and Smoot, G.F. 1983, Phys. Rev. Letters, **50**, 616.

Peebles, P.J.E. 1976, Astrophys. J. (Letters), **205**, L109.

_____. 1980, The Large Scale Structure of the Universe, (Princeton: Princeton University Press).

_____. 1984, Astrophys. J., **284**, 439.

Rivolo, A.R., and Yahil, A. 1981, Astrophys. J., **251**, 477.

_____. 1983, Astrophys. J., **274**, 474.

Rubin, V.C., Ford, W.K., and Thonnard, N. 1980, Astrophys. J., **238**, 471.

Sandage, A., and Tammann, G.A. 1984, First ESO-CERN Symp., eds. G. Setti and L. van Hove, (Geneva: CERN) p. 127.

Sandage, A., Tammann, G.A., and Yahil, A. 1979, Astrophys. J., **232**, 352.

Schechter, P.L. 1980, Astr. J., **85**, 801.

Silk, J. 1968, Astrophys. J., **151**, 459.

_____. 1974, Astrophys. J., **193**, 525.

Tonry, J.L., and Davis, M. 1981, Astrophys. J., **246**, 680.

Turner, M.S., Steigman, G., and Krauss, L.M. 1984, Phys. Rev. Letters, **52**, 2090.

Uson, J.M., and Wilkinson, D.T. 1984, Astrophys. J., **283**, 471.

Yahil, A. 1981, 10th Texas Symp. Rel. Astrophys., eds. R. Ramaty and F.C. Jones, Ann. N.Y. Acad. Sci., **375**, 169.

Yahil, A., Sandage, A., and Tammann, G.A. 1980, Astrophys. J., **242**, 448.

Yang, J. Turner, M.S., Steigman, G., Schramm, D.N., and Olive, K.A. 1984, Astrophys. J., 281, 493.

Zel'dovich, Ya. B. 1970, Astr. Astrophys., 5, 84.

DISCUSSION

E. SHAYA: What do you expect the outer contours of a pancake to look like today? Would not a pancake pull the background material onto it so that the lowest contours are more or less spherical?

A. YAHIL: Certainly, the central high density disk of the Virgo Supercluster might be a pancake, and the surrounding lower contours would be the background material that is pulled in more or less spherically. Now, the galaxies in the inner high density disk may or may not be the result of pancake fragmentation, but the pancake model does not explain how galaxies form in the outlying shells, which is the main point I was making. Furthermore, the Virgocentric infall is measured for these outlying shells, so the standard derivation of Ω_0 holds in your scenario as well.

H. MacGILLIVRAY: In support of your last remark, I can confirm that a British group (Stevenson, Shanks, Fong, and MacGillivray) have found that the amplitude of the two-point correlation function for galaxies down to B ~ 24 mag is less than predicted from scaling the relationship for bright galaxies. This would support your suggestion that cluster formation may have been a recent (i.e., late epoch) phenomenon.

O.-G. RICHTER: Do you get from your model, and the numbers resulting from it, a mass infall rate?

A. YAHIL: Yes, although you have to specify exactly what you mean by infall rate. One way is simply to look at $4\pi r^2 pv$ at points of interest, for example at what we call the edge of the central cluster (the point of maximum expansion after the first rebound, and the location of the secondary density maximum). If you do that you obtain numbers $\sim 10^5\ M_\odot$ for younger clusters, dropping off to $\sim 10^4\ M_\odot$ for older clusters. For details see Rivolo and Yahil (1983).

DYNAMICS OF THE LOCAL SUPERCLUSTER AND THE VIRGO CLUSTER

EDWARD J. SHAYA
California Institute of Technology, Pasadena

AND

R. BRENT TULLY
University of Hawaii, Honolulu

I. INTRODUCTION

This talk is a discussion of the velocity fields and the galaxy distributions in the Local Supercluster, with special emphasis given to determinations of the mass and the dynamical history of the Virgo Cluster. By examining the velocity field of the galaxies near the Virgo Cluster for the gravitationally induced retardation of expansion, one can obtain an independent check on the virial theorem estimates of the mass of the cluster. In addition, modeling of this velocity field gives us the rate of infall of galaxies into the cluster. Detailed knowledge about the accretion rates of galaxies into clusters is an important aid in understanding cluster evolution and dynamics. By examining galaxy motions throughout the rest of the Local Supercluster, one can determine the mass distribution out to large distance from Virgo. Peculiar motions of the clouds of galaxies with respect to the Virgo influenced flow will also be apparent from these studies.

One example of an analysis of the velocity field around Virgo is the Hoffman *et al.* (1980) analysis of the velocity dispersions along lines-of-sight about the direction to Virgo. They determined the mass of the Virgo Cluster to be $7 \times 10^{14} M_{\odot}$ and the turnaround radius (the shell where $v_{virgo} = 0$) to be $\theta \approx 27°$ from Virgo. This mass determination is in excellent agreement with both of the earlier virial theorem calculations (Smith 1936, Oort 1958: $M_{Virgo} = 7.5 \times 10^{14} M_{\odot}$). It is a simple matter to count up all the galaxies within this turnaround radius to determine the number of galaxies that will fall into the Virgo Cluster in the next Hubble time. It turns out that in the next $\frac{2}{3} t_o$ the number of bright galaxies in the Virgo Cluster will increase by 70%. As the cluster undergoes this significant growth, the fraction of ellipticals will drastically decrease because the infalling population is primarily composed of spiral galaxies.

II. AN INFALLING CLOUD

Brent Tully and I have determined the mass of the Virgo Cluster in a new way which is related to the Hoffman *et al.* velocity dispersion technique. The major difference is that, in this study, the lines-of-sight were chosen judiciously with the help of 3-dimensional maps of the Local supercluster to aid us. Almost contiguous to the 6° circle of the Virgo Cluster is a part of the Virgo II Cloud of galaxies known as the Virgo Southern Extention. This cloud was noted by Tully (1982) to have a high velocity dispersion compared to similar clouds in the Local Supercluster and, when viewed with the assumption that recessional velocity is proportional

to distance, appears to be elongated along the line-of-sight (the structure between the arrows in Fig. 1).

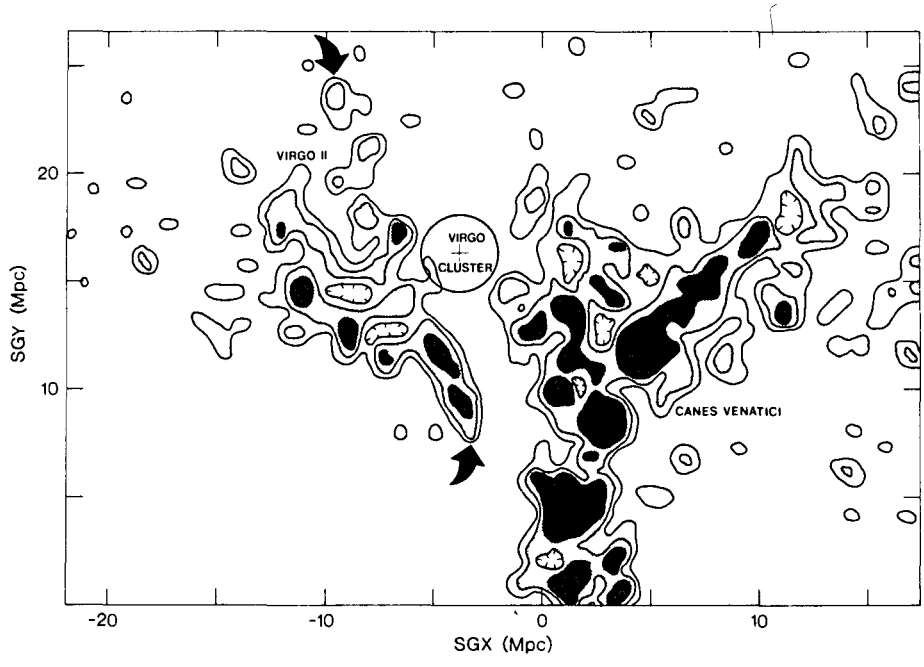


Fig. 1 – A view from the pole of the Local Supercluster of the two principal clouds which constitute the plane of the supercluster. We are located at the origin of the coordinate system. The map was plotted assuming uniform Hubble flow across the entire region. The elongated feature which points toward us (bracketed by the two arrows) is a kinematic effect caused by the breakdown of the Hubble flow near the cluster.

The higher velocity members are expected to be nearer to us and falling into the cluster and away from us and the opposite holds for the lower velocity galaxies. A simple interpretation is that this cloud of galaxies has been feeling a strong gradient in the gravitational field of Virgo. The gravitational field has caused the galaxies closer to the cluster to infall at higher velocities than the ones more distant. The magnitude of the velocity difference of each galaxy from the velocity of Virgo (here taken to be the velocity of M87) as a function of angle from the center of Virgo is plotted in Figure 2. With the M87 velocity taken for the velocity of the center of Virgo there is symmetry in the excursions of velocity differences from the Virgo velocity between the nearer and farther galaxies. Interestingly, if one insists that the velocity of the gravitational center of Virgo is at the mean unweighted velocity of the Virgo galaxies of 1004 km s^{-1} there would be an offset in the figure which would imply an orbital motion for

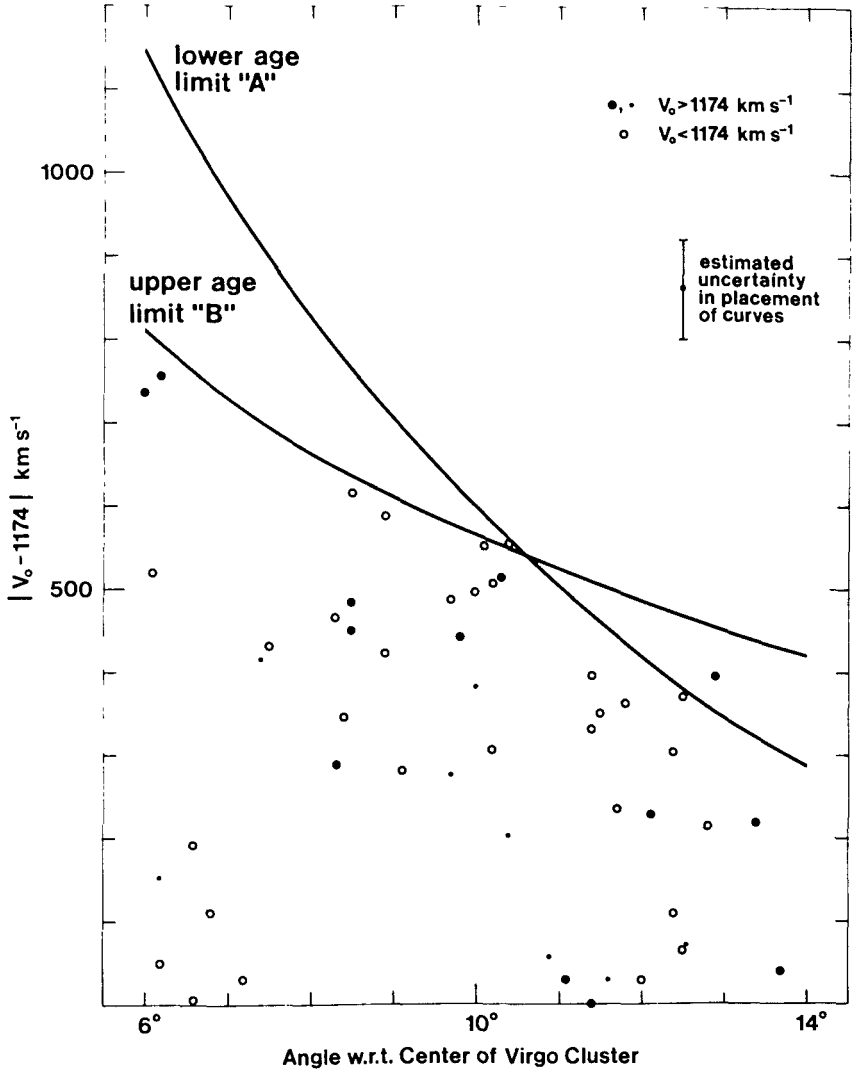


Fig. 2 – Infall velocity projected into the plane of the sky, assuming a cluster velocity of 1174 km s^{-1}. Open circles: galaxies falling toward the cluster and toward us; large dots: galaxies falling toward the cluster but away from us; small dots: galaxies expanding away from the cluster and us. Limit A: $M = 18 \times 10^{14} M_\odot, t_o = 6$ Gyr. Limit B: $M = 5 \times 10^{14} M_\odot, t_o = 50$ Gyr.

the cloud of 170 km s^{-1} around the center of Virgo.

The local maximum radial velocities for different lines-of-sight and at distances nearly equal to the Virgo distance were calculated from the Friedmann model (see Tully and Shaya 1984 for details). The model fits, shown as dotted lines in Fig. 2, are for two extreme values for the age of the universe. In Fig. 3, the solid lines enclose the masses required to fit the envelope in Fig. 2 as a function of the age of the universe. The dotted lines enclose the masses required to fit the envelopes when a velocity of 1004 km s^{-1} is taken to be the Virgo velocity. The range in mass permitted by the virial theorem is also presented in Fig. 3; agreement is found between the two techniques for ages of the universe between 10-15 Gyr.

III. VIRIAL ANALYSES

In view of the conclusions earlier that many spirals are presently falling into Virgo, the application of the virial theorem to this ensemble may seem reckless, and, one may even wonder why there would be agreement at all with the other mothods described here. But perhaps if the virial theorem is applied separately to the different morphological types, we could gain important insights on both the mass and the dynamical history of the cluster. It should be kept in mind that even if all the galaxies examined in a virial theorem analysis had just fallen in from very great distances, the application of the virial theorem would result in an overestimate of the mass by at most a factor of four because the rms escape velocity is only twice the rms velocity in any virialized system.

The Virgo ellipticals have a centrally condensed distribution (the scaleheight is about half of that in the spiral distribution – Tully and Shaya 1984) and appear to form a relaxed cluster at the core of the cluster. The situation is reminiscent of the numerical models of Rivolo and Yahil (1983) in which the earliest participants of a collapse undergo strong accelerations and phase mixing, thereby virializing in a short time (a "soft landing"), on the other hand, the later arrivals retain initial orbital phase information for significantly longer times. If the elliptical system is indeed relaxed, and since it does not sample the full cluster volume, then the mass derived from the virial theorem based only on ellipticals could be taken to be a lower limit to the total cluster mass. The spiral sample probably contains a substantial fraction of recent arrivals carrying excess amounts of kinetic energy and thus would provide an overestimate of the mass.

The virial analysis was carried out on three samples (see Table 1): (1) all 186 galaxies with known velocities in the Virgo Cluster, (b) the 75 bright ellipticals and S0 galaxies in the cluster, and (c) the just 30 ellipticals. With each of the three samples, two cases were considered. In one case, the virial analysis involved the standard mass weights with the assumption of a constant mass-to-light ratio. In the second case, all galaxies were given equal weights. As it turned out, the virial mass determination of the spirals is only about a factor of two greater than the E+S0 subsample, so in fact the mass determined by considering all galaxies, which is between the other two values, certainly can not be far off. Our best estimate for the mass

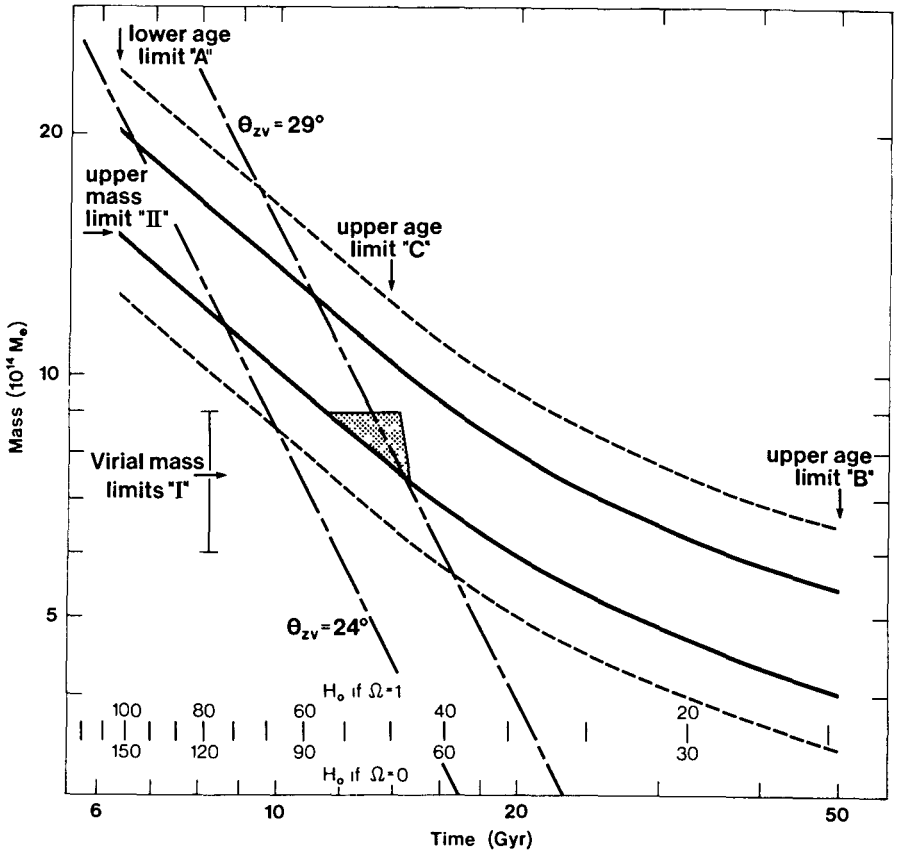


Fig. 3 – The mass-age family of models which satisfy the observed infall motions. The two solid curves correspond to models which give fits to the data displayed in Fig. 2 which are offset from the best fit by the amount shown by the error bars. The dashed curves correspond to models in agreement with a Virgo velocity given by the unweighted mean velocity of the Virgo galaxies. Age limits A and B are set by the acceptable range of slopes of the curves in Fig. 2. Mass limits I are given by the virial analysis of the Virgo Cluster. Mass limit II is a projection of the upper limit given by the virial analysis for the mass within 6° *of Virgo to a radius of* 10° *characteristic of the infalling galaxies, assuming a density fall off of* r^{-2}. *The two sloping parallel lines correspond to the* 24° *and* 29° *limits for the turnaround radius cited by Hoffman et al.*

of the cluster is a compromise between the extreme limits:

$$M_{Virgo} = 7.5 \pm 1.5 \times 10^{14} M_{\odot}.$$

An integrated blue luminosity of $1.7 \pm 0.2 \times 10^{12} L_{\odot}$ was determined by Tully and Shaya (1984) for the cluster, so the mass-to-light ratio is then:

$$M_{Virgo} = 440 \pm 100 \frac{M_{\odot}}{L_{\odot}}$$

Table 1

VIRIAL ANALYSIS OF THE VIRGO CLUSTER

Case	N_{char}	R_{Ω} (Mpc)	σ_v (km s^{-1})	M_{VT} ($M_{\odot}$)	t_c (years)
All types					
1) luminosity weights	18	0.77	750	9.6×10^{14}	
2) equal weights	186	0.76	716	8.6×10^{14}	3.6×10^{9}
E+S0					
1) luminosity weights	9	0.67	552	4.7×10^{14}	
2) equal weights	75	0.63	597	5.0×10^{14}	3.6×10^{9}
Ellipticals Only					
1) luminosity weighted	5	0.49	590	4.1×10^{14}	
2) equal weights	30	0.42	678	4.3×10^{14}	2.1×10^{9}

IV. THE VIRGOCENTRIC VELOCITY FLOW

With the aid of velocity independent distance indicators, it is now possible to get a crude map of the velocity flow over the entire supercluster. There are now over 500 spiral galaxies with velocities less than 3000 km s^{-1} for which distances can be obtained utilizing at least one of the following five relationships between the global properties of spirals: (1) $H_{0.5}^{b,i}$ versus W_{20}, (2) $B_T^{b,i}$ versus W_{20}, (3) $D_{25}^{b,i}$ versus W_{20}, (4) $B_T^{b,i}$ - $H_{0.5}^{b,i}$ versus $H_{0.5}^{b,i}$, and (5) $D_{25}^{b,i}$ versus $H_{0.5}^{b,i}$. Aaronson *et al.* (1982) derived parameters of the Local Group motion and density distribution, with the assumption that the density falls as some power of the radius, by fitting a cosmological model to the 306 galaxies for which distances have been estimated from relation (1) above. Rather than fit a model of the velocity flow and, as in Aaronson *et al.*, search for a minimum in χ^2, we choose to take the observed run of velocity with Virgocentric distance and *derive* the radial mass distribution, without any assumptions about the shape of the distribution.

Fig. 4 shows Virgocentric velocity as a function of distance from Virgo for 280 galaxies outside of the Virgo cluster and with v $\leq$ 3000 km s^{-1}. The 3 dimensional position of each galaxy was determined from the position in the sky plus one or more of the velocity independent distance methods. The two quantities of Fig. 4 were calculated assuming this is the precise location of the galaxy and all motions are directed radially to or from the center of the Virgo

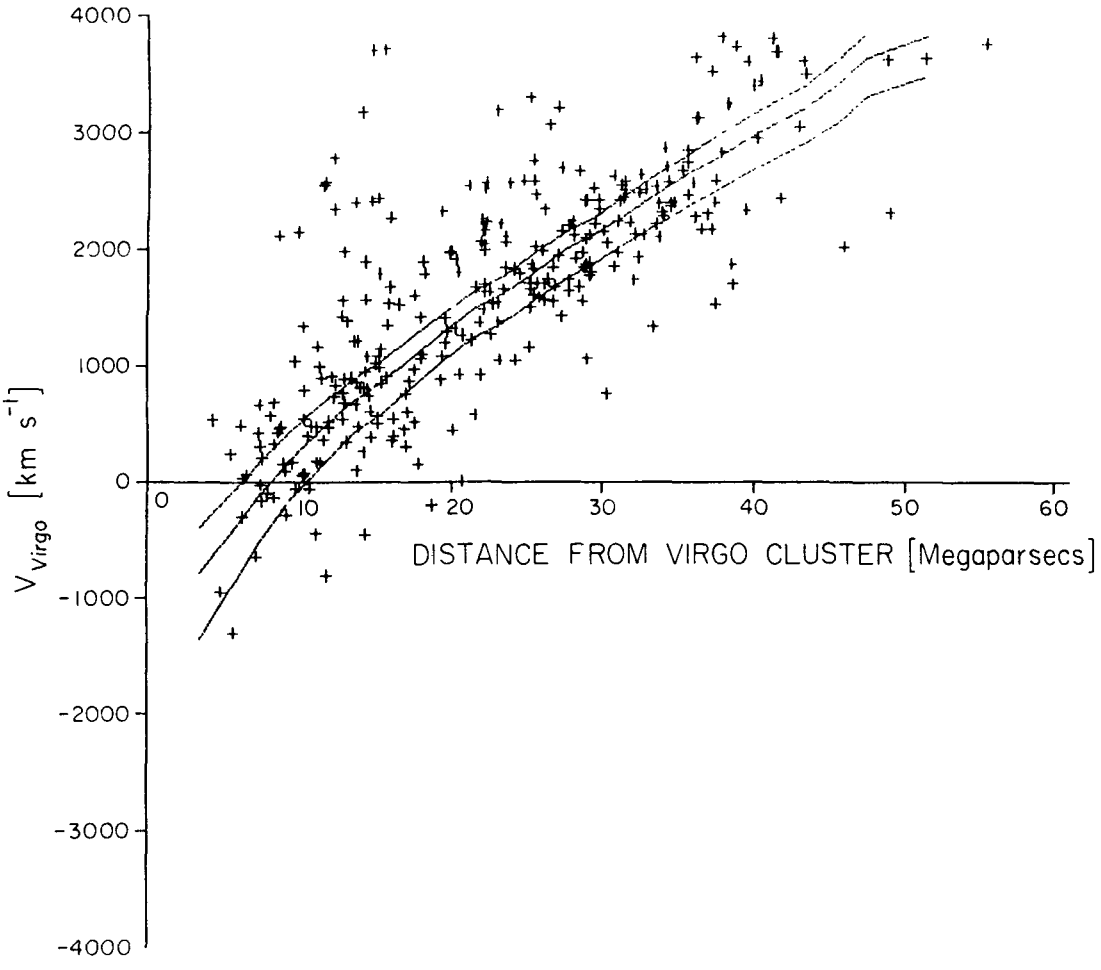


Fig. 4a – The Virgocentric velocity flow of 280 galaxies outside of the Virgo Cluster and with $v < 3000 kms^{-1}$. *Distance from Virgo and velocity with respect to Virgo are calculated assuming the distance to each galaxy is given precisely by the velocity independent distance indicators and all motions are along the radial vectors to the cluster center. The middle line is a model in which the cluster has* $8 \times 10^{14} M_{\odot}$, *and there is constant density outside of Virgo such that the mass internal to 20 Mpc is twice the Virgo mass. An age of 13 Gyr. is taken for the universe. The lower line has all masses doubled and the upper line is with all masses halved.*

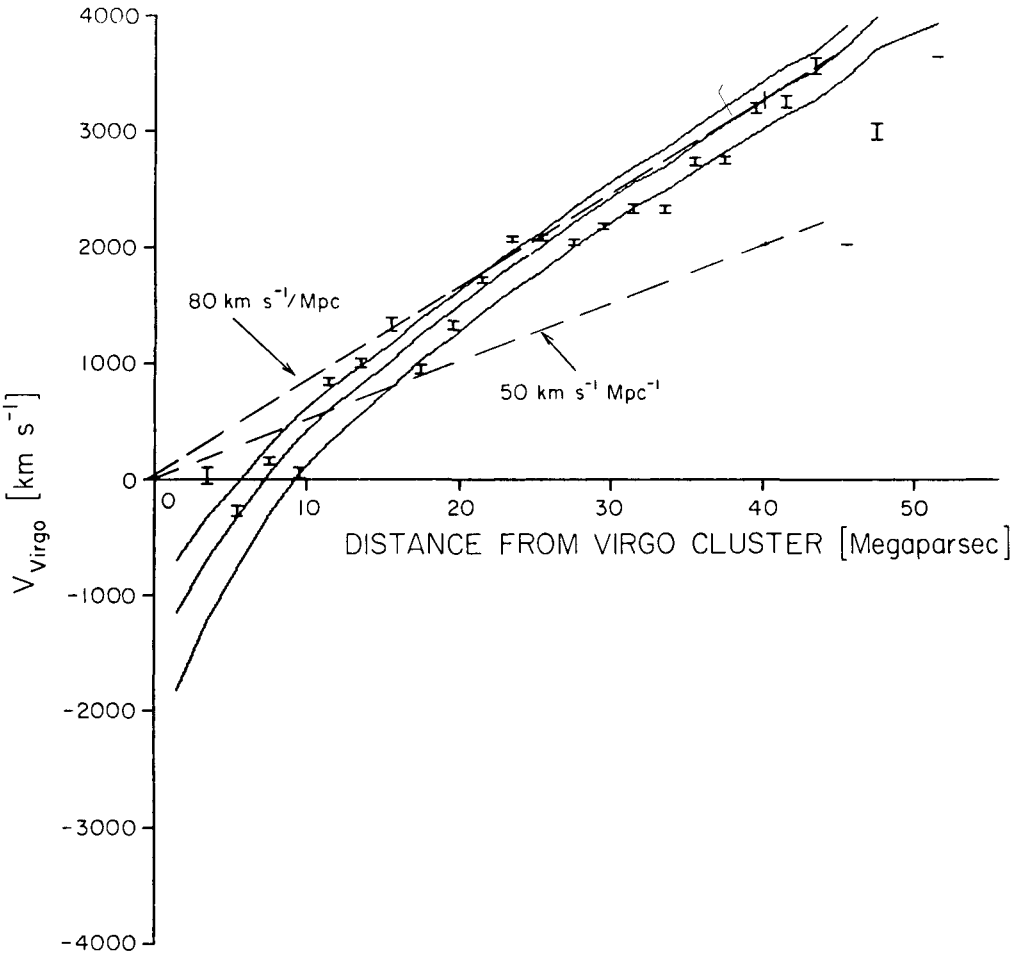


Fig 4b – The Virgocentric velocity binned into 2 Mpc intervals in radius. Each galaxy in 4a was weighted according to the uncertainty in Virgocentric velocity associated with a 25% error in distance.

Cluster. Although the scatter may at first appear discomforting, the scatter is drastically amplified by the deprojection into Virgocentric coordinates.

Monte Carlo simulations of this region reproduced the general trends in the scatter when errors in the distance of 25% (1 σ) were introduced. This is significant because 25% is the quoted error in the distance determination methods and it would, therefore, imply that peculiar motions from the smoothed Virgo influenced flow can not be even as great as 200 km s^{-1}.

The galaxies were weighted according to the spread in their calculated Virgocentric velocities if they were instead situated anywhere between -25% and +25% of their accepted distance. Mean velocities in 2 Mpc bins in radius were calculated (Fig. 4b). For a given age of the universe, each binned velocity independently defines the mass internal to that shell. In Fig. 5 are displayed the integrated mass distributions resulting from Friedmann models for each binned radius and velocity, and for two different values for the age of the universe. It should be noted that the slope in Fig. 4 at large radii is consistent with a Hubble Constant of $\approx$ 80 km s^{-1} Mpc^{-1} and, with that caveat, there can be no solutions, in this analysis, with ages older than $\frac{1}{H_0} \approx$ 13 Gyrs. As one varies t_0, a wide range of mass profiles results from the observed velocity flow. Each implies a radically different mass-to-light ratio as a function of Virgocentric radius and different total masses for the whole region.

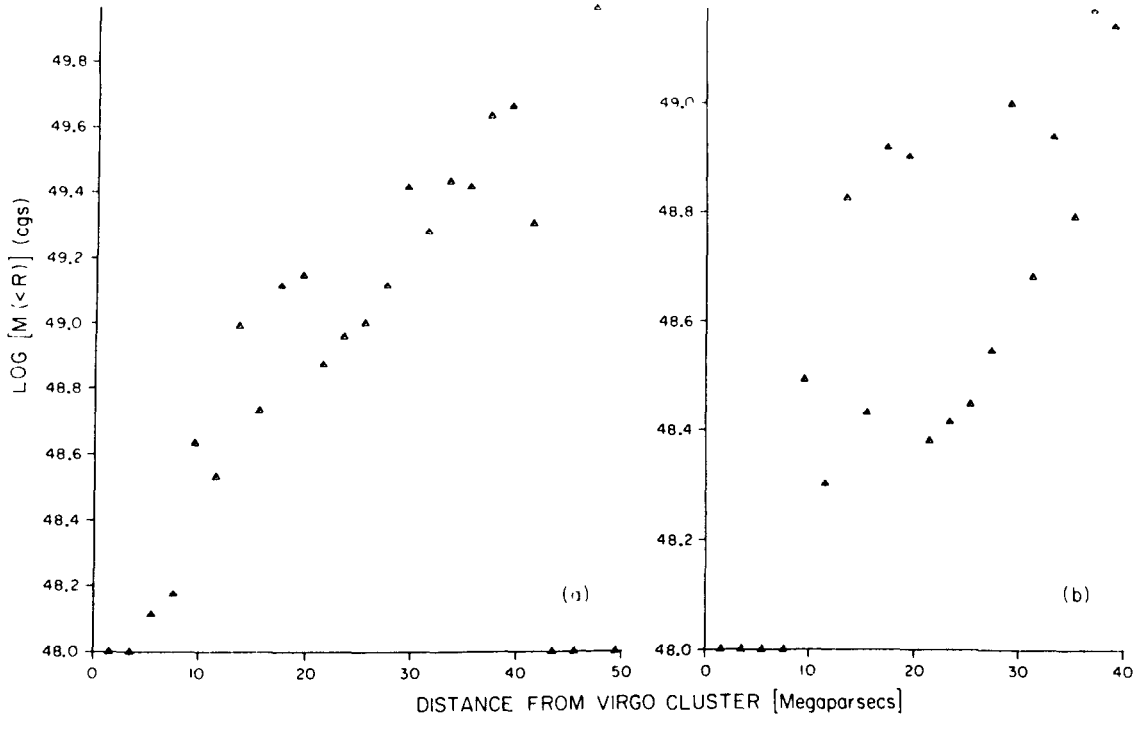


Fig. 5 – The integrated mass distribution in 2 Mpc intervals of radius for two different ages of the universe. (a) t_o = 10 Gyr; (b) t_0 = 12 Gyr. Each binned velocity in Fig. 4b independently determines the corresponding mass at that radius in this figure.

V. CONCLUSIONS

1. There is presently a large flux of predominantly spiral galaxies falling into the Virgo Cluster.

2. The infall velocities of galaxies near the cluster are consistent with the virial theorem mass determinations if the universe is between 10-15 Gyrs.

3. The virial theorem mass determined from Virgo spirals is only 2.2 times the mass determined from the Virgo ellipticals.

4. The expansion of galaxies out to recessional velocities of 3000 km s^{-1} is relatively undisturbed aside from the Virgo Cluster, and spherically symmetric about the cluster.

5. Motions deviating from the Virgo influenced flow are usually less than 200 km s^{-1}.

REFERENCES

Aaronson, M., Huchra, J., Mould, J., Schecter, P., and Tully, B. 1982, *Ap. J.*, **258**, 64.

Hoffman, G. L., Olson, D. W., and Salpeter, E. E. 1980, *Ap. J.*, **242**, 861.

Rivolo, A., and Yahil, A. 1983, *Ap. J.*, **274**, 474.

Tully, R. B. 1982, *Ap. J.*, **257**, 389.

Tully, R. B., and Shaya, E. J. 1984, *Ap. J.*, **281**, 31.

THE TERMINATION OF GALAXY FORMATION BY CLUSTER FORMATION

R. Brent Tully
Institute for Astronomy, University of Hawaii

This review will contain a Hawaiian perspective of aspects of the evolution of the Virgo Cluster and the effect of such an environment on the formation and evolution of galaxies. There will be an attempt to draw connections between five fragments of information and ideas: (i) the distribution of galaxies in the supercluster about Virgo is very clumpy, (ii) at least the outer parts of spiral galaxies probably formed relatively recently, (iii) both galaxies and larger-scale structure within the supercluster might be in, or near to, a tidally limited regime, (iv) large-scale tidal fields can dictate the morphologies of galaxies, and (v) a color-magnitude diagram might contain information on the recent evolution of the cluster.

1. A Clumpy Local Supercluster. It is becoming generally appreciated that galaxies have a strong propensity to cluster and that the fraction of isolated galaxies is extremely low. The situation in the Local Supercluster centered on the Virgo Cluster was described by Tully (1982, Ap.J. 257:389). The important result to recall is that 98% of galaxies in a zone about Virgo are contained in only 11 clouds that fill roughly 5% of the available volume.

Now, given the reasonably consistent estimates that have emerged for the mass of the Virgo Cluster and our knowledge of the velocity field of the supercluster (cf. Shaya, this proceedings), one very predictable matter is the time it will take for any given entity in the supercluster to fall into the Virgo Cluster. We can say with considerable confidence that membership in the cluster will roughly double with a doubling of the age of the universe and quadruple with a quadrupling of the age of the universe. By that time, almost the entire supercluster, as we usually think of it, will have been swallowed by the central cluster. What will happen after that depends on the mean density of the universe.

Two points: (a) It has to be appreciated that many galaxies could have fallen into the cluster relatively recently, just as many galaxies will do so in the near future. (b) Because of the clumpy distribution of galaxies, the cluster enrichment rate will be very irregular, with few galaxies arriving for long periods and many galaxies arriving in short intervals. Tully and Shaya (1984, Ap.J. 281:31) point out that right now, and for the next 3 billion years, the infall rate is very high. By happenstance, there is a major cloud falling into

the cluster today. Later, the cluster will experience a drought for roughly 8 billion years, until another large entity is captured.

2. Has Galaxy Formation Continued Until Recent Epochs? 'Recent', in the present context, is in comparison with the time it took for the initial collapse of the Virgo Cluster. Is the tidal field of the cluster a major consideration during the period of galaxy formation? Shaya and Tully (1984, Ap.J. 281:56) argued that galaxy formation at the Holmberg radius of spirals must have been going on when the universe was at least 2 billion years old, which is the epoch of the collapse of the core of the Virgo Cluster.

The arguments that lead to this minimum age for the formation of the outer disks of spirals will be reviewed. It is assumed that galaxies receive their angular momentum from a primordial cloud that is torqued by an external tidal field. The primordial cloud collapses in shells, with the collapse time of each shell governed by the density internal to the shell. It is further assumed that each shell attempts to dissipate energy and collapse to a condition of centrifugal equilibrium. Shells with a lot of angular momentum need not fall very far, while shells with little angular momentum must collapse a long way (shells with no angular momentum fall to the center). The collapse time depends directly on the radius of the shell before collapse, to the power 3/2, and inversely on the mass within the shell as collapse begins, to the power 1/2. Consequently, the minimum collapse timescale to a given radius requires a minimal turnaround radius (hence a minimal collapse factor, hence maximal angular momentum content) and maximal mass driving the collapse compared with the mass measured to exist within the specified radius after collapse (hence a maximal amount of unseen matter which could not dissipate energy and most of which remains at large radii [Fall and Efstathiou 1980, M.N.R.A.S., 193:189]). Tidal torquing provides the maximum angular momentum to matter at the limit of tidal break-up. There is a maximum amount of matter to drive the collapse if essentially all the matter is in a halo that could not dissipate energy during collapse and the matter that does dissipate energy to form the galactic disk is only a trace component. It is these extreme limits which give a minimum collapse time of 2 Gyr to the Holmberg radius and forces the conclusion that galaxy formation was an ongoing process after cluster formation had commenced.

3. Tidal Fields in the Local Supercluster. The mass that is observed to exist in the vicinity of the Virgo Cluster creates a tidal field that can be calculated. With reasonable models concerning the growth of that mass concentration, the evolution of the tidal field is constrained (Tully and Shaya 1984, cited). There

can be circumstances when the tidal field prevents the collapse of clouds that would have sufficient density to be bound if they were isolated.

We can ask if a shell of gas in a primordial cloud about a galaxy will collapse into the galaxy or if it will be stripped away. There is a mean density of the galaxy as seen by the shell and a mean density of the structure that creates the external gravitational field, and associated with each of these mass concentrations there is a collapse timescale. If the collapse timescale toward the external (or larger-scale) structure is the shorter, then the shell will be stripped from the galaxy. Consequently, an isolated galaxy can continue to accrete shells of every lower density (yet above the critical density) but accretion from a primordial cloud is inevitably discontinued once a galaxy falls into a cluster.

The process is repeated on larger scales. Groups of galaxies can be disrupted by clusters. Certain of the clouds discussed by Tully (1982, cited) are elongated in the direction of the Virgo Cluster, a condition that must be a consequence of the tidal field of the cluster. In a study in progress of the velocity fields of these clouds, and making use of distances independent of velocities, we are concluding that these clouds are not bound, though sub-units might be.

Viewed from the perspective of a single particle, the process is a race, though with predictable results. All particles in regions in excess of the critical density will eventually be caught up in a collapse. Particles in regions of smaller scale enhancements will participate in multiple collapse events while particles in the local minima may only join the large-scale collapse (hence it would be surprising if the mass-to-light ratio does not increase with scale). In any event, cluster formation inevitably brings an end to galaxy formation.

We must be approaching this moment across the whole Local Supercluster. All matter within 8 Mpc of the Virgo Cluster (if we are at 17 Mpc) is now caught up in large-scale collapse. In addition, there is action on smaller scales, with the influence of neighboring galaxies and groups certain to be important. At the present epoch within the Local Supercluster, tidal fields must be making it difficult for galaxies to retain the remnants of the primordial clouds that they formed from.

4. Galaxy Morphologies. It follows from the discussion in the previous section that a tidal field has one important effect on galaxy morphology: it can cut off gas replenishment. In the extreme, galaxies that fell into the Virgo Cluster with the initial collapse when the universe was only 2 billion years old have

been deprived of infalling gas for the last 10 billion years or so. It has been argued by Larson, Tinsley, and Caldwell (1980, Ap.J. 237:692) that galaxies will exhaust their gas on much shorter timescales through star formation. If true, then galaxies that are gas-rich today have depended on replenishment from infall. Galaxies that arrived early in clusters would be gas depleted by now. This mechanism explains the high incidence of such systems in clusters without recourse to hypotheses such a ram pressure stripping, ablation, and two-body encounters. The gas-rich galaxies found in clusters would be recent arrivals. The incidence of gas-rich systems in the Virgo Cluster can be explained if galaxies have arrived in the cluster in the recent past at the same rate that they will arrive in the near future.

Another influence of the cluster tidal field may be just as important. Galaxies presumably get their angular momentum from torquing by such tidal fields, with the angular momentum acquired at a given moment dependent on the product of the quadrupole moment of the body being torqued and the strength of the external field. As shells collapse, their quadrupole moment diminishes. If a galaxy is moving away from the external tidal field, as would generally be the case in the expanding universe, then the tidal field is falling with time as well, the coupling with the tidal field is broken, and the galaxy subsequently conserves angular momentum as it collapses and spins up.

By contrast, consider the situation if a shell is collapsing while the system as a whole is falling toward a cluster. Now, the tidal field is growing, so the shell may continue to be torqued even as it collapses and spins up. The major axis of the shell can rotate through the direction of alignment with the tidal field and a counter torque can be experienced. Numerical modeling by Shaya and Tully (1984, cited) indicates that the effect can be realized with the tidal field calculated to exist about the Virgo Cluster. A succession of collapsing shells with different degrees of torquing and counter torquing would presumably give rise to a system with relatively low angular momentum. Thus, the first generation galaxies in a cluster could be expected to have low angular momentum content. Presumably, as they are subsequently deprived of gas, such galaxies would become ellipticals.

A cluster would then be composed of systems that arrived very early that have low angular momentum and are gas depleted (ellipticals), systems that arrived moderately early that had already formed high angular momentum disks but have subsequently been deprived of gas (SOs), and systems that arrived recently that

retain their high angular momentum disks and have not had time to use up their gas (spirals).

5. The Cluster Color-Magnitude Diagram. Gas-rich and gas-poor galaxies in the Virgo Cluster are well separated on a blue-infrared color-magnitude diagram (Tully, Mould and Aaronson 1982, Ap.J., 257:527). The weak color dependency seen in the gas-poor systems is take to be principally the consequence of the metallicity dependency of the colors of red giant stars. The stronger color variations seen in the gas-rich systems can be attributed to contributions from young stars, metallicity gradients, and, perhaps, variations in the initial mass function. The galaxies on the gas-rich branch of the Virgo color-magnitude diagram could be modeled and it was found that if star formation was arrested for roughly 4 billion years the models evolved to the gas-poor branch.

In the context of the scenario that was presented earlier, it might be expected that galaxies would evolve from the gas-rich branch to the gas-poor branch once they fall into a cluster. Since the Virgo galaxies that have so far been studied photometrically lie discretely on one branch or the other, the interpretation would be that these systems have arrived in the cluster either very recently or very long ago (compared with timescales of 3-4 billion years to use up their gas and then to evolve in color). More complete Virgo samples might reveal the presence of intermediate cases, and surely intermediate cases must exist in other clusters if the ideas presented here have some validity.

DISCUSSION

R. GIOVANELLI: (a) If isolated galaxies are still growing, then gas reservoirs are being accreted. We searched for HI in the far periphery of very isolated galaxies and found none.

(b) It bothers me that the sizes of gaseous disks are remarkably similar in spirals over a wide range of local densities: isolated, in pairs, in groups, they all seem to have the same size (except in cluster cores). However, gas disks are the most vulnerable parts of galaxies: shouldn't they vary in size more smoothly as tidal effects can be severe in groups as well?

B. TULLY: (a) In previous surveys, a modest fraction of spirals do have HI extending out as far as 6 Holmberg radii.

(b) Loose groups are probably only forming today. So galaxy formation in such environments might only be drawing to a close at the present epoch. It may only be in significantly denser environments that gas replenishment was shut off long enough ago to have an effect.

R. GIOVANELLI: (1) Would you interpret spirals in clusters with deficient gas content as gas poor because of arrested disk growth?
(2) Then why do they have "normal" optical diameters and shrunken gaseous disks?

B. TULLY: (1) Yes. (2) Maybe gas replenishment has been arrested only recently in the mean and the effect is more immediate on gas content.

THE LOCAL GROUP VELOCITY AND THE VIRGO CLUSTER

R.D. Davies & L. Staveley-Smith
Nuffield Radio Astronomy Laboratories
Jodrell Bank
Macclesfield
Cheshire

The Local Group of galaxies, which includes the Milky Way and the Andromeda nebula as the principal objects, will have a velocity relative to the mean Hubble flow in the local region of the Universe. This velocity is likely to have a number of components. (1) A velocity which reflects the random motion of mass aggregates the size of the Local Group ($\sim 10^{12} M_\odot$). (2) A velocity induced by the gravitational attraction of the nearest cluster of galaxies, namely the Virgo cluster with a mass of 5.10^{14} $M_\odot$. (3) The velocity induced by more distant clusters of galaxies; these are in the recession velocity range 3000 to 6000 km s^{-1}; some of these clusters have masses approaching 10^{16} $M_\odot$ and may give rise to velocities comparable with that induced by the Virgo cluster.

We will discuss our measurements of the Local Group velocity determined relative to the backdrop of galaxies extending out to 5000 km s^{-1}. This will be compared with the discrepant result of Rubin, Thonnard, Ford & Roberts (1976) and with the measurement of the dipole component of the cosmic microwave background (CMB) which gives the Local Group velocity relative to the microwave background reference frame at $z \simeq 1000$. Our results agree with this latter derivation.

1. The Aim of the Observations The main motivation for our observations was to resolve the discrepancy between the Local Group motion obtained (a) by Rubin et al. from an optical study of the background of galaxies and (b) by observers of the dipole component of the CMB. The difference in velocity is a vector of magnitude of 800 km s^{-1} which on the face of it would seem to be much larger than measurement errors would accommodate. We chose a new approach to the measurement of the motion relative to the backdrop of galaxies. Instead of the apparent optical luminosity of galaxies (the standard candle approach), we used the HI flux integral and velocity width as an estimator of the relative distance to a galaxy. This distance indicator does not require the substantial systematic corrections necessary in the use of the optical data. We find that this HI distance indicator is comparable in accuracy with the optical indicator but does not have the potential whole-sky systematic errors due to galactic absorption and seasonal observing. Since there is no general agreement on what is the particular short-coming of the Rubin et al. result, we prefer to set this on one side and begin the exercise with a new data set and approach the subject afresh.

A second aim was to establish what fraction of the CMB dipole asymmetry was intrinsic and hence was a property of the early Universe. Such large-scale asymmetries in the CMB have been discussed (Silk & Wilson 1981, Peebles 1981, Abbott & Wise 1984). A determination of the dipole asymmetry would then lead directly to an estimate of the intrinsic fluctuations anticipated on smaller scales by the various theoretical approaches.

A third important aim of the observations was to provide an estimate of the infall velocity of the Local Group towards the Virgo cluster. This has a special cosmological significance because it gives an estimate of the mass of the Local Supercluster and hence a value for Ω, the density relative to the closure density of the Universe (e.g. Silk 1974, Peebles 1976). In our first observations (Hart & Davies 1982) we took this velocity to be the component of the total Local Group motion which lay in the direction of the Virgo cluster (410 km s^{-1}). With the larger data base which we have now accumulated it is possible to determine the infall velocity typical of any galaxy at the Local Group distance from the Virgo cluster. This value is 200 km s^{-1}, significantly less than the component of the Local Group motion in the direction of the Virgo cluster.

2. The main features of our approach

There are a number of features of our use of the HI parameters alone for distance estimates which make our result of particular interest. The most obvious is the use of the HI integrated flux of the galaxy as the distance indicator. This can be readily measured with a large radio telescope, mapping the HI distribution in larger galaxies if necessary. Two telescopes of comparable size and beamwidth, the Jodrell Bank 76m and the Parkes 64m were used to cover the sky. After calibration and intercomparison of northern and southern observations a uniform set of HI integrated fluxes is then available. These fluxes require no correction for the effect of galactic extinction as is required in optical work.

We use the easily measured velocity width of the HI integrated profile as the "third parameter" to indicate whether the galaxy is large or small. Since beginning this programme the use of the HI profile has become widespread in optical work and is often called the Tully-Fisher relation. Our approach is the HI analogue of the Tully-Fisher relation.

In any investigations involving the distribution of galaxies in depth, it is necessary to be aware of the consequences of Malmquist bias which can result in the inadvertant selection of more luminous galaxies at greater redshifts. This can bias the estimate of the Local Group motion if the distribution in galaxy

redshift is not uniform over the sky. We have obviated the effects of Malmquist bias in two ways, firstly by choosing Sbc galaxies with a small range in absolute luminosity (luminosity classes 1, 2 and 3) and secondly by ensuring that the galaxy sample was well distributed in velocity around the sky.

We have chosen a restricted range of spiral morphological types for this work. The original study (Hart & Davies 1982) was of Sbc galaxies. This has now been extended to types Sb and Sc with adequate galaxies for a Local Group solution to be made for each type. It is expected that this HI approach would give comparable accuracy for a Local Group solution to an optical approach (assuming that there was no systematic bias in the optical data) since there is a close correlation between the HI content and the optical luminosity of spiral galaxies, the more so within a given morphological type.

Finally it should be remembered that any method of distance determination based on the luminosity (whether it is optical, infrared or HI) of individual galaxies provides a distance with a (constant) fractional error. Accordingly, galaxies at twice the distance have twice the actual velocity error so that one needs four times as many galaxies in order to determine a velocity of the Local Group to the same precision. This argues for using nearby galaxies. On the other hand we want to use galaxies outside the region of the gravitational influence of the Virgo cluster at a redshift of $\sim$1000 km s^{-1} and also to include an adequate volume around us so as not to be influenced by only a few large clusters of galaxies. We have chosen on this basis a redshift range out to 6000 km s^{-1} and have the relevant HI data on some 500 galaxies.

3. The method and results The analysis uses the neutral hydrogen mass as estimated from the integrated flux and velocity width as a standard candle. We then derive a luminosity distance for each galaxy and express it as a velocity in the Hubble flow, V_H. The observed velocity of a galaxy relative to the local group V_c is then taken to be composed of the following components

$$V_c = V_H - \Delta V_G + V_{pec}$$

where ΔV_G is the component of Local Group motion in the direction of the galaxy and V_{pec} is the random line of sight velocity of the galaxy. From a series of expressions of this type we then determine V_G, the velocity of the Local Group relative to the backdrop of galaxies.

Hart & Davies (1982) used the data from 100 Sbc galaxies to derive V_G. 78 of these galaxies were sufficiently edge-on, and at adequate distance from the Virgo cluster, to be used in the solution. The Local Group motion was found to be

436 ± 55 km s^{-1} towards $\ell = 264^{o} \pm 18^{o}$, $b = 45^{o} \pm 12^{o}$. Another body of HI data for Sc galaxies was given by Rubin et al. (1976) although not used by them. A similar analysis of the Sc data gave a result of 580 ± 62 km s^{-1} towards $\ell = 245^{o} \pm 18^{o}$, $b = 35^{o} \pm 9^{o}$ in good agreement with the Sbc data. The combined result for the Local Group motion is 484 ± 55 km s^{-1} towards $\ell = 258^{o} \pm 15^{o}$, $b = 42^{o} \pm 8^{o}$. This may be compared with CMB dipole result, if interpreted in terms of a Local Group motion, of 620 ± 40 km s^{-1} towards $\ell = 265^{o} \pm 9^{o}$, $b = 35^{o} \pm 7^{o}$ (Gorenstein & Smoot 1981, Boughn et al. 1981). The HI result and the CMB result agrees well in velocity, but lie just outside their combined quoted errors in amplitude. It should be noted that the direction lies significantly (35°) away from the centre of the Virgo Cluster ($\ell = 280^{o}$, $b = 75^{o}$).

Hart & Davies (1982) took the component of the Local Group towards the Virgo Cluster to represent the infall velocity induced by the gravitational potential of the cluster. This value of 410 ± 55 km s^{-1} agrees well with values given by optical and infrared studies (Aaronson et al. 1980, Tonry & Davis 1981) for the same component of motion (although not derived from an all-sky study). This value leads to an estimate of the local density in the Universe in the range $\Omega = 0.15$ to 0.50.

The more recent Sb-Sc observations that we have made within the Local Supercluster and its surroundings indicate that this Virgocentric velocity of 410 km s^{-1} is not locally induced and therefore reflects an additional component of motion of the Local Supercluster as a whole.

The locally derived value of the motion of the Local Group relative to the Virgo cluster is 170 ± 40 km s^{-1}. This is in good agreement with the local values derived by de Vaucouleurs et al. (1981) (160 ± 40 km s^{-1}) and Yahil, Sandage & Tammann (1979) (140 ± 90 km s^{-1}) obtained by projecting their dipole solutions in the Virgo cluster direction (IAU corrections applied). The removal of the random or thermal component of this velocity is rather model dependent but it appears to give an infall amplitude of between 100 and 200 km s^{-1} if the most recent value of the mean Virgo Cluster redshift of 1094 km s^{-1} is used (Huchra, Davis & Latham 1983, corrected to IAU standard).

This result therefore favours low-Ω models unless the Local Supercluster as a whole is not a particularly overdense region.

Finally, if the total peculiar velocity of the Local Group within the Local Supercluster is subtracted from the Hart & Davies result, we obtain a velocity of

some 300 km s^{-1} towards $\ell = 303^{o}$, $b = 25^{o}$. This motion, which represents bulk motion of the whole of the Local Supercluster, is impressively aligned towards the Hydra-Centaurus supercluster at $\ell = 299^{o}$, $b = 27^{o}$, and reduces the final discrepancy with the microwave background vector to a still significant 200 km s^{-1}.

References

Aaronson, M., Mould, J., Huchra, J., Sullivan, W.T., Schommer, R.A. & Bothun, G.D., 1980. Astrophys.J., 239, 12.

Abbott, L.F. & Wise, M.B., 1984. Astrophys.J., 282, L47.

Boughn, S.P., Cheng, E.S. & Wilkinson, D.T., 1981. Astrophys.J.Lett., 243, L113.

de Vaucouleurs, G., Peters, W.L., Bottinelli, L., Gouguenheim, L. & Paturel, G., 1981. Astrophys.J., 248, 408.

Gorenstein, M.V. & Smooth, G.F., 1981. Astrophys.J., 244, 361.

Hart, L. & Davies, R.D., 1982. Nature 297, 191.

Huchra, J.P., Davis, R.J. & Latham, D.W., 1984 in proceedings of Trieste Conference on Clusters and Groups of Galaxies, p.79.

Peebles, P.J.E., 1976. Astrophys.J., 205, 318.

Peebles, P.J.E., 1981. Astrophys.J.Lett., 243, L119.

Rubin, V.C., Thonnard, N., Ford, W.K. & Roberts, M.S., 1976. Astr.J., 81, 719.

Silk, J., 1974. Astrophys.J., 193, 525.

Silk, J. & Wilson, M.L., 1981. Astrophys.J.Lett., 244, L37.

Tonry, J.L. & Davis, M., 1981. Astrophys.J., 246, 680.

Yahil, A., Sandage, A. & Tammann, G.A., 1979. in Les Houches session XXXII, Physical Cosmology, p.127.

DISCUSSION

G. HELOU: We have mapped at the VLA a fainter galaxy (14°63) of type Im IV-V, with a Gaussian integrated HI profile. We find it exhibits an overall rotation signature, although the surface HI distribution tends to be clumpy rather than smooth at a resolution of about 15 arseconds. If the dwarf is at a Virgo distance of 20 Mpc, its dynamical mass is estimated to be only about 2/3 of its observed HI mass. This is the inverse of the missing mass problem.

L. HOFFMAN: (George Helou alluded to this briefly in his comment; the discussion was halted before I could elaborate.) The dwarf 12°100 is quite unique among the Im IV, IV-V and V galaxies we have detected at Arecibo. It has the widest HI profile of the 17 such dwarfs we detected at Virgo redshifts - in fact

only one other Im_f dwarf has a Δv more than half as large. Furthermore, 12°100 is one of only two of these 17 which shows a double-horned profile. Therefore 12°100 should not be regarded as typical of the Im IV dwarfs.

(Note by the editors: This discussion refers to some part of R. Davies' talk that did not appear in his written version. For a better reference see the contribution of L. Hoffman in this volume.)

ON THE INFALL VELOCITY TOWARDS VIRGO

R.C. Kraan-Korteweg

Astronomisches Institut der Universitaet Basel

ABSTRACT

An investigation of the parameters which determine a self-consistent Virgocentric infall model reveals two stable special regions, viz. (1) a region where the observed radial velocities v_o nearly reflect the unperturbed Hubble velocities v_H and which lends itself to a determination of the Hubble constant H_o; and (2) a region where the peculiar radial velocities Δv, caused by the infall model, are about equal to our infall velocity v_{vc}; this region is particularly suited for a determination of v_{vc}. Spiral galaxies within these regions with known 21cm-line widths are used to determine values, corrected for Malmquist bias, of $H_o = 58$ km s^{-1} Mpc^{-1} and $v_{vc} = 210$ km s^{-1}.

I. INTRODUCTION

The Virgo cluster represents a mass excess which must decelerate locally the underlying expansion field. The resulting velocity field can be thought of as the sum of Virgocentric infall motions and the general linear Hubble expansion field. A quantitative understanding of the Virgocentric infall field is of great importance for the calculation of the local mass density ϱ_L within the Virgo complex and of the large-scale mean mass density ϱ_o, as well as for an understanding of the locally complex correlation between distance and recession velocity.

Under the assumption that the mass is spherically distributed about the Virgo cluster center (which is assumed in first approximation to coincide with M87), the Virgocentric infall field can be modelled with only a few observable parameters; these are the observed mean Virgo cluster recession velocity v_{obs}^{Vir} as seen from the centroid of the Local Group, the Virgocentric infall velocity v_{vc} of the Local Group, the density ration ϱ_L/ϱ_o at the position of the Local Group circle about the Virgo cluster center, and the Virgocentric density profile $\varrho(r)$. The flow pattern depends only on these four parameters; it is independent of either the Virgo cluster distance or the Hubble constant H_o. Of course, the parameters which refer to the Local Group could be replaced by those referring to any other position within the Virgo complex, but the former are most accessible to direct observation. A tacit assumption here is that all mass in the Virgo complex follows the same unique density profile $\varrho(r)$. A possible model has been discussed by Hoffmann and Salpeter (1982) which contains additional invisible matter obeying a different density profile than the visible matter; the ensuing complications are not considered here. - In the following it is also assumed that the deceleration from other mass concentrations in the vicinity of the Virgo complex is negligible in comparison to that of Virgo.

During the last years it has become possible to detect our Virgocentric infall velocity v_{vc} beyond doubt. A recent review (Tammann and Sandage, 1984) of various determinations by different methods and authors gives a best value of $v_{vc} = 220 \pm$

50 km s^{-1}. Moreover, the assumption of a selfconsistent Virgocentric infall model has found support in the observed velocity behavior of 300 galaxies within the Virgo complex (Aaronson et al., 1982).

The radial velocity pattern as seen from the (infalling!) Local Group is difficult to visualize due to the superposition of the linear expansion field and the Virgocentric infall velocities. A good illustration of the pattern, the details of which depend on the choice of the model parameters, is given by a Tonry diagram (Tonry and Davis, 1981; Sandage and Tammann, 1983). This diagram shows that the observed radial velocities differ from the expected pure Hubble velocities due to the Virgocentric flow pattern by an amount which depends on the angle α between a given galaxy and the Virgo cluster center. In particular there are two annular regions about the Virgo cluster where the observed radial velocity v_o is nearly the same as the unperturbed Hubble velocity v_H, i.e. $v_o \approx v_H$ independent of v_{vc}, and another where $v_{vc} \approx v_H - v_o$. These two regions are particularly suitable to determine from observations H_o and v_{vc}, respectively.

After a short discussion of the infall model in section II, the position and extent of the two special regions are defined in section III. In section IV a solution for H_o and v_{vc} is presented.

II. THE INFALL MODEL

The perturbed recession velocity as seen from the Virgo cluster center can be calculated for any galaxy within the Virgo complex as a function of Virgocentric distance and time by supposing a given galaxy to lie on the periphery of a Virgocentric mini-universe, the expansion history of which is defined by its mean mass density $\rho(r)$ and local expansion rate $H_o(r)$. The appropriate differential equations connecting the model parameters are published by Schechter (1980).

Once the Virgocentric velocity perturbation is known it can be transformed into a peculiar radial velocity as observed at the

Local Group by an origin transformation of the coordinate system. The total peculiar radial velocity of a galaxy, Δv, is then found by adding to the result the component of v_{vc} into the direction of that galaxy, such that

$$v_H = v_o + \Delta v, \tag{1}$$

where v_H is the unperturbed Hubble recession velocity and v_o the radial velocity observed at the Local Group. Additional possible random velocities of individual galaxies are neglected here.

It turns out that eq.(1) is double or triple valued in regions close to the Virgo cluster; the exact size of the regions depends on the size of the infall velocity v_{vc}. This is because a galaxy in front of the Virgo cluster falls away from us, whereas a galaxy beyond the Virgo cluster falls toward us, such that both galaxies may have the same observed velocity v_o. In addition a virialized galaxy at the distance of the Virgo cluster may also exhibit the velocity v_o.

The peculiar velocities Δv depend, as stated above, on the model parameters. In Table 1 two sets of parameters are laid out, which differ basicly in the value of v_{vc} in view of the fact that values of $v_{vc} \approx 220$ and $v_{vc} \approx 440$ km s^{-1} are presently still proposed in the literature.

Table I

Parameters of Two Virgocentric Infall Models

	220-model	440-model	Source
v_{obs}^{Vir}	967 km s^{-1}	967 km s^{-1}	1
v_{vc}	220 km s^{-1}	440 km s^{-1}	
ρ_L / ρ_o	3.8	3.0	2
γ	2	2	3

Sources:
(1) Kraan-Korteweg (1981)
(2) Tammann and Sandage (1984). Note that the best observed value of ρ_L / ρ_o depends on v_{vc}.
(3) γ is the exponent of the density profile assumed to have the form $\rho(r) \propto r^{\gamma}$ (Yahil et al.,1980)

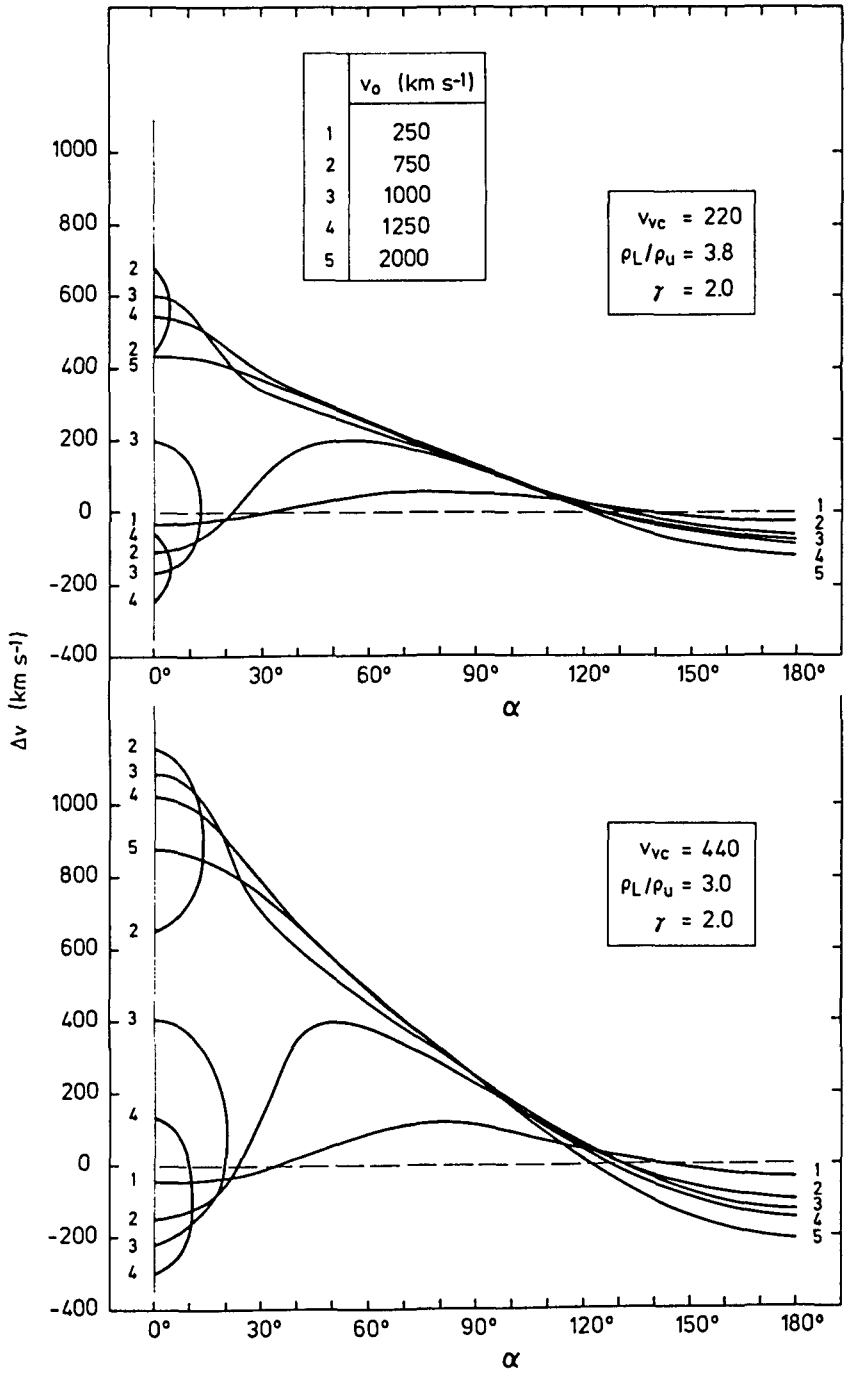


Fig.1. The peculiar velocities Δv in function of the angle α away from Virgo for the 220-model (upper panel) and the 440-model (lower panel). The different curves refer to discrete values of the observed velocity v_o = 250, 750, 1000, 1250, and 2000 km s^{-1}.

It should be noted that a good determination of the cosmic value of H_o can be obtained by dividing v_H(Virgo) by the Virgo cluster distance r(Virgo), whatever its value, - but that the resulting value of H_o is different for the two models, which imply v_H (Virgo) = 1187 and 1407 km s^{-1}, respectively.

The size of the peculiar velocities Δv for the two models of Table 1 are shown in Fig.1 in function of the angle α away from Virgo. Except for the triple valued regions, the behavior of Δv is quite similar for the two models, differing mainly in the amplitude which is determined by v_{vc}.

In the present context it is most important that Fig.1 shows that there are regions in the sky with α const where - independent of the value of v_{vc}, - Δv nearly vanishes over a wide range of v_o, or where $\Delta v \approx v_{vc}$. These two special regions are discussed in the following section.

III. SPECIAL REGIONS PREDICTED BY THE INFALL MODEL

The correlations between Δv, v_o, and α for the 220- and 440-model of Fig.1 are shown again in Fig.2a and 2b in modified form and for two special regions, i.e.

(1) $\alpha = 120 \pm 10^o$ and $600 \lesssim v_o \lesssim 2800$ km s^{-1} (Fig.2b), hereafter called the "Null Region". Here the values of the peculiar velocities Δv remain always small, in fact $\lesssim 100$ km s^{-1} even for the 440-model. This means that there is a region in the sky where $v_H \approx v_o$, regardless whether $v_{vc} = 220$ or $v_{vc} = 440$ km s^{-1}. Hence, the Null Region is particularly suitable for the determination of H_o; if the distances r_g are known for some galaxies within the Null Region it follows

$$H_o = v_H / r_g \approx v_o / r_g \qquad (2)$$

Reading off the appropriate values from Fig.2b one finds that at $v_o \approx 1000$ km s^{-1} the resulting value of H_o will be too large by 5

% on the average, and at $v_o \approx 3000$ km s^{-1} it will be too small by even less.

(2) $\alpha = 65 \pm 10^o$ and $1000 \lesssim v_o \lesssim 2800$ km s^{-1} (Fig.2a), hereafter called the "Infall Region". Here the peculiar velocities Δv happen to be close to our infall velocity v_{vc}, whatever value of v_{vc} may apply. If one knows H_o and the distances r_g to some galaxies in the Infall Region one can determine v_{vc} simply by

$$v_{vc} \approx \Delta v = v_H - v_o = r_g H_o - v_o. \qquad (3)$$

Fig.2 shows that for any individual galaxy Δv may differ from v_{vc} by $\lesssim 100$ km s^{-1} in the case of the 440-model, and by half as much for the 220-model. In any case, however, the average of several galaxies, randomly distributed over the Infall Region, will give a good determination of v_{vc}.

The usefulness of the special regions is further increased by the fact that the curves in Fig.2a and 2b are quite insensitive to variations of the adopted parameters ϱ_L/ϱ_o and γ.

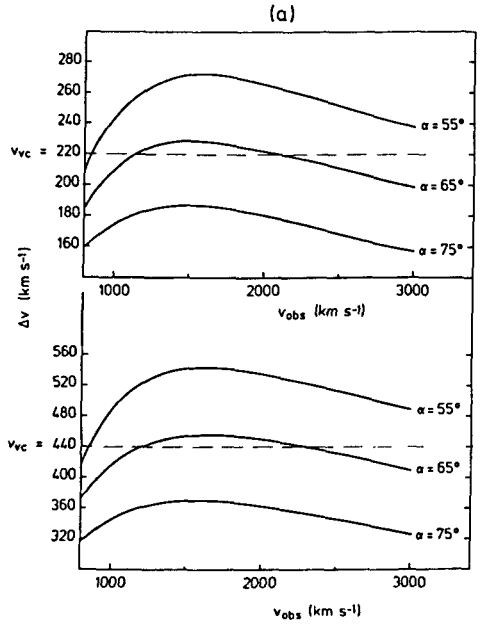


Fig.2a. The Infall Region where $\Delta v \approx v_{vc}$ for the 220-model (upper panel) and the 440-model (lower panel).

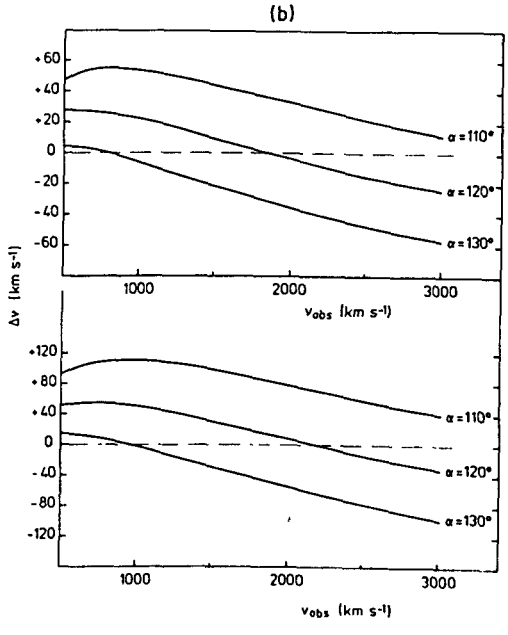


Fig.2b. The Null Region, where $\Delta v \approx 0$ for the 220-model (upper panel) and the 440-model (lower panel).

IV. THE DETERMINATION OF H_o AND v_{vc}

To proceed with the determination of the global value of H_o and of our infall velocity v_{vc}, distances are required of a sufficient number of field galaxies within the special regions. A Tully-Fisher relation for blue magnitudes of the form

$$M^{o,i}_{B_T} = -7.17 \log \Delta v_{21} - 1.83 \qquad (4)$$

was adopted as distance indicator. Here Δv_{21} is the 21cm-line width corrected to edge-on orientation. The slope of eq.(4) was taken from Richter and Huchtmeier (1984) and the zero point from Sandage and Tammann (1984).

Suitable spiral galaxies of type Sab-Sd with known 21cm-line widths and inclination $i > 45^o$ were selected from a catalogue of nearby galaxies in which the values of v_o, Δv, and v_H are given for 2810 galaxies (Kraan-Korteweg, 1985a). The catalogue contains 44 such spirals within the Null Region and 40 within the Infall Region.

The solution for H_o in the Null Region showed a pronounced dependence on v_o and therefore, - because of $v_o \approx v_H$, - on distance r_g, yielding values of H_o increasing with distance from roughly 50 (at $v_o < 1500$ km s^{-1}) to 80 (at $v_o \approx 2800$ km s^{-1}). This effect is in fact expected for a galaxy sample limited by apparent magnitude, because eq.(4) predicts the absolute magnitude M (and hence the distance modulus) only to within an intrinsic dispersion of $\sigma(M) \approx 0^m.5$. This necessarily discriminates at larger distances against galaxies which are subluminous for their line width Δv_{21}. The only distant galaxies which remain in the catalogue are overluminous for a given Δv_{21} and yield with eq.(4) too small distances and hence too large values of H_o. This effect is known as the Malmquist bias. The Null Region, which at least in first approximation is free of any systematic peculiar velocities, is particularly well suited to demonstrate how the importance of the Malmquist bias increases with increasing distance.

The solution of v_{vc} in the Infall Region by means of eq.(3) is, of course, also affected by the Malmquist bias because first H_o tends to be overestimated, as discussed in the previous paragraph, and secondly the distances r_g of the more distant galaxies are underestimated.

Instead of solving separately for H_o and v_{vc}, a combined solution was made here by determining the values of H_o and v_{vc} which give minimal scatter in a plot of (m-M) versus v_H. Only galaxies with $v_H < 1500$ km s^{-1} were used for the solution to guard against the Malmquist bias. The result is $H_o = 58 \pm 4$ km s^{-1} Mpc and $v_{vc} = 210 \pm 30$ km s^{-1}, where the indicated uncertainties are formal errors.

The result shows that present 21cm-line widths data are compatible with a relatively low value of H_o, and that the possibility can be rejected of our infall velocity v_{vc} being as high as 440 km s^{-1}.

A more detailed presentation of the method and a discussion of the results will be given elsewhere (Kraan-Korteweg, 1985b).

Partial support from the Swiss National Science Foundation is gratefully acknowledged.

REFERENCES

Aaronson, M., Huchra, J., Mould, J., Schechter, P.L., and Tully, R.B.: 1982, Astrophys.J.258, 64.

Hoffman, G.L., and Salpeter, E.E.: 1982, Astrophys.J.263, 485.

Kraan-Korteweg, R.C.: 1981, Astron.Astrophys.104, 280.

Kraan-Korteweg, R.C.: 1985a, A Catalog of 2810 Nearby Galaxies, submitted to Astron.Astrophys.Suppl.Ser.

Kraan-Korteweg, R.C.: 1985b, in preparation.

Peebles, P.J.E.: 1976, Astrophys.J.205, 318.

Richter, O.-G., and Huchtmeier, W.K.: 1984, Astron.Astrophys.132, 253.

Sandage, A., and Tammann, G.A.: 1983, in Astrophysical Cosmology, Proc.of the Vatican Study Week on Cosmology and

Fundamental Physics, ed.H.A.Brueck, G.V.Coyne, and M.S.Longair (Vatican.Pontif.Acad.Sci.) p.23.

Sandage, A., and Tammann, G.A.: 1984, Nature 307, 326.

Schechter, P.L.: 1980, Astron.J.85, 801.

Silk,J.: 1974, Astrophys.J.193, 525.

Silk,J.: 1977, Astrophys.J.59, 53.

Tammann, G.A., and Sandage, A.: 1984, preprint.

Tonry,J.L., and Davis, M.: 1981, Astrophys.J.246, 666.

Yahil, A., Sandage, A., and Tammann, G.A.: 1980, Astrophys.J.242, 448.

VII.

DISTANCE OF THE VIRGO CLUSTER AND OTHER MATTERS

THE HISTORICAL EVOLUTION OF THE VIRGO CLUSTER DISTANCE MODULUS

Otto-Georg Richter
ESO Garching

The *Virgo* cluster provides one of the most important stepping stones in the determination of the extragalactic distance scale. It distance modulus has been used to determine the Hubble constant ever since the 1920's. The original distance modulus estimate by Hubble (and coworkers) of 26.3^m has received several revisions most of which were determined by new insights into the properties of constituents of *Local Group* galaxies.

In this short contribution I have attempted to collect all the many distance modulus determinations for the *Virgo* cluster that are widely scattered in the literature. However, the resulting list (Table 1) is probably incomplete. Nevertheless it should serve as a guide to the relevant literature for the many different distance indicators that are potentially applicable to the *Virgo* cluster. In Figure 1 the individual distance moduli are plotted as a function of the publication year. The detailed interpretation is left to the reader. It seems impossible to average all the different recent values since they are drawn from different parent distributions. The controversy remains.

Until quite recently there was a 1:1 correspondence between the change in the *Virgo* cluster distance modulus and the Hubble constant. Now it has been realized that the *Local Group* may have a peculiar (infall) velocity in the direction of this cluster. Therefore, the global value of the Hubble constant will be larger than the *Virgo* cluster Hubble ratio by an amount that is not yet accurately known.

As soon as distance indicators become sufficiently accurate to determine the spatial depth of the *Virgo* cluster, a further complication of the picture may arise. Although there is also some evidence to the contrary, G. deVaucouleurs has for some time argued that the *Virgo* cluster is actually a superposition of (at least) two different aggregates, which he associates with the elliptical and the spiral populations. In Table 1 these differences have been ignored in order to keep numbers comparable. It is my belief that this question will be resolved only with the advent of the Hubble Space Telescope, the launch of which lies ahead.

Corrections and addenda to Table 1 would be gratefully acknowledged.

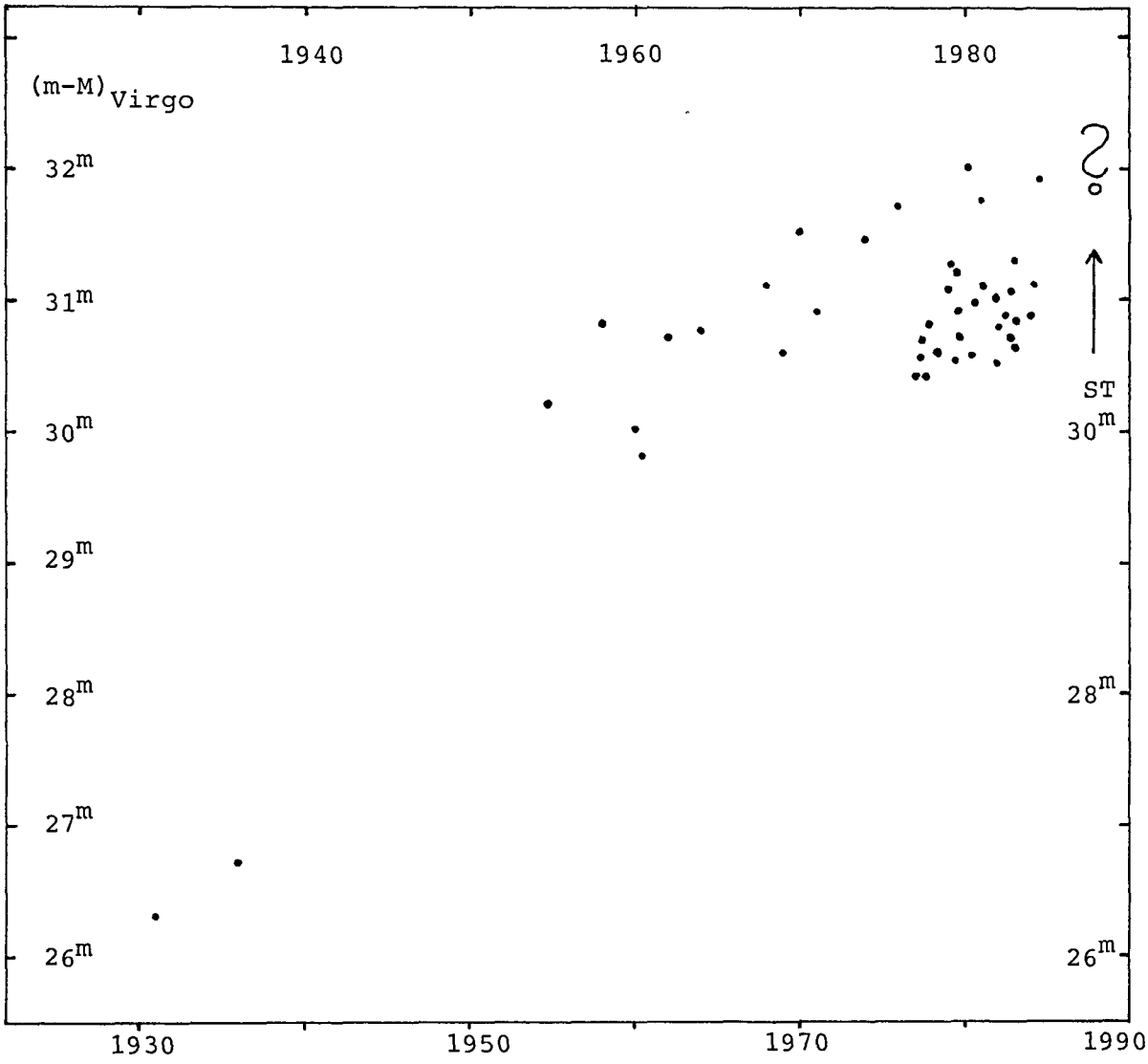


Figure 1. The *Virgo* cluster distance modulus versus the publication date.

TABLE 1
DISTANCE MODULUS DETERMINATIONS FOR THE *Virgo* CLUSTER OF GALAXIES

E. Hubble and M. Humason: 1931, *Astrophys.J.* **74**, 43	26.3
E. Hubble: 1936, in *"Realm of the Nebulae"*	26.7
W. Baum: 1955, *Publ.A.S.P.* **67**, 328	30.2
A. Sandage: 1958, *Astrophys.J.* **127**, 513	(≥) 30.8
J. Sersic: 1960, *Z.f.A.* **50**, 168	30.0
Yu.P.Pskovskii: 1960, *Sov.Astron.* **4**, 805	29.8 ± 0.7
A. Sandage: 1962, *I.A.U. Symp.* **15**, 359	30.7
E. Holmberg: 1964, *Arkiv Astron.* **3**, 419	30.76
A. Sandage: 1968, *Astrophys.J.* **152**, L149	(≥) 31.1
C.T. Kowal: 1969, *Publ.A.S.P.* **81**, 608	30.6 ± 0.3
G. deVaucouleurs: 1970, *Astrophys.J.* **159**, 435	31.5
J. Heidmann *et al.*: 1971, *Mem.R.astr.Soc.* **75**, 85	30.9 ± 0.5
A. Sandage and G.A. Tammann: 1974, *Astrophys.J.* **194**, 559	31.45 ± 0.09
A. Sandage and G.A. Tammann: 1976, *Astrophys.J.* **210**, 7	31.70 ± 0.08
G. deVaucouleurs: 1977, *Nature* **266**, 126	30.4 ± 0.3
D.A. Hanes: 1977, *M.N.R.A.S.* **180**, 309	30.4 ± 0.5
J. Heidmann: 1977, *I.A.U. Coll.* **37**, 487	30.7 ± 0.5
G.A. Tammann: 1977, *I.A.U. Coll.* **37**, 43	31.55 ± 0.12
R.B. Tully and J.R. Fisher: 1977a, *Astron.Astrophys.* **54**, 661	30.60
R.B. Tully and J.R. Fisher: 1977b, *I.A.U. Coll.* **37**, 95	30.8 ± 0.2
N. Visvanthan: 1978, *Astron.Astrophys.* **67**, L17	30.60 ± 0.39
M. Aaronson *et al.*: 1979, *Astrophys.J.* **229**, 1	31.07 ± 0.25
G. deVaucouleurs: 1979, *Astrophys.J.* **227**, 729	30.52
D.A. Hanes: 1979, *M.N.R.A.S.* **188**, 901	30.7 ± 0.3
W.E. Harris and R. Racine: 1979, *Annu.Rev.Astron.Astrophys.* **17**, 241	30.9 ± 0.3
R.C. Kennicutt: 1979, *Astrophys.J.* **228**, 696	31.20
N. Visvanathan and D. Griersmith: 1979, *Astrophys.J.* **230**, 1	31.26 ± 0.16
D. Branch *et al.*: 1980, *Bull.A.A.S.* **11**, 694	32.0 ± 0.6
B. Carney: 1980, cited in Mould *et al.* (1980)	30.53 ± 0.13
J. Mould *et al.*: 1980, *Astrophys.J.* **238**, 458	30.98 ± 0.08
D. Branch *et al.*: 1981, *Astrophys.J.* **244**, 780	31.81 ± 0.28
N. Visvanathan: 1981, *Proc.A.S.A.* **4**, 172	31.15
W.D. Arnett: 1982, *Astrophys.J.* **254**, 1	31.0 ± 0.3
G. deVaucouleurs: 1982, *Astrophys.J.* **253**, 520	30.88 ± 0.09
G. deVaucouleurs and D. Olson: 1982, *Astrophys.J.* **256**, 346	30.51 ± 0.2
D.A. Hanes: 1982, *M.N.R.A.S.* **201**, 145	30.8 ± 0.2
M. Aaronson and J. Mould: 1983, *Astrophys.J.* **265**, 1	31.08 ± 0.11
R. Buta and G. deVaucouleurs: 1983a, *Astrophys.J.Suppl.* **51**, 149	30.69 ± 0.3
R. Buta and G. deVaucouleurs: 1983b, *Astrophys.J.* **266**, 1	30.63 ± 0.2
D.A. Hanes: 1983, *Highlights of Astronomy* **6**, 227	30.8
N. Visvanathan: 1983, *Astrophys.J.* **275**, 430	31.37
L. Bottinelli *et al.*: 1984, *Astron.Astrophys.Suppl.Ser.* **56**, 381	30.88 ± 0.15
O.-G. Richter and W.K. Huchtmeier: 1984, *Astron.Astrophys.* **132**, 253	31.90 ± 0.30
R.B. Tully and E. Shaya: 1984, *Astrophys.J.* **281**, 31	31.12 ± 0.08

DISTANCE AND KINEMATICS OF THE VIRGO CLUSTER

G. de Vaucouleurs
University of Texas

Summary. The distances, structure and kinematics of various components of the Virgo cluster are reviewed. The mean distance moduli of the Virgo E cluster and the Virgo S cloud, from seven methods each, are μ_o = 30.40 ± 0.10 and 30.70 ± 0.10.

The two main components of the Virgo cluster, the concentrated E-cluster and the more diffuse S-cloud (de Vaucouleurs 1961), both within a 6° radius from a centroid close to M87 are apparently at slightly different distances from the Local Group. Leaving aside the controversial question as to whether the mean redshifts of the two components are equal or not (G. & A. de Vaucouleurs 1973; Sulentic 1977; Sandage and Tamman 1976; Kraan-Korteweg 1982; Tanaka 1984a,b) which is sensitive to the inclusion or rejection of different regions or galaxy types, there is growing evidence that the centroids of the two components are separated in space by several megaparsecs, and that at least the S-cloud shows indications of contraction in its inner regions, expansion in its outer regions, and possibly rotation in a warped plane (Tanaka 1984b).

1. Distance of the E-cluster. A new, independent estimate of the distance of the E cluster has recently been derived from a revised calibration of the absolute magnitude of B Cas (SN1572) (de Vaucouleurs 1985). The distance of 3C10, the remnant of SN1572, is, according to several recent determinations, smaller than earlier estimates had suggested. With an average distance modulus μ_o = 12.5 ± 0.25, corresponding to a distance Δ = 3.2 ± 0.4 kpc, the apparent magnitude of B Cas at maximum, corrected for absorption, was $V_o = V_M - A_V$ = - 4.1 - 1.95 = - 6.05 ± 0.2, which leads to visual and photographic absolute magnitudes M_v = - 18.55 ± 0.3 and M_{pg} = - 18.85 ± 0.3.

Then, the mean corrected magnitudes of four well-observed Type I supernovae in the Virgo E cluster, $\langle m_{pg} \rangle$ = 11.58 ± 0.22, imply a mean corrected distance modulus μ_o = 30.55 ± 0.41 and a distance of 12.9 ± 2.5 Mpc. With this distance and the mean radial velocity of the E cluster, corrected for the peculiar motion of the Local Group, V_c = 1220 ± 65 km s^{-1}, the corresponding value of the Hubble ratio is 95 km s^{-1} Mpc^{-1}, in good general agreement with many recent determinations from more distant groups and clusters.

Table 1. DISTANCE MODULI IN THE VIRGO CLUSTER

Source	Method	Virgo E	Virgo S
(1)	Brightest Globular Clusters	30.4 ± 0.3	
(2)	Color-Luminosity relation of ellipticals (corrected for zero point)	30.28 0.3:	
(3)	Luminosity function of globular clusters	30.3 0.2	
(4)	Luminosity index, magnitude and isophotal diameter of 6 spirals		30.53 ± 0.2:
(5)	Luminosity index and metric (effective) diameter of 9 spirals		30.79 0.26
(6)	Type I supernovae in 5 ellipticals	30.25 0.25	
(7)	Infra-red T-F relation and H magnitudes of 23 spirals		30.57 0.2:
(8)	Revised B-band T-F relation, magnitudes and isophotal diameters of 35 spirals		30.88 0.15
(9)	Velocity dispersion and B magnitudes of 34, E, L galaxies	30.51 0.2	
(10)	Inner ring diameters in 7 E, L and 15 spirals	30.47 0.2:	30.90 0.3:
(11)	V-band T-F relation and V magnitudes of 20 spirals		30.59 0.2
(12)	B Cas and type I supernovae in four E galaxies	30.55 0.41	
(13)	Comparison of 8 spirals 'sosies' of 14 nearby calibrators		30.66 0.2:
Unweighted means and internal mean errors		30.40 ± 0.10	30.70 ± 0.10

(1) de Vaucouleurs, Nature, 266, 126, 1977.
(2) Visvanathan, Astr. & Ap., 67, L17, 1978, corrected for extinction and zero point.
(3) Hanes, M.N.R.A.S., 188, 901, 1979, corrected for extinction and zero point.
(4-6) de Vaucouleurs, Ap. J., 227, 729, 1979, Tables 3, 4, 6.
(7) Mould, Aaronson and Huchra, Ap. J., 238, 458, 1980, corrected for zero point.
(8) Bottinelli, Gouguenheim, Paturel and de Vaucouleurs, Astr. & Ap. Suppl., 56, 381, 1984.
(9) de Vaucouleurs and Olson, Ap. J., 256, 346, 1982.
(10) Buta and de Vaucouleurs, Ap. J. Suppl., 266, 1, 1983.
(11) Visvanathan, J. Astr. & Ap., 2, 67, 1981, corrected for extinction and zero point.
(12) de Vaucouleurs, Ap. J., in press, 1985.
(13) Bottinelli, Gouguenheim, Paturel and de Vaucouleurs, unpublished.

2. Distance of the S cloud. Numerous determinations of distances to spirals in the Virgo S-cloud by a variety of distance indicators (Table 1) give consistently larger distances, leading to the conclusion that the Virgo "cluster" is really a complex system spread over a considerable depth along the line of sight. This conclusion has recently been confirmed by Tanaka (1984a) in a detailed re-analysis of the positions and velocities of several hundred galaxies in the Virgo area.

New determinations of the distances of 8 spirals in the Virgo S cloud by the method of "sosies" (Bottinelli et al. 1985) which bypasses all calibration problems (except the zero point) give a mean distance modulus μ_o = 30. 66 ± 0.2: by comparison with a dozen calibrating galaxies in the Local and nearby groups.

To assess the reality or otherwise of the distance differential between the centroids of the E-cluster and the S-cloud the zero point error of the short scale does not enter, only the internal statistical errors (~ 0.1) of the two determinations need be considered. Then the differential modulus $\Delta\mu_o$(S - E) = + 0.3 ± 0.15 appears to be significant and so is the distance difference of ~15%, or ~ 2 Mpc. Because the diameters of the two components are each of the order of 12° or ~ 20% of their distance to us, that is ~ 2-3 Mpc they will overlap to some extent. Fairall (1978) has reported a similar difference between the centroids of the early type and spiral galaxies in the Centaurus cloud where the separation is directly visible in projection on the sphere.

3. Velocity structure of the S cloud. Recent advances in the development increasingly precise distance indicators, such as the luminosity index and the 21-cm line width (see Bottinelli et al. 1983, 1984, 1985 and references therein), have reached the point where the depth of the S cloud along the line of sight may be detectable and a beginning has been made in exploring the velocity field within the Virgo cluster, at least in the S cloud (de Vaucouleurs 1982; Tanaka 1984b). Different interpretations have been proposed, the simplest involving a contracting core and an outer expanding shell, but a more complicated model, including a 'warped' plane may account better for details of the velocity structure. Further refinements in the distance indicators may soon lead to more complete and realistic dynamical models of the cluster(s) and its relations to the Local Supercluster at large.

REFERENCES

Bottinelli, L., Gouguenheim, L., Paturel, G. and de Vaucouleurs, G.
1983, Astr. Ap., 118, 4;
1984, Astr. Ap. Suppl., 56, 381;
1985, in preparation
Fairall, A. 1978, M. N. R. A. S., 183, 59P.
Kraan-Korteweg, R.C. 1982, Astr. Ap. Suppl., 47, 505.
Sandage, A. and Tammann, G. 1976, Ap. J. Lett. , 207, L1.
Sulentic, J. 1977, Ap. J. Lett., 211, L59.
Tanaka, K.I. 1984a, Pub. Ast. Soc. Japan, in press.
Tanaka, K.I. 1984b, Pub. Ast. Soc. Japan, submitted.
Vaucouleurs, G. de 1961, Ap. J. Suppl., 6, 213.
Vaucouleurs, G. and A. de 1973, Astr. Ap., 28, 109.
Vaucouleurs, G. de 1982, Ap. J., 253, 520.
Vaucouleurs, G. de 1985, Ap. J., in press.

THE VIRGO CLUSTER DISTANCE

CORRECTIONS TO GLOBAL PARAMETERS

R. Brent Tully
Observatoire de Meudon and
Institute for Astronomy, University of Hawaii

Pascal Fouqué
Observatoire de Meudon and
European Southern Observatory

Outside of the local and nearest groups, distances of individual galaxies rest on their global properties, calibrated in a statistical way.

I. INTRODUCTION :

The four observables that we use are of two kinds :

- -three are distance-dependent : blue magnitude B
  blue diameter D
  infrared magnitude H
- -one is distance-independent : HI line width W

From these, we can get three relations to determine distances :

d (B,W)	Tully and Fisher (1977)
d (D,W)	Tully and Fisher (1977)
d (H,W)	Aaronson, Huchra and Mould (1979)

But from the three distance-dependent parameters, we can build three distance-independent quantities :

color B-H	from B and H
blue surface brightness Σ_B	from B and D
"infrared" surface brightness Σ_H	from H and D

and then three new relations to determine distances :

d (H,B-H)	Tully, Mould and Aaronson (1982)

d (H,Σ_H) van den Bergh (1981)

d (B,Σ_B)

The last one is now forsaken because of a slope too close to the locus of distance uncertainties.

But before these data become useful, producing relations of low dispersion, they must be :

-corrected from observational effects : atmospheric extinction on magnitudes, resolution on HI line width.

-homogenized between various sources.

-corrected for : aperture
projection
absorption
redshift
random motions

Here are subtle effects : for example, a wrong diameter system introduces wrong aperture corrections and thus wrong corrected magnitudes.

We will deal here with aperture, projection and absorption corrections on magnitudes and diameters.

The process will be to minimize the scatter in the following distance-independent relations :

B-H (W) $\Sigma_B(W)$ $\Sigma_H(W)$ $L_B(D)$

where the last one needs a previous knowledge of distances, or to be used in a cluster. But here the slope of this relation becomes an advantage.

Our approach will be the following :

-we choose a diameter system and make the aperture corrections.

-we test the projection effects on high-latitude objects and correct them.

-we test the absorption effects and correct them.

-we test the corrected quantities for diameter effects.

If the last step shows us that no remaining bias holds, we are satisfied with our corrected global parameters.

II. DIAMETER SYSTEM :

Our requirement is that the system be measured at a constant isophotal level, in order not to introduce a distance bias.

Two commonly used systems, the Holmberg (1958) one and the UGC one, are compared in Fig. 1 to show up the problem : the ratio of both diameters

varies along the diameter range, and thus at least one of the systems is in error.

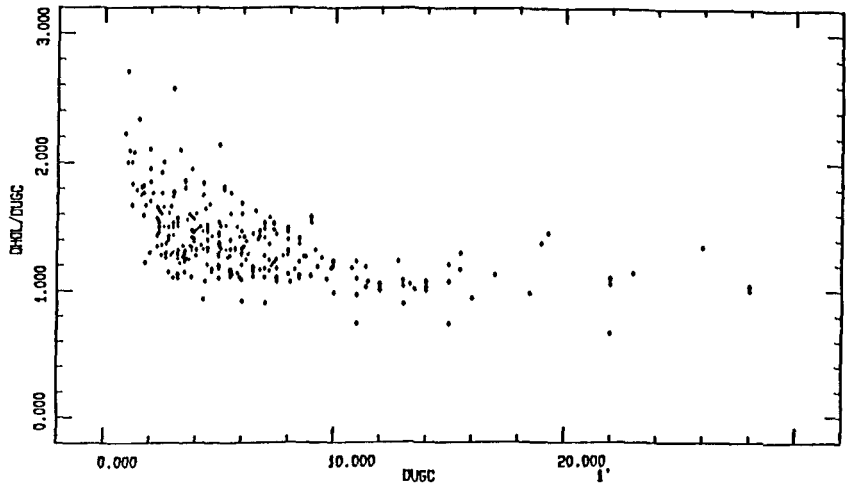


FIG. 1

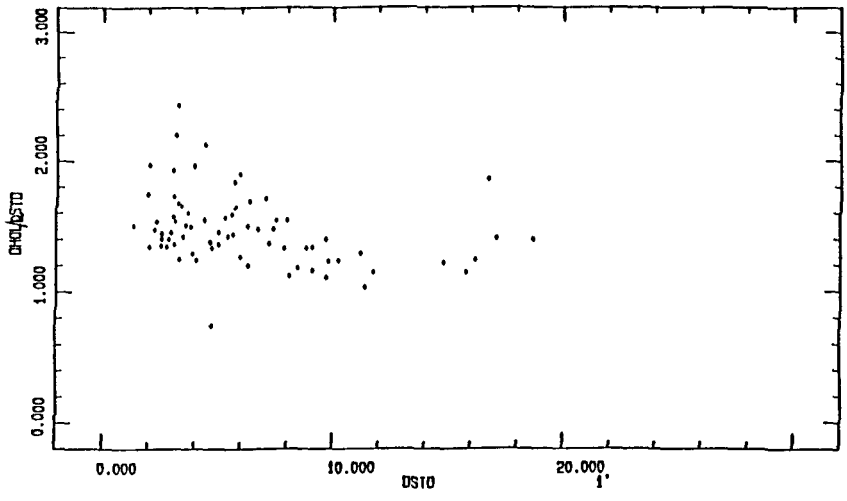


FIG. 2

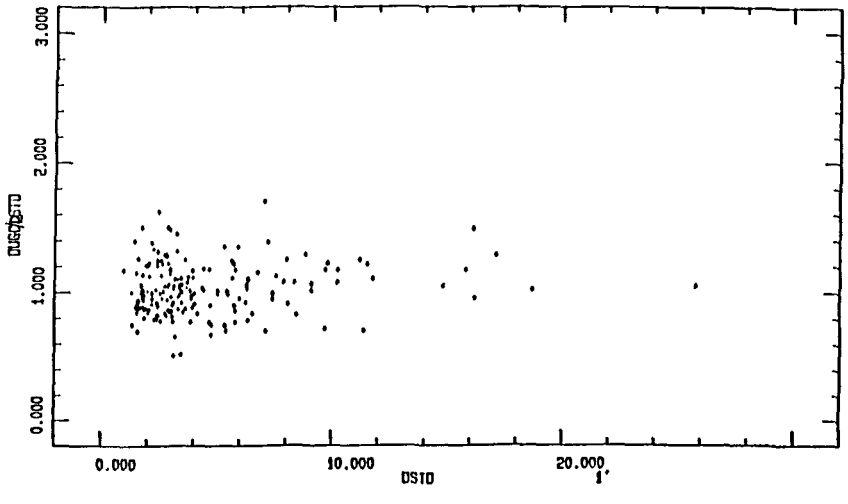


FIG 3

We have chosen in Fouqué and Paturel (1983) to compile all isophotal measurements at the 25 and 26.5 mag.arcsec^{-2} levels. We thus defined a standard system of 237 diameters. When compared to this system (thought to be bias-free), it appears that the Holmberg system is not isophotal (Fig. 2) and that UGC seems to be ok (Fig. 3). In Fouqué and Paturel (1984), we reduce the "visual" catalogues (UGC, MCG, and ESO) to the standard system by adding a 0.3' constant to the visual diameters. The conversion relations are then of the form :

$$D_{25} = k_i (D_i + 0.3')$$

where :

$$k_{MCG} = 0.98$$
$$k_{UGC} = 0.89$$
$$k_{ESO} = 0.74$$

III. PROJECTION EFFECTS ON MAGNITUDES AND DIAMETERS :

This point has formed the subject of a long controversy between, on the one hand, Holmberg (1958) and Tully (1972) that put all the correction on the magnitudes and none on the diameters, and Heidmann et al. (1972) on the other hand, that share the correction between both. It should be added that the effect on magnitudes is only due to absorption, when the effect on diameters, if any, is a combination of absorption and of a geometrical effect.

The four tests at our disposal depends on one of the corrections, or both, and can therefore disentangle the two effects :

B-H (W) depends only on B correction (H correction is assumed to be small (10% of the B one).

Σ_H(W) depends only on D correction (apart the small H correction).

Σ_B(W) and L_B(D) depends on both.

We have found that the B correction cannot be well represented by a one-parameter function (generally the optical depth). So we adopt a model where a part f of the galaxy is unabsorbed, a part f is totally absorbed, and the remaining (1-2f) contains dust homogeneously mixed with stars (model of the infinite sheet of uniform thickness). The relation between absorption and inclination then rests on two parameters, τ and f, and is given by :

$$A_B^i = -2.5 \log \left[f\,(1+e^{-\tau \sec i}) + (1-2f)\frac{1-e^{-\tau \sec i}}{\tau \sec i} \right]$$

where f=0.5 corresponds to the case of an infinite thin disk, and f=0 to the Holmberg (1958) model where dust and stars are totally mixed.

Moreover, we cut our law at 80° to take a plateau between 80° and 90°. The adopted curve is shown in Fig. 4.

But the B-H (W) test does not constrain the values of τ and f very much.

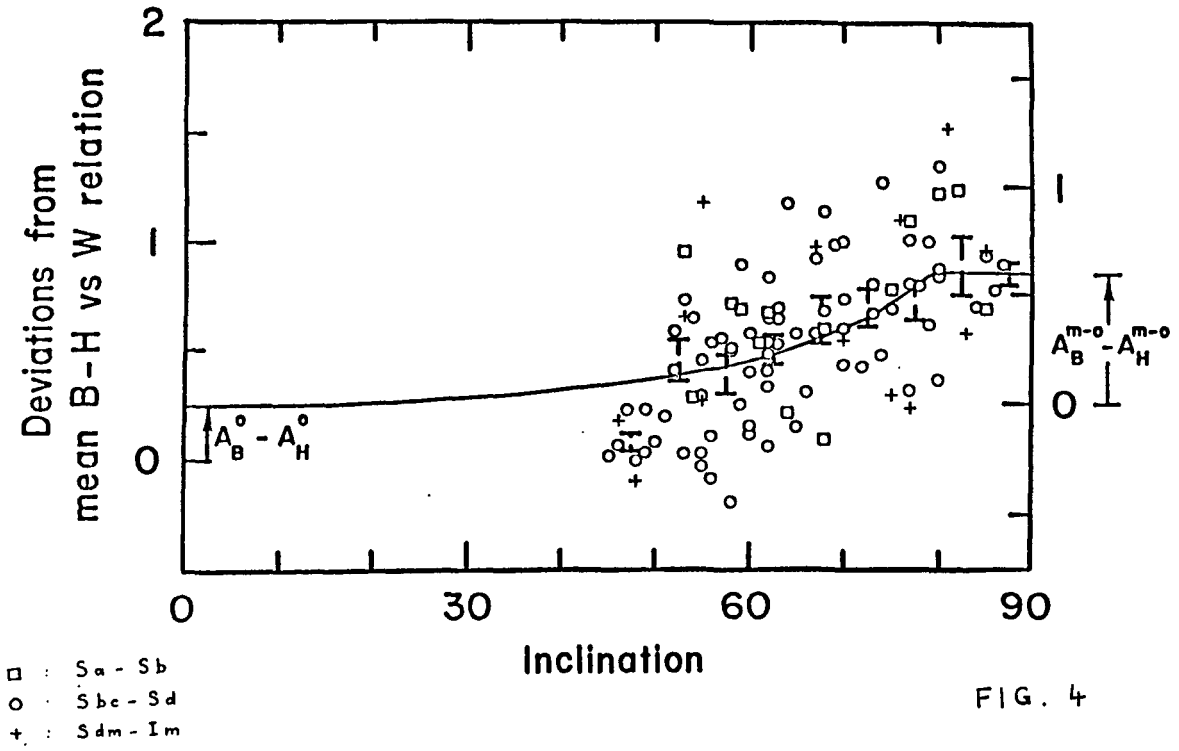


FIG. 4

Therefore, we only use these approximate values to correct the small H effect in the $\Sigma_H(W)$ test. We thus derive the D correction, adopting the RC2 relation :

$$\log D_{25}^{\star} = \log D_{25} - C \log R_{25}$$

Our preferred value, $C = 0.22 \pm 0.03$ is in perfect agreement with the RC2 one, $C = 0.235 \pm 0.045$.

Now we can use the two remaining tests, $\Sigma_B(W)$ and $L_B(D)$, corrected for the diameter effect, to better constraint the values of τ and f. The result is given in Fig. 5, where our adopted values are :

$$\tau = 0.55 \quad \text{and} \quad f = 0.25$$

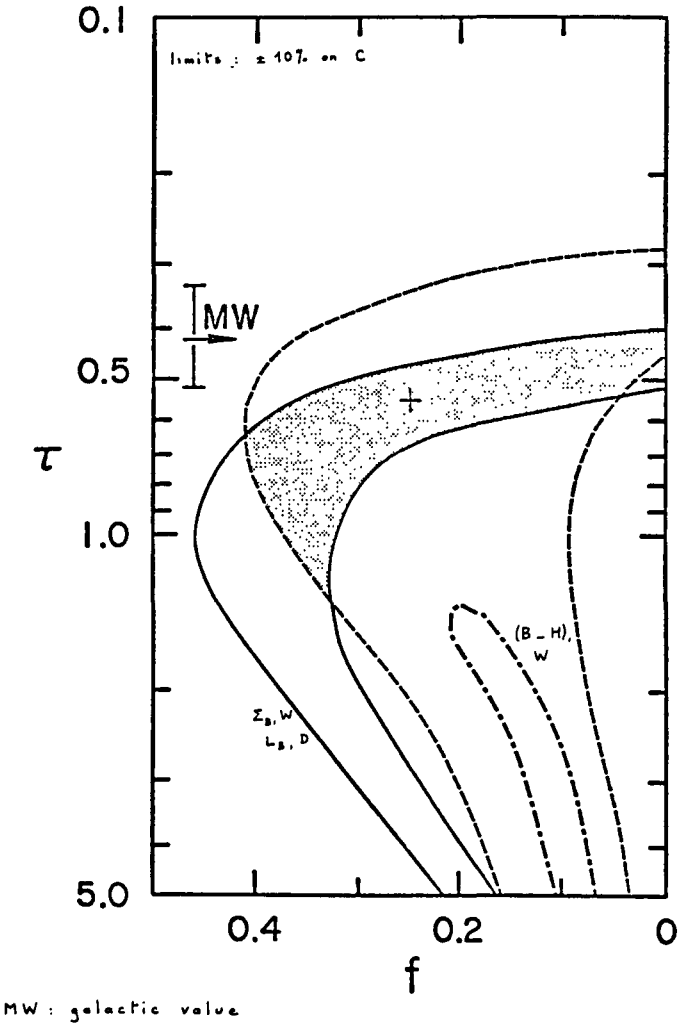
The order of magnitude of this effect is the same as in RC2, and we cannot in Fig. 4 see the type effect suggested in RSA.

IV. ABSORPTION EFFECTS :

Three different laws are currently available to describe the absorption of light by our own galaxy. They are given in RSA, RC2 and Burstein and Heiles (1978), and differ by the slope, the longitude dependence and the absorption at galactic poles. Our tests cannot deal with the last two effects, but are sensitive to the slope of the approximate csc b law. Our three models give the following slopes :

RSA : 0.132 RC2 : ~0.20 BH 78 : ~0.23

FIG. 5



The residuals of our four tests are such that :

$$\Delta (B_T^i - H_{-0.5}^i) = 0.9\, A_{B,\,true}^b \qquad \text{(we adopt } A_H = 0.1\, A_B\text{)}$$

and, adopting the RC2 relation $\log D_{25}^{i,b} = \log D_{25}^i + A_B^b K_D^{25}$:

$$\Delta \Sigma_H^i = (0.1 - 5\, K_D^{25})\, A_{B,\,true}^b$$

$$\Delta \Sigma_B^i = (1 - 5\, K_D^{25})\, A_{B,\,true}^b$$

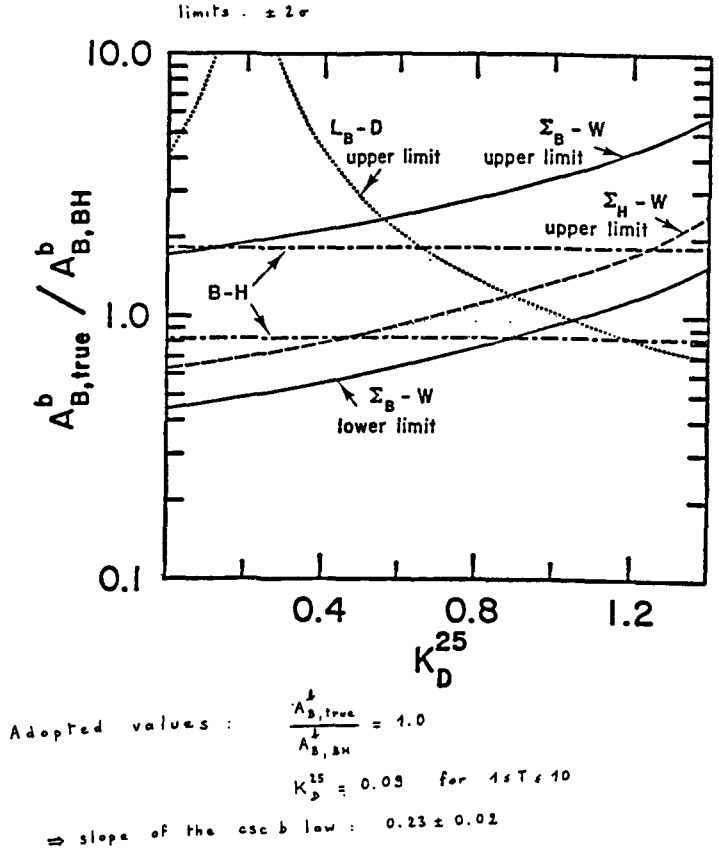
$$\Delta \log L_B^i = (0.4 - \alpha\, K_D^{25})\, A_{B,\,true}^b$$

where $\alpha = 2.1 \pm 0.2$ is the slope of the $L_B(D)$ relation.

Fig. 6 gives the results of these constraints, and our adopted values are the following, using the BH 78 model for the absorption :

$$A^{b}_{B,\,true} / A^{b}_{B,\,BH} = 1.0$$
$$K^{25}_{D} = 0.09 \text{ for spiral galaxies}$$

FIG. 6



With the RC2 absorption model, we get about the same results, what prevents us to choose between the two slightly different slopes. But the smaller slope of the RSA model is clearly excluded. We adopt a slope of 0.23 ± 0.02, which gives for our galaxy an optical depth $\tau = 0.42$, not so far from our mean adopted value 0.55 for spiral galaxies.

V. BACK TO THE DIAMETER SYSTEM :

We can now correct diameters for projection and absorption effects. Fig. 7 shows that residuals do not depend on diameters, what justifies a posteriori our choice of the standard system from Fouqué and Paturel (1983).

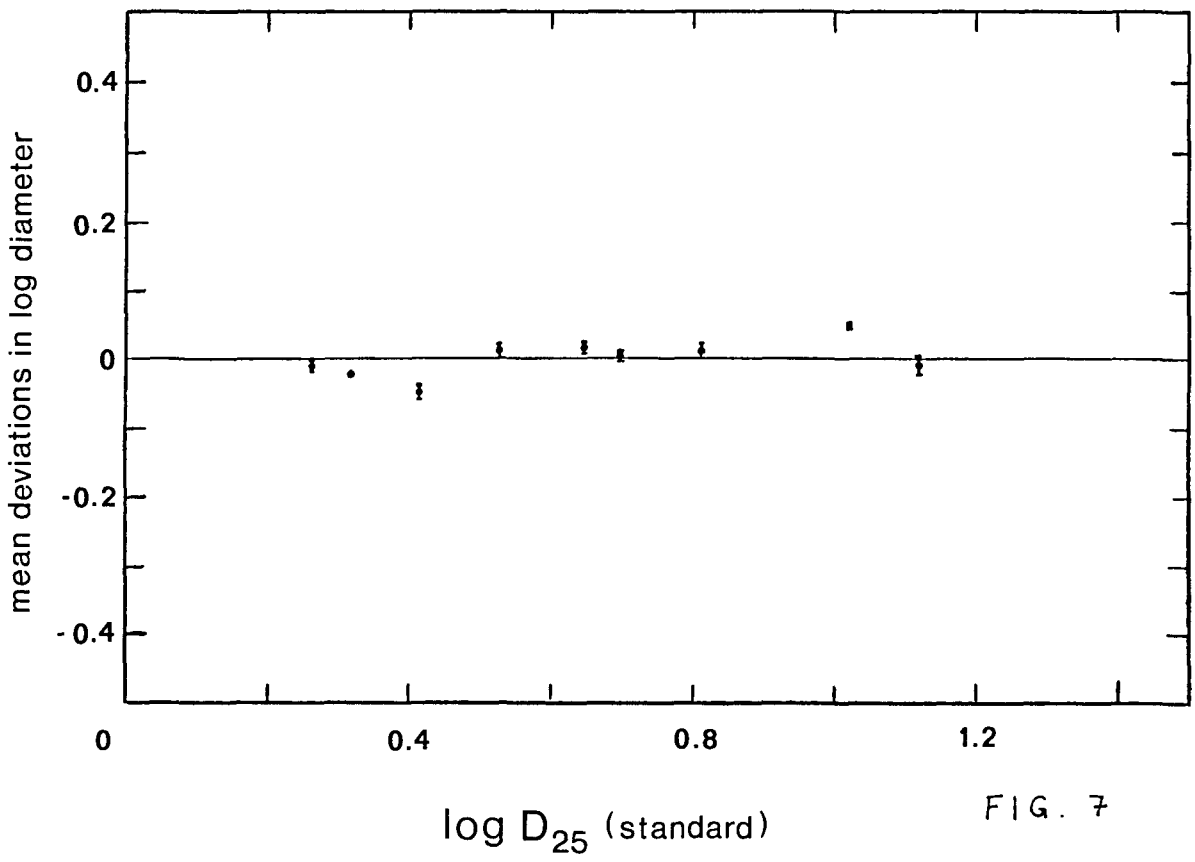


FIG. 7

References

Aaronson, M., Huchra, J., and Mould, J. 1979, Astrophys. J. 229, 1.

Burstein, D., and Heiles, C. 1978, Astrophys. Lett. 19, 19.

Fougué, P., and Paturel, G. 1983, Astron. Astrophys. Suppl. 53, 351.

Heidmann, J., Heidmann, N., and de Vaucouleurs, G. 1972, Mem. Roy. Astron. Soc. 75, 121.

Holmberg, E. 1958, Medd. Lunds Astr. Obs. (2), Nr. 136.

Tully, R.B. 1972, Monthly Notices Roy. Astr. Soc. 159, 35p.

Tully, R.B., and Fisher, J.R. 1977, Astron. Astrophys. 54, 661.

Tully, R.B., Mould, J., and Aaronson, M. 1982, Astrophys. J. 257, 527.

Van den Bergh, S. 1981, Astrophys. J. Lett. 248, L9.

DIAMETERS OF GALAXIES INSIDE AND OUTSIDE CLUSTERS

A. Bosma
Observatoire de Marseille

1. Introduction. Here I will examine the following hypothesis: spiral galaxies in clusters are smaller than those in the field due to truncation. Evidence for this comes from comparing spirals in Virgo with field spirals. In Virgo:

1. The HI diameters are smaller.
2. The percentage of galaxies with faint outer extensions is lower.
3. The micrometric diameters are more often determined by the smooth disk.
4. The blue luminosity - diameter relation may indicate smaller diameters.
5. The infrared surface brightness - 21-cm linewidth relation indicates higher surface brightnesses, or smaller diameters.

Note that from 1 - 5 we pass from truncation of the gaseous disk via that of the population I disk to truncation of the stellar disk itself. All of the above may be true, but it should be stressed that the diameter system needs improvement.

2. HI diameters. As discussed elsewhere in this volume (Kotanyi, Warmels), the HI envelopes of several Virgo spirals are much smaller than those of comparable galaxies in the field. The mean ratio of isophotal HI-size at 1.8 10^{20} atoms cm^{-2} to optical size at 25 magn. $arcsec^{-2}$ is about 20% smaller, there are no galaxies with HI envelopes extending out to 2 - 3 optical radii, and sometimes the HI-disks are very small, in particular in galaxies near to M87. Thus truncation of the outer HI envelope in some cluster spirals seems well established.

3. Faint outer extensions and disk edges. In a study of micrometric diameters of galaxies on various sky survey prints and films, Bosma and Freeman (1984, in preparation; also Bosma 1983) find the following. If a disk galaxy follows the exponential law with a central surface brightness of 21.5 in the blue (cf. Freeman 1970) we expect a growth in diameter with a factor 1.3 on the SRC-films compared to the Palomar blue prints, due to the different surface brightness levels. However, about 15 - 20 % of the galaxies we measured in the declination zone -20° to -30° show an increase in diameter by more than a factor 2. We measured also a UK Schmidt IIIaJ plate of the central part of the Virgo cluster and find only 2 out of 44 galaxies with a growth factor larger than 1.6. The galaxies with those large growth factors are mostly giant galaxies, which often show a two-zone structure in their disk. The outer zone of low surface brightness is virtually absent in the Virgo galaxies. We noted also that the disk edge in field galaxies is much more frequently defined by the young stellar population (spiral structure), while for Virgo galaxies the micrometric diameter is usually set by the smooth stellar

disk fading into the background. Both these phenomena point to truncation of the population I disk in the (Virgo-) cluster environment.

4. Diameter - luminosity relation. Data from Holmberg (1958), using H = 100 km $s^{-1}Mpc^{-1}$, show that there is no difference in the diameter - luminosity relation between Virgo galaxies and field galaxies. Yet Peterson et al. (1979, abbrev. PSS) find that for a galaxy of $M_B = -20.7$ the Holmberg radius is 18.2 kpc in Virgo, and 23.5 and 23.8 kpc in Hercules and the field (H = 50). However, here the various absorption corrections play a decisive role. To correct diameters or magnitudes the criterion is that the corrected surface brightness S = m + 5 log D is independent of inclination or axial ratio a/b. Holmberg corrects magnitudes only, PSS correct diameters only, while the RC2 recommends both. Even if one corrects to a uniform system, a problem remains with the data of PSS, since the slope of S vs. log a/b for the Hercules galaxies is much steeper than for the Virgo galaxies.

5. H-surface brightness - 21-cm linewidth relation. Kraan-Korteweg (1983) notes that the distance independent relation between $S = H_c^{-0.5} + 5 \log D_1$, and ΔV_{21}, where $H_c^{-0.5}$ is the corrected infrared magnitude, D_1 the corrected diameter in the blue, and ΔV_{21} the corrected 21-cm linewidth, differs for galaxies in the Virgo and Pegasus I clusters on the one hand, and those in the Zw 74-23 and Perseus supercluster on the other hand. Further analysis (Bosma 1984, Astron. Astrophys., submitted) shows that the latter galaxies behave like field galaxies. Most likely the diameters are the main cause of the difference. An interesting correlation exists between the residuals from a mean $S - \Delta V_{21}$ relation and those from a color $(B_T^0 - H_c^{-0.5}) - \Delta V_{21}$ relation. The Virgo and Pegasus I galaxies are, for the same ΔV_{21}, redder and of higher surface brightness than the field galaxies. This suggests that their diameters are smaller, since differences in Hubble type cannot explain the effect alone. This is confirmed by a $\log D_1 - \log \Delta V_{21}$ diagram showing that the Perseus supercluster galaxies have for the same linewidth the same diameter as the Pegasus I galaxies, despite their higher redshift. Of course this analysis rests heavily on the accuracy of the diameter sytem and the corrections, which both need drastic improvement. But if true, truncation of the stellar disk itself, at least in some cluster enviroments, cannot be excluded.

References:

Bosma, A. 1983. I.A.U. Symp. 100, p. 253, ed. E. Athanassoula. Dordrecht: Reidel
Freeman, K.C. 1970. Astrophys. J. 160, 811
Holmberg, E. 1958. Medd. Lund Obs. Ser. II no. 136
Kraan-Korteweg, R.C. 1983. Astron. Astrophys. 125, 109
Peterson, B.M., Strom, S.E., Strom, K.M. 1979. Astron. J. 84, 735

A COMPARISON OF THE VIRGO CLUSTER WITH (ONE) OTHER NEARBY CLUSTER(S)

Otto-Georg Richter
ESO Garching

The purpose of this note is to draw attention to some other clusters of galaxies that are very similar to the *Virgo* cluster and may provide a better playground for some observational studies. Furthermore, the detailed knowledge about properties in common with and different from the other clusters, could perhaps lead to a better understanding of the *Virgo* cluster proper.

Since *Virgo* is the nearest large cluster everything else to compare with is further away. Aside from this basic complication, there are some requirements as to how much information needs to be known about the other clusters in order to do a thorough comparison. We need at least some basic (optical) morphological and static parameters and, in addition, a redshift and a good measure of the velocity dispersion together with some information in other wavelength regimes, e.g., X-rays.

Of course, a comparison can be much more detailed if the relative distance moduli are small enough. Here a limit of $\Delta(m-M)_{Virgo} \leq 3^m$ is adopted. This implies a limit in (corrected) radial velocity of $v_o \leq 4500\ km\ s^{-1}$ or $z \leq 0.015$ (direction-dependant on your choice of the infall velocity of the Local Group). From the list of Noonan (1981) we then have quite a number of candidates. However, Noonan also lists groups which have to be excluded.

The small final sample is listed in Table 1. There the name of the cluster, its mean redshift, the number of available redshifts and the velocity dispersion from Noonan (1981)

Table 1 *Nearby Clusters with $z \leq 0.015$*

Cluster	Noonan, 1981			Recent			Reference
	z	n	σ_v	v_o	n	σ_v	
Virgo				1141	253	687	
Fornax I	0.0046	59	352	1395	65	352	Richter & Sadler, 1985
Centaurus	0.0107	66	871	2894	106	507	Lucey *et al.*, 1980
Hydra I	0.0114	21	765	3419	96	681	Richter & Huchtmeier, 1983
Pegasus I	0.0134	27	659	3885	31	236	Richter & Huchtmeier, 1982
2013-7100	0.0137	3	419				Vidal, 1975
1843-6321	0.0141	18	531				Fairall, 1979
Cancer	0.0145	21	755	4607	38	317	Bothun *et al.*, 1983
Klemola 27	0.0145	10	572	4253	20	551	Richter, 1984

Notes

Virgo: Velocity of *M 87*

Fornax I: *Fornax A* (*NGC 1316*) and a few other galaxies near to it (including *NGC 1365*) seem to form a background group

Cancer: Is not a single cluster, consists of several groups

and more recent sources is given. Apparently, from the parameters given by Noonan, especially the velocity dispersions, the clusters are indeed all comparable. However, more recent studies revealed that *Fornax I*, *Cancer*, *Pegasus I* and *Klemola 27* are smaller than was believed earlier. Furthermore, the *Centaurus* cluster seems to be the extreme case of a superposition of

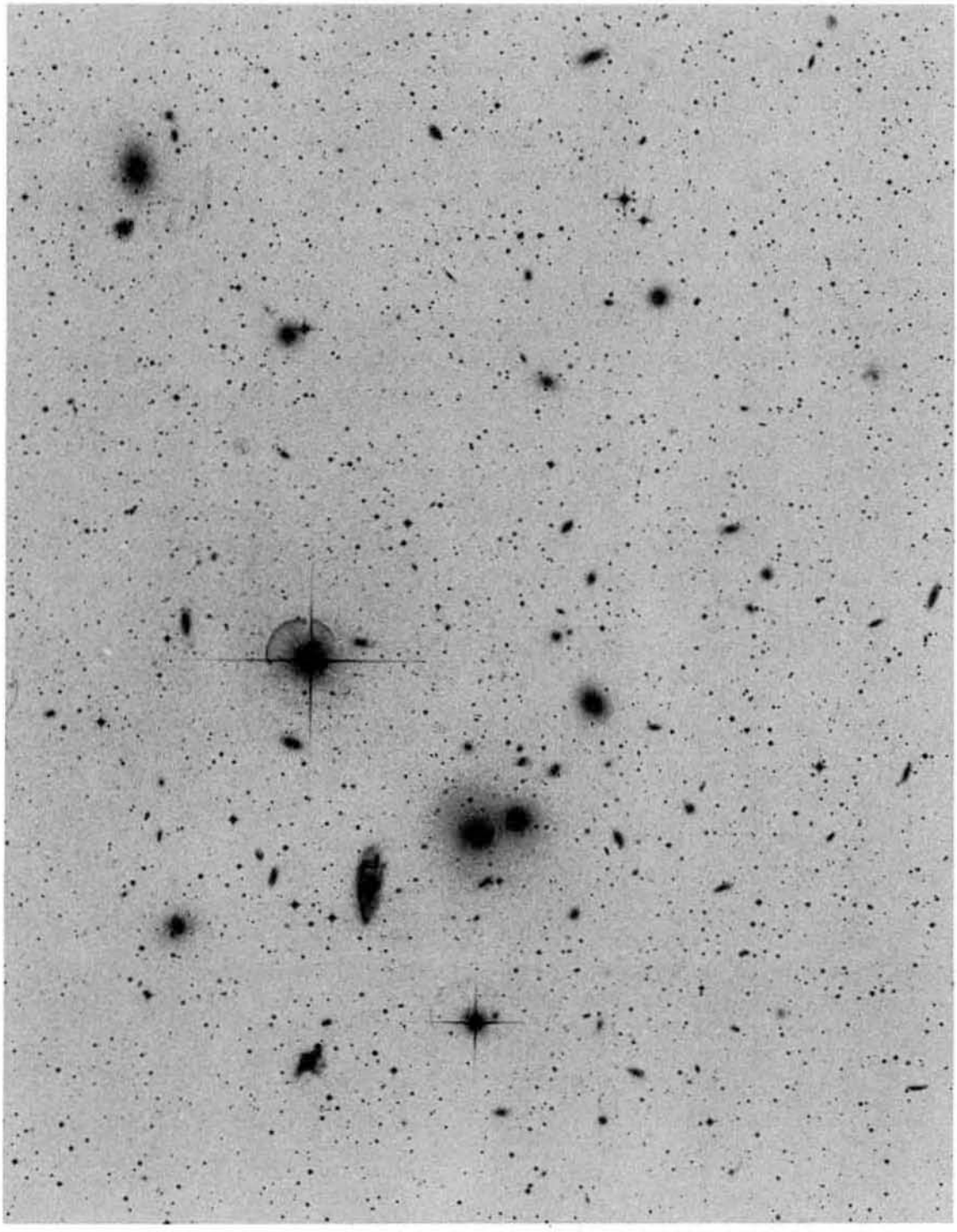


Figure 1. The central region of the *Hydra I* cluster of galaxies. Enlargement from the ESO Quick Blue Survey (field 501). For large scale photographs of the two central galaxies see Lindblad (1977).

two clusters. Finally, inspection of *2013-7100* on the southern sky surveys shows a very inconspicious and poor cluster, which, just like *1843-6321*, lacks any further information aside from that provided in the references cited in Table 1. Thus, only a single nearby cluster appears to be really comparable to *Virgo*, namely *Hydra I*, also known as *A 1060* (see Fig. 1). Similarities between the *Virgo* cluster and the *Hydra I* cluster were first pointed out by Richter et al. (1982). There are a few more distant clusters, e.g., *A 262*, *A 1367*, and the *Hercules* cluster, that may also be comparable to the *Virgo* cluster. However, the (known) number of parameters similar for *Virgo* and *Hydra I* is impressively larger than for the more distant clusters. For this reason, and because I believe that I know much more about *Hydra I* than all those other clusters, I shall concentrate here on that comparison. [I do, however, encourage observers to study the southern hemisphere clusters in order to provide the data lacking here for a more general comparison.]

The points expressed already by Richter et al. (1982) are: (1) both clusters are of Bautz-Morgan class III, (2) the ratio of their redshifts is about equal to the inverse of the ratio of their apparent diameters, (3) their total population within the first 4.5^m of the luminosity functions is comparable [≤ 210 galaxies in *Hydra I*, ≥ 176 galaxies in *Virgo* (Kraan-Korteweg, 1982)], (4) their velocity dispersions are equal within less than 1σ, (5) their X-ray luminosities are about the same, and (6) both the two dominant galaxies *M 87* and *NGC 3311* have nearly equal absolute magnitudes and they both have a very large retinue of globular clusters.

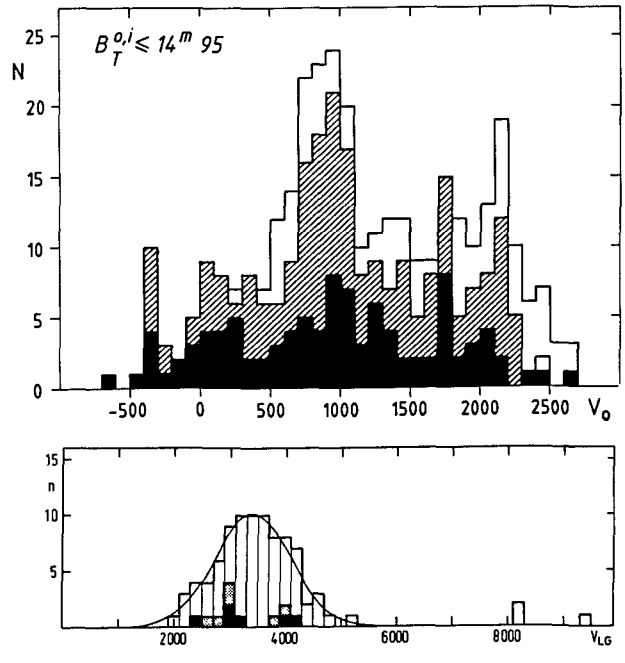


Figure 2. Radial velocity histograms for *Virgo* and *Hydra I*. Shading in the upper (*Virgo*) diagram indicates different limiting distances from the cluster centre (3°, 6° and 10°); in the lower diagram it indicates HI radial velocities.

There are also some obvious differences: (a) the central region in *Hydra I* appears to be much more densely populated than that in *Virgo* where there seems to be some empty space just around *M 87*, (b) the *Virgo* cluster's radio continuum emission is completely dominated by *M 87* whereas *NGC 3311* is only a very weak radio source (e.g., Lindblad et al., 1984), (c) the radial velocity histograms are very different in that *Hydra I* appears to be isolated in redshift space with a void behind it extending to at least 8000 $km\ s^{-1}$ while *Virgo* shows a very complex histogram (see Fig. 2). Also the (local) velocity dispersion as a function of distance from the cluster centre shows a different behaviour in the two clusters (see Fig. 3 below for *Hydra I*).

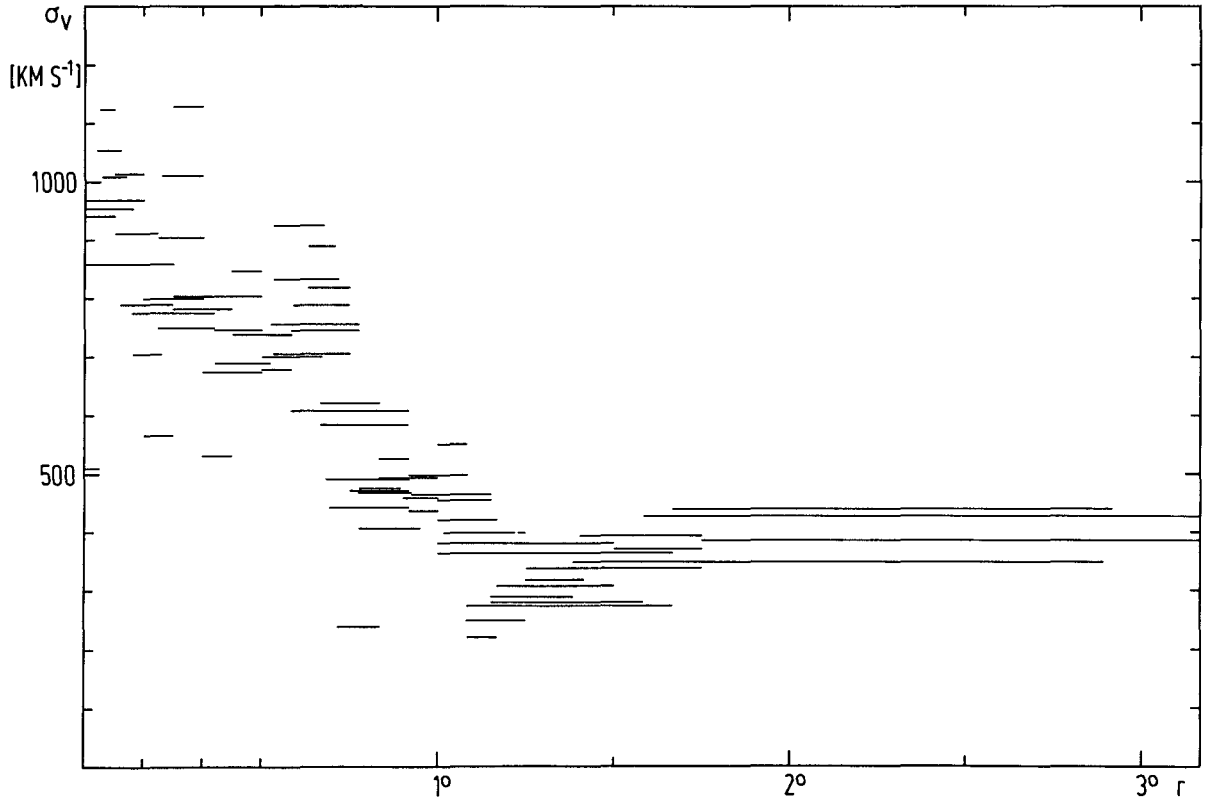


Figure 3. Line of sight velocity dispersion σ_v versus the apparent distance r from the cluster centre. The length of the bars indicates the range over which σ_v is measured. (Only samples with more than 3 galaxies are used.)

The available evidence from the data for *Virgo* and *Hydra I* suggests two not very different possible evolutionary scenarios to explain the differences between them. In the first, *Hydra I* has formed somewhat (a few Gyr) earlier than *Virgo* and is, correspondingly, further evolved. Alternatively, they may well have formed simultaneously, but *Virgo* might not yet have had time to relax to a stable configuration because of continuing infall of galaxies from its environment - the *Local Supercluster* - at a rate much higher than the corresponding figure for *Hydra I* and the *Hydra-Centaurus* supercluster. ("Is *Virgo* just a *Hydra* in its youth?") Therefore, it appears that a detailed comparative study of the kinematical and dynamical behaviour of the two clusters could lead to substantial advances in the understanding of the processes than govern galaxy formation and evolution. Such an investigation will be possible

after (1) more redshift data for *Hydra I* are available (Richter, 1985, in preparation) and (2) better means to determine individual galaxy masses are developed.

The faintness of *NGC 3311* in the radio domain contrasts with the outstanding brightness of *M 87*. This allows radio studies, including 21cm line observations, of the central region of *Hydra I* to much deeper levels than possible in the central region of *Virgo*. The VLA can probably do as good for *Hydra I* as for *Virgo*, maybe even better. Two examples are given in Fig. 4 below.

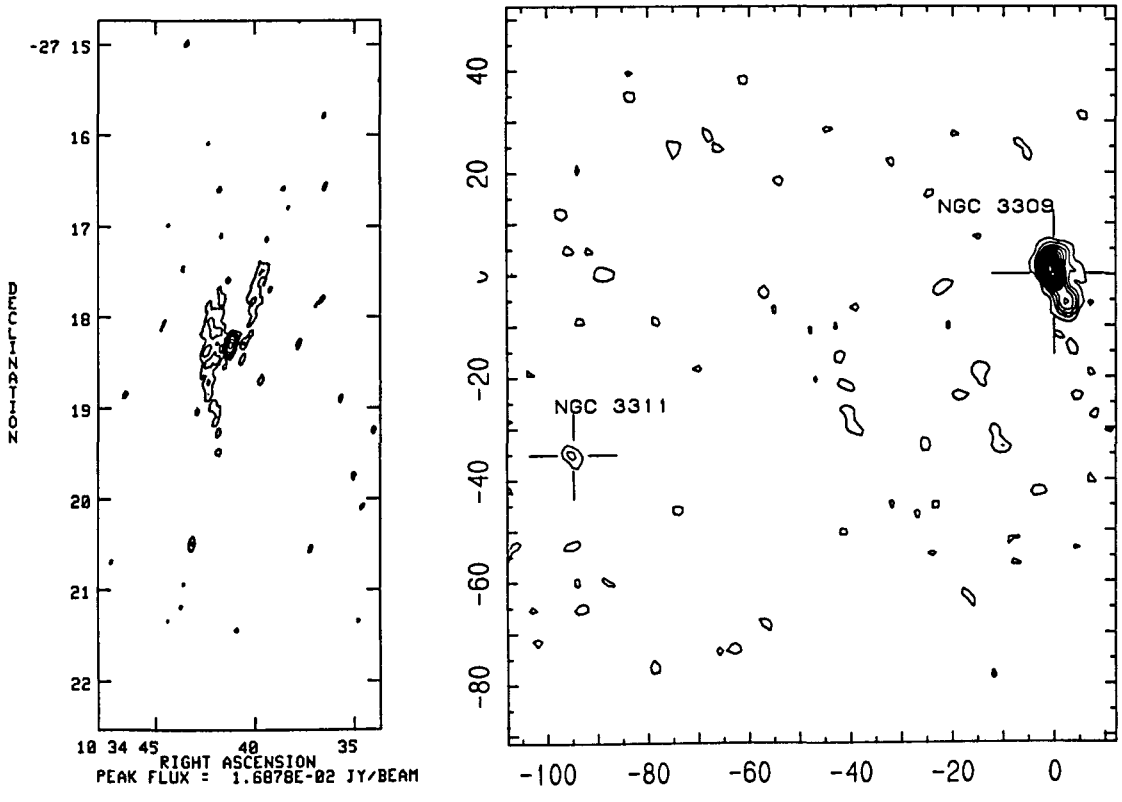


Figure 4. Left: VLA radio continuum map of *NGC 3312* at 1465 MHz (C. Kotanyi, *priv.comm.*). Right: VLA continuum map at 4895 MHz of the two central galaxies in *Hydra I* (Lindblad *et al.*, 1984).

There are a number of peculiar galaxies in both clusters that, apparently, suffer from environmental influences. The prime examples are *NGC 4438* in *Virgo* and *NGC 3312* in *Hydra I*. Eventually, by comparing the properties of these galaxies we may learn more about the different processes and how to disentangle them, such as enhanced (stimulated) or suppressed star formation, ram pressure sweeping, or buoyancy, that led to the observed disturbances.

References

Bothun,G.D., Geller,M.J., Beers,T.C. and Huchra,J.P.: 1983, *Astrophys.J.* **268**, 47

Fairall,A.P.: 1979, *Mon.Not.R.Astron.Soc.* **188**, 343

Kraan-Korteweg,R.: 1982 *Astron.Astrophys.Suppl.Ser.* **47**, 505

Lindblad,P.O.: 1977, *The ESO Messenger* **10**, 20

Lindblad,P.O., Jörsäter,S. and Sandquist,Aa.: 1984, *Astron.Astrophys.*, submitted

Lucey,J.R., Dickens,R.J. and Dawe,J.A.: 1980, *Nature* **285**, 305

Richter,O.-G.: 1984, *Astron.Astrophys.Suppl.Ser.* **58**, 131

Richter,O.-G. and Huchtmeier,W.K.: 1982, *Astron.Astrophys.* **109**, 155

Richter,O.-G. and Huchtmeier,W.K.: 1983, *Astron.Astrophys.* **125**, 187

Richter,O.-G. and Sadler,E.M.: 1985, *Astron.Astrophys.Suppl.Ser.*, in press

Richter,O.-G., Materne,J. and Huchtmeier,W.K.: 1982, *Astron.Astrophys.* **111**, 193

Vidal,N.V.: 1975, *Publ.A.S.P.* **87**, 625

DISCUSSION

H. MacGILLIVRAY: I would just like to point out one other similarity between the Hydra I and Virgo clusters. We have just obtained a deep AAT photograph of the center of the Hydra I cluster. This reveals that NGC 3311 has a rich globular cluster population, similar to M87.

THE FAR BACKGROUND OF THE VIRGO CLUSTER

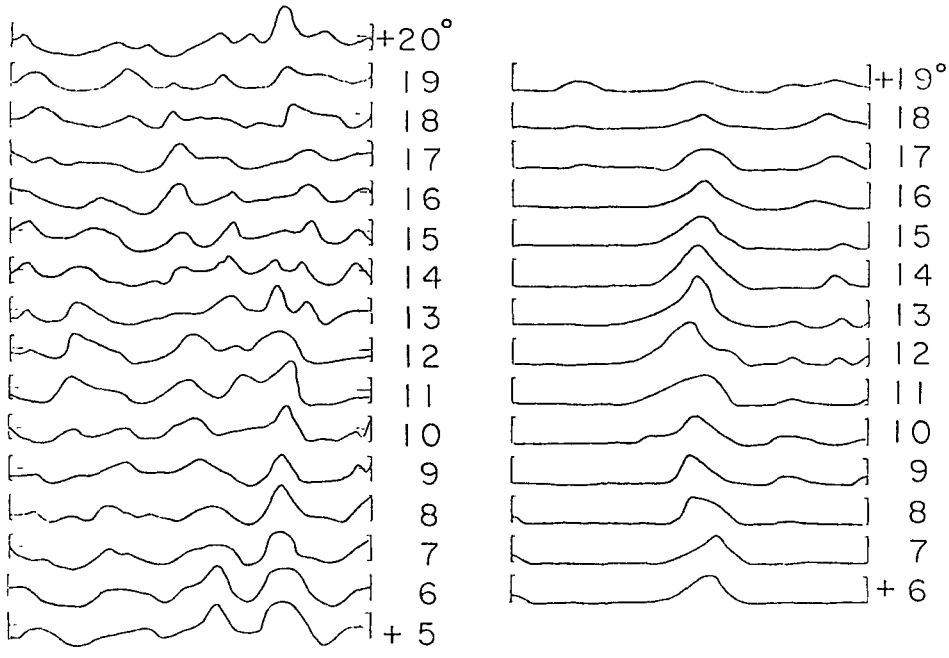
Gibson Reaves
Department of Astronomy
University of Southern California, Los Angeles, California 90089

Is it possible to put a limit on the intergalactic extinction within the Virgo cluster by comparing the projected areal density of very faint--and thus very distant--galaxies and clusters of galaxies within the area of the cluster, with the density in regions surrounding the cluster?

A large area, from $\alpha = 11^h00^m$ to 14^h00^m and from $\delta = +5^\circ$ to $+20^\circ$ (1950.0), was chosen for study. The Virgo cluster occupies the central 15% of this approximately 675 sq. deg. region.

Neither the Abell (1958) statistical sample of clusters nor the Shectman (1984) clusters picked from the Shane and Wirtanen (1967) counts display an areal distribution clearly related to that of the bright galaxies of the Virgo cluster. In both cases, the number of background clusters is too small for quantitative study. It is well known, however, that the areal density of clusters catalogued by Zwicky et al. (1961, 1963) is indeed lower in areas behind nearby clusters. In my opinion (Reaves 1974), this deficiency results largely from the observer's subjective difficulty in identification, and not from intergalactic extinction. Until this subjective effect is accurately calibrated, analyses of this kind of Zwicky's clusters should not be used for extinction studies.

The counts of galaxies by Shane and Wirtanen (1967), complete to nearly 19th mag., are numerous, and their systematic errors have been carefully studied and evaluated. We examine these counts here, qualitatively and quantitatively. Fig. 1(a) shows profiles of reduced and smoothed contoured counts of faint galaxies derived from Figs. 1 and 2 of the Shane and Wirtanen monograph. These profiles are taken at 1° intervals in declination and extend from $\alpha = 11^h00^m$ on the right, to 14^h00^m on the left. The tick marks on the scales at each end of each profile denote densities, from bottom to top, of 40, 60, and 80 galaxies per sq. deg. The highest density is over 100 at 11^h40^m on the $+11^\circ$ profile. An instructive exercise for the reader, before studying Fig. 1(b), is to attempt to find the Virgo cluster by inspection of Fig. 1(a) only. For comparison, Fig. 1(b) shows profiles of smoothed contoured counts of all galaxies in the region with $m \leq 14.0$ from Nilson (1973)--a limit chosen to make the Virgo cluster conspicuous --processed in precisely the same manner as were the Shane and Wirtanen counts in Fig. 1(a). Again, the profiles are given at 1° intervals in declination, but here the ticks represent zero below, and two above, galaxies per sq. deg. The Virgo cluster seems to have no effect on the counts of faint galaxies in Fig. 1(a).



(a) Background (b) Foreground

Fig. 1. Density Profiles. (a) Faint galaxies beyond the Virgo cluster. (b) Bright galaxies, showing the Virgo cluster.

Next, let us attempt to place a quantitative upper limit on the extinction through the Virgo cluster, again using the Shane and Wirtanen counts. From their Table VIII, we sum the counts on their 6° by 6° plates centered at declinations $+10^{\circ}$ and $+15^{\circ}$, and from right ascension $11^{h}20^{m}$ to $13^{h}40^{m}$, multiplying the sum of the counts on each by the appropriate personal, batch, smoothing and normalizing factors. The contribution to these counts by Virgo cluster members $m \leq 17.0$ has been subtracted from each field; the correction is taken as equal to 4 times the number of galaxies with $m \leq 14.0$ (Nilson 1973). This factor is based on the Kraan-Korteweg (1981) parameters in a Schecter luminosity function, and a limiting magnitude for detection of Virgo cluster dwarfs on the Lick 20-inch survey plates of 17th mag. (For any reasonable luminosity and diameter functions, it can be shown that the maximum area of occultation by images of Virgo cluster galaxies will be about 5% of the area, equivalent to only 0.05 mag. of extinction, and therefore entirely negligible here.) The results are given in Table 1, column (3). The number of bright, $m \leq 14.0$ galaxies is given in column (2). For mean areal densities in galaxies per sq. deg., divide each tabular entry by 72. Linear interpolation based on the three westerly and

TABLE 1.
Numbers of Galaxies in $+10^{o}$ plus $+15^{o}$
Declination Zones

R.A.	Cluster	Background
(1)	(2)	(3)
$11^{h}20^{m}$	20	2523
11 40	15	3552
12 00	17	3806
12 20	117	3514
12 40	67	4199
13 00	13	2508
13 20	6	3313
13 40	2	2866

three easterly fields gives a predicted count of 43 ± 7 background galaxies per sq. deg. at $12^{h}30^{m}$ (i.e., between $12^{h}20^{m}$ and $12^{h}40^{m}$) whereas the mean observed background count is 54 per sq. deg.

This result, that the observed count is greater than the (corrected) interpolated count, was unexpected, and may be explained by the extreme irregularity of the distribution of faint galaxies, and also possibly by an insufficient allowance for the contribution to the counts by compact dwarf members of the cluster. (The amount of extinction equivalent to a reduction of the counts by 10%--say, from 50 to 45 per sq. deg.--may be approximated from data in the Shane and Wirtanen paper. It comes out to be 0.1 mag.)

From these crude results, the most that one may tentatively conclude is that the extinction through the Virgo cluster is probably less than 0.2 mag. This result is consistent with those derived from a study of residuals in the corrected B - V vs. redshift relation which yield 0.1 mag. as a general upper limit for clusters (Reaves 1968, 1974).

(It is my subjective, qualitative impression, from the relative crispness and surface brightness of the photographic images of the faint galaxies beyond the Virgo cluster core, that the extinction is, in fact, much less than 0.2 mag. But I am unable at present to substantiate this impression quantitatively.)

A rough calculation shows that if there is intergalactic dust within the Virgo cluster with the same extinction properties in the visible as the interstellar dust within galaxies, then a 0.2 mag. upper limit on the extinction

restricts the total mass of intergalactic dust in the Virgo cluster to about 10^{11} solar masses. This is the same order of magnitude as the total mass of dust in the individual Virgo cluster galaxies if we assume that they are all spirals.

The conclusion of the preceding paragraph may be stated more provocatively: if the dust-free systems in the Virgo cluster were formed initially as spirals, and if they then lost their interstellar gas and dust subsequent to formation as a result of interactions with their surroundings, then, unless there is some efficient dust removing process operating, the extinction through the cluster will be about 0.2 mags. If the extinction could be shown to be significantly less than 0.2 mags.--say, 0.02 mags.--then this evolutionary hypothesis would have to be rejected.

REFERENCES

Abell, G.O. 1958, Ap.J. Suppl., 3, 211.

Kraan-Korteweg, R.C. 1981, Astron. and Ap., 104, 280.

Nilson, P. 1973, Uppsala Astr. Obs. Ann., 6 (Uppsala General Catalog of Galaxies).

Reaves, G. 1968, Pub. A.S.P., 80, 564.

_____ 1974, Sov. Astron., 18, 307.

Shane, C.D., and Wirtanen, C.A. 1967, Pub. Lick Obs., 22, Part 1.

Shectman, S.A. 1984, preprint.

Zwicky, F. et al. 1961, 1963, Catalogue of Galaxies and Clusters of Galaxies (Pasadena: California Institute of Technology), 1 and 2.

VIII.

PANEL DISCUSSION



From left to right: H. Arp, W. Forman, R. Kennicutt, M. Roberts, R. Giovanelli, B. Tully, A. Sandage

FUTURE NEEDS FOR OBSERVATIONS OF THE VIRGO CLUSTER

PANEL DISCUSSION

Panelists: H. Arp
W. Forman
R. Giovanelli
R. Kennicutt
A. Sandage
B. Tully

Chairman: M. Roberts

M. ROBERTS: The organizers of this workshop thought it would be appropriate at the end of the third day to have this panel discussion. It's a discussion which, I trust, the audience will participate in. I know, when speaking to the panelists I expressed the hope that they would be captious in their remarks with the intent of keeping the conversation going.

D. LYNDEN-BELL: May I suggest that it's a rule that each glass is emptied after the speaker has spoken... (laughter).

M. ROBERTS: I'm glad you brought that! Some of the participants in this panel required very special conditions, like wine, and I'm delighted to say that the organizers of the workshop responded instantly - they must have a basement full... (laughter).

Without further ado, and primarily because the slides were put into the slide projector in that order, I am going to call on Chip Arp to make the first remarks. This is sort of open-ended but with the general theme of the Virgo Cluster.

H. ARP: Well, Gustav remarked that it was the purpose of a workshop to make outrageous remarks. I'm sure he forgot I was in the audience... (laughter). - Having second thoughts, Gustav -?

I just want to make a few comments and start with maybe something mild: I show you the Virgo Cluster in 1967, and the reason why I go back to 1967 is

not to show that astronomers back in those days were so brilliant and perceptive, but that an effect which persists for this length of time - my friends tell me - is liable to be a real effect. I hope that's true for astronomers too. The effect that I want to talk about is the overall view of the Virgo Cluster, and I, like everyone else or many people back in those days, just plotted it out from the Shapley-Ames Catalogue and just used different symbols and so forth. I plotted a little bit larger area than has been discussed in this conference, and I was sort of struck by this continuity of particularly the brighter galaxies in the area... (Speaker shows a transparency, ed.) I did one other thing which is somewhat interesting: I just took clumps here and said, just what is the mean redshift (because there is a lot of dispersion in the redshifts) of these things, and I was interested to see that there is a kind of continuity here, 900 km/sec, 800 km/sec [around M87] down into NGC 4472, which I always considered the center of the Virgo Cluster, 1200 km/sec, and then these higher ones down here. I think this is still interesting and the thing that reminded me of this was to see Kotanyi's radio map of the Virgo Cluster and I'm going to show that in a minute. But I want to particularly point out that this is kind of Gustav's 800-900 km/sec range up around M87, and then this is his second cluster down here [around NGC 4472], which is pretty much the same as we saw - which is rather nice. Let me show you Kotanyi's which is so similar. He loaned me this. I think particularly spirals, where the radio sources are indicated by the heavy dots, indicate again this continuity. But if you're going to view this whole Virgo Cluster as a twisted chain, or something like that, you're going to have to worry about these large redshift differences.

Now, this is particularly striking - this has been known for a long time: this very very tight chain of E-galaxies. And this is the cloud of S-galaxies which surround it, which de Vaucouleurs pointed out many years ago, and which raises the problem of the redshifts of the S-galaxies and the E-galaxies, which I will come to in a minute. Before I do that, let me make one comment which has been alluded to a lot in this conference. I think it is a very important point. What does this line define? The first slide, I just happen to have it with me, which dates back from about 1970 shows just de Vaucouleurs E-galaxies plotted in the region of the Virgo Cluster, and here is the direction of the jet and the direction of the counterjet (see Figure I, ed.). I always thought that this was an exceedingly good fit... A lot of people are unaware of this.

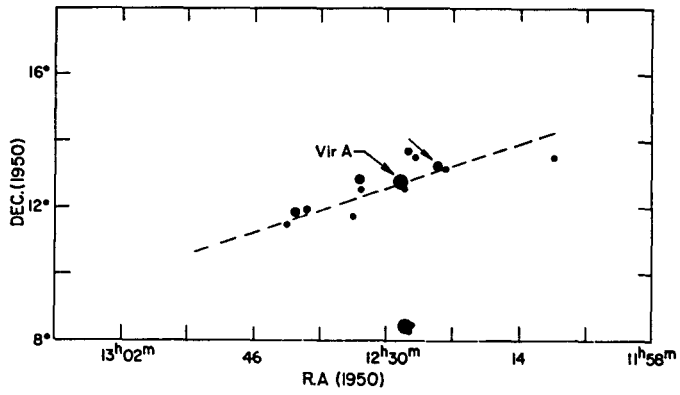


Fig. I: All E galaxies (classification by de Vaucouleurs) in the region are plotted as filled circles. The dashed line is the line of the optical jet and counterjet and also the line of the radio source components inside M87. The arrows point to strong radio sources in the area. (H. Arp 1968, Pub. A.S.P. 80, p. 138.)

M. ROBERTS: Where is the rest of the stuff?

H. ARP: Oh, this is just the E-galaxies - and I didn't even classify them, de Vaucouleurs did... (laughter). I'm just using other people's data. Well, but of course we all know that one incident doesn't make a significant thing. So, I looked around in other groups that might confirm this. I'm not going to show you all, but just this second slide which shows another example of this which is Centaurus A, the other big radio source. Again the bright galaxies form a line along the jet. I looked at 17 of the brightest radio sources and I claim that there were 15 that showed alignment along these radio directions... I think there is something very important going on. In this conference we've seen X-ray stuff, we've seen diffuse sources, we've seen compact sources, we've seen a lot of things on this line between M87 and M84. I'm sure we don't know what it means, but I think it is very important; perhaps for that reason.

Now, this line around M87 - this is the second remark I want to make - poses a real problem. This is a real paradox, because, if they (i.e., the galaxies in the line, ed.) even had dispersions of a few hundred km/sec, the line would disappear in a few times 10^8-10^9 years. So you have this really fundamental paradox of a few times 10^{10} year old galaxies, the E-galaxies, forming a line which can only exist for an order of magnitude less than that. So there is that problem, and that problem extends to all these chains that are showing up in the new catalogues of peculiar galaxies, and so forth. I would recommend to MacGillivray that he apply his methods to these chains, because it looks to me, just on viewing them, that the galaxies tend to be elongated along the line of the chain which had seemed to me was in the Markarian chain too.

The last remark I want to make is a little more serious, and that is the question about the redshifts, as I call them, in the Virgo Cluster. This is a slide from 1974/75. Now, I'm not worried about test probes of gravitational fields, or anything. What I'm asking here is the question of why is the mean redshift of the material which is bound up in morphologically classified Sc's or Sb's different from the mean redshift of morphologically classified E's? The reason I did this is because this is luminosity weighted, so that the most of the mass is tied up in ellipticals with this (...) kind of a redshift, and in spirals with this (...) kind of redshift. You can add innumerable numbers down here (i.e., add faint galaxies, ed.), and you're not going to change that because they're very small. I think that one of the nicest pictures we saw was Sandage's picture which showed that for the brighter Virgo galaxies you got E's and SO's and then, as it got fainter, the percentage of the E's and SO's dropped and you got dwarf E's and irregulars. So that by the time you're down to a factor ten, or something like this, you're really running out of true spirals. So, I think the one thing you shouldn't do - and this is my final point - is what my friend Gustav did, which is to lump the spirals and the irregulars and the Sm's together; and I'll show you why I'm afraid of that. Here are the results by Edmond Giraud for his thesis at Montpelier and also at Institut d'Astrophysique; here is the Virgo Cluster, the Perseus Cluster, the Hercules Cluster, and they all show this rather large difference for the Sb-Sc types with an excess redshift. And you notice it drops down to the dwarfs, the Sm's, and the Sd's. Now, if you average and, particulary, weight this very hard, you're going to wipe out this effect completely, which is what, I think, has happened to Gustav's material and in John Huchra's. The last confirmation of this is shown here. Those are the clusters you just saw; here is the whole sample of groups in de Vaucouleurs' catalogue, here is the Huchra and Geller catalogue; and I might say that Sulentic and I have done this in binary pairs of galaxies, where you have an elliptical and a spiral, and you always find the same thing. I think this is a real paradox, and I think it has to be grappled with, and I don't think you can get around it in Virgo!

M. ROBERTS: Would people care to make some comments on this..., audience or participants?... (silence).

R.B. TULLY: They're stunned!... (laughter)

A. SANDAGE: We were asked when Mort typed up that little invitation for all of us to sit here without knowing any of this: What would we do next, if we had lots of telescope time? What would you do next?

H. ARP: Well, I thought about the question, and I came up with an answer that surprised me. I think the most important thing is the outer regions of the Virgo Cluster galaxies, the lower surface brightness regions. And I think that Space Schmidt, which has been designed, and is all ready to go at a very small fraction of the budget of the Space Telescope, should be flown. It has a five degree field on the Virgo Cluster; it could be covered to a surface brightness three-quarters of magnitude deeper in visual range and much deeper in the ultraviolet and infrared. We would see the disturbances, the perturbations, the connections: we would get more real information on the Virgo Cluster. In my opinion that's the most important thing that could be done on the Virgo Cluster.

R.C. KENNICUTT: I saw something. Could we have your Centaurus slide back?... That is the most important thing here. You trace that line around 180° and you will hit the Virgo Cluster.

H. ARP: That is the kind of creative thinking we need...! (laughter)

M. ROBERTS: Well, I think, Chip, you have done a job in bringing out things that haven't been said. I might say that, when I first saw that publication of the line of ellipticals around M87 - aligned with the jet - I didn't believe it. And so I sat down myself and plotted it up, and lo and behold it's true! - using the data that were then available. I think, it's become much fuzzier now with more ellipticals... (R.B. Tully: Well, there can't be more ellipticals...) ...in the catalogues.

A. SANDAGE: Well, I guess since Bruno did all of the work on this Las Campanas survey, do you know what it looks like, Bruno, if you take now what the data are, rather than [plotting only galaxies brighter than] magnitude, say, -18^m?

B. BINGGELI: I think there are not more ellipticals... I mean, faint ones we classified E and not dE. We have a plot of only ellipticals and I remember there was still this... this... I'm afraid... (laughter).

A. SANDAGE: We kind of ignored that in Basel...

J.-L. NIETO: What's the probability of having such a line-up of galaxies which has been seen in the cluster?

H. ARP: Oh, I thought about that last night and... (laughter). I visualized the way that my friend Donald Lynden-Bell, if you forgive me, Don, might approach the problem. Gustav tells us there are 40,000 square degrees in the sky, and if we consider 40 square degrees around the Virgo Cluster, then we have a thousand places we can look in the sky to get a statistical fluctuation. So, I think that this clearly proves the Virgo Cluster is a statistical fluctuation... (laughter). Now, seriously, how to disprove that? Because, you see, the Virgo Cluster is a unique object. That's the point of my remark.

G. HELOU: But it's not a unique cluster. I mean, there are certainly other clusters where we can do the same kind of test.

H. ARP: That's why I went to the other radio sources! Centaurus A, 3C31, all the rest of them. And actually they all show the same effect, more or less.

G. HELOU: No, I meant the E versus S effect.

H. ARP: The E versus S? Yes, I think they do.

I might just make one more remark, and that is, it seems to me that there is an important distinction we make here between the bright galaxies and the faint galaxies. The faint galaxies are definitely more spread around. Why are the bright galaxies linearly arranged?

R. GIOVANELLI: I wanted to make a remark. Today we've heard that the Virgo Cluster may have a rotation curve; maybe it also has spiral structure...? (laughter)

D. LYNDEN-BELL: This is Arp 19.. What was it Chip? Arp 19.. what? - your spiral structure in the Virgo Cluster that has been mentioned? (Oh, Arp 1967?)

G. HELOU: There is room for Vincent Icke who has shown that under certain cosmological assumptions, if you're making galaxies in clusters and specifically E-type galaxies in clusters, you're going to make them into chains that sort of tend to line up. So that cannot be all that surprising.

H. ARP: That's right. Chaining, I think, is a phenomenon of galaxies.

D. LYNDEN-BELL: Then that has to be a short-lived phenomenon; the time scale is wrong.

J. HUCHRA: Chip, does your plot of the velocities run east to west in the same orientation as everybody else has been showing plots, for Virgo? (H. Arp: in the coordinates?) Right... Then the sense of rotation is exactly opposite what Gustav mentioned this morning, which must mean that the bright galaxies are counter-rotating to the faint galaxies.

H. ARP: No, I don't think it is contrary to what Gustav said.

I'm showing the southern extension, which most people did not talk about. Gustav was talking about essentially this..., right? Where is Gustav?

A. SANDAGE: He just walked out. (laughter)

J.-L. NIETO: Concerning the coincidence with the direction of the jet, you should not forget that the jet is bent southwards at its very end and the whole two-sided radio source is composed of two diffuse radio lobes which are a little bit southwards of the optical center. The direction is, roughly speaking, perpendicular to the jet itself. So maybe all these coincidences are just meaningless.

H. ARP: No, I think what you're talking about is the general considered drift of the diffuse material. The narrow jets are the ones that I think define a significant direction in this area, and they seem to be well defined.

J.-L. NIETO: But this is a very nuclear phenomenon at the very beginning of the jet, but outwards it's the interaction with the...

H. ARP: Oh, don't forget the radio jets in radio galaxies go out enormous distances, therefore for an enormous time...

J.-L. NIETO: Not M87 itself.

D. LYNDEN-BELL: But what you've said is important because Forman would take objection to it... You want all this gas to be static around M87 and the idea that the radio lobes on both sides are bent backwards doesn't really fit that too well.

W. FORMAN: To refer to one of the earlier questions... It's possible that your galaxy, M87, is slowly moving. I don't know..., there was a paper by...

someone who also explained also some of the H alpha filaments. The explanation which they presented was that the galaxy was simply slowly moving.

D. LYNDEN-BELL: Slowly moving being 200 km/sec?

C. KOTANYI: Yes, the H alpha filaments are exactly on the northern edge of the radio source.

M. ROBERTS: Knowing that M87 will have several hours to itself, I will use the chairman's prerogative and move on to another speaker and ask, in a random fashion, Brent... do you have anything to say? (Be captious!)

B. TULLY: The topic that I have heard described to me was what we might do next in terms of observations and increasing knowledge of the Virgo Cluster, and, I guess, the only thing that I know what to do is what I'm doing next and that biases my thoughts. The first question one wants to ask, though, is what is really the most important question we're dealing with here, and to my mind it's galaxy formation. The nice thing about the Virgo Cluster is that it has all kinds of galaxies... It's a pretty popular game now to be looking at distant clusters as we were hearing before. It seems very probable - in fact, one of the maybe disappointing things at this meeting is how good the agreement has been - that the Virgo Cluster, in fact, is a rapidly evolving system. And if that's the case, then presumably all other clusters are too. I think the information that we need first of all, some of it is very valuable, is the radio information: the 21 cm information about stripping as a function of radius. That's really crucial stuff, it seems to me, and also now the molecular stuff and anything we can get out of the IRAS observations. These are things I haven't been able to synthesize yet. But in the optical domain, I think we're just barely starting with regard to our knowledge of area photometry of galaxies; and I'm talking about large samples in a cluster, samples of a thousand, say, complete samples in the direction, say, that Okamura has been discussing: Colours (that he didn't have) and concentration indices, and scale lengths for large samples. Of course, part of my saying this is realizing that it now can be done; it can be done all the way across the visible from the U passband to one micron easily now with CCD's. I know I'm involved in something like that, and a number of other people are too, and I certainly see that as important. In particular, tomorrow I'll give a little talk about the colour magnitude diagram, and I think that there might be possibilities for that having some of the importance, say, of the HR diagram to stars. Perhaps we'll be able to trace evolution on such diagrams.

M. ROBERTS: It's sort of strange that the radio data, from your remarks I gather, are in better shape than the optical. With all the manpower in the optical...

R.B. TULLY: Well, the optical people have that potential. Of course the radio is only getting underway in a sense too, in the sense that only small numbers of galaxies have been looked at. So, I'm saying that there is capability now, both in the radio and in the optical, which hasn't been fully exploited.

M. ROBERTS: So, there are a few more theses yet to get out of the Virgo Cluster.

R.B. TULLY: Another parameter, in fact I mentioned it, is the concentration index. I think the bulge-to-disk ratio is a really important parameter to know about for large samples.

R.D. DAVIES: To someone who knows nothing about optical astronomy would you, Brent, say that it would be possible to actually get distances of individual objects? What I'm concerned about, and everything I've heard points to it, is that the stuff that we call the Virgo Cluster isn't all of the same distance. There has certainly been some statement that the W-cloud is a background object. I'm not sure that everybody agrees to that. It's possible, but it's a bit worrisome. If that's a background object, isn't the southern Cloud B at a distance that's different from the other objects? It would be good to see whether, in fact, these things are connected, whether there is a common halo. In all the discussions we've heard about hydrogen deficiencies, and so on, and the optical colours - all have assumed that that stuff is at the same distance. And indeed, if one [cloud] was 30% further away than the other, the redshifts could almost be compatible with 20% difference in distance. Isn't it possible to get some distances, say, by identifying stars? Maybe you need to do that with the Space Telescope; maybe you can do it from the ground. It depends what the modern technology is up to these days. But can you get some distances and sort out whether these groups are...

R.B. TULLY: Well, I think the situation there is... Optimistic people might think that you can get distances to individual galaxies with a given technique to 20%. And if you had several techniques you had some faith in, you might push that down 15%, a little lower perhaps, on an individual galaxy. As you say, the front to back range in the Virgo Cluster is 20% of its distance from us. It means that it's kind of a grievous problem. If

you've got several galaxies in group B you might get that down, so you were sort of convincing yourself. But that's the problem with this whole other business of analyzing whether there are expanding shells, or galaxies in the backside and frontside. It's certainly right at the limits of optimistic...

R.D. DAVIES: My question to you, though, is, are there techniques available or likely to become available? Space Telescope, ...?

D. LYNDEN-BELL: Rod, these two things are three degrees apart, maybe four degrees apart in the sky...

R.D. DAVIES: Yes, but their velocity differs...

D. LYNDEN-BELL: No, ... A and B are very similar in velocity.

R.B. TULLY: But still, they could be a large distance apart; they could be. There is no evidence there.

D. LYNDEN-BELL: Could somebody give me the velocity difference..., in fact, I got it in these notes... region A: 1057 [km/sec], region B: 963 [km/sec].

R. GIOVANELLI: We've heard in Gustav Tammann's talk this morning what the difference may be between the northern part, the part receding from us and the part coming towards us: one is at .8 and the other at 1.2 times the distance from the centre of the cluster. I think this is a difference of 50%. If one puts together all the spirals in those two clumps, we have something like probably 200 HI profiles. There sure must be enough edge-on galaxies so that we can tell apart a difference of 50%.

R.B. TULLY: Where is the difference of 50%?

R. GIOVANELLI: Well, if one is at 0.8 and one at 1.2, I guess, 1.2 divided by 0.8 will give you 1.5. I mean that is a difference of 50%...

R.B. TULLY: Where does your difference of 0.8 and 1.2 come from?

R. GIOVANELLI: From Gustav's talk this morning, I think...

D. LYNDEN-BELL: ...velocities, velocities...

R.B. TULLY: OK, but I'm saying, just in terms of the projection on the sky, if it's a more or less round thing then we're expecting 10% variations.

D. LYNDEN-BELL: If that!

A. SANDAGE: Plus or minus 10%. What do you really think Tully-Fisher can give?

R.B. TULLY: I think, 20% for galaxies that are benign, and I think that I have...

A. SANDAGE: How do you know beforehand what's benign?

D. LYNDEN-BELL: ...not in the Virgo Cluster is an important benignity!

A. SANDAGE: This is a crucial thing. Is NGC 4569 benign?

R.B. TULLY: No, I don't think that's benign.

A. SANDAGE: So you really think that Tully-Fisher can give NGC 4569?

R.B. TULLY: No, I said it's not benign.

A. SANDAGE: It's normal then...

R.B. TULLY: Benign means... (laughter)

A. SANDAGE: ...not sick. Or is sickness not important?

R.B. TULLY: Sickness is important. I am saying that I do believe that I have tests of whether I can fairly go and get a distance. I can look for example at the colour of the galaxy and see if the colour is normal (B minus H colour, for example). I can look at its surface brightness and see if that's normal, say, in plots against the line profile width. Those are relationships which are distance independent. If on such tests a galaxy is normal, then I tell you first of all that all the various techniques at my disposition give common distances, they give me the same distances.

A. SANDAGE: If you had a distance limited sample of normal galaxies, what is the intrinsic dispersion in absolute magnitude at a given line width? What is the real Tully-Fisher dispersion?

R.B. TULLY: I have only felt that I had a handle on that by looking at galaxies at a common distance, which is to say in clusters. In those cases I get these numbers that we're talking about here, 20% in distance, or .3, .4 in magnitude. If you look into the field, though, and use some other method, like redshift or model, to give you a distance, inevitably the dispersions are going up. Inevitably.

A. SANDAGE: Now, Richter and Huchtmeier got a value for that. What...

O.-G. RICHTER: The value was a bit different for Virgo and the more nearby groups. In the more nearby groups we have a scatter in the blue Tully-Fisher of roughly .6 magnitude, whereas in Virgo it goes up to .9 to 1 magnitude.

A. SANDAGE: That's the sigma?

O.-G. RICHTER: That's the sigma. That's the dispersion around the mean line. Part of that is due, for example, to this W-cloud which is at a certain distance. If we remove that from the sample, it goes already down. It may be that this larger scatter which we see in the Virgo Cluster is a hint at its physical extension. But to what extent we can use the distance indicator to sort that out, that's another question.

J. HUCHRA: That depends on the parameters of the galaxies you were using... Did you go to only highly inclined systems or did you play the game like de Vaucouleurs and take things down almost 25 degrees?

O.-G. RICHTER: Yes, we take all of them, because both extremes have their problems and their corrections, and we think that the line width correction is better under control than the intrinsic magnitude correction.

J. HUCHRA: I claim that the inclinations are disastrous, especially for face-on. And it's not even under control, it's just insane.

O.-G. RICHTER: I've made a relative statement!

M. ROBERTS: I think the value of this discussion is to show how one method, including the originator, feels about its applicability.

R.B. TULLY: I would not agree with Richter. I don't really want to get into a discussion on this, but I think that the sample that you used gave you a dispersion which is much larger than the real scatter is. Now, I don't really think that that's something that we want to go into.

O.-G. RICHTER: Well, our first sample consisted of 66 galaxies, now, meanwhile, with the sample that Walter Huchtmeier was talking about yesterday, we have doubled that number and the scatter remains roughly the same. It goes down a bit.

R.B. TULLY: Well, it's not the largeness of the sample which is a problem; it's in the other sense. I would make the claim that there are too many galaxies in your original sample - I don't know what you got now - that shouldn't be considered. So, I mean we could talk about that, but there is a whole bunch of dangers that you can get into and which can increase the dispersion. I don't think that it is as high as you suggest.

A. SANDAGE: Could we go back to Rod's point... Is there any possible way to get distances, or what are the possible methods? That's certainly a crucial one which is in the front running. There is another one and that's the resolution into brightest resolved red/blue stars. And if you look at the local galaxies where that can be calibrated with the Cepheids you get some idea how stable that is. You and Sidney Wolfe were looking into the A supergiants, we've been looking into the red supergiants and brightest blue variables. And that gives a dispersion of about $0^{m}.4$ plus or minus, or a spread of $0^{m}.4$ with only about 12 calibrators; so the sigma is still not known. But if it's really $0^{m}.4$ in absolute magnitude, that's 20% in distance. Now, I think that the Virgo Cluster spirals can, in fact, be resolved almost from the ground: almost from Palomar, but certainly from Hawaii, and certainly from ESO, and certainly from Campanas. But the apparent magnitude of the brightest blue stars will be about 21^{m}, I think - maybe 22^{m} - but their absolute magnitudes seem really now to be very stable at $-10^{m}.0$. It's certainly possible to do that from the ground, but you have to have very very good seeing, and you have to choose the galaxies so that the background disk luminosity, the continuum luminosity that you are trying to resolve the stars against, is small. But that's a next thing to do if you have lots of telescope time and could sit and wait for the good seeing. One should really try to determine the apparent magnitude of the brightest blue stars. And how do you know they're going to be the brightest ones? - because these are the irregular variables that only have half a magnitude or a magnitude variation. You have to have 20 years' observations

to get the maximum. Fortunately those exist in M101 and M33, but you have to have long-range programmes to do that. So, that's not feasible with the amount of telescope time that's available. No telescope time allocation committee is going to permit that. So, you've got to find some other way, and that other way may be the red supergiants at -8^m to -9^m. I think we were very optimistic believing that this was independent of the absolute magnitude of the parent galaxies. It certainly is somewhat degenerate but not completely.

B. TULLY: Maybe what you can observe best, though, are the stars that are just at the upper envelope of stability in the blue, like Humphries' upper envelope, just below the Hubble-Sandage stars. So you can see the brightest blue stars, and you look a few times and you see which ones are varying, and then you see at which magnitude they become stable.

A. SANDAGE: That's right. But the brightest blue ones which are just slightly above vary on time scales of several years. So it depends, I guess, on how steep in the luminosity function you're going to hit the wall. And since you're after the brightest stability ones, and you know you're at the Eddington limit then... and that seems very stable at $-10\overset{m}{.}0$ with certain calibrations of the Cepheids. But that, I think, could be done from the ground..., but you shake your head.

R. KENNICUTT: Merely if you do the brightest variables... Remember the distance of Virgo, especially your distance: a third of a second of arc is probably 30 parsecs. That means the brightest stars you're going to see are Magellanic star clusters and h and Chi Persei. The Pleiades are stellar in M101.

A. SANDAGE: But they won't vary! That's the reason why you use the blue variables.

R. KENNICUTT: Then you need 20 years to do it.

R. GIOVANELLI: What about the H-magnitudes, John? How many H-magnitudes are available?

J. HUCHRA: Well, that's a situation which can be improved, relatively trivially. We stopped observing not because we ran out of H-magnitudes that we could get, but rather because we started to run out of cluster galaxies that we can do from Arecibo. It's a little different.

R. GIOVANELLI: How many H-magnitudes are there?

J. HUCHRA: In existence?

R. GIOVANELLI: In the Virgo Cluster...

J. HUCHRA: Oh, in the Virgo Cluster. We've only been doing the edge-on spirals, so there must be maybe forty, and not all of those have real high-class 21cm profiles.

R. GIOVANELLI: There are several hundred HI profiles; certainly 150...

J. HUCHRA: But remember, edge-on. Mark and Jeremy and I pretty much stuck to the requirement of the galaxy to be more edge-on than 45° and not interacting and of late enough type. And if you go to those kinds of requirements, there are 170, maybe 200 spirals total in Virgo of about 16th magnitude. If you cut in the inclination requirements, and you cut in the morphological type requirements, and in the "not-4438-requirements", that cuts the number down to about 40 or 50. I think we have reasonable data on about 30 right now.

H. ARP: What about the globular clusters? What is the potential accuracy for distance indicators from the globular clusters?

A. SANDAGE: Zero!

J. HUCHRA: That's dangerous, real dangerous...

R.B. TULLY: I think the studies of globular clusters tell you more about globular clusters than they do about distances.

A. SANDAGE: Who else said zero? (laughter)

M. ROBERTS: Let me finish the subject of what should be done over the next few years... What is your feeling on how Virgo is doing?

R. GIOVANELLI: I came here sort of ringing a bell. I recognize there is a lot of alarming effects going on in this cluster, and not only this one. Lots of spirals are getting blasted by something - extragalactic medium, whatever. Several talks have been given on HI, it was not only the last one by Guiderdoni. Well, we have to think of the fact that if this is happening, it

has happened very recently. I believe that galaxies in this cluster are being stripped; their gas is going somewhere else; it's certainly leaving the disk, it's not visible anymore; maybe it leaves the galaxy and migrates into the intracluster medium. Something is going to happen to these galaxies; I don't think that there are enough mass losses that are going to replenish them and put them back to be well-behaved spirals as they were before. Now the problem with this is that then we're looking at something very special now. I think that most SO's - and most people would probably agree with me - were not generated that way. They didn't become SO's after having been stripped in a cluster environment. There are too many lines of evidence that indicate that SO's have been that way for a long time. There are SO's out there in the periphery of superclusters where nothing, not even the fastest travel times, could have brought them there after being in the core of a cluster. So, are we living in a very special time? Are we living in a time for spirals that are starting to get stripped? It's a little unsettling. It's a little anti-copernican, if you want. We happen to be living in this very special time when spirals are falling into the clusters and are becoming SO's. I don't like it... I really don't have any...

D. LYNDEN-BELL: Isn't that just a measure of the density of the Virgo Cluster...? There is a certain G ρ defined by the density of the Virgo Cluster..., and later there will be another cluster which has another ρ which will do it then...

R. GIOVANELLI: It seems to be happening in Coma; it seems to be happening in a lot of other clusters that have a relatively...

D. LYNDEN-BELL: If you go further out in Coma you presumably find the density lower.

R. GIOVANELLI: What happened to the spirals that fell in, say, half a billion years ago...? We see that the majority of spirals in the cluster quarter are being swept at a very fast pace. If you sort of integrate this over the time of...

R. KENNICUTT: But they're gas poor; it's not the same thing as being swept. (silence... laughter)

W. FORMAN: ...May I go back to Don's comment..., you know, it is exactly just the time scale of the Virgo Cluster. It happens to be Virgo's turn. Those

spirals may well be falling in. If you look at Coma, it was presumably much denser aggregated; it made more E and SO galaxies, and perhaps, as you went out in shells, the distance of stuff that is falling in at different times... You have to go a lot further out before you get to the kinds of densities of spirals you see in Virgo; it's just much further out in Coma.

R. GIOVANELLI: I just came here with the intention of dropping the brick on my toe, which I just did 6 months ago. Literally. Well, there are a few other things... I want to raise problems about this interpretation! There is something else that looks a little funny. HI is swept in cluster spirals, at least that's what it looks like from the sample that we've seen. We see that there is correlation between the HI deficiency and the ultraviolet deficiency. Galaxies that are swept seem to have their star formation quenched; the correlation with the ultraviolet is particularly telling; something happened just very recently. The correlation with the B-V also indicates that galaxies which are gas-poor are making much fewer stars. Now, the CO still seems to be there, but why are the CO clouds not making stars anymore? Is there a problem with the quality of the samples? I seem to see that in your samples (Judy and Kenney's samples) there is a large preponderance of late spirals. Is there a bias in the way you selected the galaxies? I would like to see more observations of CO content in maybe very early type spirals, like Sa's, both in the field and in the cluster, and see what happened to those. ...Could you comment on that, Judy?

J. YOUNG: I spoke mostly about Sc's today, we have the most field galaxy data on Sc's. Within Virgo, I did look at the centres of 8 Sa's and Jeff has plans to look at more Sa's. I wouldn't agree with the statement that star formation has been quenched in the galaxies. I do raise the point about the deficiency versus U-B correlation; one needs to know how that correlates with type, because the deficiency is somewhat type-dependent within a cluster - just due to the a morphological segregation. So, that's just an issue which has to be addressed. I think star formation in the outer parts needs to be looked at more carefully by looking at colour gradients in galaxies. Gradients were certainly talked about today, but there aren't good data in any galaxy, and in the very outer parts where the HI has been stripped, it would be nice to know if the colour gradients imply that star formation has just turned off there, and not in the inner parts of the galaxy where one still sees the CO, or that it has for some reason turned off in the outer parts and been lessened somewhat in the center. I guess the IRAS data certainly imply that; although, without having a comparison sample of the same types one doesn't

know what the normalization is but that star formation might be down. People are talking about a factor of 2, and the CO contents, H2 masses that we are implying are accurate to a factor of two only. So, we can't make the statement that all this data isn't consistent... Maybe Jeff can speak about whether his planned sample has any very early types in it.

J. KENNEY: Well, it has a couple of SO/a types. I did show data today on NGC 4569 and NGC 4579 which some people classify as Sab's. So those are the earliest type ones that I've done. A problem with this will be that it takes a long time to check even some of these brighter galaxies, so that I will not be able to get data far out in the disks in more than, say, 20 galaxies. I plan to look at perhaps an additional 20 but don't expect to detect them out of the disk.

D. LYNDEN-BELL: Everybody is talking as though when you take gas out of the galaxy its type is inviolate. I am unhappy that that might not be true by half a type, or something.

J. HUCHRA: That's because if you really do quench star formation instantaneously... it's something like an Sc that was forming stars at a continuous rate, in 10^9 years it turns into the colours of an SO. It takes almost no time at all to change colour. The surface brightness will go down by about a magnitude, maybe a magnitude and a half. That's the instantaneous approximation and almost certainly is not what's going on in these galaxies in Virgo. As Rob will say, there are no smoking guns.

D. LYNDEN-BELL: I wasn't claiming that there were smoking guns...

J. HUCHRA: 10^9 years isn't really enough time for the spiral pattern to turn into a pumpkin. When people do try to look at underlying disks in these spirals, such as Schweizer, you still see the spiral patterns quite well in the underlying old population in the infrared light, so that morphology will still be there.

D. LYNDEN-BELL: Do we know whether the pitch angle is the same as it was?

J. HUCHRA: You're asking a lot!

D. LYNDEN-BELL: Yes! But that's the sort of thing that the morphologist is going to use.

J. YOUNG: But we're also talking about, I believe, stripping of low density gas in the outer parts of galaxies, and that doesn't necessarily affect what most of the optical disk is doing. The most extreme cases do strip, it does appear in NGC 4569, gas that is within the optical disk; that one sees at least on the photographs. I don't know...

R. KENNICUTT: The optical disks are affected. I didn't show slides today. When you look at a galaxy in Virgo the star formation rate total is down by a factor of five, say. It isn't that there are simply five times fewer HII regions, all clumped to the center of the galaxy. The characteristic luminosity of the entire HII region population is depressed by roughly the same factor, so the disk is affected. And I think you raised a very important point. When I tried to do these optical correlations, asking the question of is the star formation in a Virgo Sc different from the field Sc was almost a self-defeating game to play, because, when Allan Sandage classified the thing as an Sc part of it went into a classification of something he calls resolution of the disk. And I think Fred raised the point that what we need is some - whether it be photometric - index that is inviolate to stripping, some dynamical index - either large data sets on dynamical properties, rotation curves, or, perhaps, just the bulge ratios, although there you have to be careful to find those as well - to try to look, at least from the optical point of view, at the question of environment independent type. You can't separate them...

R. GIOVANELLI: To some extent, I think, the diameter of the disk is a good indication. It has been mentioned by several groups here that the best diagnostic tool for the hydrogen content of a spiral is the size of the disk. Shostak and others, and yesterday's talk of Chantal and today's talks of Guiderdoni and Martha and others have been stressing the fact that it would be a good idea to use sizes. This sort of hybrid surface density of the HI is almost type independent. We're talking about HI deficiencies of a factor of 10. If you move from one morphological type to the other, even if you make an error of 3 morphological types - if you agree that the galaxy is a spiral, but is not an S0, a generic spiral, you can say that if that spiral is deficient by a factor of ten, it is not the result of the misclassification. That galaxy really has a funny disk; something happened to its gas. In fact, I would like to encourage people who do comparisons of hydrogen contents - especially those who prefer to use hydrogen mass-to-luminosity ratios - to use also the other one. Just as an exercise; it doesn't take so much work.

Instead of using just M_H/L's. With the L's you always put in the bulge, and that bulge changes the luminosity. When you use that bulge luminosity you're sort of entering a very large spread, a very large arbitrary scattering relation. I think we have some ways of measuring when something really has happened, something peculiar has happened to the galaxy. The sizes of the disk are very very good. They are not so artistic...

A. SANDAGE: I think what you and Martha and the others have shown about what you've said is probably the second, or first, most unexpected thing for me in this conference: that "independent morphological type". That's the reason why, yesterday, I kept always asking what the morphologial type was, because one had thought the HI content went with type. So your proof is absolutely self-consistent. I just am still amazed that you get a line which has no scatter with Sa, Sb, Sc with your surface brightness of HI. And so what to do next? What I think I am going to do next is try to see if I can understand that in the following way. Strictly on morphological grounds one can divide the Sa's into three groups. One with absolutely smooth arms, no evidence of gas or star formation, and no dust. One intermediate group that has some dust and the ones that are closer to Sb, but they're still called Sa. Now that's been done, and that list has been given to Huchtmeier for the HI and it's my understanding that in those three morphological groups the HI content is absolutely correlated: hardly any HI in the smooth arm Sa's, lots of HI in the other types. Now, if I go back and do what Martha suggested and look at the disk and divide by the surface area, if you're right, everything is going to come together. But I'd be very surprised if that does.

R. GIOVANELLI: There was a paper some years ago on the HI content of low surface brightness spirals and they were found, surprisingly, to be very hydrogen abundant, by a factor of three or four. If you just take the hydrogen mass to luminosity ratio, that's what you get. You take just the size of the disk, they just fall in in the sequence of all the other late spirals, just very nicely.

J. HUCHRA: Something else that might be important are the rotation curves. You can think about the masses of the galaxies. This is something which is not going to change much in the stripping process. And those kinds of things are probably easier to measure than many of these other properties.

M. ROBERTS: Let me go to Bill and ask...

W. FORMAN: I have a somewhat different perspective than some of the people sitting here, namely the X-ray telescopes now are gone. Some of questions looking not just to the next observing season but to the years beyond - perhaps it's a prejudice because it's the kind of thing that one can see in the X-ray, but the questions that interest me have, I think, implications for both the optical and for the radio observations - are just listed here: the cluster gas - where does it come from? In Virgo the gas that you see, in the centre of the cluster, is comparable to the mass that sits in galaxies. It's a lot of gas. The gas has half solar abundance of iron. Some of it was primoridal, and huge amounts of iron were expelled in the initial generations of stars; or the abundance was comparable but huge amounts of mass were blown out of the galaxies. Now where did it really come from, when did it come out? If you go to something like Coma, it's even perhaps a bit more perplexing. The mass of gas is several times the mass that you now see in stars. You really have huge amounts of gas, and it too has half solar abundance of heavy elements, of iron. It would be interesting to now start looking backwards in redshift to see what you expect..., how do you get that, what kind of energies do you need to make all those heavy elements, and what do these early galaxies look like? It could be absolutely spectacular.

D. LYNDEN-BELL: Can I ask the question of how much extra gas is there if you just consider not the whole Virgo Cluster but the region over which you see the gas? Surely that's a much bigger factor?

W. FORMAN: I think the answer is that in the core of the Virgo Cluster, not out to three degrees, but out to, say, one degree, one and a half degrees, the mass that you see in gas is comparable to the mass in the galaxies in that region.

D. LYNDEN-BELL: ...in that region, I see. So, in practice it's a very small fraction of the total involved...

W. FORMAN: ...of that total out to some marginal degrees. That would be true. In Coma, though, I would guess the situation would be somewhat worse. The mass of gas is getting to be some number times 10^{14} solar masses. So in rich clusters it's ten percent of the virial mass.

...In coming back to M87, the question would be: what is M87? Well, in some sense it dominates as cD; it has a peculiar population of globular clusters. Where did they come from? The other question that I would like to

be able to answer is how the X-rays behave in time... If you look at the galaxies and clusters presumably producing all this extra gas, huge amounts of energies did generate all this iron. What was happening to the galaxies in the field? Where did that gas go? Did they make an intergalactic medium?

The other question that's fairly interesting: there seem to be cooling flows at the centres of clusters, around the cD's certainly. There may well be cooling flows around these other coronae. This is a general source of gas, material that can accrete, that can affect radio sources in essentially all early type galaxies, perhaps more prevalent in the centre of rich clusters. The other thing I would like to mention is that certainly in X-rays one is struck that there are a lot of other clusters like Virgo and one has the problem that, no matter how good your data is, you always come to the question in Virgo, - am I seeing something peculiar? - just a statistical fluctuation? You can go to more other clusters now with the same kinds of central galaxies, Abell 1060, 262 Centaurus. They all contain, at least speaking in X-ray terms, these bright galaxies that seem to dominate the cluster. One certainly should be able to begin to look at these and see whether or not the kinds of properties that one sees in Virgo are the same; whether there are some of the clouds that formed the same kind of galaxies as in Virgo, or whether we actually begin to see something different.

C. KOTANYI: I agree rather with Arp that indeed Virgo is special, it is unique in being the closest system. This has implications! I would say that things like stripping are second order, so we will have a hard time to notice that in other systems. We have to go to small details which you don't see there. So, Virgo remains really the touchstone of...

B. TULLY: It should be pointed out in fact that that statement is not correct. There are two other pretty good clusters within the Virgo distance. And we talked about how little work has been done on the Virgo cluster at the beginning of this conference. And so I'd like to mention these other two clusters. There is the Fornax cluster, which at least people have heard about... (laughter)

A. SANDAGE: We got the proper plates for the whole Fornax Cluster too! If anybody would like to volunteer to do the same as Bruno has done on the Virgo Cluster...

B. TULLY: And then there is the other cluster that has received so little attention that it's disgraceful and that's the Ursa Major cluster. It has some different properties, like zero elliptical galaxies. But it is a cluster at the same distance.

W. FORMAN: That's quite a different property! There couldn't be any blinds, could there? (laughter)

D. LYNDEN-BELL: But that's the blind test at once. You must give the positions in this cluster to Chip, and the positions of another cluster full of ellipticals to Chip, and see which one he chooses to have the lines in.

M. ROBERTS: There are still two more participants to participate. I'd like to call Allan now... to see if you have any comments?

A. SANDAGE: Well, the three oldest people at this conference are me, you and Chip, and we all suffered together. But at that time Walter Baade was still alive and the whole, I think, of what the three of us have done has been influenced a tremendous amount by that time when he was just indicating the population concept. And going through life for the last thirty years... all elliptical galaxies are exactly the same age! No variation whatsoever. Now, that's not what most of you believe. And it has been very hard to overcome your teacher's hammer on your head. So - I agree with Brent - why do you study the Virgo Cluster? You study the Virgo Cluster to try to find something about the formation and the evolution of galaxies, and I think the Virgo Cluster is an incredibly important place to look for that. So what now can you do with reasonable amounts of telescope time is to ask the question, are all stars in all elliptical galaxies essentially the same age or aren't they. The whole problem of where the dE's come from and where the Im's fit in is now extremely ripe for work. First of all, I think, there ought to be a massive survey of the profiles of Im's and Sm's; there are not all that many in the Virgo cluster. Now, if dE's really are the daughter products of some more massive parent; and it seems that they have to be if stars are going to form in such a system - you can't imagine how stars are going to form in something whose parent was as low density as Draco; - so, if dE's are daughters: how long ago did they become daughters? Well, the study then of the stellar content of dE's - are they young stars, or are they just like globular clusters where everything is exactly the same age? - is extremely easy with the techniques and just a few nights at the telescope. I got four slides (reproduced here in Figure II, ed.) which show what could be done four

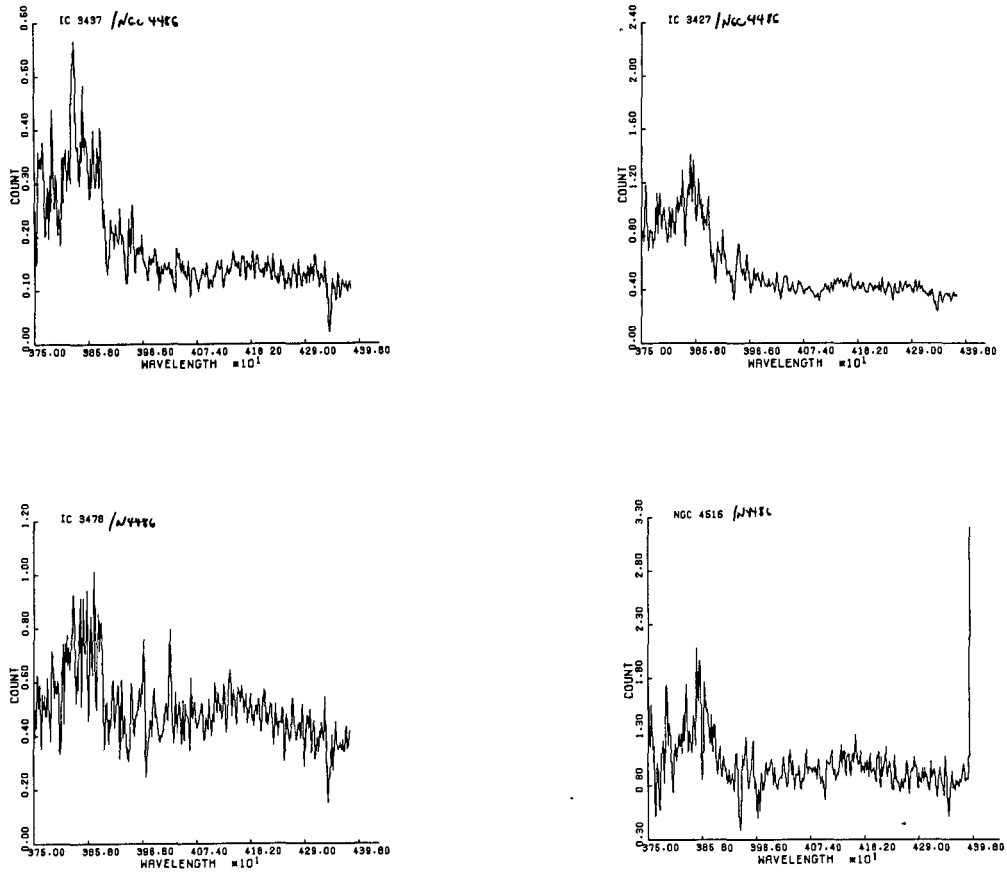


Fig. II: Spectra of 4 Virgo dwarf ellipticals divided by the spectrum of M87 (courtesy of A. Sandage).

years ago in this business. These are spectra of dE's which were bright enough to get at Palomar with the Reticon as it existed at that time, and these spectra are the product of one night's observing with Alan Dressler on a few of the brightest dE's that were found at the beginning of the catalogue work. Now what is plotted here - this is IC3437 (upper left in Figure II, ed.) - is the spectrum of that divided by the spectrum of M87, and it goes from 3700 Å to 4400 Å. What you see immediately is that, whatever the ratio is, it's pretty level until you get to about 3960 Å and then it takes off like a bomb. That's the ultraviolet excess. Now, is that the Fraunhofer line blanketing, metallicity effect, or what? Every single dwarf that we've got has that effect. That's the U-B blueing as the absolute magnitude of the dE gets fainter. What it looked like to me on the screen when these spectra came up was that the equivalent width of the hydrogen lines was increasing as you got fainter and fainter objects at the telescope. This would suggest that it's not metallicity Fraunhofer line blanketing, but more and more A stars

coming into the spectrum. Now, we haven't done anything with these for four years, but it would be extremely easy now with the detectors available to do a mass study and get the equivalent widths of the hydrogen lines and the metal lines. Tully has undoubtedly done all of this. Let's see the next one. They all show this. That's less, although if you take the division of the counts it's about the same ultraviolet excess. That's IC3427 divided by M87, and there the jump is a little less, that's a brighter galaxy. And the next one is again an IC galaxy, exactly the same features; that is the ultraviolet excess. And finally the fourth one... it's an absolutely common feature. OK, What is it? That's a question I think is amenable to a tremendous PhD thesis with one night at a telescope. So, that's one thing. Part of this is to pick the nucleated ones, to see if they look like globular clusters. Two nights at the telescope could get you a sample of thirty and see if the distribution of metallicity is the same as in globular clusters. We know they're composed of stars. What kind of stars? What's the age? All of that's amenable to working, and that's what I think would answer the question whether dE's have had recent star formation or whether they are like Baade told us always, that twenty billion years ago it all began in a burst and then hardly anything has happened in the ellipticals. So, I think all of that could be done in just a very few months. That's what I think I would do next.

H. ZINNECKER: I just wanted to comment on my interest in this. I mean, if you manage to get the optical minus infrared fluxes then this is also a means to address this question.

A. SANDAGE: That's right, Hans. I guess I would have asked you yesterday why you chose the infrared and interpreted it as metallicity. What is the feature in the spectrum that is changing as the metal abundance changes? We know what it is in the ultraviolet, it's the Fraunhofer line blanketing...

H. ZINNECKER: But, I mean, if the metallicity gets higher the giant branch gets cooler, and so it gets redder. So the infrared colour J-K is sensitive to metallicity and this has been calibrated for globular clusters. If I know that the things are red in J-K, then I have an indication that it is metal rich. Now, if the B-K colour does not agree with this metallicity, then I have to interpret the blueness of B-K in a different way. So, in a way, J-K and B-K are orthogonal axes, one is metallicity and one is some sort of an age indicator. But only for part of the...

A. SANDAGE: That's true if you a priori know that you are dealing with a globular cluster-like population whose subgiant/giant branch goes redward. But you could equally well be dealing with a 10^9 year old population where you have M stars of luminosity class III, normal HR diagram of only a billion years old.

H. ZINNECKER: That's why I tried to look through all these other systems, for instance the Magellanic Cloud type clusters, some of which are younger, and if we knew better what the Searle-Wilkinson-Bagnuolo classes meant, then we could address this question in better terms. I believe Hodge has tried to show that the Searle-Wilkinson-Bagnuolo intermediate age clusters are rather young, say, only 10^9 years old. So from that we know that, for instance, you could only expect carbon stars, red stars, if they were less than 10^9 years old. So if they are too red - and they could have carbon stars - then we would know they're young. Since they do not seem to show carbon stars at a significant level, I excluded significant star formation younger than 10^9 years. There may be some declining star formation rate, that's not excluded...

A. SANDAGE: I think that your program is extremely valuable. It's exactly along this line of trying to find the age and it would be interesting if you could add the ultraviolet to it as well.

J.-L. NIETO: I just wanted to ask you what's the size of the aperture through which you got the spectrum of M87?

A. SANDAGE: This is a good question... About 10 seconds of arc for both square aperture 10 seconds on a side.

M. ROBERTS: You don't need new telescopes for this... you could do it tomorrow.

A. SANDAGE: No you need a new time allocation committee. (laughter)

M. ROBERTS: I'd like to call upon Rob to...

R. KENNICUTT: I'm getting hungry, so... (laughter)

D. LYNDEN-BELL: ...you EAT galaxies? (laughter)

R. KENNICUTT: Right... Let me play a bit of the devil's advocate with regard to sweeping. We've heard all sorts of platitudes all through this conference that the most important thing about studying Virgo is to understand the formation and evolution of galaxies. But we know from studies of clusters that the cluster environment does have a profound effect on the formation of galaxies. We know that the ratio of ellipticals to spirals is very different in clusters, and the ratio is higher the richer one goes in clusters. We know that the ratio of SO's to spirals is very different. There is no reason to expect that the ratios of different spiral types shouldn't be affected. Certainly - I'm convinced too - there is sweeping going on. But I'm afraid that we're also sweeping under the rug perhaps a very fundamental piece of information about galaxy evolution, especially galaxy formation. So, if you now want to accept as an operational hypothesis that ram pressure sweeping is the explanation, I think it's time to test that hypothesis. There are three projects that one could do to improve on what we have now. One we've talked about a lot is optical data, disk to bulge ratios, disk surface brightnesses especially. So, I won't go into that. There are a couple of other things, though. One is studies of individual galaxies. We've been talking of nothing but statistics of one kind or another, so, don't forget that if you go to the Virgo Cluster and pick a random Sc galaxy, anywhere in the cluster, it would probably be indistinguishable from a large number of field galaxies. You only see these transient statistics. You see them most strongly in the HI diagrams, but there are lots of normal galaxies in Virgo. There are galaxies in the Coma Cluster, the most hostile of all environments, which if anything are more gas rich and more star formation rich than field galaxies. It's hard to understand, if sweeping is so efficient, how these other galaxies can survive. Maybe one way to do it is to start looking at individual objects. That's the second project. John said that I said there are no smoking guns. Well, if I said that I misquoted several people... Typically what happens in this game is that whenever someone writes a paper about sweeping, they present one or two of their favourite objects for recently stripped spirals. Here is a list. If somebody wants to go out and make the front pages of the New York Times I guess maybe this is what you do. I won't go into details. Many of them are favourites. They sort of come in two classes. One are things with very abnormal X-ray, radio continuum or HI morphologies; the kinds of things Chris was talking about. There is another class, the so-called anemics. What's unusual about those is that they clearly have the disk to bulge morphologies of late type galaxies but the gas contents and star formation properties of early type galaxies. There are extreme cases - objects with virtually no bulges at all... few percent of the light..., but with the gaseous and stellar populations of Sa or Sb galaxies...

I think it's important, at the same time, not to ignore the field when studying Virgo as hard as we have. A lot of the processes that we see in Virgo, including the most extreme examples of "stripping", go on in the field and, I guess, I'll finish up with a couple of slides of NGC 1961. The slides were provided to me by Seth Shostak who was the principal author of a paper that came out about a year ago, which was "NGC 1961 - Evidence of a ram pressure swept spiral". It is probably as good a case for sweeping as I have seen anywhere, including any of the examples we've discussed so far. Here's the HI distribution. By the way, NGC 1961 is the galaxy which Vera Rubin and Ken Ford and Norbert Thonnard got into the New York Times for announcing it was the most massive spiral in the Universe. There is a strong asymmetry in HI crowding up on one side of the galaxy. The galaxy has a very peculiar optical morphology and very peculiar emission line velocities. That's the sort of the head-tail morphology in HI. The next slide shows the velocity field of the HI. That's not so unusual, but it is again, you see, evidence for some distortions up here, lots of spiral arms here but they are again more evidence for asymmetric velocities indicative of sweeping. If you make a radio continuum map, there is a fairly sharp ridge over here, a ridge in the continuum emission. The Einstein maps of this galaxy, long integrations, show an X-ray ridge over here, at least that's the claim in the paper. It's a rather tough case, it's a velocity of several thousand km/sec. There is quite a rapid change in colour at the edge if you look at the blue and red plates.

So, you want a good smoking gun, a recently stripped galaxy, that's it. There is only one problem with 1961. You know from the NGC number it is not in the Virgo Cluster. In fact, you can hardly find a more isolated galaxy: it's sort of over here... (speaker is drawing on blackboard, ed.). There are a couple of little galaxies over here; some of them at the same redshift, some not, I don't know... There may be a small group, but that's it. This thing [NGC 1961] has a virial mass just from the optical rotation curve of something in excess of 10^{12} or maybe 10^{13} solar masses, in fact, somebody probably knows, but from what I knew it is 10^{12}. It has an HI mass of 10^{10} solar masses. Presumably that 10^{10} solar mass is being removed from it now by this invisible intercluster medium. By the way, you don't see any X-ray gas in here...

A. SANDAGE: Intergalactic medium...

R. KENNICUTT: Well, nothing in X-rays. According to the calculations that Shostak et al. made, you need a density of intercluster gas of ten to the...

Now, I'm not a theoretician...(laughter). Look, I can't work out what you need, but let's do a little, you know, sort of my level of thinking. For a momentum conservation alone you got to have mucho solar masses of this stuff (...) to remove this stuff (...). So you've got probably several hundred billion solar masses of hot intergalactic gas that have to be here. Where it comes from, heaven knows, right? There is not enough mass of gas in these galaxies to make it. So you've got an invisible intercluster medium that is stripping this thing, that is being fed by invisible galaxies. Imagine to confine a cloud like this gravitationally requires invisible mass of probably 10^{14} to 10^{15} [solar masses]. You need an invisible Virgo Cluster here to strip this. Now one of two things is right. In my mind, either something else is going on than sweeping - a suggestion a few people have made, even brought up in this paper..., well, maybe a collision of an intergalactic cloud, HI cloud or something... This thing is so big that one galactic rotation time out here is something like a billion years. So maybe some lump, strange warp has developed. Anyway, if that's the explanation and it can happen in NGC 1961, it might happen in a few of these cases in Virgo as well. The other interpretation is - this could be one of the most important observations anyone has ever made - maybe this is the missing mass! Right? Here is this invisible thing without even a cluster. So, here is the last thing I will raise both in statistics and individual galaxies. It's important to look in the field as well. If you come up with a scenario for producing some of these fantastic smoking guns in Virgo, you are going to have to explain how galaxies like 1961 can be created without the benefit of having a Virgo Cluster around them as well.

H. ARP: Can I make a post-script to this? The reason why my attention was drawn to this galaxy - something you didn't mention - there are long luminous filaments coming out which are going off in this direction. Just as a suggestion, what about having an explosion on the edge of that galaxy?

R. KENNICUTT: (raising an eyebrow) ...Yeah... (laughter).

R. GIOVANELLI: Since you're talking about one shot things, there is another galaxy. The name is NGC 7214. Two or three years ago, Martha and I stumbled over this galaxy, a nice Sc irregular, pretty irregular for a spiral, and, well, we found that the HI profile was very funny. It looked something like this... (speaker is drawing on blackboard).

M. HAYNES: Which is just the way NGC 1961 looks.

R. GIOVANELLI: We decided to map this thing. We had a beam which is about this big, not terribly good. However, the hydrogen of this galaxy was like that (speaker is drawing on blackboard), very similar to NGC 1961. Then we went to the VLA and we mapped this thing, and there is a nice star here, and then there is something smaller here, which in Arecibo we couldn't resolve because our beam was too big... Well, it turns out that if you look at the gas in here, it's split, and there is another nice galaxy right behind this one. I think it's very dangerous to just look at one case alone...

R. KENNICUTT: That's not my paper! That's one of yours... (laughter)

R. GIOVANELLI: Just behind NGC 1961 there could be another guy who is doing something to it just like NGC 7214 and it could be the source for the gloom that Chip was talking about not so long ago. So I think there is a...

H. ARP: This is hidden light to match the hidden mass!

M. ROBERTS: In keeping with Rob's opening remarks about hunger, which I think is shared by many of us, I shall adjourn this and point out that all you can say about the wine is that we [the panelists] started earlier and I trust there will be copious quantities at the dinner this evening.

IX.

SUMMARY

SUMMARY

D. Lynden-Bell
Institute of Astronomy, Cambridge

If the objects clustering are much smaller than the scale considered and their motions are not relativistic and gravity is the only important influence, then there exists a regime in which the only important constant of nature is Newton's G. At time t after the start of the big bang there is a natural density given by $(G\rho)^{-\frac{1}{2}} \sim t$ and so

$$\rho \sim 1/Gt^2 \qquad (1)$$

Actually, most of the time is spent near the minimum density to which the big bang expansion leads before collapse. For bound non-dissipative systems $\rho_{min} = 1/8\rho$.

We have seen in this Conference that the Virgo cluster is young and is growing. Equation (1) may lead us to believe that there may be a super Virgo, nine times less dense when the universe is three times older. Were there structures at nine times the current density at $1+z = 3$?

An $\Omega = 1$ universe is necessary to make such statements strictly true but the local overdensity makes such statements very close to truth because locally in the Virgo cluster the world is close to such a piece of such a universe.

This has been largely an observational conference and there are no **direct** observations of the dark matter that dominates the dynamics of the Virgo cluster and the outer parts of normal galaxies. We must not forget that we have been talking about less than a tenth of what we believe must be present. Anyone who studies dynamics needs to know what is happening to the dark haloes that dominate the mass. The dark haloes of galaxies are large floppy, low-density structures easily distorted by tides. Tides between haloes are much more important than tides between galaxies not just because the haloes are more massive, but more importantly, because they are much less dense. Even if we consider only the distortions of the visible galaxies, then Prof. Setti's heavy halo will have a great influence on me, not just directly, but more importantly his halo will bend my halo, which will then distort me. Such effects enhance tides by another factor three over and alone those expected because Setti's halo is heavier than he is. In considering the dynamics of the Virgo cluster we should consider in greater detail what is happening to these haloes and at what stage the tides tear off the haloes to generate the great pools in which the surviving galaxies swim. This is the mass that leads to the observed M/L_B ratios of 150 to 750 times solar. While

haloes have been somewhat neglected in this conference, it has not been lacking in excitement. Three major observational advances have come from large campaigns on the Virgo cluster:

1. The Las Campanas survey has shed new light on the luminosity function of galaxies. The luminosity functions of all high surface brightness galaxies have been traced well past their maxima but the r.m.s. spreads in magnitudes are a magnitude or so; no good standard candles have appeared.

The dwarf galaxies by contrast have low surface brightness with $\rho \propto M$ and have luminosity functions that rise inexorably as the luminosity is reduced.

With the large number of dE galaxies observed, it is possible to pinpoint their concentration toward a point to the NW of M87, clearly different from M87 itself around which the X-ray gas is concentrated.

2. The impact of all the velocity data gathered by Huchra among others, has shown that the old separation of Ellipticals from Spirals is no longer a problem. However, the velocity of the dE galaxies agrees with M87 and both are displaced from the mean of all galaxies by some 200 km/sec. The velocity dispersion differs in different parts of the Virgo cluster, the group to the south around NGC4472 being noticeably cooler than the group around the centre close to M87. However, the local mean dispersion is nowhere as great as the overall dispersion, showing that there are probably systematic streaming motions. Although Tammann found a hint of rotation, problems to do with the elimination of high velocity background galaxies to the North of Virgo West complicate the picture. The elliptical velocity distribution is nearly gaussian while that of the spirals is approximately a rectangular distribution with a greater dispersion. It seems agreed that this difference is due to the fact that many of the spirals are still falling in in great lumps and some have just completed their first transit of the cluster.

3. Many different investigations converged to the demonstration by criteria independent of galaxy type that Virgo cluster galaxies do react to their environment. They show less neutral hydrogen overall and particularly in their outer parts. In nearly every case the observations are explicable as a result of ram pressure stripping but there are two results that stand against this trend. i) the molecular CO distribution in Virgo Galaxies is not different from field galaxies of the same type in the systems so far investigated; ii) the Sm and dwarf irregular galaxies which one might expect to be most stripable do <u>not</u> show the expected gas deficit.

However, the outer parts of large spirals show both the deficits in neutral hydrogen and the older smooth stellar population expected.

We deduced that Virgo was a young growing cluster and the Conference was full of the excitement of a young and growing subject.

LIST OF PARTICIPANTS

LIST OF PARTICIPANTS

H. ARP
Max-Planck Institut für Astrophysik
Karl-Schwarzschild-Str. 1
D-8046 Garching bei München
B.R.D.

L. ATHANASSOULA
Observatoire de Marseille
2, Place le Verrier
F-13248 Marseille Cedex 4
France

C. BALKOWSKI
Observatoire de Meudon
DAPHE
F-92195 Meudon Principal Cedex
France

B. BINGGELI
Astronomisches Institut
Venusstrasse 7
CH-4102 Binningen
Schweiz

A. BOSMA
Observatoire de Marseille
2, Place le Verrier
F-13248 Marseille Cedex 4
France

L. BOTTINELLI
Observatoire de Meudon
Dept. de Radioastronomie
F-92195 Meudon Principal Cedex
France

N. CALDWELL
Aura Inc.
Casilla 603
LA SERENA
Chile

R.D. DAVIES
Nuffield Radio Astronomy
Laboratories
University of Manchester
Jodrell Bank, Macclesfield
Cheshire SK11 9DL
U.K.

T. DE JONG
University of Amsterdam
Astronomical Institute
Roeterstraat 15
NL-1018 WB Amsterdam
The Netherlands

W. FORMAN
Smithsonian Observatory
60 Garden Street
Cambridge, MA 02138
U.S.A.

G. GAVAZZI
Istituto di Fisica Cosmica
Via Bassini 15
I-20133 Milano
Italy

R. GIOVANELLI
National Astronomy & Ionosphere
Center
Arecibo Observatory
P.O. Box 995
Arecibo, PR 00613
U.S.A.

L. GOUGUENHEIM
Observatoire de Meudon
Dept. de Radioastronomie
F-92195 Meudon Principal Cedex
France

B. GUIDERDONI
CNRS
Institut d'Astrophysique
98 bis, Bd Arago
F-75014 Paris
France

M.P. HAYNES
Cornell University
Astronomy Department
Space Science Building
Ithaca, NY 14853
U.S.A.

G. HELOU
JPL, Caltech
Mail Code 230-205
4800 Oak Grove Dr.
Pasadena, CA 91109
U.S.A.

L. HOFFMAN
Lafayette College
Dept. of Physics
Easton, PA 18042
U.S.A.

J.P. HUCHRA
Center for Astrophysics
60 Garden Street
Cambridge, MA 02138
U.S.A.

W.K. HUCHTMEIER
Max-Planck-Institut für
Radioastronomie
Auf dem Hügel 69
D-5300 Bonn 1
B.R.D.

R.D. JOSEPH
Imperial College of Science and
Technology
Blackett Laboratory
Prince Consort Road
London SW7 2BZ
U.K.

J. KENNEY
University of Massachusetts
Dept. of Physics & Astronomy
GRC 517D
Amherst, MA 01002
U.S.A.

R.C. KENNICUTT, Jr.
University of Minnesota
Department of Astronomy
116 Church Street S.E.
Minneapolis, MN 55455
U.S.A.

C. KOTANYI
National Radio Astronomy Observatory
P.O. Box 0
Socorro, NM 87801
U.S.A.

R.C. KRAAN-KORTEWEG
Astronomisches Institut der
Universität Basel
Venusstrasse 7
CH-4102 Binningen
Schweiz

D. LYNDEN-BELL
Institute of Astronomy
Madingley Road
Cambridge CB3 0HA
U.K.

H.T. MacGILLIVRAY
Royal Observatory
Blackford Hill
Edinburgh EH9 3HJ
Scotland

J.-L. NIETO
Observatoire de Toulouse
14 Avenue Edouard Belin
F-31400 Toulouse
France

S. OKAMURA
Kiso Observatory
Mitake-mura, Kiso-gun
Nagano-ken
397-01 Japan

G. REAVES*
University of Southern California
Department of Astronomy
University Park
Los Angeles, CA 90089
U.S.A.

M.S. ROBERTS
National Radio Astronomy Observatory
Edgemont Road
Charlottesville, VA 22901
U.S.A.

B. ROCCA-VOLMERANGE
CNRS
Institut d'Astrophysique
98 bis, Bd Arago
F-75014 Paris
France

A. SANDAGE
Mt. Wilson & Las Campanas
Observatories
813 Santa Barbara Street
Pasadena, CA 91101
U.S.A.

E. SHAYA
Caltech
Mail Code 105-24
Pasadena, CA 91125
U.S.A.

A. SMITH
European Space Agency - ESTEC
Space Science Department
Postbus 299
NL-2200 AG Noordwijk
The Netherlands

J. SOUVIRON
CEN-SACLAY, DPhG/SAP
Service d'Astrophysique
F-91191 Gif-sur-Yvette, Cedex
France

J.R. STAUFFER
Dominion Astrophysical Observatory
5071 W. Saanich Road
Victoria, B.C. V8X 4M6
Canada

G.A. TAMMANN
Astronomisches Institut der
Universität Basel
Venusstrasse 7
CH-4102 Binningen
Schweiz

R.B. TULLY
Institute for Astronomy
University of Hawaii
2680 Woodlawn Drive
Honolulu, HI 96822
U.S.A.

G. DE VAUCOULEURS*
University of Texas
Department of Astronomy
RLM 15.212
Austin, TX 78712
U.S.A.

L. VIGROUX
CEN-SACLAY, DPhG/SAP
Service d'Astrophysique
F-91191 Gif-sur-Yvette, Cedex
France

S. WAGNER
Stettiner Str. 2
D-6900 Heidelberg
B.R.D.

R.H. WARMELS
Kapteyn Laboratorium
University of Groningen
Postbus 800
NL-9700 AV Groningen
The Netherlands

A. YAHIL
Institute of Astronomy
Madingley Road
Cambridge, CB3 0HA
U.K.

J.S. YOUNG
Five College Radio Astronomy
Observatory
University of Massachusetts
619 I GRC Tower B
Amherst, MA 01003
U.S.A.

H. ZINNECKER
Royal Observatory
Blackford Hill
Edinburgh EH9 3HJ
Scotland

PARTICIPANTS FROM E.S.O:

P. ANGEBAULT

D. BAADE

S. CRISTIANI

M.-H. DEMOULIN-ULRICH

R. DE SOUZA

S. D'ODORICO

P. FOUQUE (La Silla)

P. GROSBØL

S. JÖRSÄTER

F. MATTEUCCI

A. MOORWOOD

O.-G. RICHTER

E. SADLER

G. SETTI

M. TARENGHI

L. WOLTJER

R. ALBRECHT (ST-ECF)

T. COURVOISIER (ST-ECF)

*) Contrib. in absentia